Solubilization and stabilization of natural molecules in green and edible formulations

Dissertation

Zur Erlangung des Grades
Doktor der Naturwissenschaften (Dr. rer. Nat.)
der Fakultät für Chemie und Pharmazie
Universität Regensburg

vorgelegt von

Nadja Ulmann

aus Regensburg, November 2023

Diese Doktorarbeit entstand im Zeitraum von Januar 2021 bis November 2023 am Institut für physikalische und theoretische Chemie der Universität Regensburg unter Betreuung von Prof. Dr. Werner Kunz.

Abgabe der Doktorarbeit: 22.11.2023

Prüfungsausschuss:

Vorsitzender:	Prof. Dr. Oliver Tepner
1.Gutachter:	Prof. Dr. Werner Kunz
2.Gutachter:	Prof. Dr. Hubert Motschmann
3.Prüfer:	Prof. Dr. Joachim Wegener

Acknowledgements

This PHD thesis would not have been possible without the support of numerous people.
First of all, I would like to express my gratitude to my supervisor Prof. Dr. Werner Kunz for giving me the opportunity to carry out the dissertation on this interesting topic and for his permanent support during these years.
I am also grateful for the intermittent cooperation with BASF. In particular, I am thankful to Mireia Subinya Albrich, Roland Heinrich Staff, Matthias Kellermeier, Johanna Medert and Stephan Saum for the regular online discussions and for the insight into the company. On this account, I also want to thank the SKH GmbH for enabling this cooperation.
A part of the experimental work was performed by the bachelor students and interns Martin Rosenhammer, Julian Schiller, Jennifer Winter, Nicole Neubauer, Anna Saridis and Hugo Cuvilliers, to whom I am especially thankful.
Moreover, I thank my colleagues, Hellmuth Schönsteiner, Franziska Wolf, Theresa Ferstl, Dr. Peter Karageorgiev, Rosemarie Röhrl, Dr. Marcel Flemming, Dr. Theresa Höß, Bianca Heiligtag, Dr. Eva Müller and Prof. Dr. Rainer Müller for their support. I am also cordially thanking Philipp Schmid and Pierre Baudin for the conduction of the SAXS experiments.
I thank Dr. Johnny Hioe and Prof. Dr. Dominik Horinek for the cooperation. Thank you for the enlightening discussions, Johnny.
I thank all members of our chair, my lab partners Lea Rohr, Michael Schmidt and Verena Huber, Thomas Gruber, my office partner Adrien Fusina, Johnas Blahnik and Patrick Denk!
Dr. Didier Touraud, I am deeply thankful to you for our numerous scientific and funny discussions, for your help and for your encouragement!

My deepest thanks are reserved to my mother, father, brother and boyfriend, who always supported me in numerous ways!

Abstract

A broad hydrotropic action of aromatic sodium carboxylates – among them many polyphenols – was discovered. Based on their amphiphilicity and on specific molecular interactions, aromatic sodium carboxylates turned out to act as salting-in and -out agents in the (anti-)hydrotrope range for the small slightly hydrophobic di(propylene glycol) n-propyl ether. Sodium cinnamate and salicylate were even comparable to the biological solubilizer sodium cholate but still significantly weaker than the common surfactant sodium dodecyl sulfate.

Aside of this, in the presence of aromatic solutes, aromatic sodium carboxylates exerted a distinct solubilizing mode, which was strongly driven by the carboxylate's electronic system. Thus, the water-solubility of riboflavin, lumichrome, riboflavin 5'-monophosphate sodium salt, vitamin K3, folic acid and caffeine was increased considerably. Using a sodium polyphenolate, even the water-insoluble nutraceutical curcumin could be dissolved in water in minor amounts. Especially in the case of riboflavin and folic acid, the water-solubility was improved strongly by up to 2000 times using sodium 3,4-dimethoxycinnamate and sodium ferulate, respectively. In the case of riboflavin and lumichrome, the water-solubility correlated eminently with the conjugated electronic system of the solubilizer. In the case of folic acid and vitamin K3, the amphiphilicity of the solubilizer was more important than its electronic system. Moreover, some of the aromatic solutes were even able to increase the water-solubility of aromatic sodium carboxylates, while being solubilized by the carboxylates themselves. Nuclear magnetic resonance measurements of riboflavin with aromatic sodium carboxylates in deuterated dimethyl sulfoxide confirmed this mutual hydration. Reversible copigmentation of riboflavin, lumichrome, riboflavin 5'-monophosphate, vitamin K3 and folic acid with electron-rich aromatic sodium carboxylates indicated the formation of charge transfer complexes. Complementary dynamic light scattering, surface tension, nuclear magnetic resonance and nuclear Overhauser effect analysis contradicted the presence of larger aggregates and confirmed the formation of π-stacked complexes in the case of riboflavin, riboflavin 5'-monophosphate, lumichrome, vitamin K3 and folic acid.

Out of the polyphenolate cations tested, sodium was the best for the solubilization of riboflavin. Nevertheless, the better water-soluble choline polyphenolates enabled to keep still similar molar solubilizer/riboflavin ratios and to solubilize even more riboflavin in water.

Sodium ferulate turned out as the compromise, if a simultaneously high water-solubility of riboflavin, folic acid and vitamin K3 is desired. Moreover, despite of a similar solubilizing mechanism for riboflavin, vitamin K3, folic acid and caffeine, sodium ferulate managed to solubilize the four drugs in one formulation largely over their solubility in pure water. Thereby, sodium ferulate, caffeine and vitamin K3 turned out to undergo facilitated hydrotropy, enabling a synergistic improvement in caffeine's and vitamin K3's water-solubility.

The photodegradation of vitamin K3 could not be prevented by the presence of sodium polyphenolates. In contrast, riboflavin's photodegradation was considerably slowed down by a factor of 2-4 by sodium polyphenolates above a molar polyphenolate/riboflavin ratio of 6 in diluted aqueous solutions comprising riboflavin near the maximum concentration allowed in non-alcoholic beverages. If samples with high aromatic sodium carboxylate concentrations ($\geq$ 0.37 mol·kg^{-1}) were exposed to the sun, even more than 80 % of the initial riboflavin content were conserved for at least 8 weeks in the presence of sodium polyphenolates and even in the presence of the non-radical scavenger and non-antioxidant sodium cinnamate. Moreover, sodium polyphenolates were compatible with a common sports drink formulation from BASF, where they kept their photostabilizing effect on riboflavin.

Aside of the hydrotropic properties of aromatic sodium carboxylates, they also provide a cosurfactive support for the standard surfactant sodium dodecyl sulfate. Thus, sodium ferulate decreased the critical micellar concentration of sodium dodecyl sulfate, increased the structuring of the micellar solution, and increased the solubility of the hydrophobic solute Sudan blue II relatively to the pure surfactant solution. Moreover, the cosurfactive action of sodium ferulate coexists with its hydrotropic solubilizing power for aromatic solutes. Thus, riboflavin and Sudan blue II could be solubilized simultaneously in an aqueous solution composed of varying concentrations of sodium dodecyl sulfate with 0.37 mol·kg^{-1} sodium ferulate. Although, sodium ferulate decreased the critical aggregate concentration and increased the structuring of an aqueous solution comprising the "biological surfactant" sodium cholate, the solubility of the hydrophobic solute Sudan blue II and of riboflavin was decreased due to the presence of sodium ferulate and sodium cholate, respectively. The similar salting-in power of sodium cinnamate to sodium cholate in cloud point measurements of a water/di(propylene glycol) n-propyl ether mixture and the absence of a critical micellar concentration in conductivity measurements suggested that this lack of a cosurfactive action of sodium ferulate originates from the more hydrotropic and rigid character of cholate. Nevertheless, Sudan blue II and riboflavin could be dissolved in one pot at concentrations exceeding the ones in pure water. Thus, sodium ferulate's cosurfactive support for sodium dodecyl sulfate and sodium cholate and the compatibility of sodium ferulate's hydrotropic and cosurfactive properties constitute a green way to create less toxic and edible formulations of poorly water-soluble aromatic and hydrophobic solutes.

Moreover, because riboflavin was revealed to stack parallelly in its crystalline form, and due to the low influence of the ribityl chain on riboflavin's water-solubility, riboflavin's solubility was found to be mainly restricted by its stacking and not by hydrogen bonding among the ribityl chain. Thus, it was not surprising that the aromatic L-tryptophane, caffeine, saccharine, L-proline, L-histidine and indoxyl sulfate solubilized riboflavin in water, too. Consequently, not only polyphenolates, but also other π-conjugated compounds can act as solubilizers for

riboflavin. Therefore, the molecules need not necessarily to be amphiphilic. Finally, riboflavin's water-solubility can be tuned by altering the polarity of the solvent and its hydrogen bonding network, too.

List of Abbreviations

Ca.	Circa	**max.**	Maximum
CAC	Critical aggregate concentration	**MHC**	Minimum hydrotrope concentration
CMC	Critical micelle concentration	**N**	Number of measurements
COSMO-RS	Conductor like screening model for real systems	**NMR**	Nuclear magnetic resonance
COSY	Correlation spectroscopy	**NOESY**	Nuclear Overhauser effect spectroscopy
DLS	Dynamic light scattering	**PTT**	Phase transition temperature
e.g.	Exempli gratia	**SAXS**	Small angle X-ray scattering
HMBC	Heteronuclear multiple bond correlation	**UV-Vis**	Ultraviolet-visible
HPLC	High pressure liquid chromatography	**Vis.**	Visible
HSQC	Heteronuclear single quantum coherence	**1D**	One dimensional
LC-MS	Liquid chromatography-mass spectrometry	**2D**	Two dimensional
LCST	Lower critical solubilization	**Vit.**	Vitamin

Abbreviations for compounds:

ATP	Adenosine 5'-triphosphate disodium salt	**NaH_2PO_4**	Sodium dihydrogen phosphate
CDRF	Cyclodehydroriboflavin	**NaOH**	Sodium hydroxide
CMF	Carboxymethylflavin	**Na-4-OH-Prop**	Sodium 3-(4-hydroxyphenyl)-propionate
DMSO(-d_6)	(deuterated) Dimethyl sulfoxide	**Na-2,4-Pentadienoate**	Sodium (2E,4E)-5-phenyl-2,4-pentadienoate
DPnP	Di(propylene glycol) n-propyl ether	**NaSCN**	Sodium thiocyanate
FAD	Flavin adenine dinucleotide	**Naterephthalate**	Disodium terephthalate
FMF	Formylmethylflavin	**NaValerate**	Sodium 5-phenylvalerate
FMN	Flavin mononucleotide	**OH**	Hydroxy
HCl	Hydrochloric acid	**OMe**	Methoxy
LC	Lumichrome	**PTFE**	Polytetrafluoroethylene
LF	Lumiflavin	**Resveratrol-Tri-PO_4**	Trisodium resveratrol triphosphate
NaButyrate	Sodium 4-phenylbutyrate	**RF**	Riboflavin
NaCHC	Sodium cyclohexane carboxylate	**RF-PO_4**	Riboflavin 5'-monophosphate
NaCl	Sodium chloride	**SDS**	Sodium dodecyl sulfate
Na-3,5-DiCF3-Benz	Sodium 3,5-bis(trifluoromethyl) benzoate	**SXS**	Sodium Xylene Sulfonate
Na-DL-Mandelate	Sodium DL-mandelate	**Tetra-Na-NADPH**	β-Nicotinamide adenine dinucleotide tetrasodium salt

Abbreviations for sodium polyphenolates are displayed in Table 2 in section 2.6.

Signs and units:

$\boldsymbol{\delta}$	Chemical shift	**AU**	Arbitrary units
$\boldsymbol{\delta_{calc}}$	Chemical shift calculated with an increment table	**rpm**	Rounds per minute
$\boldsymbol{\delta_{exp}}$	Experimental chemical shift	**ppm**	Parts per million
J	Coupling constant	**wt.%**	Weight percent
		vol.%	Volume percent
		w/w	Weight to weight ratio

Table of Contents

1 Introduction

Nowadays, food additives are indispensable for human's and animal's nutrition. Coloring and flavoring agents are widely used to mimic certain ingredients, to highlight the freshness of products or to create a new taste in order to attract people. Similarly, proteins, sugar substitutes or vitamins are commonly added to food and beverages to improve the endurance during sports, to prevent a gain in weight or to simply support the immune system. Thus, the common yellow coloring agent and essential vitamin, riboflavin, has an enormous importance for the coloring of food and beverages but also for the nutritional supplemental industry.[1–6] Unfortunately, riboflavin's poor water-solubility and quick photodegradation into non-bioactive compounds as well as its photosensitizing power set a limit to its usage as coloring agent for beverages and food.[1,7–10] Analogously, the industrially relevant vitamins, vitamin K3 and folic acid, are also poorly water-soluble and photosensitive. The fast photodegradation and low solubility of vitamins, organic colorants and drugs represents still a challenging task, as the photostability and solubility often correlate with absorption and bioavailability. Hence, special preparation techniques, solubilizers and certain stabilizers or storage conditions are required. However, solubilizers and stabilizers must be food-approved, lowly toxic, biodegradable and should not alter the color, taste, or bioavailability of the solute in the final formulation. Moreover, to keep a drug's or a vitamin's function, the solute must be solubilized sufficiently without too strong interactions with the solubilizing agents, which is by far not trivial.

Currently, the perception of people undergoes a transformation leading to the augment usage of natural and biobased solvents, solubilizers and stabilizers for food and beverages, which are most preferably not processed after extraction or at least undergo rather green processing. The most common bio-based solvents for food, beverages and pharmaceuticals are water and vegetable oils. Thus, biobased microemulsions of low toxicity composed of water as major outer phase, of an oily component such as limonene or rape seed oil, and of a lowly toxic natural surfactant are widely investigated as potential food and pharmaceutical formulations to solubilize hydrophobic solutes. Although surfactants for such microemulsion are chosen to be lowly toxic and natural, such as lecithin, sucrose monopalmitate or tweens, the strongly pronounced amphiphilicity of surfactants makes them irritant for membranes.[11–14]

Since the last century, hydrotropes are investigated as less toxic, less membrano-destructive and better biodegradable substitutes to surfactants. Thus, hydrotropes are better candidates to dissolve slightly hydrophobic compounds in food, beverages and pharmaceutical formulations. Nevertheless, especially food approved efficient hydrotropes are rare.

Polyphenols as natural antioxidant molecules present in grains, vegetables, fruits, tea and coffee are part of the humans' and animals' daily dietary with an uptake of approximately 25 mg up to 1 g per day.[15–17] Polyphenols comprise many health benefits, such as being anti-diabetic,

antimicrobial, antimutagenic, and anticarcinogenic.[16,18,19] Hence, these phytochemicals gained importance during the last years and their potential application covers a wide range from pharmaceuticals and human nutrition to cosmetics.[16,19] Thus, according to the European Food Safety Authority (EFSA) certain polyphenolic acids are allowed in flavor industry for normal usage under 0.05 wt.% and maximum usage under 0.2 wt.%.[20] Yet, despite their highly praised health benefits and despite their amphiphilic molecular backbone and several potential hydrogen bonging sites, which indicate hydrotropic properties, the solubilizing properties of (poly)phenolic acids were never thoroughly investigated. As cheap, easily available, biodegradable, edible antioxidants and radical scavengers, polyphenolic acids appeared as potential natural multifunctional solubilizers.[10,21–23]

In this research, salts of polyphenolic acids and related aromatic and non-aromatic carboxylates were examined for their solubilizing power regarding the solubilization of poorly water-soluble compounds, whose solubility is limited by hydrogen bonding, self-stacking or/and hydrophobicity. A major focus was set on the importance of the amphiphilic character and aromaticity on the solubilizing power. Especially, the solubility problem of riboflavin and strategies to overcome it were broadly investigated using not only polyphenolic acid derivatives, but also other aromatic and non-aromatic solubilizers. Additionally, polyphenolic acids and derivatives were used to improve the water-solubility of lumichrome, riboflavin-5'-monophosphate, vitamin K3, folic acid, caffeine and curcumin. The compatibility of riboflavin, vitamin K3, caffeine and folic acid in an aqueous sodium ferulate solution was evaluated to see if the solutes would compete for the polyphenolate due to similar interactions of the four aromatic solutes with the hydrotrope. To see, if polyphenolic acid derivatives can act simultaneously as solubilizing and stabilizing agents, the photostabilizing power of some aromatic sodium carboxylates on riboflavin and vitamin K3 was evaluated.
Additionally, the cosurfactive potential of one polyphenolate – sodium ferulate – was investigated in the presence of the standard surfactant sodium dodecyl sulfate and in the presence of the biosurfactant sodium cholate. Finally, the compatibility of sodium ferulate's complexation of aromatic solutes and its cosurfactive behavior was evaluated in the sodium dodecyl sulfate and sodium cholate system using the solutes riboflavin and Sudan blue II as triggers for the two different solubilizing modes of sodium ferulate.

2 Fundamentals

2.1 Green solvents

In 1998, Paul T. Anastas and John C. Warner dealt comprehensively with the terminus “Green chemistry” stating that “Green chemistry is the utilization of a set of principles that reduces or eliminates the usage or generation of hazardous substances in the design, manufacture and application of chemical products.”[24] Anastas and Warner defined Green Chemistry via the introduction of 12 principles:

1. Prevention of waste – 2. Atom economy – 3. Less hazardous chemical synthesis – 4. Designing saver chemicals – 5. Safer solvents and auxiliaries – 6. Design for energy efficiency – 7. Use of renewable feedstocks – 8. Reduce derivatives – 9. Catalysis – 10. Design for degradation – 11. Real-time analysis for pollution prevention –12. Inherently safer chemistry for accident prevention. Nowadays, the termini sustainable and clean chemistry are often used as a substitute for “Green Chemistry”.

For economic reasons, the implementation of Green Chemistry is by far not easy as the criteria should meet up with the availability, price and stability of the chemicals. Moreover, all of the twelve principles cannot be retained simultaneously and thus one needs to decide which of the principles should be prioritized for a certain application. Therefore, the terminus green is always set in relation to other processes.[25,26]

2.2 Food additives

The increasing population requires food production to become cheaper and to meeting up the same quality standards at the same time. Food additives are deployed to preserve food and thus to prevent its spoilage and to keep its taste, texture, odor and color. However, food additives are also used to make food and beverages more attractive, to make them look safe to eat, or to simulate high contents of certain substances, such as fruits or vitamins in juices. Thus, food additives are also a tool for marketing. In the European Union, regulatory guidelines are listed in the Codex Alimentarius to prevent an overuse of food additives and thus keep side effects low. The Codex Alimentarius established the International Numbering System (INS), which assigns one “E-number” to each food additive, as long chemical names might be confusing for the costumer.

Further food additive legislations are given by the US Food and Drug Administration (FDA) or United Kingdom Food Standards Agency.[27,28]

2.3 Solubilizing agents

Surfactants, hydrotropes and cosolvents are applied to increase the solubility of target compounds. Surfactants are schizophrenic molecules with a clear separation of a hydrophobic tail and a hydrophilic head group. Due to their amphiphilic structure, surfactants self-assemble via the formation of micelles, cylindrical structures or bicontinuous phases. Depending on the formulation and surfactant concentration, surfactants form also liquid crystalline phases. Although surfactants are widely used as solubilizing agents for the preparation of emulsions and microemulsions, their strong foaming tendency and their strongly membranophilic properties makes the usage of most surfactants for food, beverages and for pharmaceutical applications unattractive – except if foaming is desired.[29–31]

In 1916, Neuberg defined "hydrotropes" as compounds being able to increase the water-solubility of poorly soluble compounds. Comprising an amphiphilic structure due to a hydrophobic tail and a hydrophilic head group, hydrotropes in principle resemble surfactants.[32] Thus, such as surfactants, hydrotropes lower the surface tension of water.[29] However, the amphiphilicity is usually less pronounced in the case of hydrotropes. Consequently, more than a hundred times higher hydrotrope concentrations are required to reach a comparable surface tension as with a surfactant. Moreover, hydrotropes must not necessarily tend to self-assemble in the absence of a hydrophobic solute, do not form liquid crystals and foam significantly less than most surfactants.[29,33] In the case of a self-aggregation of a hydrotrope in the absence of a solute at the so-called critical aggregate concentration (CAC), the formed aggregates are claimed to be more dynamic than surfactant derived micelles.

Another important term when speaking of hydrotropes is the so-called minimum hydrotrope concentration (MHC), which corresponds to the minimum concentration of a hydrotrope required for solubilization of a hydrophobic solute. Owing to the rather weakly pronounced amphiphilicity of hydrotropes, the CAC and MHC usually are around 10^{-1} mol·L^{-1}.[34] Thus, larger amounts of hydrotropes are required to have a comparable solubilizing effect to surfactants. However, hydrotropes are usually less toxic and less membrane-permeable than surfactants.[35,36] As the solubility of a poorly water-soluble solute is increased in a non-linear way by hydrotropes, the effectiveness of a hydrotrope can be obtain from the Setschenow constant $K_{setschenow}$ from equation 1.[37]

$$log(\frac{S}{S_{MHC}}) = K_{setschenow}(c - c_{MHC}) \quad (1)$$

S = solubility of the solute at any hydrotrope concentration, S_{MHC} = solubility of the solute at the MHC, c and c_{MHC} are the corresponding hydrotrope concentrations

Because this thesis was part of a cooperation with the company BASF, the effectiveness was quantified in a more applicative manner. With respect to the solute's solubility in pure water s_0, a molar hydrotrope to solute ratio was calculated from the ratio of the applied hydrotrope

concentration c^H and the solute's water-solubility s in the presence of the hydrotrope at the concentration c^H, see equation 2.

$$ratio = \frac{c^H}{s - s_0} \quad (2)$$

Typical hydrotropes are sodium salts of short alkylbenzene sulfonates, such as xylenesulfonate (SXS) and cumenesulfonate, monoethers of ethylene glycols or higher polyols. The action of these compounds as hydrotrope, cosolvent or surfactant depends on the alkyl chain length.[29] Other typical hydrotropes are nicotinamide, urea, γ-valerolactone, citrate, and caffeine.[32]

Currently, hydrotropes are proposed to have three modes of action. Firstly, hydrotropes might form a complex with the solute. Secondly, hydrotropes might act as chaotropic agents by changing the water-structure locally and thus reduce the hydrophobic effect. The third mechanism includes the formation of aggregates or pre-clusters.[34,38]

The usage of hydrotropes is favorable for several reasons: 1) Chemical modification of hydrophobic drugs is not required to make them water-soluble. 2) Potentially toxic organic solvents can be prevented. 3) The time and energy demanding process of emulsification to solubilize drugs is not required. 4) Hydrotropy is highly selective.[32]

Moreover, the usage of mixtures consisting of several hydrotropic agents may reduce the toxicity of one specific hydrotrope even more due to a lower amount of it in the total formulation.[39]

Further, it is important to distinguish hydrotropes from cosolvents, which, in principle, resemble hydrotropes. Cosolvents are water-miscible organic solvents used in liquid drug formulations to increase the solubility of poorly water-soluble substances. In contrast to hydrotropes and surfactants, cosolvents have no structuring potential and thus have no minimum cosolvent concentration. However, a clear border between hydrotropes and cosolvents does not exist.[29]

If hydrotropes show a solubility dependent solubilizing power, facilitated hydrotropy might occur. This is a phenomenon, whereby the solubility of a hydrotrope is increased using another hydrotrope or cosolvent leading to a synergistic enhancement of a hydrotrope's effectiveness or/and efficacy due to an alteration of the MHC or increase of the hydrotrope's solubility.[39] Similarly, cosurfactants can be used to lower the critical micelle concentration (CMC) and to increase the surface-active efficiency/efficacy and solubilizing power of surfactants.[31]

2.4 Hofmeister Series – Salting-in and -out properties

Hofmeister was the first one to categorize the ionic effects, which influence protein solubilization in 1888. He found that the specific ionic effect correlates with the charge density of ions.[40,41] Later, studies revealed the Hofmeister Series to have a strong correlation with salting-in/out of hydrophobic substances, denaturation of proteins, hydrogen bonding of

substances, hydration of the ions as well as ion pairing and surface tension, see Figure 1.[42–45] According to Collins, small highly charged ions, such as phosphates, sulfates and carboxylates, were named “kosmotropes”. Kosmotropes are likely to be hydrated. Large polarizable low charge ions were named “chaotropes” and are less hydrated than kosmotropes. The charge density and not the absolute charge is decisive, because e.g. the very large and polarizable polyoxometalates are known to be superchaotropic, although having charges of about IV or even V.[44,46] Based on the theory of Yizhak Marcus, kosmotropic and chaoptropic behavior of ions can be quantified with three parameters: Size of the anion, entropy of the water structure and effect of ions on the number of water molecules in the surroundings.[41,47] This is certainly important for biological systems, as the transmembrane transport of biological electrolytes, such as sodium and potassium, depends on their hydration shell.[47]

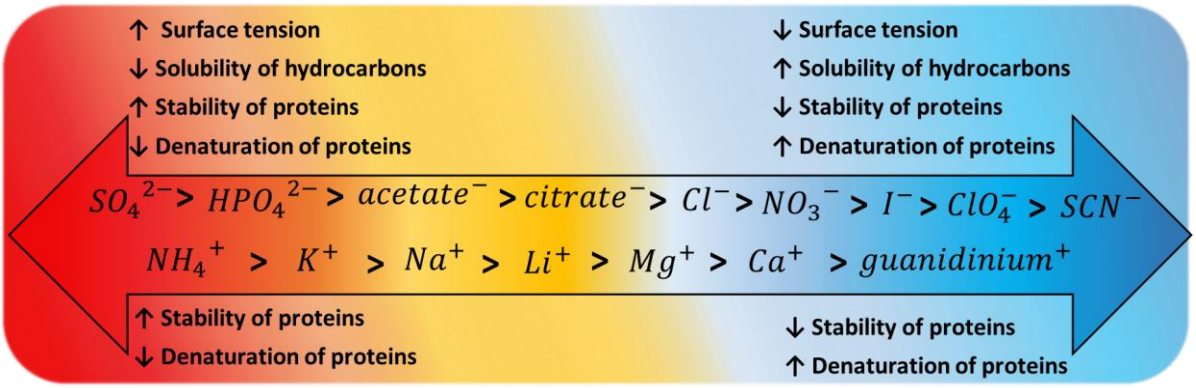

Figure 1: Cations and anions from the Hofmeister Series[48–50]

An elegant method for the quantification of salting-in and -out properties, was introduced by Grundl et al., who analyzed the effect of various charged and non-charged organic molecules on the phase transition temperature (PTT) of binary di(propylene glycol) n-propyl ether (DPnP)/water mixtures, see Figure 2.[51] At low temperatures, the hydrogen bond network enables DPnP to be solubilized in water leading to a monophasic system. At high temperatures, the hydrogen bonds between water and DPnP are disrupted due to higher Brownian molecular motion. As a consequence, DPnP is dehydrated and the water/DPnP solution becomes a heterogenous system. The lowest temperature of this clouding is called lower critical solubilization temperature (LCST).

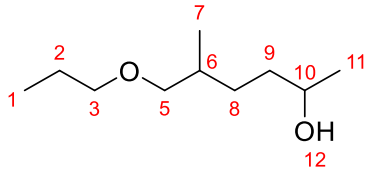

Di(propylene glycol) n-propyl ether
(DPnP)

Figure 2: Molecular structure of DPnP

In this research, the PTT of the binary water/DPnP (45/55 (w/w)) mixture near the LCST was investigated. Salting-in leads to an increase of the PTT of the binary system, while salting-out induces a decrease of the PTT.[52] For a linear increase/decrease of the PTT of the water/DPnP system with increasing additive concentration, the slope defines the magnitude of the salting-in/-out properties of additives, see equation 3.

$$PTT(c_{additive}) = PTT(c_0) + m \cdot c_{additive} \quad (3)$$

$PTT(c_0)$ = 15 °C = PTT of the pure water/DPnP (45/55 (w/w)) mixture[51]
m = magnitude of the additives' salting-in or -out power in °C·mol·mmol^{-1}
$c_{additive}$ = additive concentration

As the PTT can be easily determined with a heating plate and a thermometer by the eye, the determination of the PTT for a quantification of the salting-in/-out properties of compounds is convenient because it is a fast, simple, low cost, barely energy demanding and non-toxic method.[51]

2.5 π-Stacking

In general, the term π-stacking refers to a non-covalent interaction of aromatic molecules comprising π-orbitals. As a consequence, aromatic molecules undergo reversible complexation at distances larger than typical Van-der-Waals radii.[53]
Since the early age, three models were developed to describe stacking phenomena: The Solvophobic Model, the Electron Donor-Acceptor Model and the Atomic Charge Model. The Solvophobic Model considers stacking as a purely entropically driven phenomenon. However, this model is not applicable for stacking phenoma of rather non-polar aromatic molecules in organic solvents, and stacking involves enthalpic contributions, too. The Electron Donor-Acceptor Model proposes electronic interactions of a molecule with electron acceptor groups and another molecule comprising electron donor groups, which lower and increase the energy of the lowest unoccupied molecular orbital (LUMO) and higher occupied molecular orbital (HOMO), respectively. The resulting charge transfer complexes or π-π*complexes are characterized by a broadened UV-Vis-spectrum and charge transfer transitions in the UV-Vis-region. However, in contrast to the excited state, charge-transfer interactions are only minorly important in the ground state and not all stacking interactions are coupled with a charge-transfer transition. The Atomic Charge Model is based on an inhomogeneous distribution of the charge in the aromatic ring leading to an syn-alignment of distinct charges.[54] Although the stacking-interactions are not entirely understood up to know, basic rules on the understanding of π-π-interactions were formulated by Hunter and Sanders in the 1990s. They stated that π-interactions can be described best using a modification of the Atomic Charge Model. They

proposed repulsion of the π-electrons and attraction between the π-electrons and σ-framework to be the origin of the final geometry of a π-complex. Thus, the π-electron density induces a quadrupole moment with a partial negative charge above the aromatic faces and a partial positive charge in the periphery leading to attractive electrostatic interactions, see Figure 3. Van-der- Waals interactions and the solvophobic effect are supposed to dominate the magnitude of the interaction.[54] However, the electrostatic model of Hunter and Sanders neglected short range effects and induction by substituents claiming that electron-withdrawing substitutents reduce π-repulsion and thus enhance π-stacking, while electron-donating substituents reduce the tendency of aromatic molecules for π-stacking. Yet, calculations of Sherrill et al. showed that substitution of benzene rings with electron-withdrawing groups promotes stacking.[55,56] A proposal of Wheeler and Houk was to treat substituents in the benzene dimer as direct interaction partner for the aromatic ring with no involvement of the π-system of the substituted benzene.[57] Nevertheless, it is still unclear, whether the electrostatic or dispersion effects play a key role in π-π-interactions. Certainly, factors determining the strength and dynamics of π-stacking are geometric configurations/sterics, substituents and polarizability of aromatic molecules as well as the polarity and hydrogen bonding capacity of the solvent.[58]

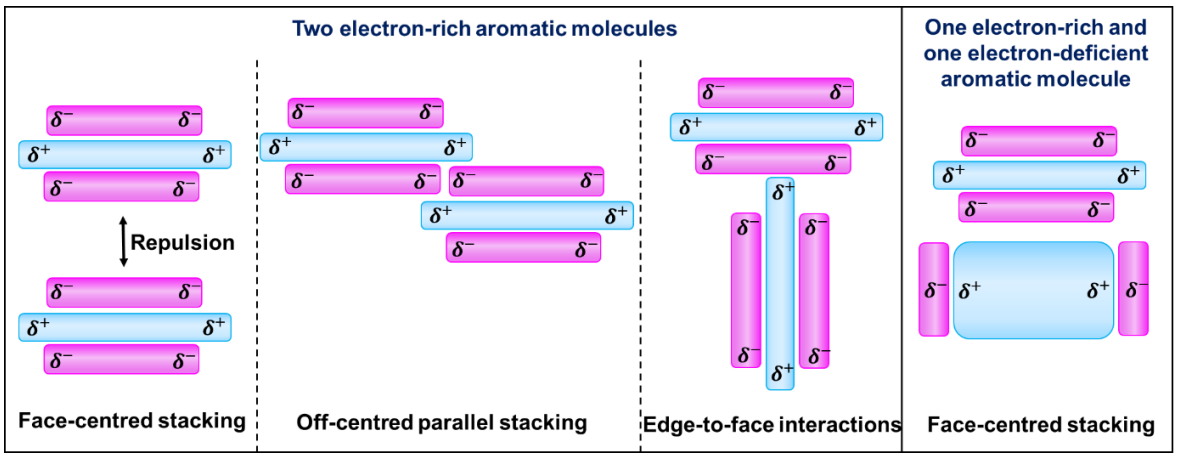

Figure 3: Possible orientations of aromatic molecules based on electrostatic considerations. Adapted from [59].

As many biological compounds, such as amino acids, vitamins, flavonoids, anthocyanins, but also drugs, are aromatic, π- π-interactions could play a crucial role in the organization and functionalization of various biochemical systems. Thus, attractive π- π-interactions are known to stabilize the deoxyribonucleic acid (DNA), to influence the folding of proteins and to be essential for protein-ligand recognition. Moreover, the mechanism of cofactor binding by the flavoenzymes is known to involve a stacking interaction between an aromatic residue of tyrosine, tryptophan or histidine at the cofactor binding site and the isoalloxazine ring of the flavin.[60,61] Thus, π-stacking in combination with other non-covalent interactions can even alter the redox-potential of flavins from -210 mV up to 600 mV.[62]

Due to the non-destructive and reversible binding mechanism, π-complexation states a great potential for controlled drug release via π-stacked micellization of aromatic surfactants, for the design of sensors and molecular receptors and for DNA sequencing.[58]

2.6 Polyphenolic acids

Together with flavonoids, coumarins, stilbenes, tannins, lignans as well as lignins, phenolic acids – including polyphenolic acids – constitute the most abundant secondary polyphenols.[19,20] Making up around one third of the phenolic compounds digested by humans, phenolic acids are essential for humans' and animals' dietary.[19] Polyphenolic acids are a subgroup of phenolic acids, comprising either a benzoic or cinnamic acid backbone. Thus, polyphenolic acids can be separated into two groups: hydroxycinnamic acids and hydroxybenzoic acids.

Seeds, leaves of vegetables and skin of fruits and grasses are especially rich in polyphenolic acids. The reason therefore is probably that these bio-compounds are partially responsible for the stability of plant cell walls, where the acids are oligomerized and bound to other molecules via ester, ether or amide bonds as lignin.[19,63] Generally, hydroxy substituted cinnamic and benzoic acids are mainly associated with sugars to form glucosides or bound to other organic acids and thus are rarely present in their free and monomeric form.[16,19,64] The most common hydroxycinnamic acids are caffeic, p-coumaric and ferulic acids, which frequently occur in foods esterified with quinic acid or glucose.[16] Free polyphenolic acids can be obtained from plants via basic, acidic or enzymatic hydrolysis.[19,63]

In plants, polyphenolic acids are mainly produced starting from L-phenylalanine or L-tyrosine.[65,66] Large scale production is achieved via biotechnological synthesis and extraction from plants.[19,67]

Polyphenolic acids are involved in protein synthesis, photosynthesis, nutrient uptake and regulation of enzyme activity.[68] The main role of phenolic compounds in plants is probably the protection of the plant from exterior biological and physical stress and diseases. However, they also contribute to the coloration and taste of the plants.[63] Further, plants use polyphenolic acids as a tool to control nutrition uptake of plants in the surrounding and thus as a kind of communication between plants, which is called allelopathy. Hence, polyphenolic acids adsorb to clay minerals, undergo complexation with sesquioxides, influence the uptake of phosphorus by cucumbers and enable the fixation of dinitrogen by soil bacteria.[68–70]

Further, polyphenolic acids may also alter the color, sensory quality, nutritional and antioxidant properties in food.[63,71,72] Thus, in spite of the low phenolic acid content (≈ 0.17 %) compared to the proteins and carbohydrates (> 80 %) in cereals, the consistence of dough and the texture of baked bread depends on the phenolic acid content. The reason is assumed to be the reductive capacity of polyphenolic acids influencing the formation of disulfide bonds, which are

responsible for the gluten network formed by proteins. Hydrophobic interactions of polyphenolic acids with amino acids, such as the one of ferulic acid with tryptophan in dough, could also contribute to the texture, taste and color of food.[63] Hence, ferulic acid was found to influence the precipitation of milk and soybean milk due to agglomeration of casein at concentrations near 0.5 % (m/v). Additionally, 0.2 %(m/v) ferulic acid act as a preservative in milk and soybean milk and improve also the milk's quality due to the repression of volatile fatty acid formation.[73,74]

Further, polyphenolic acids exert anti-diabetic properties, as they are also involved in the production of insulin and inhibit α-glucosidase and α-amylase, which convert carbohydrates into glucose.[63,75,76] Adisakwattana et al. found that the methoxy group on the aryl ring boosts the antidiabetic action of polyphenolic acid.[77] The sweetening and bitterness inhibiting potential of ferulic and caffeic acid and their salts in aqueous 0.001 to 0.2 wt.% solutions suggests the usage of polyphenolic acids in anti-diabetic treatment.[78] In general, most polyphenolic acids are antimicrobial, anti-inflammatory, antimutagenic and antithrombic.[19,79,80]

Moreover, polyphenolic compounds are the main source for antioxidants delivered by plants exhibiting even higher antioxidant properties than some antioxidant vitamins.[81,82] Several antioxidant tests, including the Folin-Ciocalteau reagent, Ferric Reducing Antioxidant Power measurements, the 2,2-diphenyl-1-picrylhydrazyl (DPPH) assay, the 2,2'-azino-bis(3-ethylbenzothiazoline-6-sulfonic acid) (ABTS) assay and Differential Pulse Voltammetry showed that the number and position of hydroxy and methoxy groups and the type of the antioxidant side chain (antioxidant effect: COOH < CH_2COOH < CH=CHCOOH) determine their antioxidant efficiency.[83–85]

Currently, three main radical scavenging mechanisms are proposed for the antioxidant action of polyphenolic acids: 1. Due to the conjugation of the carboxylate to the aryl ring, polyphenolic acids are able for hydrogen donation. The hydrogen transfer is a one-step reaction and depends on the O-H-bond dissociation enthalpy. 2. Polyphenolic acids can quench radicals via electron donation. The electron donation is a two-step reaction and relates to the ionization potential and proton dissociation enthalpy. 3. Polyphenolic acids are also capable of sequential proton-loss electron transfer which is ruled by the proton affinity and electron transfer enthalpy. All three quenching mechanisms might even occur simultaneously, whereby the type of quenching depends on the solvent properties.[84] Because of their antioxidant properties, polyphenolic acids are regularly used in therapeutics, anti-aging cremes, sun cremes and other cosmetic formulations, but also in food industries. Especially, ferulic acid is widely used as cosmetic additive.[19,86]

A disadvantage of the antioxidant activity of polyphenolic acids is their easy oxidation, which can occur enzymatically and non-enzymatically and leads to the formation of the more reactive quinones and semiquinones. Subsequent Michael-type addition results mainly in the

dimerization or oligomerization of polyphenolic acids, which is responsible for a brown coloration.[63,87,88]

The degradation products after oxidation of ferulic acid (ferulic acid dimers) were proved to have antioxidant properties, too. However, the dimers showed lower antioxidant activity than two monomers.[89] In spite of such a degradation, phenolic acids are important food components due to their lipid oxidation inhibiting, antioxidant and radical scavenging properties, as they can stabilize other important compounds, see Figure 4.[90]

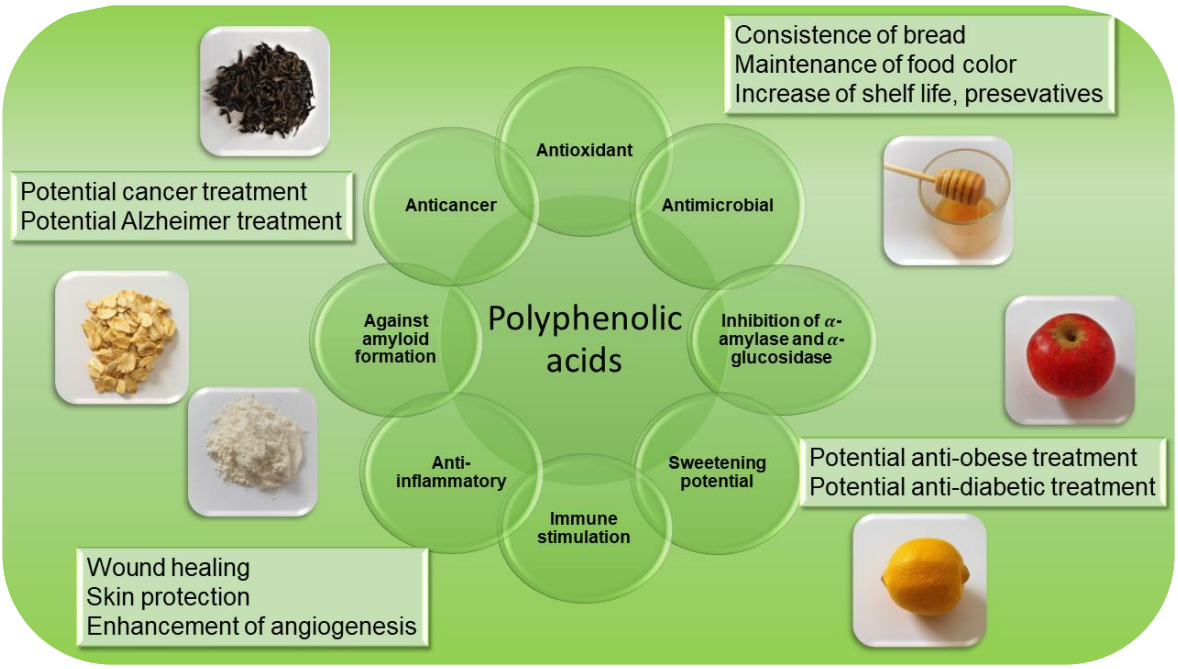

Figure 4: Occurrence, properties and possible applications of polyphenolic acids [19,73,91–97]

The daily dietary intake of polyphenolic acids via digestion of vegetables, fruits and plant-based beverages accounts for about 500-800 mg per person. Thereof, 700 mg cinnamic acid derivatives and 100 mg benzoic acid derivatives are consumed. Nevertheless, the uptake of polyphenolic acids can vary from 6 to 987 mg per day. 200 mL of roast and ground coffee were assumed to supply already 20-675 mg chlorogenic acid, which is an esterified form of caffeic acid.[17,98,99]

Upon intake, polyphenolic acids are absorbed easily in the intestine involving Na^+-dependent and independent mechanisms.[89] Methoxylated cinnamate derivatives reach the blood stream more easily and in an unchanged form, while hydroxylated cinnamates mainly undergo sulfonation or glucuronidation in the liver.[100–102] Thus, there is almost no unmodified ferulic acid in the blood stream and its metabolites are excreted instantly via the urine.[103,104] In contrast, 3,4-dimethoxycinnamic acid undergoes less metabolic modifications as the methoxy group inhibits the activity of first-pass liver enzymes, which are responsible for sulfonation and glucuronidation reactions. Owing to its more lipophilic character, 3,4-dimethoxycinnamic acid penetrates the intestinal wall also more easily than ferulic acid by several times, leading to a fast increase of the 3,4-dimethoxycinnamic acid concentration in the blood shortly after

indegestion.[100–102,105] The metabolized products of polyphenolic acids are excreted via the feces and urine.[106]

Being an essential part of the humans' nutrition and providing in the same time various health benefits, polyphenolic acids are nutraceuticals.[107] In general, most benzoic and cinnamic acid derivatives and salts are of low toxicity, see Table 1. Hence, benzoic acid and its derivatives are already common food additives exhibiting no toxicity in the applied concentrations (normal usage up to 500 $mg \cdot kg^{-1}$; maximal usage up to 2000 $mg \cdot kg^{-1}$).[20]
In animal husbandry, polyphenolic acids are also omnipresent. Thus, the usage of polyphenolic acid-rich grasses and food, such as durum wheat bran consisting mainly of ferulic acid, improved the production, quality and shelf-life of dairy products and the quality of meat.[73,74,108]

Table 1: LD_{50} values for benzoic acid and cinnamic acid and their derivatives via the oral administration.

Compound	LD_{50} ($mg \cdot kg^{-1}$)
Benzoic acid	≥ 2250 (rat)[109]
Sodium benzoate	≥ 2000 (rat) [110]
Cinnamic acid	≥ 5000 (rat)[111]
Sodium cinnamate	3250 (mice)[111]
3,4-Dihydroxycinnamic acid	800 (mice)[112]
Salicylic acid	891 (rat)[113,114]
Sodium salicylate	1600 (rat)[113,114]
Ferulic acid	300-2000 (rat)[115]
Sodium ferulate	3200 (mice)[116]
Vanillic acid	≥ 5020 (rat)[117]
Syringic acid	≥ 2000 (rat)[118]
Veratric acid	≥ 800 (rat)[119]

In this research, polyphenolic acids are considered as small compounds comprising a carboxylic acid group and an aromatic moiety substituted with methoxy and/or hydroxy groups, see Figure 5 and Table 2. Judging from their molecular structure, polyphenolic acids were supposed to have hydrotropic properties due to their amphiphilic backbone, rather large interaction surface and hydrogen bonding sites. Due to their planarity, sodium polyphenolates might perform stacking with other aromatic compounds. However, polyphenolic acids are often regarded as solutes themselves due to their low solubility in water (< 1 wt.%).[120] Being absorbed into the blood system after digestion (pH: 7.35-7.45), polyphenolic acids (pka~4) are negatively charged in the body.[121–124] Consequently, the anionic form of polyphenolic acids is predominant in the body. Therefore, the low solubility of polyphenolic acids was evaded in this research using polyphenolate salts. As sodium is the major cation of extracellular fluid in the body, which plays a key role in the regulation of myocardial and neurological functions, and due to cost reasons, mostly the solubilizing properties of the more water soluble sodium polyphenolates were studied.[125,126]

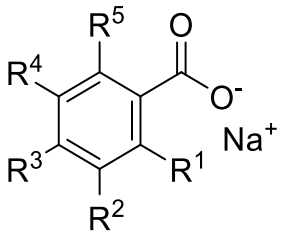

Sodium benzoate and derivatives*

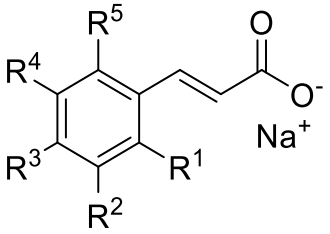

Sodium cinnamate and derivatives**

Figure 5: Molecular backbone of polyphenolic acids. The nomination and abbreviation of these derivatives (and **) are given in Table 2.*

Table 2: Abbreviations of sodium polyphenolates used in this research. Note: NaBenz and NaCinn are no polyphenols. See Figure 5 for the molecular backbone.

Corresponding acid	Abbreviation	R^1	R^2	R^3	R^4	R^5
Benzoic acid	NaBenz	H	H	H	H	H
Salicylic acid	Na-2-OH-Benz	OH	H	H	H	H
3-Hydroxybenzoic acid	Na-3-OH-Benz	H	OH	H	H	H
4-Hydroxybenzoic acid	Na-4-OH-Benz	H	H	OH	H	H
o-Anisic acid	Na-2-OMe-Benz	OMe	H	H	H	H
m-Anisic acid	Na-3-OMe-Benz	H	OMe	H	H	H
p-Anisic acid	Na-4-OMe-Benz	H	H	OMe	H	H
Gallic acid	Na-3,4,5-TriOH-Benz	H	OH	OH	OH	H
Syringic acid	Na-4-OH-3,5-DiOMe-Benz	H	OMe	OH	OMe	H
2,3-Dihydroxybenzoic acid	Na-2,3-DiOH-Benz	OH	OH	H	H	H
Protocatechuic acid	Na-3,4-DiOH-Benz	H	OH	OH	H	H
2,4-Dihydroxybenzoic acid	Na-2,4-DiOH-Benz	OH	H	OH	H	H
3,5-Dihydroxybenzoic acid	Na-3,5-DiOH-Benz	H	OH	H	OH	H
2,3-Dimethoxybenzoic acid	Na-2,3-DiOMe-Benz	OMe	OMe	H	H	H
Veratric acid	Na-3,4-DiOMe-Benz	H	OMe	OMe	H	H
2,4-Dimethoxybenzoic acid	Na-2,4-DiOMe-Benz	OMe	H	OMe	H	H
3,5-Dimethoxybenzoic acid	Na-3,5-DiOMe-Benz	H	OMe	H	OMe	H
Vanillic acid	Na-4-OH-3-OMe-Benz	H	OMe	OH	H	H
Cinnamic acid	NaCinn	H	H	H	H	H
o-Coumaric acid	Na-2-OH-Cinn	OH	H	H	H	H
m-Coumaric acid	Na-3-OH-Cinn	H	OH	H	H	H
p-Coumaric acid	Na-4-OH-Cinn	H	H	OH	H	H
4-Methoxycinnamic acid	Na-4-OMe-Cinn	H	H	OMe	H	H
Caffeic acid	Na-3,4-DiOH-Cinn	H	OH	OH	H	H
Ferulic acid	Na-4-OH-3-OMe-Cinn	H	OMe	OH	H	H
3,4-Dimethoxycinnamic acid	Na-3,4-DiOMe-Cinn	H	OMe	OMe	H	H
Sinapinic acid	Na-4-OH-3,5-DiOMe-Cinn	H	OMe	OH	OMe	H
Phloroglucinol carboxylic acid	Na-2,4,6-TriOH-Benz	OH H	OH	H	OH	

2.7 Riboflavin

In 1933, riboflavin (RF) – also known as 7, 8-dimethyl-10-ribityl-isoalloxazine, lactoflavin, ovoflavin, uroflavin, vitamin G, lyochrome or hepatoflavin[1,127] – was first isolated from yeast, egg white, and whey by Kuhn and Wagner-Jauregg, see Figure 6 A. Simultaneously, the coenzyme flavin mononucleotide – riboflavin-5'-phosphate – was discovered in yeast by Warburg and Christian, see Figure 6 B for its sodium salt.[1] RF is the precursor of the flavocoenzymes flavin adenine dinucleotide (FAD) and flavin mononucleotide (FMN = riboflavin-5'-phosphate), which are biologically active in combination with flavoproteins (dehydrogenases, oxidases, monooxygenases, reductases). Hence, RF is involved in the maintenance of our body.[6,128–130] Thus, compounds with a RF basic framework (flavocoenzymes) are essential for biochemical reactions in living cells, because they participate in redox reactions due to their action as electron, hydrogen atom or even hydride ion transporters.[8,62,131]

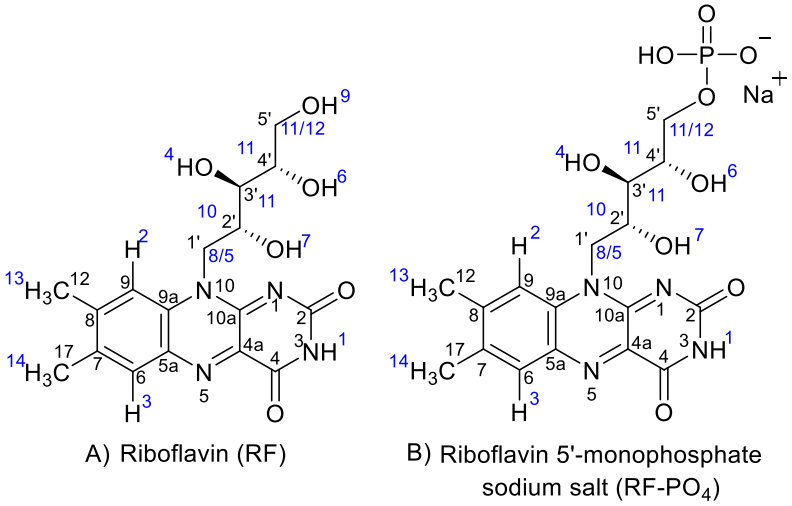

Figure 6: Molecular structures of A) riboflavin and B) riboflavin 5'-monophosphate sodium salt (RF-PO_4). For NMR analysis, the carbon atoms are labelled with small black numbers, protons are labelled with blue numbers.

In general, flavoenzymes are crucial for the citric acid cycle, the catabolism of amino acids with a branched chain, the biosynthesis and regulation of cofactors and hormones, the chromatin remodeling and thus DNA repair, the folding of proteins and cell apoptosis.[131] Besides this, the conversion of tryptophan into niacin and the conversion of vitamin B6 and B9 into their active forms is also supported by flavins.[6,130,132] Further, RF is involved in the activation of macrophages and thus is essential for the function of our immune system.[133,134]

Consequently, deficiency of RF, or vitamin B2, can lead to a sore throat, loss of hair, skin inflammation and further deficiency might even cause anemia and malfunctions of nerves.[131,134–141] Being such an important compound, RF is widely used for pharmacological treatments as displayed in Figure 7.

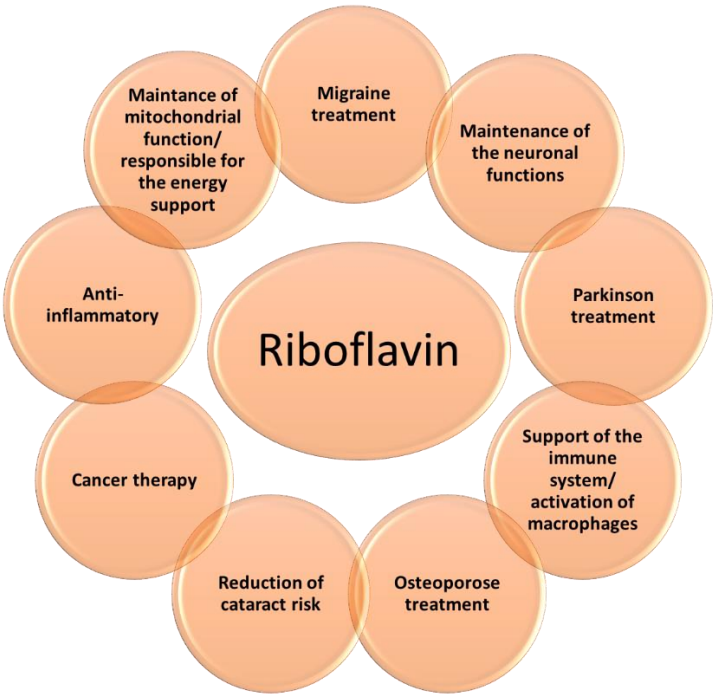

Figure 7: Pharmacological importance of riboflavin [2,4–6]

After digestion, RF is directly absorbed, while the coenzymes FAD or FMN are digested with carrier proteins, which undergo denaturization in the stomach prior to dephosphorylation and absorption in the small intestine.[131] After absorption, the free RF can be metabolized to FMN by riboflavin kinase and further to FAD by adenylyltransferase in erythrocytes or leukocytes.[4,131] Free RF in the plasma (concentrations in the range of nmol·L^{-1}) associates with albumin or globulins. [62,131,142] The flavo-content after absorption accounts for 50 % of free RF, 40 % FAD and 10 % FMN.[62]

RF is synthesized in all plants and by most microorganisms.[6] However, in humans, RF is only synthesized in the large intestine with the help of microflora in lower amounts than required.[6,131] Therefore, the consumption of RF via meat, fish, leafy vegetables, eggs or milk and cheese is essential for humans.[8,127,131,143] The average recommendation of RF daily intake accounts for 1.3 mg per day for men and 1.1 mg per day for women.[131] Although approximately 30 mg RF are absorbed per meal, a poisoning with the vitamin is improbable because excessive RF is excreted via the urine.[131,144] Thus, RF is widely used as nutritional supplement, yellow coloring agent for ice creams, bakeries, confectionery, and beverages, meats and dairy products as well as for pharmaceutical applications such as in anti-migraine treatment.[2,145] As the water-solubility of riboflavin 5'-monophosphate (RF-PO_4) is about 350 times higher than the one of RF, the phosphorylated RF analogue is often used as yellow coloring agent instead of RF.[28] RF-PO_4 is dephosphorylated before the absorption in the small intestine and thus absorbed as RF after digestion. Consequently, the only difference between the two flavins is the price, because RF is cheaper than RF-PO_4.[62] As coloring agents, RF and sodium riboflavin-5'-phosphate are also known under E101.[28] In 2021, 207 tons of RF pigments – corresponding

to 115 million US dollars - were consumed only for beverage industries.[145] Global players in RF production are Guangji Pharmaceutical, DSM, BASF and Shanghai Acebright Pharmaceuticals.[146,147] About 9000 tons of RF are produced annually.[148,149]

Due to the huge demand on RF, new techniques for RF production for the biotechnological and chemical synthesis of RF are always in development. The fermentation is not only a one-step reaction but also cheap, whereby chemical synthesis requires usually several reaction steps followed by purification which drive the costs high. Thus, a typical synthetic RF production pathway has only a yield of about 60 %, while creating a lot of waste and requiring 25 % more energy compared to the fermentative production. Hence, the most common way of RF production are the biotechnological methods. Microbia like *Ashbya gossypii, Bacillus subtilis* or *Candida spp.* are typical producers for RF.[6,150] With the usage of proline-resistant *Bacillus subtilis* strains up to 26.5 $g \cdot L^{-1}$ RF could be synthesized within 70 h.[151]

Although RF is thermostable, it is highly photolabile.[8,127,152] Thus, within some hours more than 80 % the RF in milk can be destroyed when exposed to the sun.[8] The absorption maximum in the visible range at 450 nm leads to the fastest destruction of RF via subsequent cleavage of the ribityl chain.[1,8] Which degradation products are formed, depends on several conditions. RF is first exited to its singlet state, from where it can undergo intersystem crossing to its excited triplet state having a life time of 1 ms, see Figure 8.[8,153–155]

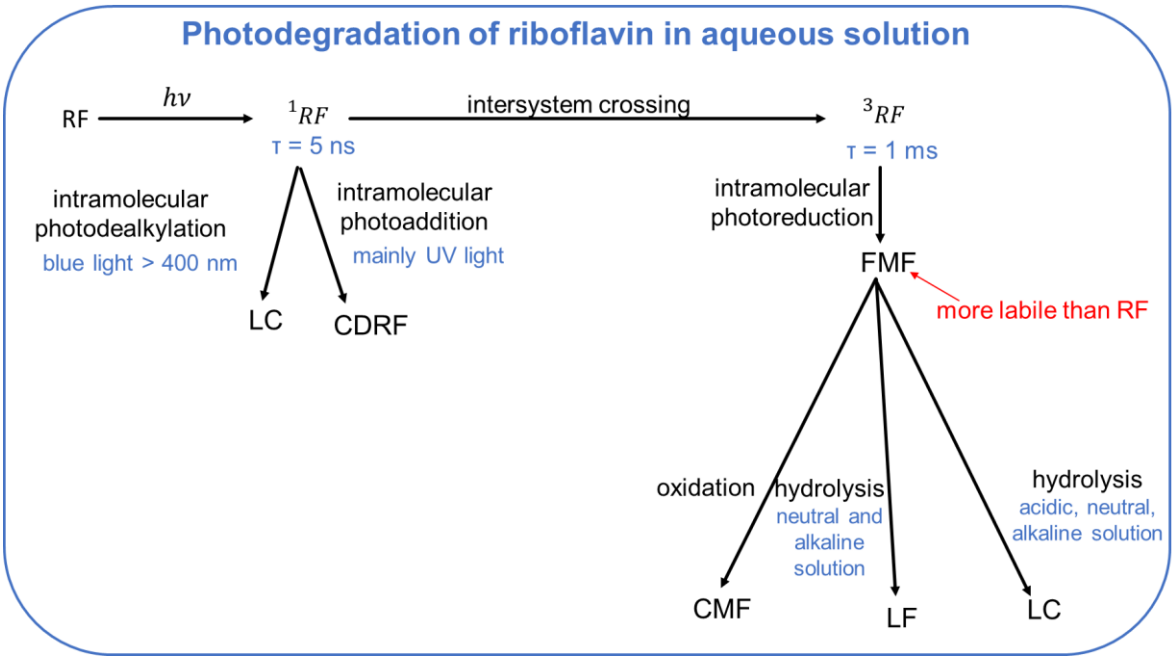

Figure 8: Photodegradation of RF in aqueous solution.[8,154–160]

The major degradation products of RF in aqueous medium upon illumination with visible light are lumichrome (LC) and lumiflavin (LF), both being biologically inactive and photosensitive, see Figure 9.[8,154,161,162] In alkaline medium, LF is the major product, whereas LC is formed at all pH-values. Minor degradation products are formylmethylflavin (FMF), carboxymethylflavin (CMF) and cyclodehydroriboflavin (CDRF), see Figure 9.[154] FMF is even more photosensitive

than RF and either hydrolyzed to LC and LF or oxidized to CMF.[158,163,172–174,164–171] Due to its fast degradation FMF is usually present at low concentrations.[154,155,158] CDRF formation is favored in phosphate and sulfate buffers with a pH value < 8, see Figure 9. At neutral pH (6-7), RF reaches its maximum photostability.

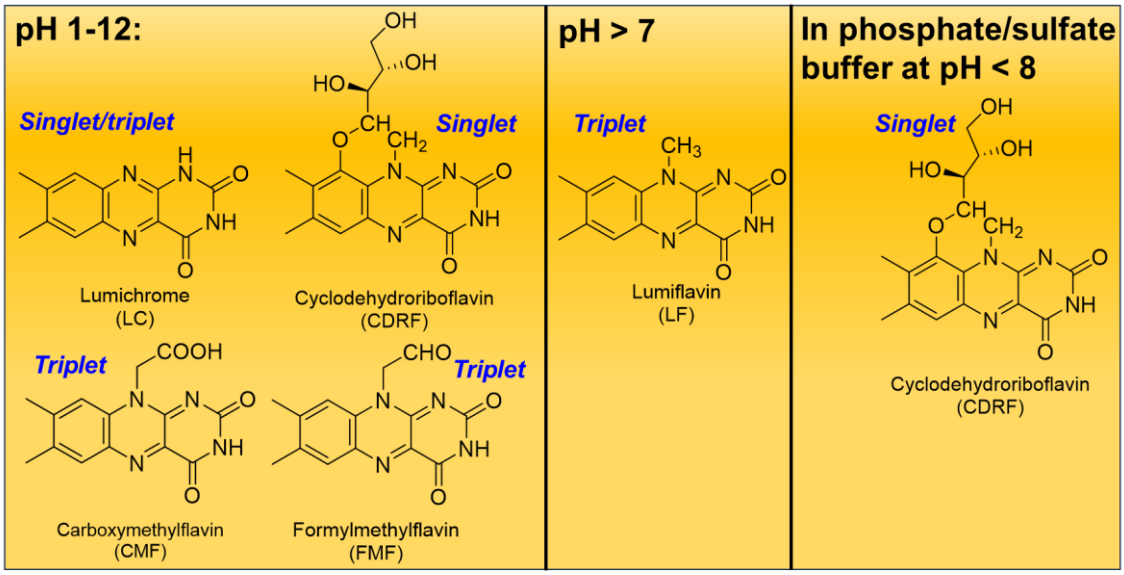

Figure 9: Common photoproducts upon riboflavin's degradation

The rate of RF's photodegradation was found to depend on the solvent's polarity, as certain ribityl chain conformations might be favored in some solvents compared to others.[175] In polar solvents, RF is less photolabile than in organic ones.[8,176,177] Moreover, of hydrogen phosphate ions and chloride ions increasing the ionic strength of the solvent promote the photodegradation of RF probably due to the formation of RF-anion exciplex interactions.[178]
Another problem of RF's high photosensitivity is the photosensitization of other vitamins, carbohydrates, lipids, proteins, and amino acids in food and beverages by RF, which subsequently is converted to its un-excited state.[8] In beer, the photosensitization of other compounds by RF leads to an off-flavor.[10,179] Further, the formation of singlet oxygen via quenching of RF by triplet oxygen can lead to the oxygenation of fatty acids or induce a reaction of amino acids, which results in the spoilage of oils and dairy products.[8] Moreover, the presence of RF leads to the destruction of many polyphenols, folate, methionine, cysteine, histidine, tyrosine, tryptophan, thiamine and ascorbate.[8,10,142,179]

Another obstructive property of RF is its solubility. Though being referred to the water-soluble vitamins, RF's water-solubility amounts to 70-100 mg·L^{-1} (at 27 °C).[8] Even by short boiling, the solubility of RF in water cannot exceed 1000 mg·L^{-1} being stable against precipitation for 1 day. Its solubility in other polar protic solvents such as amyl alcohol, cyclohexanol, benzyl alcohol, phenol or amyl acetate and the ones reported in Table 3 is mostly even worse. Further, RF is also not soluble in ether, acetone, chloroform or benzene. Only formic acid enables to dissolve

about 1 wt.% RF.[1,180] Consequently, RF is an important vitamin with poor water-solubility, high photolability and photodestructive capacity.

Although the solubility of RF is sufficient for many applications, it limits the yield of RF in biotechnological and chemical synthesis. Moreover, a higher solubility might also increase RF's bioavailability upon supplementation or injection. Thus, the search for new solubilizers for RF is an ongoing task.[1,8,180]

*Table 3: Solubility of riboflavin in different solvents. *For water in (mmol·kg^{-1})*

Solvent	c(RF) (g·L^{-1})	c(RF) (mmol·L^{-1}) *
Dimethyl sulfoxide	0.100 (25 °C)[181]	0.266
Water*	0.083 ± 0.006 (30 °C) [182]	0.22 ± 0.02
	0.070 to 0.100 (27 °C)[8]	0.19 to 0.27
Ethanol	0.045 (27 °C) [1,180]	0.12
Acetone	0.036 ± 0.009 (30 °C) [182]	0.10 ± 0.02
Methanol	0.033 ± 0.002 (30 °C) [182]	0.088 ± 0.005

The common hydrotropes, urea and nicotinamide, are known to increase the solubility of RF in water at neutral pH as well as in methanol, dimethyl sulfoxide and N-methylformamide. Urea turned out as less efficient solubilizer than nicotinamide. As nicotinamide and urea increased RF's solubility more strongly in solvents capable of both donation and acceptance of hydrogen bonds, Coffman and Kildsig supposed that the solubilization of RF by these two hydrotropes proceeds via an alternation of the solvent's hydrogen bonding affinity. Though Coffman and Kildsig observed a bathochromic shift of RF's absorption spectrum in the presence of nicotinamide, they first interpreted it as a "change of the solvent's nature".[182] However, the bathochromic shift might also originate from the formation 1:1 and 1:2 sandwich complexes of RF and nicotinamide in an aqueous solution as proposed by classical molecular dynamics. Thus, Van der Waals interactions between RF and its solubilizer are probably important for the solubilization of RF.[35] Still, relatively high concentrations of nicotinamide are required to solubilize 10 times more RF than in pure water.[182] Further, RF's photodegradation in pure water follows first order kinetics, while nicotinamide induces second order kinetics.[158,183] Hence; nicotinamide is not appropriate to the usage as RF solubilizing agent.

Further, RF was found to form complexes with several aromatic compounds, such as adenine, caffeine and other purines, tryptophan, indole, serotonin, chlortetracycline, hydroquinone and phenols.[107,127,174] The observation of an isosbestic point in UV-Vis measurements of RF in the presence of the aromatic Schaeffer's salt and in the presence of sodium salicylate as well as molecular modelling of RF in the presence of the compounds tiron and β-naphthol proposed stacking of these aromatic compounds with RF at distances of 3.0 to 5.0 Å.[60,184]

All these observations and simulations show that the solubilization of RF and its interaction with other molecules is not trivial.

2.8 Vitamin K3

Vitamin K3 or menadione is a synthetic derivative of the lipophilic K vitamins, see Figure 10. It is metabolically activated in the liver to become a co-factor in the activation of vitamin K-dependent proteins.[185] These proteins are the reason why vitamins of the K group are important for the coagulation of blood during hemostasis, for cell growth and proliferation, as well as for inflammatory reactions in the body. Moreover, the K vitamins are responsible for the maintenance of the bone strength and bone metabolism.[186] Although green vegetables make up 40-50 % of the total vitamin K intake, fruits and vegetable oils, such as soybean, cottonseed, canola and olive oil, are important natural sources for vitamin K. Low amounts of the vitamin are also present in animal products, such as fish, liver, milk or eggs.[187,188] While vitamin K1 stands for one compound – phylloquinone –, the term vitamin K2 (menaquinone) represents a variety of compounds comprising 4-13 isoprene units, see Figure 10. Almost all forms of vitamin K2 are produced by anaerobic bacteria. MK-4, comprising four isoprene units, is the only form of vitamin K2 being present in fish, liver or eggs and not in bacteria, and accounts for the main part of vitamin K2 resorbed by humans.[186,189,190] As the requirement for vitamin K1 and K2 is low, supplementation with these vitamins is not common for adults and minorly exerted on infants.[188] Yet, their synthetic derivative vitamin K3 is extensively used as an supplement in animal husbandry, see Figure 10.[189]

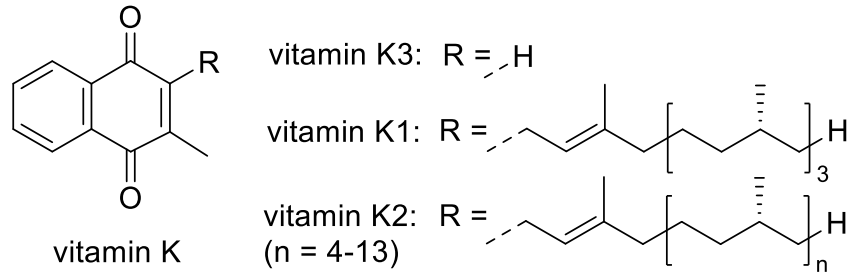

Figure 10: Molecular structure of vitamin K1, K2 and K3

Crystalline menadione sodium bisulfite or menadione nicotinamide bisulfite complexes are already widely used for the supplementation of poultry, swine and fish.[185,191] Especially in poultry industry, antibiotics may inhibit the healthy development of intestinal microorganisms required for the synthesis of K vitamins or interfere directly with vitamin K metabolism.[188] Vitamin K3 is not only used to prevent blooding upon injuries, but also to support the fast bone growth process of animals in husbandry.[185,192] As vitamin K3 is converted to MK-4 in the liver, it has the same biological benefits as vitamin K2.[189] A benefit of vitamin K3 is its at least sparing solubility in water (151 $mg \cdot L^{-1}$), which facilitates the feeding with this vitamin.[193] However, vitamin K3 is known to cause neonatal hemolytic anemia and liver damage in humans and thus has probably the same effect on other animals.[188] As vitamin K3 is considerably cheaper than its natural relatives K1 and K2, it is still widely used in animal husbandry.[188] Usual dosage forms for vitamin K3 are pellets, extrusion and mash.[191,194] Moreover, vitamin K3 is added to

drinking water because it enhances the chromium exposure of domesticated animals, which increases their lifetime, improves reproduction, and reduces metabolic problems, stress, and illness.[185,195]

However, vitamin K3's sparing solubility in aqueous solutions and the low photostability is probably the reason, why pellets and extrusion are the usual dosage forms of vitamin K3 to animals.[196] Although vitamin K3's solubility can be tuned using water-ethanol mixtures, the solubility of vitamin K3 does not only depend on the solvent's polarity and hydrogen bonding capacity, but also on specific intermolecular interactions. This leads to an entropy driven and mostly endothermal solvation of vitamin K3 in dichloromethane, 1,2-dichloroethane, methyl acetate, acetone, acetonitrile, n-butanol, n-propanol, 2-propanol, cyclohexane and methanol.[197] As vitamin K3 stacks with other vitamin K3 molecules in its crystalline form and cocrystallized in a π-stacked manner with aromatic compounds, it was assumed that the huge interaction surface provided by the stacking of the planar vitamin K3 molecules in its crystalline state might be one reason for its limited solubility in water.[198]

2.9 UV-Vis-spectroscopy

Ultraviolet-visible (UV-Vis) spectroscopy enables the quantification and quality control of molecules via interactions between electromagnetic radiation in the ultraviolet (10-400 nm) and visible (400-750 nm) region with matter. Upon illumination with light, valence electrons from the bonding, non-bonding and anti-bonding orbitals are excited to higher energetic levels causing a reduction of the intensity of the absorbed wavelengths, see Figure 11.

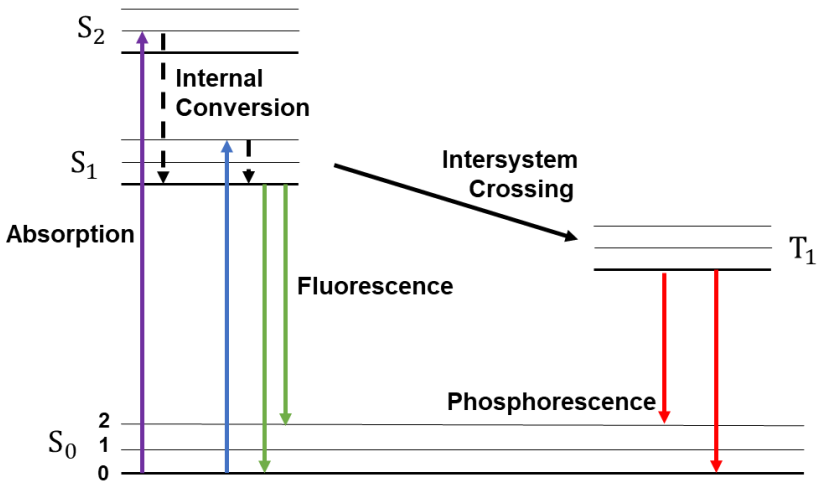

Figure 11: Schematic representation of electronic transitions in a molecule.[199]

Which wavelengths are absorbed by a molecule depends strongly on the molecule's structure. The excited state is usually stable for 10^{-13}-10^{-3} s. The ground state is regained through spontaneous or stimulated emission of radiation (fluorescence, phosphorescence) or through radiationless processes (e.g., internal conversion of energy in order to obtain a thermal

equilibrium). Due to vibrational relaxation, dissipation or solvent reorganization processes, the emitted energy or light is always less energetic than the absorbed one. As a larger conjugated system corresponds to a smaller gap between the outermost electron levels, the absorption spectrum of a molecule experiences a bathochromic shifted with increasing size of the conjugation.

Lambert and Beer found a relation that correlates to the intensity of an absorption with the concentration and thickness of the cuvette.[200,201] However, the Lambert-Beer law is not necessarily valid for analyte concentrations > 10 mmol·kg^{-1}, as analyte-solvent and analyte-analyte interactions might alter the linear correlation.[201] Due to Van-der-Waals, hydrogen bonding and other electrostatic forces, the solvent can influence the absorption of molecules. In the law of Lambert-Beer, this solvent effect is covered by ***ε***.

$$A = -\log(T) = -\log\left(\frac{I}{I_0}\right) = \varepsilon \cdot c \cdot d \tag{4}$$

A = absorbance, T = transmittance, I = remaining light intensity, I_0 = initial light intensity
ε *= molar extinction coefficient, c = concentration, d = thickness of the illuminated layer*

2.10 High pressure liquid chromatography

High pressure liquid chromatography (HPLC) is a method for the separation of molecules (amino acids, carbohydrates, lipids, nucleic acids, proteins, steroids, …), which can be used for qualitative and quantitative analysis. An HPLC device consists of a solvent depot, an autosampler, a high-pressure pumping system, a column, a detector, and a computer system. The separation process takes place in a silica gel column made of stainless steel, which can be 20-100 cm long having a diameter of 2-6 mm. Distinct types of columns are available. Normal phase columns consist of a polar stationary phase of silica gel. Via modification of normal phase columns using covalently bound alkyl chains (C12, C18, …, phenyl, diphenyl, diols) reversed phase (with non-polar coating) or even chiral columns are prepared. Depending on the molecule and on its matrix, different columns are used to obtain optimal separation.
Inside, the column is packed with particles of a pore size in the µm range. The analytes are separated due to distinct adsorption affinity to a stationary phase (liquid or solid adsorbent in the column) and due to their solubility in the mobile phase (eluent), Therefore, the analytes must be soluble in the eluent, which is pumped through the column with high pressure (10-400 atmospheric pressure) and a flow of 0.1–5 cm·s^{-1}.
The speed and degree of the distribution of the analytes between the stationary and mobile phase can be further controlled via variation of the temperature, eluent flow, and constitution of the eluent. Instead of isothermal HPLC, where a constant flow is maintained during the

measurement, gradient elution – corresponding to a variation of the solvent composition during the elution – is often used to accelerate the separation of analytes.[202,203] Using gradient elution, the polarity can be adjusted via variation of the portion of polar and less polar solvents. Common eluents are water, acetonitrile, methanol, isopropanol or hexane.[204] The water phase can be basic or acidic to prevent the presence of multiple peaks due to incomplete deprotonation or protonation of basic and acidic functional groups.

The time required to pass the column and to reach the detector is called retention time and is characteristic for each compound.[202,203]

Depending on the column and detector, HPLC enables the detection of several compounds in mircomolar to picomolar concentrations within one measurement. Typical detectors for HPLC are UV-Vis-absorption detectors, fluorescence detectors, electrochemical detectors, refractive index detectors, mass spectrometric detectors, evaporative light scattering detectors, radioactive detectors and chemiluminescent nitrogen detector.[205] In this research, the UV-Vis-absorption detector was used. The retention time and the UV-Vis-spectrum of a signal provided qualitative information on the analytes, whereas the area beneath a peak in the chromatogram was used to quantify the analytes after calibration.

2.11 Nuclear Magnetic Resonance spectroscopy

Nuclear Magnetic Resonance (NMR) spectroscopy is a common non-destructive technique for the elucidation of molecular structures, interactions between compounds and for the quantification of analytes in solutions and in the solid-state. This spectroscopic method requires a magnetic moment of an atom's nucleus μ, which causes a nuclear spin with a *spin angular momentum P,* see equation 5. Atoms with a nuclear spin I = 0, such as ^{12}C and ^{16}O are not analyzable with NMR because they have no spin angular momentum and thus no *nuclear magnetic moment*. Only atoms with an odd number of protons and/or neutrons and thus with a nuclear spin I > 0 can be analyzed with NMR spectroscopy. The most common nuclear spin I = ½ can be found in ^{1}H, ^{19}F, and ^{31}P with 100 % abundance and in ^{13}C, ^{15}N, ^{29}Si with lower abundance.

$$\mu = P \cdot \gamma = \frac{\gamma \cdot h \cdot \sqrt{I(I+1)}}{2\pi} \quad (5)$$

h = Planck's constant, γ = gyromagnetic ratio

γ is a specific constant for each nucleus, which depends on the mass, charge and g-factor of an atom. Thus, NMR can even distinguish between isotopes.

In the ground state, all nuclei are in the same level of magnetic energy E, which depends on μ and B_0, see equation 6. Being exposed to an exterior homogenic magnetic field B_0, the nucleus of an atom performs precessional motion with the Larmor frequency, which is directly proportional to B_0 and m. The nuclear magnetic moments can adopt $(2I+1)$ possible

orientations with magnetic quantum numbers m ranging from - I to + I with $\Delta m = \pm 1$. This degeneration of the energy levels is called Zeeman effect. Thus, atoms with most common spin I = ½ can adopt two magnetic quantum numbers ½ and -½ being parallel and antiparallel to B_0, respectively. As m can change only by ± 1, the energetic difference between the parallel and antiparallel orientation of the nuclear spin is explained by equation 7.

$$E = -\mu \cdot B_0 = -\gamma \cdot h \cdot m \cdot B_0 / (2\,\pi) \quad (6)$$

$$\Delta E = \gamma \cdot h \cdot B_0 / (2\,\pi) \quad (7)$$

The energetic level of a nucleus can be altered upon irradiation with radiofrequency perpendicular at the resonance (Larmor) frequency to B_0 causing a spin-flip. Through relaxation phenomena such as via emission of heat, the nucleus can return to its ground state again. The higher B_0, the higher the energetic difference between the levels ΔE, the better the resolution.[206]

The equilibrium between the population of the ground N_0 and excited states N_1 can be expressed via the Boltzmann equation.

$$\frac{N_1}{N_0} = e^{-\frac{\Delta E}{k_B T}} \quad (8)$$

T = temperature, k_B = Boltzmann constant

High concentrations of the analyte are required to obtain a sufficient signal to noise ratio, which rises with the square root of the number of scans.

Aside of the strength of the exterior magnetic field B_0 and of γ, the chemical environment of the nucleus defines ΔE. The nucleus is shielded from the external magnetic field B_0 by its electron shell and by neighbored nuclei. Thus, the local magnetic field B_{local} induced by the electrons and nuclei in a nucleus' surrounding leads to an effective magnetic field B_{effect} distinct of B_0. Practically, ΔE is expressed as chemical shift δ (ppm) referring to the excitation frequency of an internal standard $\nu_{reference}$, which is usually tetramethyl silane. The chemical shift of the internal standard is set to 0 ppm.

$$\delta = \frac{\nu_{sample} - \nu_{reference}}{\nu} \quad (9)$$

ν_{sample} = *excitation frequency of the sample*, ν = *frequency of magnetic field B_0*

Depending on the electronegativity of the neighbored atoms and on the distance, the chemical shift of the nucleus can be increased in the presence of electron demanding neighbors (deshielding) and decreased in the presence of electron pushing neighbors (shielding). This interaction of the nucleus with other ones is called spin-spin coupling or scalar coupling and can lead to a splitting of the signals. While the position of the signal provides information about

the type of atom, the integral of the signals in ^{1}H-NMR are proportional to the number of protons and hence can be used for quantification purposes.[202]

Although one-dimensional (1D) NMR spectroscopy is a powerful technique, the spectra can get complicated for larger molecules, such as for many drugs or proteins. To be still able to identify molecules, two-dimensional (2D) NMR spectroscopy is used complimentary. Such as in 1D NMR, the sample is excited by a radio-pulse leading to a spin-flip of the nuclei with a magnetic moment. In contrast to 1D NMR, the signal is not recorded right away. After a certain evolution time t_1, in which the nuclear spins of the molecules rearrange, a second pulse is used to create a position dependent reorganization of the spins prior to detection after the time t_2, see Figure 12 . By varying the time of evolution, the system can be probed at distinct partially relaxed equilibria, which depend on the surrounding of the nucleus by electrons and by other nuclei in the sample. The 2D NMR spectrum is retrieved by plotting the two time domains t_1 and t_2 against the signal's intensity and subsequent Fourier transformation.[207] 2D NMR provides information about the protons (Correlation Spectroscopy (COSY)) and carbons (Heteronuclear Single Quantum Coherence (HSQC), Heteronuclear Multiple Bond Correlation (HMBC)) in the direct neighborhood to a nucleus. Only nuclei next to each other in the same molecule can be detected.

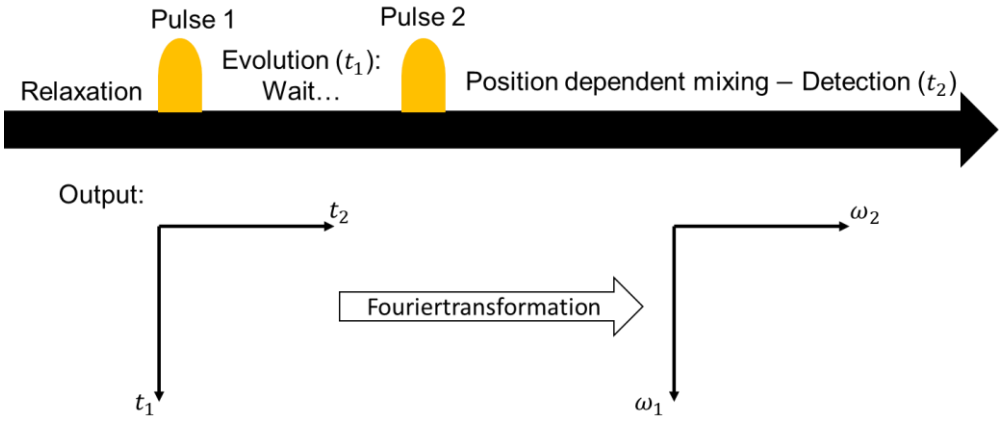

Figure 12: Schematic representation an 2D NMR experiment.

If information about the proximity of two nuclei positioned on distinct molecules or of further separated nuclei on one molecule is desired, Nuclear Overhauser Effect Spectroscopy (NOESY) is the method of choice. Although NOESY is also a 2D NMR technique. The principle deviates slightly from the one of COSY, HSQC and HMBC. "The nuclear Overhauser effect (NOE) is defined as the change of a spin's signal due to magnetization transfer through cross relaxation in a dipolar coupled system or simply defined as the dipole-dipole relaxation effect, which causes transfer of magnetization from one nucleus to another."[208] Thus, the integrated intensity of one NMR changes if another nucleus is saturated by a radiofrequency.[209] As the NOE correlates with the Brownian motion, small molecules give rise to positive signals, while

larger ones lead to negative signals due to slower tumbling.[208] Like this, NOESY enables the observation of intra- and intermolecular interactions.

2.12 Dynamic Light Scattering (DLS)

Light – when regarding it as an electromagnetic wave – can induce electron density oscillation within a molecule. Hence, the molecule can be regarded as an oscillating dipole that emits the light with which it was irradiated. This electric oscillation in the molecule depends on the polarizability. For bigger molecules (> 20 nm), an irradiation with light can even induce several oscillating dipoles. All these dipoles can emit light having a distinct phase to the one of the irradiation. The irradiated light can then interfere. Such an interference pattern comprises information about the particle as the emitted light is no longer isotropic but has the same wavelength.[210]

In the case of DLS, Brownian motion (a thermic effect) causes a permanent random movement of the particles in the solution. This leads to a shift of the initial angular frequency ω_0 by $\Delta\omega$ – called Doppler Effect. A movement of the particle in direction to the detector results in a positive $\Delta\omega$, a movement in the opposite direction in a negative $\Delta\omega$. As the Brownian motion is random, a Lorentzian shaped distribution of the scattered angular frequencies around ω_0 can be observed. The angular frequency half width at half height $\Delta\omega_{1/2}$ of the Lorentzian curve was found to be related to the diffusion coefficient *D* that characterizes the Brownian motion of particles.[210,211]

$$\Delta\omega_{1/2} = D \cdot q^2 \tag{10}$$

Theoretically, one could calculate the *D* if being able to record the Lorentzian curve precisely. However, due to the law of conservation it was not possible to slim such spectra. This problem was solved by the usage of digital correlators. Fourier transformation can be used to switch from spectral analysis into the time delay τ dependent analysis of the second-order intensity autocorrelation $G_2(\tau)$. [212] The intensity of the scattered beam $I(t)$ is measured at a random time *t*, whereas the intensity $I(t+\tau)$ is monitored at a time delay τ. $G_2(\tau)$ represents the average of the two intensities over a large number of times t. A short time delay corresponds to a strong correlation of $G_2(\tau)$, as the intensity decays exponentially with the time. For long τ the correlation vanishes. No correlation corresponds to $G_2(\tau) = \langle I(t)\rangle^2$.

$$G_2(\tau) = \langle I(t) \cdot I(t+\tau)\rangle \tag{11}$$

In case of monodisperse particles, $G_2(\tau)$ depends on the decay rate of the intensity Γ. A and B are instrumental factor with B < A. A normalization of $G_2(\tau)$ via division by $\langle I(t)\rangle^2$ leads to $g_2(\tau)$. The decay rate Γ is linked to the diffusion coefficient.[210,213,214]

$$G_2(\tau) = A + B \cdot exp[-2 \cdot \Gamma \cdot \tau] \tag{12}$$

$$g_2(\tau) = 1 + \beta \cdot exp[-2 \cdot \Gamma \cdot \tau] \quad (13)$$

$$\Gamma = \mathrm{D} \cdot q^2 \quad (14)$$

Thus, the diffusion coefficient can be calculated from the autocorrelation function $g_2(\tau)$. With the Stokes-Einstein equation it is possible to derive the hydrodynamic radius R_H from the diffusion coefficient. However, this relation accounts only for non-interacting spherical particles.[214,215]

$$D = \frac{k_B \cdot T}{6 \cdot \pi \cdot \eta \cdot R_H} \quad (15)$$

k_B = *Boltzmann constant*

T = *temperature*

η = *dynamic viscosity of the solvent*

The experimental setup of DLS is displayed in Figure 13.

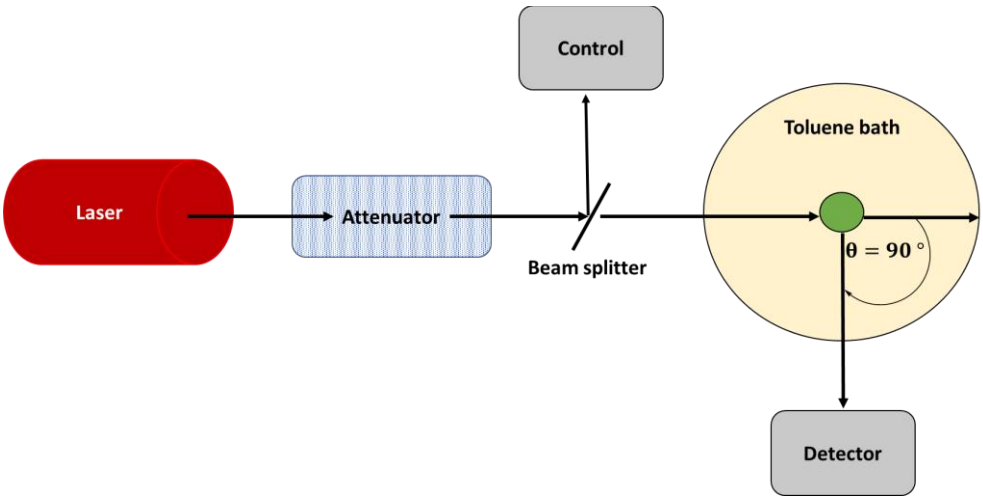

Figure 13: Setup for dynamic light scattering measurements

3 Experimental

3.1 Chemicals

Deionized Millipore water (18 MΩ·cm) was taken from a Millipore purification system from **Merck Millipore** (Billerica, MA USA).

Riboflavin (97 %) and cyanin chloride (Rotichrom TLC) were purchased from **Carl Roth** (Karlsruhe, Germany).

Riboflavin was provided by **BASF SE** with a purity greater than 97.0 g / 100 g according to Ph. Eur.

Riboflavin (Lot. 35FLH), folic acid (> 98.0 %), menadione (> 98.0 %, T, HPLC) sodium 3-hydroxybenzoate (99.0 %), cyclohexane carboxylic acid (> 98.0 %), sodium 4-hydroxybenzoate (98.0 %), 2-methoxybenzoic acid (> 98.0 %, GC), 3-methoxybenzoic acid (> 98.0 %, GC), 4-methoxybenzoic acid (> 99.0 %, GC), sodium vanillate (98 %), trans-2-hydroxycinnamic acid (> 98.0 %, HPLC), 2,3-dihydroxybenzoic acid (> 98.0 %, HPLC), 2,4-dihydroxybenzoic acid (> 98.0 %, HPLC), 3,4-dihydroxybenzoic acid (> 98.0 %), 3,5-dihydroxybenzoic acid (> 98 %), 2,3-dimethoxybenzoic acid (> 98.0 %, GC), 2,4-dimethoxybenzoic acid (> 99 %), 3,4-dimethoxybenzoic acid (> 98.0 %), 3,5-dimethoxybenzoic acid (> 98.0 %, GC), syringic acid (97.0 %), trans-m-coumaric acid (> 98.0 %, GC), caffeic acid (> 98.0 %), trans-4-methoxycinnamic acid (> 98.0 %, GC), sinapinic acid (98.0 %, GC), 3-(4-hydroxyphenyl)-propionic acid (98.0 %), 3,4-dimethoxycinnamic acid (> 98.0 %), (2E,4E)-5-phenyl-2,4-pentadienoic acid (> 98.0 %, GC), 5-phenylvaleric acid (> 99.0 %), sodium terephthalate (99.0 %, HPLC), phloroglucinol (> 99.0 %, anhydrous HPLC), diphenic acid (> 98.0 %, GC, T), coumalic acid (> 97.0 %, GC, T), sodium DL-mandelate (> 99.0 %, T, HPLC), biotin (> 98.0 %, T), β-Nicotinamide adenine dinucleotide reduced disodium trihydrate (98.0 %), vanillyl alcohol (> 98.0 %, GC), ethyl vanillin (> 98.0 %, GC), adenosine (> 99.0 %, T, HPLC), pyridoxine hydrochloride (98.0 %, T, HPLC), thiamine hydrochloride (99 %, HPLC), L-histidine (> 99.0 %, HPLC), rutin hydrate (>94 %, T, HPLC), hesperidin (> 90 %, T, HPLC), L-tryptophan (> 98 %, HPLC), caffeine, (> 98.0 %, T, HPLC), ellagic acid dihydrate (> 98.0 %, T, HPLC) and 3-indole propionic acid (> 98.0 %, T) were purchased from **TCI Chemicals** (Eschborn, Germany).

Gallic acid (98.0 %, for synthesis), 4-phenylbutyric acid (99 %), sodium dihydrogen phosphate dihydrate (p.A.) and sodium dodecyl sulfate (99 %), acetonitrile (HPLC grade, LiChrosolv®), sodium citrate tribasic dihydrate (p.A.), potassium hydroxide pellets (p.A), carboxymethylcellulose sodium salt high viscosity (substrate for cellulase, 800-3100 mPas), hydrochloric acid (1 $mol \cdot L^{-1}$ aqueous solution), triacetin (> 99 %, FG) and methanol (HPLC grade, LiChrosolv®) were purchased from **Merck** (Darmstadt, Germany).

Riboflavin 5'-monophosphate sodium salt (73-79 %, < 10.5 % H_2O; 3.8-6.5 % Na (anhydrous)), trans-ferulic acid (99 %), trans-cinnamic acid (> 99 %, FCC, FG), 4-hydroxycinnamic acid (> 98.0 %), sodium benzoate (99 %, p.A.), sodium salicylate (99.5 %, reagent plus), sodium thiocyanate (99.99 %), sodium xylene sulfonate (< 9.0 % sodium sulfate), 2,4,6-trihydroxybenzoic acid monohydrate (90 %, predominantly 1,3,5-benzenetriol), tyrosol (> 98.0 %), DPnP (Dowanol, ≥ 98.5 %, isomeric mixture), tannic acid (according to Ph. Eur.), phenylsuccinic acid (98 %), sodium phenyl phosphate dibasic hydrate (from rice), adenine (≥ 99 %), adenosine 5'-triphosphate disodium salt (99 %, from microbia, 10 % H_2O (Carl Fischer)), L-tyrosine (reagent grade ≥ 98 %, HPLC), L-proline (99 %, FCC, FG), saccharine (98 %), pyroglutamic acid (99.0 %, T), γ-valerolactone (99 %, FCC, FG), Sudan blue II (98 %), meglumine (USP testing specification), L-arginine (98% reagent grade), acetone (p.A.), ethanol (p.A.), dimethyl sulfoxide (99.9 %, ACS reagent), hydrochloric acid (37 %), calcium phosphate dibasic (> 98.0-105.0 %), potassium dihydrogen phosphate (≥ 99.0 %, ACS reagent), potassium sorbate (99.0 %, p.A.), D-(+)-glucose (≥ 99.5 %, GC), D-(-)-fructose (≥ 99.0 %, HPLC, suitable for microbiology), potassium 3-indoxylsulfate (quality: 200), citric acid (99 %), L-ascorbic acid (99 %), trifluoroacetic acid (99.0 %, suitable for HPLC), calcium L-lactate pentahydrate (USP testing specification) and lumichrome were purchased from **Sigma Aldrich** (Darmstadt, Germany).

Sodium hydroxide pellets (p.A., AnalaR Normapur), sodium chloride (99.6 %) and potassium chloride (99.5-101.0 %, AnalaR NormaPur) were obtained from **VWR** (Ismaning, Germany). 3,5-Bis(trifluoromethyl)benzoic acid (98 %) was purchased from **Thermo Scientific Fisher** (Germany).

Sodium dodecyl sulfate (ultrapure) was purchased from **AppliChem GmbH** (Darmstadt, Germany).

Sodium cholate (99 %, loss upon drying: 3.9 %) and choline hydroxide (46 wt.% aqueous solution) were purchased from **Alfa Aesar (**Kandel, Germany).

Drinking water (Natürliches Mineralwasser, natriumarm, ohne Kohlensäure, sodium: 13.2 mg, potassium 1.0 mg, magnesium: 32.9 mg, calcium 67.6 mg in 1 liter) was purchased from **Adelholzener Alpenquellen GmbH** (Siegsdorf, Germany). White sugar for the model sports drink from BASF was purchased from **Südzucker** (Mannheim, Germany). Capsules comprising oligomeric proanthocyanidins complex 200 were purchased from **Greenline Products** (200 mg OPC (95 %) + 250 mg vitamin C).

Fulvic acid (> 90 %) was purchased from **Molekula Group** (Darlington, United Kingdom).

Resveratrol triphosphate (≥ 90 % phosphorylated, ≥ 50 % triphosphorylated, 10 % water (Carl Fischer) was purchased from **Ajinomoto OmniChem** (Wetteren, Belgium).

Deuterated dimethyl sulfoxide (99.8 %) and deuterium oxide (99.96 %) were purchased from **Deutero** (Kastellaun, Germany).

Sodium ferulate (99.54 %) for NMR analysis was purchased from **BDLpharm** (Kaiserslautern, Germany).

The laboratory material used is listed in Table 4.

Table 4: List of all materials used in this research

Name	Description	Company
Indicator paper pH 10-1	Universal	VWR international (Ismaning, Germany)
Syringe filter 0.2	0.2 µm PTFE and cellulose acetate; membrane, diameter 13 mm or 25 mm	VWR international (Ismaning, Germany)
Syringe filter 0.45	0.45 µm PTFE or cellulose acetate; membrane, diameter 25 mm	VWR international (Ismaning, Germany)
HPLC vials	Brown glass 1.5 mL ND9 with screw caps	Carl ROTH (Karlsruhe, Germany)
NMR tubes	NMR tubes borosilicate length 8 inch	Deutero (Kastellaun, Germany)
DLS tubes	Tube, culture, disposable, 10x75mm, borosilicate	Corning Incorporated (New York, USA)
Pipettes	1 mL	VWR international (Ismaning, Germany)

If not stated differently, all experiments were performed at room temperature (23°C) in Millipore water. If not state otherwise, water was used as synonym for Millipore water. The pH-value of the samples was tested with indicator paper to be between 6 and 7.5.

3.2 Investigation of the hydrotropic properties of polyphenolic acid salts

3.2.1 Sodium polyphenolates as salting-in and -out agents

3.2.1.1 Phase transition temperature measurements of the binary water/DPnP system

Sodium salt solutions of ranging from 0–500 mmol·kg^{-1} were prepared in the binary water/DPnP ((45/55 (w/w)) system. Some sodium polyphenolates and related compounds were synthesized via neutralization of the corresponding acid with self-made aqueous sodium hydroxide solution and subsequent removal of water via lyophilization for up to 4 days, see Table 5. The water content was determined with Coulometric Karl Fischer by means of an 899 Coulometer from Metrohm with platinum electrodes from Metrohm (Herisau, Switzerland). Taking into account the salt's water content, the required amount of salt (NaBenz, Na-4-OH-3-OMe-Cinn, Na-3,4,5-TriOH-Benz, Na-2-OMe-Benz, Na-2,3-DiOMe-Benz, sodium 3-(4-hydroxyphenyl)-propionate (Na-4-OH-Prop), Na-3-OH-Benz, Na-4-OH-Benz, Na-4-OH-3-OMe-Benz) was mixed with water and 1.65 g of DPnP to have a final water/DPnP of the composition (45/55 (w/w)).

The residual samples (Na-3,4-DiOH-Benz, sodium 3,5-bis-(trifluoromethyl)-benzoate (Na-3,5-DiCF3-Benz), NaCinn, Na-2-OH-Cinn, Na-4-OH-Cinn, Na-4-OMe-Benz, NaCHC) were prepared via neutralization of the corresponding acid with 1 mol·L^{-1} self-made sodium hydroxide solution. Then residual amount of water and 1.65 g DPnP was added, to obtain 3 g of a water/DPnP mixture (45/55 (w/w)).

Additionally, sodium cholate (0–300 mmol/kg) and sodium dodecyl sulfate (0–200 mmol/kg) samples were prepared analogously by addition of the salts to water and DPnP to obtain 3 g samples of the water/DPnP (45/55 (w/w)) mixture.

PTT measurements of the binary water/DPnP system (45/55 (w/w)) were conducted via heating of the samples in a water bath from their homogeneous state at 0 °C (ice bath) to their cloud point by means of a heating plate from Heidolph Instruments (MR Hei-Standard, 825 W, Schwabach, Germany). The PTT was determined with a thermometer (error +/- 1 °C) as turbidity by the eye. The sample comprising Na-3,5-DiCF3-Benz was prepared once. The residual samples were prepared in triplicate.

Table 5: Sodium polyphenolates synthesized via lyophilization with the determined water content (Coulometric Karl Fischer)

Salt	water content/wt.%
Na-3,4,5-TriOH-Benz	10.6
Na-4-OH-3-OMe-Cinn	1.0
Na-2-OMe-Benz	0.4
Na-2,3-DiOMe-Benz	0.3
Na-4-OH-Prop	1.9

3.2.1.2 Surface tension measurements of sodium polyphenolates and similar compounds

Stock solutions of Na-4-OH-3-OMe-Cinn (70026 mg·L^{-1}), Na-3,5-DiCF3-Benz (98985.6 mg·L^{-1}) and NaCinn (93704 mg·L^{-1}) were prepared via neutralization of the corresponding acid with 1 mol·L^{-1} self-made sodium hydroxide (p.A) solution and addition of the residual amount water. In the case of NaBenz (90899 mg·L^{-1}), Na-2-OH-Benz (90899 mg·L^{-1}) and sodium dodecyl sulfate (SDS) (8000.2 mg·L^{-1}) the sodium salt was directly dissolved in water. All samples were prepared in duplicate except of the one comprising SDS, which was prepared only once.

All surface tension curves were obtained from a Krüss (Hamburg, Germany) Tensiometer K100 at 25 °C by means of the Wilhelmy Ring Method with a platinum-iridium-ring. The measurement device diluted the 40 mL stock solutions automatically down to 0.1 mg·L^{-1} with help of the dosing system Dosino 800 from Metrohm (Herisau, Switzerland) to obtain a surface tension curve. Each concentration was measured 5 times (deviation < 0.5 mN·m^{-1}). For the curvature correction, the Harkins & Jordans method (accuracy of 0.8 %) was used.

To know the concentration in mol·L^{-1}, the density of the stock solutions was measured with a DMA5000 Density Meter from Anton Paar (Ostfildern-Scharnhausen, Germany) at 25 °C prior to the surface tension determination. Via the vibration of a U-shaped capillary, filled with the sample, its density was calculated by the measurement device.

3.2.1.3 DLS measurements of sodium polyphenolates and related aromatic salts in water and in the binary water/DPnP system

For the DLS measurement see section 3.6. All samples were measured for 120 s. Only Na-4-OH-Prop in pure water at 10 °C was measured for 60 s.

The samples comprising Na-3,5-DiCF3-Benz, NaCinn, Na-2-OH-Benz, NaBenz, NaCHC, Na-4-OH-Prop and Na-4-OMe-Benz in pure water and in the binary water/DPnP system were prepared at 25 °C. The reference sample (binary water/DPnP solution) and the Na-4-OH-Benz and Na-3,4-DiOH-Benz samples were prepared at 10 °C due to turbidity at 25 °C. After addition of all compounds as described in section 3.2.1.3.1 and 3.2.1.3.2, the samples were stirred at 450 rpm at the corresponding temperature for 20 min for entire dissolution.

All samples were filtered with 0.2 µm polytetrafluoroethylene (PTFE) syringe filters in clean borosilicate tubes at the corresponding preparation temperature. The samples comprising Na-3,5-DiCF3-Benz, NaCinn, Na-2-OH-Benz, NaBenz, NaCHC, Na-4-OH-Prop, Na-4-OMe-Benz, Na-4-OH-Benz and Na-3,4-DiOH-Benz as well as the reference were measured in pure water and in the binary water/DPnP system at 10 °C. The samples comprising Na-3,5-DiCF3-Benz, NaCinn, Na-2-OH-Benz, NaBenz, NaCHC, Na-4-OH-Prop and Na-4-OMe-Benz in water and in the binary water/DPnP system were additionally measured at 25 °C. All samples were prepared in duplicate.

3.2.1.3.1 Sodium polyphenolates and related compounds in pure water

0.5 mol·kg^{-1} NaCinn, Na-3,5-DiCF3-Benz, NaCHC, Na-4-OMe-Benz and Na-3,4-DiOH-Benz solutions were prepared by equimolar neutralization of the corresponding acid with 2 mol·L^{-1} self-made sodium hydroxide solution and addition of the residual water to obtain a total water content of 3 g. 0.5 mol·kg^{-1} NaBenz, Na-2-OH-Benzl, Na-4-OH-Benz and Na-4-OH-Prop samples and a 0.6 mol·kg^{-1} Na-2-OH-Benz sample were prepared via direct dissolution of the salt in 3 g water.

3.2.1.3.2 Sodium polyphenolates and related compounds in the binary DPnP/water system

0.5 mol·kg^{-1} NaCinn, Na-3,5-DiCF3-Benz, NaCHC, Na-4-OMe-Benz, Na-3,4-DiOH-Benz solutions in the binary water/DPnP system (45/55 (w/w)) were prepared by equimolar neutralization of the corresponding acid with 2 mol·L^{-1} self-made sodium hydroxide solution and addition of the residual water to have in total 1.35 g water. Then, 1.65 g DPnP was added.

The 0.5 mol·kg^{-1} NaBenz, Na-2-OH-Benz, Na-4-OH-Benz and Na-4-OH-Prop samples and the 0.6 mol·kg^{-1} Na-2-OH-Benz sample were prepared via direct dissolution of the salt in a mixture of 1.35 g water and 1.65 g DPnP. Additionally, a reference sample was prepared from 1.35 g water and 1.65 g DPnP.

3.2.1.4 Nuclear magnetic resonance measurements of sodium ferulate in the binary water/DPnP system

A sample of 0.2 mol·kg^{-1} Na-4-OH-3-OMe-Cinn in the binary water/DPnP (45/55 (w/w)) mixture was prepared by direct dissolution of the salt (99.54 %; BDLpharm) in 1.35 g water and 1.65 g DPnP. To have a reference for Na-4-OH-3-OMe-Cinn, deuterium oxide was saturated with the salt via stirring at 450 rpm at 23 °C for 1 h. The latter sample was filtered through 0.45 µm PTFE syringe filters. An ^{1}H-NMR spectrum of both solutions was recorded. To have a reference for DPnP, an ^{1}H-NMR spectrum of pure DPnP was recorded, too. Therefore, 0.8 mL of each sample were filled into a borosilicate NMR tube. The NMR measurements were conducted at 25 °C. ^{1}H-NMR, COSY and NOESY experiments were conducted with a Bruker Avance III HD 400 (400.13 MHz) NMR-spectrometer with a 5 mm BBO 400S1 BBF-H-D probe head with a Z-gradient at the Central Analytical NMR department of the University of Regensburg.

3.2.2 Hydrotropic solubilization of aromatic compounds with polyphenolic acid salts

3.2.2.1 Riboflavin

3.2.2.1.1 Solubilization of riboflavin in water

The water-solubility of riboflavin from three distinct distributors with maximum two different batches (Carl Roth, BASF, TCI) was determined in triplicate. For saturation, an excess of riboflavin was added into 2 g of water. After 2 min of ultrasonication (Bransonic 220, 120 W, frequency: 50 kc), the samples were stirred at 450 rpm at 23 °C in the dark for 2 h. The samples were filtered with 0.45 µm PTFE syringe filters. For UV-Vis-measurements, the sample were diluted 1:3 (w/w) with water on the balance.

3.2.2.1.2 Solubilization of riboflavin in presence of polyphenolic acids and their corresponding sodium salts

Stock solutions (0.50 mmol·kg^{-1}) of ferulic and cinnamic acid as well as of the corresponding sodium salts were prepared in 0.5 L volumetric flasks via stirring overnight. Stock solutions of vanillic acid and its sodium salt were prepared at the same concentration in 1.0 L volumetric flasks via stirring for 1 h. All stock solutions were diluted with water to 0.40 mmol·kg^{-1}, 0.25 mmol·kg^{-1} and 0.10 mmol·kg^{-1} samples. After addition of an excess of RF, the samples

were stirred in the dark for 1 h and filtered through 0.45 µm PTFE syringe filters. After 1:3 dilution with water on the balance, the absorbance at 449 nm was measured with a UV-Vis-spectrophotometer, see section 3.2.2.4. The samples were prepared in duplicate.

3.2.2.1.3 Hydrotropic solubilization of riboflavin with sodium polyphenolates and related compounds

Aqueous solutions of sodium polyphenolates and related compounds (Na-2-OMe-Benz, Na-3-OMe-Benz, Na-4-OMe-Benz, Na-2,3-DiOH-Benz, Na-3,4-DiOH-Benz, Na-3,5-DiOH-Benz, Na-2,4-DiOH-Benz, Na-2,3-DiOMe-Benz, Na-2,4-DiOMe-Benz, Na-3,4-DiOMe-Benz, Na-3,5-DiOMe-Benz, Na-4-OH-3,5-DiOMe-Benz, Na-3,4,5-TriOH-Benz, Na-2,4,6-TriOH-Benz, NaCHC, NaCinn, Na-2-OH-Cinn, Na-3-OH-Cinn, Na-4-OH-Cinn, Na-4-OMe-Cinn, Na-3,4-DiOH-Cinn, Na-4-OH-3-OMe-Cinn, Na-3,4-DiOMe-Cinn, Na-4-OH-3,5-DiOMe-Cinn, Na-4-OH-Prop, Na-3,5-DiCF3-Benz, NaButyrate, NaValerate, Na-2,4-Pentadienoate, disodium diphenate, sodium coumalate, sodium D,L-mandelate, disodium phenyl succinate) were dissolved in water via neutralization of the corresponding carboxylic acid with self-made sodium hydroxide solution and addition of the residual amount of water. The residual samples (NaBenz, Na-2-OH-Benz, Na-3-OH-Benz, Na-4-OH-Benz, Na-4-OH-3-OMe-Benz, disodium terephthalate (Naterephthalate), sodium thiocyanate (NaSCN), sodium dihydrogen phosphate (NaH_2PO_4), SDS, sodium xylene sulfonate (SXS), tyrosol, phloroglucinol, tannin, disodium phenyl phosphate) were prepared via direct dissolution of the salt in the required amount of water. A compound was defined to be insoluble in water, if it was not completely solubilized after stirring at 450 rpm for 1 h. For saturation, RF was added in excess to all samples, even to heterogenous ones. After ultrasonication for 2 min (Bransonic 220, 120 W, frequency: 50 kc), all samples were stirred at 450 rpm in the dark for 1 h and filtered with 0.45 µm PTFE syringe filters.

The samples comprising 0.4-1.62 $mol \cdot kg^{-1}$ of this compound were prepared only once. The samples comprising NaH_2PO_4 between 3 and 4 $mol \cdot kg^{-1}$ were also prepared only once. Samples with Na-2,4,6-TriOH-Benz, Na-2,4-Pentadienoate, NaValerate, NaButyrate and tyrosol were prepared in triplicate. The residual ones were prepared in duplicate. For the quantification of RF, see section 3.2.2.4.

3.2.2.1.4 Effect of riboflavin's type on the solubilization power of sodium polyphenolates

The water-solubility of RF in aqueous sodium vanillate solutions ranging from 0-240 $g \cdot kg^{-1}$ Na-4-OH-3-OMe-Benz was determined for a batch from Carl Roth and for two batches from BASF via saturation. Therefore, an excess of RF was added to the clear aqueous sodium vanillate solutions. The samples were ultrasonicated for 2 min (Bransonic 220, 120 W, frequency:

50 kc), stirred at 450 rpm in the dark for 1 h and filtered through 0.45 µm PTFE syringe filters. Then, the RF concentration was determined as described in section 3.2.2.4.
Additionally, 0.2 mol·kg^{-1} aqueous solutions of NaBenz, Na-4-OH-3-OMe-Benz, Na-2-OH-Benz, Na-2-OH-Benz, Na-4-OH-3-OMe-Cinn and Na-3,4-DiOMe-Cinn, which were prepared via dissolution of the salt in water or by neutralization with 1 mol·L^{-1} self-made sodium hydroxide solution, were saturated analogously with RF.

3.2.2.1.5 Change of riboflavin's absorption spectrum in presence of sodium ferulate

An aqueous 0.37 mol·kg^{-1} Na-4-OH-3-OMe-Cinn solution was prepared via neutralization of ferulic acid with 1 mol·L^{-1} self-made sodium hydroxide solution and addition of the required amount of water. After an excess of RF was added, the sample was ultrasonicated for 2 min (Bransonic 220, 120 W, frequency: 50 kc), stirred at 450 rpm in the dark for 1 h and filtered through 0.45 µm PTFE syringe filters. The sample was diluted with Millipore water to obtain twelve distinct concentrations of Na-4-OH-3-OMe-Cinn from 370 to 0.19 mmol·kg^{-1}. The UV-Vis-absorbance spectrum from 250-750 nm of each sample was recorded with a Lambda18 spectrophotometer (Überlingen, Germany). Therefore, the samples were filled in 3 mL quartz cuvettes (10 mm with a transmission from 200-2500 nm) from Hellma (Müllheim, Germany). Millipore water served as reference.

3.2.2.1.6 Effect of distinct cations on the solubilization efficiency of polyphenolates

0.37 mol·kg^{-1} ferulate solutions were prepared via neutralization of ferulic acid with choline hydroxide solution (46 wt.%), meglumine, arginine, self-made sodium hydroxide and self-made potassium hydroxide and addition of the residual amount of water. After saturation with RF via ultrasonication for 2 min (Bransonic 220, 120 W, frequency: 50 kc) and subsequent stirring at 450 rpm in the dark for 1 h, the samples were filtered with 0.45 µm PTFE syringe filters. The RF concentration was determined via UV-Vis-measurements as section 3.2.2.4. The sample comprising choline ferulate was prepared in duplicate. The residual samples were prepared in triplicate.

3.2.2.1.7 Hydrotropic solubilization of riboflavin by means of choline polyphenolates in water

Choline salt solutions comprising choline gallate, vanillate, 3,5-dihydroxybenzoate, ferulate, cinnamate or 3,4-dimethoxybenzoate were prepared via neutralization of the corresponding carboxylic acid with aqueous choline hydroxide solution (46 wt%) and addition of the residual amount of water. All tested choline salts were dissolved after stirring at 450 rpm for 15 min. Then, RF was added in excess and the samples were ultrasonicated for 2 min (Bransonic 220, 120 W, frequency: 50 kc) and stirred at 450 rpm in the dark for 1 h. After filtration through

0.45 µm PTFE syringe filters, RF was quantified as reported in section 3.2.2.4. The samples were prepared in duplicate.

3.2.2.1.8 Crystallization of riboflavin

3.2.2.1.8.1 Synthesis and microscope images of riboflavin crystals

2 g of a water/acetonitrile (50/50 (w/w)) solution were saturated with RF and cinnamic or 3,4-dimethoxycinnamic acid by stirring at 450 rpm at 23 °C for 4 h. After filtration through 0.45 µm PTFE syringe filters, 0.2 mL of the samples were filled in a narrow 1.5 mL vessel and overlayed with 2 mL of acetonitrile. After one month, microscope images of the crystals were taken with a bright-field microscope with an Eclipse E400 biological microscope from Nikon (Tokio, Japan).

A Nikon L Plan SLWD objective lens with a 20 times magnification and a numerical aperture of 0.35 or a Nikon LU Plan objective lens with a 10 times magnification and a numerical aperture of 0.30 with a WD17.3 lens enabling a magnification of 200 and 100 times, respectively, were used for the enlargement. A camera (EOS 50D) from Canon (Tokio, Japan) was mounted on the microscope with an adapter from LMscope (Graz, Austria).

3.2.2.1.8.2 Single crystal X-ray analysis

Single Crystal X-Ray Analysis was conducted by the central analytical department at the University of Regensburg. A suitable crystal with was mounted on a MITIGEN holder with inert oil on a XtaLAB Synergy R, DW system, HyPix-Arc 150 diffractometer. The temperature during the data collection was 123.01(10) K. The structure was solved with the ShelXT 2018/2 (Sheldrick, 2018) solution program using dual methods and Olex2 1.5-alpha as the graphical interface.[216] The model was refined with ShelXL 2018/3 (Sheldrick, 2015) using full matrix least squares minimization on $\boldsymbol{F^2}$.[216–221] The radiation type was Cu K_α. Details on the crystal and fitting parameters are given in section 7.2 in the Appendix.

3.2.2.1.9 Cocrystallization attempts for riboflavin and sodium polyphenolates

Sodium salt solutions were prepared via neutralization of the corresponding polyphenolic acid with 1.0 or 6.0 $mol \cdot L^{-1}$ sodium hydroxide solution and stirring for 30 min at 450 rpm. The samples were saturated with RF via addition of an excessive amount of RF followed by stirring at 450 rpm in the dark for 1 h and filtration through 0.45 µm PTFE syringe filters.

3.2.2.1.9.1 Liquid diffusion method via usage of an antisolvent

Concentrated sodium polyphenolate/RF or polyphenolic acid/RF solutions were carefully overlayed with a precipitant solvent, see Figure 14. At the turbid phase border of the two

solvents, cocrystals should be formed due to the slow diffusion of the antisolvent into the RF solution.[222]

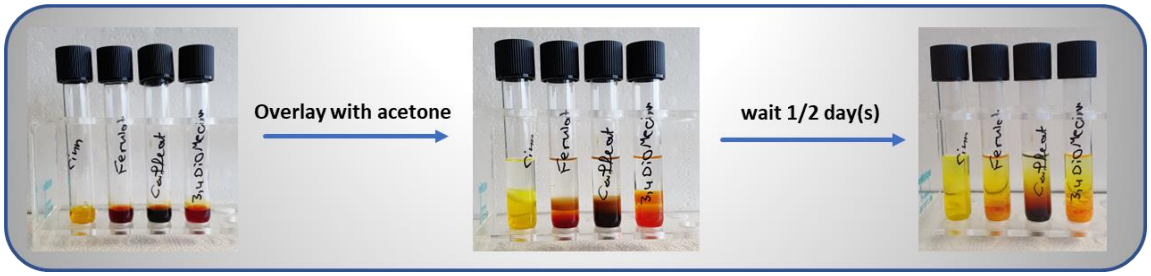

Figure 14: Experimental procedure for crystallization via the liquid diffusion method with an antisolvent. From left to right: NaCinn, sodium ferulate, sodium caffeate, Na-3,4-DiOMe-Cinn.

Preparation of RF/sodium polyphenolate solutions:

0.5 mL stock solutions (0.50 M NaCinn, 0.37 M sodium ferulate, 0.4 M sodium caffeate, 1.5 M Na-3,4-DiOMe-Cinn) were saturated with RF. 0.5 mL of the stock solutions were overlayed with 2.5 mL acetone, ethanol or acetonitrile.

Crystallization of RF with polyphenolic acids from Dimethyl sulfoxide:

Dimethyl sulfoxide (DMSO) was saturated with 3,4-dimethoxycinnamic acid, ferulic acid, vanillic acid or cinnamic acid via stirring at 450 rpm at 23 °C overnight. The turbid samples were then saturated with RF. After filtration, 0.2 mL of the DMSO stock solution was overlayed with 2.5 mL of water.

Crystallization of RF with polyphenolic acids from water/acetonitrile (50/50 (w/w)):

A water/acetonitrile (50/50 (w/w)) solution was saturated with vanillic, ferulic, cinnamic or 3,4-dimethoxycinnamic acid and RF via stirring at 450 rpm for 4 h at 23 °C After filtration through 0.45 µm PTFE syringe filters, 0.2 mL of the samples was overlayed with 2 mL of acetonitrile.

3.2.2.1.9.2 Slow cooling of a saturated solution

3 mL of a solvent (water, ethanol, water/ethanol (50/50 (w/w)), methanol, acetonitrile or acetone) were saturated with RF and NaCinn or sodium vanillate under stirring at 450 rpm at 45 °C in the dark for 1 h. After hot filtration with 0.45 µm PTFE filters, the clear solutions were let to cool down to 4 °C slowly within one week in a water bath in the dark.

3.2.2.1.9.3 Slow evaporation of the solvent from saturated solutions

Evaporation of water: 5 mL of aqueous solutions (0.50 M NaCinn, 0.37 M sodium ferulate, 1.5 M Na-3,4-DiOMe-Cinn) were saturated with RF. The water was slowly removed via rotary evaporation at 50 °C. The clear solutions were cooled slowly in a warm water bath to 20 °C.

Evaporation of ethanol: 5 mL of a binary water/ethanol (50/50 (w/w)) solution was saturated with sodium ferulate and RF at 45 °C within 1 h. Ethanol was partially removed via slow rotary evaporation at 50 °C, so that no precipitation occurred. Then the sample was cooled slowly to 20 °C in a warm water bath so that crystals should be formed slowly.

3.2.2.1.9.4 Crystallization via slow neutralization

0.37 mol·kg^{-1} sodium ferulate solution saturated with RF was put in a 50 mL round bottom flask, which was connected with another 50 mL round bottom flask comprising concentrated hydrochloric acid via a glass tube, see Figure 15. Concentrated hydrochloric acid was then slowly evaporated into the flask comprising sodium ferulate and RF by keeping 23 °C for 1 day, 30 °C for 2 days and 45 °C for 1 day.

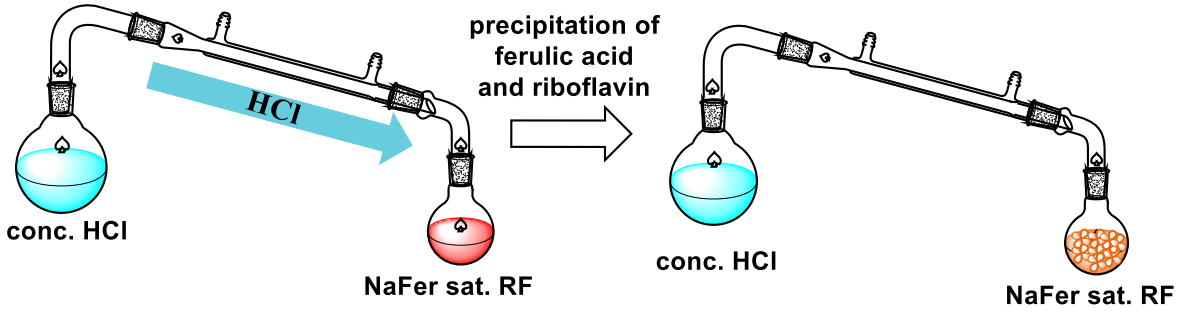

Figure 15: Experimental setup for the precipitation of sodium ferulate/riboflavin cocrystals.

3.2.2.1.10 Surface tension measurements in presence of riboflavin

The stock solutions comprising NaCinn, NaBenz, Na-4-OH-3-OMe-Cinn, Na-2-OH-Benz from section 3.2.1.2 were saturated with RF via ultrasonication for 2 min (Bransonic 220, 120 W, frequency: 50 kc) and stirring at 450 rpm at 23 °C in the dark for 1 h. The samples were then filtered through 0.2 µm PTFE syringe filters. Surface tension measurements were conducted as reported in section 3.2.1.2. The samples were prepared in duplicate.

3.2.2.1.11 DLS measurements in absence and presence of riboflavin

An aqueous 0.37 mol·kg^{-1} solution of Na-4-OH-3-OMe-Cinn was prepared via neutralization of the corresponding acid with 1 mol·L^{-1} self-made sodium hydroxide solution and addition of the residual amount of water. Aqueous solutions of NaBenz and Na-2-OH-Benz at a concentration of 1 mol·kg^{-1} were prepared via dissolution of the salts in the required amount of water. After 30 min all salts were dissolved. These samples were measured in triplicate.

Then the same samples were saturated with RF via addition of an excess of RF and subsequent ultrasonication for 2 min (Bransonic 220, 120 W, frequency: 50 kc) followed by stirring at 450 rpm in the dark for 1 h. Additionally, a 1 mol·kg^{-1} Na-3,4-DiOMe-Cinn sample was prepared via neutralization of the corresponding acid with 1 mol·L^{-1} self-made sodium hydroxide solution and saturation with RF. To have a reference, pure water was saturated with RF. The saturated RF samples were filtered through 0.45 µm PTFE syringe filters. For the DLS measurement setup see section 3.6.

3.2.2.1.12 Small angle X-ray scattering measurements

Aqueous sodium polyphenolate solutions (0.30 mol kg^{-1}) were prepared without and saturated with RF (NaCinn, Na-3,4-DiOH-Cinn, Na-4-OH-3-OMe-Cinn and Na-2-OH-Benz). To see, whether RF induced structuring in water, one sample of water saturated with RF was prepared, too. Additionally, the small angle X-ray scattering (SAXS) spectrum of pure Millipore water was recorded to subtract the background induced via the solvent.

All SAXS measurements were carried out by Philipp Schmid from the inorganic department at the University of Regensburg and Dr. Pierre Bauduin at the Institute de Chimie Séparative de Marcoule (ICSM) in Marcoule in France. The measurements were performed at 22 °C. The samples were filled in 2 mm quartz glass capillaries. SAXS measurements were conducted on a bench built by XENOCS. The radiation was Mo-Kα1 (λ(Mo) = 0.071 nm). The scattering was measured using a large online scanner detector with a diameter of 345 mm from MAR Research using an off-center detection, the q-range (0.2 to 40 nm^{-1}) was large. A 12:∝ multilayer Xenocs mirror (for Mo radiation) coupled to two sets of scatter less FORVIS slits served for the collimation and led to a 0.8 mm × 0.8 mm X-ray beam at the sample position. The measurement of the empty cell and subtraction of the detector noise served for background corrections. The intensity was normalized by means of a high-density polyethylene film. A sealed capillary with silver behenate was used as the scattering vector calibration standard. Experimental resolution was $\Delta q/q = 0.05$. Via the software FIT2D the data was pre-evaluated.

3.2.2.1.13 Nuclear magnetic resonance measurements

3.2.2.1.13.1 Riboflavin and aromatic sodium salts

All NMR experiments were conducted in deuterated dimethyl sulfoxide (DMSO-d_6). Samples consisting of both RF and NaBenz, Na-3-OH-Benz, Na-4-OH-Benz, Na-4-OH-3-OMe-Benz or NaCinn were saturated with RF leading to the ratio reported in Table 6. For saturation of DMSO-d_6 with RF and the aromatic sodium salts, an excess of the compounds was added and the samples were stirred at 450 rpm in 1 g DMSO-d_6 for 1 h. Only in the case of NaCinn in presence of RF at the molar ratio 1, the sample was diluted with DMSO-d_6 after filtration through 0.45 µm PTFE syringe filters and then saturated with NaCinn again. All samples were filtered through 0.45 µm PTFE syringe filters.

To see if the chemical shift of RF and of the additives depends on the additive to RF ratio, four distinct molar Na-2-OH-Benz/RF ratios were prepared (Ratio 2: DMSO-d_6: 1.993 g, Na-2-OH-Benz: 0.009 g, RF: 0.010 g; Ratio 5: DMSO-d_6: 2.017 g, Na-2-OH-Benz: 0.024 g, RF: 0.011 g; Ratio 10: DMSO-d_6: 1.966 g, Na-2-OH-Benz: 0.113 g, RF: 0.026 g; Ratio 50: DMSO-d_6: 3.012 g, Na-2-OH-Benz: 0.243 g, RF: 0.011 g). The samples were stirred at 450 rpm until a clear solution was obtained within 20 min.

Reference samples of all sodium salts were prepared by saturation of DMSO-d_6 with the respective aromatic sodium salt and filtration through 0.45 µm PTFE syringe filters.
The analyzed samples with the contained compounds and the resulting molar ratio of the sodium salts to RF are listed in Table 6. ^{1}H-NMR, ^{13}C-NMR, COSY, NOESY, HSQC and HMBC spectra of these sample were recorded. For the measurement setup see section 3.5.

Table 6: Preparation of the samples for NMR analysis and corresponding molar ratio of the sodium salt to riboflavin

Sample	Molar ratio (additive/RF)	Reference
NaBenz/RF	2	NaBenz
Na-2-OH-Benz/RF	2	Na-2-OH-Benz
Na-2-OH-Benz/RF	5	Na-2-OH-Benz
Na-2-OH-Benz/RF	10	Na-2-OH-Benz
Na-2-OH-Benz/RF	50	Na-2-OH-Benz
Na-3-OH-Benz/RF	11	Na-3-OH-Benz
Na-4-OH-Benz/RF	2	Na-4-OH-Benz
Na-4-OH-3-OMe-Benz/RF	1	Na-4-OH-3-OMe-Benz
NaCinn/RF	0.4	NaCinn
NaCinn/RF	1	NaCinn

Additionally, an aqueous 3 mol·kg^{-1} Na-3,4-DiOMe-Cinn solution, prepared via neutralization of the corresponding acid with 6 mol·L^{-1} sodium hydroxide solution, was saturated with RF via ultrasonication for 2 min, stirring at 450 rpm in the dark for 1 h and subsequent filtration through 0.45 µm PTFE filters. A NOESY spectrum of this sample was recorded as explained in section 3.5.

3.2.2.1.13.2 NMR measurements of riboflavin phosphate sodium salt

To obtain maximum resolution, deuterium oxide was saturated with sodium ferulate and/or RF-PO_4 via stirring at 450 rpm at 23 °C in the dark for 1 h. The samples were then filtered through 0.45 µm PTFE syringe filters. ^{1}H-NMR, NOESY, ^{13}C-NMR, HMBC and HSQC measurements were conducted. For ^{13}C-NMR measurements, an insert with DMSO-d_6 was inserted to have a reference peak. For the measurement setup see section 3.5.

3.2.2.1.14 Photostability of riboflavin in aqueous sodium polyphenolate solutions

3.2.2.1.14.1 Riboflavin in diluted aqueous sodium polyphenolate solutions

The photodegradation of RF was monitored for aqueous 3 g samples consisting of a fixed initial amount of RF (48 mg·kg^{-1}) in presence of Na-4-OH-3-OMe-Cinn, Na-3,4-DiOH-Cinn, Na-3,4-DiOMe-Cinn, Na-4-OH-3,5-DiOMe-Benz, Na-4-OH-3-OMe-Benz, Na-2-OH-Benz, NaCinn, NaBenz, NaSCN and NaH_2PO_4 as well as in presence of choline cinnamate (choline Cinn). In the case of NaCinn, Na-3,4-DiOH-Cinn, Na-4-OH-3-OMe-Cinn and Na-4-OH-3-OMe-Benz, the molar additive/RF ratios 6, 25 and 50 were analyzed. In the case of Na-3,4-DiOMe-Cinn, Na-

4-OH-3,5-DiOMe-Benz, and choline Cinn, the ratios 50 and 25 were analyzed. In the case of NaBenz, Na-2-OH-Benz, NaSCN and NaH_2PO_4 only the ratio 50 was analyzed.

Samples comprising Na-4-OH-3-OMe-Benz, Na-2-OH-Benz, NaBenz, NaSCN and NaH_2PO_4 were prepared via direct dissolution of the salt in water. Samples comprising Na-4-OH-3-OMe-Cinn, Na-3,4-DiOH-Cinn, NaCinn, Na-4-OH-3,5-DiOMe-Benz and Na-3,4-DiOMe-Cinn were prepared via neutralization of the corresponding polyphenolic acid with self-made 1 $mol \cdot L^{-1}$ sodium hydroxide solution in 100 mL water in a 0.5 L volumetric flask via stirring at 450 rpm for 20 min. The sample comprising choline cinnamate was prepared via neutralization of cinnamic acid with an aqueous 46 wt.% choline hydroxide solution. Then, 0.48 mg RF were added to all samples, the flasks were filled up with water and stirred in the dark at 450 rpm overnight to obtain a clear stock solution. The final samples were obtained via 1:2 dilution of this stock solution on the balance. A reference sample consisting of 48 $mg \cdot kg^{-1}$ RF in pure water was prepared analogously.

Then several 30 mL snap glasses were filled with 3 g of the sample and closed, so that one snap glass served for an analysis after a certain time.

The samples were illuminated with an LED-plant lamp (400-800 nm; 30 Watt-150 Watt corresponding to a halogen lamp), see Figure 16. After 1 or 2 h, the sample was filtered with 0.2 µm PTFE filters into vials without prior dilution. RF and the aromatic additives were quantified via HPLC analysis, see section 3.7. Samples comprising Na-4-OH-3-OMe-Cinn and NaCinn at ratios 25 and 50 and the reference sample were prepared in duplicate. The residual samples were prepared once.

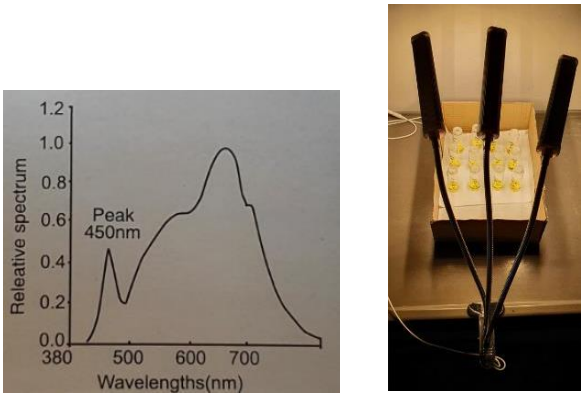

Figure 16: Left: UV-Vis-spectrum of the LED-plant lamp (400-800 nm; 30 Watt - 150 Watt corresponding to a halogen lamp) used for the photostability experiments; right: Experimental setup for photostability experiments, which was covered by a carton box to prevent exterior light sources.

3.2.2.1.14.2 Color stability of riboflavin in concentrated aqueous sodium polyphenolate solutions

Aqueous solutions comprising 3.00 $mol \cdot kg^{-1}$ NaBenz, 1.00 $mol \cdot kg^{-1}$ Na-4-OH-3-OMe-Benz, 0.58 $mol \cdot kg^{-1}$ NaCinn, 0.37 $mol \cdot kg^{-1}$ Na-4-OH-3-OMe-Cinn or 2.10 $mol \cdot kg^{-1}$ Na-3,4-DiOMe-Cinn were prepared via dissolution of the required amount of salt (NaBenz, Na-4-OH-3-OMe-Benz) or via neutralization of the acid (NaCinn, Na-4-OH-3-OMe-Cinn, Na-3,4-DiOMe-Cinn)

with self-made 1 mol·L^{-1} or 6 mol·L^{-1} sodium hydroxide solution and addition of the residual amount of water. 6.5 g of each solution were prepared in triplicate. After saturation RF via ultrasonication for 2 min (Bransonic 220, 120 W, frequency: 50 kc) and subsequent stirring at 450 rpm in the dark for 1 h, the samples were filtered through 0.45 µm PTFE syringe filters.
The samples were separated in two 20 mL snap glasses, each comprising 3 g of the concentrated solutions, so that one of the two samples was stored in a dark box, while the other one was stored next to the window exposed to the sun from April to August. Like this identical samples were compared.
In certain time intervals, the samples were analyzed with a Lambda18 spectrophotometer (Überlingen, Germany) using 3 mL quartz cuvettes (10 mm with a transmission from 200-2500 nm) from Hellma (Müllheim, Germany). Millipore water served as reference. For the quantification of RF see section 3.2.2.4. The samples were prepared in triplicate.

3.2.2.1.14.3 Photostability of riboflavin in concentrated aqueous sodium polyphenolate solutions

The photostability RF in an aqueous 0.37 mol·kg^{-1} Na-4-OH-3-OMe-Cinn, 0.60 mol·kg^{-1} Na-3,4-DiOH-Cinn, 1.05 mol·kg^{-1} Na-4-OH-3-OMe-Benz and in an aqueous 0.59 mol·kg^{-1} NaCinn solution was analyzed. The sodium salt solutions were prepared via neutralization of the corresponding polyphenolic acids with self-made 1 mol·L^{-1} sodium hydroxide solution and addition of the residual amount of water or via direct dissolution of the salt in water and stirring at 450 rpm for 20 min. For saturation with RF, an excess of RF was added. The samples were then ultrasonicated for 2 min (Bransonic 220, 120 W, frequency: 50 kc) and stirred at 450 rpm in the dark for 1 h. After filtration with 0.45 µm PTFE syringe filters into 20 mL snap glasses, the samples were closed and illuminated with an LED-plant lamp (400-800 nm; 30 Watt-150 Watt corresponding to a halogen lamp) for 24 h, see Figure 16. As RF was stable, the samples were then stored next to the window exposed to the sun from May until October.
After dilution of 1-2 drops of the samples with water on the balance, RF and the aromatic additives were quantified via HPLC analysis, see section 3.7. The samples were then closed again and stored next to the window. The measurements were conducted only once.

3.2.2.1.14.4 Preparation of samples for LC-MS analysis

A sample of pure water saturated with RF was illuminated with the LED plant lamp from Figure 16 for 5 h analyzed.
Additionally, a sample comprising Na-4-OH-3-OMe-Cinn and another one comprising NaCinn with the molar additive/RF ratio 25 after 15 h of illumination from section 3.2.2.1.14.1 were analyzed.

To understand the browning of sodium caffeate samples, a solution of 0.40 mol·kg^{-1} Na-3,4-DiOH-Cinn in water was prepared via equimolar neutralization of caffeic acid with 1 mol·L^{-1} sodium hydroxide solution and let stay open for 4 h while stirring at 450 rpm in the dark.
The analysis was conducted at the central analytical department at the University of Regensburg with the Liquid Chromatography-Mass Spectrometry (LC-MS) technique with the Q-TOF 6540 UHD from Agilent.

3.2.2.1.14.5 Oxygen content measurements

10 g samples comprising Na-4-OH-3-OMe-Cinn, Na-3,4-DiOH-Cinn, Na-4-OH-3-OMe-Benz, Na-3,4,5-TriOH-Benz, Na-2-OH-Benz, Na-4-OH-Benz, Na-3,4-DiOH-Benz, Na-2,3-DiOH-Benz, and Na-3,5-DiOH-Benz were prepared. Therefore, the corresponding acid was neutralized with self-made 1 mol·L^{-1} sodium hydroxide solution or the salt was directly dissolved in water.
Further, samples comprising RF were prepared. Therefore, first, 10 g of aqueous Na-2-OH-Benz, Na-3,5-DiOH-Benz, Na-3,4-DiOH-Benz, Na-2,3-DiOH-Benz, Na-3,4-DiOH-Cinn and Na-3,4,5-TriOH-Benz solutions were prepared via neutralization with self-made 1 mol·L^{-1} sodium hydroxide solution or the salt was direct dissolution in water. Then, an excess of RF was added and the sample were ultrasonicated for 2 min (Bransonic 220, 120 W, frequency: 50 kc) followed by stirring at 450 rpm in the dark for 1 h. The samples were filtered with 0.45 µm PTFE syringe filters into 20 mL snap glasses.
Additionally, three samples comprising 90 mg·kg^{-1} RF in pure Millipore water were prepared via dissolution of 45 mg RF in 0.5 L water in a volumetric flask via ultrasonication for 2 min (Bransonic 220, 120 W, frequency: 50 kc) followed by stirring at 450 rpm in the dark for 1 h until entire dissolution of RF.

Measurement: To reach an oxygen-equilibrium, all samples including the ones comprising pure water were stirred at 250 rpm in open snap glasses for 2 h in order to prevent oxygen bubbles due to too fast agitation. After 1 h without agitation to reach equilibrium, the oxygen content was measured within 5 min, when a constant value was obtained. The oxygen content was determined with the Clark electrode „AQUA-DO_2 with an oxygen TPS ED1 sensor (version number: V1.0 T3520). For zero-point calibration a sodium sulfite solution (2 g on 100 mL of water) was used, while air was set as 100 %. The oxygen saturation could be measured from 0-250 % with a resolution of 0.1 % and an accuracy of ±0.3 %.

Before measuring the samples, the oxygen content of pure Millipore water was measured as the oxygen content depends on the partial oxygen pressure, which changed every day. All obtained values were divided by the oxygen content of Millipore water to obtain a relative value. All samples were prepared in triplicate.

3.2.2.1.15 Compatibility of riboflavin/sodium polyphenolate solutions with a sports drink model

Carboxymethylcellulose was dissolved in water under stirring by boiling for 5 min. All salts were dissolved in water (51 g drinking and 430 g deionized water). The hot carboxymethylcellulose solution was united with the salt solution and the residual amount of drinking water was added, see Table 7.

Table 7: Preparation of the sports drink model of BASF, pH 3.5.

Substance	Mass (g)
Carboxymethylcellulose sodium salts high viscosity	1.000
Boiling drinking water	300.000
Solubilization within 5 min under stirring	
Drinking water	51.000
Deionized water	430.000
Calcium phosphate dibasic	0.216
Potassium dihydrogen phosphate	0.350
Sodium citrate tribasic hydrate	0.486
Sodium chloride	0.800
Sodium benzoate	0.150
Potassium sorbate	0.200
Citric acid	2.500
Sugar	61.000
Ascorbic acid	0.150
Drinking water (for rinsing)	152.123
Total:	999.75

Aqueous RF/sodium polyphenolate concentrates were prepared by saturation of the respective aqueous polyphenolate solution with RF via ultrasonication for 2 min followed by stirring at 23 °C in the dark for 1 h. All samples were filtered with 0.45 µm PTFE filters. The concentration of the solutions is given in Table 17 in section 4.1.2.1.9. After dilution to a RF concentration of 50 $mg \cdot kg^{-1}$ with the sports drink, one part of the samples was stored in closed snap glasses in the dark in order to prevent kinetic effects of precipitation. The other part was stored at ambient light next to the window to have an idea of the coloration loss in the sports drink with illumination. The samples were checked every day by the eye if there is a change in color or if precipitation is formed. To ensure comparability, all samples were prepared on the same day.

3.2.2.1.16 Solubility of calcium lactate

The solubility of calcium lactate in pure water was determined via successive addition of the salt until it was no longer solubilized. Then the solubility of calcium lactate in a 0.37 $mol \cdot kg^{-1}$ sodium ferulate solution was determined via stepwise addition of pure calcium lactate to the aqueous sodium ferulate solution until the solubility limit of the calcium salt was reached. If particle were visible by the eye, the solubility limit was supposed to be reached.

3.2.2.2 Lumichrome

To determine the water-solubility of LC, 3 g of water were saturated with LC via ultrasonication for 2 min, (Bransonic 220, 120 W, frequency: 50 kc) followed by stirring at 450 rpm for 1 h. The samples were filtered with 0.45 µm PTFE syringe filters.

All samples comprising 0.2 mol·kg^{-1} of a solubilizer (NaCinn, NaButyrate, NaValerate and Na-2,4-Pentadienoate, Na-4-OH-3-OMe-Cinn, Na-4-OH-3-OMe-Benz, Na-3,4-DiOMe-Cinn, NaBenz, NaCHC) were prepared either via dissolution of the salt in water or via neutralization of the corresponding acid with self-made 1 mol·L^{-1} sodium hydroxide solution and addition of the residual amount of water followed by stirring at 450 rpm for 20 min. Samples comprising 0.37 mol·kg^{-1} Na-4-OH-3-OMe-Benz, Na-4-OH-3-OMe-Cinn and Na-3,4-DiOMe-Cinn were prepared analogously via neutralization. For a saturation, LC was added in excess and the samples were ultrasonicated for 2 min (Bransonic 220,120 W, frequency: 50 kc). After stirring at 450 rpm in the dark for 1 h, the saturated samples were filtered with 0.45 µm PTFE syringe filters. All samples were prepared in triplicate. For the quantification of LC, see section 3.2.2.4.

3.2.2.3 Riboflavin-5'-monophosphate sodium salt

The water-solubility of riboflavin 5'-monophosphate sodium salt in water was determined in triplicate. 1 g of water were saturated with RF-PO_4 via ultrasonication for 2 min (Bransonic 220, 120 W, frequency: 50 kc) and subsequent stirring at 450 rpm in the dark for 3 h. The samples were filtered with 0.45 µm cellulose acetate and PTFE syringe filters.

Additionally, 0.37 mol·kg^{-1} sodium polyphenolate solutions (Na-4-OH-3-OMe-Cinn, Na-4-OH-3-OMe-Benz and Na-3,4-DiOMe-Cinn) were prepared via neutralization of the corresponding acid with self-made 1 mol·L^{-1} sodium hydroxide solution and addition of the residual amount of water followed by stirring at 450 rpm for 20 min. In the case of Na-3,4-DiOMe-Cinn, the sample was stirred, to achieve only a neutralization, as the compound was not soluble in water. After addition of an excess of RF-PO_4, the samples were ultrasonicated for 2 min (Bransonic 220, 120 W, frequency: 50 kc) and stirred at 450 rpm in the dark for 3 h. The long stirring process was necessary, to reach an equilibrium. The samples were filtered through 0.45 µm cellulose acetate and PTFE syringe filters. All samples were prepared in triplicate.

For the quantification and calibration of RF-PO_4, see section 3.2.2.4.

3.2.2.4 Quantification of riboflavin, lumichrome and riboflavin 5'-monophosphate via UV-Vis-absorbance measurements

The samples were diluted with Millipore water on the balance to recalculate the dilution factor with equation 21 from section 3.4.The absorption of RF, LC and RF-PO_4 was recorded at 449 nm, 386 nm and 445 nm, respectively, with a Lambda18 spectrophotometer (Überlingen, Germany). The diluted samples were filled in 3 mL quartz cuvettes (10 mm with a transmission from 200-2500 nm) from Hellma (Müllheim, Germany) with Millipore water as reference. Using

the calibration curves from section 7.1 in the Appendix and equation 22 from section 3.4, the concentration of RF and LC was calculated.

The purchased RF-PO_4 consisted had a purity of 73-79 wt.%. To prevent overestimations of RF-PO_4's water-solubility, its purity was rounded down to 70 %. The residual 30 % were supposed to have no contribution to the absorbance at 445 nm. After multiplication with the factor 0.7 the experimentally determined solubility of sodium RF-PO_4 was 49 ± 4 g·kg^{-1} and matched roughly with the solubility of 30-39 g·L^{-1} at 25 °C provided by literature.[1,223] Hence, the concentration of RF-PO_4 was determined with equation 23 by multiplication with the factor 0.7, see section 3.4.

The calibration curves were prepared in triplicate using the Lambda18 spectrophotometer (Überlingen, Germany).

Calibration curve for riboflavin:

In a 250 mL volumetric flask, 0.02 g of RF were dissolved in Millipore water to obtain a stock solution. This stock solution (≈ 0.2 mmol·kg^{-1}) was diluted with water to obtain concentrations of 0.06, 0.05, 0.04, 0.03, 0.02 and 0.01 mmol·kg^{-1} of RF. The calibration curves are displayed in Table A 1 in the Appendix.

Calibration curve for lumichrome:

Due to its low solubility in water, sodium ferulate was used as solubilizers for the preparation of the LC stock solutions. The amount of ferulate in the samples was considered for the calculation of LC's concentration. An aqueous sodium ferulate solution (20 g of a 0.37 mol·kg^{-1}) was prepared via neutralization of ferulic acid with an equimolar amount of 1 mol·L^{-1} sodium hydroxide solution and addition of the residual water via stirring at 450 rpm in a closed vessel for 20 min. After dissolution of 4 mg LC via stirring at 800 rpm at 23 °C for 20 min, this stock solution was diluted with water on the balance to obtain LC concentrations of 10, 20, 40, 50 and 60 µmol·kg^{-1}. The calibration curves are given Table A 2 in the Appendix.

Calibration curve for riboflavin 5'-monophosphate sodium salt:

A stock solution of 20.9 mmol·kg^{-1} RF-PO_4 was prepared via dissolution of ca. 0.02 g of RF-PO_4 in 2 g of water. This stock solution was diluted with water to obtain 80, 60, 50, 40, 30, 20, and 10 µmol·kg^{-1} RF-PO_4 solutions. The calibration curves are given in Table A 3 in the Appendix.

3.2.2.5 DLS measurements in absence and presence of lumichrome and riboflavin phosphate

Aqueous solutions of Na-4-OH-3-OMe-Cinn and Na-3,4-DiOMe-Cinn at 0.37 mol·kg^{-1} were prepared via neutralization of the corresponding acid with 1 mol·L^{-1} self-made sodium hydroxide solution and addition of the residual amount of water. LC and RF-PO_4 were added in excess. Then, the samples were ultrasonicated for 2 min (Bransonic 220, 120 W, frequency: 50 kc) and stirred at 450 rpm in the dark for 1 h. Additionally, pure Millipore water was

saturated with only LC or only RF-PO_4, to know the structuring of the pure compounds. All saturated samples were filtered with 0.2 µm PTFE syringe filters. The samples comprising RF-PO_4 were additionally filtered through 0.2 µm cellulose acetate filters. The samples were prepared in triplicate. For the DLS measurement setup see section 3.6.

3.2.2.6 Calculation of the change of the molar Gibbs energy of solubilization

The change of the molar Gibbs energy of solubilization was calculated from the water-solubility of solute in pure water and in aqueous sodium carboxylate solutions with equation 16-18.

$$\Delta\Delta G = R \cdot T \cdot \ln\left(\frac{c_W(RF)}{c_W(X)}\right) \quad (16)$$

ΔΔG = *change of the molar Gibbs energy of solubilization of riboflavin upon substitution of lumichrome with a ribityl chain and substitution of ribose with an isoalloxazine ring*
R* =** *ideal gas constant in J mol^{-1} K^{-1},* ***T* =** *296.15 K,* ***c_W(RF) = *solubility of riboflavin in water*
c_W(X) = *solubility of lumichrome or ribose in water*

$$\Delta\Delta G^*(X) = R \cdot T \cdot \ln\left(\frac{c_{NaPP}(X)}{c_{water}(X)}\right) \quad (17)$$

$$\Delta\Delta G^{**} = \Delta\Delta G^*(RF) - \Delta\Delta G^*(LC) \quad (18)$$

ΔΔG*(X) *= change of the molar Gibbs energy of solubilization of RF or LC due to the presence of sodium polyphenolates and related compounds*
c_{NaPP}(X) *= water-solubility of RF or LC in presence of 0.2 mol·kg^{-1} sodium polyphenolates and related compounds*
c_{water}(X) *= solubility of RF or LC in pure water*
ΔΔG** *= difference of the change of ΔΔG*(X) of LC and RF in presence of sodium polyphenolates and related compounds*

3.2.2.7 Vitamin K3

3.2.2.7.1 Preparation of aqueous aromatic sodium carboxylate solutions analyzed with UV-Vis-spectroscopy

3 g of water were saturated with vitamin K3, ultrasonicated for 2 min (Bransonic 220, 120 W, frequency: 50 kc) and stirred at 450 rpm at 23 °C in the dark for 1 h.
Additionally, aqueous 3 g samples comprising 0.37 mol·kg^{-1} and 0.5 mol·kg^{-1} NaCHC were prepared via neutralization of the corresponding acid with 1 mol·L^{-1} self-made sodium hydroxide solution and addition of the residual amount of water. After saturation with vitamin K3, the samples were also ultrasonicated for 2 min (Bransonic 220, 120 W, frequency: 50 kc) and stirred at 450 rpm at 23 °C in the dark for 1 h. All saturated samples were filtered through

0.45 µm PTFE syringe filters. The samples were diluted with Millipore water on the balance to recalculate the dilution factor with equation 21 from section 3.4. The solubility of vitamin K3 was determined as described in section 3.2.2.7.5.1. All samples were prepared in triplicates.

3.2.2.7.2 Preparation of aqueous sodium carboxylate solutions analyzed with NMR spectroscopy

1.5 g to 3 g samples of Na-4-OH-3-OMe-Cinn, Na-3,4-DiOMe-Cinn, Na-2,4-Pentadienoate, NaCinn, NaValerate and NaButyrate ranging from 0.1 mol·kg^{-1} to 0.58 mol·kg^{-1} were prepared by neutralization of the corresponding acid with 1 mol·L^{-1} self-made sodium hydroxide solution and addition of the residual amount of water. In the case of Na-2,4-Pentadienoate, a 0.05 mol·kg^{-1} sample was prepared additionally. Moreover, samples comprising 1.0, 2.0 and 3.0 mol·kg^{-1} Na-3,4-DiOMe-Cinn were prepared. Samples comprising 0.37-1.0 mol·kg^{-1} NaBenz were also prepared via direct dissolution of the salt in water.

Regardless whether the sodium salt was completely dissolved, after stirring for 20 min, all samples were saturated with vitamin K3 via ultrasonication for 2 min (Bransonic 220, 120 W, frequency: 50 kc) followed by stirring at 450 rpm in the dark at 23 °C for 1 h. The samples were filtered through 0.45 µm PTFE syringe filters. Then, 0.8 mL of the sample were filled into an NMR tube. Via ^{1}H-NMR measurements, the solubility of vitamin K3 was determined, see section 3.2.2.7.5.2.

In the case of the 3 mol·kg^{-1} Na-3,4-DiOMe-Cinn samples, Nuclear Overhauser Effect Spectroscopy was performed, too, see section 3.2.2.7.5.2 for the preparation. All samples were prepared in triplicates.

3.2.2.7.3 Shift of the absorption wavelength

The aqueous 0.37 mol·kg^{-1} sodium ferulate sample saturated with vitamin K3 from section 3.2.2.7.2 was successively diluted with water on the balance, so that all resulting samples had a constant molar ferulate to vitamin K3 ratio of 19.4. Like this 7 mmol·kg^{-1}, 17 mmol·kg^{-1}, 56.5 mmol·kg^{-1}, 87.5 mmol·kg^{-1} and a 190.9 mmol·kg^{-1} sodium ferulate solutions were obtained. After each dilution a UV-Vis-spectrum from 300-800 nm was recorded with a Lambda18 spectrophotometer (Überlingen, Germany) using 3 mL quartz cuvettes (10 mm with a transmission from 200-2500 nm) from Hellma (Müllheim, Germany) against Millipore water as reference sample. Additionally, the UV-Vis-spectrum of a 1:3 diluted sample of vitamin K3 (saturation) in water was recorded. Further, a pure aqueous sodium ferulate was prepared at 33.8 mmol·kg^{-1} via neutralization of the required amount of ferulic acid with 1 mol·L^{-1} self-made sodium hydroxide solution.

3.2.2.7.4 Photostability of vitamin K3 in presence of NaBenz, Na-4-OH-3-OMe-Cinn and Na-3,4-DiOMe-Cinn

Aqueous samples comprising 0.37 mol·kg^{-1} of NaBenz, sodium ferulate and Na-3,4-DiOMe-Cinn were prepared via dissolution of NaBenz in water and neutralization of the two polyphenolic acids with 1 mol·L^{-1} self-made sodium hydroxide solution. Water saturated with vitamin K3 served as reference. 13 g of each sample were prepared, so that the sample could be divided into two 6 g samples after the filtering process. The samples were saturated with vitamin K3 via ultrasonication for 2 min (Bransonic 220, 120 W, frequency: 50 kc) and stirred at 450 rpm at 23 °C in the dark for 1 h. All saturated samples were filtered through 0.45 µm PTFE syringe filters. 6 g of each sample were stored in the dark and 6 g of the sample were stored next to the window in a 20 mL snap vessel. The experiments were performed from May to June, so that the samples next to the window were exposed to the sun. The samples were prepared in triplicate.

In certain time intervals, 1 g of each sample were filtered with 0.45 µm PTFE syringe filters to remove vitamin K3's water-insoluble degradation product and precipitation due to a potential degradation. The content of vitamin K3 in pure water and in presence of NaBenz was observed with UV-Vis-spectroscopy, see section 3.2.2.7.5.1. Therefore, the sample was diluted with water on the balance. The samples comprising Na-4-OH-3-OMe-Cinn and Na-3,4-DiOMe-Cinn were analyzed via NMR spectroscopy without prior dilution, see section 3.2.2.7.5.2. Therefore, 0.8 mL of the sample were filled into an NMR tube.

3.2.2.7.5 Quantification of vitamin K3

3.2.2.7.5.1 Quantification of vitamin K3 via UV-VIS-spectroscopy

The absorption of vitamin K3 was recorded at 336 nm with a Lambda18 spectrophotometer (Überlingen, Germany) using 3 mL quartz cuvettes (10 mm with a transmission from 200-2500 nm) from Hellma (Müllheim, Germany). Millipore water served as reference sample. With the calibration curves and equations 21 and 22 from section 3.4, the concentration of vitamin K3 was calculated.

All calibration curves were prepared in triplicate. For the calibration, 0.05 g of vitamin K3 were dissolved in Millipore water in a 1 L volumetric flask by ultrasonication for 5 min (Bransonic 220, 120 W, frequency: 50 kc) and stirring at 450 rpm at 23 °C in the dark for 1 h. This stock solution (0.3 mmol·kg^{-1}) was diluted with water to have concentrations of 0.3, 0.25, 0.20, 0.15, 0.10 and 0.05 mmol·kg^{-1} of vitamin K3. The calibration curves are reported in Table A 4 in the Appendix.

3.2.2.7.5.2 Quantification of vitamin K3 via NMR spectroscopy

All NMR experiments were performed in non-deuterated Millipore water. ^{1}H-NMR and NOESY experiments were performed at a Bruker Avance III HD 400 (400.13 MHz) NMR-spectrometer with a 5 mm BBO 400S1 BBF-H-D probe head with a Z-gradient. The devices were prepared by the central analytical NMR department of the University of Regensburg. The concentration of vitamin K3 was determined with the relation from equation 19.

$$\frac{c(polyphenolate)}{c(vitamin\ K3)} = \frac{Integral\ (polyphenolate)}{Integral\ (vitamin\ K3)} \quad (19)$$

$\boldsymbol{c}(\boldsymbol{polyphenolate}) =$ *concentration of polyphenolate (mol·kg^{-1})*

$\boldsymbol{c}(\boldsymbol{vitamin\ K3}) =$ *concentration of vitamin K3 (mol·kg^{-1})*

$\boldsymbol{Integral}\ (\boldsymbol{polyphenolate}) =$ *Integral of one polyphenolate proton*

$\boldsymbol{Integral}\ (\boldsymbol{vitamin\ K3}) =$ *Integral of one proton of vitamin K3*

3.2.2.8 Folic acid

3.2.2.8.1 Solubilization of folic acid in aqueous sodium carboxylate solutions

The solubility of folic acid in pure water was determined via saturation of 2 g water with folic acid by ultrasonication for 2 min (Bransonic 220, 120 W, frequency: 50 kc) and subsequent stirring at 450 rpm at 23 °C in the dark for 1 h. The samples were filtered with 0.2 µm PTFE syringe filters into vials.

Additionally, 2 g of sodium salt solutions (0.2 mol·kg^{-1} NaCHC, NaBenz, NaButyrate, NaValerate, NaCinn, Na-2,4-Pentadienoate, Na-4-OH-3-OMe-Benz, Na-4-OH-3-OMe-Cinn, Na-3,4-DiOMe-Cinn and 0.37 mol·kg^{-1} Na-4-OH-3-OMe-Benz, Na-4-OH-3-OMe-Cinn, Na-3,4-DiOMe-Cinn) were prepared via neutralization of the corresponding acid with 1 mol·L^{-1} self-made sodium hydroxide solution and addition of the residual amount of water or by direct dissolution of the salt in water. After stirring at 450 rpm for 20 min, an excess of folic acid was added to all samples. Then, the samples were ultrasonicated for 2 min (Bransonic 220, 120 W, frequency: 50 kc) and stirred at 450 rpm at 23 °C in the dark for 1 h. All samples comprising solubilizers were filtered with 0.45 µm PTFE syringe filters and diluted with water on the balance in order to recalculate the dilution factors with the help of equation 21 in section 3.4. Then the samples were filtered with 0.2 µm PTFE syringe filters into vials. The concentration of folic acid was determined via HPLC measurements with a UV-Vis-detector using the elution method from Table A 125 in the Appendix. For details on the HPLC measurement see section 3.7. All samples were prepared in triplicate

Calibration for folic acid:

Due to its low solubility, 0.01 g folic acid was dissolved in 10 g of water using 3.68 wt.% sodium vanillate as solubilizer via stirring in the dark for 20 min. This stock solution was then diluted with water to 5 µmol·kg^{-1}–750 µmol·kg^{-1} samples on the balance. The amount of vanillate in the samples was considered for the calculation of the folic acid concentration. All samples were prepared in triplicate, see Table A 136 in the Appendix.

3.2.2.8.2 Intermolecular interactions – NOESY measurements

To investigate the proximity of folic acid and aromatic sodium carboxylate salts, a NOESY spectrum of an aqueous 3 mol·kg^{-1} Na-3,4-DiOMe-Cinn solution was recorded. The 3 mol·kg^{-1} Na-3,4-DiOMe-Cinn solution was synthesized via neutralization of the corresponding polyphenolic acid with 6 mol·L^{-1} sodium hydroxide solution and addition of the residual amount of water via stirring for 30 min at 450 rpm. After addition of an excessive amount of folic acid, the sample was ultrasonicated for 2 min (Bransonic 220, 120 W, frequency: 50 kc) and stirred at 450 rpm at 23 °C in the dark for 1 h. After filtration through 0.45 µm PTFE syringe filters, the ^{1}H-NMR and NOESY spectrum were recorded, see section 3.5.

3.2.2.9 Caffeine

A 0.37 mol·kg^{-1} sodium vanillate solution, which was prepared via dissolution of the salt in water, was saturated with caffeine. Additionally, a 0.37 mol·kg^{-1} sodium ferulate solution, prepared via neutralization of the corresponding acid with 1 mol·L^{-1} sodium hydroxide solution, was saturated with caffeine. To know the water-solubility of caffeine, additionally, 2 g of water were saturated with caffeine.

For saturation, an excess of caffeine was added. After ultrasonication for 2 min (Bransonic 220, 120 W, frequency: 50 kc), the samples were stirred at 450 rpm at 23 °C in the dark for 1 h. Then, the samples were filtered through 0.45 µm PTFE syringe filters. An ^{1}H-NMR spectrum of the samples was recorded as described in section 3.5. The samples were prepared once. Caffeine was quantified with equation 20.

$$\frac{n(water)}{n(solute)} = \frac{Integral\ (water)}{Integral\ (solute)} \quad (20)$$

n(water) *= mole of water;* ***n(solute)*** *= mole of the solute;*

Integral() *= Integral of one proton of the solute molecule or water*

3.2.2.10 Compatibility of riboflavin, vitamin K3, folic acid and caffeine in an aqueous sodium polyphenolate solution

22 g of a 0.37 mol·kg^{-1} sodium ferulate solution were prepared via neutralization of the polyphenolic acid with 1 mol·L^{-1} self-made sodium hydroxide solution and stirring at 450 rpm

for 20 min until entire dissolution. Respectively 2 g of the solution were separated in eleven small snap glasses. The solutions were saturated with all combinations of RF, vitamin K3, folic acid and caffeine, see Table 8. Therefore, an excessive amount of the drugs was added to reach turbidity. The samples were ultrasonicated for 2 min (Bransonic 220, 120 W, frequency: 50 kc) and stirred at 450 rpm at 23 °C in the dark for 1 h. After filtration through 0.45 µm PTFE syringe filters, an ^{1}H-NMR spectrum of the samples was recorded as described in section 3.5. RF, vitamin K3, folic acid and caffeine were quantified via the integrals in the NMR spectrum using equation 20 from the previous section. To have more accuracy, the integrals were averaged if several separated peaks were present for one compound. To the same purpose some samples were prepared twice, see Table 8.

Table 8: Samples prepared to test the compatibility of drugs in a sodium ferulate solution

Sample	Saturation with	Number of experiments
1	RF, vitamin K3	1
2	RF, folic acid	2
3	RF, caffeine	1
4	Vitamin K3, folic acid	1
5	Vitamin K3, caffeine	2
6	Folic acid, caffeine	1
7	RF, vitamin K3, folic acid	1
8	RF, vitamin K3, caffeine	1
9	RF, folic acid, caffeine	2
10	Vitamin K3, folic acid, caffeine	2
11	RF, vitamin K3, folic acid, caffeine	2

Additionally, a sample of pure water saturated with vitamin K3 and caffeine was prepared in triplicate. Therefore, an excess of both solute was added to 2 g of water. After ultrasonication for 2 min (Bransonic 220, 120 W, frequency: 50 kc) and stirred at 450 rpm at 23 °C in the dark for 1 h. After filtration through 0.45 µm PTFE syringe filters, an ^{1}H-NMR spectrum of the samples was recorded as described in section 3.5. The drugs were quantified using equation 20 from the previous section. To have more accuracy, the integrals were averaged if several separated peaks were present for one compound.

3.2.3 Sodium ferulate as potential cosurfactant and π-complexer

3.2.3.1 General sample preparation

Preparation of sodium ferulate solutions: Solutions comprising sodium ferulate in pure water were prepared via neutralization of ferulic acid with 1 mol·L^{-1} sodium hydroxide solution and stirring for maximum 20 min until entire dissolution.

Preparation of pure SDS or sodium cholate solutions: Solutions comprising SDS or sodium cholate in pure water were prepared via direct dissolution of the salt in the required amount of water.

Preparation of sodium ferulate solutions with SDS or sodium cholate: Solutions comprising 0.37 mol·kg^{-1} sodium ferulate with varying concentrations of SDS or sodium cholate were prepared. Therefore, first, a pure aqueous sodium ferulate solution was prepared, as described above. Then, the corresponding amount of SDS or sodium cholate was added and the samples were stirred at 450 rpm at 23 °C. After stirring for maximum 1 h, all samples were homogeneous.

Saturation: Therefore, an excess of the corresponding colorant (RF or Sudan blue II) was added. Then, the samples were ultrasonicated for 2 min (Bransonic 220, 120 W, frequency: 50 kc) and stirred at 450 rpm at 23 °C in the dark for 1 h. Then, all samples were filtered through 0.2 µm PTFE syringe filters.

3.2.3.2 Solubility of riboflavin and Sudan blue II in aqueous solutions

For quantification purposes and for more accuracy, 2-10 g samples were prepared depending on the concentration of SDS and sodium cholate.

Solutions comprising SDS or sodium cholate (0.1-0.4 mol·kg^{-1} or 0.1-0.6 mol·kg^{-1}) in pure water were prepared via direct dissolution of the salt in the required amount of water and were saturated with RF, or with Sudan blue II or with RF and Sudan blue II.

Solutions comprising 0.37 mol·kg^{-1} sodium ferulate with SDS or sodium cholate concentrations ranging from 0.37-370 mmol·kg^{-1} were also prepared and saturated with RF, or with Sudan blue II or with RF and Sudan blue II.

For comparison, pure water was saturated with Sudan blue II. Additionally, a sample consisting of pure water saturated with RF and Sudan blue II was prepared. An aqueous 0.37 mol·kg^{-1} sodium ferulate solution was also saturated with Sudan blue II.

Both colorants were quantified with a Lambda18 spectrophotometer (Überlingen, Germany). For the quantification of RF see section 3.2.2.4. As Sudan blue II is not water-soluble at all, and because the low solubility in the investigated solutions did not allow a sufficient dilution (max. 1:20) with unpolar solvents to keep the solvochromic effect of water low, a calibration with Sudan blue II was not conducted. Therefore, the Sudan content was measured as net-

absorbance at 643 nm against water as blank after dilution of the samples with water on the balance Therefore, diluted samples were filled in 3 mL quartz cuvettes (10 mm with a transmission from 200-2500 nm) from Hellma (Müllheim, Germany). The total absorbance of Sudan blue II was calculated by multiplying the measured absorbance with the dilution factor from equation 21 from section 3.4. All samples were prepared in triplicate.

3.2.3.3 DLS measurements

For DLS measurements, 3.5 g of a 0.37 mol·kg^{-1} aqueous sodium ferulate solution, 3.5 g of a 0.37 mol·kg^{-1} aqueous SDS solution and 3.5 g of an aqueous solution comprising 0.37 mol·kg^{-1} SDS and sodium ferulate were prepared. After measuring the DLS curves of these solutions, they were saturated with RF and DLS curves were again recorded. For details on the DLS measurement see section 3.6. All samples were prepared in triplicate.

3.2.3.4 Conductivity measurements

Samples consisting of 20 g water and 0.37 mol·kg^{-1} sodium ferulate or SDS or SDS and sodium ferulate were filled into a tempering measuring cell. The same samples were prepared and saturated with either RF, Sudan blue II or with both colorants. The conductivity was measured at 25 °C with a WTW Cond730 conductivity meter with TetraCon325 electrode via successive dilution of the samples with Millipore water using a burette. After each dilution, the system was left to equilibrate for 30 s. The samples were prepared in triplicate.

3.3 Solubilization of Riboflavin

3.3.1.1 Solubilization of riboflavin in presence of riboflavin 5'-monophosphate sodium salt in water

An excess RF-PO_4 and RF was added to 1.5 g of water. After ultrasonication for 2 min (Bransonic 220, 120 W, frequency: 50 kc), the samples were stirred at 450 rpm in 10 mL snap glasses in the dark for 1 h. After filtration through 0.45 µm PTFE syringe filters followed by filtration through 0.2 µm cellulose acetate filters, the concentration of RF-PO_4 was determined, see section 3.2.2.4. The sample were prepared in quadruplicate.

3.3.1.2 Attempt for disruption of RF-RF π-stacking via thermal energy

In the case of NaBenz, Na-4-OH-3-OMe-Benz, Na-2-OH-Benz, NaBenz and SDS solutions, the salt was directly dissolved in 2 g water. In the case of Na-3,4-DiOMe-Cinn, NaValerate and NaButyrate, 2 g samples were prepared via neutralization of the corresponding acid with self-made 1 or 6 mol·L^{-1} sodium hydroxide solution and addition of the residual amount of water followed by stirring at 450 rpm for 20 min. A list of the samples is reported in Table 9. Na-3,4-DiOMe-Cinn was never entirely soluble. In the case of Na-2-OH-Benz and NaBenz, the

concentration was far beneath the sodium salt's solubility, as RF precipitated fast otherwise. The residual solubilizer concentrations were near their solubility limit. Then, all samples were saturated with RF via ultrasonication for 2 min (Bransonic 220, 120 W, frequency: 50 kc) followed by stirring at 450 rpm at 90 °C or 23 °C in the dark for 1 h. The samples saturated at 90 °C were let to cool down in the dark to 23 °C for 1 h so that insoluble RF and sodium salts precipitated. All samples were filtered with 0.45 µm PTFE syringe filters. The RF concentration was determined via UV-Vis-measurements as reported in section 3.2.2.4. The samples were monitored for 4 weeks to prevent a kinetic retardment of the precipitation after cooling the samples down to 23 °C. Only the sample comprising NaBenz precipitated on the next day. Therefore, it was filtered and measured again. All samples were prepared in triplicate.

Table 9: Preparation of aqueous sodium salt solutions for solubilization of RF at 90 °C and at 23 °C.

Neutralization of the acid with NaOH		**Usage of the salt**	
Salt	**c (mol·kg^{-1})**	**Salt**	**c (mol·kg^{-1})**
Na-3,4-DiOMe-Cinn	3.000 – 0.200 – 0.130	**NaBenz**	3.000
Na-2,4-Pentadienoate	0.100	**Na-4-OH-3-OMe-Benz**	0.858
NaValerate	0.400	**Na-2-OH-Benz**	0.937
NaButyrate	0.400	**SDS**	0.400 – 0.200

3.3.1.3 Solubilization of riboflavin by means of other aromatic additives

Aqueous 0.37 mol·kg^{-1} additive solutions were prepared via direct dissolution of the compounds in water. If the additives were not soluble at this concentration samples with lower concentrations were prepared, see Table 10. 2 g samples were prepared in the case of 0.37 mol·kg^{-1} solutions and 10 g samples in the case of lower additive concentrations.

Samples comprising L-proline, trisodium resveratrol triphosphate (Resveratrol-Tri-PO_4), saccharine, pyroglutamic acid, γ-valerolactone, thiamine hydrochloride (Thiamine x HCl) , pyridoxine hydrochloride (Pyridoxine x HCl), L-histidine, L-tyrosine, biotin, rutin, hesperidin, L-tryptophan, adenosine, adenine, caffeine, β-nicotinamide adenine dinucleotide tetrasodium salt (Tetra-Na-NADPH), adenosine triphosphate (ATP), D-(+)-glucose and D-(-)-fructose from 0.1 to 0.4 mol·kg^{-1} and samples comprising fulvic acid from 0.01 to 0.1 mol·kg^{-1} were prepared via direct dissolution of the compounds in water at the concentration stated in Table 10. As vitamin K3 (Vit. K3), folic acid, ellagic acid, vanillyl alcohol and ethyl vanillin were scarcely water-soluble, 3 g of water were saturated with the additive, so that the maximum concentration of the potential solubilizer was reached. Additionally, samples sodium saccharine, NaPyroglutamate, Thiamine + NaOH, Pyridoxine + NaOH and 3-indole propionic acid were prepared via neutralization of saccharine, pyroglutamic acid, thiamine hydrochloride, pyridoxine hydrochloride, and 3-indole propionic acid with 1 mol·L^{-1} sodium hydroxide solution and addition of the residual amount of water. The sample comprising indoxyl sulfate was

purchased as potassium salt, which was too basic. Therefore, the salt was neutralized with an aqueous 1 mol·L^{-1} hydrochloric acid solution to pH 2 and 7.

Prior to the saturation with RF, the pH-value of each sample was controlled with indicator paper, see Table 10. Regardless whether the compound was soluble after 30 min of stirring, all samples were saturated with RF via ultrasonication for 2 min (Bransonic 220, 120 W, frequency: 50 kc) and subsequent stirring at 450 rpm in the dark for 1 h. The samples were filtered with 0.45 µm PTFE syringe filters. The RF content was determined as reported in section 3.2.2.4. The samples were prepared once, in duplicate or triplicate, see Table 10.

Table 10: Solubilization of RF in water by means of natural additives. N = number of measurements

Compound	c(compound) (mmol·kg^{-1})	N	Compound	c(compound) (mmol·kg^{-1})	N
Pyridoxin x HCl	370 (pH 3)	3	**Vit. K3**	Saturation (pH 6)	3
L-Proline	370 (pH 6)	3	**Folic acid**	Saturation (pH 6)	3
Resveratrol-Tri-PO_4	185 (pH > 8)	3	**Ellagic acid**	Saturation (pH 6)	3
Saccharine	370 (pH 2)	3	**Vanillyl alcohol**	Saturation (pH 6)	3
Pyroglutamic acid	370 (pH 1)	3	**Ethyl vanillin**	Saturation (pH 5)	3
γ-valerolactone	370 (pH 7)	3	**NaSaccharine**	370 (pH 7-8)	3
Thiamin x HCl	300 (pH 3)	3	**NaPyroglutamate**	370 (pH 3)	3
L-Histidine	80 (pH 7-8)	3	**Pyridoxine + NaOH**	370 (pH 8)	3
L-Tyrosine	80 (pH 6)	3	**Thiamine + NaOH**	80 (pH 8)	3
Biotin	50 (pH 4)	3	**Caffeine**	80 (pH 6)	3
Rutin	80 (pH 6)	3	**Caffeine**	370 (pH 6)	1
Hesperidin	80 (pH 6)	3	**Tetra-Na-NADPH**	100 (pH 7-8)	2
Adenosine	80 (pH 6)	3	**L-Tryptophan**	80 (pH 6)	3
Adenine	80 (pH 6)	3	**Indoxyl sulfate**	100 mM (pH 2)	3
ATP	80 (pH 3)	2	**Indoxyl sulfate**	100 mM (pH 7)	3
3-Indole propionic acid	100 mM (pH 5)	3			

Additionally, 10 mmol·kg^{-1} solutions of anthocyanin/proanthocyanidins comprising 3.000 g water and 0.0194 g cyanin chloride or 0.0219 g grape seed extract (distributor unknown, green grapes) or 0.4369 g of an OPC complex 200 from Greenline Products (200 mg OPC (95 %) + 250 mg vitamin C) were prepared. After stirring at 450 rpm for 1 h, the products were not dissolved. Still, the samples were saturated with RF via ultrasonication for 2 min (Bransonic 220, 120 W, frequency: 50 kc) and stirring at 450 rpm in the dark for 1 h. After filtration through 0.2 µm PTFE syringe filters, the RF content was determined via HPLC analysis, see section 3.7.

3.3.1.4 Solubilization of riboflavin in the ternary system water/ethanol/triacetin

3.3.1.4.1 Solubilization of riboflavin

Binary water/ethanol solutions from 0-100 % ethanol, binary ethanol/triacetin solutions from 40-100% ethanol, ternary water/ethanol/triacetin solutions at a fixed water/ethanol ratio of 1:1 with a triacetin content from 0 to 90 % and ternary water/ethanol/triacetin solutions at a fixed ethanol/triacetin ratio of 6:4 with varying water content from 0 to 100 % were prepared in 10 % steps. 5 g of each solution were saturated with RF via ultrasonication for 2 min (Bransonic 220, 120 W, frequency: 50 kc) and stirring at 450 rpm at 23 °C for 1 h. After filtration of the samples with 0.2 µm PTFE syringe filters, the samples were diluted with the corresponding solvent (water, ethanol, binary or ternary water/ethanol/triacetin solution) on the balance. RF was quantified as reported in section 3.3.1.4.3. The samples were prepared in duplicate.

3.3.1.4.2 Photodegradation of riboflavin

Binary ethanol/water mixtures consisting of 18 g and ranging from 0 to 100 % ethanol were prepared in 10 % steps. Additionally, binary ethanol/triacetin solutions ranging from 40-100% ethanol were prepared in 10 % steps. After an excessive amount of RF was added to 5 g of the samples, they were ultrasonicated for 2 min (Bransonic 220, 120 W, frequency: 50 kc) and stirred at 450 rpm at 23 °C for 1 h. All samples were filtered with 0.2 µm PTFE-filters.

The remaining 13 g of the prepared binary solutions were used for dilution of the saturated samples on the balance and also as blank for the quantification of RF via UV-Vis-measurements, see section 3.3.1.4.3.

If RF was sufficiently soluble, the samples were diluted with the corresponding binary mixture to have an absorbance of 1.0 AU to have the comparable initial concentrations of RF. If RF's solubility was lower, the samples were not diluted. These samples were illuminated for 300 min with a LED plant lamp, see Figure 16 in section 3.2.2.1.14.1. The UV-Vis-spectrum was recorded every 30 min in order to obtain the kinetics of the photodegradation. To evaluate the main degradation product, the absorbance of the samples was measured from 300-700 nm. RF was quantified without further dilution as reported in section 3.3.1.4.3.

3.3.1.4.3 Quantification of riboflavin in water/ethanol/triacetin solutions via UV-Vis measurements

The absorbance of RF at 449 nm was measured with the UV-Vis Lambda19 spectrophotometer (Überlingen, Germany) in 3 mL quartz cuvettes (10 mm with a transmission from 200-2500 nm) from Hellma (Müllheim, Germany) with the corresponding binary or ternary solution or ethanol as blank. The content of RF was determined by means of calibration curves in the corresponding solution of water/ethanol/triacetin.

Calibrations:

Calibration curves for RF were recorded for distinct binary and ternary mixtures of water, ethanol and triacetin. Therefore, 5 mg RF were dissolved in 250 mL of the corresponding mixture. The following mixtures were investigated: a binary water/ethanol solution from 0-100 % ethanol in 10 % steps, in a binary ethanol/triacetin solution from 40-100 % ethanol in 10 % steps, a ternary water/ethanol/triacetin system at a fixed water/ethanol ratio of 1:1 increasing the triacetin content in 10 % steps from 0 to 90 % and a ternary water/ethanol/triacetin system at a fixed ethanol/triacetin ratio of 6:4 increasing the water content in 10 % steps from 0 to 100 %. After ultrasonication for 2 min (Bransonic 220, 120 W, frequency: 50 kc) and stirring at 450 rpm at 23 °C for 10 min, RF was dissolved. The samples were diluted on the balance to have 0.5, 0.4, 0.3, 0.2, 0.1 mmol·kg^{-1} RF solutions. All calibration curves were prepared in duplicate. The averaged calibration curves are reported in Table A 5-Table A 8 in the Appendix.

3.4 Equations for the quantification of solutes

$$f = \frac{m_{sample} + m_{water}}{m_{sample}} \tag{21}$$

m_{sample} *= weight of water in the sample*

m_{water} *= weight of water*

$$c_{compound} = \frac{absorbance - b}{m} \cdot f \tag{22}$$

$$c_{RF-PO4} = 0.7 \cdot \frac{absorbance - b}{m} \cdot f \tag{23}$$

$c_{compound}$ *= concentration of the compound*

f *= dilution factor, see equation 21*

b *= intercept of the calibration curve*

m *= slope of the calibration curve*

c_{RF-PO4} *= concentration of RF-PO₄*

3.5 Measurement setup for NMR

The samples (0.8 mL) were filled into an NMR tube. The NMR measurements were conducted in the dark. Proton Nuclear Magnetic Resonance (^{1}H-NMR), 13-Carbon Nuclear Magnetic Resonance (^{13}C-NMR), Correlation Spectroscopy (COSY), Heteronuclear Multiple Bond Correlation (HMBC) experiments, Heteronuclear Single Quantum Coherence (HSQC) experiments and Nuclear Overhauser Effect Spectroscopy (NOESY) experiments were performed at a Bruker Avance III HD 400 (400.13 MHz) NMR-spectrometer with a 5 mm BBO 400SB BB-H-D or with a 5 mm BBO 400S1 BBF-H-D probe head with a Z-gradient at the Central Analytical NMR department of the University of Regensburg.

3.6 DLS measurement setup

All samples were filtered with 0.2 µm PTFE syringe filters into clean borosilicate DLS tubes and measured at 25 °C in a toluene bath if not stated differently. The borosilicate glass tubes were reflux distilled with acetone for 20 min and dried in a desiccator to prevent disturbance by dust particles. The DLS correlation curves were retrieved with an ALV/CGS-3 goniometer (Langen, Germany) with an ALV/LSE-5004 correlator and with an ALV correlator software at an angle of 90 ° and a laser wavelength of 632.8 nm (22 mW HeNe, vertical polarized).

3.7 Measurement setup for HPLC

An HPLC device from Waters with two Waters 515 pumps, a Waters 717 autosampler and a Waters 2487 UV-VIS-detector with an RP-18 column from Knauer (Eurosphere-100, 5 µm, 100 Å, 250 mm x 4.6 mm) or an RP-18 column 4.6 Nucleodur C18 Isis (5 µm, octadecyl especially cross-linked, multi-endcapping, 250 mm x 4.6 mm) were used for the analysis. The absorbance from 230-800 nm was measured with a 2998 PDA Detector from waters with a resolution of 1.2 nm. Prior to analysis, all samples were filtered with 0.2 µm PTFE-filters into vials. If not stated differently, the samples were injected (10 µL) three times. Maintaining a flow of 1 mL·min^{-1}, the elution took place at pH 2 at 40 °C with water comprising 0.1 vol.% trifluoroacetic acid as polar mobile phase and acetonitrile as non-polar mobile phase. The elution methods are given in Table A 124, see section 7.13. The concentration of the compound was determined via the area beneath a peak at one wavelength using equation 24 and calibration curves from sections 7.13.2-7.13.4 in the Appendix.

$$c_{compound} = \frac{area - b}{m} \cdot f \qquad (24)$$

$\boldsymbol{c_{compound}}$ *= concentration of the compound (mmol·kg^{-1})*

$\boldsymbol{f}$ *= dilution factor, see equation 21 in section 3.4*

$\boldsymbol{area}$ *= averaged peak area of RF (V·s) at 445 nm*

$\boldsymbol{b}$ *= intercept of the calibration curve (V·s)*

$\boldsymbol{m}$ *= slope of the calibration curve (V·kg·mmol^{-1})*

4 Results and Discussion

4.1 Polyphenolic acid salts as solubilizing agents

4.1.1 Polyphenolates as salting-in and -out agents

4.1.1.1 Phase transition temperature measurements in the binary water/DPnP system

Though being involved in various biological processes in plants, such as protein synthesis, photosynthesis, nutrient uptake, regulation of enzyme activity, disease cure, plant defense as well as allelopathy, the potential salting-in and -out effect of polyphenolic acids was rarely investigated.[63,68–70,79,224] The amphiphilic backbone of polyphenolic acids could be decisive for their uptake through lipophilic membranes and influence their way of interactions with target molecules. Thus, the salting-in/-out properties of distinct natural sodium polyphenolates and related molecules were investigated via phase transition temperature measurements in the binary water/DPnP (45/55 (w/w)) system. This system was chosen due to its low PTT with DPnP, which can be seen as representative for a solute in a plant. Additionally, PTT measurements in presence of Na-3,5-DiCF3-Benz and NaCHC were performed, to analyze the influence of more hydrophobic substituents and the influence of the aromatic aryl ring. On top of that, the PTT measurements in presence of SDS and sodium cholate were conducted to compare aromatic sodium carboxylates to a common surfactant and to a biosemulsifier.[225,226]

Regarding the PTT curves in Figure 17, all sodium salts tested decreased or increased the PTT linearly with the additive concentration. To quantify the salting-in/-out power, the salts are ordered according to their slope – the *m*-value – in Table 11. Almost all additives exhibited a salting-in effect. Still, some salts were salting-out. More precisely, Na-4-OH-3-OMe-Benz, Na-2-OMe-Benz and Na-3,4-DiOH-Benz exhibited only a slight salting-out effect, while Na-2,3-DiOMe-Benz and Na-3,4,5-TriOH-Benz showed a considerable salting-out effect corresponding to 25 % and 50 % of the salting-out power of sodium chloride.[51] Regarding Table 11, the following was concluded:

A) Having an *m*-value twice as high as NaSal, having a higher m-value than the biosurfactant sodium cholate and a similar m-value to SDS, Na-3,5-DiCF3-Benz was the most salting-in polyphenolate-like compound tested. Thus, the hydrophobic trifluoromethyl groups induce salting-in properties comparable to a standard surfactant and better than a biosurfactant, which itself can be considered only like a hydrotrope.[227,228]

B) NaCinn was the only compound possessing similar and slightly stronger salting-in power than Na-2-OH-Benz, because out of the sodium benzoate and cinnamate derivatives, NaCinn

was the most amphiphilic one. Natural sodium polyphenolates, Na-4-OH-Prop, NaBenz and NaCHC exhibited a weaker salting-in power on DPnP than the standard hydrotrope Na-2-OH-Benz.[227,229] Hence, natural polyphenolates can be considered to act maximum in a hydrotrope range.

C) An increase of the amphiphilicity by an elongation of the carboxylate side chain increases the salting-in effect on DPnP in water (Na-4-OH-3-OMe-Benz → Na-4-OH-3-OMe-Cinn; NaBenz → NaCinn, Na-4-OH-Benz → Na-4-OH-Cinn; except of Na-2-OH-benz and Na-2-OH-Cinn).

D) The more hydroxy or methoxy groups were present on the aryl ring, the weaker was salting-in power (Na-4-OH-Benz > Na-3,4-DiOH-Benz > Na-3,4,5-TriOH-Benz; Na-2-OMe-Benz > Na-2,3-DiOMe-Benz). A modification of NaBenz and NaCinn with a hydroxy group reduced the salting-in power of sodium polyphenolates more in para position than in meta and this more than in ortho position (Na-3-OH-Benz > Na-4-OH-Benz, Na-2-OH-Cinn > Na-4-OH-Cinn). The reason therefore is probably the deterioration of the amphiphilicity due to the polar hydroxy or methoxy group. The only exception of this trend was Na-2-OH-Benz, because the hydrogen bond formed between the ortho hydroxy group and the carboxylate leads to a more developed amphiphilicity and to a stronger salting-in effect of Na-2-OH-Benz compared to NaBenz.[230]

E) Further, Na-4-OMe-Benz exerted a stronger salting-in power on DPnP than Na-4-OH-Benz. Similarly, the salting-out properties of Na-3,4-DiOH-Benz were diminished upon an induction of a methoxy group (Na-4-OH-3-OMe-Benz). Presumably, the weaker hydration of the methoxy group together with an increased lipophilicity compared to the hydroxy group led to the stronger salting-in and weaker salting-out behavior of Na-4-OMe-Benz and Na-4-OH-3-OMe-Benz, respectively.

In contrast, an ortho methoxy group (Na-2-OMe-Benz) revoked the salting-in behavior compared to NaBenz and Na-2-OH-Benz. Probably, the methoxy group hinders the hydration at the carboxylate and deteriorates the amphiphilicity compared to NaBenz and Na-2-OH-Benz.

F) Na-4-OH-Prop was found to be less salting-in than Na-4-OH-Cinn. The only difference between the two molecules is the rotational restriction on the side chain in case of the aromatic Na-4-OH-Cinn. Regarding the theory on the quantification of salting-in/-out properties by Marcus, the water-structuring entropy should be higher for a weaker salting-in compound.[47] Thus, the weaker salting-in effect of Na-4-OH-Prop might correlate with its flexible side chain enabling a higher water-structuring entropy than in the Na-4-OH-Cinn sample.

G) Additionally, the induction of a conjugation to NaCHC leading to the planar and more rigid NaBenz weakened the salting-in power. The stronger salting-in character of NaCHC compared to NaBenz was affirmed by molecular dynamics of Raschke and Levitt, who revealed a weaker binding of the first hydration shell to cyclohexane compared to benzene.[231]

H) Unexpectedly, sodium cholate was found to have salting-in properties similar to Na-2-OH-Benz, too. This suggests rather hydrotrope like behavior of the biosurfactant sodium cholate. Yet, regarding the PTT curve of sodium cholate, one can also see the difference to sodium polyphenolates and related compounds. Sodium cholate curve exhibits two distinct slopes. The second lower slope might indicate an aggregation of sodium cholate, as more cholate molecules were required to increase the PTT further. Such a behavior is rather typical for surfactants than for hydrotropes and was observed for SDS in the comparable binary water/propylene glycol propyl ether system by Häckl, too.[232] Aqueous systems comprising SDS and cholate are further discussed in further in section 4.1.3.[233]

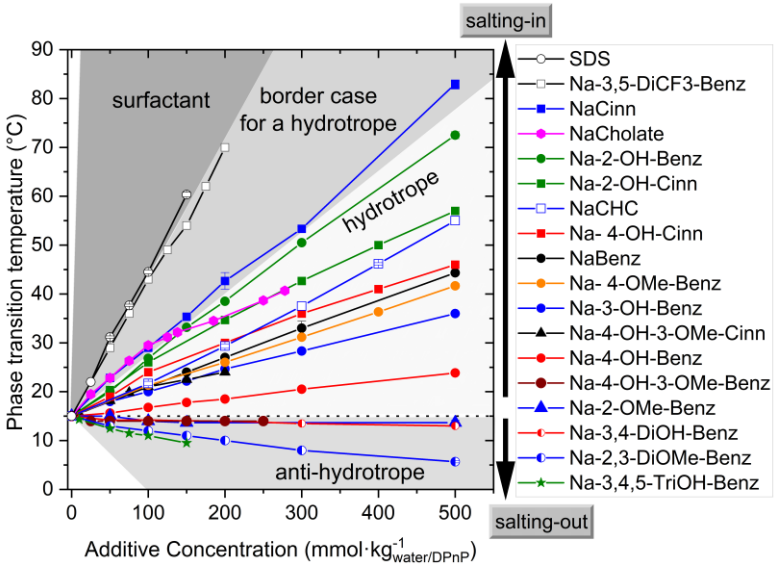

Figure 17: Shifts of the PTT of a binary water/DPnP mixture (45/55 (w/w)) in presence of sodium polyphenolates, similar compounds and in presence of the two surfactants sodium cholate and sodium dodecyl sulfate. All samples were prepared in triplicate.[233]

Table 11: Salting-in/-out properties of sodium polyphenolates, similar compounds and in presence of the two surfactants sodium cholate and sodium dodecyl sulfate represented by the m-value corresponding to the slope of the curves from Figure 17 in the binary water/DPnP (45/55 (w/w)) system.[233]

Salt	m (°C·mol·mmol^{-1})	Salt	m (°C·mol·mmol^{-1})
SDS	8.46	**Na-4-OH-3-OMe-Cinn**	1.29
Na-3,5-DiCF3-Benz	7.55	**Na-4-OH-Prop**	1.27
NaCinn	3.75	**Na-3-OH-Benz**	1.16
NaCholate	3.68 (first slope)	**Na-4-OH-Benz**	0.51
Na-2-OH-Benz	3.26	**Na-4-OH-3-OMe-Benz**	-0.06
Na-2-OH-Cinn	2.35	**Na-2-OMe-Benz**	-0.06
NaCHC	2.26	**Na-3,4-DiOH-Benz**	-0.10
Na-4-OH-Cinn	1.72	**Na-2,3-DiOMe-Benz**	-0.51
NaBenz	1.65	**Na-3,4,5-TriOH-Benz**	-1.02
Na-4-OMe-Benz	1.48		

The different factors determining the salting-in/-out behavior of sodium polyphenolates and related compounds are summarized in Figure 18. Obviously, the observations of the PTT measurements in the binary water/DPnP (45/55 (w/w)) system follow the predictions from the

definition of classical hydrotropy. [32,234] This was expected, because, NaCinn was the strongest natural salting-in compound and comprised an m-value being just 1.15 times higher than the one of the classical hydrotrope Na-2-OH-Benz.[227]

Being one of the first to categorize salting-in/-out properties in aqueous glycol ether systems, Grundl et al. found short carboxylate sodium salts to be salting-out.[51] However, compared to the carboxylate, the huge organic residue induced distinct salting-in/-out properties in the case of sodium cinnamate and benzoate derivatives. This is in line with the observations from Mehringer et al, who reported a correlation of hydrophobic residue of organic salts to their salting-in power.[42,51]

To summarize, polyphenolic acids can adopt different salting-in/-out properties via substitution with hydroxy and/or methoxy groups or by a change in the aromaticity. The salting-out properties of sodium polyphenolates are rather weak compared to the one of the classical inorganic salting-out agent sodium chloride.[51] The strong dependence of the salting-in/-out properties of sodium polyphenolates on the substitution of the aryl ring might be the reason for broad occurrence of polyphenolic acids plants and for their involvement in nutrition control and uptake of plants.[69] As proteins and their aggregates can exhibit an LCST, sodium polyphenolates or similar organic compounds might assist the solubilization and stabilization of proteins against precipitation in biochemical systems.[235–238] Thus, the conformational change of the major allergen protein in egg white, reported by Lu et. al, might be also induced by the weak salting-in character of ferulic acid leading to a reduced binding to IgE and resulting in a depression of the allergenic potential of proteins.[63,239] The assumption of a further role of polyphenolic acids as solubilizers is even more affirmed by the similar salting-in power of NaCinn and Na-2-OH-Benz to the biological solubilizer sodium cholate.[226] Hence, polyphenolic acids as well as their anionic salts might have a secondary function as solubilizing agents, which might assist their primary biological role in plants.[233]

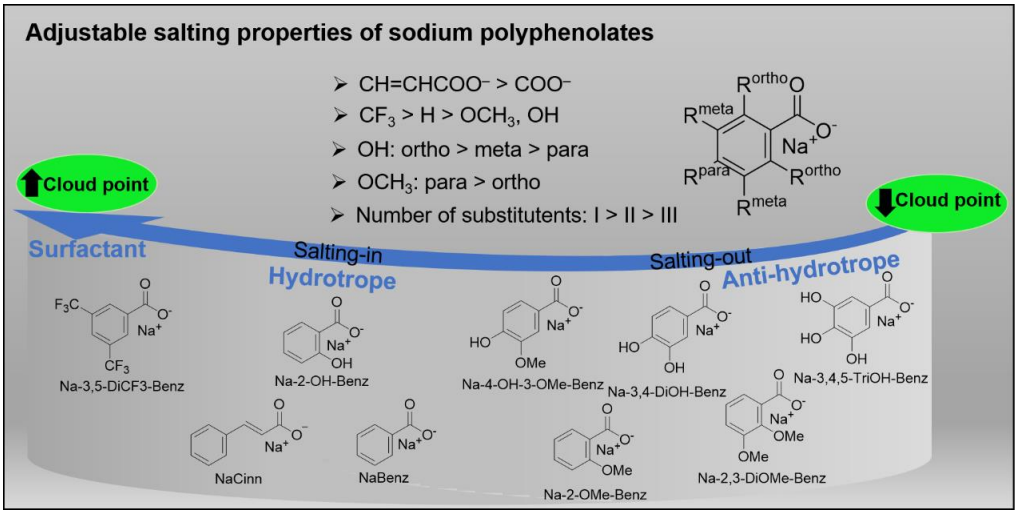

Figure 18: Schematic representation of factors determining the salting-in/-out behavior of sodium polyphenolates.[233]

4.1.1.2 Interfacial behavior of sodium polyphenolates in aqueous solution

4.1.1.2.1 Surface tension

Due to their amphiphilic backbone aromatic sodium carboxylates were supposed to reduce the surface tension of water. This might be decisive for the hydrotropic action of sodium polyphenolates. Therefore, concentration dependent surface tension measurements at the water/air interface of aqueous solutions comprising the surfactant SDS, comprising the most hydrophobic polyphenolate-like compound Na-3,5-DiCF3-Benz, and of aqueous solutions comprising the natural compounds NaCinn, Na-4-OH-3-OMe-Cinn, Na-2-OH-Benz and NaBenz were recorded, see Figure 19. The surface-active efficiency corresponding to the concentration needed to reach a certain surface tension of the tested compounds decreases in the following order: SDS > Na-3,5-DiCF3-Benz > NaCinn > Na-4-OH-3-OMe-Cinn > Na-2-OH-Benz > NaBenz. The surface-active effectiveness corresponding to the maximum reduction in surface tension that can be achieved, decreases as follows: Na-3,5-DiCF3-Benz > SDS > NaCinn >Na-4-OH-3-OMe-Cinn > Na-2-OH-Benz > NaBenz.

Regarding both, the surface-active efficiency and effectiveness, NaBenz, NaCinn and Na-4-OH-3-OMe-Cinn exhibit a similar surface affinity to the hydrotrope Na-2-OH-Benz.

In contrast, Na-3,5-DiCF3-Benz decreased the surface tension more strongly than the natural organic sodium salts tested and cannot be classified as a common hydrotrope. Still, for surface tension reductions similar to the surfactant SDS, much higher concentrations (> 10^{-1}) were required. Hence, Na-3,5-DiCF3-Benz states an intermediate case between a surfactant and a hydrotrope. Although the order of the surface-active efficiency of Na-3,5-DiCF3-Benz, NaCinn, NaBenz and Na-2-OH-Benz was in line with their salting-in power from section 4.1.1.1, Na-4-OH-3-OMe-Cinn was more efficiently acting on the surface tension than NaCinn despite being less salting-in than NaCinn. Thus, the surface activity correlates usually, but not necessarily with the solubilization of the small hydrocarbon DPnP.

Further, the CAC and CMC of the organic sodium salts and of SDS, respectively, were determined, see Table 12. Because of surface active impurities, the CAC of the organic sodium salts in Figure 19 corresponds to the break point, whereas the CMC of SDS corresponds to the intercept of the two linear parts of the curve. As expected, the CACs of Na-4-OH-3-OMe-Cinn, NaCinn and NaBenz are in the range of the common hydrotropes Na-2-OH-Benz and sodium xylene sulfonate. This confirms once more the hydrotropic behavior of polyphenolates comprising salting-in properties.[240,241] However, the CAC of Na-4-OH-3-OMe-Cinn was beneath the one of Na-3,5-DiCF3-Benz and NaCinn despite the stronger action of the latter two compounds on the PTT, see section 4.1.1.1. Moreover, the CAC of Na-2-OH-Benz was higher than the one of NaBenz, while Na-2-OH-Benz exhibited a greater m-value in the PTT measurements from section 4.1.1.1. Obviously, the onset of the aggregation corresponding to

the CAC does not correlate with the hydrotropic solubilization of DPnP. Otherwise, the PTT curves should exhibit a change in the slope at the CAC. A reasonable explanation for the lack of a correlation between the order of the solubilizers' CACs and PTT measurements would be the weak tendency of aromatic sodium carboxylates for self-aggregation. This would imply specific molecular interactions of DPnP with the salting-in agents.[233]

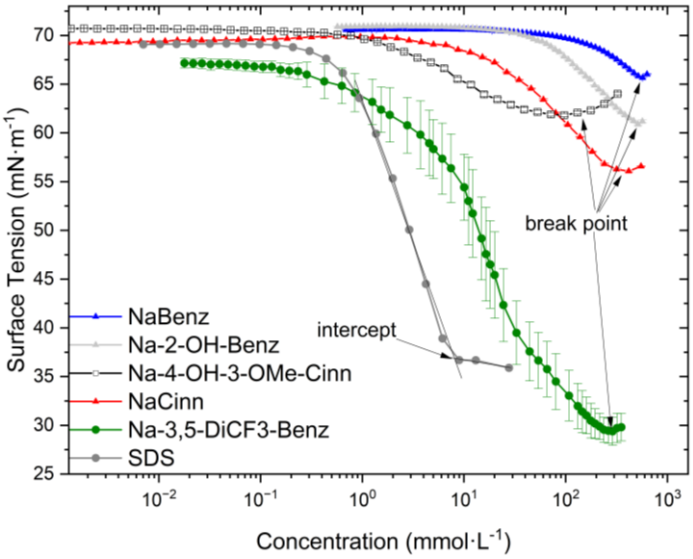

Figure 19: Surface tension measurements of different sodium salts relative to sodium dodecyl sulfate in Millipore water at 25 °C. SDS was measured once. The residual samples were prepared in duplicate.[233]

Table 12: Experimental critical micelle concentration (CMC) or critical aggregate concentration (CAC) and the ones reported in literature of sodium carboxylate salts and of the surfactant SDS as well as of the hydrotrope SXS. Due to impurities in the purchased compounds, the CAC was determined at the break point of the curves from Figure 19.[233]

	Experiment	**Literature**
Compound	**CMC/CAC (mmol·L^{-1})**	**CMC/CAC (mmol·L^{-1})**
Sodium xylene sulfonate	-	450 [242]
Na-2-OH-Benz	514	640 (30 °C)[243]
NaBenz	432	480 [34]
NaCinn	367	-
Na-3,5-DiCF3-Benz	≈ 289	-
Na-4-OH-3-OMe-Cinn	177	-
SDS	8.08	8.25 [244]

4.1.1.2.2 Dynamic light scattering measurements

To further evaluate the aggregation potential of sodium polyphenolates in aqueous solution, DLS measurements of pure water comprising sodium polyphenolate(-like) compounds and of the binary water/DPnP mixtures (45/55 (w/w)) comprising sodium polyphenolate(-like) compounds were conducted at 25 °C, see Figure 20 B. The same samples were additionally measured at 10 °C to investigate the thermal effect on the structuring ability near to the PTT of the water/DPnP mixture without additives, see Figure 20 C. The samples comprising Na-4-OH-Benz and Na-3,4-DiOH-Benz were measured only at 10 °C due to turbidity at 25 °C. The binary water/DPnP mixture (45/55 (w/w)) without additives served as reference. Due to turbidity above 14 °C and for an easier handling, this reference sample was only measured at 10 °C, see Figure 20. In congruence to the prediction of self-assemblies of DPnP in water by [245], the DLS correlation function of the reference samples exhibited a well-developed correlation function reaching a plateau at 0.9 without significant fluctuations. Consequently, DPnP should be actually considered as a solvo-surfactant comprising structuring abilities between a hydrotrope and surfactant.[246]

In contrast, sodium polyphenolates and related compounds in pure water did neither induce self-aggregation at 10 °C nor at 25 °C, as the correlation functions were strongly fluctuating, see Figure 20 A below and Figure A 1 in the Appendix. Although NaCinn, NaBenz and the 0.6 mol·kg^{-1} Na-2-OH-Benz sample were measured above their CAC, the correlation functions were strongly fluctuating beneath 0.2. Thus, according to DLS measurements, sodium benzoate and cinnamate derivatives do not form self-assemblies in pure water. This is in line with the postulation of Shimizu that hydrotropes should not tend to self-aggregation in the absence of a solute to act as a good solubilizer.[33]

All samples comprising 55 wt.% DPnP exhibited correlation functions between 0.2 and 0.85, which showed slight or no fluctuations, see Figure 20 B. All sodium polyphenolates and related compounds showed a visible effect on the DLS correlation functions relatively to the reference sample at 25 °C and 10 °C: Na-3,4-DiOH-Benz < reference < Na-4-OH-Benz < NaCHC < NaBenz ≈ Na-4-OH-Prop ≈ Na-4-OMe-Benz < NaSal < NaSal (0.6 M) ≈ Na-3,5-DiCF3-Benz ≈ NaCinn. This was expected, because the structurally similar propylene glycol n-propyl ether was reported to form self-assemblies of a very flexible interface, implicating an easy access of propylene glycol n-propyl ether (or here DPnP) for the solubilizer and solvent.[245,247]

At both temperature tested, an inverse correlation of the self-assemblies' size and of the structuring's development with the salting-in power of the compounds was observed. Thus, the only the salting-out agent Na-3,4-DiOH-Benz measured increased the size of the nano-structures and the correlation function relatively to the reference. Additionally, an increase of the polyphenolate concentration in case of Na-2-OH-Benz, resulted in a higher PTT and thus

stronger salting-in of DPnP, while the DLS correlation function was decreased. Hence, an increased salting-in of DPnP reduced nano-structuring degree in the solution.

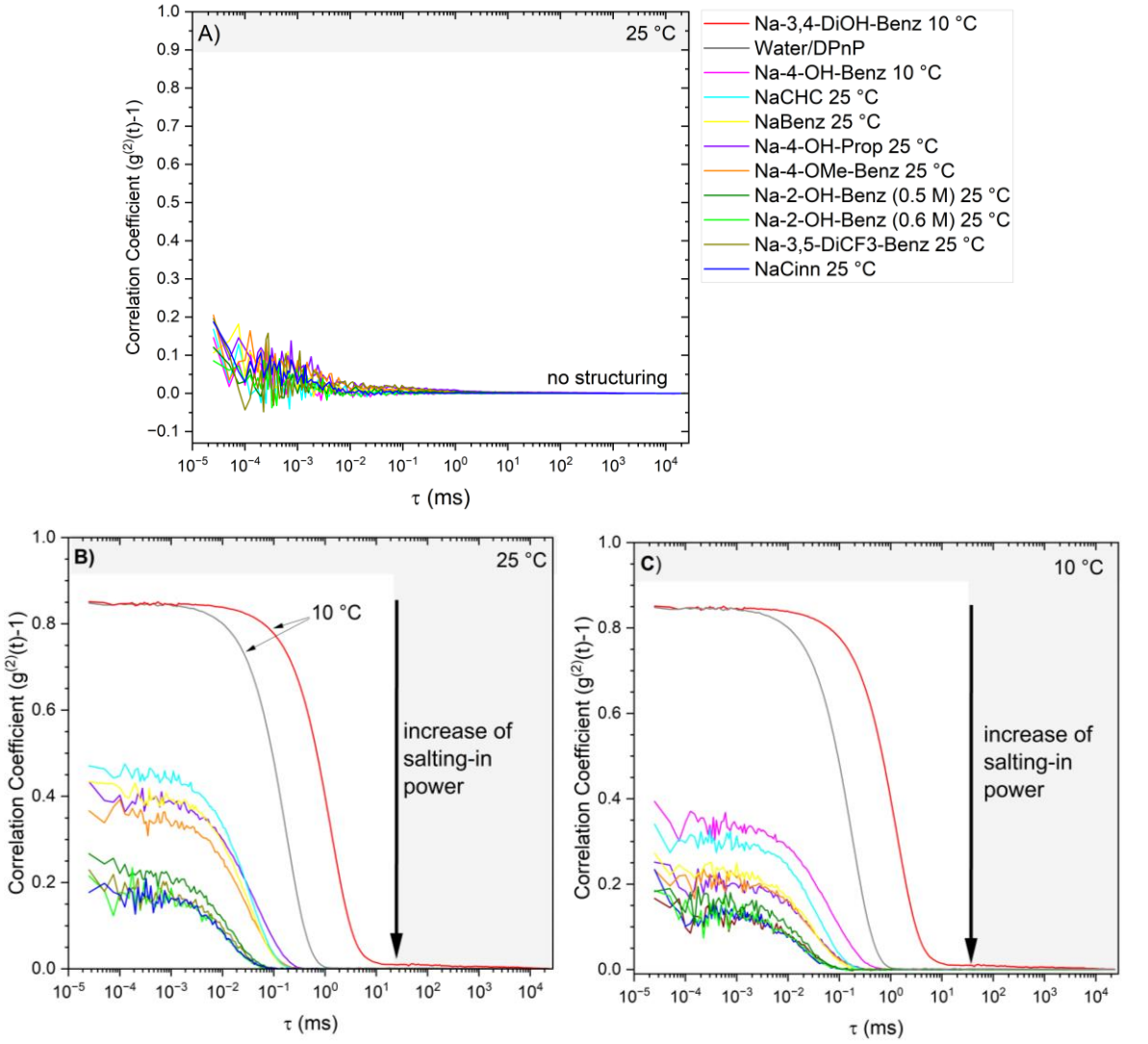

Figure 20: A) DLS correlation functions of 0.5 mol·kg^{-1} sodium polyphenolates and related compounds in pure water at 25 °C. B) DLS correlation functions of 0.5 mol·kg^{-1} sodium polyphenolates and similar compounds in a water/DPnP (45/55 (w/w)) system at 25 °C. C) DLS correlation functions of 0.5 mol·kg^{-1} sodium polyphenolates and similar compounds in a water/DPnP (45/55 (w/w)) system at 10 °C. The samples comprising Na-3,4-DiOH-Benz, Na-4-OH-Benz and the reference sample – a pure water/DPnP mixture (45/55 (w/w)) – were only measured at 10 °C due to turbidity in the water/DPnP system at 25 °C. Additionally, Na-2-OH-Benz was measured at 0.6 mol·kg^{-1} in water and in the water/DPnP system. τ = lag time, time delay for the detection. The samples were prepared in duplicate.[233]

Additionally, the correlation functions were less pronounced and stronger fluctuating at 25 °C, while a lower temperature reduced the nano-structuring in the water/DPnP system. Thus, the nearer the PTT of the sample to the temperature applied during the DLS measurement, the more defined is the correlation function and the larger the size of the observed aggregates. The reason therefore is presumably, the accumulation of DPnP at locally high concentrations prior to the macroscopic phase separation. This is logical, because micellization is also based on unfavorable interactions between water leading to a reduction of the contact with the solvent. Hence, sodium benzoate and cinnamate derived sodium polyphenolates improve the favorable interaction of DPnP with water and reduce the structuring tendency of DPnP in water.

Yet, the ability of NaBenz and NaCHC to reduce the DLS correlation function of the water/DPnP system does not correlate with their salting-in power form section 4.1.1.1. One reason therefore might be that small size of the two compounds could enable an inclusion of them into the DPnP nano-assemblies. Probably, because of its higher flexibility and due to its weaker binding affinity to water, NaCHC induced a more pronounced correlation function than NaBenz.[231]

Still, the DLS measurements of sodium polyphenolates and related compounds show that DPnP was not solubilized via developed aggregation but rather due to specific molecular interactions. Finally, the absence of nano-structuring of sodium polyphenolates and related sodium salts in pure water and the destruction of the nano-structuring in presence of DPnP compared to the water/DPnP without additives correlate to the hydrotrope theory of Shimizu.[33] Hence, the hydrotropic action of sodium polyphenolates is independent of their self-assemble properties in the pure water.[233]

4.1.1.3 Nuclear Magnetic Resonance measurements

Surface tension and DLS measurements from the previous two sections revealed that the solubilization of DPnP in water is not increased due to an aggregative potential of sodium polyphenolates but rather because of specific molecular interactions. To investigate the interactions of sodium polyphenolates with DPnP in aqueous solutions, ^{1}H-NMR and NOESY measurements of a 0.2 mol·kg^{-1} Na-4-OH-3-OMe-Cinn in the binary water/DPnP (45/55 (w/w)) system were performed, see section 7.4 in the Appendix. Na-4-OH-3-OMe-Cinn was used, because it was one of the best solubilizing agents for aromatic compounds in the section 4.1.2.1.1 and because its corresponding acid is known to be present in food and is used for skincare products.[94,248]

Regarding the ^{1}H-NMR spectrum of Na-4-OH-3-OMe-Cinn, Na-4-OH-3-OMe-Cinn's protons were minorly influenced by the presence of DPnP, see Figure A 3-Figure A 5 as well as Table A 24 in the Appendix. DPnP induced a slight change of the scalar coupling of Na-4-OH-3-OMe-Cinn's protons (H2: doublet of doublet → doublet; H1: doublet → singlet). The dissolution of DPnP in water comprising 0.2 mol·kg^{-1} of sodium ferulate led to a change of the chemical shift and of splitting of almost all protons of DPnP, see Figure A 2-Figure A 5, Table A 26. However, the origin of this is rather the interaction of DPnP with water. Nevertheless, cross-peaks of Na-4-OH-3-OMe-Cinn (Ha, H1, H2, H3, Hb) with several protons of DPnP (H1, H11, H3, H5, H9, H10 and H2) in the NOESY spectrum indicated that Na-4-OH-3-OMe-Cinn and DPnP are at least intermittently not further away from each other than 5 Å, see Figure 21 and Figure 22 .[249] However, more details about the specific interactions of DPnP with sodium ferulate were not accessible with NMR measurements.

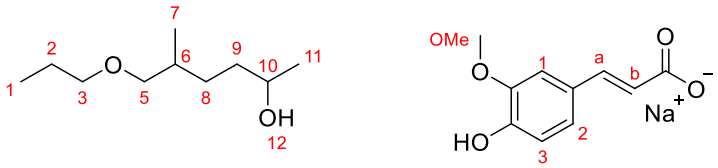

Di(propylene glycol) n-propyl ether (DPnP)

Sodium ferulate (Na-4-OH-3-OMe-Cinn)

Figure 21: Numeration of the protons of DPnP and sodium ferulate for ^{1}H-NMR analysis.

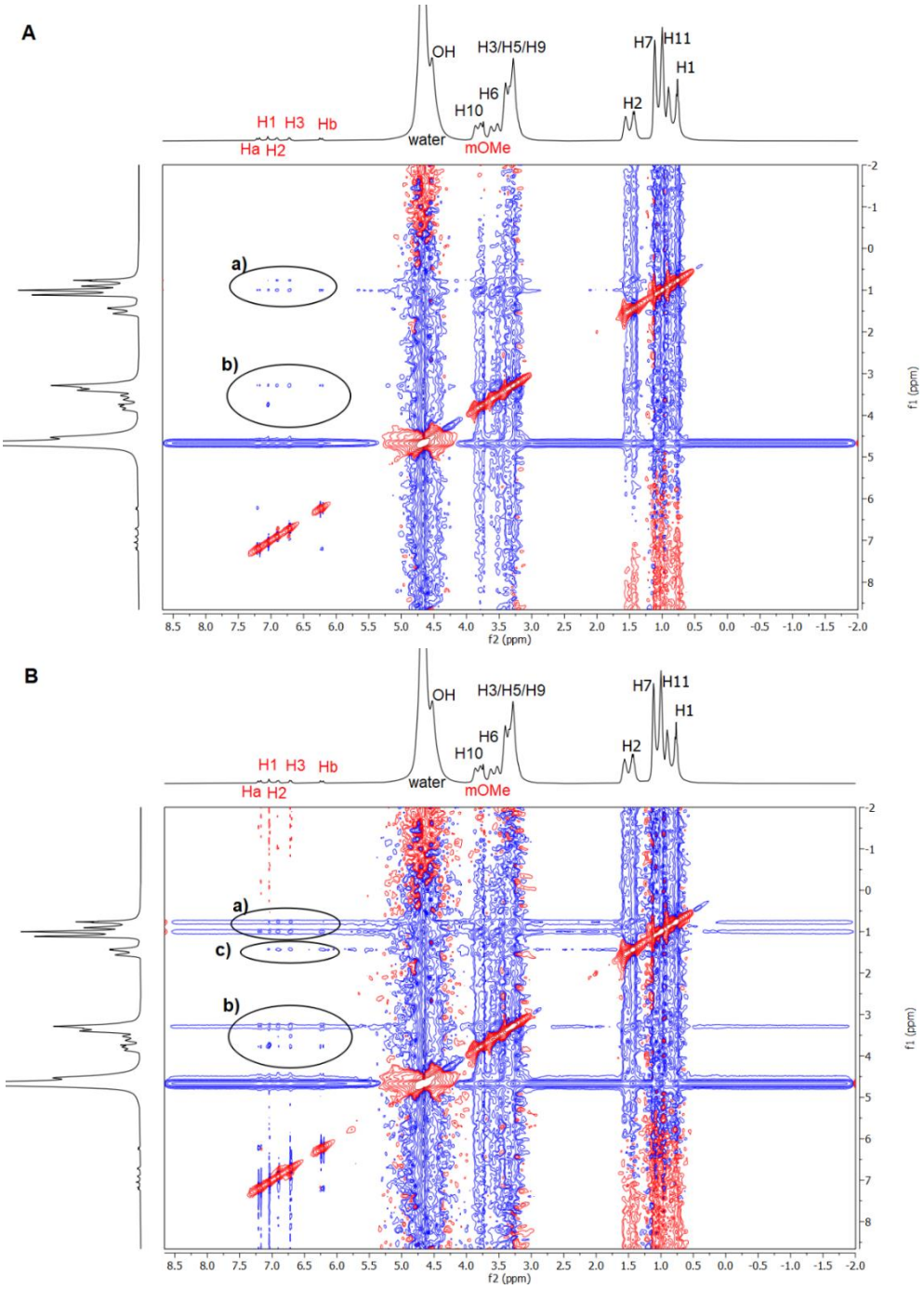

Figure 22: NOESY spectrum of a water/DPnP (45/55 (w/w)) mixture containing 0.2 mol·kg^{-1} Na-4-OH-3-OMe-Cinn Red: Protons of Na-4-OH-3-OMe-Cinn; black: Protons of DPnP. a) Cross-peak of Na-4-OH-3-OMe-Cinn's aromatic protons (Ha, H1, H2, H3, Hb) with H1 and H11 of DPnP; b) Cross-peak of Na-4-OH-3-OMe-Cinn's aromatic protons (Ha, H1, H2, H3, Hb) with H3, H5, H9 and H10 of DPnP, c) Cross-peak of Na-4-OH-3-OMe-Cinn's aromatic protons (Ha, H1, H2, H3, Hb) with H2 of DPnP. A) Low zoom; B) Strong zoom.[233]

4.1.1.4 Conclusion

Using simple PTT measurements, the salting-in/-out properties of the tested sodium polyphenolates were found to depend on the hydrophobic chain length. The salting-in/-out properties of sodium polyphenolates turned out to be precisely adjustable in the (anti-)hydrotrope range, depending on the functionalization of the aryl ring. Complimentary surface tension and DLS measurements of sodium polyphenolates in pure water confirmed the hydrotropic character of polyphenolates having a salting-in character.

Moreover, DLS and NMR measurements indicated a specific molecular interactions of polyphenolates with DPnP in water instead of highly structured aggregation. In line with this, the solubilizing properties of sodium polyphenolates in the water/DPnP system correlated to the classical hydrotrope theory.[32,42,234]

Regarding additionally the salting-in effect, the DLS correlation functions as well as the surface tension properties of the typical plant hormones indole-3-acetate and indole-3-butyrate in the same aqueous DPnP system, one can conclude that the tendency of the hydrotropes to form self-assemblies is independent of the hydrotropic solubilization of DPnP.[233,250]

As superchaotropic globular boron cluster anions having salting-in properties were exposed as membrane carriers (for cationic and neutral peptides, amino acids, neurotransmitters, vitamins, antibiotics and drugs) other salting-in agents might have also the potential to transport target molecules through membranes.[251] Exhibiting comparable salting-in power to sodium cholate, polyphenolates might assist biological solubilization processes and thus have a secondary biological function.[252]

4.1.2 Hydrotropic solubilization of aromatic compounds with polyphenolates

4.1.2.1 Riboflavin

4.1.2.1.1 Aqueous solubilization of riboflavin with sodium polyphenolates

A water-solubility of 0.27 ± 0.02 mmol·kg^{-1} is sufficient for the application of RF as coloring agent and for an ordinary supplementation with this vitamin. Yet, RF's low solubility might be disadvantageous for the yield in its biochemical synthesis, which correlates with the reactants' and products' solubility. Further, a RF solubilizer might also enable the high RF concentrations needed for injections, prevent precipitation of RF or improve the vitamin's bioavailability.[6,127,150] Due to RF's lability in alkaline medium, solubilizers for RF should maintain an acidic or neutral pH value.[8,253]

Based on a patent of lithium, potassium and sodium gallate as promising solubilizers for RF for pharmaceutical injection formulations, sodium polyphenolates were approached as potential solubilizers.[254] It was supposed that polyphenolic acids and/or their salts might solubilize RF via aggregation and/or via stacking.

Regarding the results from section 4.2.1, aggregation of polyphenolates around RF was supposed to be improbable due to the rather polar moieties of RF. Instead, RF's poor solubility in water should be overcome via weakening the stacking of RF with other RF molecules. As the polyphenolic compounds 3,4-dimethoxycinnamic acid, sodium benzoate and salicylate, were reported to stack in the crystal, to stack with theobromine and caffeine, respectively, they were supposed to stack with RF, too.[255–257] Due to their high natural abundance and low toxicity, polyphenolic acids and their corresponding salts, would be even applicable in food and beverage formulations as well as in pharmaceutical products.[258] The solubility of RF was determined via UV-Vis-absorbance measurements after saturation with RF.

First, vanillic, ferulic and cinnamic acid were tested as solubilizing agents for RF, see Figure 23. However, RF's water-solubility was either minorly or not increased at all. Better solubilization of RF was supposed to be realized by increasing the concentration of the solubilizer. Therefore, the acids were neutralized with sodium hydroxide to obtain the more water-soluble sodium polyphenolates. Sodium was used, as it is the major cation in the extracellular fluid.[125,126] As polyphenolic acids are known to be resorbed into the blood with a pH-value of 7.35-7.45, where their deprotonated form should be prevalent, sodium polyphenolates constitute important salts for biochemical systems.[105,124] The pH-value of all sodium polyphenolate solution was tested with indicator paper to be around 7, to exclude a pH effect on the solubility of RF.

Regarding Figure 23, sodium ferulate, vanillate and cinnamate behaved equally to their corresponding acids for concentration in the mircomolar range. However, when applied at higher concentrations, sodium polyphenolates solubilized RF more efficiently in water. Thus,

with one of the best solubilizers, Na-3,4-DiOMe-Cinn, the solubility of RF was increase by more than 2000 times at a molar additive/RF ratio of 7.8, see Table A 53 in the Appendix.

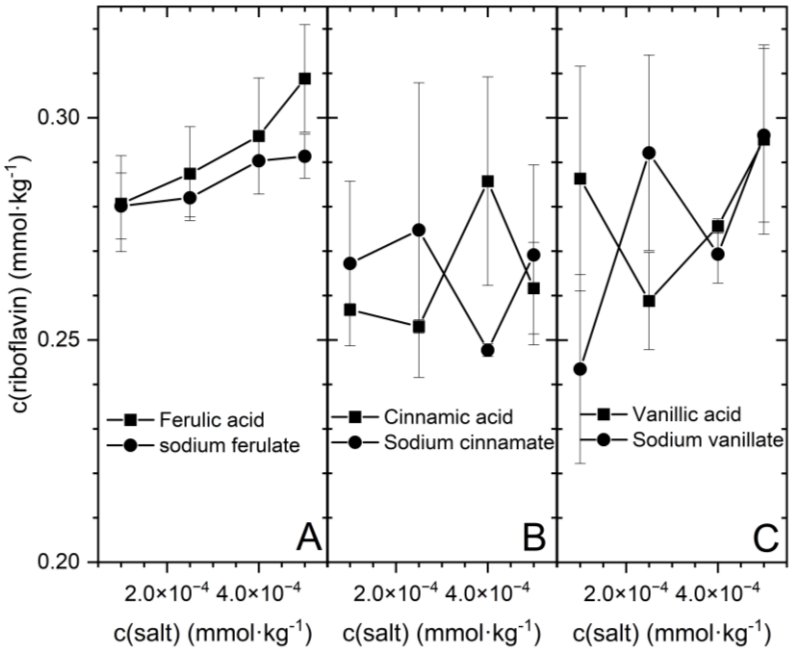

Figure 23: Solubilization of RF by means of polyphenolic acids and their corresponding sodium salts.

To further analyze the underlying mechanism of RF's solubilization in water, the RF solubilizing properties of polyphenolate-related compounds, of a salting-in and -out agent, of a common hydrotrope and of a surfactant were compared to the ones of sodium polyphenolates.

In general, the solubility of RF in water increased exponentially with the concentration of sodium cinnamate and benzoate derivatives, such as it is typical of amphiphilic solubilizers, see Figure 24 A and B.[225]

In correlation with the amphiphilic character, the curves obtained with NaBenz and its derivatives exhibited a slightly reduced linearity in the log-log-plot compared to the ones obtained with the more amphiphilic sodium cinnamate derivatives, see Figure 24 C and D. Thus, all substituted and unsubstituted sodium cinnamates were revealed as more potent solubilizers for RF in water than the corresponding sodium benzoates (NaCinn > NaBenz; Na-2/3/4-OH-Cinn > Na-2/3/4-OH-Benz; Na-4-OMe-Cinn > Na-4-OMe-Benz; Na-3,4-DiOMe-Cinn > Na-3,4-DiOMe-Benz; Na-4-OH-3-OMe-Cinn > Na-4-OH-3-OMe-Benz; Na-3,4-DiOH-Cinn > Na-3,4-DiOH-Benz; Na-4-OH-3,5-DiOMe-Cinn > Na-4-OH-3,5-DiOMe-Benz), see Figure 24 A-D. A break point that might indicate a minimum hydrotropic concentration (MHC) corresponding to the onset of the solubilization, was not observed in the log-log-plot, see Figure 24 C and D. However, NaBenz and NaCinn as well as their derivatives were exposed as classical hydrotropes in section 4.1.1 and hydrotrope must not necessarily have a MHC.[33]

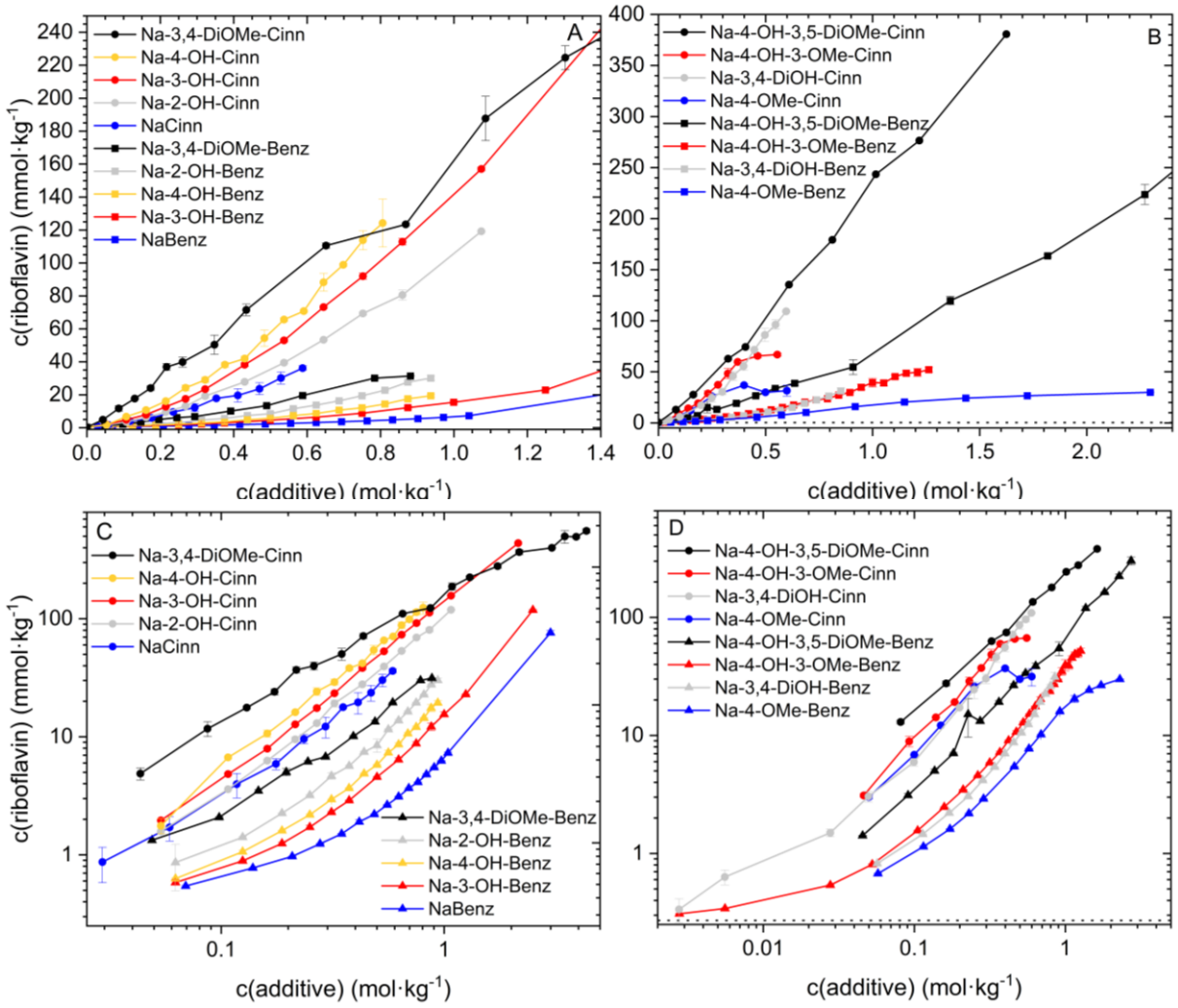

Figure 24: Water-solubility of riboflavin in presence of different sodium cinnamates and benzoates. A) Monosubstituted and dimethoxy substituted compounds, B) Mono-, di- and trisubstituted compounds. C and D correspond to the diagram A and B in a log-log-plot, respectively.

Although the log-log-plot did not reveal the presence of an MHC, the molar solubilizer/RF ratio in the plot from Figure 25 decreased rapidly with the solubilizer's concentration after a maximum ratio was reached. The higher this ratio in Figure 25, the more solubilizer molecules per one RF molecule were present in the solution. Consequently, the maximum ratio corresponds to the solubilizer concentration, which exhibits the lowest efficiency for the solubilization of RF in water. For each additive, this maximum ratio was different and each additive reached this point of its lowest RF solubilizing efficiency at a different additive concentration. Therefore, this concentration might correspond to a MHC, above which the molar additive/RF ratio decreases and thus the solubilizing efficiency increases. For the additives in Figure 25, the maximum ratio and thus the worst efficiency was reached at additive concentrations < 0.21mol·kg^{-1}. Yet, the CACs of NaBenz and NaCinn as well as their derivatives obtained from surface tension measurements were usually >> 0.2 mol·kg^{-1}, see section 4.1.1.2.1. On the other side, a CAC and MHC of hydrotropes does not necessarily have to be equal.

After reaching a minimum ratio, often, the solubilizer/RF ratio did not change upon further increasing the additive concentration. Only, in some cases, the molar additive/RF ratio increased again after reaching a minimum molar ratio (Na-4-OH-3-OMe-Cinn, Na-4-OMe-Benz, Na-4-OMe-Cinn, Na-2,3-DiOH-Benz, Na-2,4-DiOH-Benz). Commonly, the solubility limit of sodium polyphenolates in water was the onset of the anew increase of the molar solubilizer/RF ratio (Na-4-OH-3-OMe-Cinn, Na-4-OMe-Cinn, Na-2,3-DiOH-Benz and Na-2,4-DiOH-Benz). Consequently, the loss on solubilizing efficiency with increasing additive concentration originates from the lack of the solubilizer's water-solubility. Still, the solubility of the polyphenolate did not correlate with its solubilizing power. According to Kunz et al., this discrepancy between their solubilizing power and water-solubility is not unusual for hydrotropes.[29] Thus, so far, the solubilization trend is in line with the classical hydrotrope theory, where mostly the hydrotrope's amphiphilic character is decisive for the solubilization.[32,33,37,259]

However, the best molar solubilizer/RF ratios were obtained with Na-2,4,6-TriOH-Benz (4.5 at 0.08 M), Na-4-OH-3,5-DiOMe-Cinn (4.2 at 1.02 M), Na-3,4-DiOMe-Cinn (5.8 at 1.09 M) and Na-4-OH-3-OMe-Cinn (6.2 at 0.37 M) and not with entirely amphiphilic solubilizers (NaCinn, NaBenz, NaButyrate, NaValerate), see Figure 25. Hence, the highest solubility of RF (560 ± 20 mmol·kg^{-1}) was reached with an aqueous 4.34 mol·kg^{-1} Na-3,4-DiOMe-Cinn solution, although the compound cannot be regarded as flawlessly amphiphilic. Therefore, amphiphilicity is not the main criterium to be suitable as RF solubilizer.

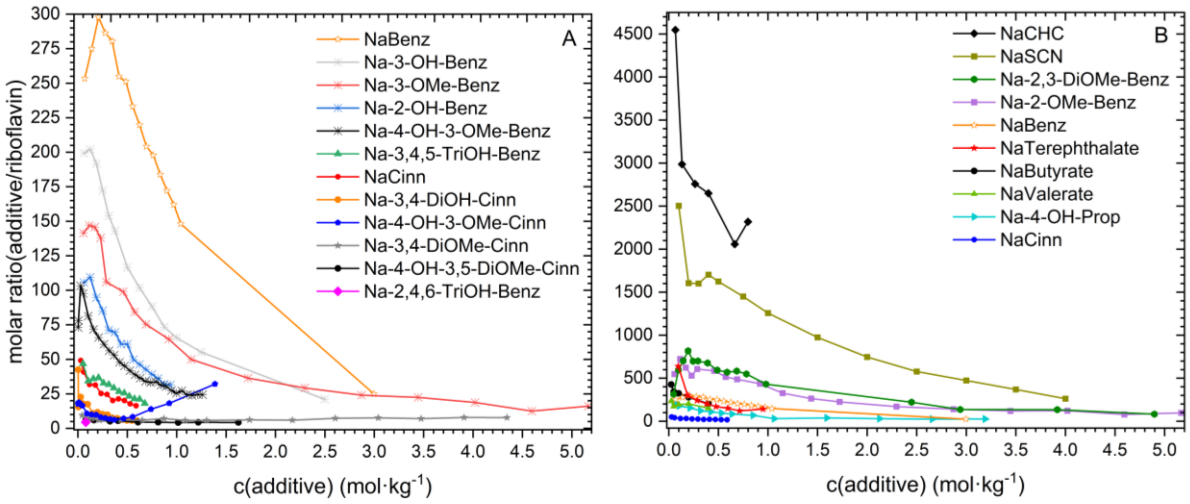

Figure 25: Molar solubilizer to riboflavin ratio versus the solubilizer concentration in water. The ratio was determined by division of the additive concentration by the riboflavin solubility after subtraction of the solubility of riboflavin in pure water, see equation 2 in section 2.3. A: Medium to good sodium salts; B: Good to bad solubilizers. In the case of insoluble sodium polyphenolates, the ratio was calculated from the added amount of the polyphenolate and the measured riboflavin concentration.

Analogously, the substitution of benzoate/cinnamate with a hydroxy group in meta and para position improved also the solubilization power for RF in water, although the solubilizer's amphiphilicity was reduced by this substitution. For instance, Na-3,4-DiOH-Cinn solubilized ca. 2.5 times more RF than NaCinn at an additive concentration of 0.3 mol·kg^{-1}. Analogously, at a

concentration of ca. 0.4 mol·kg^{-1}, Na-3,4,5-TriOH-Benz solubilized even at least 8 times more RF in water than NaBenz.

Further, the solubilization power of the additives increased with increasing number of hydroxy groups bound to the sodium benzoate and cinnamate aryl ring (Na-3,4,5-TriOH-Benz > Na-3,5-DiOH-Benz > Na-3,4-DiOH-Benz > Na-4-OH-Benz > Na-3-OH-Benz > NaBenz; Na-2,4,6-TriOH-Benz > Na-2,4-DiOH-Benz > Na-2-OH-Benz > Na-4-OH-Benz > NaBenz; Na-3,4-DiOH-Cinn > Na-4-OH-Cinn > Na-3-OH-Cinn > NaCinn), see Figure 26 A-C. Successive substitution of the sodium benzoate and cinnamate backbone with methoxy groups increased the solubilization power of the additives, too (Na-3,4-DiOMe-Cinn > Na-4-OMe-Cinn > NaCinn; Na-3,5-DiOMe-Benz > Na-3,4-DiOMe-Benz > Na-4-OMe-Benz > Na-3-OMe-Benz > NaBenz), see Figure 26 D.

Although the substitution of the benzoate and cinnamate backbone with methoxy and hydroxy groups on meta and para position reduces the amphiphilic character of the solubilizers relatively to the unsubstituted benzoate and cinnamate, meta and para substituted compounds solubilized more RF than NaBenz and NaCinn. Consequently, the solubilization mechanism for RF is not the same as for DPnP from section 4.1.1, where the salting-in/-out properties of sodium cinnamate and benzoate derivates on DPnP were predictable with regard to the amphiphilic character of the additives. For the aqueous solubilization of RF with sodium polyphenolates, the amphiphilic character has apparently only a minor effect on their solubilization properties.

Nevertheless, again in correlation to the classical hydrotrope theory, a mono- and di-substitution of benzoate with a methoxy group in ortho and ortho/meta position reduced the solubilization power relatively to NaBenz because of a reduction of the solubilizer's amphiphilicity (NaBenz > Na-2-OMe-Benz > Na-2,3-DiOMe-Benz), see Figure 26 D. Probably, the hydration of the carboxylate is impeded due to the sterical demand and due to the hydrophobic character of this functional group. In line with this, hydroxy groups in the ortho position increased the solubilizer's amphiphilicity and thus increased the solubilization efficiency of the compounds enormously (Na-2,4,6-TriOH-Benz, Na-2,4-DiOH-benz, Na-2,3-DiOH-Benz; Na-2-OH-Benz), see Figure 26 B. To be exact, Na-2-OH-Benz solubilized 3-5 times more RF than NaBenz over the whole concentration range tested. Two hydroxy groups in ortho position increased the solubilization power compared to NaBenz so strong that Na-2,4,6-TriOH-Benz was even more efficient than the best sodium cinnamate derivates (Na-3,4-DiOMe-Cinn, Na-4-OH-3,5-DiOMe-Cinn) tested, Figure 28 A. Sodium benzoates substituted with hydroxy group(s) in ortho position are probably enormously potent RF solubilizers, because the intermolecular hydrogen bond between the adjacent carboxylate and the hydroxy group in ortho position leads to an increased amphiphilicity and better hydration.[230]

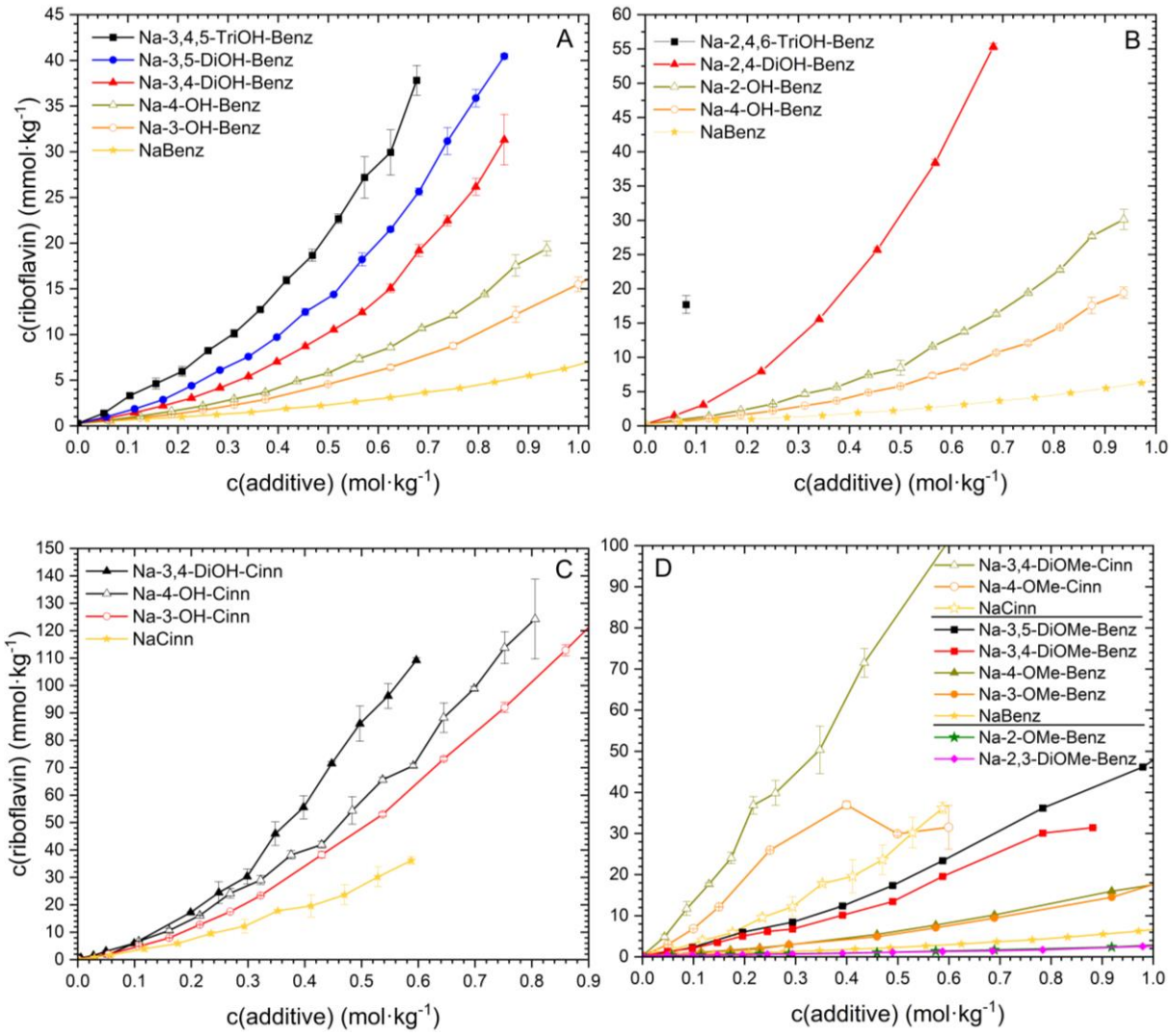

Figure 26: Water-solubility of RF depending on the number of hydroxy and methoxy groups on the aryl ring of a sodium benzoate or cinnamate salt. A and B: Dependence on the number of hydroxy groups on a sodium benzoate backbone; C: Dependence on the number of hydroxy groups on a sodium cinnamate backbone; D: Dependence on the number of methoxy groups on a sodium cinnamate and benzoate backbone.

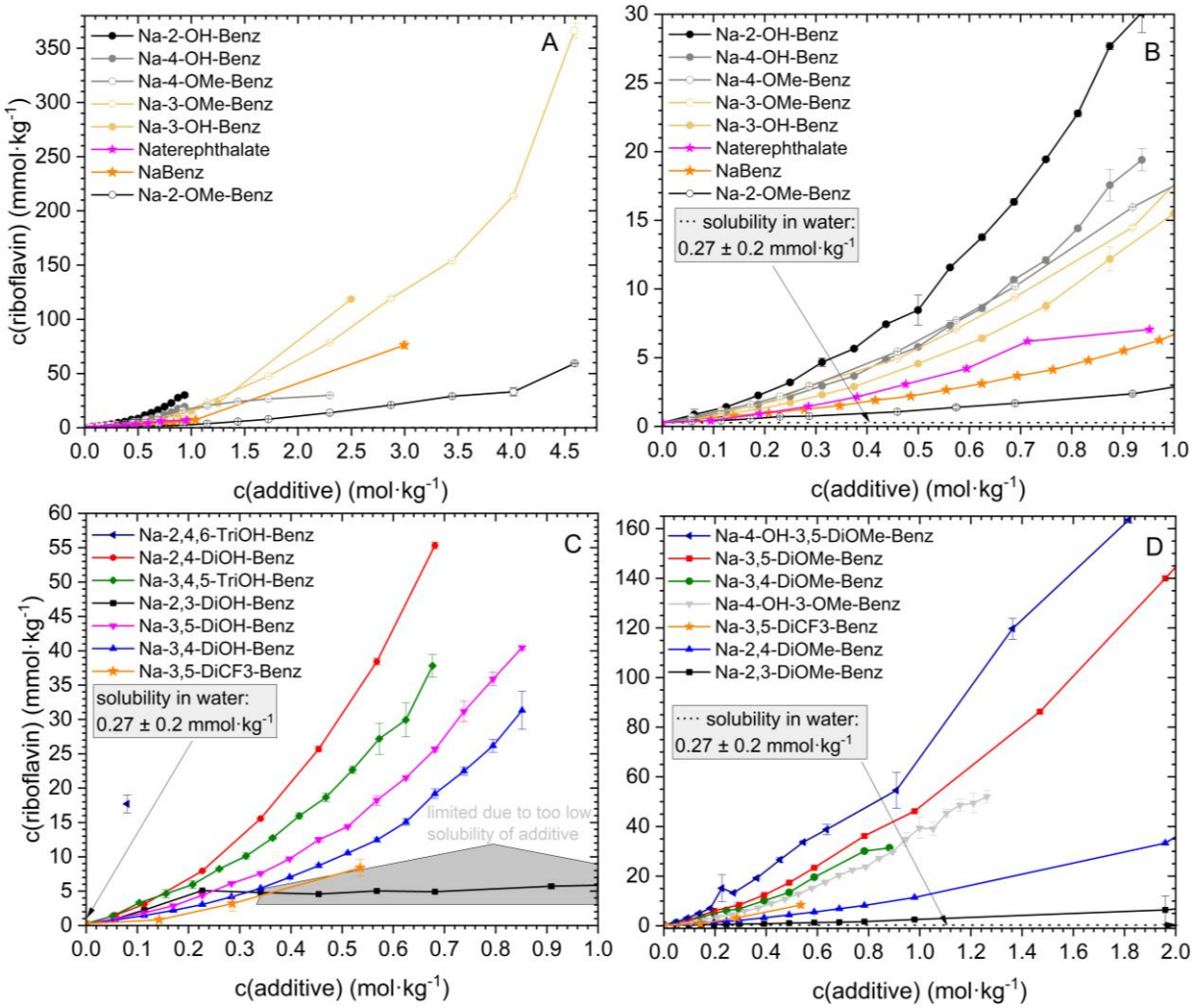

Figure 27: A: Water-solubility of riboflavin in presence of mono-substituted sodium benzoates; B: Enlarged view of A; C: Water-solubility of riboflavin in presence of di-/tri-hydroxy and trifluoromethyl-substituted benzoates; D: Water-solubility of riboflavin in presence of di-/tri-methoxy- and trimethylfluoro-substituted sodium benzoates.

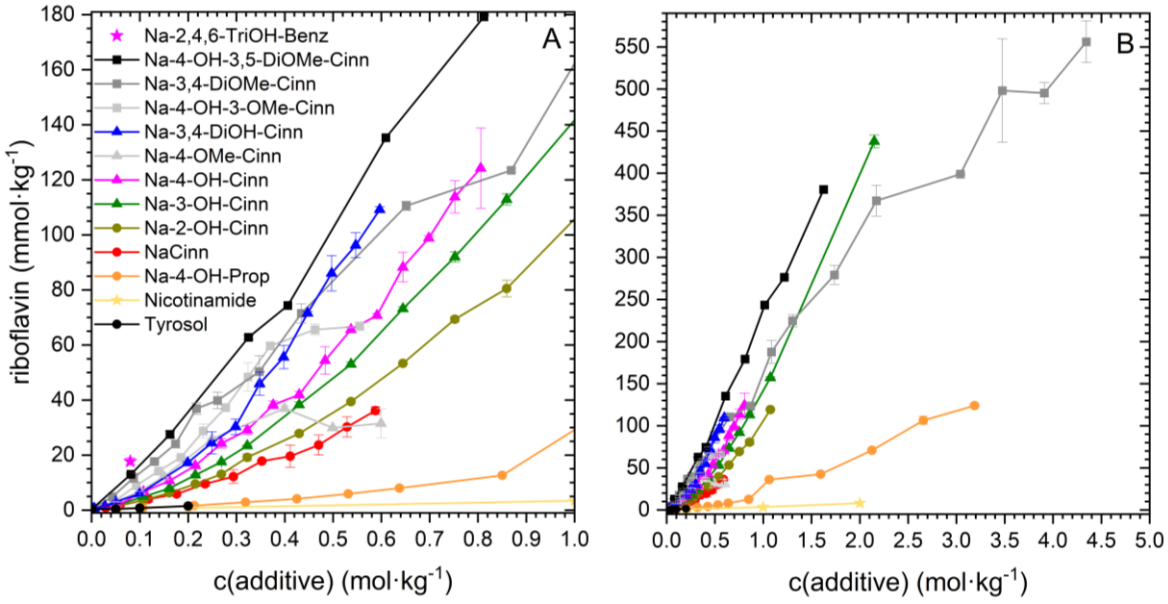

Figure 28: Water-solubility of riboflavin in water in presence of sodium cinnamate derivatives, sodium 2,4,6-trihydroxybenzoate and sodium nicotinate. A: Solubilization curves for 0-1 mol·kg-1 of the additives; B: Solubilization curves for 0-5 mol·kg-1 of the additives. The values for nicotinamide were taken from Coffman and Kildsig.[182]

Further observations in the solubilization of RF by sodium polyphenolates in water:

A) In the case of a mono-substitution of NaBenz and NaCinn with one methoxy or hydroxy group, a para substitution led to a better solubilizer for RF than a meta one and this more than an ortho substitution (Na-4-OH-Benz > Na-3-OH-Benz; Na-4-OH-Cinn > Na-3-OH-Cinn > Na-2-OH-Cinn; Na-4-OMe-Benz > Na-3-OMe-Benz > Na-2-OMe-Benz), see Figure 27 A and B and Figure 28.

B) For meta and para position for solubilizers with a benzoate backbone, methoxy groups were revealed to improve the solubilization power more strongly than hydroxy groups (Na-4-OMe-Benz > Na-4-OH-Benz; Na-3-OMe-Benz > Na-3-OH-Benz; Na-4-OMe-Cinn > Na-4-OH-Cinn), see Figure 27 A and B and Figure 28.

C) Further, additives comprising directly neighbored functional groups solubilized less RF than additives comprising functional groups apart from each other (Na-2,4-DiOH-Benz > Na-2,3-DiOH-Benz; Na-3,5-DiOH-Benz > Na-3,4-DiOH-Benz; Na-3,5-DiOMe-Benz > Na-3,4-DiOMe-Benz; Na-2,4-DiOMe-Benz > Na-2,3-DiOMe-Benz), see Figure 29 and Figure 27 C and D.

D) At the same concentrations, the aromatic tyrosol solubilized less RF in water than Na-4-OH-Benz. Therefore, the carboxylate group of polyphenolates can promote their solubilizing properties for RF in water, but it is not crucial for the solubilization.

The findings A, C and D indicate that hydration influences the aqueous solubilization of RF. Thus, probably, the approach of non-neighbored functional groups on the aryl ring by water is sterically easier as non-neighbored hydroxy and methoxy groups have a larger interaction surface with water than neighbored ones. However, according to point B, hydration alone cannot be the main driving force for the aqueous solubilization of RF by sodium polyphenolate. Otherwise, hydroxy groups – as (i) less hydrophobic, (ii) better hydrated and (iii) better hydrogen bond partners – should always solubilize more RF than methoxy groups.

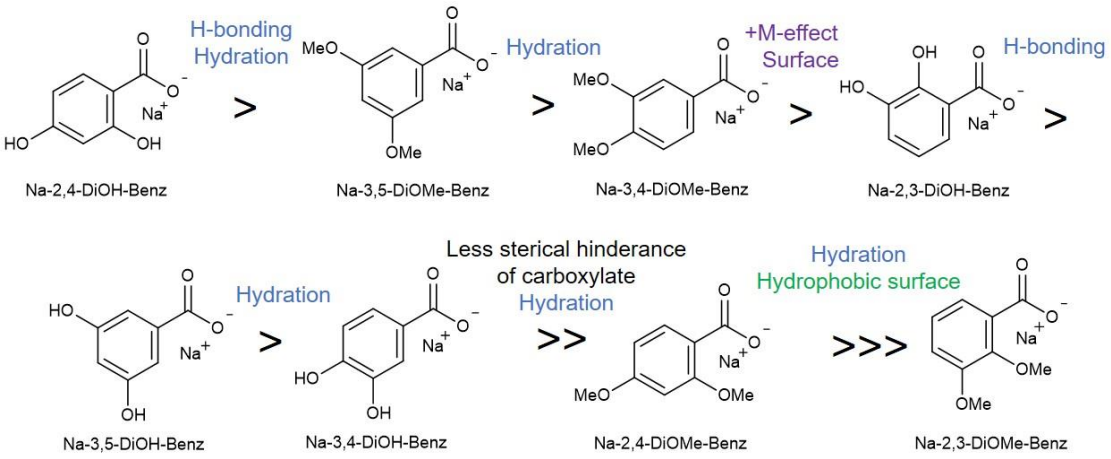

Figure 29: Solubilization power of di-substituted sodium benzoates for riboflavin in water with the possible reason, why the righter compound is more efficient than the one to its left. The corresponding solubilization curves are displayed in Figure 27 C and D.

The following observations suggest a great importance of the solubilizers π-system and thus a great importance of the planarity for the RF-solubilization performance of sodium polyphenolates:

i) With increasing positive mesomeric and lower negative inductive effect of the functional groups on the aryl ring (OMe > OH > CF3 > COO^-), the solubilization power of the aromatic solubilizers for RF in water increased, see Figure 27 B-D above. Thus, the hydrophobic Na-3,5-DiCF3-Benz – proofed via surface tension and cloud point measurements of DPnP in water in section 4.1.1 –, solubilized less RF than Na-3,5-DiOH-Benz and Na-3,5-DiOMe-Benz. Sodium terephthalate solubilized less RF than Na-4-OH-Benz and Na-4-OMe-Benz.

ii) Regarding the strong influence of the size of the solubilizers conjugated electronic system, the superior solubilization power of sodium cinnamates to the one of sodium benzoates might also originate from the larger π-system of cinnamates leading to a larger planar potential interaction surface.

iii) An enlargement of the size of the conjugated electronic system when going from Na-4-OH-Prop to Na-4-OH-Benz to Na-4-OH-Cinn improved the solubilization power for RF, see Figure 28. Further, tyrosol solubilized RF despite of its reduced amphiphilicity compared to Na-4-OH-Cinn and Na-4-OH-Benz, see Figure 28 Additionally, 0.08 $mol \cdot kg^{-1}$ phloroglucinol solubilized 1.7 ± 0.2 $mmol \cdot kg^{-1}$ RF in water, although it was less efficient than Na-2,4,6-TriOH-Benz. Thus, the presence of a carboxylate group improves the solubilizing power but is not essential for the RF solubilizing properties of sodium polyphenolates.

To evaluate the solubilization mechanism in the solubilization of RF by means of sodium polyphenolates in water further, (i) a salting-out agent and (ii) one salting-in agent , (iii) two standard hydrotropes (nicotinamide, sodium xylene sulfonate), (iv) a standard surfactant as well as polyphenolate-like compounds with (v) different chain lengths and (vi) variation of the electron conjugation were analyzed, see Figure 30. The observations are listed below:

A) Though just minorly in comparison to sodium polyphenolates, but the salting-in and -out agents NaSCN and NaH_2PO_4 increased and decreased, respectively, the solubility of RF compared to pure water. Still, even NaBenz solubilized largely more RF in water than NaSCN.

B) Despite its lipophilic methyl groups, SXS exhibited a RF-solubilizing power comparable to NaBenz. The reason therefore, is probably the weaker hydration of a sulfonate group compared to a carboxylate group that might compensate the larger hydrophobic residue of SXS.[42] On the contrary, sodium phenyl phosphate, which should be strongly hydrated at its phosphate group, was one of the worst solubilizers in Figure 31, though causing a basic pH at which RF should be even more soluble than at the neutral pH-value of NaBenz solutions. Thus, the hydration of the solubilizer's head group seems to influence the solubilization power.

C) The surfactant SDS increased the solubility of RF in water more than the salting-in agent NaSCN and more than NaBenz. Still, the less amphiphilic NaCinn solubilized > 4 times more RF than SDS at an additive concentration of 0.4 mol·kg^{-1}.

D) An elongation of the hydrophobic side chain increased the RF solubilizing power of aromatic additives (NaBenz < NaButyrate < NaValerate). Yet, the aqueous solubility of RF depended minorly on the hydrophobic chain length of the solubilizers. Thus, NaValerate solubilized only about 29 % more RF than NaButyrate and NaButyrate solubilized only 24 % more RF than NaBenz at an additive concentration of 0.4 mol·kg^{-1}.

E) Na-4-OH-Prop was exposed as better solubilizing agent than the more amphiphilic NaValerate and NaButyrate. Further, Na-2,4-Pentadienoate and the less amphiphilic Na-4-OH-3-OMe-Cinn exhibited a similar RF solubilizing power. This proves once more that a flawless amphiphilic character is not necessary to act as good RF solubilizer.

F) Apparently, the substitution of NaBenz of the aryl ring with a carboxylate group (NaTerephthalate) improved the solubilizing properties. Yet, two carboxylate groups on the side chain (Na-Phenylsuccinate) weakened the solubilizing efficiency compared to NaBenz. Analogously, the modification of the side chain with a hydroxy group (Na-DL-Mandelate), worsened the solubilizing power compared to NaBenz. Hence, carboxylate and hydroxy groups, which increase the solubilizers amphiphilicity led to a weaker solubilizing power.

G) In spite of the same chemical formula, NaBenz and Na-2,4-Pentadienoate solubilized more RF than NaCHC and NaValerate, respectively, see Figure 30. Thus, over the whole tested solubilizer range, the concentration dependent RF solubilization efficiency of the solubilizer (molar ratio of additive/RF) was increased 6 to 20 times when comparing NaValerate with Na-2,4-Pentadienoate, and 2 to 4.5 times when comparing NaCHC to NaBenz, see Table A 27, Table A 28, Table A 59 and Table A 60. The only difference between the solubilizers was the size of their π-system. Consequently, the induction or enlargement of the solubilizer's electronic π-system improved the solubilizing properties of the additives more than the elongation of the hydrophobic side chain described in point D. The reason for this effect might be the correlation of the molecules' conjugated electronic system with their planarity, which increases the potential interaction surface through dispersive interactions.

H) Regarding subpoint G, the weaker RF solubilization power of nicotinamide compared to NaBenz might result from the electronegative nitrogen atom in the pyridine ring, which leads to a depletion of the electron density in the aryl ring, as it is already known for pyrimidine rings comprising not only one but two nitrogen atoms in their aromatic ring.[260] A depletion of the electron density by oxygen in the aryl ring, is probably also the reason for the weak solubilization of RF in presence of NaCoumalate.

Observations A and B from above indicate once more that an increased hydration of the solubilizer can improve the solubility of RF in water. According to the points C to F, the size of the hydrophobic part, which correlates with the solubilizers' amphiphilicity and would be decisive for the inclusion of RF into potential sodium polyphenolate aggregates, can but does not necessarily have to determine the additives' RF solubilizing power. Instead, the conjugated electronic system of the additives is the domineering factor in the solubilization of RF in water. The larger the π-system of the solubilizer was, the more RF was solubilized in water and the more efficient was the solubilizer (low molar additive/RF ratio). Hence, a substitution of the sodium benzoate and cinnamate backbone with functional groups exhibiting a positive mesomeric and a low minus inductive effect improved the RF solubilizing properties relatively to NaBenz and NaCinn. Further, the solubilizer's conjugated electronic system turned out as even more important than the retention of the solubilizer's amphiphilic character. Regarding the points C to H, the strong dependence of the RF solubilizing power on the size and type of the solubilizers' conjugated electronic system, which correlates with the additive's planarity, indicates that dispersive interactions are dominant in the solubilization of RF.

As the solubilization of RF was strongly driven by the size of the aromatic π-system of the solubilizer, sodium diphenate and tannin were tested. Consisting of two NaBenz units, NaDiphenate was expected to double the solubility of RF. However, NaDiphenate exhibited even weaker solubilizing properties than NaBenz, see Figure 30.

Analogously, tannin – an oligomeric form of 10 gallic acid molecules – turned out as less efficient solubilizer than Na-3,4,5-TriOH-Benz, when regarding tannin's solubilizing power in its "monomeric" form, see Table A 66 in the Appendix. As a rubbery precipitate was observed within some hours in presence tannin, solubilization of RF with tannin would not be possible anyway. Because the space demand of the solubilizer and solute was found to matter in the solubilization of RF-PO_4, RF and LC, see section 4.1.2.1.9, tannin and diphenate are probably too bulky for a strong interaction with RF.

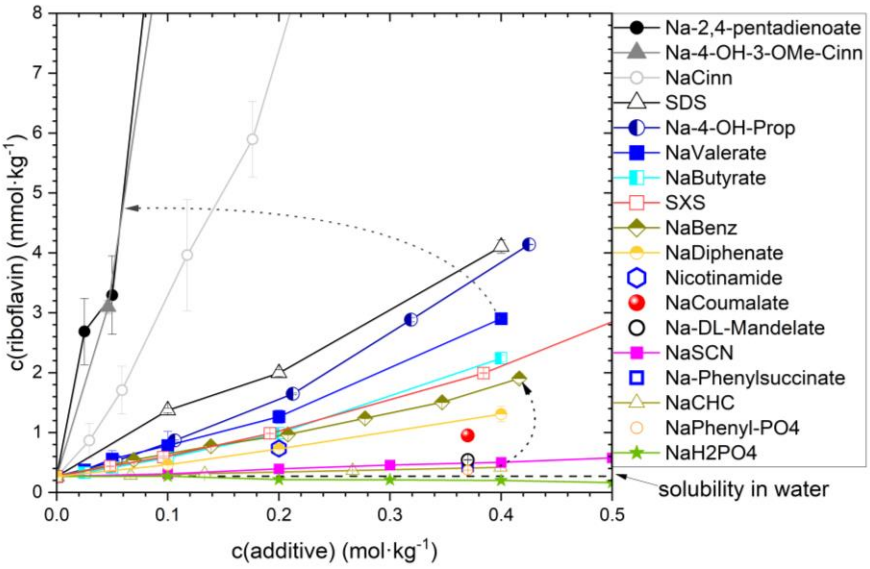

Figure 30: Water-solubility of RF in presence of aromatic sodium salts, of sodium cyclohexane carboxylate, of a surfactant, of a salting-in and salting-out agent in water. Riboflavin's solubility in pure water is indicated by a dashed line. The curved arrows mark the induction of a larger electronic system. The values for nicotinamide were taken from Coffman and Kildsig.[182]

In Figure 31, all additives tested as solubilizing agents for RF in water are ordered according to their solubilizing efficiency (molar additive/RF ratio).

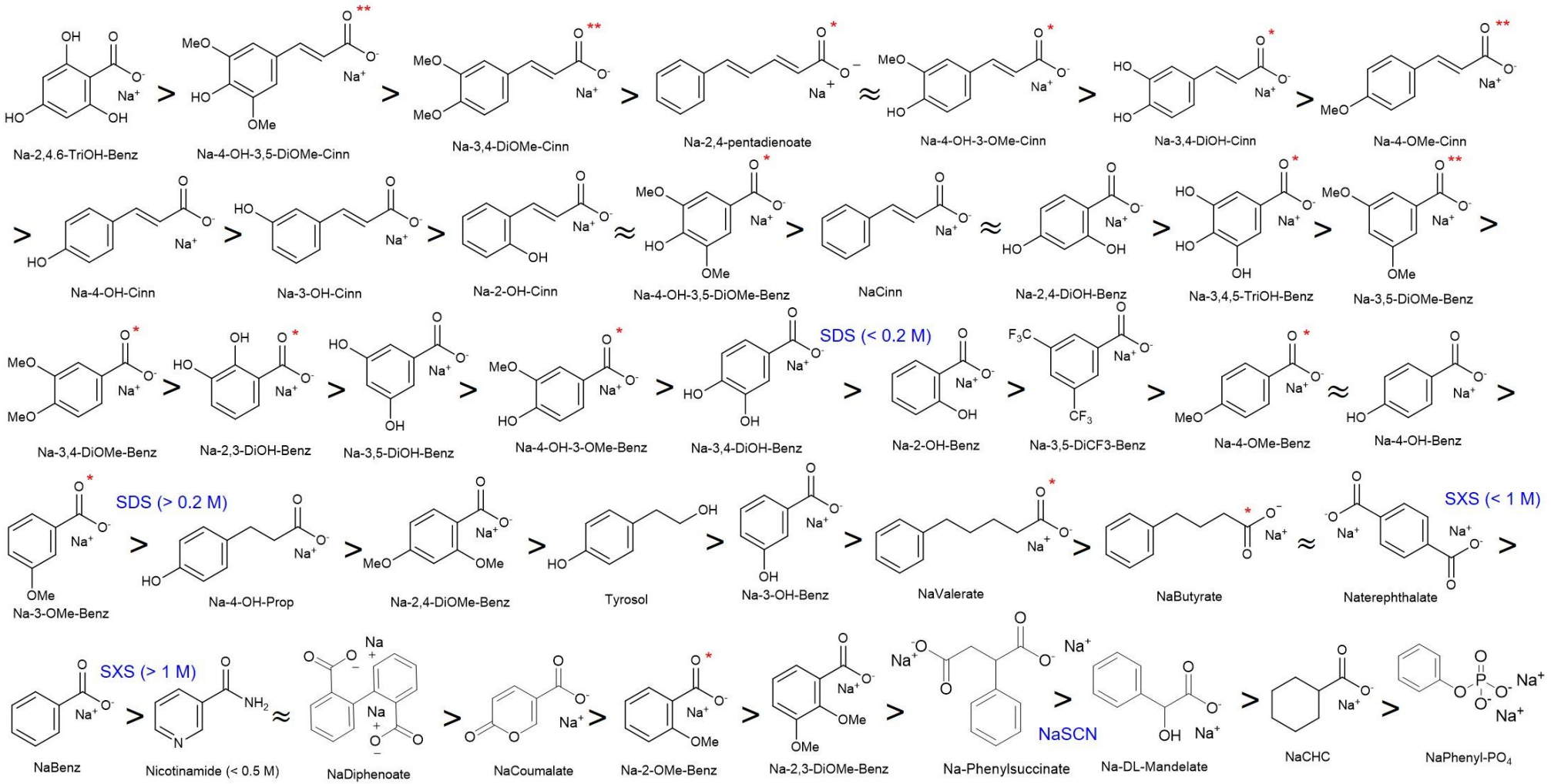

Figure 31: Riboflavin solubilizers – sodium benzoates and cinnamates as well as related compounds, sodium dodecyl sulfate, sodium thiocyanate, nicotinamide[182] *and sodium xylene sulfonate – in the aqueous medium ordered according to their riboflavin solubilizing efficiency. Sometimes the slope of the solubilization curves changed with the concentration, therefore the solubilization power was regarded above 0.2 mol·kg*$^{-1}$ *of the additive concentration. For polyphenolic compounds, which were not tested above 0.2 mol·kg*$^{-1}$*, at least a linear increase of the riboflavin solubility was assumed to categorize the compound. All samples (nicotinamide not tested) exhibited ca. pH 7, tested with indicator paper, to exclude a pH contribution to the solubilization. *Riboflavin further increased the aqueous solubility of the compound, too. **Not only the compound itself solubilized riboflavin, but riboflavin solubilized the totally insoluble compound in water, too. M = mol·kg*$^{-1}$

Aside of the strong dependence of RF's aqueous solubility on the solubilizer's aromatic system, a concentration dependent bathochromic shift of RF's absorption spectrum was observed in presence of "electron-rich" additives. The change of RF's absorption spectrum by the presence of sodium polyphenolates corresponds to a so-called copigmentation. This phenomenon is often mentioned in relation with anthocyanins. It originates frequently from a non-covalent complexation of a colored solute with a non-colored solubilizer leading to an intensification or alteration of the solute's color.[261–263]

In Figure 32, the shift of RF's absorption spectrum is depicted for differently concentrated aqueous solutions comprising sodium ferulate and RF at a constant molar ferulate/RF ratio of 7.4. Due to the effect of polyphenolates on RF's absorption spectrum, the samples' coloration changed from yellow (absorbance mainly in the blue region) to orange, red (absorbance in the green/blue region) and almost to black with rising polyphenolate and RF concentration, see Figure 32 on the top right a-f. For RF in high concentrated aqueous solution of sodium benzoate derivatives, a maximum reddish coloration was observed. Moreover, for most aromatic sodium carboxylates, the samples' color changed significantly only for additive concentrations > 0.1 mol·kg^{-1}. Interestingly, the absorption maxima of RF at 371 and 445 nm were not affected by sodium polyphenolates, see Figure 32.

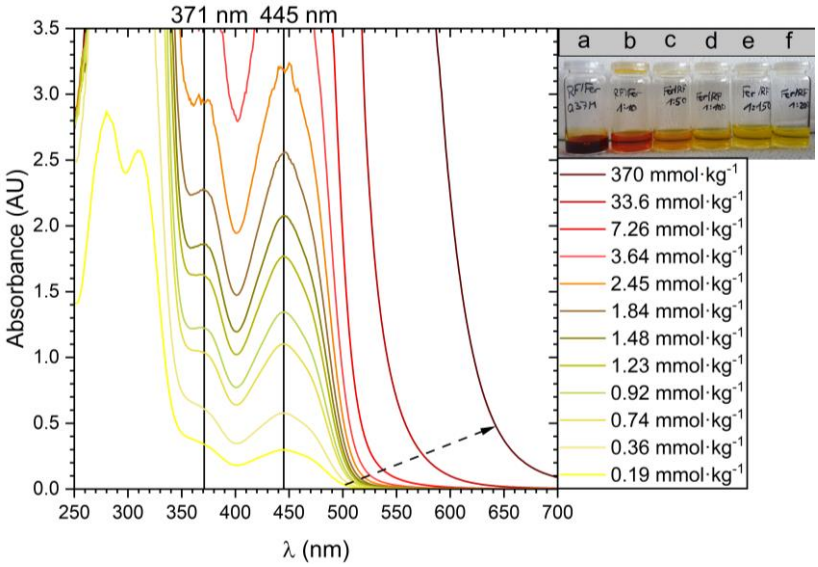

Figure 32: Change of the absorption spectrum of riboflavin in presence of different sodium ferulate concentrations in water with the two absorption maxima at 371 and 445 nm. The molar ratio of sodium ferulate to riboflavin in each sample was 7.4. a: 370 mmol·kg^{-1}, b: 33.6 mmol·kg^{-1}, c: 7.26 mmol·kg^{-1}, d: 3.64 mmol·kg^{-1}, e: 2.45 mmol·kg^{-1}, f: 1.84 mmol·kg^{-1} sodium ferulate.

Further "electron richer" additives led to a stronger bathochromic shift than "electron poor" additives at the same concentration after saturation with RF. However, the molar solubilizer/RF ratio was lower for "electron richer" additives and thus the statistical probability for the contact of RF with the additives was also lower for "electron-rich" solubilizers. Nevertheless, the effect of "electron richer" additives on RF's absorption spectrum was considerably greater (NaBenz < Na-4-OH-Benz ≈ Na-2-OH-Benz < Na-4-OH-3-OMe-Benz < Na-4-OH-3-OMe-Cinn < Na-3,4-DiOMe-Cinn), see Figure 33 A. A dependence of the sample's coloration on the conjugated

electronic system of the solubilizer is typical for π-stacked complexation, which indicates the formation of charge transfer complexes.[264]

Additionally, a variation of the hydrophobic chain length (NaButyrate → NaValerate) did not change the sample's coloration, but the induction of a conjugated electronic system changed the color from yellow to orange-red (NaValerate → Na-2,4-Pentadienoate), see Figure 33 B. Although the solubilization of a compound via the inclusion into aggregates or micelles might change the extinction coefficient, the absorption spectrum of the sample should not change considerably in the lateral dimension. Hence, the solubilization of RF by means of sodium polyphenolates cannot be driven by classical aggregation, where RF would be embedded into a core of potential sodium polyphenolate aggregates.
Further, the absorption spectrum and thus the coloration of pure RF in water was regained when the concentrated solutions comprising RF and "electron rich" solubilizers (Na-4-OH-3-OMe-Benz, Na-4-OH-3-OMe-Cinn, NaCinn, Na-2,4-Pentadienoate, Na-3,4-DiOMe-Cinn) were diluted sufficiently. Thus, the slope of the calibration curves for RF was equal in absence and presence of polyphenolates for an absorbance between 0-1 AU. Therefore, the change of RF's absorption spectrum did not impede the quantification of RF. Moreover, the reversible bathochromic shift of RF's absorption spectrum indicates rather weak interactions of sodium polyphenolates with RF.

A)  **B)** 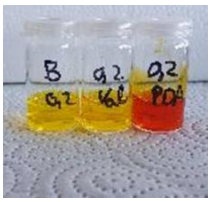

Figure 33: A) From left to right: pure RF in water (saturation) and 0.2 mol·kg^{-1} NaCHC, NaBenz, Na-4-OH-Benz, Na-2-OH-Benz, Na-4-OH-3-OMe-Benz, Na-4-OH-3-OMe-Cinn, Na-3,4-DiOMe-Cinn in water saturated with RF. From left to right the solubilization efficiency of the additive increases. B) From left to right: 0.2 M NaButyrate, 0.2 M NaValerate, 0.2 M Na-2,4-Pentadienoate.

On top of that, not only RF was solubilized by sodium polyphenolates, but RF was able to increase the water-solubility of some sodium polyphenolates (Na-4-OH-3-OMe-Cinn, Na-3,4-DiOH-Cinn, Na-4-OH-3,5-DiOMe-Benz, Na-4-OH-3-OMe-Benz, Na-3,5-DiOMe-Benz, Na-3,4-DiOMe-Benz, Na-2,3-DiOH-Benz, Na-4-OMe-Benz, Na-3-OMe-Benz, Na-2-OMe-Benz, Na-2,4-DiOH-Benz, Na-3,4,5-TriOH-Benz, NaValerate, NaButyrate, Na-2,4-Pentadienoate), see Table 13. In some cases, RF solubilized even water-insoluble sodium polyphenolates (Na-3,4-DiOMe-Cinn, Na-4-OH-3,5-DiOMe-Cinn and Na-4-OMe-Cinn), see compounds marked with * and ** in Figure 31 and Table 13. Hence, the solubilization of RF and many sodium polyphenolates in water is mutual. Further, some of the best RF solubilizing agents turned out to be never entirely solubilized in water. Thus, Na-3,4-DiOMe-Cinn solubilized > 2.8 times RF than the water-soluble and more amphiphilic NaCinn at an additive concentration of 0.35 mol·kg^{-1}. Consequently, the solubilization properties of sodium polyphenolates cannot be

categorized by their water-solubility. Analogously, solubilizing also aromatic solutes, whose solubility is restricted by their π-stacking, A. Fusina recently found that, the more water-soluble hydrotropic polyphenol, pyrogallol, solubilized the aromatic solute quercetin less efficiently than the less water-soluble phloroglucinol.[265] These observations are in line with the fact that often neither the change of the water structure nor the change in the hydration of the solute.[29,266]

Table 13: Water-solubility of some sodium polyphenolates and related sodium salts in absence and presence of RF. The solubility was determined only roughly, as it was deducted from the samples prepared for the solubilization curves in this in this section and not determined accurately.

Sodium polyphenolate	Solubility in pure water (mol·kg^{-1})	Solubility with RF (mol·kg^{-1})
Na-2-OMe-Benz	1.15	5.17
Na-3-OMe-Benz	0.29	5.17
Na-4-OMe-Benz	0.29	2.87
Na-2,3-DiOH-Benz	0.23	2.27
Na-3,4-DiOMe-Benz	0.20	0.88
Na-3,5-DiOMe-Benz	≈ 0	3.92
Na-4-OH-3-OMe-Benz	1.11	1.26
Na-4-OH-3,5-DiOMe-Benz	1.82	2.73
Na-4-OMe-Cinn	≈ 0	0.60
Na-4-OH-3-OMe-Cinn	0.37	1.39
Na-3,4-DiOH-Benz	0.45	0.60
Na-3,4-DiOMe-Cinn	≈ 0	> 4.34
Na-4-OH-3,5-DiOMe-Cinn	≈ 0	> 1.63
Na-3,4,5-TriOH-Benz	0.57	0.68
Na-2,4-Pentadienoate	≈ 0.1	> 0.2
NaValerate	0.05	> 0.4
NaButyrate	0.05	> 0.4

As, (i) RF and sodium polyphenolates increased their water-solubility mutually, as (ii) copigmentation of them was observed and because (iii) the absorption spectrum/yellow coloration of RF was regained upon dilution with water, the solubilization of RF by means of sodium polyphenolates constitutes an extended reversible copigmentation. Moreover, the mutual solubilization of RF and many sodium polyphenolates and the copigmentation of RF with sodium polyphenolates proof interaction of the electronic π-system of RF and polyphenolates via π-stacking. Further, the mutual solubilization indicates that this RF-sodium polyphenolate complex exhibits an improved hydration compared to the separate biomolecules in water, which was additionally confirmed by ^{1}H-NMR experiments of RF in presence of aromatic sodium carboxylates in DMSO-d_6 in section 4.1.2.1.7.

Although hydration and the solubilizers' amphiphilicity contribute to the sodium polyphenolates' solubilizing power, the extension of the additives aromatic π-system increased the RF solubilizing power most. In the following the arguments for and against an aggregative solubilization of RF by means of sodium polyphenolates, for and against the hydration of the

solubilizer as driving force in this solubilization and for and against dispersion forces leading to π-stacking are discussed, see also Table 14.
To summarize, the water-solubility of RF depended extraordinarily on the size and type of the aromatic π-system of the solubilizer. Still, the solubilization of RF can be modified by the solubilizer's amphiphilicity and salting-in character. Sodium polyphenolates do not necessarily have to be water-soluble to exhibit great RF solubilizing properties, as two insoluble polyphenolates belong to the best solubilizers tested (Na-3,4-DiOMe-Cinn, Na-4-OH-3,5-DiOMe-Cinn).

To further evaluate the sodium polyphenolate's ability for aggregation and accumulation at interfaces, surface tension and DLS measurements of sodium polyphenolates in absence and presence of RF were compared, see section 4.1.2.1.5. NMR measurements and cocrystallization attempts were also applied to understand the interaction of RF with sodium polyphenolates on molecular scale, see sections 4.1.2.1.6 and 4.1.2.1.7.

Table 14: Pro (↑) and contra (↓) arguments for a solubilization of riboflavin (RF) in water with sodium polyphenolates via aggregation, π-stacking and hydration as main solubilization mechanism. Minimum hydrotrope concentration (MHC), critical aggregate concentration (CAC), sodium xylene sulfonate (SXS), sodium dodecyl sulfate (SDS), for residual abbreviations see Figure 31. +M = positive mesomeric effect; -I = negative inductive effect.

Aggregation	π-stacking	Hydration
↑Many polyphenolates are amphiphilic ↑All sodium cinnamates > sodium benzoates	↑All sodium cinnamates > sodium benzoates	↑ Salting-in/out agent in-/decrease the solubility of RF ($NaSCN/NaH_2PO_4$)
↑After reaching a critical polyphenolate concentration (maximum of the additive/RF ratio) the solubilizing efficiency improves considerably. → might correspond to an MHC	↓No break point in the log-log-plot ↓Theoretical MHC region obtained from the maximal additive/RF ratio at polyphenolate concentrations < 0.21 mol·kg^{-1}, but typical CACs of are > 0.2 mol·kg^{-1}	
↑Dependence of RF's solubility on the hydrophobic chain length of the solubilizer (SDS > NaValerate > NaButyrate > NaBenz)	↑Weak dependence on the hydrophobic chain length (NaButyrate → NaValerate: +29 %) ↑Most aromatic solubilizers better than surfactant SDS	
	↑Deterioration of amphiphilicity improves solubility of RF (Na-3,4,5-TriOH-Benz > NaBenz) ↑Solubility increases with increasing +M and decreasing -I-effect (OMe > OH > CF3 > COO^-) ↑Increase of aromatic π-system improves solubility (Na-4-OH-3-OMe-Cinn ≈ Na-2,4-Pentadienonate >> NaValerate; Na-4-OH-Cinn >> Na-4-OH-Benz > Na-4-OH-Prop) ↑Induction of conjugation improves solubility (NaBenz >> NaCHC) ↑Electronegative substituent in the aromatic ring lowers solubility (Nicotinamide < NaBenz) ↑Even without a carboxylate group tyrosol solubilized RF → aromaticity sufficient for a solubilization	↑Solubility of RF rises with increasing number of OH-groups ↑para > meta > ortho substitution with OH- and OMe-groups (except Na-2-OH-Benz) ↑Compounds with non-neighbored OH/OMe-groups are better solubilizers than those with adjacent groups ↓OMe > OH on the aryl ring, although OMe more lipophilic ↑Hydratable carboxylate improves solubility of RF (Tyrosol < Na-4-OH-Benz) ↓Totally insoluble compounds Na-3,4-DiOMe-Cinn and Na-4-OH-3,5-DiOMe-Cinn more efficient solubilizers than water-soluble NaBenz, Na-2-OH-Benz and Na-3,4,5-TriOH-Benz
	↑Red-shift of RF's absorption spectrum for high concentrated sodium polyphenolate/RF solutions ↑Red-shift upon induction of a conjugation (NaValerate → Na-2,4-Pentadienoate) →Reversible copigmentation ↑Mutual solubilization of RF and sodium polyphenolates	↑In spite of lipophilic methyl groups, SXS with its less hydrated sulfonate group is a comparable solubilizer to NaBenz [42] ↓Mutual solubilization ↓Mutual solubilization even with totally insoluble sodium polyphenolates

4.1.2.1.2 Effect of riboflavin's type on the solubilization power of sodium polyphenolates

As already the solubility of RF in pure water depended on the distributor and batch (Figure 114 in section 4.2.1), the solubilizing power of sodium polyphenolates might differ on the type of RF, too. Therefore, the trend for the solubilization of RF by means of sodium polyphenolates was compared for RF from two distinct distributors (Carl Roth and BASF) and for two distinct batches from BASF. A solubilization curve of RF in water with sodium vanillate as solubilizer was recorded with the RF from Carl Roth and with two RF batches from BASF, see Figure 34. All three types of RF led to an exponential increase of RF's solubility in dependence of sodium vanillate. However, RF from Carl Roth was not only the most soluble in pure water, but better solubilized by vanillate than the RF from BASF, too. Further, the solubility of RF in presence and absence of vanillate depended even on the batch of RF (red and blue curve). Thus, the solubility of RF in pure water and at different sodium vanillate concentrations from batch 2 equaled always 75-86 % of batch 1. Hence, the difference between the solubilization curves in percent was ca. constant over the whole concentration range in Figure 34.

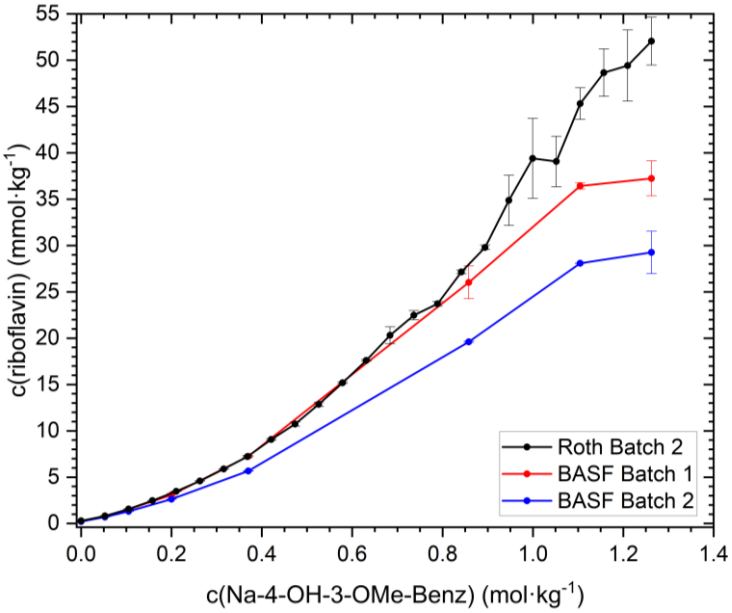

Figure 34: Water-solubility of riboflavin from Carl Roth and from two different riboflavin batches from BASF by means of sodium vanillate in water at 23 °C.

When regarding the solubility of RF in 0.2 mol·kg^{-1} sodium polyphenolate and NaBenz solutions, the solubilizing properties of sodium polyphenolates differed upon distributor and batch, too, see Figure 35. Nevertheless, the trend of the solubilizing power did not vary with the distributor and batch, see Figure 35 (NaBenz < Na-4-OH-Benz < Na-2-OH-Benz < Na-4-OH-3-OMe-Benz < Na-4-OH-3-OMe-Cinn < Na-3,4-DiOMe-Cinn). Although the order of the solubilizing power of sodium polyphenolates was not influenced by the type of RF, the solubility of RF differed ca. 20 % upon the type of RF. Still, except for Na-2-OH-Benz, the distance between the three types of RF in percent stayed approximately constant for all additives, see Figure 36.

Consequently, the type of RF determines RF's solubility in pure water and the extent, to which solubilizers can dissolve the vitamin. One possibility for the distinct solubilities of RF might be impurities. The crystalline structure of RF might also influence the solubility of RF. In any case, further investigations on the correlation of RF's water-solubility and its crystalline state should be carried out in the future, as the controlled solubilization of RF might be useful for a controlled release of this vitamin in drug therapies.

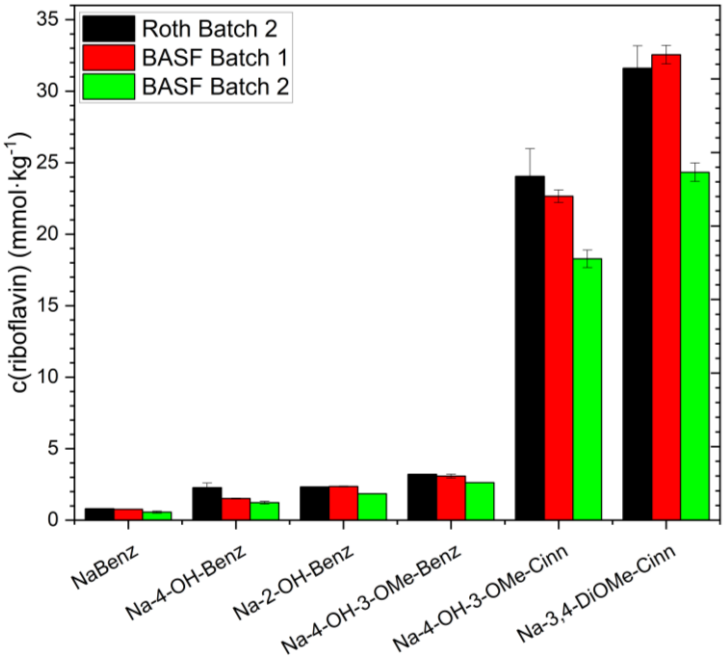

Figure 35: Water-solubility of different types of RF (from Carl Roth and two batches from BASF) in presence of sodium benzoate and cinnamate salts at 23 °C.

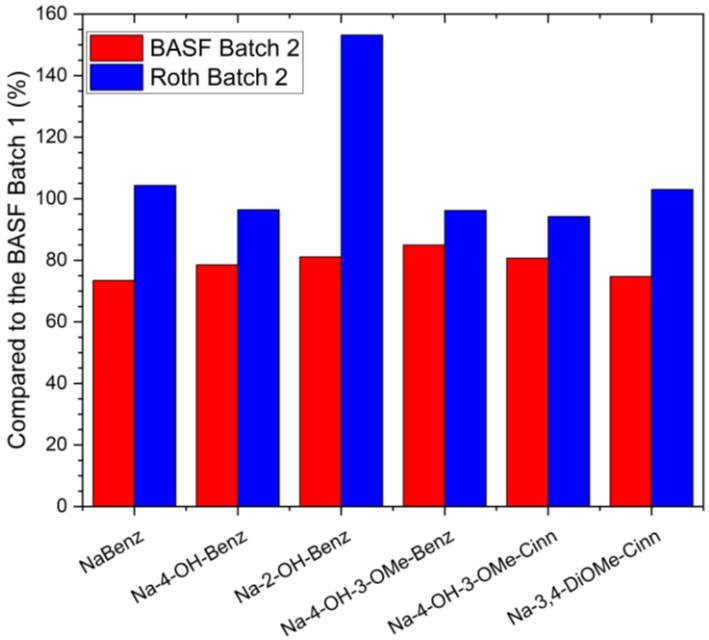

Figure 36: Water-solubility of riboflavin from Carl Roth and batch 2 BASF compared to batch 1 from BASF at a solubilizer concentration of 0.2 mol·kg^{-1}. The data were calculated from the solubility of RF in Figure 35.

4.1.2.1.3 Effect of distinct cations on the solubilization efficiency of polyphenolates

Due to different dissociation constants, polarizability and hydration, the type of cation might influence the solubilizing power of polyphenolates for RF in water. Therefore, two potentially edible inorganic cations (sodium and potassium) and three potentially edible or pharmaceutical admitted organic cations were compared, see Figure 37. Because sodium ferulate (Na-4-OH-3-OMe-Cinn) – one of the best RF solubilizers from section 4.1.2.1.1 – was soluble up to 0.37 mol·kg^{-1}, the water-solubility of RF in presence of other ferulate salts was tested at the same concentration.

Though meglumine, arginine and potassium ferulate were not soluble at 0.37 mol·kg^{-1}, the solutions were still saturated with RF, hoping for a mutual solubilization of RF and the solubilizer as it was observed in the case of sodium polyphenolates in section 4.1.2.1.1. The compounds exerted the following solubilization power: **Sodium > choline > potassium > arginine > meglumine.**

Obviously, the small and less polarizable cations sodium and choline promoted the solubilizing power of ferulate more than the larger potassium, arginine and meglumine. Despite of several hydroxy groups and one amine group as potential hydrogen bonding partner and despite of meglumine's high solubility in water, meglumine exerted the weakest solubilizing power among the five cations. Additionally, the weak performance of arginine ferulate compared to potassium, choline and sodium ferulate, amine and hydroxy groups on the cation weakened the solubilizing power of the polyphenolates. Thus, hydrogen bonding sites on the cations probably do not necessarily improve the solubilizing power of polyphenolates.

However, the priority was to find the best cation for polyphenolates in potentially edible formulations, thus the reasons for the weak solubilizing performance of potassium, arginine and meglumine were not further investigated. The solubilization power of choline polyphenolates for RF in water was investigated in section 4.1.2.1.4.

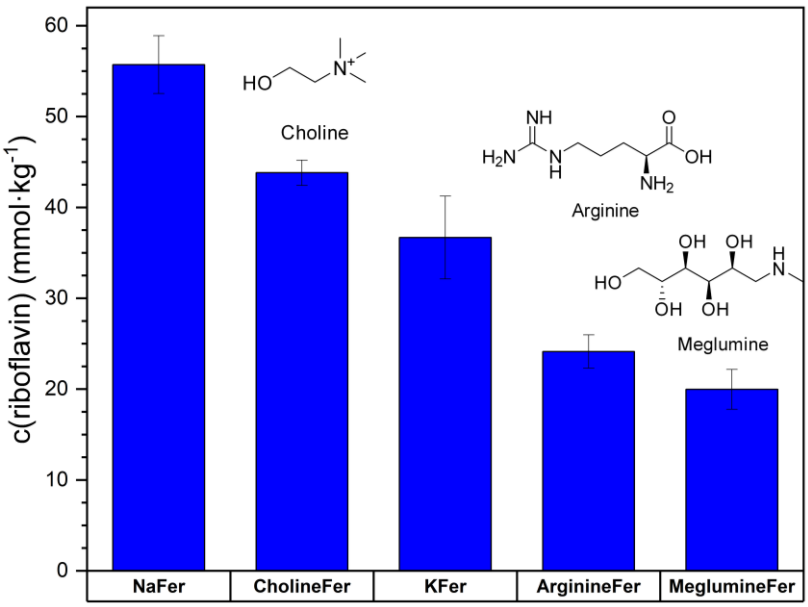

Figure 37: Water-solubility of riboflavin in presence of 0.37 mol·kg^{-1} ferulate (Fer) with different cations in water. For exact solubility see section 7.6 in the Appendix.

4.1.2.1.4 Aqueous solubilization of riboflavin using choline polyphenolates

As gallate exhibited distinct RF-solubilizing power depending on the inorganic cation (K^+ > Li^+ > Na^+), the influence of choline as small hydrophilic organic cation on the solubilization performance of polyphenolates was examined for some polyphenolates and related compounds.[254] Choline was chosen, as the resulting solution would combine the vitamin RF with two nutraceuticals – polyphenolates and choline.[267]

The water-solubility of RF is presented in Figure 38 as a function of the choline and sodium polyphenolate concentration. As in the case of sodium polyphenolates, choline polyphenolates increased the solubility of RF in water exponentially. Hence, polyphenolates and not their cationic counterions are crucial for the strong effect on RF's solubility. The best molar choline salt/RF ratio for the solubilization of RF in water by means of choline polyphenolates and cinnamate is reported in Table 15. The best molar ratio among the tested choline salts was reached with a 0.64 mol·kg^{-1} choline ferulate solution (ratio 8), see Table 15. However, a 0.37 mol·kg^{-1} sodium ferulate solution exhibited still a better molar ferulate/RF ratio of 6.2, see Table A 51 in the Appendix. Generally, choline salts showed slightly lower solubilization efficiency for RF. Nevertheless, choline and sodium polyphenolates exhibit roughly comparable RF solubilizing powers for concentrations < 0.6 mol·kg^{-1}. Due to their better water-solubility compared to sodium polyphenolates, much more RF was solubilized using choline salts.

Table 15: Water-solubility of riboflavin at the best molar choline salt/RF ratio. Prior to the calculation of the molar ratio, RF's water-solubility was subtracted, see equation 2 from section 2.3.

Choline salt	c(choline salt) (mol·kg^{-1})	c(RF) (mmol·kg^{-1})	Molar ratio
3,5-DiOH-Benz	0.47	8.7 ± 0.4	55.1
4-OH-3-OMe-Benz	0.52	10.3 ± 0.5	51.3
3,4,5-TriOH-Benz	1.46	31.8 ± 0.5	46.4
3,4-DiOMe-Benz	0.035	1.0 ± 0.1	46.4
Cinn	0.04	1.9 ± 0.3	23.9
4-OH-3-OMe-Cinn	0.64	80 ± 7	8.0

Further, the solubilization efficiency of choline polyphenolates seems to decrease for high choline salt concentrations (> 0.6 mol·kg^{-1}), as the exponential increase of RF's solubility flattens out for high choline salt concentrations, see Figure 38. Thus, for concentrations > 0.6 mol·kg^{-1}, the molar choline polyphenolate/RF ratio increased again, see Figure 39. On the contrary, the slope of the solubilization curves in presence of sodium polyphenolates stayed more or less similar for the whole concentration range tested. Consequently, for high concentrations, sodium polyphenolates are better RF solubilizers enabling a lower molar solubilizer/RF ratio than the corresponding choline salts (except for gallate), see Figure 39.

However, sodium polyphenolates have a limited solubility in water, whereas choline salts were enormously water-soluble (> 2 mol·kg^{-1}) Thus, sodium ferulate has a solubility of 0.37 mol·kg^{-1}, while at least 5 mol·kg^{-1} choline ferulate can be solubilized in water. Consequently, the better water-soluble choline salts enabled a greater enhancement of RF's aqueous solubility, see Figure 38. Thus, choline ferulate increased the water-solubility of RF by at least 800 times compared to pure water at 5.05 mol·kg^{-1} of the solubilizer, while sodium ferulate (0.56 mol·kg^{-1}) increased the solubility only by 233 times due to sodium ferulate's limited water-solubility, see Table A 51 in the Appendix. Analogously, a 0.59 mol·kg^{-1} sodium cinnamate solution solubilized only 127 times more RF than pure water, whereas in a 5.97 mol·kg^{-1} choline cinnamate solution RF's solubility was increased 523-fold. However, the solubility limit of choline salts was not tested, as the samples were very viscos for high choline polyphenolate concentrations.

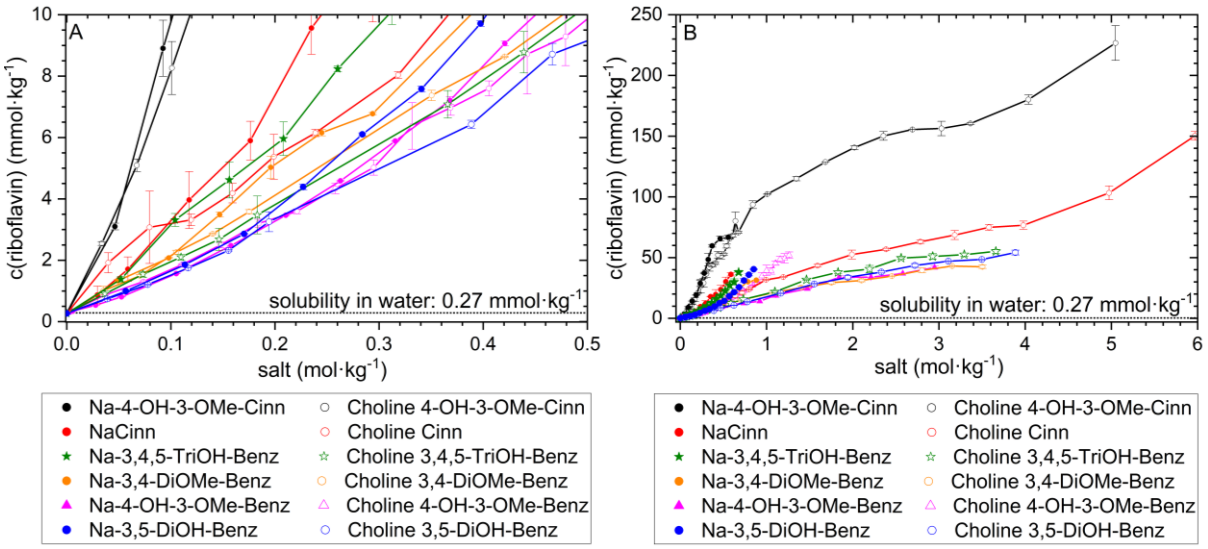

Figure 38: Aqueous solubility of riboflavin in presence of sodium and choline salts of ferulic, cinnamic, gallic, veratric, vanillic, and 3,5-dihydroxybenzoic acid. A: enlarged view; B: entire view.

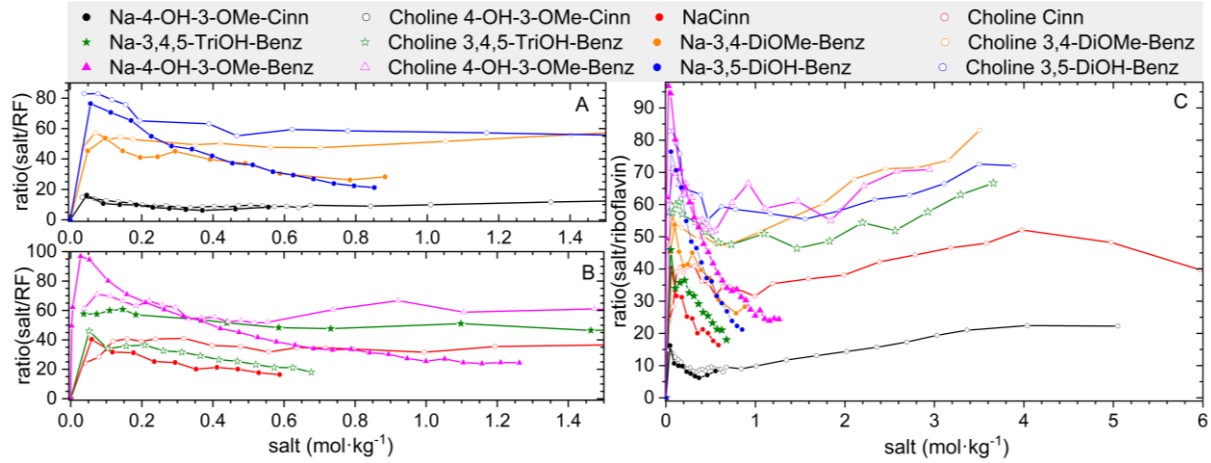

Figure 39: Molar ratio of sodium and choline salts of ferulic, cinnamic, gallic, veratric, vanillic, and 3,5-dihydroxybenzoic acid to riboflavin corresponding to the solubilization efficiency for riboflavin in water. A and B: enlarged view, C: entire view from 0-6 mol·kg^{-1}.

Despite a similar solubilization efficiency of choline and sodium polyphenolates for concentrations < 0.6 mol·kg^{-1}, the solubilization efficiency of 3,4,5-trihydroxybenzoate and 3,4-dimethoxybenzoate as well as 3,5-dihydroxybenzoate and 4-hydroxy-3-methoxybenzoate was switched for the corresponding choline salts, see Figure 40. Probably, choline enables a better hydration of the polyphenolates and thus the methoxy substituted compounds comprising a stronger positive mesomeric effect, are better solubilizers than the hydroxy substituted ones.[268] Then, for sodium polyphenolates, the better hydration of hydroxy groups compared to methoxy groups leads to the greater solubilization power of hydroxy substituted compounds.

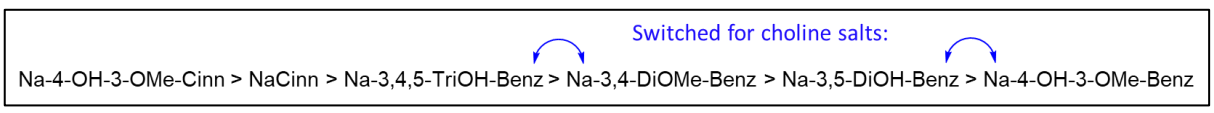

Figure 40: Solubilizing efficiency of choline and sodium polyphenolates for riboflavin in water.

Finally, choline polyphenolates are promising solubilizing agents for riboflavin, which increase RF's solubility exponentially. Yet, the usage of choline salts would probably not be desired for food or beverages, as they exhibit a fishy odor. However, choline and polyphenolates are nutraceuticals and choline polyphenolates have higher antioxidant capacity compared polyphenolic acids.[268] Therefore, choline polyphenolates might constitute potential RF solubilizers for pharmaceuticals and nutritional supplements.

4.1.2.1.5 Evaluation of the structuring potential of polyphenolates in presence of riboflavin in aqueous solution

4.1.2.1.5.1 Surface-active behavior of sodium polyphenolates in presence of riboflavin

In case of an aggregative solubilization of RF by sodium polyphenolates and in case of a significant abstraction of the amphiphiles from pure polyphenolate aggregates to form a RF/polyphenolate complexes, the absolute surface tension and the CAC of sodium polyphenolates might be altered. Hence, surface tension curves in Millipore water in absence and presence of RF were recorded, see Figure 41. The break point of the surface tension curves corresponds to a CAC. Keeping the hydrotrope/RF ratio constant, RF induced neither a depletion nor an accumulation of polyphenolates at the water/air interface. The CAC was not altered, too. Consequently, surface tension measurements indicate a CAC of sodium polyphenolates in the absence and presence of RF but provide neither an evidence for a solubilization of the vitamin via aggregation of polyphenolates nor an evidence for a huge demand of polyphenolates for RF's solubilization.

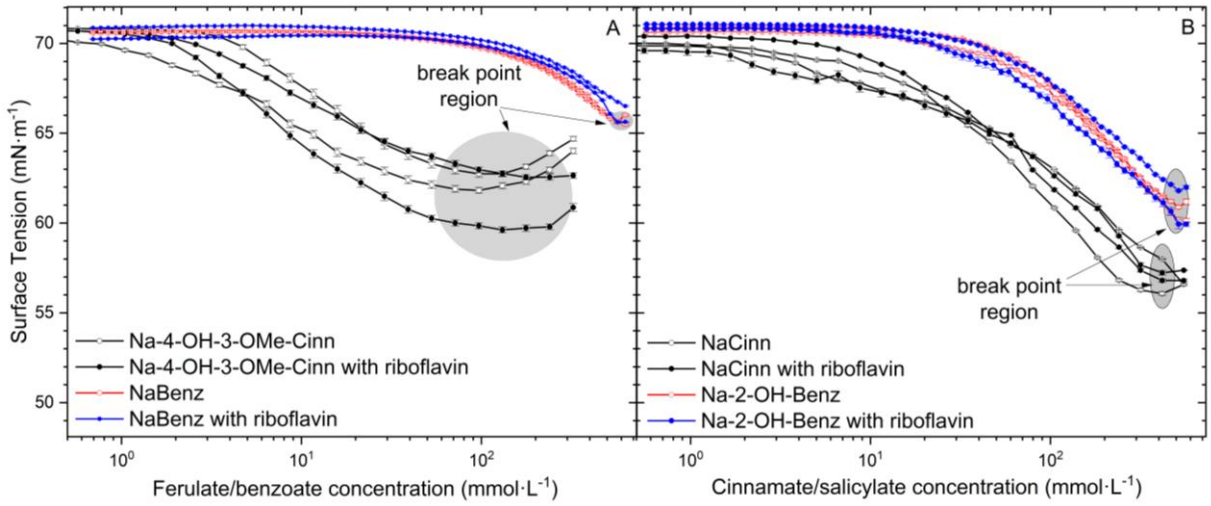

Figure 41: Surface tension curves of sodium ferulate and benzoate (A) as well as sodium cinnamate and salicylate (B) in absence and presence of riboflavin. The stock solution (sample of highest concentration) was saturated with riboflavin. Thus, the molar hydrotrope/riboflavin ratio was constant for each surface tension curve. The samples were prepared in duplicate, thus for each sample two curves are displayed.

4.1.2.1.5.2 DLS measurements of sodium polyphenolate in absence and presence of riboflavin

As the surfactant SDS solubilized a considerable amount of RF in water and because the solubility of RF increased slightly with increasing amphiphilicity of its solubilizer, the solubilization of RF by means of polyphenolates might involve aggregation at least partially, see section 4.1.2.1.1. Thus, DLS measurements of RF in water, of sodium polyphenolates and NaBenz in water and of aqueous sodium polyphenolate/NaBenz solutions saturated with RF were conducted. As Na-3,4-DiOMe-Cinn was never entirely solubilized in water, a sample without RF was not analyzed. As Na-4-OH-3-OMe-Cinn, had a limited water-solubility, the sample comprising this polyphenolate was prepared at its water-solubility (0.37 mol·kg^{-1}). The other sodium salts were prepared at 1 mol·kg^{-1}, to be largely over the CAC of the sodium salts.[233] Na-3,4-DiOMe-Cinn and Na-4-OH-3-OMe-Cinn were chosen, because these compounds belong to the four best solubilizers tested in section 4.1.2.1.1. NaBenz and Na-2-OH-Benz were chosen because of their totally amphiphilic structure. Though NaCinn is also perfectly amphiphilic, samples comprising NaCinn crystallized fast on the glass of the DLS tube leading to a correlation function > 1.

No or slight structuring with considerable fluctuations was detected for the aqueous NaBenz, Na-4-OH-3-OMe-Cinn, Na-3,4-DiOMe-Cinn and Na-2-OH-Benz. RF alone had no structuring potential in pure water according to DLS. In the case of NaBenz, RF even nullified the slight nano-structuring in the 1 mol·kg^{-1} NaBenz sample, whereas RF exhibited no effect at all on the samples comprising Na-4-OH-3-OMe-Cinn. Na-2-OH-Benz and Na-3,4-DiOMe-Cinn. Consequently, RF has either no or a structure breaking effect.

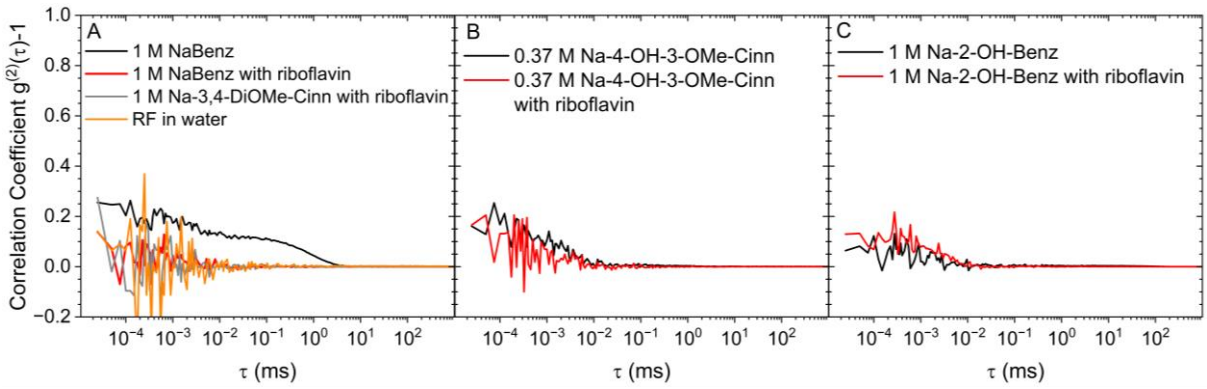

Figure 42: Dynamic light scattering correlation functions of A: riboflavin, sodium benzoate, sodium benzoate saturated with riboflavin and sodium 3,4-dimethoxycinnamic acid in water; B: sodium ferulate and sodium ferulate saturated with riboflavin in water; C: sodium salicylate and sodium salicylate saturated with riboflavin in water; at 25 °C. M = mol·kg^{-1}

Although, DLS is not as precise as SAXS or Small Angle Neutron Scattering, DLS allows evaluating the magnitude of structuring. Yet, slight structuring or small complex formation are usually not visible in DLS correlation curves. Therefore, SAXS spectra of pure RF in water (saturation), and 0.3 mol·kg^{-1} sodium polyphenolate solutions without and saturated with RF

were measured against water as reference. However, the scattering light density of water and of the solutes was in a similar range, see Figure A 7 in section 7.10 in the Appendix. Therefore, the contrast between the scattering of water and the scattering of sodium polyphenolates was too small to yield reliable results. If the concentration of sodium polyphenolates would be at least 1 mol·kg^{-1}, the contrast might be sufficient. However, the best RF solubilizing sodium polyphenolates were not soluble at this concentration. Only Na-3,4-DiOMe-Cinn was soluble above 4 mol·kg^{-1}, but only in presence of RF. Therefore, a reference sample without RF would not be accessible for Na-3,4-DiOMe-Cinn and the measurement would not be reliable. Hence, SAXS measurements are not appropriate for the analysis of potential aggregation in aqueous sodium polyphenolate/RF solutions. A better method for obtaining more certain information about potential aggregation might be Small Angle Neutron Scattering. However, this method is rather expensive and was not exerted, as the results from section 4.1.2.1.1 show clearly a greater effect of the electronic contribution than of the amphiphilic one.

4.1.2.1.5.3 Conclusion

The absence of a pronounced correlation in DLS and the absence of an effect of RF on the surface tension and CAC of Na-4-OH-3-OMe-Cinn, NaCinn, Na-2-OH-Benz and NaBenz negated the inclusion of RF into aggregates. Moreover, sodium polyphenolates increased RF's water-solubility already at low additive concentrations (<0.21 mol·kg^{-1}), while the CACs of them were mostly above 0.2 mol·kg^{-1}. On top of that, the bad solubilizing performance of the surfactant SDS compared to sodium polyphenolates confirmed that the amphiphilicity of polyphenolates cannot be the solubility determining factor. Thus, classical aggregation of sodium polyphenolates, which would be comparable to surfactants, does not occur. Instead, probably small complexes of RF and polyphenolates are formed.

4.1.2.1.6 Attempt for cocrystallization of riboflavin and aromatic sodium carboxylates

To get more insight into the arrangement of RF and sodium polyphenolates in the solution, cocrystallization of RF with different sodium phenolates or phenolic acids was attempted. Distinct methods for the synthetization of cocrystals were tried, see section 3.2.2.1.9.

However, RF and aromatic sodium carboxylate salts or carboxylic acids crystallized always apart from each other. Aromatic sodium carboxylates/carboxylic acids crystallized always in colorless transparent needles or plates, while RF crystallized as orange and mostly non-transparent needles, which were ingrown via the edges, see Figure 43.

As the aqueous solubility of ferulic acid is low compared to the one of sodium ferulate, another idea was to precipitated sodium ferulate slowly from an aqueous sodium ferulate solution saturated with RF, see section 3.2.2.1.9.4. The precipitation of ferulate equals a reduction of

the solubilizing agent for RF. Thus, RF should be precipitated, too, and hopefully via the formation of RF-sodium ferulate cocrystals. However, the orange crystals were either not clear or too small for an analysis, see Figure 44. The failure to synthesize cocrystals indicates that the interactions of RF and sodium polyphenolates are weak and dynamic.

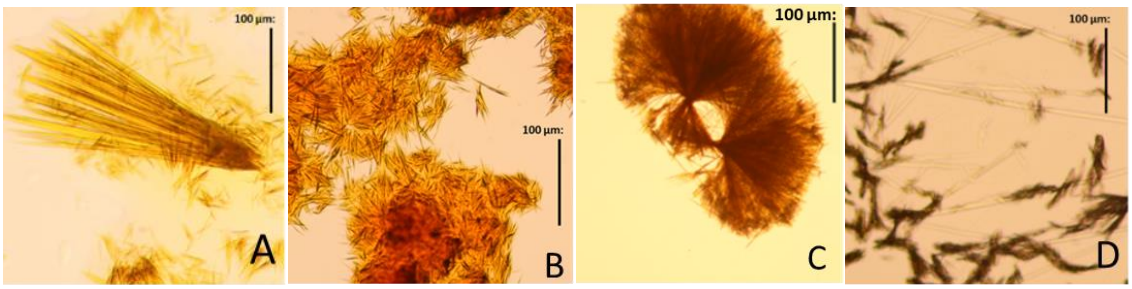

Figure 43: A) Na-3,4-DiOMeCinn/RF stock solution overlayed with acetone: Needles grown together radially 0.29 mm x ≤0.01 mm; B) Sodium caffeate/RF stock solution overlayed with acetone: Needles grown together radially. C) NaCinn/RF stock solution overlayed with acetone: Needles grown together radially; D) Colorless crystals: pure NaCinn

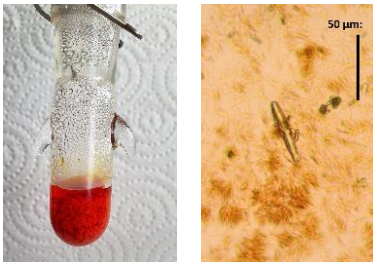

Figure 44: Left: 0.37 mol·kg^{-1} sodium ferulate saturated with RF after precipitation with HCl. Right: Many tiny needle-shaped ferulic acid and RF crystals were obtained.

4.1.2.1.7 Insight in the interaction of riboflavin and aromatic sodium carboxylates via NMR spectroscopy

NMR measurements of RF, of sodium polyphenolates, NaCinn and NaBenz as well as NMR measurements of RF in presence of sodium polyphenolates/NaCinn/NaBenz were conducted to further evaluate the interactions of RF and sodium polyphenolates. Regarding the exponential increase of RF's water-solubility in presence of polyphenolates and similar compounds from section 4.1.2.1.1, deuterium oxide would have been the most reasonable solvent for the NMR experiments. However, the solubility of RF in deuterium oxide was as so low as in water, so that the NMR signals were too noisy in ^{1}H-NMR and not visible at all in ^{13}C-NMR. Other typical NMR solvents, such as deuterated acetonitrile, chloroform, methanol, ethanol, benzene and acetone solubilized either less or no RF at all. Only in DMSO-d_6, RF, polyphenolates, NaBenz and NaCinn were sufficiently soluble for ^{1}H-NMR and barely enough soluble for ^{13}C-NMR experiments. Although DMSO-d_6 is totally distinct from water and might even suppress inter- and intramolecular hydrogen bonding, the reduced proton exchange in

DMSO-d_6 gave access to the hydroxy groups of RF and polyphenolates and to RF's amine group.[269] Therefore, DMSO-d_6 was used for almost all NMR measurements regarding RF, see section 7.11.1 and sections 7.11.3-7.11.8 in the Appendix. Only for the NOESY measurement of the 3 mol·kg^{-1} Na-3,4-DiOMe-Cinn sample saturated with RF, water could be used.

To still evaluate the interaction of RF with sodium polyphenolates in an aqueous medium, additionally NMR measurements of the better water-soluble RF-PO_4 in absence and presence of sodium ferulate were performed in deuterium oxide. This was possible, because RF-PO_4 comprises the same isoalloxazine ring as RF and RF-PO_4 was also solubilized by sodium polyphenolates, see section 4.1.2.2. Due to the high water-solubility of RF-PO_4, all NMR signals in ^{1}H- and ^{13}C-NMR were well resolved, see sections 7.11.2 and 7.11.9 in the Appendix.

To reach maximum resolution, all NMR samples were prepared via saturation of the deuterated solvent with RF, RF-PO_4 and/or sodium polyphenolates/cinnamate/benzoate. The signals of all NMR spectra were assigned via the splitting, integrals, cross-peaks in the Correlation Spectroscopy (COSY), Nuclear Overhauser Effect Spectroscopy (NOESY), Heteronuclear Single Quantum Coherence (HSQC) and Heteronuclear Multiple Bond Correlation (HMBC) NMR spectrum, via comparison with simulation in ChemDraw 20.0, MestReNova (from 2020) and via a comparison with NMR assignments from the literature. In some cases, an increment table was used to calculate the chemical shift of the protons/carbons.[270–273] The NMR spectra and the peak assignment are reported in section 7.11 in the Appendix.

In section 4.2.1, cross-peaks in the NOESY spectrum were used to study the intra- and intermolecular interactions of RF with itself and RF-PO_4 with itself. π-Stacking and a bent ribityl chain were indicated by NOESY measurements of RF-PO_4 in pure water, while the NOESY spectrum of RF did not exhibit such indications. In case of strong intermolecular interactions of RF or RF-PO_4 with sodium polyphenolates, a change of the chemical shift $\Delta\delta$ in the ^{1}H- and ^{13}C-NMR spectrum was supposed relatively to the ^{1}H- and ^{13}C-NMR spectra of the pure compounds. Therefore, $\Delta\delta$ was calculated from ^{1}H-NMR and ^{13}C-NMR, see section 7.11 in the Appendix. Further, cross-peaks in NOESY NMR spectra were used to evaluate the intermolecular interactions of RF or RF-PO_4 with sodium polyphenolates in DMSO-d_6 and deuterium oxide, respectively. As, Na-2-OH-Benz was sufficiently soluble in DMSO-d_6, the dependence of the ^{1}H- and ^{13}C-NMR signals on the molar ratio of Na-2-OH-Benz and RF was also analyzed, see section 4.1.2.1.7.2 below. The observations are briefly reported one after another in the sections 4.1.2.1.7.1-4.1.2.1.7.7 for each aromatic sodium salt and summarized and interpreted in section 4.1.2.1.7.8.

4.1.2.1.7.1 Riboflavin in presence of sodium benzoate

A saturation of DMSO-d_6 with NaBenz and RF resulted in a molar ratio of NaBenz/RF of two. In Figure 45 the change of chemical shift of RF's and NaBenz's protons and carbons with the numeration of the protons/carbons compared to the pure compounds in DMSO-d_6 is displayed for a molar NaBenz/RF ratio of 2.

^{1}H-NMR: The splitting of NaBenz's protons was altered by the presence of RF, see Figure A 18, Figure A 19 and Table A 81 in section 7.11.3 in the Appendix. The chemical shift of NaBenz's aromatic protons was not considerably influenced by the presence of RF (≤ 0.04 ppm), see Figure 45 on the right. Analogously, out of RF's protons on the isoalloxazine ring, only the aromatic proton H2 was deshielded by 0.15 ppm due to the presence of NaBenz, whereas the other protons on the isoalloxazine ring were not affected at all, see Figure 45 on the left. Further, RF's hydroxy groups were broadened (H4, H6, H7) and the signal of the outermost hydroxy group (H9) disappeared, see Table A 82 in section 7.11.3 in the Appendix. RF's hydroxy group signals of H6, H7 were merged, see Figure A 19 in section 7.11.3 in the Appendix. The reason for the deshielding and change of the splitting of the ribityl chain's residual protons (H12, H11, H10) originated most probably from the entire or partial deprotonation of RF's hydroxy groups, see Figure 45 on the left and Figure A 19 in section 7.11.3 and Figure A 8 in section 7.11.1 in the Appendix.

^{13}C-NMR: NaBenz's carbon atoms on the ortho and meta position (C2/6, C3/5) were deshielded by ≤ 0.2 ppm, whereas the residual ones were shifted by > 0.4 ppm, see Figure 45 right and Table A 83 in section 7.11.3 in the Appendix. The para carbon atom of NaBenz C4 was shifted most by 0.9 ppm upfield. Further, the change of the chemical shift of NaBenz's carbons increased from ortho to meta to para (C2/6 < C3/5 < C4) due to the presence of RF, see Figure 45 on the right. Regarding RF, not only its carbon atoms on the ribityl chain were obviously shifted by 0.42-0.58 ppm, but also all carbons (except of C9a) in the isoalloxazine ring, see Figure 45 on the right and Table A 84. C9 was shifted most by 0.52 ppm out of the carbons in the isoalloxazine ring.

Summary: In ^{1}H-NMR, only the exchangeable hydroxy group protons were deshielded significantly, whereas the residual protons of RF and NaBenz were not or just minorly affected by the presence of NaBenz or RF. On the other side, the electro-magnetic environment of almost all carbon atoms of both molecules was changed minorly to significantly (mainly deshielded).

NOESY: The NOESY spectrum of RF in presence of NaBenz revealed a proximity of NaBenz's protons H2 and H1 to RF's protons H11 on the ribityl chain, see Figure 46.

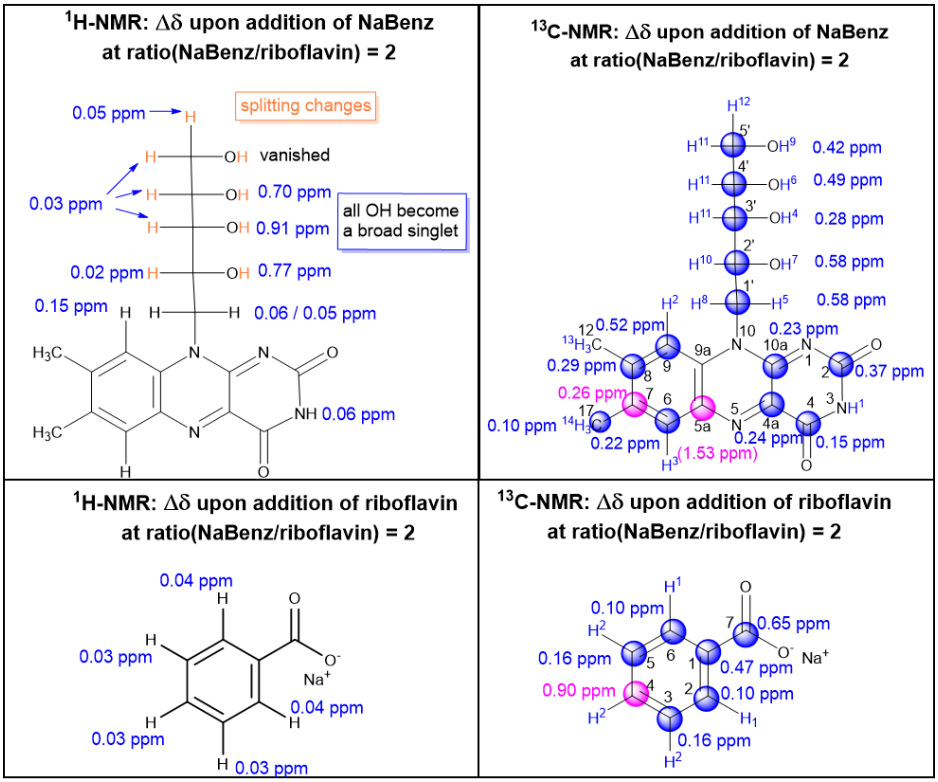

Figure 45: Change of chemical shift of riboflavin's signals in presence of NaBenz and change of the chemical shift Δδ of NaBenz's signals in presence of RF in DMSO-d_6 in ^{1}H- and ^{13}C-NMR at a molar ratio of NaBenz/RF = 2. Blue: shifted downfield/deshielded; magenta: shifted upfield/shielded; orange: changed splitting. The corresponding NMR spectra and peak attribution are given in section 7.11.3 in the Appendix.

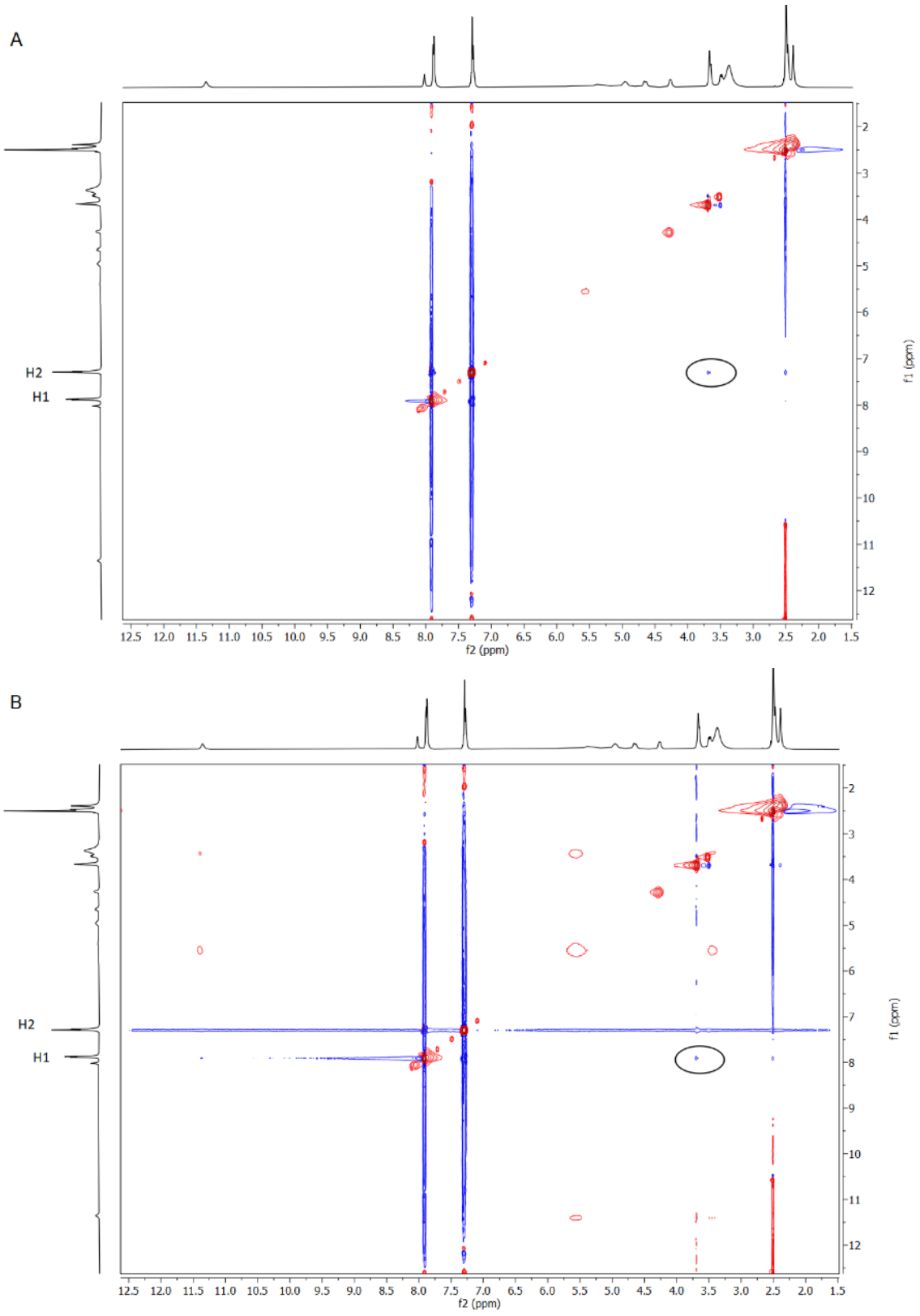

Figure 46: NOESY spectrum of sodium benzoate and riboflavin in DMSO-d_6 at a molar ratio of NaBenz/RF = 2. A) The circled cross-peak indicates an interaction of H11 of RF with H2 of NaBenz; B) Stronger zoom revealed the circled cross-peak, which indicated an interaction of H11 of RF with H1 of NaBenz.

4.1.2.1.7.2 Riboflavin in presence of sodium salicylate

As Na-2-OH-Benz was sufficiently soluble in DMSO-d_6, the dependence of the chemical shift of RF's and Na-2-OH-Benz's proton and carbon atoms on the molar Na-2-OH-Benz/RF ratio was accessible. Therefore, ^{13}C- and ^{1}H-NMR spectra of Na-2-OH-Benz in presence of RF in DMSO-d_6 at four different molar Na-2-OH-Benz/RF ratios (2, 5, 10 and 50) were conducted, see section 7.11.4 in the Appendix. A graphical overview of the maximum change of the protons' and carbons' chemical shift and the numeration of the atoms are displayed in Figure 48.

^{1}H-NMR: The superimposed ^{1}H-NMR spectra of RF and Na-2-OH-Benz in DMSO-d_6 at distinct molar ratios are reported in Figure 47 A-C. As DMSO-d_6 suppresses proton exchange, the exchangeable protons of RF and Na-2-OH-Benz gave rise to sharp signals with a well resolved splitting, see Figure 47 A and B yellow/blue curve.[269] Yet, with increasing Na-2-OH-Benz/RF ratio, the exchangeable protons of RF underwent deshielding up to 0.46 ppm as well as peak broadening, which finally resulted in a loss of the splitting, see Figure 47 A, B and Figure 48 on the left. The hydroxy group of Na-2-OH-Benz underwent also peak broadening and a crescent deshielding with increasing RF/Na-2-OH-Benz ratio by up to 1.10 ppm, Figure 47 A and Figure 48 on the left. The reason for the peak broadening is that water-free DMSO-d_6 still contains traces of residual water due to its hygroscopicity.[274] Apparently, the residual water in DMSO-d_6 was not sufficient for a hydration or peak broadening of pure compounds' exchangeable protons. Yet, the traces of water were sufficient for a hydration of RF's ribityl chain and Na-2-OH-Benz's hydroxy group, when Na-2-OH-Benz and RF were dissolved in DMSO-d_6 together.

Further, with increasing molar RF/Na-2-OH-Benz ratio, RF induced a crescent shielding of Na-2-OH-Benz's aromatic protons by 0.1-0.23 ppm, see Figure 47 C. The protons H2 and H4 next to Na-2-OH-Benz's hydroxy group were shielded most, see Figure 48 on the left. Analogously, Na-2-OH-Benz induced at least a slight deshielding of all protons of RF except of the methyl groups, see Figure 48 on the left.

The coupling constants of Na-2-OH-Benz in presence of RF did not correlate with the mole ratio of RF/Na-2-OH-Benz, see Table A 86 in section 7.11.4 in the Appendix. In case of RF, only the coupling constants of the non-exchangeable protons H5/H8 were weakened due to the Na-2-OH-Benz, see Table A 88-Table A 91 in section 7.11.4 in the Appendix.

^{13}C-NMR: Almost all carbon atoms of RF and Na-2-OH-Benz were shifted due to the presence of Na-2-OH-Benz and RF, respectively. Na-2-OH-Benz's carbon atoms were shielded or deshielded by 0.37-1.79 ppm, see Figure 48 on the right. The carbon atoms of RF's ribityl chain were deshielded by 0.22-0-55 ppm and the ones on the isoalloxazine ring were mainly deshielded by 0.04 ppm-1.68 ppm., see Figure 48 on the right.

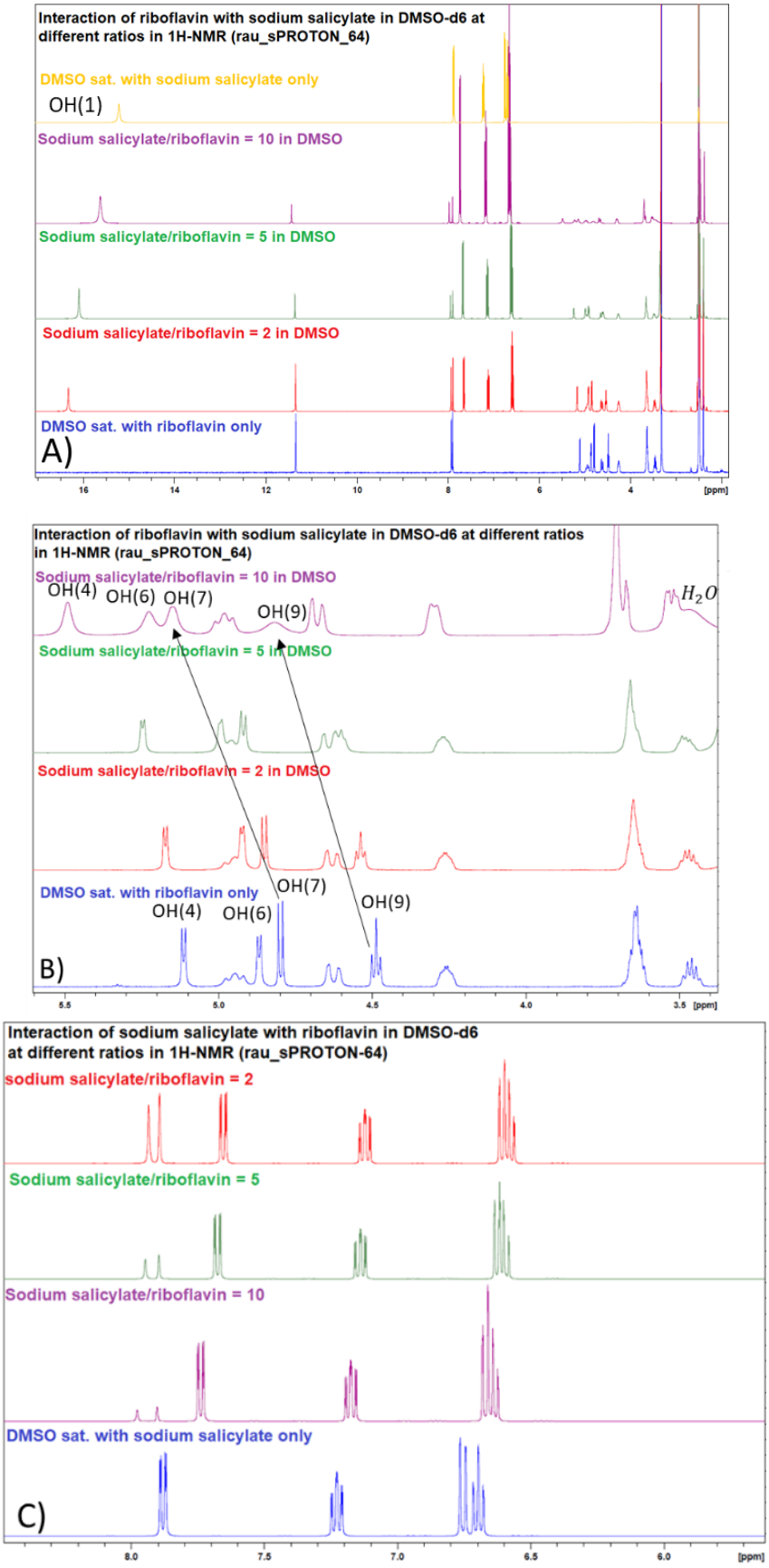

Figure 47: ^{1}H-NMR signals of RF and Na-2-OH-Benz in DMSO-d_6 at different molar ratios of Na-2-OH-Benz/RF. The pure spectra of RF and Na-2-OH-Benz are displayed in blue, yellow and purple. A) Full spectrum with the hydroxy group of sodium salicylate. B) View of the hydroxy groups on ribityl chain of RF. C) View of the aromatic protons of Na-2-OH-Benz.

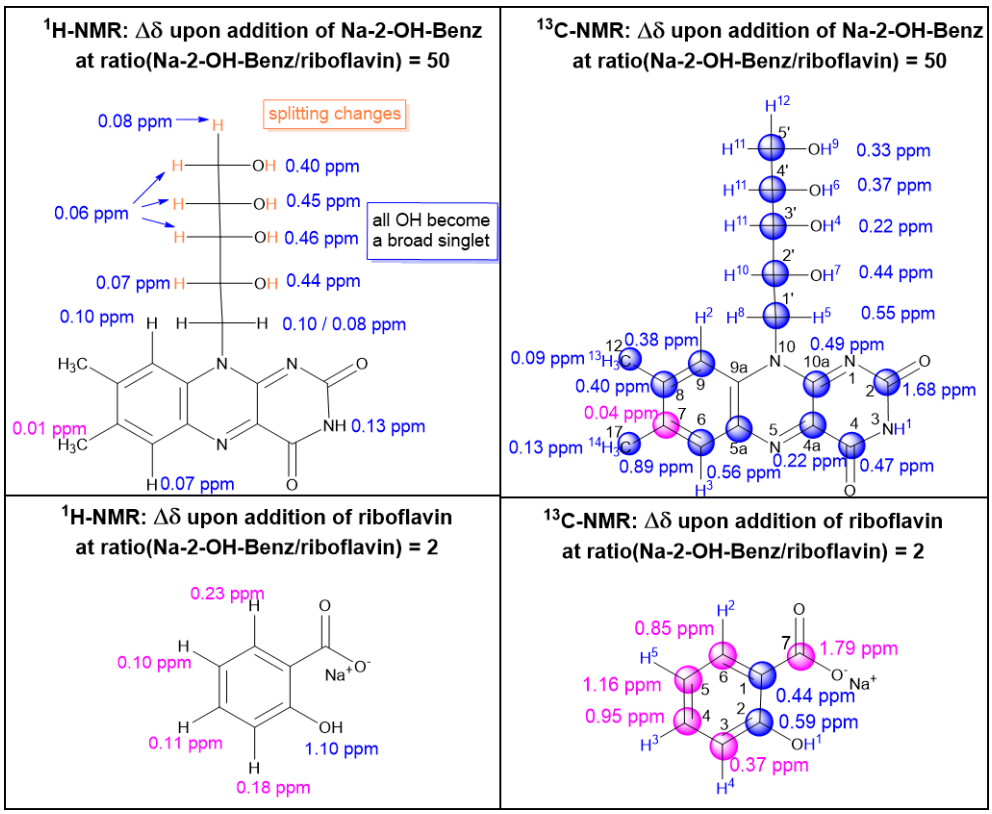

Figure 48: Change of chemical shifts of riboflavin's and sodium salicylate's protons and carbons in ¹H-NMR ¹³C-NMR in presence of Na-2-OH-Benz and RF, respectively, at different molar ratios. Blue: deshielding/ shift to low field; Pink: shift to high field; orange: changed splitting. The corresponding NMR spectra and peak attribution are given in section 7.11.4 in the Appendix.

In the following, the change of the chemical shift of RF's and Na-2-OH-Benz's protons is displayed as a function of the molar ratio of the two molecules, see Figure 49. The change of the chemical shift of all of Na-2-OH-Benz's and RF's protons increased more or less linearly with the molar RF/Na-2-OH-Benz and Na-2-OH-Benz/RF ratio, respectively. In the plot of Δδ of Na-2-OH-Benz against the molar RF/Na-2-OH-Benz ratio, a break point is present at the ratio 5, see Figure 49 A. A break point is also present in the plot of Δδ of RF against the molar Na-2-OH-Benz/RF at ratio 10, see Figure 49 B.

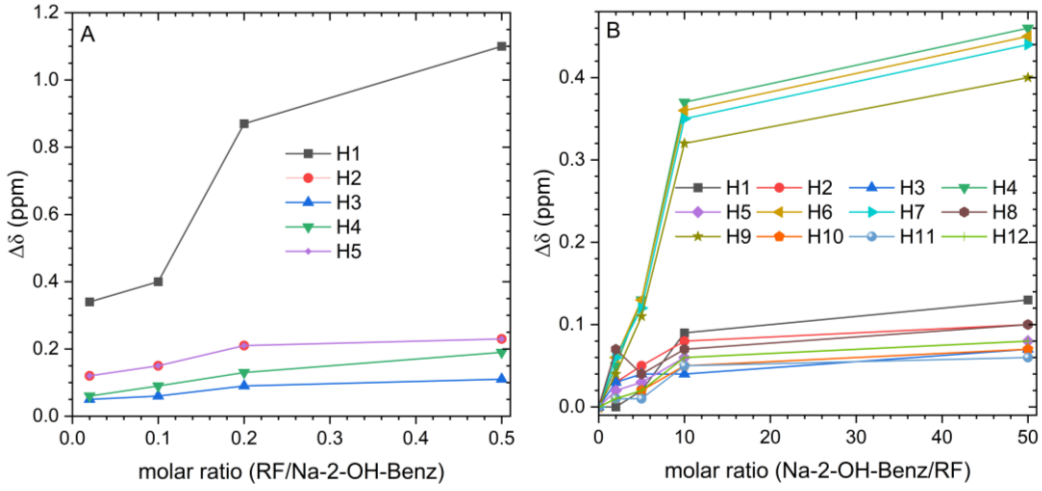

Figure 49: A: Shielding of sodium salicylate's protons depending on the ratio of riboflavin/Na-2-OH-Benz. H2 and H5 of Na-2-OH-Benz have an equal change of the chemical shift, hence the curves overlap. B: Deshielding of riboflavin's protons depending on the ratio of Na-2-OH-Benz/RF.

Further, in Figure 50 and Figure 51, the change of the chemical shift of RF's and Na-2-OH-Benz's carbon atoms at different molar ratios of Na-2-OH-Benz to RF is visualized. Almost all carbons of RF were deshielded more strongly the more Na-2-OH-Benz was present, see Figure 50 A and B. On the contrary, only 2 carbons of Na-2-OH-Benz were deshielded due to the presence of RF, while the other carbons were shielded. Up to a break point at a molar Na-2-OH-Benz/RF ratio of 10, the chemical shift of almost all carbon atoms of RF changed linearly with the ratio of Na-2-OH-Benz/RF, see Figure 50. Analogously, all Na-2-OH-Benz's carbons were shifted linearly up to a Na-2-OH-Benz/RF ratio of 5 see Figure 51.

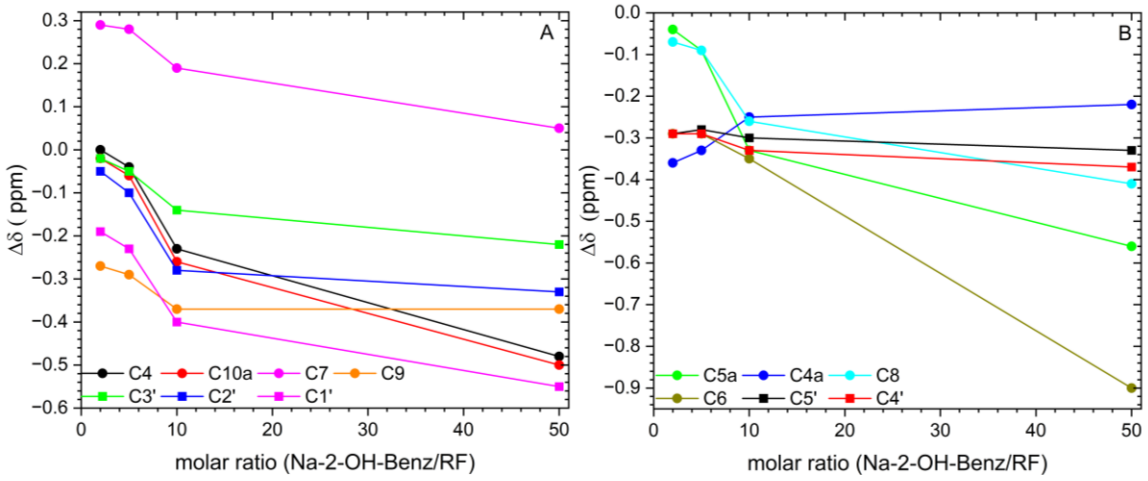

Figure 50: Change of chemical shift of riboflavin's carbons depending on the ratio of Na-2-OH-Benz/RF, for the exact values see section 7.11.4. Negative: Deshielding; positive: Shielding.

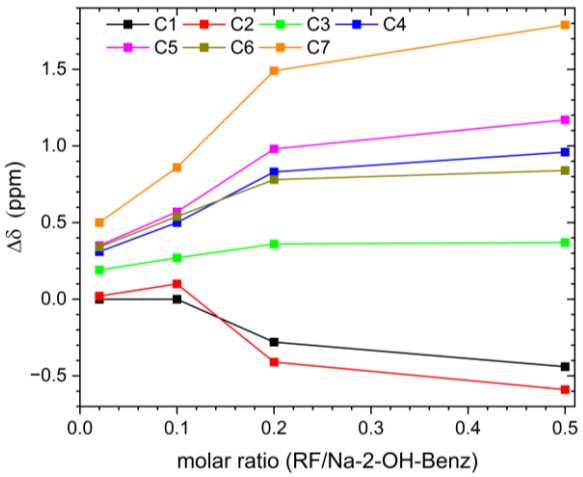

Figure 51: Change of chemical shift of sodium salicylate carbons depending on the ratio of riboflavin to sodium salicylate. The change of the chemical shift, for the exact values see section 7.11.4. Negative: Deshielding; positive: Shielding.

Summary: Until a break point, almost all signals of RF's and Na-2-OH-Benz's protons and carbons changed linearly with the molar Na-2-OH-Benz/RF or RF/Na-2-OH-Benz ratio, respectively.

NOESY spectrum: The cross-peak of RF's aromatic proton H2 with the ribityl chain protons H11 and H12 (area (a) in Figure 52) indicates a curved conformation of the RF's ribityl side chain in presence of Na-2-OH-Benz. The cross-peak of the RF's amine group and its hydroxy groups (area (b) in Figure 52), demonstrates once more the hydration of the exchangeable groups of RF in presence of Na-2-OH-Benz.

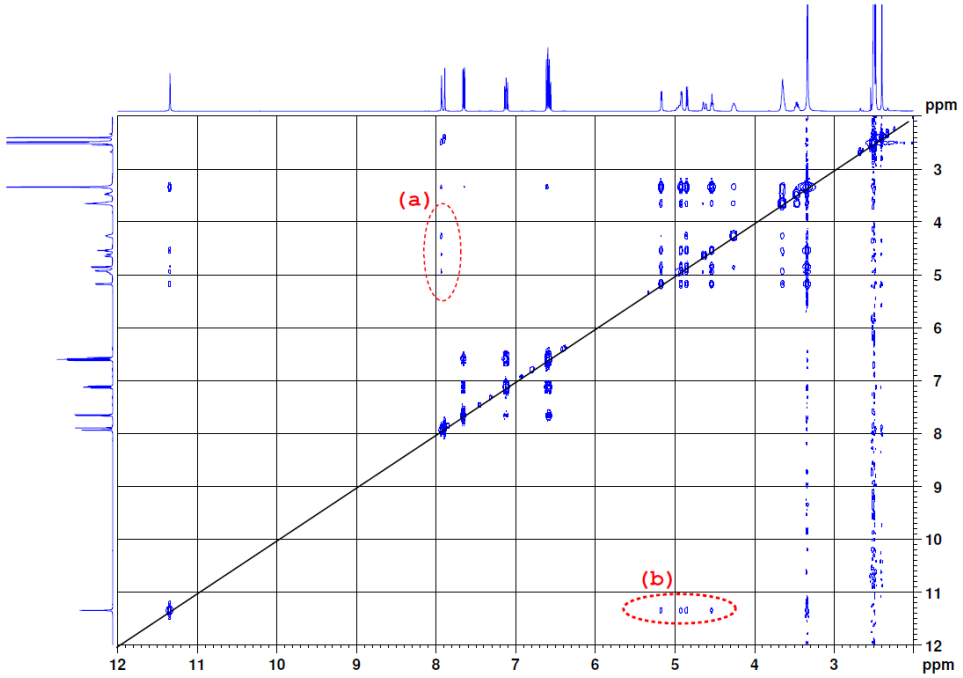

Figure 52: NOESY NMR spectrum of riboflavin in presence of sodium salicylate in DMSO-d_6 with a molar ratio of Na-2-OH-Benz/riboflavin of 2. a) Interaction of H2 of RF with H11/H12/H8/H5 of RF; b) Interaction of amine group with hydroxy groups of RF due to hydration in presence of sodium salicylate.

4.1.2.1.7.3 Riboflavin in presence of sodium 3-hydroxybenzoate

The saturation of DMSO-d_6 with Na-3-OH-Benz and RF resulted in a molar Na-3-OH-Benz/RF ratio of 11. The change of chemical shift of RF and Na-3-OH-Benz's protons and carbons and the numeration of the protons/carbons are given in the structures displayed in Figure 53.

^{1}H-NMR: RF's ribityl chain was completely deprotonated in presence of Na-3-OH-Benz, see Figure 53 on the left and Figure A 36 in section 7.11.5 in the Appendix. Consequently, the splitting of the non-exchangeable protons H11, H12 and H10 was lost and the corresponding signals gave rise to singlets. The protons in RF's isoalloxazine ring H2 (0.18 ppm) and H3 (0.06 ppm) were shifted only slightly in presence of Na-3-OH-Benz, see Figure 53. Analogously, out of Na-3-OH-Benz's protons, only the hydroxy group proton was deshielded by 0.20 ppm, see Figure 53.

^{13}C-NMR: The carbons on RF's ribityl chain were deshielded slightly to considerable by 0.11 – 0.18 ppm, see Figure 53 on the right. Further, almost all carbon atoms on RF's isoalloxazine ring were shifted in different directions, see Figure 53 on the right. Regarding Na-3-OH-Benz, all of its carbon atoms were shifted by > 0.1 ppm, see Figure 53 on the right. All carbon atoms

except of C1 were deshielded. The change of the carbon atom's chemical shift increased from ortho to meta to para.

Summary: In ^{1}H-NMR, only the exchangeable protons of RF and Na-3-OH-Benz experienced a considerable change of the chemical shift due to the presence of Na-3-OH-Benz and RF, respectively. In contrast, almost all carbons of RF and all carbon atoms of Na-3-OH-Benz were shifted due to the presence of Na-3-OH-Benz and RF, respectively.

NOESY: The cross-peak of Na-3-OH-Benz's hydroxy group and RF's aromatic protons H2 and H3 revealed that Na-3-OH-Benz is indeed directly next to RF, see area (b) in Figure 54. If RF and Na-3-OH-Benz perform stacking, then the cross-peaks of the hydroxy group of Na-3-OH-Benz and with the ribityl chain protons H5, H8, H10, H11 and H12 of RF indicate again a curved conformation of the ribityl side chain in presence of sodium polyphenolates, see area (a) in Figure 54.

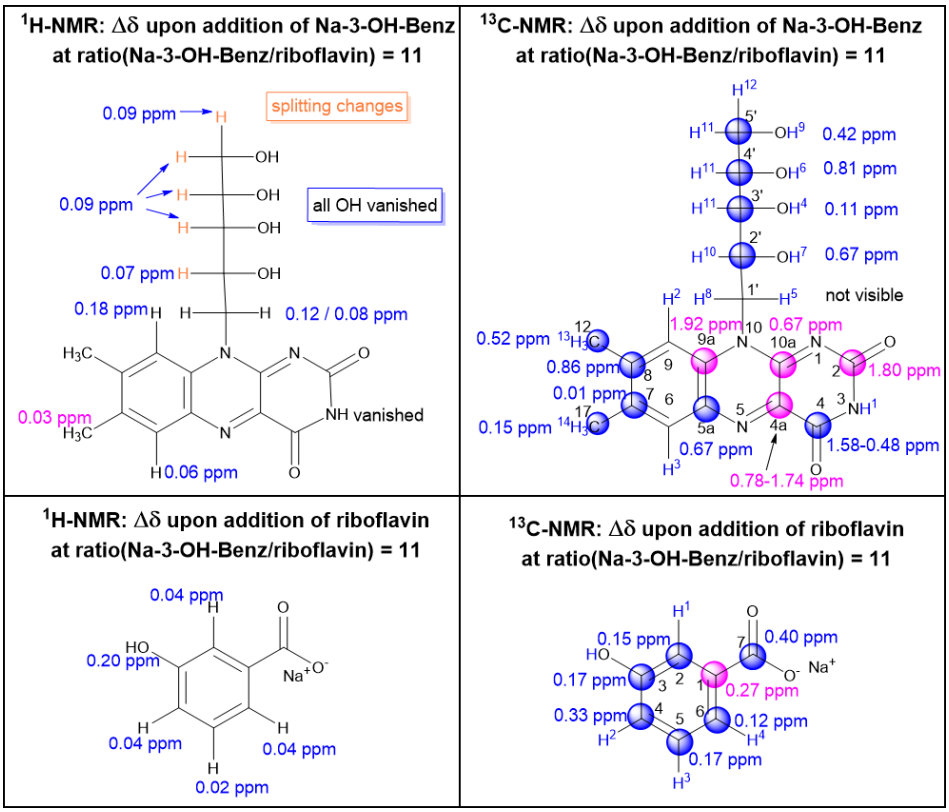

Figure 53: Change of chemical shift Δδ of riboflavin's protons and carbons in presence of sodium 3-hydroxybenzoate in DMSO-d_6 in ^{1}H- and ^{13}C-NMR and vice versa at a molar ratio of Na-3-OH-Benz to RF of 11. Blue: shifted downfield/deshielded; magenta: shifted upfield/shielded, orange: changed splitting. The shift of C9a of RF is not certain, as the signal in the spectrum of pure RF in DMSO-d_6 was hardly visible. The peak attribution and change of the chemical shift are given in section 7.11.5 in the Appendix.

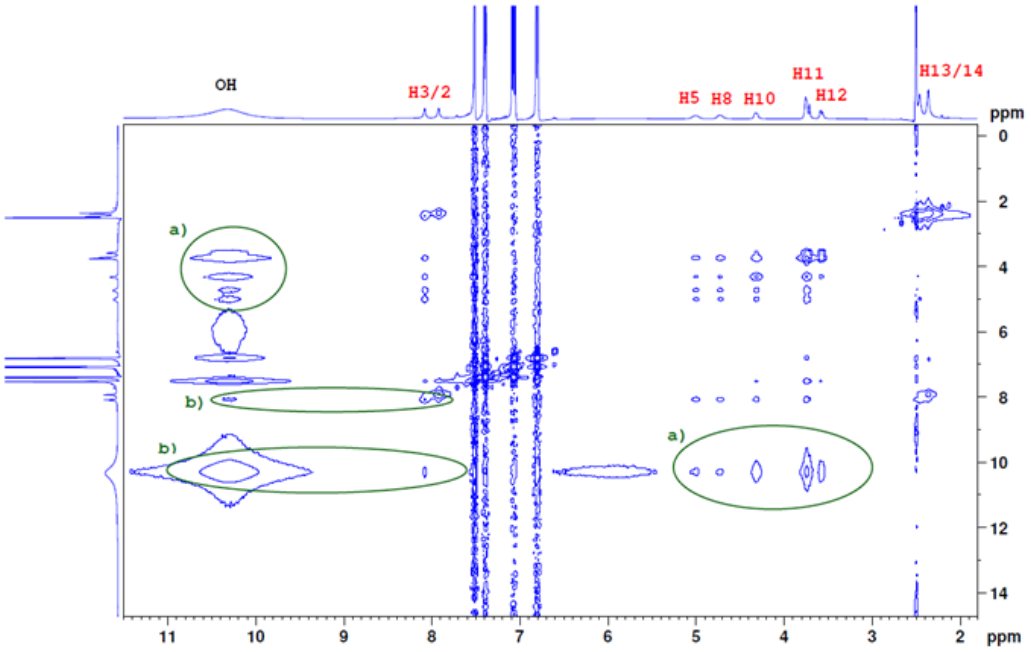

Figure 54: NOESY NMR spectrum of riboflavin in presence of sodium 3-hydroxybenzoate in DMSO-d_6 at the molar ratio of Na-3-OH-Benz/riboflavin = 11. a) Interaction of ribityl side chain (H5, H8, H10, H11, H12) of RF with the hydroxy group of Na-3-OH-Benz. b) Interaction of one aromatic protons (H2/3) of RF with the hydroxy group of Na-3-OH-Benz.

4.1.2.1.7.4 Riboflavin in presence of sodium 4-hydroxybenzoate

A saturation of DMSO-d_6 with Na-4-OH-Benz and RF led to a molar Na-4-OH-Benz/RF ratio of 2. The change of chemical shift of RF and Na-4-OH-Benz's protons and carbons relatively to the pure compounds in DMSO-d_6 and the numeration of the protons and carbons are given in the structures displayed in Figure 55. First, many of RF's protons were broadened and lost their splitting pattern due to the presence of Na-4-OH-Benz. As the ^{1}H-NMR spectrum of pure Na-4-OH-Benz was also distorted, probably the purchased Na-4-OH-Benz contained traces of paramagnetic impurities, which destroyed the coupling of RF's protons. Nevertheless, an evaluation of Na-4-OH-Benz's influence on RF's protons was possible.

^{1}H-NMR: All exchangeable protons of RF were either deshielded or disappeared. The aromatic proton H2 of RF was slightly deshielded by 0.14 ppm, whereas H3, H11, H10, H8, H5 and H14 were not or only scarcely deshielded, see Figure 55 on the left. Regarding Na-4-OH-Benz, only its hydroxy group was shielded by 0.20 ppm. Its residual protons were shielded slightly, see Figure 55 on the left. Obviously, both Na-4-OH-Benz and RF were hydrated strongly by the residual water in DMSO-d_6 if the compounds were present in DMSO-d_6 together. Due to this hydration, a change of the splitting and coupling constants of the protons on the ribityl chain was induced, see Figure 55 below, Table A 102 in section 7.11.6 and Table A 77 section 7.11.1 in the Appendix.

^{13}C-NMR: Most of RF's carbon atoms in the isoalloxazine ring were deshielded by up to 0.50 ppm. Only the methyl groups were shielded. The methyl group of RF (C12) was shifted most by 1.92 ppm upfield, see Figure 55 on the right. Further, all carbon atoms on the ribityl chain were deshielded by 0.24-0.53 ppm. Regarding the carbon atoms of Na-4-OH-Benz, the one on the hydroxy group (C4) and the one on the carboxylate group (C7) were shifted most by 0.21 ppm and 0.14 ppm upfield, respectively. The change of the chemical shift of Na-4-OH-Benz's carbon atoms increased from ortho to meta to para. The same order was observed for NaBenz and Na-3-OH-Benz in the previous sections 4.1.2.1.7.1. and 4.1.2.1.7.3.

Summary: Only exchangeable protons of RF and Na-4-OH-Benz were influenced by the presence of the Na-4-OH-Benz and RF, respectively. The reason was that the presence of RF and Na-4-OH-Benz led to a hydration of Na-4-OH-Benz and RF, respectively. Except of few carbon atoms, the presence of RF and Na-4-OH-Benz resulted in a change of almost all of Na-4-OH-Benz's and RF's carbon's chemical shift, respectively.

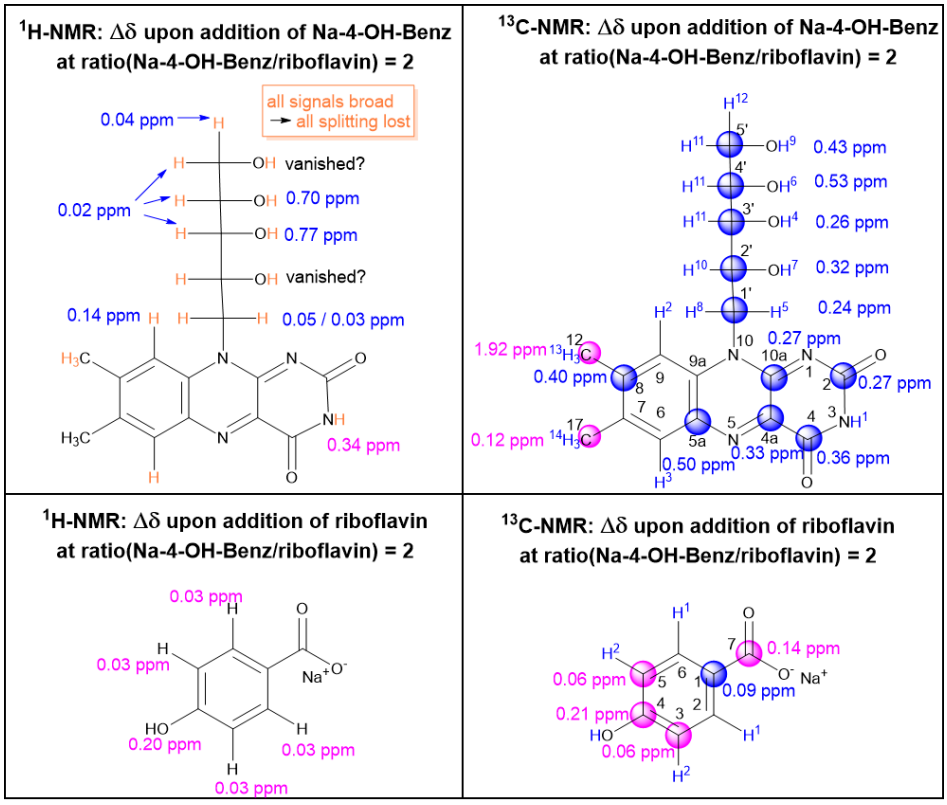

Figure 55: Change of chemical shift Δδ of riboflavin's protons and carbons in presence of sodium 4-hydroxybenzoate in DMSO-d_6 in ^{1}H- and ^{13}C-NMR and vice versa. The molar ratio Na-4-OH-Benz to riboflavin equals 2. Blue: shifted downfield/deshielded; magenta: shifted upfield/shielded; orange: changed splitting. The corresponding NMR spectra and peak attribution are given in section 7.11.6 in the Appendix.

NOESY: The cross-peaks of RF's amine and RF's hydroxy groups with water show again the hydration of the two molecules, when being present in DMSO-d_6 together with Na-4-OH-Benz, see area (a) in Figure 56. The cross-peak of RF's H5 with the aromatic proton H2 of Na-4-OH-Benz shows the proximity of Na-4-OH-Benz to the ribityl chain of RF see area (b) in Figure 56.

Hence, RF and Na-4-OH-Benz must be close to each other in the solution and induce a strong hydration of each other.

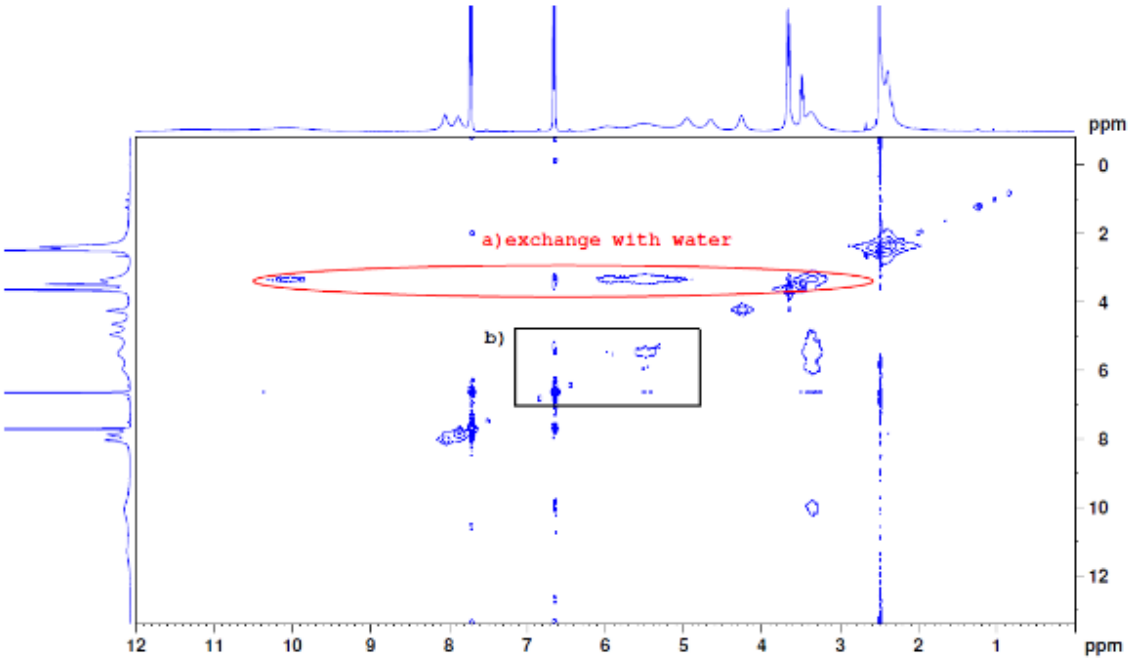

Figure 56: NOESY NMR spectrum of riboflavin with sodium 4-hydroxybenzoate in DMSO-d_6 at a molar ratio of Na-4-OH-Benz/RF = 2. a) Cross-peak between water and RF's amine and hydroxy groups. b) Cross-peak between H2 of Na-4-OH-Benz and H5 of RF.

4.1.2.1.7.5 Riboflavin in presence of sodium vanillate

The saturation of DMSO-d_6 with sodium vanillate and RF resulted in a molar ratio of sodium vanillate to RF of 1.3. The change of chemical shift of RF and Na-4-OH-3-OMe-Benz's protons and carbons relatively to the pure compounds in DMSO-d_6 and the numeration of the protons/carbons are given in the structures displayed in Figure 57.

^{1}H-NMR: Sodium vanillate did not induce a significant shift of the protons in RF's isoalloxazine ring. Thus, the aromatic proton H2 of RF was the only one being shifted downfield by 0.12 ppm, see Figure 57 on the left. Regarding the protons on RF's ribityl chain, the splitting changed and the signals and exchangeable hydroxy groups were deshielded and broadened (H4/H6) or disappeared (H7/H9), see Figure 57 on the left. Presumably due to the hydration, the coupling of H5 with H8 on the ribityl side chain decreased compared to pure RF in DMSO-d_6 (12.17 Hz with vanillate, 13.65 Hz pure RF in DMSO-d_6). The hydroxy group of sodium vanillate was slightly deshielded by 0.14 ppm and broadened due to the presence of RF, whereas the residual protons of sodium vanillate were scarcely influenced by the presence of RF, see Figure 57 on the left.

^{13}C-NMR: Though the change of the chemical shift in ^{1}H-NMR was only significant for the exchangeable groups, all carbon atoms of RF (except C9a as uncertain signal) and all carbons

of sodium vanillate were shifted in presence of vanillate and RF, respectively. Due to the presence of sodium vanillate, the carbon atoms on the ribityl side chain of RF were deshielded by 0.18-0.49 ppm. Additionally, sodium vanillate induced a shift of all carbon atoms on the aromatic isoalloxazine ring of RF. C2, C4, C9 were even shifted by 1.97 ppm upfield, 2.94 ppm downfield and 0.47 ppm downfield, respectively. Regarding sodium vanillate, all carbon atoms were shifted noticeably. The carbon C3 next to the methoxy group of vanillate was shifted most (1.01 ppm upfield).

Summary: Non-exchangeable protons of RF and sodium vanillate were not significantly influenced by the presence of sodium vanillate and RF, respectively. In contrast, all hydroxy groups of RF and sodium vanillate were either broadened and deshielded or deprotonated due to the presence of the other vanillate and RF, respectively. Further, RF and sodium vanillate induced mutual a change in the electro-magnetic environment of almost all carbon atoms of vanillate and RF, respectively.

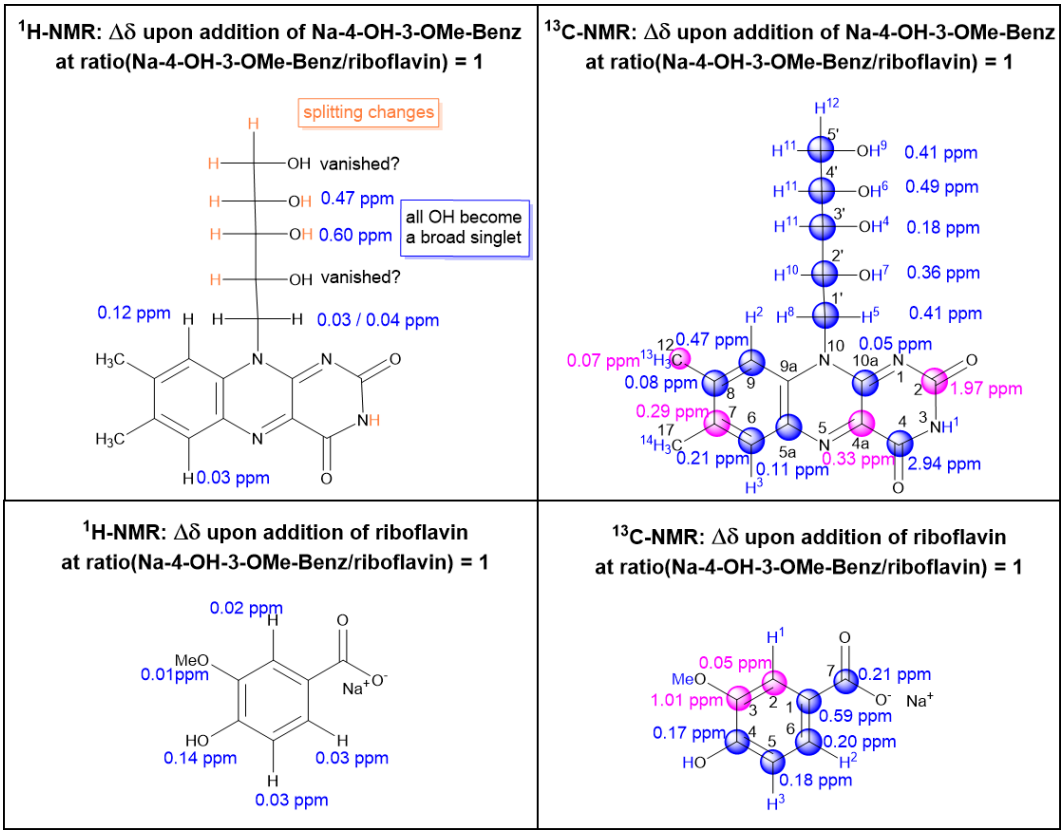

Figure 57: Change of chemical shift Δδ of riboflavin's protons and carbons in presence of sodium vanillate in DMSO-d_6 in ^{1}H- and ^{13}C-NMR and vice versa. The ratio sodium vanillate to RF equals 1.3. Blue: shifted downfield/deshielded; magenta: shifted upfield/shielded; orange: changed splitting. The corresponding NMR spectra and peak attribution are given in section 7.11.7 in the Appendix.

NOESY NMR: At least one of RF's methyl groups gave rise to a cross-peak with the protons H11 on RF's ribityl chain, see Figure 58. Thus, the ribityl chain is probably curved in presence of sodium vanillate.

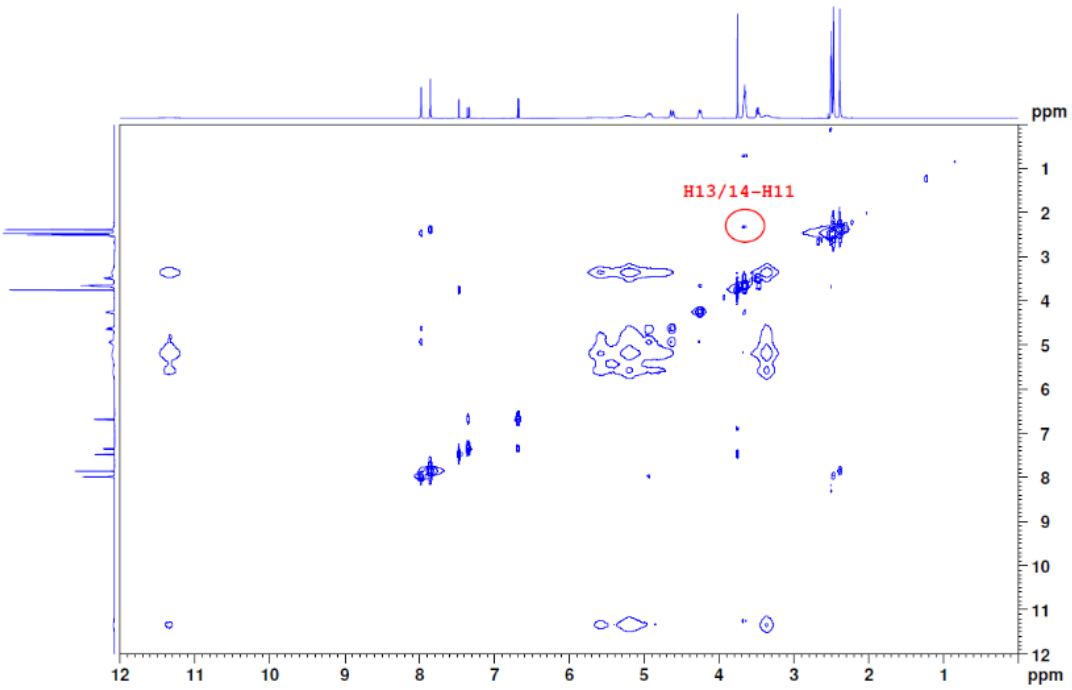

Figure 58: NOESY NMR spectrum of riboflavin in presence of sodium vanillate in DMSO-d_6 at a molar vanillate/riboflavin ratio of 1.3. Red: Cross-peak of H13 and/or H14 of riboflavin with H11 of riboflavin.

4.1.2.1.7.6 Riboflavin in presence of sodium cinnamate

The NMR spectra of NaCinn in DMSO-d_6 and of NaCinn in presence of RF in DMSO-d_6 at the molar NaCinn/RF ratios of 1 and 0.4 and the peak attribution are given in section 7.11.8 in Appendix. Due to the low solubility of NaCinn in DMSO-d_6, the signal to noise ratio was low in ^{13}C-NMR. Still, some signals could be attributed. The maximum change of chemical shift of RF and NaCinn's protons and carbons relatively to the pure compounds in DMSO-d_6 with the numeration of the protons/carbons is displayed in Figure 59.

^{1}H-NMR: The presence of RF induced only a slight shift of NaCinn's side chain protons H2 and H1 by 0.08 and 0.02 ppm downfield. NaCinn's splitting and coupling constants were not altered by the presence of RF, see Table A 109 in section 7.11.8 in the Appendix. Analogously, RF's protons on the isoalloxazine ring were just marginally influenced by NaCinn. Only, H2 and H3 were scarcely deshielded, see Figure 59 on the left. The exchangeable protons on the ribityl chain were deshielded by up to 0.36 ppm, broadened and two signals disappeared completely, see Figure A 51 and Figure A 52 in section 7.11.8 in the Appendix. Hence, NaCinn led to a hydration of RF.

^{13}C-NMR: Even after saturation, the signals of RF's carbon atoms and some of NaCinn were very noisy. Therefore, for some carbon atoms of RF two (C2, C10a, C4a) or even three (C1) signals would be possible. For C4, C2 and C9a, the shift was not determined as the signal was too uncertain. Regarding RF, almost all carbon atoms were shifted due to the presence of NaCinn. C6 in the isoalloxazine ring was shifted most by 1.05 ppm downfield, see Figure 59

on the right. The carbons on the ribityl chain were all deshielded by 0.22 to 0.38 ppm. For C1 several signals were obtained. Hence it was either shielded by 0.43 ppm or deshielded by 0.83 ppm. Further, the NaCinn's carbon atoms on the side chain were shifted most (0.37 ppm, 1.19 ppm) and were the only carbons of NaCinn being shielded, see Figure 59 on the right. All other carbons were deshielded, out of which the C1 on the carbonyl group was deshielded the most by 1.07 ppm.

Summary: The change of the chemical shift of RF's non-exchangeable and NaCinn's protons induced by the presence of NaCinn and RF, respectively, was extremely weak. Yet, the hydroxy groups of RF were obviously deprotonated due to the presence of NaCinn. In ^{13}C-NMR, the carbon atoms of NaCinn and RF were clearly shifted due to the presence of RF or NaCinn, respectively. However, due to the low signal to noise ratio, the change of RF's carbon atoms in ^{13}C-NMR must be regarded cautious.

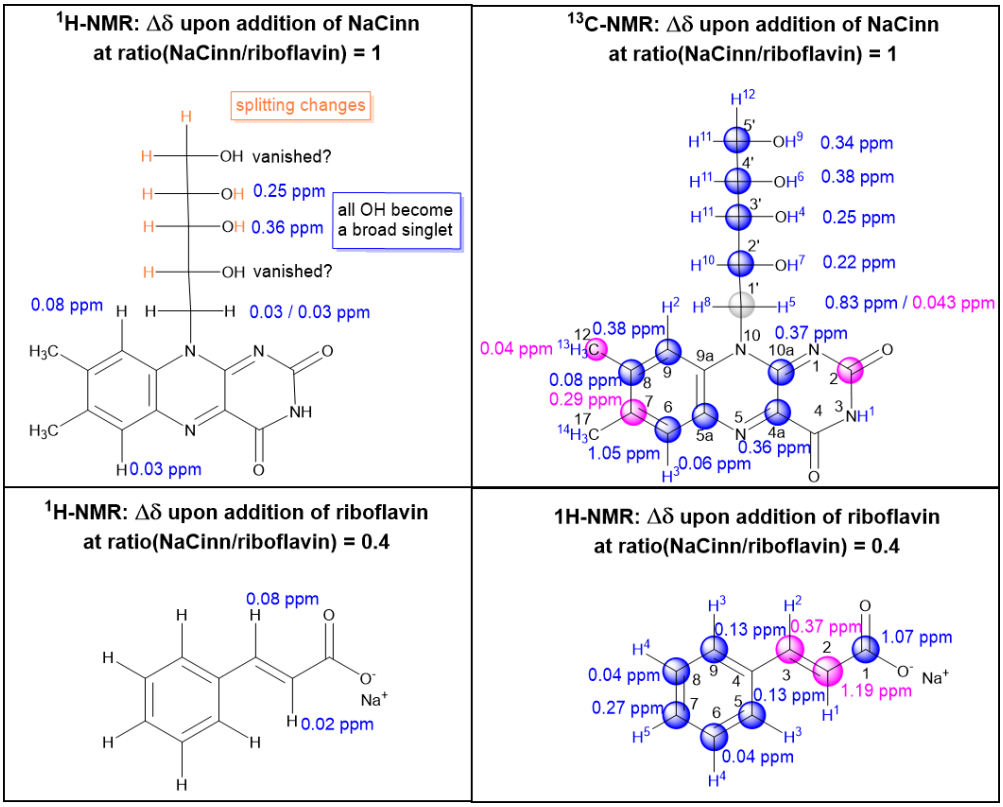

Figure 59: Change of chemical shift Δδ of riboflavin's protons and carbons an in presence of sodium cinnamate in DMSO-d_6 in ^{1}H- and ^{13}C-NMR and vice versa. The molar ratio of NaCinn to RF equals 1 for the shifts of the protons of RF and 0.4 for the shift of the protons of NaCinn. Blue: shifted downfield/deshielded, magenta: shifted upfield/shielded, orange: splitting changed. The corresponding NMR spectra and peak attribution are given in section 7.11.8 in the Appendix. C2 of RF was probably shielded, but it disappeared in the noise, therefore a certain change of the chemical shift was not determined.

NOESY: Unusual cross-peaks of RF and NaCinn were not observed in the NOESY NMR spectrum of NaCinn with RF at a molar ratio of 1, see Figure A 57 and Figure A 58 in section 7.11.8 in the Appendix.

4.1.2.1.7.7 Sodium riboflavin 5'-monophosphate in presence of sodium ferulate in deuterium oxide

To evaluate the change of the chemical shift of RF due to the presence of the sodium polyphenolates, NMR spectra of RF-PO_4, comprising the same molecular backbone, with the water-soluble sodium ferulate in deuterium oxide at a molar ferulate/RF-PO_4 ratio of 5.5 were recorded, see section 7.11.9 in the Appendix for the spectra and peak attribution. To have a reference peak in ^{13}C-NMR, a tube with DMSO-d_6 was inserted. The numeration of the protons and carbon atoms of sodium ferulate and RF-PO_4 is reported in Figure 60 on the right. The change of the chemical shift of RF-PO_4's and sodium ferulate's protons and carbon atoms due to the presence of sodium ferulate and RF-PO_4, respectively, is displayed in the same figure.

^{1}H-NMR: Due to proton exchange in deuterium oxide, all exchangeable groups were not visible and were not regarded for the evaluation. The non-exchangeable protons of RF-PO_4 were shifted only slightly due to the presence of sodium ferulate (≤ 0.15 ppm), see Figure 60 on the right. On the other side, the non-exchangeable protons of sodium ferulate were obviously shielded by 0.15-0.34 ppm, see Figure 60 on the left.

^{13}C-NMR: Sodium ferulate induced a change of all of RF-PO_4's carbon atoms, see Figure 60 on the right. C5' was the only carbon on the ribityl phosphate chain, which was shielded. The residual carbons on the ribityl phosphate chain were deshielded. In the isoalloxazine ring, the aromatic carbons C8, C4a, C4, C6 were shifted most (up to 1.14 ppm) due to the presence of sodium ferulate. Both methyl groups of sodium RF-PO_4 were deshielded slightly by 0.12 ppm. Regarding sodium ferulate, all of its carbon atoms were shielded due to the presence of RF-PO_4 (0.3-0.56 ppm), see Figure 60 on the right.

Summary: Although the protons of RF-PO_4 were not considerably affected by sodium ferulate, all of RF-PO_4's carbon atoms were visibly shifted in up- or downfield. In case of sodium ferulate, all of its protons and carbon atoms were shielded considerably due to the presence of RF-PO_4.

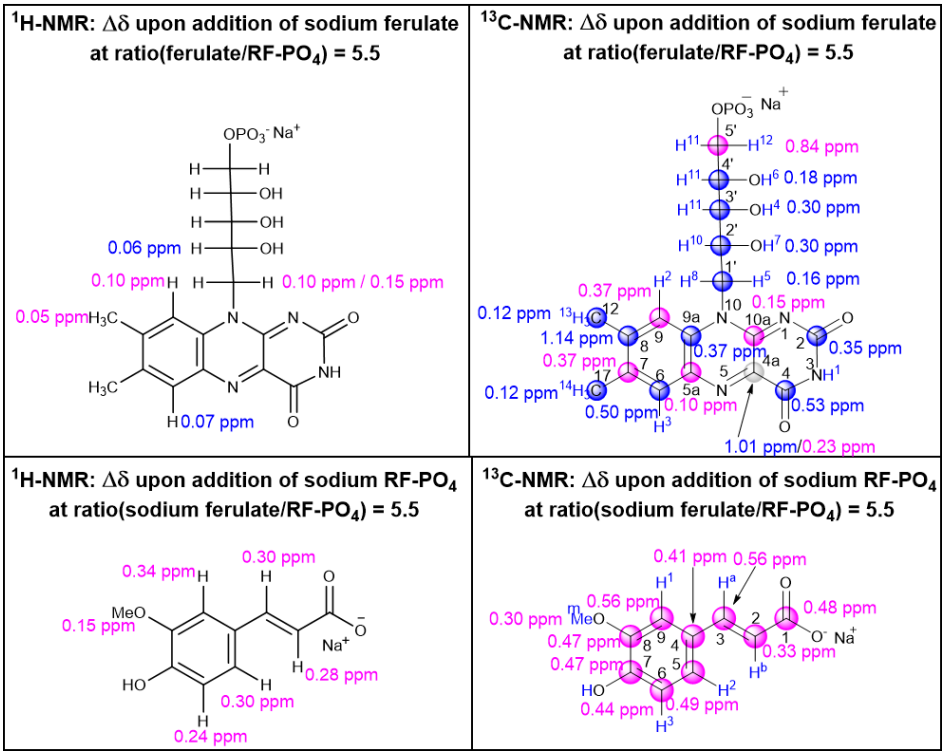

Figure 60: Change of chemical shift Δδ of the protons and carbon atoms of riboflavin 5'-monophosphate sodium salt and sodium ferulate due to the presence of sodium ferulate and riboflavin 5'-monophosphate sodium salt, respectively, in deuterium oxide. The molar ratio sodium ferulate to RF-PO$_4$ equals 5.5. Blue: shifted downfield/deshielded and magenta: shifted upfield/shielded. For the corresponding NMR spectra and peak attribution see section 7.11.9 in the Appendix

NOESY: The NOESY spectrum of RF-PO$_4$ in presence of sodium ferulate comprises artefacts distributed symmetrically around the peak on the diagonal line. These artefacts were even present after repetition of the experiment and new preparation of the sample. At the distinct molar ratio of sodium ferulate/RF-PO$_4$ of 10, the artefacts were still present. An analysis with Rotating frame Overhauser Enhancement Spectroscopy led also to the same artefacts. A possibility was that sodium ferulate comprised paramagnetic impurities, which gave rise to such artefacts. Yet, a change of the distributor of the sodium ferulate salt (abcr, sodium ferulate 95 %) did not prevent the artefacts in presence of RF-PO$_4$. Therefore, only certain cross-peaks are marked in the NOESY spectrum in Figure 61. The cross-peak of the aromatic proton H2 of RF-PO$_4$ with the protons H11 and H12 on the ribityl phosphate chain indicates a curved ribityl phosphate chain in presence of sodium ferulate, see area (a) in Figure 61. The proton H2 has also a common cross-peak with water, which might result from the curved ribityl phosphate chain due to its strong hydration because of the hydroxy groups and phosphate group, see area (b) in Figure 61. Additionally, the cross-peak of the proton H3 on the isoalloxazine ring with H8, H10, H11 and H12 on the ribityl phosphate chain of RF-PO$_4$ indicates a stacking of RF-PO$_4$ with itself and a curved ribityl phosphate chain, see areas (a) and (b) in Figure 61. Further, the cross-peak of one of RF-PO$_4$'s protons H11 and H12 on the ribityl phosphate chain with the methoxy group of sodium ferulate was observed, see area (c)

in Figure 61. Thus, in spite of the strong hydration of the ribityl phosphate chain, sodium ferulate seems to be in the near environment of the curved chain.

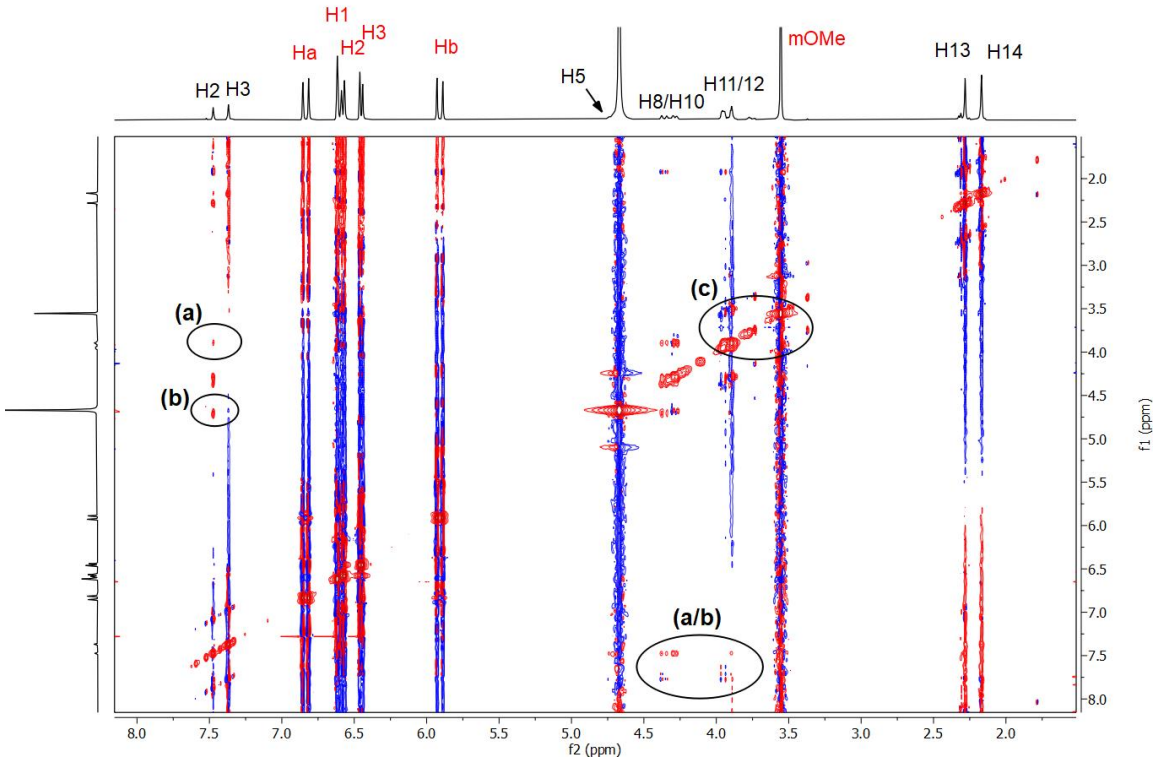

Figure 61: NOESY NMR spectrum of riboflavin 5'-monophosphate sodium salt in presence of sodium ferulate at a molar ratio of sodium ferulate/RF-PO_4 = 5.5 in deuterium oxide. a) H2 with H11/12 of RF-PO_4; b) H2 of RF-PO_4 with deuterium oxide; a/b) H3 of with H8/H10/H11/H12 of RF-PO_4; c) H11/H12 of RF-PO_4 with the methoxy group of sodium ferulate.

4.1.2.1.7.8 Summary

In Figure 62, the protons and carbons atoms of RF, sodium benzoate derivatives and of NaCinn experiencing a change of the chemical shift due to the presence of benzoate derivatives/cinnamate and RF, respectively, are marked.

^{1}H-NMR: Because the purchased DMSO-d_6 was water-free, the exchangeable protons of RF and Na-2-OH-Benz, Na-3-OH-Benz, Na-4-OH-Benz and Na-4-OH-3-OMe-Benz in DMSO-d_6 exhibited sharp signals of a well-defined splitting pattern, see in section 7.11 in the Appendix. Yet, all sodium polyphenolates as well as NaBenz and NaCinn induced a deshielding and peak broadening of the hydroxy groups and of the amine group of RF in DMSO-d_6, see section 7.11 in the Appendix. Sometimes, only the splitting was lost, while the presence of NaBenz, Na-4-OH-Benz, sodium vanillate and NaCinn resulted in a disappearance of some of RF's hydroxy group signals. On the other side, RF induced a peak broadening and deshielding of the hydroxy groups of Na-2-OH-Benz, Na-3-OH-Benz, Na-4-OH-Benz and sodium vanillate, too, see section 7.11 in the Appendix. As DMSO is hygroscopic, even "water-free" DMSO-d_6 contains residual amounts of water.[274] Usually, such low amounts of water do not lead to a hydration of exchangeable groups. Thus, RF or sodium polyphenolates alone in DMSO-d_6 were not

sufficiently hydrated to endure a loss of their exchangeable groups. Yet, apparently the traces of water were attracted by RF and the sodium salts, if the compounds were dissolved in DMSO-d_6 together.

Additionally, a cross-peak of the non-exchangeable aromatic proton H2 on the isoalloxazine ring of the RF-analogue RF-PO_4 with water was present in the NOESY spectrum of RF-PO_4 in presence of sodium ferulate in deuterium oxide, while there was no such cross-peak in the NOESY spectrum of pure RF-PO_4 in absence of sodium ferulate. This means, RF-PO_4 and sodium ferulate induced a mutual hydration of each other in deuterium oxide, too. These observations are in line with the mutual increase of the water-solubility of RF and sodium polyphenolates observed in section 4.1.2.1.1.

Due to the hydration of the ribityl chain in presence of sodium polyphenolates, the non-exchangeable protons (H11, H12, H10, H8, H5) were also deshielded in presence of most sodium polyphenolates. Analogously, on the phosphate chain of RF-PO_4, all carbon atoms were deshielded except of the one directly next to the phosphate group (C5'). Thus, the hydration of RF and RF-PO_4 by sodium polyphenolates induced deshielding of RF's and RF-PO_4's protons and carbon atoms on the ribityl chain. However, nor the degree of proton exchange (deprotonation/deshielding) neither the change of the chemical shift correlated with the solubilization power of sodium polyphenolates for RF in water from section 4.1.2.1.1

Further, the non-exchangeable protons of RF and RF-PO_4 were affected only scarcely by all aromatic sodium carboxylate salts. Analogously, the aromatic protons of NaBenz, Na-2-OH-Benz, Na-3-OH-Benz, Na-4-OH-Benz, sodium vanillate and NaCinn were shifted only marginally ($\leq$ 0.23 ppm), too. In the case of NaCinn, the side chain protons H1 and H2 were also only slightly deshielded (0.02 and 0.08 ppm). Consequently, in DMSO-d_6, the non-exchangeable protons of RF and the ones of the aromatic sodium carboxylates experienced only a slight change of the electro-magnetic field due the presence of the aromatic salt and RF, respectively. Regarding the NMR experiments with RF-PO_4 in deuterium oxide, all protons of sodium ferulate were shielded by 0.15-0.34 ppm, see Figure 60 in section 4.1.2.1.7.7. Still, sodium ferulate did not induce a noticeable change of the chemical shift of RF-PO_4's aromatic protons. Nevertheless, the slight change of the chemical shift shows specific interactions between RF or RF-PO_4 and aromatic sodium carboxylates.

^{13}C-NMR: RF induced a slight change of the chemical shift of almost all carbon atoms of aromatic sodium carboxylates. Only in the case of Na-4-OH-Benz and NaCinn, not all carbon signals were shifted by the presence of RF, see Figure 45, Figure 48, Figure 53, Figure 55, Figure 57 and Figure 59 on the right. Analogously, RF-PO_4 induced a shielding of all of sodium ferulate's carbon atoms. Yet, such as in proton NMR, there was no correlation between the shift's direction or value and the aqueous solubilization power of the compounds for RF, see section 4.1.2.1.1. This might be due to the fact that the solubilization of RF seemed also to

depend on the hydration of its solubilizer and NMR experiments were carried out in DMSO-d_6 and not in water, where the solubilization curves were recorded.

Further, out of the carbon atoms in Na-4-OH-3-OMe-Benz, the one next to the methoxy group (C3) was shifted most due to the presence of RF. Interestingly, methoxy groups improved the aqueous RF solubilizing power of sodium polyphenolates, see section 4.1.2.1.1. Additionally, for NaBenz, Na-3-OH-Benz and Na-4-OH-Benz, the chemical shift in ^{13}C-NMR was changed due to the presence of RF in DMSO-d_6 more for the carbon atoms in para than meta position and for carbon atoms in meta position more than in ortho position, see Figure 45, Figure 53 and Figure 55 in the sections 4.1.2.1.7.1, 4.1.2.1.7.3 and 4.1.2.1.7.4. This correlates to the increase of the solubilization efficiency by a substitution of sodium polyphenolates with hydroxy/methoxy groups from ortho to meta to para from section 4.1.2.1.1. Moreover, the aromatic sodium salts led also to a change of almost all of RF's and RF-PO_4's carbons' chemical shift. Hence, the interaction of RF or RF-PO_4 with sodium polyphenolates seemed to include the entire carbon backbone.

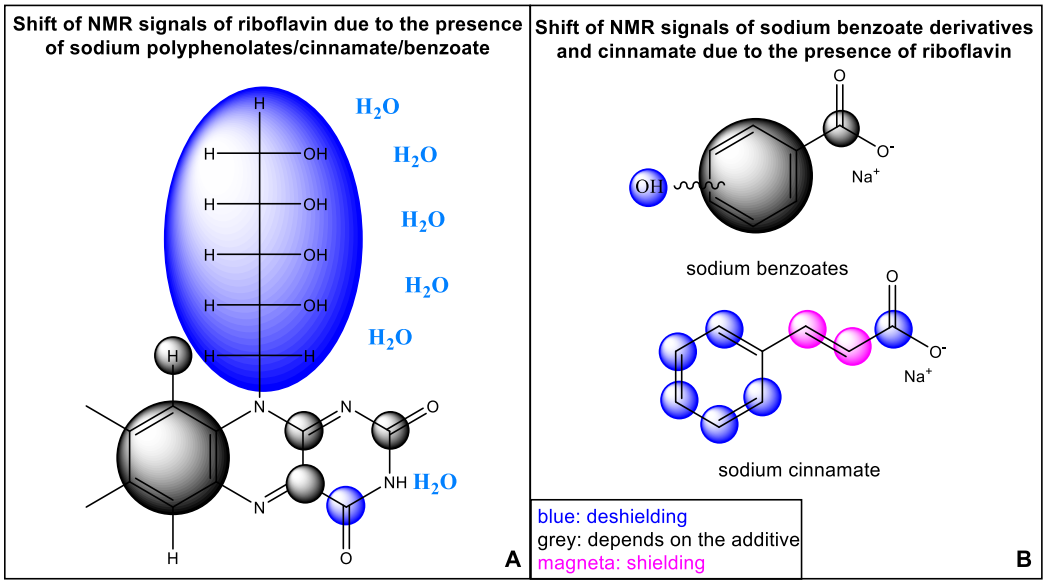

Figure 62: Change of the chemical shift of riboflavin's proton and carbon atoms due to the presence of sodium polyphenolates, sodium cinnamate or benzoate in DMSO-d_6. B: Change of the chemical shift of the protons and carbons of sodium benzoate derivatives, benzoate and of cinnamate due to the presence of riboflavin in DMSO-d_6

Note: In the case of HOMO-LUMO interactions, which are supposed to be the origin of charge transfer complexes, the electron density of both complexants should theoretically increase and lead to a shielding of the protons.[275,276] However, some protons were deshielded. One reason therefore might be the oversize of RF compared to polyphenolates and that the aromatic backbone of RF comprises heteroatoms, which might complicate the HOMO-LUMO interaction. Yet, the main reason for this inconsistent shielding or deshielding of the protons and carbons is probably that the π-system driven solubilization of RF and the copigmentation were observed in aqueous samples, while NMR experiments were carried out in DMSO-d_6. DMSO-d_6 is known to interact strongly with other compounds via hydrogen bonding and to

weaken intermolecular interactions. Consequently, DMSO-d_6 might hinder the attractive interactions of RF with sodium polyphenolates.

NOESY: A NOESY spectrum of an aqueous 3 mol·kg^{-1} Na-3,4-DiOMe-Cinn solution saturated with RF, where the signal to noise ratio was good, could be recorded, see Figure 63. As NOESY has a detection limit of 5 Å and common distances for π-stacked compounds are 3.46-3.85 Å, the cross-peaks of RF's and Na-3,4-DiOMe-Cinn's protons along the entire molecules affirm a π-stacked arrangement of RF and Na-3,4-DiOMe-Cinn in aqueous solution, see Figure 63.[249,277–280]

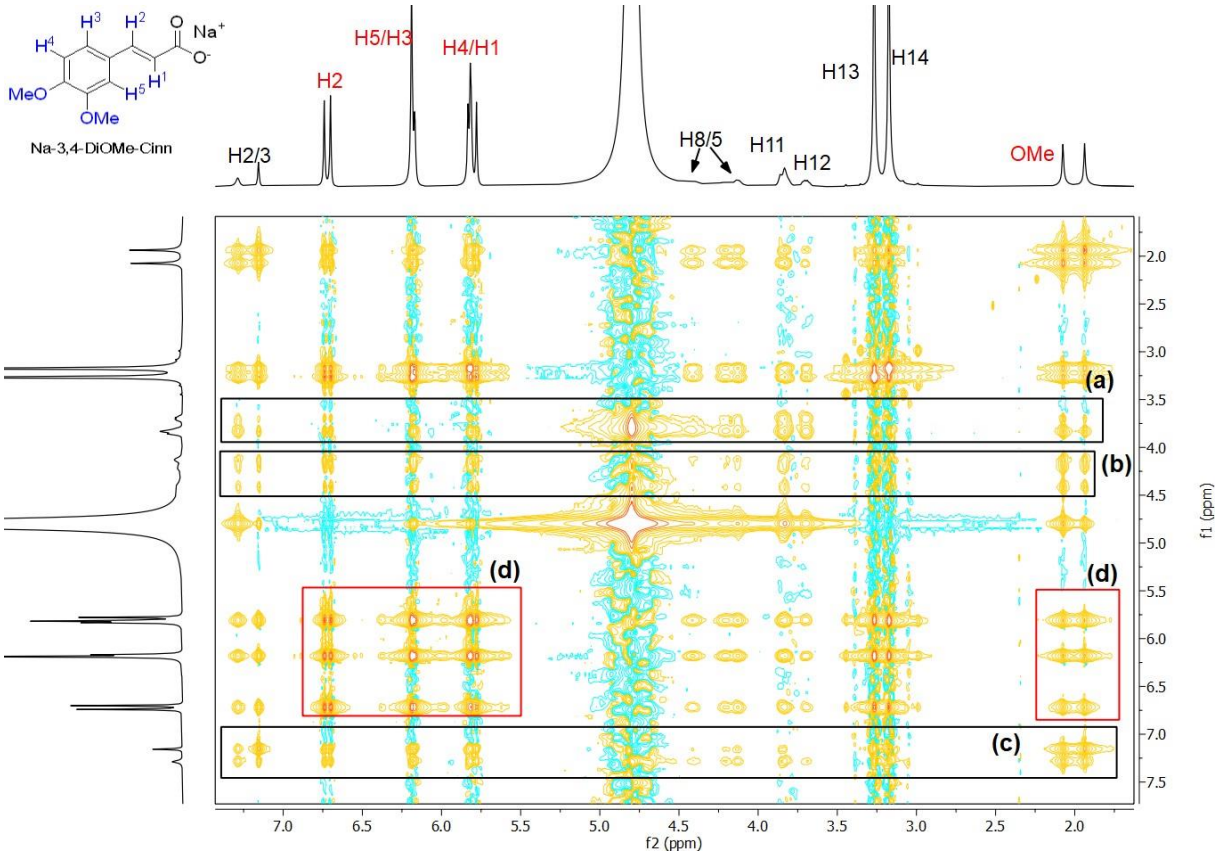

Figure 63: NOESY spectrum of an aqueous 3 mol·kg^{-1} sodium 3,4-dimethoxycinnamate solution saturated with riboflavin. a) Cross-peaks of the ribityl chain protons H12 and H11 with H5/8, H2/3, H13/14 of RF and with H2, H5, H3, H4, H1 and with the methoxy groups of Na-3,4-DiOMe-Cinn; b) Cross-peaks of H8/5 of riboflavin with H11, H12, H2/3, H13/14 of RF and with H2, H5, H3, H4, H1 and with the methoxy groups of Na-3,4-DiOMe-Cinn; c) Cross-peaks of the aromatic protons H2/3 of RF with H13/14, H11, H12, H8/5 of RF and with H2, H3 H5, H4, H1 and with the methoxy groups of Na-3,4-DiOMe-Cinn; d) all protons of Na-3,4-DiOMe-Cinn interact with each other.

Further, the NOESY NMR spectrum of Na-2-OH-Benz with RF in DMSO-d_6 and the one of sodium vanillate with RF in DMSO-d_6 indicated a curved ribityl side chain of RF in presence of these sodium polyphenolates, see Figure 64 A and B. The NOESY spectrum of RF and Na-3-OH-Benz revealed a proximity of the non-exchangeable protons of RF's ribityl side chain (H12, H11, H10, H8, H5) to the hydroxy group of Na-3-OH-Benz, see Figure 64 C. As RF and sodium polyphenolates perform π-stacking (see section 4.1.2.1.1), the cross-peak of Na-3-OH-Benz's hydroxy group with H2 of RF might be induced due to the proximity of these protons because of a stacked arrangement of the two molecules. If so, then the interaction of Na-3-OH-Benz's

hydroxy group with the non-exchangeable ribityl side chain protons indicated again a curved conformation of the ribityl side chain. Additionally, the cross-peaks of at least one proton of Na-3-OH-Benz, NaBenz and Na-4-OH-Benz showed that RF and sodium polyphenolates are directly next to each other when being dissolved in DMSO-d_6, see Figure 64 D, E.

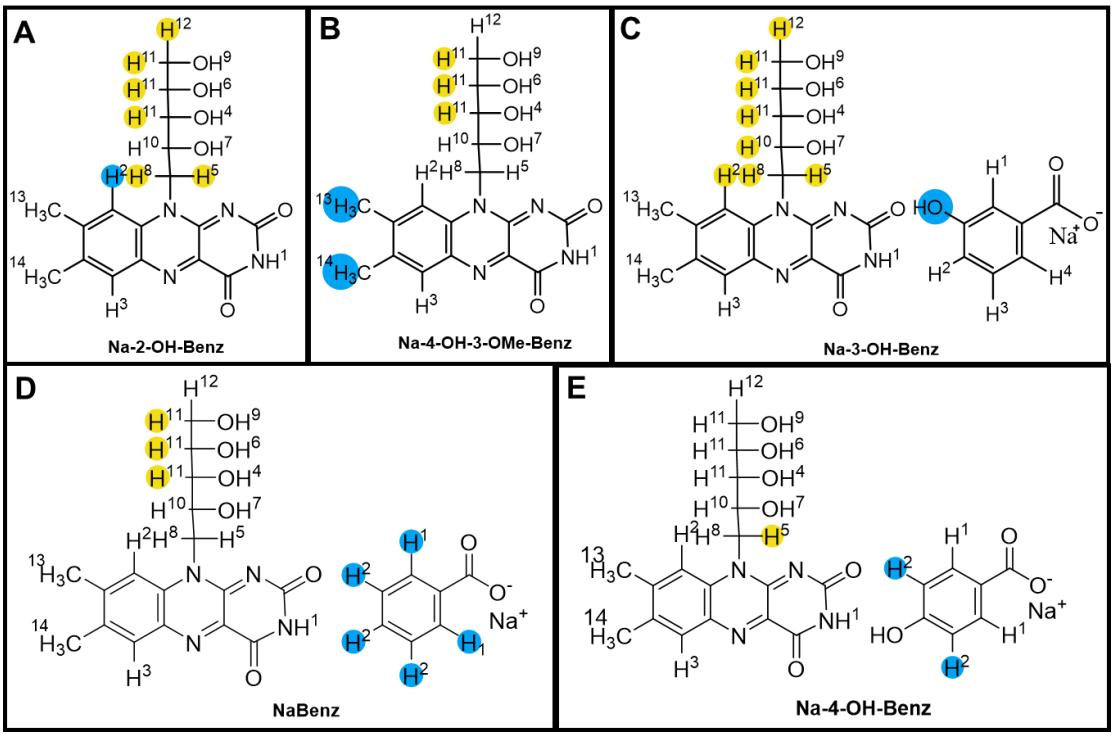

Figure 64: Interactions derived from the NOESY spectra: A-C) Indications for a curved ribityl side chain from the NOESY NMR spectra in DMSO-d_6: A) RF in presence of Na-2-OH-Benz at a molar ratio of Na-2-OH-Benz/RF = 2. B) RF in presence of an equimolar amount of sodium vanillate. C) RF in presence of Na-3-OH-Benz at a molar ratio of Na-3-OH-Benz/RF = 11. C-E) Indications for direct proximity of RF to sodium polyphenolates: D) RF in presence of NaBenz with a molar NaBenz/RF ratio = 2, E) RF in presence of Na-4-OH-Benz with a molar Na-4-OH-Benz/RF ratio = 2. See section 4.1.2.1.7.2 for A, section 4.1.2.1.7.5 for B, section 4.1.2.1.7.3 for C, section 4.1.2.1.7.1 for D and section 4.1.2.1.7.4 for E.

In conformity to this, the NOESY spectrum of the well water-soluble riboflavin analogue RF-PO_4 confirmed a curved ribityl phosphate chain in deuterium oxide in the presence of sodium ferulate, see Figure 65 A below. Additionally, cross-peaks in the NOESY spectrum of RF-PO_4 in the absence and presence of sodium ferulate indicated π-stacking of RF-PO_4 with other RF-PO_4 molecules, see Figure 65 B and Figure 119 in section 4.2.1. As RF and RF-PO_4 both comprise the same aromatic backbone, RF probably also performs stacking with other RF molecules in aqueous solution of aromatic sodium carboxylates, see section 4.2.1.

Further, the cross-peak of sodium ferulate's methoxy group with H11/H12 of RF-PO_4 demonstrates once more the proximity of the ribityl chain to polyphenolates, see Figure 65 C.

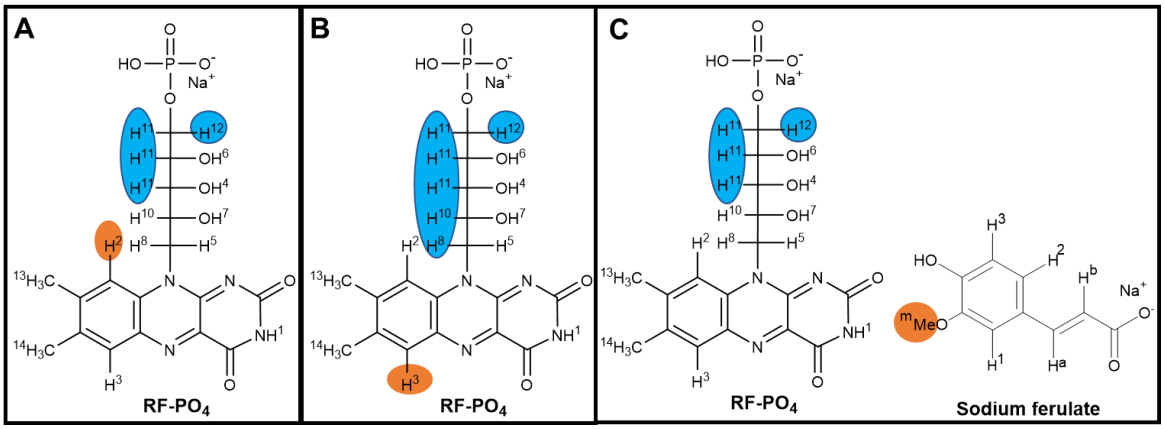

Figure 65: Intramolecular interactions of RF-PO_4 and intermolecular interaction of RF-PO_4 with sodium ferulate retrieved from cross-peaks in the NOESY NMR spectrum from Figure 61. The blue protons interact with the orange proton. Molar ratio of sodium ferulate/RF-PO_4 = 5.5. A) Indication of a curved ribityl phosphate chain; B) Indication of anti-stacking; C) Indication of a proximity of sodium ferulate's methoxy group and the ribityl phosphate chain.

To summarize, although the chemical shift of RF's and of the aromatic sodium salts' protons changed only slightly for non-exchangeable protons, almost all signals of their exchangeable protons were shifted, broadened or disappeared. Additionally, almost all carbon atoms of RF and of the aromatic sodium salts were influenced by the presence of the sodium salts and RF, respectively. Consequently, the entire molecules are affected by the prevalent interactions, and RF and sodium polyphenolates are stronger hydrated when being dissolved together than when being dissolved separately in DMSO-d_6 and deuterium oxide.

Moreover, concentration dependent measurements of RF's and Na-2-OH-Benz's chemical shift revealed a break point (molar Na-2-OH-Benz/RF ratio), above which the slope of the curves flattened out, see Figure 49-Figure 51 in section 4.1.2.1.7.2. As stacking of sodium polyphenolates and RF was already proofed in the section 4.1.2.1.1, this break point might correspond to a saturation concentration for a complexation. With its three aromatic rings, RF is larger than Na-2-OH-Benz and thus about two times more Na-2-OH-Benz might be required to reach this break point for RF. The low dependence of the chemical shift on the ratio of RF and Na-2-OH-Benz indicated weak interactions of the RF and Na-2-OH-Benz in DMSO-d_6. Similarly, the small change of the chemical shift by the presence of aromatic sodium carboxylates or RF affirms weak interactions of the tested aromatic sodium salts with RF and RF-PO_4 in DMSO-d_6 and deuterium oxide This observation correlates to the one of reversible copigmentation of RF and some sodium polyphenolates, which also indicated weak interactions of RF and aromatic sodium carboxylates, see section 4.1.2.1.1.

(i) The change of the chemical shift of almost all carbon atoms of RF, of RF-PO_4 and of the aromatic sodium salts, when being in dissolved together, (ii) the relatively weak changes of the non-exchangeable protons' chemical shift, (iii) the break point of the linear increasing change of the chemical shift of the protons and carbons of RF and Na-2-OH-Benz at the molar Na-2-OH-Benz/RF ratios 10 and 5, (iv) the increasing change of the chemical shift of NaBenz's, Na-

3-OH-Benz's and Na-4-OH-Benz's carbon atoms from ortho to meta and para position and (v) the strong change of the chemical shift of sodium vanillate's methoxy group due to the presence of RF are further indications for π-stacking of RF/RF-PO_4 with the aromatic sodium salts.

As sodium polyphenolates solubilize RF, and because a curved ribityl chain was observed in the presence of three sodium polyphenolates, the high solubility of RF-PO_4 in water might be not only due to the phosphate group, but also due to the curved ribityl phosphate chain. In case of a curved ribityl chain, RF and RF-PO_4 would be more compact, so that water bonding network should be less disturbed. Consequently, the mutual increase of the aqueous solubility of RF and sodium polyphenolates might partially arise from the conformational change of RF's ribityl chain, which itself could originate from π-stacking of RF and sodium polyphenolates.

4.1.2.1.8 Photostabilization of riboflavin in aqueous polyphenolate solutions

As described in section 2.7, RF is highly photolabile, which results either in a degradation of the vitamin yielding mainly to lumichrome or in the loss of other vitamins or antioxidants due to their photosensitization by RF.

Polyphenolic acids are well-known for their antioxidant and radical scavenging properties. They were reported to quench RF's single and triplet state in aqueous water/acetonitrile solutions, on diffusion scale.[10,83,84] Their antioxidant properties often correlate with their radical scavenging power.[84] As choline polyphenolates exhibit even stronger antioxidant properties than the corresponding polyphenolic acids, the corresponding sodium polyphenolates were supposed to provide a photostabilizing effect on RF, too.[268]

As π-complexation of vitamin K3 with 1-hydroxy-2-naphthoic and 6-hydroxy-2-naphthoic acid was already documented to slow down the photodegradation of the aromatic vitamin, the π-complexation of RF and sodium polyphenolates might enable further photoprotection of RF.[196] Being directly attached to riboflavin in the π-complex, polyphenolates might quench the vitamin's excited singlet or/and triplet state directly after RF's excitation.[10] Moreover, the extension of RF's absorption spectrum due to stacking with polyphenolates might open further relaxation pathways to RF. Besides this, polyphenolates presumably induce a change and rigidity to RF's ribityl chain, which might alter the hydrogen bonding ability of the sugar chain and provide another possibility to RF's photostabilization. The effect of polyphenolates on the ribityl chain might thereby correlate to the π-stacking of riboflavin and polyphenolates. As polyphenolates and RF copigmented only at high concentrations, extended π-complexation of the biocompounds might occur only at high concentrations of both compounds due to a higher collision probability in solution. If the π-complexation of RF and polyphenolates is indeed

reversible upon dilution and if one can expect a potential effect of π-complexation on RF's photostability, a photostabilization of RF by polyphenolates might depend on both of the compounds' concentration. Therefore, it was necessary to test the photostability of riboflavin in lowly concentrated (=diluted) and highly concentrated aqueous polyphenolate solutions.

RF's photostability was monitored using HPLC with a UV-Vis-detector in diluted aqueous polyphenolate solutions and in some concentrated polyphenolate solutions to see if there is a distinct stabilization process in the diluted and concentrated regime. RF's photostability was then compared to the one in pure water. Additionally, the photoproducts of RF in pure water and the photoproducts of RF being photodegraded in an aqueous ferulate and cinnamate solution were determined via LC-MS analysis at the central analytical department of the University of Regensburg. To get a better insight into the photoprotective mechanism of sodium polyphenolates for RF, the oxygen content of aqueous sodium polyphenolate solutions with and without riboflavin was additionally measured by means of a Clark electrode. To the same purpose, the photostability of RF was evaluated in the presence of NaBenz, NaCinn and choline cinnamate.

4.1.2.1.8.1 Diluted aqueous systems

For the diluted systems, the photodegradation of RF in aqueous solution was monitored in the presence of different antioxidant and non-antioxidant derivatives of NaBenz and NaCinn as well as in presence of one salting-in and -out agent at the three molar additive/riboflavin ratios 6, 25 and 50. Ratio 6 and 25 were investigated because like this the photodegradation of RF could be compared to the concentrated sodium ferulate, caffeate, cinnamate and vanillate samples saturated with RF in section 4.1.2.1.8.2. Because NaCinn accelerated the photodegradation of RF unexpectedly, additionally, the photostability of RF in presence of choline cinnamate was measured. The initial concentration of RF in all diluted samples was 48 $mg \cdot kg^{-1}$ and thus near RF's maximum amount allowed in non-alcoholic beverages (≈ 50 $mg \cdot kg^{-1}$) to see if polyphenolates would be applicable for the stabilization of RF in beverage formulations. After all, sodium polyphenolates might be used for the stabilization and solubilization of RF in food, beverage and pharmaceutical products.

At all three tested molar ratios, sodium polyphenolates induced a photostabilization of RF in an aqueous neutral solution, see Figure 66-Figure 68. The photostabilization increased with increasing molar polyphenolate to RF ratio (ratio: 6 < 25 < 50), as it would be expected in the case of a quenching reaction, which prevents the photodestruction of RF through a degradation of the stabilizer. Although antioxidant properties of polyphenolic acids depend on the position, type and number of methoxy and hydroxy groups on the aryl ring and on the length of the aromatic backbone (COOH < CH_2COOH < CH=CHCOOH), the photostabilizing effect at ratios 6 and 25 was similar for all polyphenolates tested.[84] Though the photostabilization of RF at ratio 50 did also not depend on the position and number of the

hydroxy and methoxy groups on the aryl ring, sodium benzoate derivatives exhibited slightly weaker photostabilizing properties than sodium cinnamate derivatives, see Figure 66. Thus, substituted sodium benzoate derivatives enabled a conservation of 2-2.7 times more RF than in pure water after 8 h of illumination with an LED-plant lamp, while sodium cinnamate derivatives allowed keeping 3-4 times more RF compared to the pure water sample after the same time. This is in line with the higher antioxidant and scavenging properties of cinnamic acid derivatives compared to benzoic acids derivatives.[84]

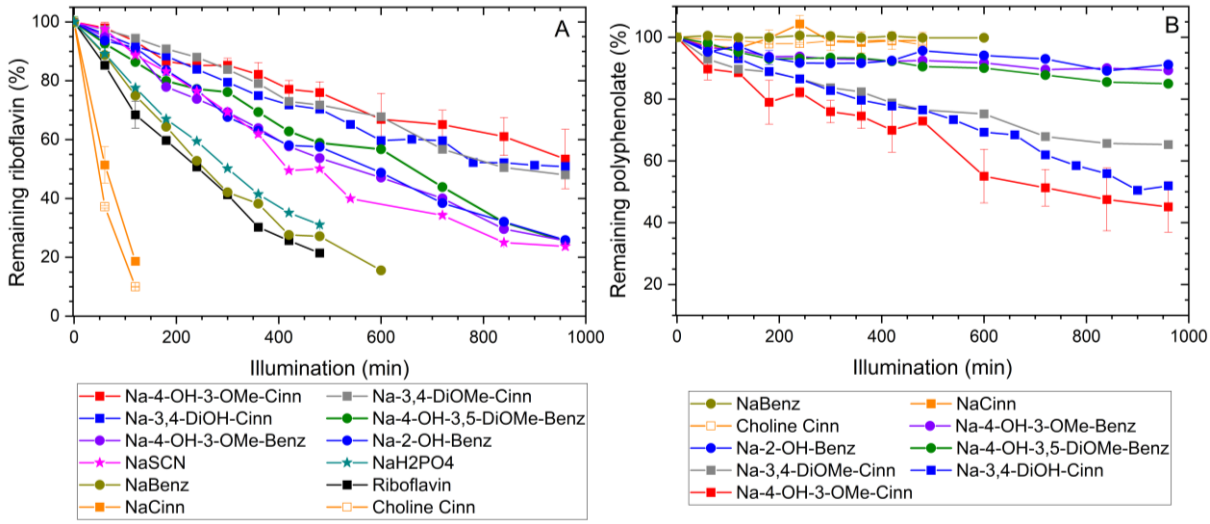

Figure 66: A) Photodegradation of riboflavin in pure water and in aqueous systems comprising of sodium or choline salts of sodium benzoate and cinnamate as well as their derivatives, in presence of sodium thiocyanate and sodium dihydrogen phosphate. B) Degradation of benzoate and cinnamate derivatives upon illumination of the samples. All samples comprised 48 mg·kg^{-1} riboflavin at a molar additive/riboflavin ratio of 50.

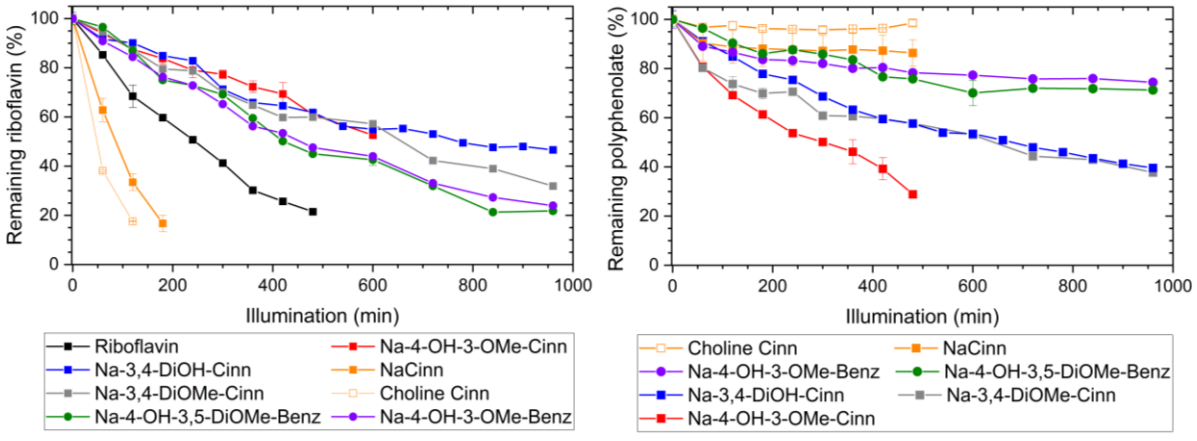

Figure 67: A) Photodegradation of riboflavin in pure water and in aqueous systems comprising of sodium or choline salts of sodium benzoate and cinnamate as well as their derivatives. B) Degradation of benzoate and cinnamate derivatives upon illumination of the samples. All samples comprised 48 mg·kg^{-1} riboflavin at a molar additive/riboflavin ratio of 25.

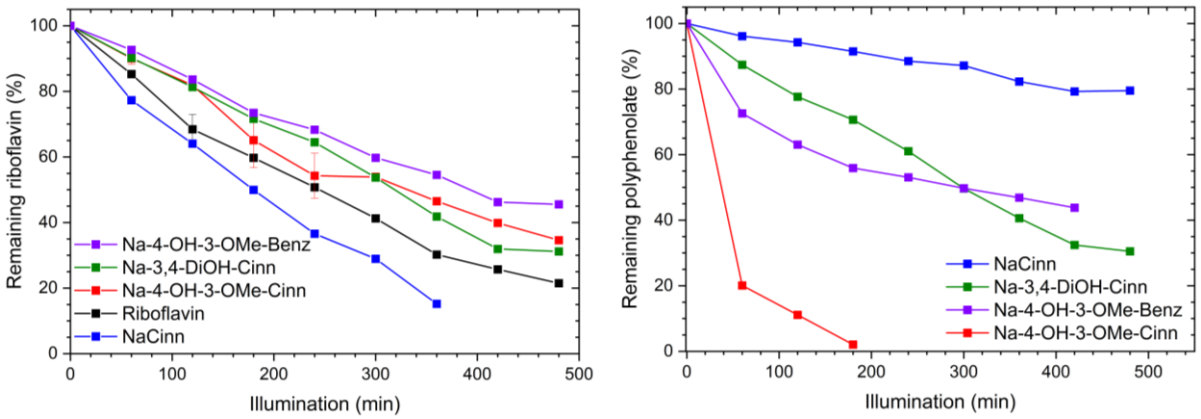

Figure 68: A) Photodegradation of riboflavin in pure water and in aqueous systems comprising of sodium or choline salts of sodium benzoate and cinnamate as well as their derivatives. B) Degradation of benzoate and cinnamate derivatives upon illumination of the samples. All samples comprised 48 mg·kg^{-1} riboflavin at a molar additive/riboflavin ratio of 6.

Further, owing to its antioxidant properties, the salting-in agent, NaSCN, performed similarly to sodium benzoate derivatives.[281] However, NaSCN exhibited a weaker RF solubilizing potential (section 4.1.2.1.1) and its photostabilizing properties are still worse when compared to sodium cinnamate derivatives. Hence, NaSCN was not further investigated.

Consequently, the strongest photostabilization of RF in the diluted polyphenolate-RF systems was observed in presence of Na-3,4-DiOMe-Cinn, Na-4-OH-3-OMe-Cinn and Na-3,4-DiOH-Cinn, see Figure 66-Figure 68. Regarding the color of the sample comprising Na-4-OH-3-OMe-Cinn at the molar sodium ferulate/RF ratio 6, one can see that already the lowest stabilizer/RF ratio resulted in a considerable preservation of the initial color, see Figure 69.

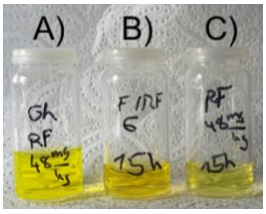

Figure 69: Color change of RF after illumination with an LED plant lamp for 15 h. A) Fresh water saturated with RF, B) Aqueous sample comprising sodium ferulate and RF at a molar ratio of 6 after illumination for 15 h C) RF in pure water after illumination for 15 h.

However, all Na-3,4-DiOH-Cinn samples turned brown already after few hours and even if stored in the dark, see Figure 70 right. Even in absence of RF, aqueous Na-3,4-DiOH-Cinn solutions turned brownish after few hours in the dark. The reason was an oxidation of caffeate, see section 4.1.2.1.8.3. Thus, Na-3,4-DiOMe-Cinn and Na-4-OH-3-OMe-Cinn are the best photostabilizers for RF in diluted aqueous neutral medium.

Comprising no antioxidant power, NaBenz and the salting-out agent Na_2PO_4 did not influence RF's photodegradation speed, see Figure 66 A. Yet, sodium and choline cinnamate accelerated the photodegradation of RF and even more with increasing cinnamate/RF ratio, see Figure 66 A-Figure 68 A. Thus, after 2 h of illumination > 80% of RF were lost compared to the fresh cinnamate samples leading to a total discoloration, see Figure 70 left.

A)  B) 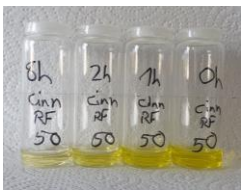 C) 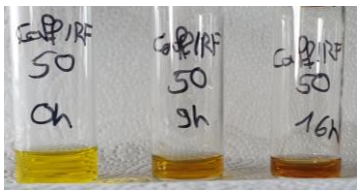

Figure 70: Color change of aqueous riboflavin (48 mg·kg^{-1}) samples at pH 7 upon illumination of the samples with an LED-plant lamp: A, B: In presence of sodium cinnamate at a molar NaCinn/RF ratios of 25 (A) and 50 (B). From left to right: for 8 h, 2 h, 1 h and 0 h. C: In presence of sodium caffeate at a molar caffeate/RF ratio of 50. From the left to the right: 0 h, 9 h and 16 h.

As mentioned above, polyphenolates might stabilize RF via the photosensitization of the polyphenolates leading to their degradation. Thus, the concentration of the polyphenolates as well as the one of NaBenz and NaCinn was monitored during the photoexperiments.

Having no influence on the photodegradation speed of RF, NaBenz was not degraded during the whole illumination process, see Figure 66 B. Analogously, NaCinn and choline cinnamate seemed to be completely stable at the molar ratios 25 and 50, see Figure 66 B and Figure 67 B. Yet, the analysis of the cinnamate samples with ratio 6 showed that cinnamate is clearly degraded in presence of RF, although cinnamate exhibited no photoprotective effect on RF at all, see Figure 68 B. Consequently, the apparent stability of cinnamate at the ratios 25 and 50 was certainly covered by the excess of NaCinn and choline cinnamate compared to RF. As the samples comprising NaCinn and choline cinnamate behaved more or less equally, the acceleration of RF's photodegradation was dependent on the cinnamate anion and not on the cation. LC-MS analysis of the NaCinn samples comprising 48 mg·kg^{-1} RF at an NaCinn/RF ratio of 25 after 15 h of illumination showed that NaCinn reacted with RF. Many distinct adducts of RF with two and up to four cinnamate molecules were formed in addition to the usual photodegradation products of RF – LC and CDRF, see Table A 121 in the Appendix.

Further, all polyphenolates tested, degraded during the illumination, see Figure 66-Figure 68. The order of the polyphenolate's degradation at the molar ratio 50 was: NaBenz < NaCinn < Na-4-OH-3-OMe-Benz ≈ Na-4-OH-3,5-DiOMe-Benz < Na-2-OH-Benz < Na-3,4-DiOMe-Cinn ≈ Na-3,4-DiOH-Cinn < Na-4-OH-3-OMe-Cinn. Thus, the higher the antioxidative properties of the polyphenolate, the faster the degradation of the polyphenolate. This is logical, as the antioxidant properties of polyphenolic acids correlate with their scavenging ability.[84]

4.1.2.1.8.2 Concentrated systems

The photostability of RF was also investigated in aqueous solutions of highly concentrated aromatic sodium carboxylates. In particular, aqueous 3.00 mol·kg^{-1} NaBenz, 0.58 mol·kg^{-1} NaCinn, 1.00 mol·kg^{-1} Na-4-OH-3-OMe-Benz, 0.37 mol·kg^{-1} Na-4-OH-3-OMe-Cinn and 2.10 mol·kg^{-1} Na3,4-DiOMe-Cinn solutions were saturated with RF and stored next to the window or in a dark box for 17 weeks. Sodium vanillate and ferulate are well-known quenchers of RF's excited singlet and triplet state, while NaBenz and NaCinn possess no quenching

ability.[10] The concentration of the potential stabilizer was chosen as high as possible to have comparable molar stabilizer/RF ratios. The aromatic sodium carboxylate solutions were prepared either at the limit of their water-solubility (Na-4-OH-3-OMe-Cinn, NaCinn, Na-4-OH-3-OMe-Cinn) or to have at least ≈ 70 % water content (NaBenz, Na-3,4-DiOMe-Cinn), so that the system could count as an aqueous solution. The molar sodium carboxylate to RF ratios ranged only from 5 to 35, although the absolute concentrations of the aromatic sodium carboxylate and RF ranged from 0.37 and 3 mol·kg^{-1}. The reason therefore is an increase of the solubilizing efficiency with the concentration of the aromatic sodium carboxylate due to its hydrotropic solubilization of RF, see section 4.1.2.1.1.

First, no precipitate was observed for neither of the five aqueous aromatic sodium carboxylate solutions saturated with RF during the storage process. Only, in the presence of NaBenz, a minor amount of RF precipitated already after 5 weeks of storage in the dark due to oversaturation. But further RF was not lost after 5 weeks.

The color of the concentrated aqueous sodium polyphenolate solutions saturated with RF, in particular sodium vanillate, ferulate and Na-3,4-DiOMe-Cinn, after 17 weeks of storage in the dark and next to the window was the same as the one of the fresh samples, see Figure 71. However, the NaCinn and NaBenz samples stored next to the window exhibited a darker coloration with longer storage, while the samples stored in the dark became a bit brighter than the fresh samples. Thus, regarding only the evolution of the samples' color, NaBenz and NaCinn seemed to exhibited either a weaker or no photostabilizing effect on RF, while the true sodium polyphenolates preserved the color in the concentrated regime. Nevertheless, after dilution of the samples stored next to the window for 17 weeks with water to comparable concentrations of RF, the color of all five aromatic sodium carboxylate solutions was almost similar for the human eye. Therefore, the absolute RF content was determined via the absorbance at 449 nm with a UV-Vis-spectrophotometer after calibration, see Figure 72 A.

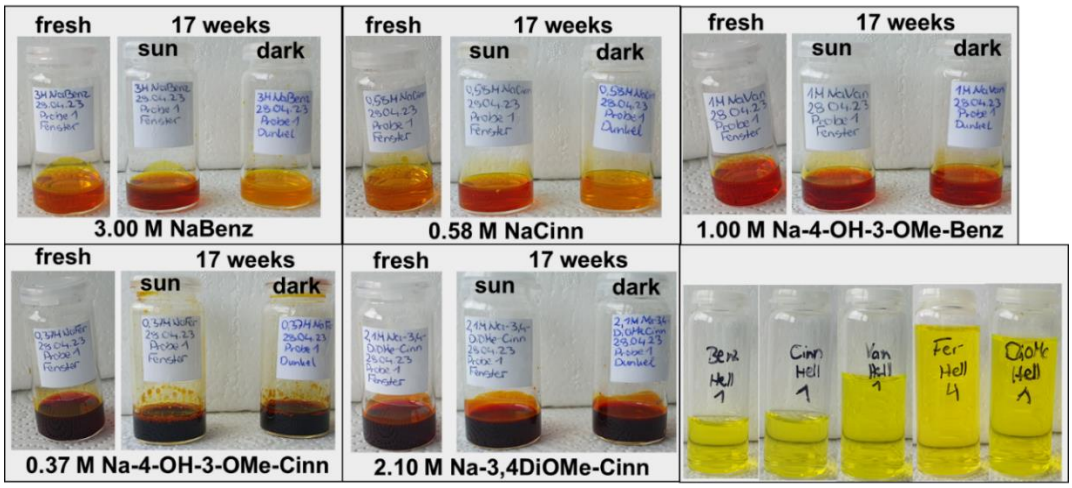

Figure 71: Aqueous aromatic sodium carboxylate solutions saturated with riboflavin freshly prepared and after storage next to the window exposed to the sun and storage in the dark for 17 weeks. Bottom right: Color of the concentrated samples stored next to the window for 17 weeks after dilution with water (0.6 mmol·kg^{-1} riboflavin).

In contrast to RF in the diluted solutions from the previous section, no or almost no RF was lost in the concentrated Na-4-OH-3-OMe-Benz, Na-3,4-DiOMe-Cinn, Na-4-OH-3-OMe-Cinn and NaCinn samples for up to 8 weeks. Only in the presence of NaBenz, RF photodegraded in a rather linear manner. Regarding the remaining RF content relatively to the fresh samples in Figure 72 B, Na-4-OH-3-OMe-Benz, Na-4-OH-3-OMe-Cinn and Na-3,4-DiOMe-Cinn obviously preserved the sample's yellow coloration totally for at least 4 months. In line with the absence of a photostabilization of RF in the diluted NaBenz sample from the previous section, RF was photodegraded fastest in the concentrated NaBenz solution.

Unexpectedly, NaCinn retarded RF's photodegradation. Thus, after 4 months being exposed to the sun, ca. 90 % of RF was left. This observation goes against the acceleration of RF's photodegradation in the diluted aqueous NaCinn solution, see section 4.1.2.1.8.1 and Table A 121 in the Appendix.

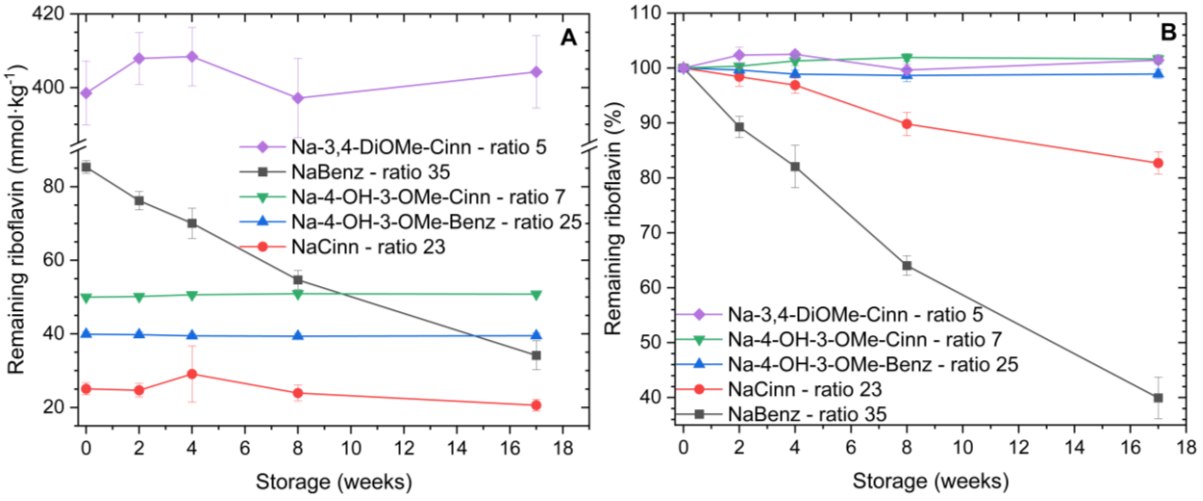

Figure 72: Color-stability of riboflavin in concentrated aromatic sodium carboxylate solutions at molar stabilizer/RF ratios between 5 and 35 stored next to the window. The theoretical concentration of RF is given as absolute concentration (A) and relatively to the RF content in the corresponding fresh solution. The concentrations were: 3.00 mol·kg^{-1} NaBenz - 0.58 mol·kg^{-1} NaCinn – 1.00 mol·kg^{-1} Na-4-OH-3-OMe-Cinn - 0.37 mol·kg^{-1} Na-4-OH-3-OMe-Cinn - 2.10 mol·kg^{-1} Na3,4-DiOMe-Cinn.

For more clarity, the UV-Vis-spectra of the concentrated aromatic sodium carboxylate solutions saturated with RF were recorded from 300 to 550 nm during the storage in the dark and next to the window, see Figure 73. In the presence of Na-4-OH-3-OMe-Benz, Na-4-OH-3-OMe-Cinn, Na-3,4-DiOMe-Cinn, NaCinn and NaBenz, RF was entirely stable for at least 4 months when being stored in the dark.

In correlation to the undisturbed photodegradation of RF in the concentrated NaBenz sample, the UV-Vis-spectrum of the NaBenz sample resembled the theoretically main photoproduct of RF in neutral aqueous solutions – lumichrome – more, with proceeding storage next to the window, see Figure A 92 in the Appendix. In conformity to the photostabilization of RF in concentrated aqueous NaCinn, Na-4-OH-3-OMe-Benz, Na-4-OH-3-OMe-Cinn and Na-3,4-DiOMe-Cinn solutions, the UV-Vis-spectrum of these samples did not change qualitatively.

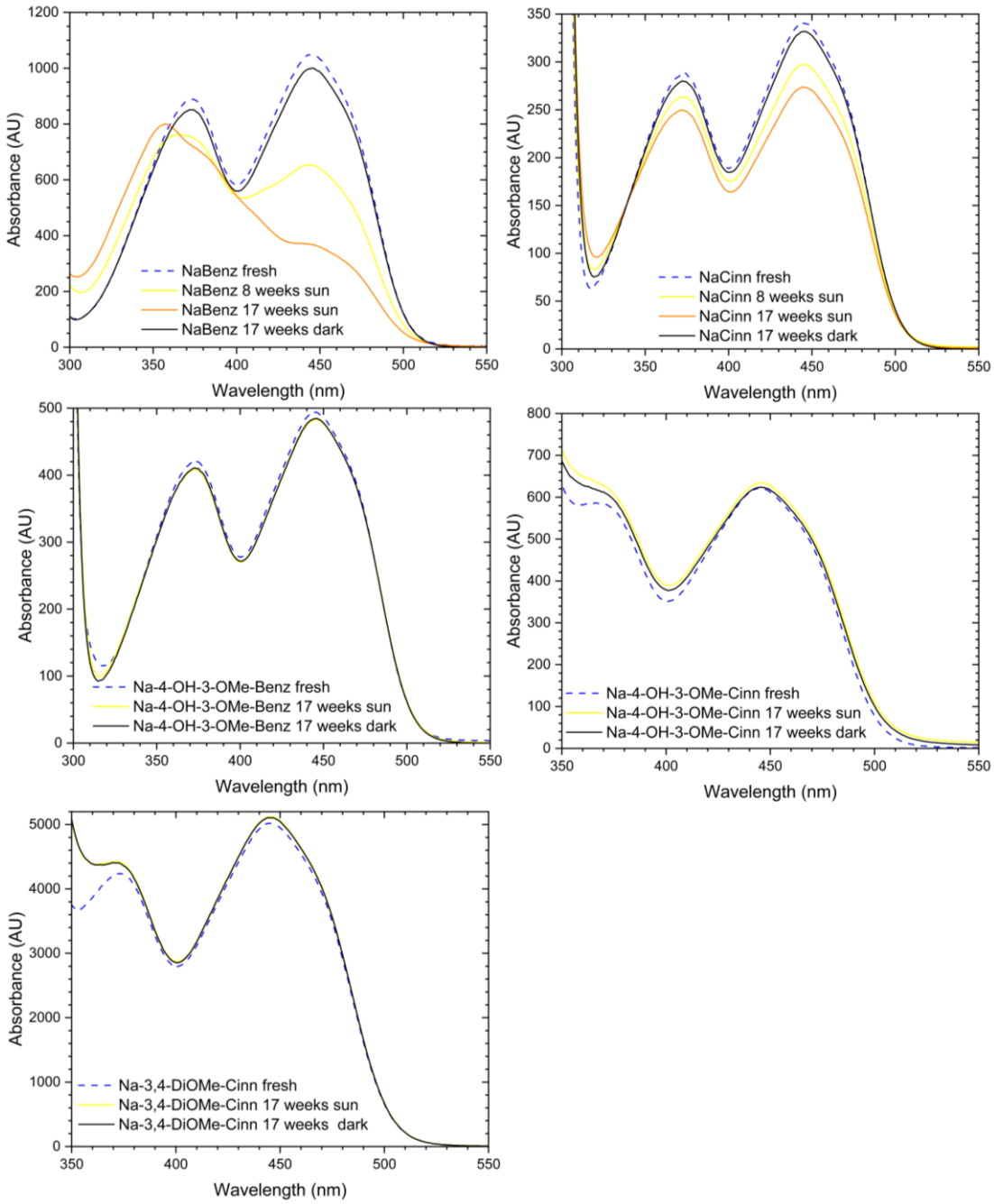

Figure 73: UV-Vis-spectra of riboflavin in aqueous sodium carboxylate solutions directly after the preparation and 8 or 17 weeks after storage in the dark and next to the window exposed to the sun.

As RF is primarily photodegraded upon successive cleavage of its ribityl chain, some photoproducts have the same or similar UV-Vis-spectrum as RF. Hence, despite the considerable stabilization of the sample's color in highly concentrated NaCinn, Na-4-OH-3-OMe-Benz, Na-4-OH-3-OMe-Cinn and Na-3,4-DiOMe-Cinn solutions, other molecules absorbing at the same wavelength might be present in the samples.

Therefore, the photostability of RF in some highly concentrated aqueous solutions of aromatic sodium carboxylates was additionally analyzed via HPLC with a UV-Vis-detector.

A sample with Na-3,4-DiOMe-Cinn was not prepared, as its photostabilizing effect on RF resembled the one of Na-4-OH-3-OMe-Cinn in the diluted and concentrated systems. Samples

comprising NaBenz were also not analyzed, as NaBenz had no considerable effect on RF's photodegradation in the diluted and concentrated samples. In particular, a 0.37 mol·kg^{-1} sodium ferulate (Na-4-OH-3-OMe-Cinn), a 0.60 mol·kg^{-1} sodium caffeate (Na-3,4-DiOH-Cinn), a 1.05 mol·kg^{-1} sodium vanillate (Na-4-OH-3-OMe-Benz), and a 0.59 mol·kg^{-1} NaCinn solution saturated with RF were illuminated with an LED plant lamp for one day and then stored next to the window. The aromatic sodium carboxylate solutions were prepared at their solubility limit to have maximum probability for π-complexation due to the high polyphenolate concentration. Saturation of the Na-4-OH-3-OMe-Cinn, Na-3,4-DiOH-Cinn Na-4-OH-3-OMe-Benz and NaCinn samples resulted in 56.2 ± 0.3 mol·kg^{-1}, 32.51 ± 0.08 mol·kg^{-1}, 27.6 ± 0.1 mol·kg^{-1} and 43.3 ± 0.2 mol·kg^{-1} RF, respectively. Despite of a strong variation of the absolute sodium salt concentrations, the molar sodium salt/RF ratio ranged only from 6, 10, 22 to 27 for Na-4-OH-3-OMe-Cinn, Na-3,4-DiOH-Cinn, NaCinn and Na-4-OH-3-OMe-Benz, respectively. Hence, regarding the molar ratio, the concentrated samples can be compared to the diluted ones from the previous section. This time not just RF, but also the stabilizer was quantified via the UV-Vis-absorption of the analytes after separation with HPLC, see Figure 74.

No or almost no RF was lost in the concentrated aromatic sodium carboxylate samples after illumination of the samples for 24 h with an LED plant lamp, see Figure 74 A and C. Hence, RF in these concentrated aromatic sodium carboxylate samples was more stable than dissolved RF in pure water from the previous section. The closed sample were then exposed to the sun for several weeks by putting them next to the window during summer. Congruent to the quantification of RF via simple UV-Vis-measurements, all samples still comprised > 84 % RF after 8 weeks being exposed to the sun.

After 12 weeks of exposure to the sun, Na-4-OH-3-OMe-Benz turned out as the best stabilizing agent (91 ± 1 % remaining riboflavin), followed by Na-3,4-DiOH-Cinn (76.6 ± 0.3 % remaining riboflavin), Na-4-OH-3-OMe-Cinn (ca. 80 % remaining riboflavin) and NaCinn (54.1 ± 0.3 % remaining riboflavin). Because Na-4-OH-3-OMe-Cinn was one of the best stabilizers in the diluted systems, the sample comprising ferulate was analyzed until almost all RF was destroyed, which happened after 24 weeks of exposure to the sun (11 % remaining riboflavin). The stronger photostabilizing effect of Na-4-OH-3-OMe-Benz compared to Na-3,4-DiOH-Cinn and Na-4-OH-3-OMe-Cinn indicated that the stabilization of the phenoxyl radical formed during the free radical scavenging reaction of polyphenolic acids is not decisive for the photostabilization of RF in concentrated aqueous polyphenolate systems.[83,268]

Analogously, the photostabilizing effect of NaCinn confirmed that a stabilization of the quinone or phenoxyl radical state by methoxy/hydroxy groups is not required for the antioxidant and scavenging action of polyphenolic acids towards RF in concentrated in the concentrated regime.

Regarding the stabilizers themselves, more than 94 % of NaCinn and Na-4-OH-3-OMe-Benz of their initial amount were left in the samples after 12 weeks of exposure to the sun, see Figure

74 B and D. In contrast, the content of Na-4-OH-3-OMe-Cinn and Na-3,4-DiOH-Cinn corresponded to ≤ 25 % of the initial stabilizer concentration, see Figure 74 B and D. Thus, the photostabilization of RF in concentrated polyphenolate solutions does not necessarily involve a degradation of the stabilizer. The strong loss of Na-4-OH-3-OMe-Cinn and Na-3,4-DiOH-Cinn can be explained by their strong antioxidant properties, as sodium ferulate and caffeate solutions stored in the dark turned brownish in absence of RF after few days due to the dimerization and trimerization of ferulate and caffeate via autooxidation, see section 4.1.2.1.8.3.[89,97,282,283] The assumption of the oligomerization of ferulate and caffeate was affirmed by the increasing foaming potential upon gentile shaking of the samples with longer storage of the samples. Nevertheless, the browning of sodium ferulate seemed to be slowed down by the presence of RF, which was not the case for sodium caffeate.

In contrast, the concentrated samples comprising Na-4-OH-3-OMe-Benz and NaCinn saturated with RF did neither show an increasing foaming potential nor did they exhibit a distinct coloration after 12 weeks of storage next to the window.

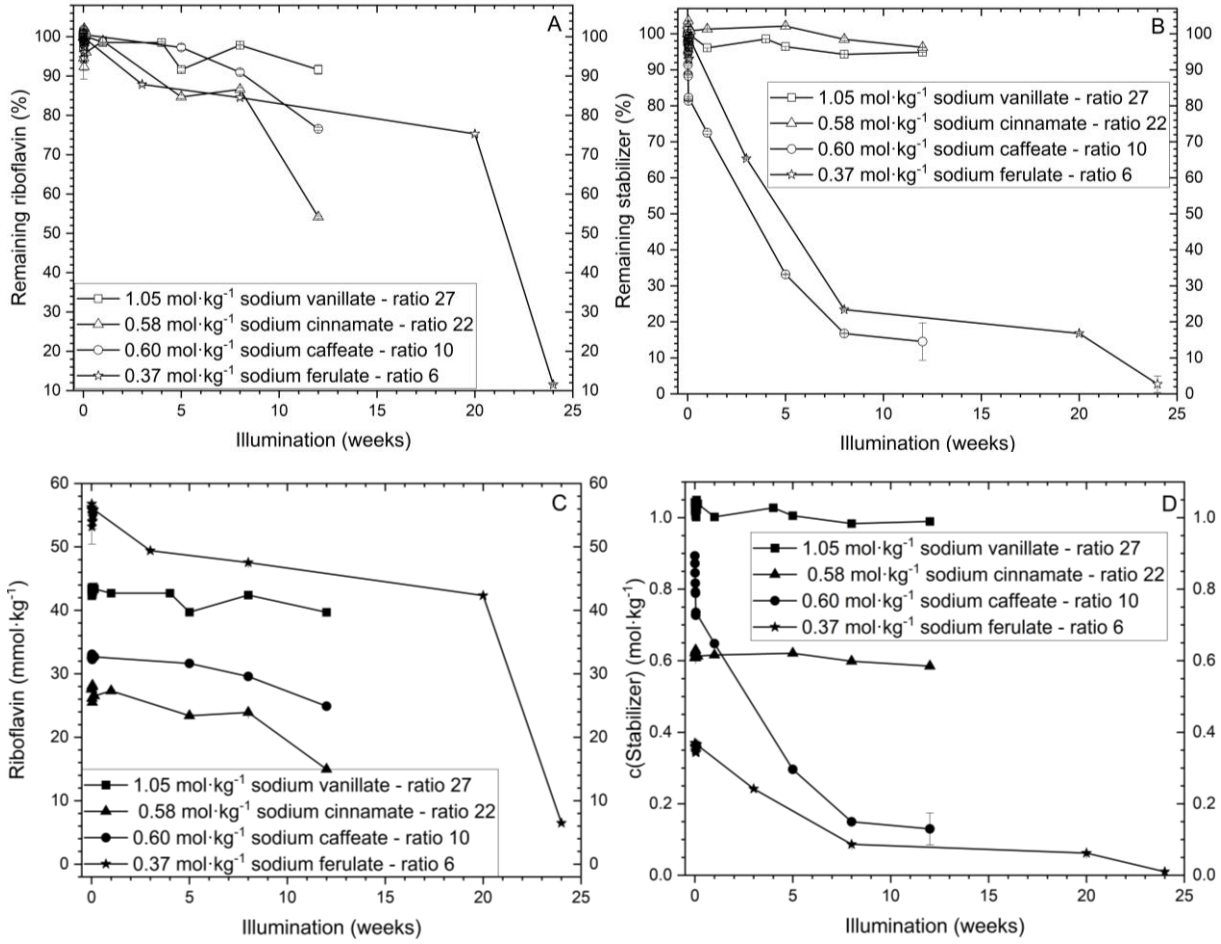

Figure 74: Photodegradation of riboflavin in aqueous concentrated solutions of aromatic sodium carboxylate salts. Despite the strong variation of the four stabilizers' concentrations, similar molar stabilizer/riboflavin ratios were obtained via saturation of the aqueous stabilizer solutions with riboflavin. A) and B) percent of riboflavin and stabilizer left relatively to the fresh samples. C) and D) corresponding concentration of riboflavin and of the stabilizer during the storage.

Though RF's photodegradation was slowed down considerably in relative terms, the huge amount of RF in the concentrated samples might cover up the relative loss of this vitamin. Consequently, the absolute loss of RF will be considered in the following. Note that the improvement of RF's photostability in concentrated aqueous systems is compared to the one in diluted aqueous system, although the diluted samples were only illuminated with a weak LED plant lamp, while the concentrated samples were exposed to the sun during summer. Thus, RF was exposed to a more intense light in the concentrated samples. Therefore, RF's photostability in aqueous concentrated aromatic sodium carboxylate solutions compared to the diluted ones was even underestimated.

In the concentrated Na-4-OH-3-OMe-Benz solution, no RF was lost for at least 8 weeks of storage next to the window, see Figure 74 above. After 12 weeks, only 3.6 $mmol \cdot kg^{-1}$ RF was degraded, while at least 13 $mmol \cdot kg^{-1}$ RF should have been lost with the same degradation speed of RF as in the diluted Na-4-OH-3-OMe-Benz sample with the molar ratio 25. Thus, at comparable molar ratios, RF was 3.6 times more stable in the concentrated sodium vanillate (c(vanillate) = 1.05 $mol \cdot kg^{-1}$; molar ratio: 27) solution than in the diluted one (c(vanillate) = 0.0032 $mmol \cdot kg^{-1}$; molar ratio: 25).

Similarly, RF was completely stable in the concentrated Na-3,4-DiOH-Cinn sample for at least 5 weeks. After 8 weeks, 2.9 $mmol \cdot kg^{-1}$ of RF were destroyed although having only a molar ratio of 10. In the diluted Na-3,4-DiOH-Cinn sample with a Na-3,4-DiOH-Cinn/RF ratio of 25 after 8 weeks of storage, 5.8 $mmol \cdot kg^{-1}$ RF should have been. Thus, at the beginning of RF's photodegradation, the concentrated system was 2 times more efficient than the diluted Na-3,4-DiOH-Cinn sample at higher molar stabilizer/RF ratio.

Analogously, 1.5 times more RF was left in the concentrated Na-4-OH-3-OMe-Cinn system than it would have been theoretically in the diluted system after 8 weeks at the same molar ratio of 6. The remaining RF in the concentrated ferulate system after 20 weeks of exposure to the sun (75 %; 42.34 ± 0.01 $mmol \cdot kg^{-1}$) corresponded even to 2.5 times more RF than RF would have been left with the degradation speed in the diluted system at the same molar ratio of 6. However, once ferulate was degraded completely, RF was almost instantly destroyed after 24 weeks, see Figure 74 C and D.

Comparing the diluted NaCinn sample at the molar ratio 25 with the concentrated one comprising a molar ratio of 22 after 5 weeks, 27.7 $mmol \cdot kg^{-1}$ RF should be destroyed completely if the degradation was as fast as in the diluted system. However only 4.23 $mmol \cdot kg^{-1}$ RF were degraded in the concentrated sample. Moreover, in pure water theoretically at least 10 $mmol \cdot kg^{-1}$ RF would be lost after 5 weeks. Thus, RF was at least 2.5 times more stable in a concentrated aqueous NaCinn solution than in pure water.

Consequently, concentrated neutral aqueous solutions of aromatic sodium carboxylate salts, and thus also sodium polyphenolates exerted a strong photostabilizing effect on RF for at least

5 to 12 weeks depending on the stabilizer. The stabilizers were not necessarily degraded due to the stabilization of RF.

4.1.2.1.8.3 LC-MS analysis of the photodegradation products

In neutral to acidic aqueous solutions, RF is mainly photodegraded to lumichrome. Cyclodehydroriboflavin and carboxymethylflavin are also formed via formylmethylflavin as intermediate.[178] However several other compounds may be formed, see Figure 9.[8]

Because polyphenolates exhibited a photoprotective effect on RF in diluted and concentrated aqueous solutions, they might also alter the photodegradation products of the vitamin. Regarding the potential application of polyphenolates as solubilizers and stabilizers in food and beverages, it is important to know the primary degradation products in presence of polyphenolates. Hence, the diluted sodium ferulate and NaCinn samples at the molar additive/RF ratio 25 were analyzed via LC-MS after illumination with an LED-plant lamp for 15 h. The degradation products of RF, sodium ferulate and cinnamate in the diluted systems at ratio 25 were assigned via the molar mass obtained from LC-MS and due to their characteristic absorption spectrum. To have a reference the photoproducts of RF formed in pure water were also determined. The absorption spectrum of CDRF, CMF and FMF resembled the one of RF because all three compounds consist of the same aromatic unit.[165,284,285] Only the absorption spectrum of LC was different, see Figure A 92 in the Appendix.

LC-MS analysis revealed LC as main degradation product, if RF dissolved in pure water (saturation) was illuminated with an LED-plant lamp for 5 h. CDRF, 3-(7,8-Dimethyl-2,4-dioxo-3,4-dihydrobenzo[g]pteridine-10(2H)-yl) propanoic acid, FMF and CMF were also detected in minor amounts, see Table A 119 in the Appendix. Thus, all expected photoproducts induced via successive cleavage of the ribityl chain were formed.

The main photoproduct of the samples comprising RF and sodium ferulate or NaCinn was also LC, see Table A 120 and Table A 121 in the Appendix. Minor amounts of CDRF, CMF and FMF were also formed.

Knowing the elution order and the UV-Vis-spectrum of RF, CDRF, CMF and LC from LC-MS analysis, CDRF, CMF and mainly LC could be identified in the chromatograms of all photodegraded polyphenolate/RF solutions in the diluted and concentrated regime, see Figure A 93-Figure A 101 in the Appendix. Consequently, sodium polyphenolates can be expected to have no significant influence on the main photodegradation products of RF in aqueous neutral medium.[8,158,163,178]

Sodium ferulate was found undergo dimerization and trimerization during the illumination of the aqueous ferulate/RF sample, see Table A 120 in the Appendix. Additionally, the formation of adducts consisting of one RF molecule with two or three ferulate molecules was detected.

In contrast to sodium ferulate, NaCinn reacted exclusively with RF leading to adducts consisting of one RF molecule and two or three cinnamate molecules, see Table A 121 in the Appendix. This explains, why the photodegradation of RF was accelerated in the presence of NaCinn in the diluted systems from section 4.1.2.1.8.1.

To see, why the sodium caffeate samples turned brown during the storage in the dark, an aqueous sample of 0.40 mol·kg^{-1} sodium caffeate was let open for 4 h while stirring continuously. LC-MS analysis revealed the formation of at least two distinct caffeic acid dimers, see Table A 122 in the Appendix. The reason therefore is the dimerization of caffeate, which usually occurs enzymatically in plants but can also be due to autooxidation.[282,283,286]

Dimerization and trimerization of polyphenolic acids is a natural process that takes place via the formation of quinones and semiquinones as intermediates and is responsible for the brown coloration of fruits and vegetables upon cutting them. [83,286–290] For ferulic acid it was revealed that half of its antioxidant potential was lost upon dimerization.[89] This is also the reason, why RF degraded in the concentrated sodium ferulate sample despite the formation of ferulic acid oligomers after almost all sodium ferulate was lost, see Figure 74 in section 4.1.2.1.8.2.
Despite the lack of studies regarding the absorption of polyphenolic acid dimers/trimers into the blood, they are of natural occurrence. Thus, dehydrodiferulic acid is present in wheat germ, young shoots of *Lolium multiflorium* and rice endosperm. Moreover, plant cell walls comprise ferulic acid dimers in small amounts, where they are supposed to act as antimicrobial and antifungal agents to protect the plants.[290–292] Aside of this, ferulate oligomers are supposed to participate in the termination of the expansion of cell wall growth and cell wall stiffening, to influence the thermal stability of cell wall adhesion and the texture of cooked fruits and vegetables, to influence the gelling properties of pectins and arabinoxylans.[293] Recently, polyferulic acid was investigated as potential active ingredient for cancer therapy and claimed to have no considerable toxic potential.[97]
Hence, the oligomerization of sodium polyphenolates due to autooxidation and due to the photosensitization by RF should not constitute a problem for the application of polyphenolates as solubilizing and stabilizing agents for RF in aqueous medium in food, beverage and pharmaceutical formulations.

4.1.2.1.8.4 Oxygen content in aqueous solutions of potential riboflavin stabilizers

After excitation to its triplet state, RF can react with triplet oxygen to singlet oxygen. Singlet oxygen was reported to be responsible for the degradation of RF to 2,3-butanedione and to be involved in reactions photosensitized by RF.[8,154,294] Thus, a high oxygen content might be partially responsible for the photodegradation of RF in aqueous solutions. In section 4.1.1,

polyphenolates were discussed as salting-in/-out agents for the hydrophobic di(propylene glycol) n-propyl ether. Simple inorganic salts are able to reduce the oxygen content in water slightly.[295] Hence, together with their antioxidant properties, salting-out properties of sodium polyphenolates might reduce the oxygen content in aqueous solutions and thus protect RF not only by their radical scavenging properties but also via the reduction of the oxygen content.[233] Therefore, the oxygen content of aqueous solutions comprising distinct sodium polyphenolates or the non-antioxidant NaCinn was determined with a Clark electrode. The results were compared to sodium chloride (NaCl), to see if the organic sodium carboxylates have a similar effect on the oxygen saturation of aqueous solutions as the inorganic salt.

Sodium polyphenolates showed distinct impact on the oxygen content, see Figure 75 A. While some sodium salts decreased the oxygen content strongly, others did not induce any change at all. The sodium salts can be order according to the oxygen saturation: pure water = Na-2-OH-Benz = Na-4-OH-Benz = Na-3,5-DiOH-Benz = NaCinn = Na-4-OH-3-OMe-Benz = NaCl > Na-4-OH-3-OMe-Cinn > Na-2,3-DiOH-Benz > Na-3,4-DiOH-Benz > Na-3,4-DiOH-Cinn > Na-3,4,5-TriOH-Benz. For compounds decreasing the oxygen content, the oxygen content was lower when being applied at higher concentrations. At least two hydroxy groups or one hydroxy group next to a methoxy group were necessary to see a reduction of the oxygen content. With increasing number of hydroxy groups on the aryl ring, the oxygen content was reduced more strongly. Hydroxy groups acted stronger on the oxygen content than methoxy groups. Substituted cinnamates reduced the oxygen content more strongly than the corresponding benzoates. The reason therefore is probably that Na-4-OH-3-OMe-Benz and Na-3,4-DiOH-Benz comprise a smaller conjugated electronic system compared to the corresponding cinnamates, which is crucial for the stabilization of the phenoxyl radical and for the action of polyphenolates as antioxidants.[83,84]

Further, the oxygen content was different depending on the position of the hydroxy group on the aryl ring (Na-3,5-DiOH-Benz, Na-2,3-DiOH-Benz and Na-3,4-DiOH-Benz). Neighbored hydroxy groups induced a strong reduction of the oxygen content while separate ones did not induce any change.

The salting-out of oxygen by inorganic salts and NaCl is known to be considerably less pronounced than the reduction of the oxygen content by some of the polyphenolates, see Figure 75 A. Moreover, the reduction of the oxygen content in aqueous solutions by inorganic salts was reported to be independent of the ion strength and typical salting-out properties and to originate rather from specific interactions.[51,295] Hence, the decrease of the oxygen content by sodium polyphenolates with at least two hydroxy groups does not correlate with their salting-out properties, see section 4.1.1. Instead, the oxygen reduction by sodium polyphenolates correlated to their antioxidant properties. The antioxidant properties of polyphenolic acids with neighbored hydroxy groups are known to be stronger than the ones of polyphenolates with non-neighbored hydroxy groups. Moreover, as in our oxygen content measurements, the

antioxidant properties of polyphenolic acids increase with increasing number of hydroxy groups.[85] Hence, sodium polyphenolates do not exert a salting-out effect on oxygen, but react with it due to their antioxidant properties.

Because riboflavin is also an antioxidant, the oxygen content of water and some aqueous sodium polyphenolate solutions was also measured in after saturation with riboflavin, see Figure 75 B. However, riboflavin did not alter the oxygen content in water nor in the polyphenolate solutions tested. (The reason for the lower oxygen content in the Na-3,4-DiOH-Benz and Na-3,4-DiOH-Cinn sample saturated with riboflavin was that the oxygen content was already strongly fluctuating without riboflavin, see Figure 75 B.)

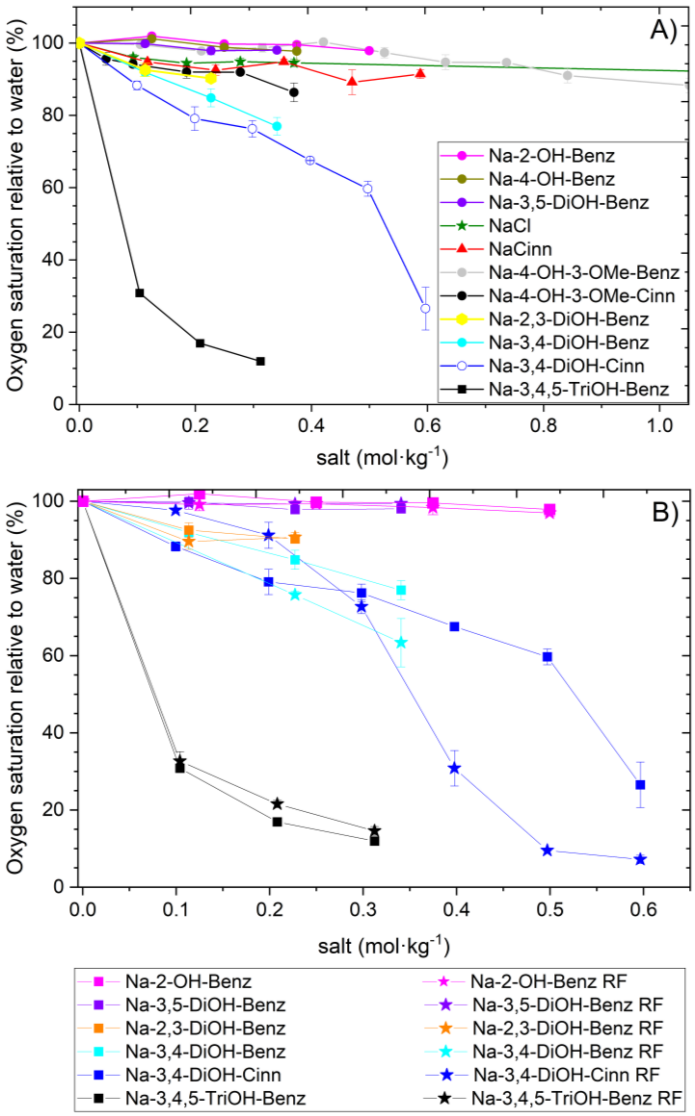

Figure 75: A) Oxygen content of organic aromatic sodium carboxylate salt and sodium chloride solutions B) Oxygen content of organic aromatic sodium carboxylate salt in absence and presence of riboflavin (saturation).

4.1.2.1.8.5 Conclusion

As expected, RF's photodegradation was impeded by the presence of sodium polyphenolates. With increasing polyphenolate/RF ratio (6 < 25 < 50), sodium polyphenolates exerted a stronger photostabilizing effect on RF in diluted aqueous sodium polyphenolate samples comprising 48 $mg \cdot kg^{-1}$ RF. Like this, RF could be preserved 2-4 times longer in aqueous solution.

In spite of comparable molar stabilizer/RF ratios, in concentrated aqueous sodium polyphenolate solutions, RF's photostability was completely superior to the one in the diluted solutions. Hence aqueous concentrated sodium vanillate, ferulate, 3,4-dimethoxycinnamate, and caffeate solutions enabled to preserve > 84 % of the initial RF concentrations even after 8 weeks of exposure to the sun by storage next to the window. This considerable photostabilization of RF in the concentrated sodium polyphenolate systems is in line with the fact that only polyphenolic acid concentrations > 0.3 $mol \cdot L^{-1}$ enabled to quench 90 % of RF's excited singlet state and thus prevented the population of the excited triplet state almost completely.[10]

However, the strong photostabilization of RF in the concentrated aqueous NaCinn sample, with NaCinn being neither an antioxidant nor a radical scavenger, showed that radical scavenging properties of sodium polyphenolates are probably not the only reason for the considerable photostabilization of RF in the concentrated polyphenolate regime. Therefore, the oxygen content in the diluted and concentrated samples was analyzed. The polyphenolate concentration in the diluted polyphenolate/RF solutions was less than 10 $mmol \cdot kg^{-1}$, while polyphenolate concentrations higher 0.1 $mol \cdot kg^{-1}$ were required to decrease the oxygen content considerably. Hence, the photostabilization of RF in the diluted systems did not originate from the oxygen reducing properties of sodium polyphenolates, see sections 4.1.2.1.8.1 and 4.1.2.1.8.4. Instead, the reduction of the oxygen content in the diluted polyphenolate/RF samples was found to be based on the antioxidant activity of polyphenolates reported in literature, see section 4.1.2.1.8.4. Additionally, Na-4-OH-3-OMe-Cinn was as efficient as Na-3,4-DiOH-Cinn in the diluted system, although Na-3,4-DiOH-Cinn decreased the oxygen content much more. Hence, not a reduction of the oxygen content, but radical scavenging properties as in the case of polyphenolic acids are responsible for the photostabilizing effect of polyphenolates on RF in the diluted regime, see Table 16.[10,179] This is also the reason, why NaBenz and NaCinn had no photostabilizing effect on RF in the diluted systems, see section 4.1.2.1.8.1.

In the concentrated systems, the oxygen content did not correlate either with the photostabilizing power of Na-3,4-DiOH-Cinn, Na-4-OH-3-OMe-Cinn and Na-4-OH-3-OMe-Benz, see Table 16. However, RF's photodegradation was slowed down considerably in the concentrated systems, while it was only slightly slowed down in the diluted samples. With ferulic, caffeic and vanillic acid and their corresponding choline salts being already known for

their scavenging properties, a photostabilization of RF was expected.[10,268] Yet, these three sodium polyphenolates behaved similarly in the concentrated samples, while Na-4-OH-3-OMe-Benz was less photoprotective than Na-4-OH-3-OMe-Cinn and Na-3,4-DiOH-Cinn in the diluted samples. Additionally, NaCinn stabilized RF in the concentrated system despite the absence of quenching abilities and oxygen lowering properties, while NaCinn destabilized RF in the diluted system due to a reaction, see Table 16. Hence, in contrast to the diluted polyphenolate systems, the scavenging properties cannot be the only reason for the considerable photostabilization of RF in concentrated sodium polyphenolate solutions.

Table 16: Observations from oxygen content measurements and photo-degradation experiments of riboflavin in presence of sodium polyphenolates and cinnamate in the diluted and concentrated system.

Compound	Oxygen content	Concentrated system	Diluted system
NaCinn	No change	Stabilization	Destabilization
Na-4-OH-3-OMe-Benz	No change	Stabilization	Weak stabilization
Na-4-OH-3-OMe-Cinn	Nearly no decrease	Stabilization	Strong stabilization
Na-3,4-DiOMe-Cinn	Not analyzed	Stabilization	Stabilization
Na-3,4-DiOH-Cinn	Strong decrease	Stabilization	Strong stabilization

While Na-4-OH-3-OMe-Cinn and Na-3,4-DiOH-Cinn degraded during the illumination of the concentrated RF/polyphenolate samples, Na-4-OH-3-OMe-Benz and NaCinn protected RF being stable themselves, see Figure 74 D in section 4.1.2.1.8.2. Obviously, RF's photostabilization in the concentrated system does not include a destruction of the photoprotectant. Thus, the photostabilization of RF in the concentrated polyphenolate systems did neither correlate with the oxygen content, nor with the radical scavenging properties of sodium polyphenolates, see Table 16.[84]

As NaCinn exerted a photostabilizing effect on RF while having no antioxidant properties, and because NaCinn is almost not photodegraded, its stabilizing effect on RF can result from two possibilities. On the one hand, the π-complex of RF and NaCinn (see section 4.1.2.1.1) might absorb the photodestructive wavelengths and allow a non-photodestructive relaxation to RF's ground state.[296] On the other hand, the proximity of NaCinn and RF in the π-complex might impede inter- and intramolecular hydrogen bonding of RF's ribityl chain (see section 4.1.2.1.7.8), which is responsible for its photodegradation.[8]

Although NaCinn stabilized RF in highly concentrated samples, this solubilizer should be avoided for RF, as it reacted with RF and accelerated its photodegradation in the diluted aqueous samples. Despite of its photostabilizing power, Na-3,4-DiOH-Cinn should be also avoided in formulations comprising RF, if a change in the product's color is not desired. As NaBenz exerted no photostabilizing properties at all, this compound can be used only for to assist the solubilization of RF. With regard to their photostabilizing power, sodium ferulate, vanillate and 3,4-dimethoxycinnamate are promising solubilizing agents for riboflavin in aqueous neutral solutions, see Figure 76. As concentrated sodium polyphenolate solutions

saturated with RF regained their photolability upon simple dilution with water, RF's reactivity required for its biochemical redox activity should not be blocked by the photostabilization of the RF in concentrated polyphenolate solutions.

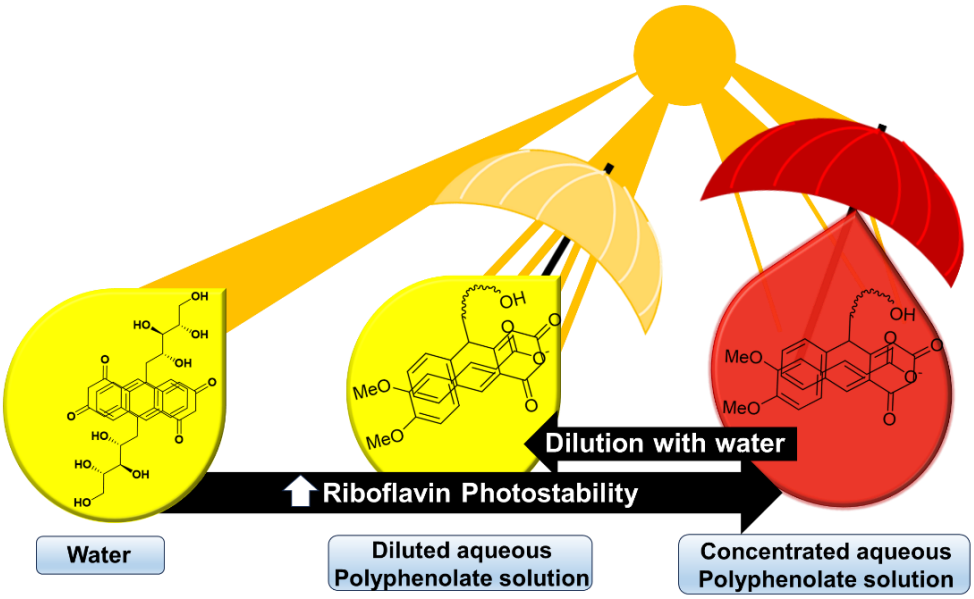

Figure 76: Schematic representation of RF's photostabilization by sodium polyphenolates

4.1.2.1.9 Compatibility of sodium polyphenolates with beverage ingredients

As sodium polyphenolates are omnipresent in human daily nutrition, because their LD_{50} values are rather high (Table 1 in section 2.6) and because benzoic acid and its derivatives are already food admitted (normal usage up to 500 $mg \cdot kg^{-1}$; maximal usage up to 2000 $mg \cdot kg^{-1}$).[20], sodium polyphenolates constitute potential solubilizing and stabilizing agents for food, beverages and pharmaceuticals. Especially in sport beverage formulations, RF is commonly used due to its vitamin functions and because of its yellow color.

As seen in section 4.1.2.1.1 and 4.1.2.1.8, precipitation and photodegradation of RF comprising beverages could be prevented or at least slowed down using sodium polyphenolates. Yet, sodium polyphenolates comprise a carboxylate group and OH- as well as OMe-groups, which might interact via complexation with divalent cations.[297] Such an interaction might lead to the precipitation of the sodium polyphenolates and also cause a precipitation of RF. Moreover, an acidic pH value of many beverages might cause precipitation of sodium polyphenolates due to a shift of the acid-base equilibrium to the protonated side, which would cause a loss of the polyphenolate's solubilizing power. Therefore, the compatibility of the sodium polyphenolate/RF mixtures was tested using the sports drink recipe of BASF. Like this, the compatibility of divalent cations, the pH resistance and the compatibility with other beverage ingredients could be simultaneously tested. Therefore, concentrated solutions comprising aromatic sodium carboxylates saturated with RF were diluted with the sports drink formulation from BASF to obtain a final RF concentration of 50 $mg \cdot kg^{-1}$ (max.

permitted RF content in non-alcoholic beverages[3]). The stability against discoloration and precipitation of the samples stored next to the window and in the dark was monitored by the eye for 3 weeks to prevent kinetically retarded precipitation, see Figure 77 and Table 17.
Although the pH in the sports drink was ca. 3.5, dilution led to polyphenolic acid concentrations below their water solubility and precipitation was not observed in most samples. Moreover, sodium precipitation and discoloration were not observed for most sodium polyphenolate formulations for several days. As suggested from the photostability measurements of RF in diluted aqueous solutions of NaBenz and NaCinn from section 4.1.2.1.8.1, the samples comprising NaBenz and NaCinn were discolored already after 2 days exposed to the sun and after 11 days of storage in the dark. Consequently, NaBenz and NaCinn did not alter the photostability of RF compared to the sports drink.
Analogously to the results from section 4.1.2.1.8, sodium caffeate should not be used for the stabilization of RF, as the samples turned brown. In line with the photostabilizing power of sodium polyphenolates observed in section 4.1.2.1.8.1, sodium polyphenolates prevented the total discoloration of the samples for at least 6 days. Sodium vanillate and 3,4-dimethoxycinnamate turned out as the best stabilizing agents, preventing total discoloration for 12 days and 17 days, respectively. Except of the samples comprising NaBenz, NaCinn and Na-3,4-DiOH-Cinn, samples stored in the dark kept their color for at least three weeks. Consequently, sodium polyphenolates should be compatible with common beverage formulations and keep their photostabilizing effect on RF.

As most of the tested aromatic sodium carboxylates did not precipitate in presence of calcium, the concentration of this divalent cation might be too low. To be sure that calcium would no induce precipitation, the water-solubility of the usual, well-soluble and fast dissolving calcium source in beverages, calcium lactate, was determined in pure water and in an aqueous 0.37 mol·kg^{-1} sodium ferulate solution, which was saturated with RF. The solubility of calcium lactate in water was 84-85 g·L^{-1} = 15 399 mg·L^{-1}. This corresponds to > 10 times more Ca^{2+} ions than in drinks fortified with calcium.[298–302] The solubility of calcium lactate was not altered by sodium ferulate or RF. Consequently, even at high concentration of the divalent calcium ion, its interaction with polyphenolates should not constitute a problem for formulation of beverages.[297]

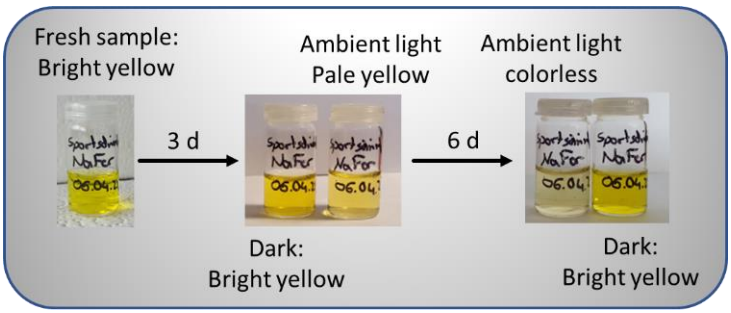

Figure 77: Example for the judgement of the color due to photo-degradation of RF in presence of sodium polyphenolates (here sodium ferulate) in the sports drink formulation from BASF, see Table 17

*Table 17: First until fourth column: polyphenolate (NaPP) , its concentration in the stock solution saturated with RF prior to dilution, the molar ratio and RF concentration in the solutions prior to dilution; the NaPP concentration in the stock solution was chosen due to the following criteria: *max. solubility without RF; ** max. solubility with RF; # best ratio; C only soluble in combination with RF; + higher concentrations too viscos for stirring/filtration; (X): vanillate: for higher c(salt) precipitation of salt after several days - Na-4-OMe-Benz: for higher c(salt) worse ratio – ferulate/Na-2-OH-Benz: for higher c(salt) precipitation of salt after several days. After dilution with the sports drink, all samples comprised 50 mg·kg^{-1} RF. Fifth column: ✓✓= Instant solubilization; ✓= White precipitation (NaCinn, Na-3,4-DiOMe-Cinn), but solubilized upon short shaking; ✗ = Instant precipitation of salt as needles, no re-solubilization after further dilution and shaking. The last two columns describe the observed coloration change of the diluted samples during three weeks of storage at ambient light and in the dark. Most samples did not undergo a color change when being stored in the dark. ✓= good photo-stabilization; ✓✓= very good photo-stabilization; ✗ = no photo-stabilization or acceleration of photo-degradation or brown coloration. For the judgement of the coloration see Figure 77.*

Salt	Salt(mol·kg^{-1})	Ratio(NaPP/RF)	RF(mmol·kg^{-1})	Precipitation?	Ambient light	Dark
NaBenz*,#	3.00	24.8	120.86	✓✓	1 d: Very pale yellow 2 d: Colorless✗	11 d: Pale yellow✗
Na-2-OH-Benz(X)	2.00	13.0	150.46	✓✓	3 d: Pale yellow 6 d: Colorless✓✓	
Na-4-OH-Benz*,#	2.93	14.0	209.51	✓✓	3 d: Pale yellow 6 d: Colorless✓✓	
Na-2-OMe-Benz*,#	0.92	432.9	2.37	✓✓	14 d: Pale yellow 18 d Colorless✓✓	
Na-4-OMe-Benz#	1.15	57.0	20.39	✗	-	
Na-3,4-DiOMe-Benz,#**	0.88	36.5	31.38	✓✓	14 d: Pale yellow 18 d: Colorless✓✓	
Na-3-OH-4-OMe-Benz*,#	1.05	24.5	45.32	✓✓	12 d: Colorless✓✓	
Na-4-OH-3,5-DiOMe-Benz#	2.73	9.0	325.24	✓✓	3 d: Pale yellow 6 d: Colorless✓	
Na-3,4,5-OH-Benz*,#	0.57	21.3	27.19	✓✓	4 d: Pale yellow 6 d: Colorless✓	
NaCinn,#**	0.59	16.4	36.18	✓	1 d: Very pale yellow 2 d: Colorless✗	11 d: Pale yellow✗
Na-4-OH-3-OMe-Cinn*,#	0.37	6.2	59.70	✓✓	3 d: Pale yellow 6d: Colorless✓	

Na-3,4-DiOH-Cinn,#**	0.40	7.2	51.35	✓✓	Few hours: Brown×	Few hours: Brown×
Na-3,4-DiOMe-Cinn+,C	1.3	6.0	224.62	✓	2 d: Less yellow 10 d: Pale yellow✓✓ 17 d: colorless	White precipitate (salt) after 8 d×
Na-2-OH-Cinn+,C	1.07	9.0	119.19	✓✓	6 d: Instantly colorless✓✓	
Na-4-OH-Cinn*,#	0.74	7.0	107.97	✓✓	3 d: Pale yellow✓ 6 d: Colorless	

4.1.2.1.10 Conclusion

RF was successfully solubilized with polyphenolates. Leading to a slightly worse molar solubilizer to RF ratio than sodium polyphenolates, the better water-solubility of choline polyphenolates compared to sodium polyphenolates enabled higher absolute water-solubility of RF. Still, so far, sodium polyphenolates are the best solubilizing agents for RF. Hence, the best sodium polyphenolates Na-4-OH-3,5-DiOMe-Cinn and Na-3,4-DiOMe-Cinn solubilized > 228 and > 176 times more RF in water than the well-known salting-in agent NaSCN at an additive concentration of 1 mol·kg^{-1}. The hydrotrope SXS solubilized also less RF than most polyphenolates tested. Moreover, the standard surfactant SDS solubilized less RF than most substituted sodium benzoate derivatives and less RF than all sodium cinnamates. Hence, at its highest concentration tested, SDS (0.4 mol·kg^{-1}) solubilized > 18 times, > 14 times and > 14 times less RF than Na-4-OH-3,5-DiOMe-Cinn, Na-3,4-DiOMe-Cinn and Na-4-OH-3-OMe-Cinn, respectively. Even nicotinamide, which is commonly applied as solubilizer for RF, solubilized > 72 times and > 55 times less RF than Na-4-OH-3,5-DiOMeCinn and Na-3,4-DiOMe-Cinn, respectively, at an additive concentration of 1 mol·kg^{-1}.[182]

Thus, the increase of RF's aqueous solubility by sodium polyphenolates is superior to the one of a common salting-in agent, of a hydrotrope, of a surfactant and even superior to the one of the common RF solubilizer nicotinamide.[182,254] Finally, gallate, which was patented as potent RF solubilizer for injections, increased RF's aqueous solubility 4.15 times and 2.9 times less than Na-4-OH-3,5-DiOMe-Cinn and Na-3,4-DiOMe-Cinn at 0.67 mol·kg^{-1} of the additive (corresponding to the water-solubility of sodium gallate in the presence of RF due to the mutual increase in solubility).[254]

The best sodium polyphenolates from this research, Na-3,4-DiOMe-Cinn, Na-4-OH-3,5-DiOMe-Cinn, Na-4-OH-3-OMe-Cinn and Na-2,4,6-TriOH-Benz, increased the solubility of RF > 2000 times, > 1400 times, > 240 times and > 65 times at the highest tested additive concentration of 4.34 mol·kg^{-1}, 1.62 mol·kg^{-1}, 0.56 mol·kg^{-1} and 0.08 mol·kg^{-1}, respectively, see Table 18.

In presence of the same four sodium polyphenolates, the best molar additive/RF ratios were obtained, see Table 18. In mass ratios, Na-4-OH-3-OMe-Cinn, Na-3,4-DiOMe-Cinn, Na-4-OH-3,5-DiOMe-Cinn and Na-2,4,6-TriOH-Benz enabled the best solubilization efficiency of 3.6, 3.5, 2.7 and 2.3, respectively.

The solubilization curve of the water-insoluble Na-3,4-DiOMe-Cinn with RF could not be continued, because the samples were too viscous and stirring with a magnetic agitator was not possible anymore. The RF solubility curves in presence of Na-4-OH-3,5-DiOMe-Cinn were not continued, because this polyphenolate was rather expensive. Na-2,4,6-TriOH-Benz was not tested either until its solubility limit, as it was supposed that this compound is usable only for pharmaceutical terms such as Na-2-OH-Benz. Thus, Na-4-OH-3,5-DiOMe-Cinn and Na-

2,4,6-TriOH-Benz might result in an even better additive/RF ratio, if solutions with higher additive concentrations would be saturated with RF.

These best sodium polyphenolates increased RF's water-solubility even comparable to a covalently bound sodium phosphate group (RF-PO_4 103 ± 8 mmol·kg^{-1}).

The molar additive/RF ratio decreased, when samples with higher additive concentration were saturated with RF. Thus, lower additive concentrations were not sufficient to reach a low number of additive molecules per one RF molecules. If aqueous samples comprising high additive concentrations were saturated with RF and then diluted with water to keep the low molar additive/RF ratio, neither RF nor the polyphenolates precipitated. Precipitation did not occur for at least 4 weeks. Thus, once RF was solubilized by sodium polyphenolates, it did not precipitate even after dilution.

Table 18: Maximum solubility of RF and best molar ratio obtained with the most efficient sodium polyphenolates for the aqueous solubilization of riboflavin at the given additive concentration.

Additive	Solubility of riboflavin	ratio(additive/riboflavin)
Na-2,4,6-TriOH-Benz	**18 ± 1 mmol·kg^{-1}** at 0.08 mol·kg^{-1}	**4.5** at 0.08 mol·kg^{-1}
Na-4-OH-3,5-DiOMe-Cinn	**380 mmol·kg^{-1}** at 1.62 mol·kg^{-1}	**4.2** at 1.02 mol·kg^{-1}
Na-3,4-DiOMe-Cinn	**560 ± 20 mmol·kg^{-1}** at 4.34 mol·kg^{-1}	**5.8** at 1.09 mol·kg^{-1}
Na-4-OH-3-OMe-Cinn	**67 ± 2 mmol·kg^{-1}** at 0.56 mol·kg^{-1}	**6.3** at 0.37 mol·kg^{-1}

The trends observed from the solubilization of RF with sodium polyphenolates and structurally related compounds in water are depicted in Figure 78. The solubilizing power of polyphenolates was found to be mostly independent of their amphiphilicity. A strong solubilizing power was observed, when the polyphenolate was substituted with functional groups exerting a positive mesomeric effect. Reversible copigmentation coupled with a mutual solubilization of RF and some polyphenolates, and the independence of the solubilizing power on the polyphenolate's water-solubility pointed to π-stacking of RF and polyphenolates instead of classical aggregative solubilization. In accordance to this, (i) the lack of a correlation in DLS, (ii) the absence of an effect of RF on surface tension curves of polyphenolates, (iii) the bad performance of SDS compared to most polyphenolates and (iv) the absence of an MHC in the solubilization curves denied an aggregation driven solubilization of RF. Instead, (i) NMR measurements showing again the mutual hydration of polyphenolates and RF, (ii) the alteration of the chemical shift of most aromatic carbon and proton atoms and (iii) cross-peaks in the NOESY spectrum indicating a distance of Na-3,4-DiOMe-Cinn and RF in water < 5 Å confirmed π-stacking of RF and polyphenolates.

π-Stacking of RF and polyphenolates is probably also the reason for the better performance of polyphenolates being substituted symmetrically with hydroxy and/or methoxy groups on the aryl ring. Thus, A. Fusina evidenced also a better solubilizing power of the more symmetric phloroglucinol to solubilize quercetin in water by π-complexation than of the actually better

water-soluble and pyrogallol.[265] Presumably, a symmetric arrangement of the substitutents on the hydrotropes' aryl ring leads to a more homogeneous distribution of the delocalized electrons in the aryl ring and thereby facilitates π-stacking.

The reason for the mutual solubilization of RF and polyphenolates originates probably from the complexation and partially from an altered ribityl side chain conformation due to the stacking. In general, the interaction of RF and polyphenolates appeared to be rather weak, as the copigmentation was easily reversible and RF did not alter the surface tension of aqueous aromatic sodium carboxylate solutions. A comparison of RF from Carl Roth with two distinct batches from BASF revealed that not only the solubility of RF in pure water but also the solubility of RF in presence of sodium polyphenolates is dependent on the distributor and batch. Thus, the solubility of RF varied up to 20-50 % depending on the distributor/batch of RF, see section 4.1.2.1.2 and 4.2.1. Reasons therefore might be impurities or distinct crystal structures of RF. Nevertheless, the magnitude of the solubilizing power of sodium polyphenolates was still roughly maintained.

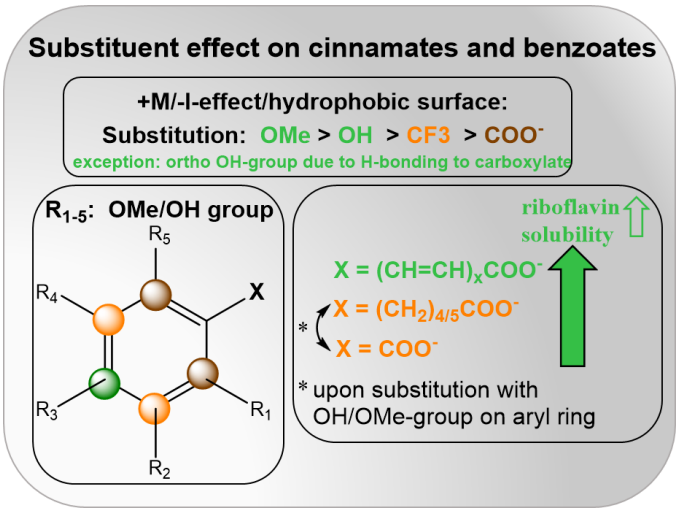

Figure 78: Effect of a functionalization of an aryl backbone, as present in natural sodium polyphenolates, on their riboflavin solubilizing power in water. The solubilization power increases from brown to orange and green. pH ≈ 7 (indicator paper)

Further, analogous to their corresponding acids, sodium polyphenolates photostabilized RF about 2-4 times compared to pure water in diluted solutions comprising 48 mg·kg^{-1} RF and for several weeks in concentrated solutions, see section 4.1.2.1.8. Although the photostabilizing mechanism was not elucidated, samples in the diluted regime were found to follow distinct rules than the one in the concentrated regime. Thus, the stabilizing power of aromatic sodium carboxylates in the diluted samples followed the antioxidative power of polyphenolic acids, as cinnamate derived polyphenolates stabilized RF better than benzoate derived ones and NaBenz and NaCinn exerted no photostabilizing effect. On the contrary, the photostabilization of RF in samples comprising high concentrations of polyphenolates or NaCinn was independent of the antioxidative power, as the non-antioxidant and non-scavenger NaCinn

photostabilized RF. As the copigmentation of RF and polyphenolates was reversible, the strong photostabilization of RF in aqueous concentrated polyphenolate and NaCinn solutions might be induced by the stacking.

The reversible photostabilization of RF by sodium polyphenolates via simple dilution might be useful for pharmaceutical practice. Thus, polyphenolate enriched injections or capsules with RF would be completely stable against photodegradation and oxidation of RF and stable against photosensitization of other pharmaceutically active molecules by RF, while RF would regain its bioactivity upon dilution in the blood cycle.

Finally, sodium polyphenolates were compatible with the sports drink beverage formulation from BASF, where they kept their photostabilizing power on RF. Consequently, aromatic sodium carboxylates constitute cheap, edible, and green bi-functional solubilizers for RF, preventing not only the photodegradation of RF, but also photosensitization of other valuable ingredients in aqueous beverages, see Figure 79.

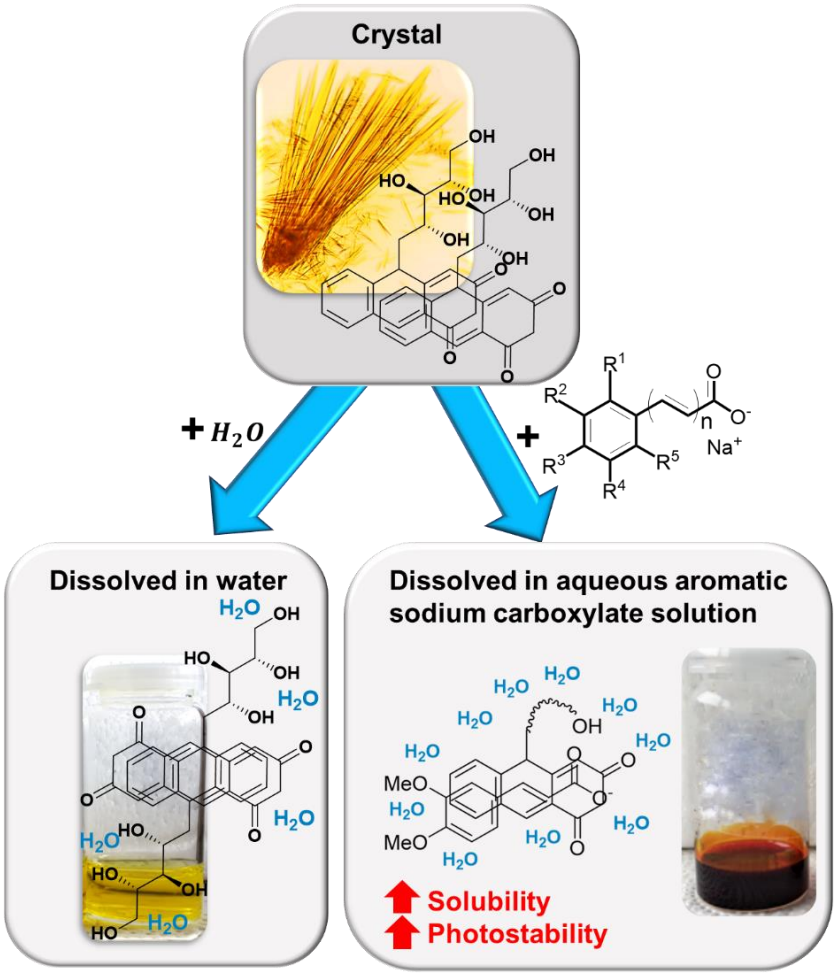

Figure 79: Molecular arrangement of RF in the crystal and in aqueous solution

4.1.2.2 Lumichrome and sodium riboflavin 5'-monophosphate

To further understand the function of the ribityl chain, three aqueous solutions comprising 0.37 mol·kg^{-1} medium or good sodium polyphenolates saturated with LC or RF-PO_4 were prepared. The change of the sample's color from transparent (LC in water) to yellow and orange in the case of lumichrome in presence of Na-4-OH-3-OMe-Benz and Na-3,4-DiOMe-Cinn, revealed an interaction of LC with the two sodium polyphenolates, see Figure 80 a-c. In the case of RF-PO_4 the samples exhibited similar coloration (orange – red – almost black) as the ones comprising RF and sodium polyphenolates. Thus, LC and RF-PO_4 both underwent copigmentation with sodium polyphenolates, such as RF did, see section 4.1.2.1.1. Consequently, LC and RF-PO_4 must be in direct contact with sodium polyphenolates in aqueous solution and not just surrounded by polyphenolates.

Figure 80: a) Lumichrome in water (saturation), b) Lumichrome in 0.858 mol·kg^{-1} Na-4-OH-3-OMe-Benz (saturation) at Na-4-OH-3-OMe-Benz's solubility limit in water, c) Lumichrome in 3 mol·kg^{-1} Na-3,4-DiOMe-Cinn as maximum possible concentration of Na-3,4-DiOMe-Cinn due to impedance of the stirring and filtering process for higher concentrations (saturation).

To further analyze the interaction of sodium polyphenolates with RF's isoalloxazine ring, other sodium polyphenolate-like compounds were tested as solubilizers for LC, too, see Figure 81 left. When applied at 0.2 mol·kg^{-1}, all aromatic solubilizers, which increased RF's solubility, increased the water-solubility of LC. The solubilizers can be ordered according to their LC solubilizing power: NaBenz < NaCHC < NaButyrate < NaValerate < Na-4-OH-3-OMe-Benz < NaCinn < Na-2,4-Pentadienoate < Na-4-OH-3-OMe-Cinn < Na-3,4-DiOMe-Cinn, see Figure 81. NaBenz was better for RF than CHC, and Na-3,4-DiOMe-Cinn and Na-2,4-Pentadienoate had a similar solubilization power for RF, whereas CHC was better for LC and Na-3,4-DiOMe-Cinn was better than Na-2,4-Pentadienoate for LC, see Figure 81 right. Nevertheless, the overall solubilization trends were the same for RF and LC, see Figure 81 right and section 4.1.2.1.1.

NaValerate solubilized 66 % more LC than NaButyrate. However, despite the improvement of LC's water-solubility by an elongation of the hydrophobic chain, this increase was nothing compared to the increase of LC's solubility via introduction of a total conjugation (NaValerate→Na-2,4-Pentadienoate), see Figure 81. Moreover, despite of its lower amphiphilic character NaCinn solubilized even 208 % more LC than NaButyrate, and Na-2,4-Pentadienonate increased the solubility of LC by > 1300 % more than NaValerate. Hence, a conjugation of the solubilizer – leading to its planarity and to a huger interaction surface – boosts the solubility of LC in water. Consequently, just as in the case of RF, the solubilization

power increased with increasing chain length and even more in presence of a conjugation over the entire molecule.

Remarkably, the factors for the increase of LC's and RF's water-solubility were also in the same scale, see Figure 81 right. This and the almost identical order of the additives according to their solubilizing power indicate that the isoalloxazine ring is implemented strongly into the underlying solubilization mechanism of LC or RF with sodium polyphenolates. Thus, the isoalloxazine ring is crucial for the interaction with sodium polyphenolates. This is in line with the observation of reversible copigmentation of RF and LC with sodium polyphenolates, with the strong dependence of RF's and LC's solubility on the extension of the polyphenolates' conjugated electronic system and with the NMR measurements of RF and RF-PO_4 in presence of aromatic sodium carboxylates.

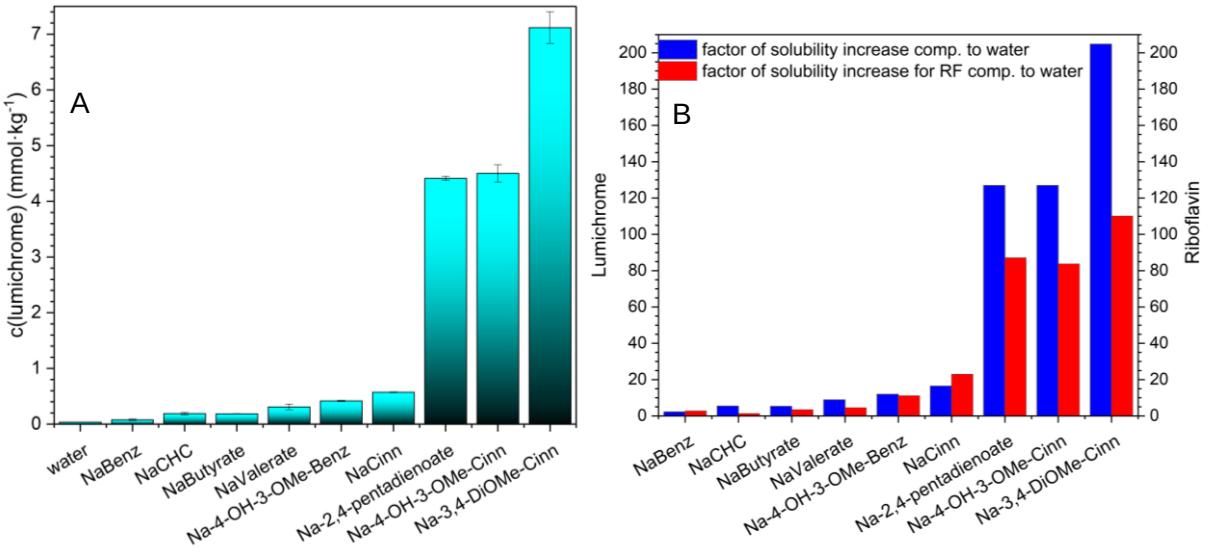

Figure 81: A) Water-solubility of lumichrome in water and in presence of 0.2 mol·kg^{-1} sodium polyphenolates and related compounds in water. Exact value in Table A 75 in section 7.8. B) Solubility increase of lumichrome and riboflavin by means of sodium polyphenolates relatively to the water-solubility of lumichrome (blue) and riboflavin (red), respectively.

Because the investigated system was very simple, a comparison of the difference of the change of the free solubilization energy of RF and LC $\Delta\Delta G^{**}$ in presence of sodium polyphenolate(-like) compounds via equation 17 and 18 from section 3.2.2.6 allowed evaluating the function of the ribityl chain in the interactions between the isoalloxazine ring and sodium polyphenolates, see Figure 82 A. The hugest difference between LC and RF was observed for NaCHC. The small NaCHC, having no conjugated electronic system, can only interact via hydrophobic interactions and hydrogen bonding with LC and RF. Compared to RF, NaCHC is rather small. Hence, imagining the solubilization of LC and RF via aggregation of NaCHC around LC or RF, much more NaCHC molecules would be needed in case RF than in case of the smaller LC molecule. Therefore, the solubility of LC was increased more by NaCHC than the one of RF.

Further, though having the same molecular backbone as NaCHC, the conjugated NaBenz increased the solubility of RF more than the one of LC. Consequently, the interactions via the

electronic system are strong enough to compensate the sterical disturbance of the ribityl chain for the solubilizer to approach RF. This finding was reinforced by the smaller $\Delta\Delta G^{**}$ for Na-2,4-Pentadienoate than for NaValerate. Although Na-2,4-Pentadienoate increased LC's solubility more than the one of RF, the electronic interactions with the isoalloxazine ring were strong enough to compensated the sterical hinderance by the ribityl chain at least a bit compared to NaValerate, see Figure 82 A. Hence, not only the stacking or dispersive interactions at the isoalloxazine ring, but also arrangement of the two solubilizers around the small LC compared to the bigger RF might be the reason for the much better performance of the latter NaCHC and NaValerate solubilizers with LC. Above all RF is harder to be embraced into aggregative structures.

In general, it is evident that for sterical demanding compounds, ΔG of RF and LC differed more than for smaller solubilizers (Na-4-OH-3-OMe-Cinn > Na-4-OH-3-OMe-Benz, NaValerate > NaButyrate; Na-2,4-Pentadienoate > NaCinn; Na-3,4-DiOMe-Cinn > Na-4-OH-3-OMe-Cinn), Figure 82 A. Rather small solubilizers seemed still to be able to approach RF when comprising a conjugated electronic system over the entire molecule. Thus, the ribityl chain of RF hinders the interaction of the isoalloxazine ring with the solubilizers.

Moreover, the effect of sodium vanillate, ferulate and 3,4-dimethoxycinnamate on the water-solubility of RF was compared to the effect of these compounds on LC's and RF-PO_4's water-solubility. The solubility of RF, LC and RF-PO_4 in presence of 0.37 mol·kg^{-1} sodium 3,4-dimethoxycinnamate, ferulate and vanillate is displayed in Figure 82 C.

The solubilization power of Na-3,4-DiOMe-Cinn and Na-4-OH-3-OMe-Cinn differed by 26 % in the case of LC, whereas it was similar in the case of RF and even flipped in the case of the RF-PO_4. Thus, an increasing sterical demand of the solubilizer (vanillate → ferulate → 3,4-dimethoxycinnamate) and of the solute (RF → LC → RF-PO_4) led to a weaker increase of the solute's water-solubility. Remembering the NMR results from section 4.1.2.1.7.8, which indicated a curved conformation of the ribityl side chain of RF and RF-PO_4 in presence of sodium polyphenolates, the ribityl and ribityl phosphate side chain probably hinders the approach of polyphenolates to the isoalloxazine ring. This is probably also one reason, why amphiphilic compounds increase the solubility of the smaller and less hydrophilic LC more than the solubility of the sterically more demanding RF.

Although the water-solubility of RF-PO_4 was increased by sodium polyphenolates, it was not in the scale of RF and LC, see Figure 82 C. Thus, 0.37 mol·kg^{-1} sodium vanillate increased the water-solubility of RF-PO_4 by 1.7 times, and 0.37 mol·kg^{-1} Na-4-OH-3-OMe-Cinn and Na-3,4-DiOMe-Cinn increased the water-solubility of RF-PO_4 only by 3 and 2.6 times, respectively. On the contrary, the water-solubility of RF was increased by 206 times with 0.37 mol·kg^{-1} Na-4-OH-3-OMe-Cinn and 220 times with 0.37 mol·kg^{-1} Na-3,4-DiOMe-Cinn.

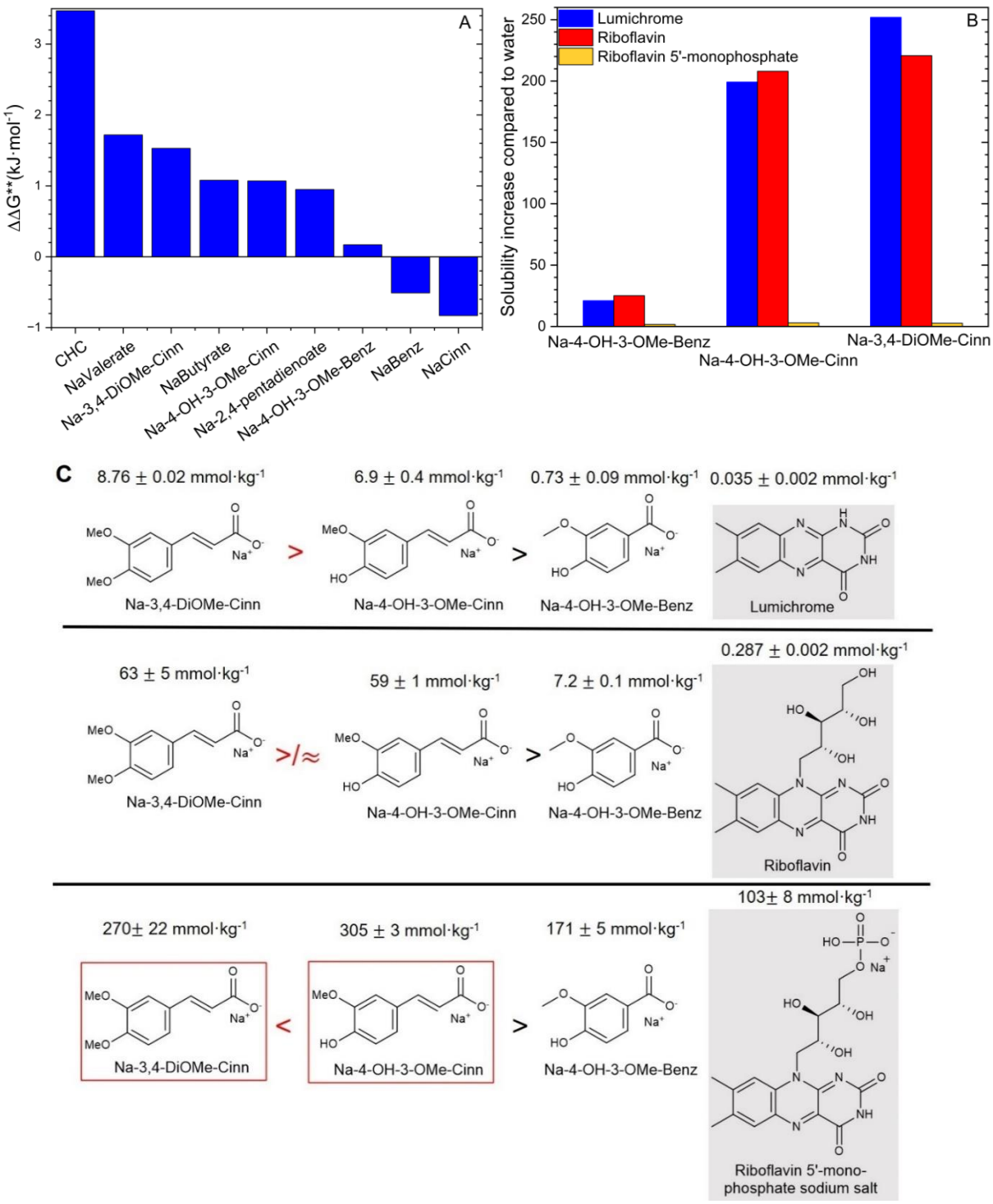

Figure 82: A: Change of the molar Gibbs enthalpy for the solubilization △△G upon introduction of a ribityl chain to LC in presence of sodium polyphenolates and structurally related compounds for aqueous 0.2 mol·kg^{-1} solutions of the solubilizer. B: Factor for the increase in solubility of lumichrome, riboflavin and riboflavin 5'-monophosphate via dissolution in a 0.37 mol·kg^{-1} sodium vanillate, ferulate and 3,4-dimethoxycinnamate solution compared to their corresponding solubility in water. C: Influence of the side chain on the isoalloxazine ring on the solubility of LC, RF and RF-PO$_4$ in presence of 0.37 mol·kg^{-1} aqueous sodium polyphenolate solutions.

The reason for the low increase of RF-PO$_4$'s water-solubility compared to the one of RF is presumably of RF-PO$_4$'s high solubility in pure water due to the strong hydration of its phosphate group.[42] Thus, RF-PO$_4$ (103 ± 8 mmol·kg^{-1}) is around 350 times more water-soluble than RF. Consequently, for a similar increase of RF-PO$_4$'s solubility as of RF's and LC's

solubility, 350 times more solubilizer molecules would be required than in the case of RF or LC. Hence, the solubility of RF-PO_4 cannot be increased by a similar factor as in the case of RF or LC, whose aqueous solubility differs only by a factor of 8. Moreover, although the water-solubility of RF was increased more than the one of sodium RF-PO_4, the absolute solubility of RF did not exceed the one of RF-PO_4. Even in presence of 0.37 mol·kg^{-1} Na-4-OH-3-OMe-Cinn, less RF was solubilized than sodium RF-PO_4 in pure water. Only high concentrations of Na-3,4-DiOMe-Cinn and Na-4-OH-3,5-DiOMe-Cinn were able to increase RF's water-solubility above the one of RF-PO_4 in pure water, see Table A 53 and Table A 54 in section 7.5 in the Appendix.

Despite the apparently low relative increase of RF-PO_4's water-solubility by sodium polyphenolates, the absolute solubility was increased strongly. Hence, 0.37 mol·kg^{-1} of Na-4-OH-3-OMe-Cinn and Na-3,4-DiOMe-Cinn were sufficient to solubilize up to 305 ± 3 mmol·kg^{-1} and 270 ± 22 mmol·kg^{-1} RF-PO_4 in water, corresponding to 145.9 g·kg^{-1} and 129.1 g·kg^{-1}, respectively. Consequently, the molar ratio and especially the weight ratio of sodium polyphenolates to RF-PO_4 was almost up to 10 times lower in the case of RF, see Table 19. Thus, the application of sodium polyphenolates as solubilizing agents is not just interesting for RF, but also for RF-PO_4, especially because a minimum weight ratio of 0.55 was reached in presence of 0.37 mol·kg^{-1} Na-4-OH-3-OMe-Cinn.

Table 19: Molar ratio and weight ratio of sodium polyphenolate (NaPP) to RF and sodium polyphenolate to RF-PO_4 after saturation of 0.37 mol·kg^{-1} sodium polyphenolate solutions with RF and RF-PO_4. ratio = c(RF)/c(polyphenolate) or ratio = c(RF-PO_4)/c(polyphenolate).

NaPP	Molar ratio (NaPP/RF-PO_4)	Molar ratio (NaPP/RF)	Weight ratio (NaPP/RF-PO_4)	Weight ratio (NaPP/RF)
Na-4-OH-3-OMe-Benz	2.2	51.4	0.86	26.0
Na-4-OH-3-OMe-Cinn	1.2	6.3	0.55	3.6
Na-3,4-DiOMe-Cinn	1.4	5.9	0.66	3.6

As the solubilization of LC and RF-PO_4 with sodium polyphenolates was not exactly the same as the one of RF, DLS measurements of LC and RF-PO_4 in water in absence and presence of two of the best riboflavin-solubilizers (Na-4-OH-3-OMe-Cinn and Na-3,4-DiOMe-Cinn) were conducted to definitely exclude solubilization of LC and RF-PO_4 via an inclusion in aggregates. The concentration of the polyphenolates was 0.37 mol·kg^{-1} corresponding to the solubility of Na-4-OH-3-OMe-Cinn in water. Regarding Figure 83, the correlation functions were strongly fluctuating around the baseline for the samples comprising LC and for the ones comprising RF-PO_4. Consequently, DLS measurements showed no indications for potential self-assemblies of sodium ferulate and 3,4-dimethoxycinnamate in presence of LC or RF-PO_4. This was expected, as the interaction of RF, LC and RF-PO_4 with sodium polyphenolates are based on their π-system.

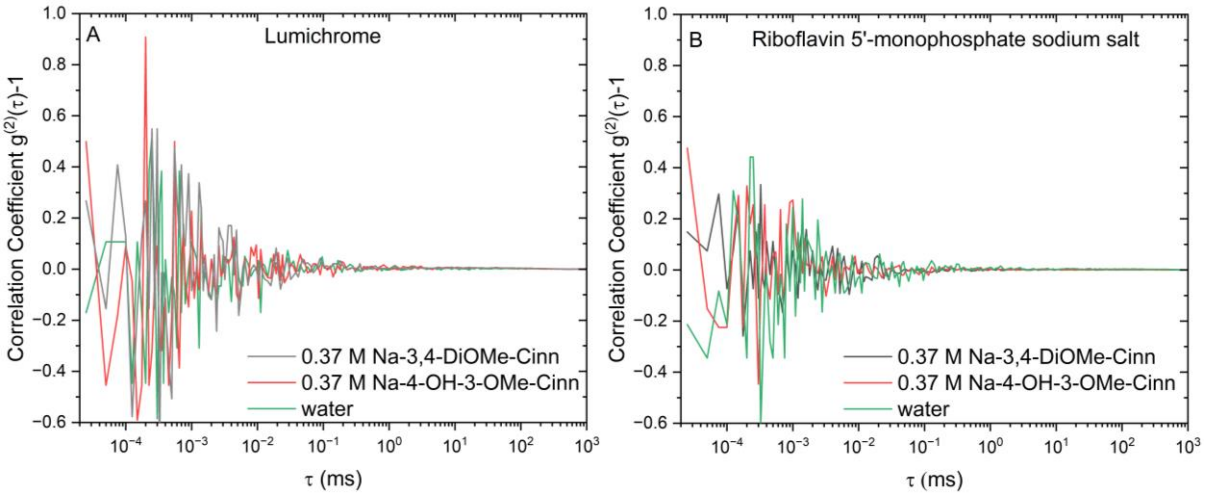

Figure 83: DLS correlation curves of lumichrome (A) and riboflavin 5'-monophosphate sodium salt (B) in pure water and in water in presence of 0.37 mol·kg^{-1} sodium ferulate and 3,4-dimethoxycinnamate. (0.37 mol·kg^{-1} is the solubility of sodium ferulate in water).

4.1.2.3 Vitamin K3

4.1.2.3.1 Solubilization

Similar to RF and LC, vitamin K3 exhibits a poor water-solubility probably due to stacking of the planar vitamin K3 molecules in the crystal, see Figure 84.[198] As aromatic sodium carboxylates turned out as efficient hydrotropes for RF, LC and RF-PO_4, sodium polyphenolates as cheap, natural, potentially edible, water-soluble antioxidants might also act on the water-solubility of vitamin K3. Of advantage for the usage of polyphenolic acids or their salts in animal husbandry would be that durum wheat bran, which consists mainly of ferulic acid, administered to cows is known to improve the milk and cheese production and to improve the milk's quality as well as its shelf-life.[73,74] Moreover, ferulic acids is already patented as feed supplement for beef cattle due to its positive effect on the meat quality.[108] Comprising further various health benefits, polyphenolic acids might constitute important solubilizing and stabilizing agents for vitamin K3 and thus facilitate the liquid administration of vitamin K3 in animal husbandry.[19,73,91–97]

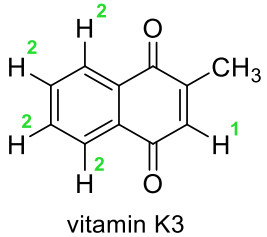

Figure 84: Molecular structure and nomination of the protons of vitamin K3 for NMR analysis.

Zhu et al. observed cocrystallization of vitamin K3 with the aromatic 1-hydroxy-2-naphthoic acid and 6-hydroxy-2-naphthoic acid via π-stacking, which was accompanied by copigmentation and an increased water-solubility of vitamin K3 in aqueous phosphate buffer

at pH 6.8.[196] Comprising a similar aromatic backbone, sodium polyphenolates might also increase the water-solubility of vitamin K3, as they already did in the case of RF, LC and RF-PO_4, see sections 4.1.2.1.1 and 4.1.2.2. Hence, the water-solubility of vitamin K3 in absence and presence of several polyphenolate(-like) compounds with distinct sizes of the conjugated electronic system was measured with the help of UV-Vis- or quantitative NMR spectroscopy. Only the solubility of vitamin K3 in pure water and in NaCHC solutions was determined via UV-Vis-measurements, as the solubility of the vitamin was below the detection limit of ^{1}H-NMR. Prior to the quantification of vitamin K3, the samples' color allowed making already conclusions on the interactions with aromatic sodium carboxylates. Saturation of water with vitamin K3 resulted in a colorless sample due to the absorption of vitamin K3 in the ultraviolet region. Yet, copigmentation leading to a redshift of the absorbance spectrum was observed for the samples comprising NaCinn, Na-2,4-Pentadienoate, NaValerate and NaButyrate, Na-4-OH-3-OMe-Cinn and Na-3,4-DiOMe-Cinn saturated with vitamin K3, see Figure 85 A.[188] Only, NaCHC and NaBenz did not induce a change in the color, see Figure 85 A. On the contrary, Na-4-OH-3-OMe-Cinn, Na-3,4-DiOMe-Cinn induced even a red coloration after saturation with vitamin K3, see Figure 85 A. Thus, vitamin K3's electronic π-system was near enough to the π-system of aromatic sodium carboxylates in aqueous solution to experience a change of the absorption spectrum.[263,303] The bathochromic shift of the absorption spectrum was dependent on the concentration of vitamin K3 and on the concentration of the aromatic sodium salts, see Figure 85 B. Hence, upon simple dilution with water, the UV-spectrum of vitamin K3 in water was regained, although the molar ratio of the aromatic sodium salt to vitamin K3 ratio did not change, see Figure 85 B.

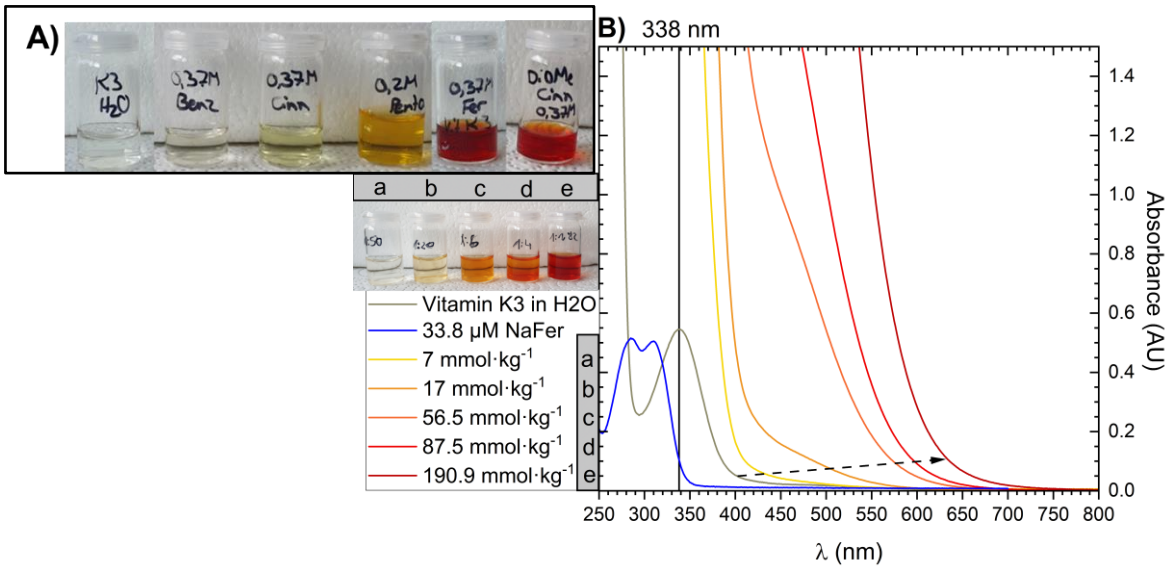

Figure 85: A) From left to right: Vitamin K3 in pure water, vitamin K3 in an aqueous 0.37 mol·kg^{-1} sodium benzoate, sodium cinnamate, sodium 5-phenyl-2,4-pentadienoate, sodium ferulate, sodium 3,4-dimethoxycinnamate solution. All samples were saturated with vitamin K3. B) UV-Vis-spectrum of sodium ferulate (NaFer), vitamin K3 (saturation) and vitamin K3 in presence of sodium ferulate at a constant molar ratio of 19.4 at distinct sodium ferulate concentrations.

Further, the solubility of vitamin K3 in aqueous sodium carboxylate solution was determined via UV-Vis-absorbance measurements after saturation with vitamin K3. The vitamin's water-solubility in presence of aromatic and one non-aromatic sodium salts at neutral pH (tested with indicator paper) is displayed in Figure 86. As Na-2,4-Pentadieonate was not solubilized above 0.2 mol·kg^{-1}, the solubilization curve could not be obtained for higher concentrations. The water-solubility of vitamin K3 amounted to 0.68 ± 0.03 mmol·kg^{-1}. All sodium salts, including the ones undergoing no copigmentation with vitamin K3, increased the water-solubility of vitamin K3 in a rather exponential manner, see Figure 86 A) and B). The solubilizers are ordered according to their solubilizing power in Figure 86 at the bottom.

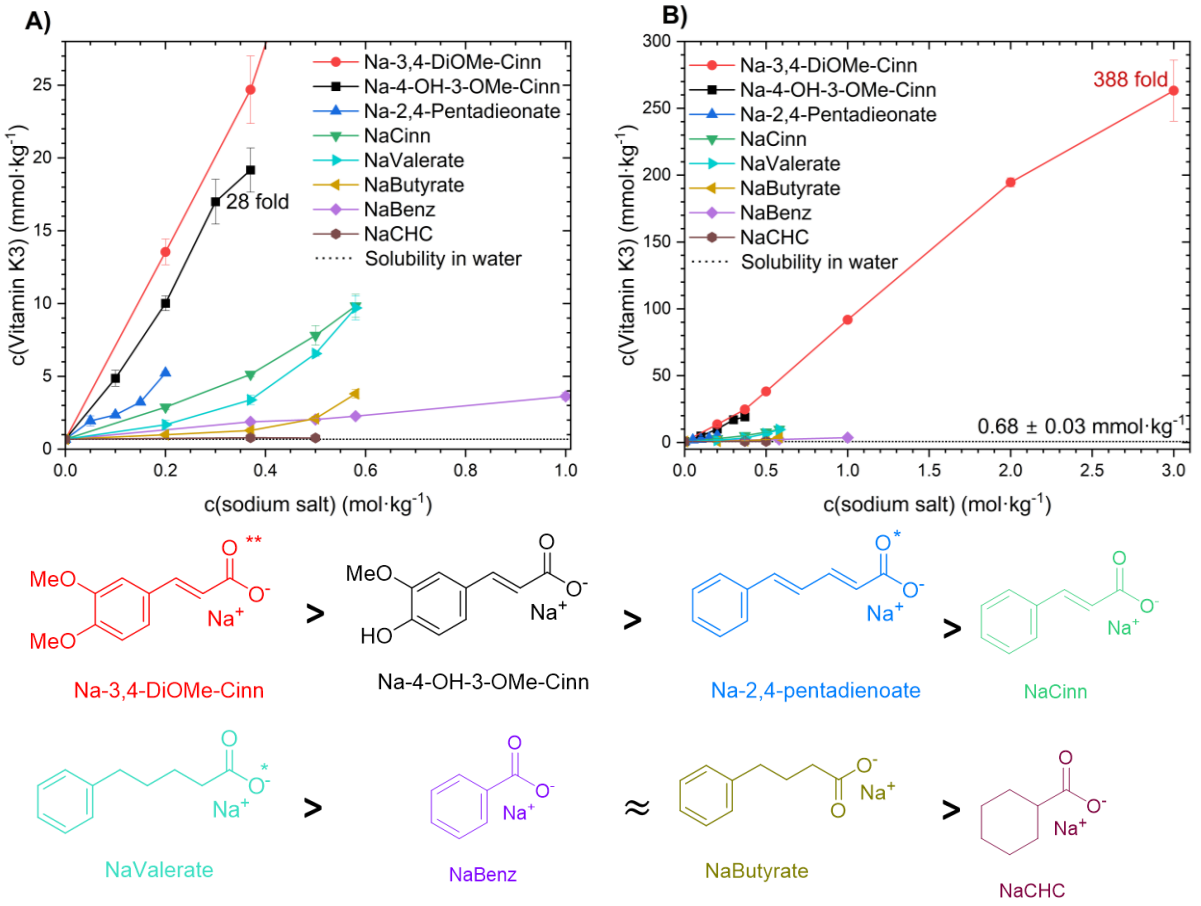

Figure 86: Top: Solubility of vitamin K3 in water in absence and presence of aromatic sodium salts and sodium cyclohexane carboxylate. A) Enlarged view; B) entire view. Bottom: Performance for the solubilization of vitamin K3 in water. Top left: best solubilizing agent, Bottom right: worst solubilizing agent.

The solubility of vitamin K3 increased with increasing conjugation and with the hydrophobic chain length (NaBenz < NaCinn < Na-2,4-Pentadieonate; NaButyrate < NaValerate). As in the case of RF in section 4.1.2.1.1, the non-aromatic NaCHC increased the solubility of vitamin K3 scarcely (+13 % at 0.5 mol·kg^{-1} NaCHC), while the aromatic NaBenz tripled the water-solubility of vitamin K3, when applied at the same concentration. Analogously, an extension of the conjugation to the carboxylate side chain was sufficient to increase vitamin K3's water-solubility by 3 times in the case of Na-2,4-Pentadieonate compared to NaValerate.

Although an increased amphiphilicity improved the solubility of vitamin K3 (NaBenz < NaButyrate < NaValerate), even the less amphiphilic but completely conjugated NaCinn solubilized significantly more vitamin K3 than NaValerate. The equal solubility of vitamin K3 in presence of 0.58 mol·kg^{-1} NaCinn and NaValerate can be explained by the limitation of NaCinn's water-solubility to 0.58 mol·kg^{-1}.

Further, Na-4-OH-3-OMe-Cinn and Na-3,4-DiOMe-Cinn solubilized vitamin K3 more efficiently than the more amphiphilic Na-2,4-Pentadieonate. Thus, a disruption of the solubilizer's amphiphilicity via implementation of a hydroxy and methoxy group to the aryl ring improved the solubilizing properties of the sodium salt. Consequently, the solubilizing mechanism of vitamin K3 is not in line with the one of DPnP from section 4.1.1. Instead, the aqueous solubilization of vitamin K3 by means of aryl carboxylates is strongly promoted by the size of the aromatic system and only minorly influenced by amphiphilicity.

Additionally, aromatic sodium carboxylate salts did not only solubilize vitamin K3, but were solubilized by the vitamin, too. Thus, Na-3,4-DiOMe-Cinn was never entirely soluble in water, but vitamin K3 enabled to keep 3 mol·kg^{-1} of the sodium salt in water for at least one month. Analogously, the water-solubility of Na-2,4-Pentadienoate was increased from 0.1 mol·kg^{-1} to approximately 0.2 mol·kg^{-1} in presence of the vitamin being stable against precipitation for at least 1 day. The solubility of NaValerate was also increased from 0.5 mol·kg^{-1} to at least 0.58 mol·kg^{-1} being stable for at least 1 day. The reversible bathochromic shift of vitamin K3's absorption spectrum, the mutual solubilization and the strong dependence of vitamin K3's water-solubility on the size of the aromatic π-system coupled with a lower dependence on the solubilizer's amphiphilicity point to an interaction of the planar aromatic sodium carboxylates with vitamin K3 via π-stacking.

Out of the solubilizers tested, 3 mol·kg^{-1} Na-3,4-DiOMe-Cinn increased the solubility of vitamin K3 up to 388 times followed by 0.37 mol·kg^{-1} sodium ferulate increasing vitamin K3's water-solubility 28 times. The molar polyphenolate to vitamin K3 ratios were 11.5 and 19.4, respectively. Thus, sodium benzoate and cinnamate derivatives enabled to solubilize by several factors more vitamin K3 than 1-hydroxy-2-naphthoic acid and 6-hydroxy-2-naphthoic. Nevertheless, the experiments are not completely comparable, as Zuh et al. adjusted a fixed molar ratio of the solubilizer and vitamin K3. Thus, 1-hydroxy-2-naphthoic acid and 6-hydroxy-2-naphthoic might even perform better. Still, the solubilizers of Zuh et al. would be maximum suitable for pharmaceutical applications, while sodium polyphenolates might be applied for food and nutritional supplement.[196]

Compared to dichloromethane (the best solvent for vitamin K3), the 3 mol·kg^{-1} Na-3,4-DiOMe-Cinn solution solubilized 53 times less vitamin K3 per mole of the corresponding solvent. However, comparing only the vitamin K3/dichloromethane ratio to the one of vitamin K3/Na-3,4-DiOMe-Cinn, Na-3,4-DiOMe-Cinn was only 2.45 times worse than the potentially carcinogenic dichloromethane.[197]

Moreover, the solubilizing power of the 3 mol·kg^{-1} Na-3,4-DiOMe-Cinn solution was approximately the same as the one of a binary water/ethanol (28/72 (w/w)) mixture, while the water/hydrotrope ratio was 18.5 in the case of a 3 mol·kg^{-1} Na-3,4-DiOMe-Cinn solution and 1 in the case of the binary water/ethanol mixture.[193] Hence, the Na-3,4-DiOMe-Cinn solution was even more efficient than water/ethanol mixtures.

4.1.2.3.2 NMR analysis

To evaluate the interaction of vitamin K3 with aromatic sodium carboxylates further, the change of the proton's chemical shift was investigated depending on the concentration of the best solubilizer Na-3,4-DiOMe-Cinn in non-deuterated water. Therefore, the change of the chemical shift of Na-3,4-DiOMe-Cinn's protons upon saturation with vitamin K3 was determined for a 0.2 mol·kg^{-1} and for a 3 mol·kg^{-1} Na-3,4-DiOMe-Cinn solution, see Figure 87. The presence of vitamin K3 led to a slight shielding of all protons of Na-3,4-DiOMe-Cinn's by 0.08 – 0.17 ppm. Thus, all protons of Na-3,4-DiOMe-Cinn were exposed to a slightly increased electron density after saturation with vitamin K3. The aromatic protons H3, H4 and H5 were affected most, see Figure 87. Although the molar Na-3,4-DiOMe-Cinn to vitamin K3 ratio was 1.3 times lower for a 3 mol·kg^{-1} solution saturated with vitamin K3 than for the 0.2 M Na-3,4-DiOMe-Cinn solution, vitamin K3 showed almost no effect on the protons of Na-3,4-DiOMe-Cinn in the 3 mol·kg^{-1} solution, Figure 87 top. The reason therefore is probably stacking of Na-3,4-DiOMe-Cinn with other Na-3,4-DiOMe-Cinn molecules due to the high concentration of this polyphenolate.[255] In any case, vitamin K3 induced an upfield shift of Na-3,4-DiOMe-Cinn's protons and thus increased the electron density of its protons.

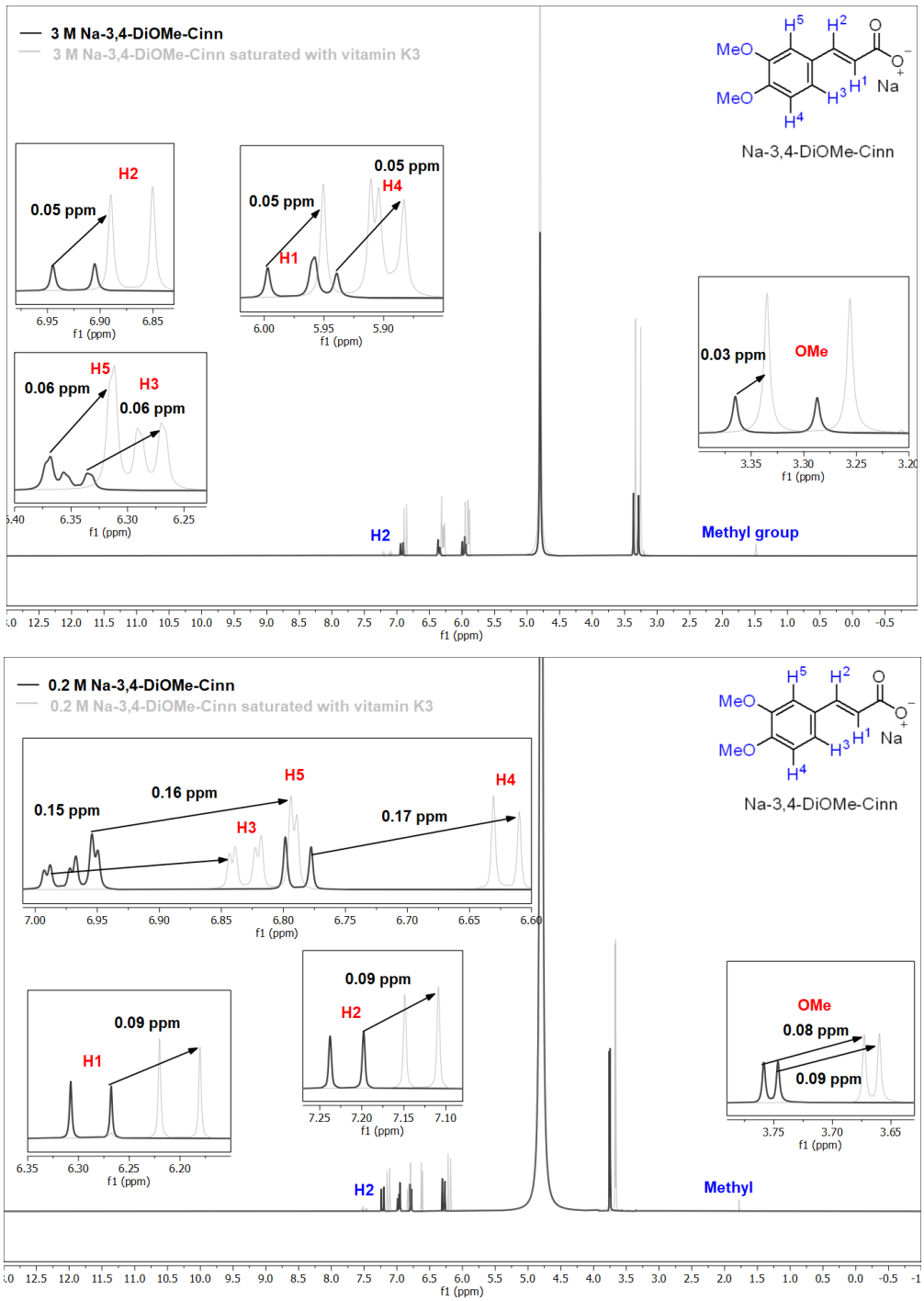

Figure 87: ^{1}H-NMR spectrum of an aqueous 3 mol·kg^{-1} (top) and 0.2 mol·kg^{-1} (bottom) sodium 3,4-dimethoxycinnamate solution in the absence of vitamin K3 and saturated with vitamin K3. Red: protons of 3,4-dimethoxycinnamate; blue: protons of vitamin K3. Proton H1 of vitamin K3 was covered by the aromatic protons of 3,4-dimethoxycinnamate. Water peak: 4.8 ppm.

Further the chemical shifts of vitamin K3's protons were evaluated when increasing the concentration of different aromatic sodium carboxylates see Figure 88 top. The chemical shift of vitamin K3's methyl group decreased with the concentration depending on the type of solubilizer, see Figure A 71-Figure A 76 in Appendix. Hence, all aromatic solubilizers increased the electron density of vitamin K3's protons. The ^{1}H-NMR spectrum of pure vitamin K3 in water after saturation was not analyzable, as the signal to noise ratio was too low. Hence, the change of vitamin K3's protons' chemical shift was determined via comparison of its protons' chemical

shifts in presence of 0.2 mol·kg^{-1} Na-3,4-DiOMe-Cinn in water to vitamin K3's protons in an aqueous 3 mol·kg^{-1} Na-3,4-DiOMe-Cinn solution, see Figure 88 at the top. The protons of vitamin K3 were shielded more strongly with increasing concentration of Na-3,4-DiOMe-Cinn. The shift of H1 was not detectable due to an overlap of this protons with the ones of Na-3,4-DiOMe-Cinn. However, H2 and the methyl group of vitamin K3 were clearly shielded by ca. 0.36 ppm, see Figure 88 top. Though the aromatic protons of H3, H4 and H5 of Na-3,4-DiOMe-Cinn's were also shielded with increasing Na-3,4-DiOMe-Cinn concertation, the reason for this strong shielding was the strong change of Na-3,4-DiOMe-Cinn's concentration and not the presence of vitamin K3, see Figure A 70 in the Supplementary Material.

The change of the chemical shift of Na-3,4-DiOMe-Cinn's protons upon saturation with vitamin K3 for a 0.2 mol·kg^{-1} solution and the change of vitamin K3's protons upon the increase of the Na-3,4-DiOMe-Cinn concentration from 0.2 mol·kg^{-1} to 3 mol·kg^{-1} are visualized in Figure 88 at the bottom. Apparently, the aromatic protons of vitamin K3 and its Na-3,4-DiOMe-Cinn were affected most by the interaction of vitamin K3 with Na-3,4-DiOMe-Cinn. This correlates with the observation from section 4.1.2.3.1 that the size of the conjugated electronic system is important to act as an efficient solubilizer for vitamin K3 in water. As Na-3,4-DiOMe-Cinn was present in solution in 10 to 14 times higher concentration than vitamin K3, Na-3,4-DiOMe-Cinn showed a greater impact on the chemical shift of vitamin K3. Finally, the shielding of the protons of vitamin K3 and of aromatic sodium carboxylates in NMR point to an increased electron density of the protons, which confirms the stacking of vitamin K3 and its aromatic solubilizers.

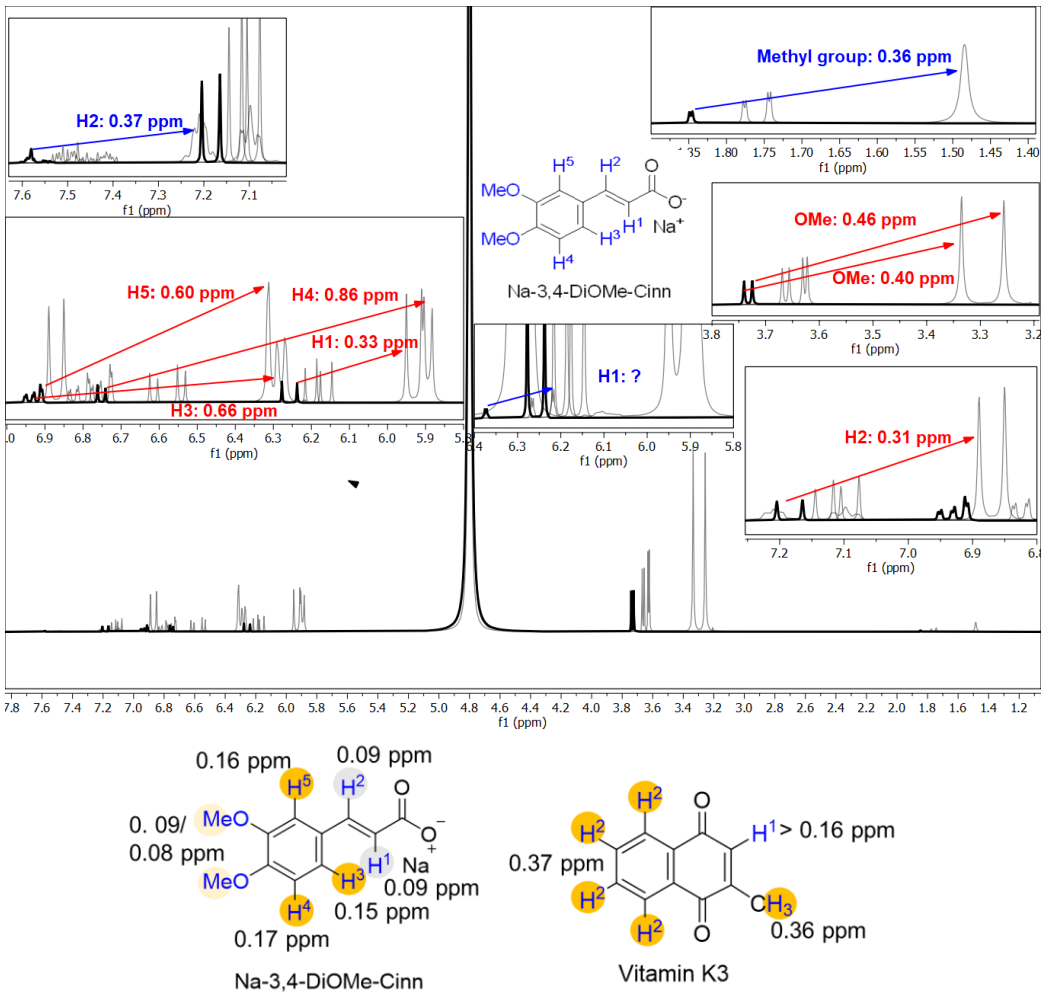

Figure 88: Top: Superimposed ^{1}H-NMR spectra of aqueous 0.2 mol·kg^{-1}(–), 0.37 mol·kg^{-1} (–), 0.5 mol·kg^{-1} (–), 3 mol·kg^{-1} ( ) sodium 3,4-dimetoxycinnamate solutions saturated with vitamin K3. Bottom left: Change of the chemical shift of Na-3,4-DiOMe-Cinn' protons in a 0.2 mol·kg^{-1} aqueous solution upon saturation with vitamin K3; bottom right: Change of the chemical shift of vitamin K3's protons when regarding the 0.2 mol·kg^{-1} and 3 mol·kg^{-1} solution saturate with vitamin K3. Yellow: strongest change; grey: least change.

As the aromatic protons of Na-3,4-DiOMe-Cinn were affected most by the presence of vitamin K3, a NOESY NMR spectrum of an aqueous 3 mol·kg^{-1} Na-3,4-DiOMe-Cinn solution saturated with vitamin K3 was recorded to evaluate the proximity of the two aromatic compounds after the solubilization. The NOESY spectrum exhibited several cross-peaks, see Figure 89. Although, Na-3,4-DiOMe-Cinn's protons interacted with the protons of other Na-3,4-DiOMe-Cinn molecules, the reason therefore was probably the high concentration of Na-3,4-DiOMe-Cinn, as the same cross-peaks were also observed in the absence of vitamin K3, see Figure A 77 in the Appendix.

The protons giving rise to cross-peaks between Na-3,4-DiOMe-Cinn and vitamin K3 are visualized in Figure 89 at the bottom. Because H1 of vitamin K3 was covered by H3 and H5 of Na-3,4-DiOMe-Cinn, cross-peaks were not visible for H1, see Figure 88 at the top. Yet, the protons of vitamin K3's methyl group exhibited cross-peaks with all protons of Na-3,4-DiOMe-Cinn, see Figure 89. Similarly, the protons H2 of vitamin K3 gave rise to cross-peaks with all

protons of Na-3,4-DiOMe-Cinn (H3, H4, H5, 2xOMe) except for the ones on the carboxylate side chain (H1, H2).

As NOESY enables a view of maximum of 5 Å and typical distances for π-stacked compounds are 3.46-3.85 Å, NOESY and NMR measurements affirm the existence of specific molecular π-interactions between vitamin K3 and aromatic sodium carboxylates.[249,277–280]

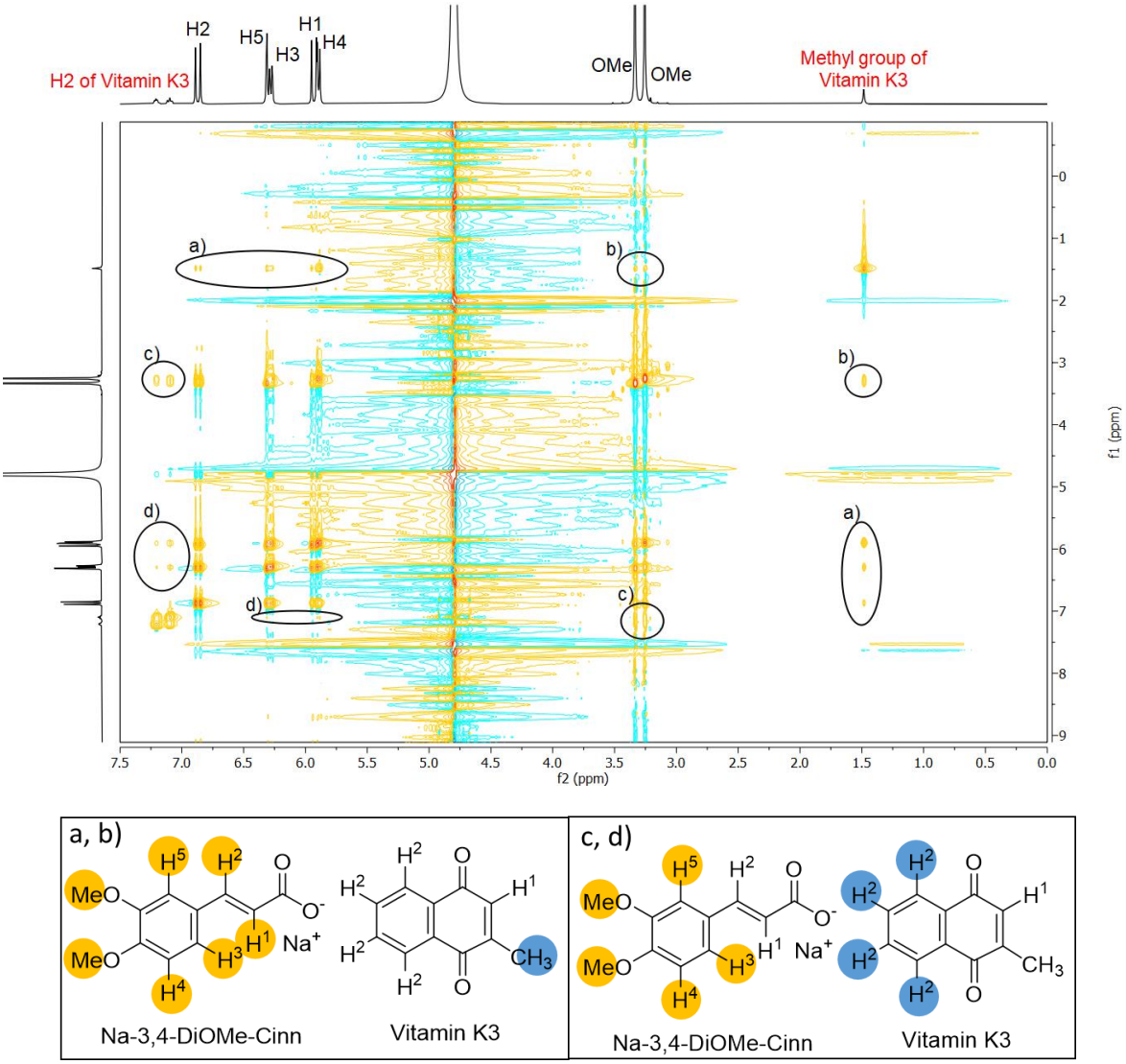

Figure 89: Top: NOESY NMR spectrum of an aqueous 3 mol·kg^{-1} sodium 3,4-dimethoxycinnamate solution saturated with vitamin K3. The cross-peaks of vitamin K3's protons with the ones of dimethoxy cinnamate (a-d) are visualized below. The blue protons have a cross-peak with the yellow marked protons. Conclusions for H1 of vitamin K3 were not possible, as the proton was covered by the signal of H3 and H5 of Na-3,4-DiOMe-Cinn.

4.1.2.3.3 Photostabilization of vitamin K3 in aqueous sodium polyphenolate solutions

Another disadvantage of the handling of vitamin K3 is its light induced dimerization, see Figure 90. Zhu et al. observed a photostabilizing effect of 1-hydroxy-2-naphthoic acid on vitamin K3 in aqueous solution. They claimed that π-stacking of the vitamin with the acid was the reason for the prevention of this dimerization and thus inactivation the vitamin function.[196]

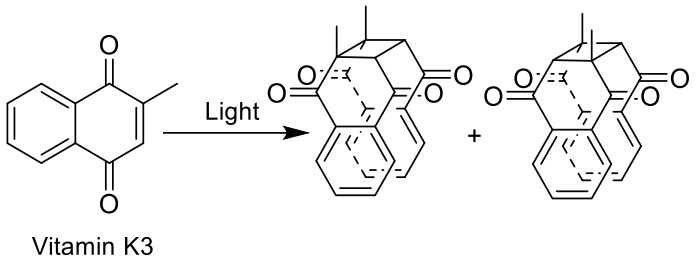

Figure 90: Dimerization of vitamin K3

The copigmentation and NMR analysis of vitamin K3 with sodium polyphenolates proofed π-stacking of vitamin K3 with phenolic acids, see sections 4.1.2.3.1 and 4.1.2.3.2. Moreover, sodium polyphenolates slowed down the photodegradation of RF in diluted aqueous solutions and concentrated sodium polyphenolate solutions enabled even a longtime stabilization of RF against photodegradation, which seemed to be independent of the polyphenolates' radical scavenging properties. Thus, sodium polyphenolates might exhibit a photostabilizing effect on vitamin K3, too. Therefore, content of vitamin K3 was monitored in pure water, in an aqueous 0.37 mol·kg^{-1} NaBenz, Na-4-OH-3-OMe-Cinn and Na-3,4-DiOMe-Cinn solution by means of NMR and UV-Vis-spectroscopy. 0.37 mol·kg^{-1} solutions of the sodium carboxylates were used as this is the maximum water-solubility of Na-4-OH-3-OMe-Cinn to have comparable samples. After saturation with vitamin K3, one part of the samples was stored in the dark, while the other part was put next to the window exposed to the sun. The stability in presence of NaBenz was investigated, because NaBenz and NaCinn had a photostabilizing effect on RF in the concentrated solutions without antioxidant properties, see section 4.1.2.1.8.2. Na-3,4-DiOMe-Cinn and Na-4-OH-3-OMe-Cinn were chosen, because they were the best solubilizers in section 4.1.2.3.1.

The sample comprising vitamin K3 in pure water became slightly turbid exhibiting a pink touch already after few hours of exposure to the sun, see Figure 91. The reason therefore was the dimerization of vitamin K3 leading to the formation of the water-insoluble dimer.[196]

Figure 91: Stability of vitamin K3 in pure water: A) after 4 h; B) After one day.

The sample comprising 0.37 mol·kg^{-1} NaBenz saturated with vitamin K3 turned turbid and pink, too. Additionally, a reddish precipitate was observed. Presumably, the precipitate was formed only in presence of NaBenz and not in pure water because the concentration of vitamin K3 in presence of NaBenz was higher.

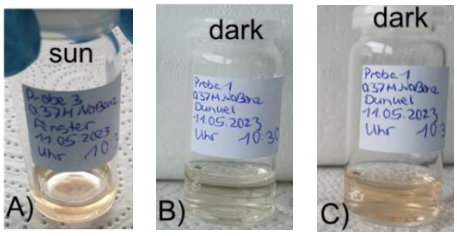

Figure 92: Stability of vitamin K3 in an aqueous 0.37 mol·kg^{-1} sodium benzoate solution: A) Exposed to the sun after 24 h; B) stored in the dark after 9 days; C) stored in the dark after 44 days.

Regarding vitamin K3 in pure water, almost 50 % of vitamin K3 (0.32 mmol·kg^{-1}) were degraded after 30 h of storage next to the window, see Figure 93. The samples stored in the dark underwent also a loss of vitamin K3. Yet, the degradation of vitamin K3 in the dark was slower and neither turbidity nor pink coloration or precipitation were observed on the samples stored in the dark.

NaBenz had no influence on the degradation of vitamin K3. Thus, about 0.4 mmol·kg^{-1} vitamin K3 was lost after 30 days in the samples stored in the dark and next to the window, see Figure 93. The reason therefore might be the absence of radical scavenging properties or too weak attractive interactions with vitamin K3.

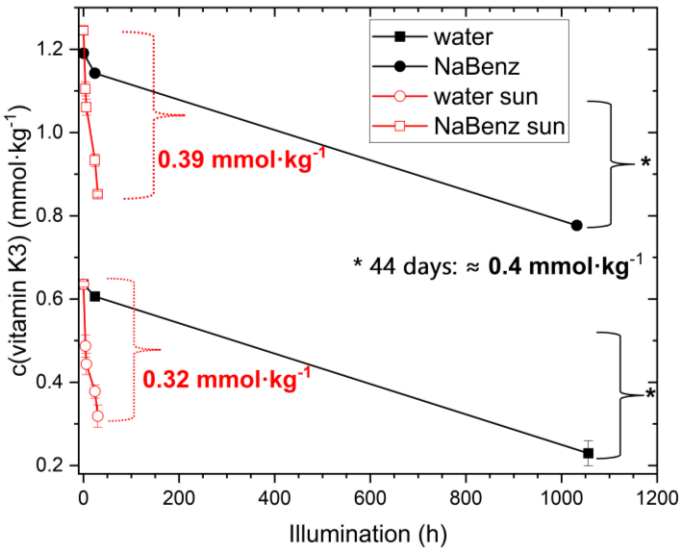

Figure 93: Stability of vitamin K3 in water and in an aqueous 0.37 mol·kg^{-1} sodium benzoate solution (NaBenz) when stored in the dark and next to the window exposed to the sun.

The 0.37 mol·kg^{-1} Na-4-OH-3-OMe-Cinn solution stabilized vitamin K3 in relative terms. Yet, after 7 days of storage next to the window, 5.52 mmol·kg^{-1} vitamin K3 were lost, while with the degradation speed of vitamin K3 in pure water only 1.16 mmol·kg^{-1} should have been lost, see Figure 96 B. The samples stored next to the window and the ones stored in the dark exhibited an oily film on the surface already after 4 days and were completely turbid after 9 days, see Figure 94 and Figure 96 A. Na-4-OH-3-OMe-Cinn samples stored in the dark lost vitamin K3 as fast as the ones stored next to the window, see Figure 94. The reason for the rapid degradation of the Na-4-OH-3-OMe-Cinn was the oxidation of sodium ferulate leading to its oligomerization and thus to a loss of the solubilizer.[293] Hence, sodium ferulate is not an appropriate hydrotrope for vitamin K3's solubilization for more than four days.

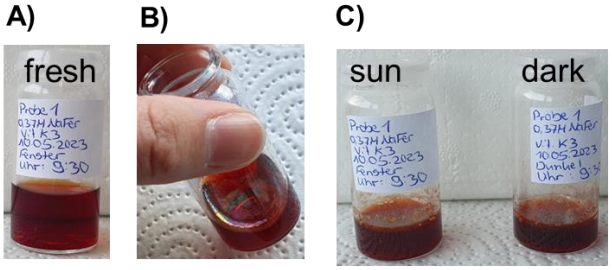

Figure 94: Stability of vitamin K3 in an aqueous 0.37 mol·kg^{-1} sodium ferulate solution: A) fresh sample; B) oily film observed for samples stored next to the window and in the dark after 4 days; C) after 9 days of storage.

In contrast, the samples comprising vitamin K3 in presence of 0.37 mol·kg^{-1} Na-3,4-DiOMe-Cinn were stable against precipitation and turbidity for at least 26 days. On day 27, a slight turbidity and precipitate were observed, which did not proceed considerably when regarding the samples after 44 days of storage, see Figure 95.

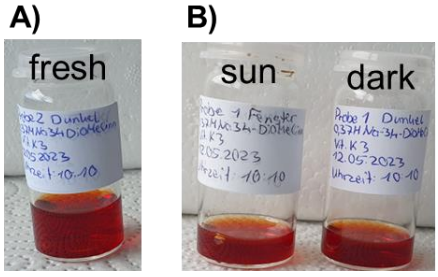

Figure 95: Stability of vitamin K3 in an aqueous 0.37 mol·kg^{-1} sodium 3,4-dimethoxycinnamate solution: A) fresh sample; B) after 44 days of storage.

In relative terms, Na-3,4-DiOMe-Cinn stabilized vitamin K3 considerably. Even after one month, still 84 ± 4 % of vitamin K3 (21.1 ± 0.7 mmol·kg^{-1}) were present in the samples stored in the dark and next to the window, see Figure 96 A and C. In absolute terms, Na-3,4-DiOMe-Cinn slowed down the photodegradation of vitamin K3 just slightly, see Figure 96 B. Thus, with the photodegradation speed of the pure water sample, 4.48 mmol·kg^{-1} vitamin K3 should have been degraded. However, in presence of 0.37 mol·kg^{-1} Na-3,4-DiOMe-Cinn, 13 % less vitamin K3 was degraded, see Figure 96 B. (Note: The sample comprising vitamin K3 in pure water was analyzed on a cloudy day, while the one comprising Na-3,4-DiOMe-Cinn was exposed to the bare sun.)

Regarding the samples stored in the dark, less vitamin K3 was lost than in the samples stored next to the window; see Figure 96 C. Thus, in the samples stored in the dark, still 97 ± 2 % vitamin K3 was present after 27 days, and 90 ± 2 % vitamin K3 was present after 36 days, see Figure 96 C. Still in absolute terms, theoretically 0.79 mmol·kg^{-1} vitamin K3 would have been lost in pure water after 27 days, while 0.74 mmol·kg^{-1} vitamin K3 were lost in the Na-3,4-DiOMe-Cinn sample, see Figure 96 D. Thus, vitamin K3 was slightly stabilized in the Na-3,4-DiOMe-Cinn solution for almost one month. However, after one moth, the degradation of vitamin K3 was accelerated, leading to a faster loss of the vitamin then it would have been in the pure water sample.

Finally, Na-3,4-DiOMe-Cinn can be used to increase the solubility of vitamin K3 considerably for ca. 1 month without considerable precipitation of the vitamin. However, for longtime storage, the samples should be stored in the dark.

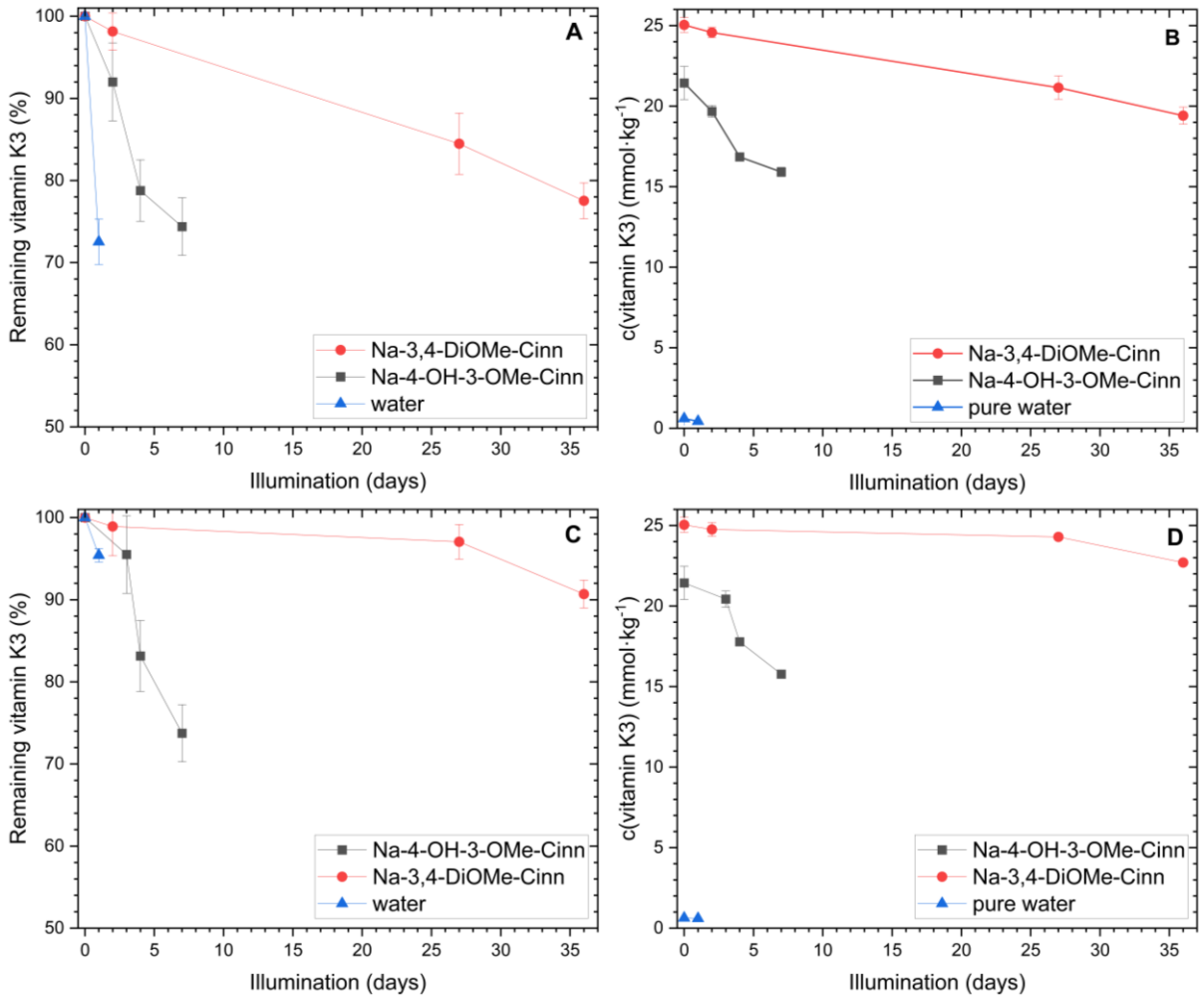

Figure 96: Stability of vitamin K3 in pure water and in an aqueous solutions comprising 0.37 mol·kg^{-1} sodium ferulate and 3,4-diemthoxycinnamate. A) and B) Samples were stored next to the window exposed to the sun; C) and D) Samples were stored in a dark box.

4.1.2.3.4 Conclusion

As vitamin K3 was solubilized in aqueous medium by the aromatic 1-hydroxy-2-naphthoic acid and 6-hydroxy-2-naphthoic acid due to π-stacking, the better water-soluble aromatic sodium polyphenolates were supposed to act similarly.[196] Indeed, all tested sodium benzoate and cinnamate derivatives increased the water-solubility of vitamin K3 exponentially. An extension of the conjugated π-electron system was more dominant for the solubilization of vitamin K3 in water than the hydrophobicity of the solubilizer. Additionally, aromatic sodium carboxylates with an extended electronic π-system underwent reversible copigmentation with vitamin K3 leading to a bathochromic shift of vitamin K3's absorption spectrum. Although the solubilizing efficiency increased with increasing concentration of the aromatic sodium salts, neither the vitamin nor the solubilizer precipitated upon dilution of the samples with water, as it was the case for RF in section 4.1.2.1.1. NMR analysis of Na-3,4-DiOMe-Cinn solutions saturated with vitamin K3 showed stronger shielding of the protons placed directly on the aryl rings and revealed a distance ≤ 5 Å between the two bio-compounds in solution. Taking additionally into account the typical π-stacking distances (3.46-3.85 Å), π-stacked complexation of vitamin K3 with aromatic sodium carboxylates in aqueous solution was concluded from NOESY measurements.[277,279,280] The complexation is probably also the reason for the mutual solubilization observed for vitamin K3 and some aromatic sodium carboxylates.

The best solubilizing agents tested, sodium 3,4-dimethoxycinnamate and sodium ferulate, increased vitamin K3's water-solubility 388 times and 28 times, respectively. In contrast, cocrystallization of vitamin K3 with 6-hydroxy-2-naphthoic acid from the research of Zhu et al. allowed increasing the water-solubility of vitamin K3 only 1.5 times.[196] Moreover, 3 $mol \cdot kg^{-1}$ Na-3,4-DiOMe-Cinn enabled a higher absolute water-solubility of vitamin K3 than a covalently bound bisulfite group, which is usually used for improving vitamin K's solubility in animal husbandry.[304]

As sodium polyphenolates, cinnamate and benzoate stabilized the photolabile RF in aqueous neutral medium at high concentrations of the stabilizer probably due to π-interactions, they were thought to exert photostabilizing properties on vitamin K3, too.[84] Thus, relatively to vitamin K3 in pure water, the stability of vitamin K3 was observed for samples comprising 0.37 $mol \cdot kg^{-1}$ sodium ferulate, 3,4-dimethoxycinnamate and NaBenz stored in the dark and exposed to the sun. However, the three aromatic salts did not alter the stability of vitamin K3 in the dark and under light. Thus, sodium ferulate can be used only for the solubilization of vitamin K3 for four days, as oxidation of ferulate led to a fast precipitation and turbidity of the sample stored in the dark and next to the window. Sodium 3,4-dimethoxycinnamate, as the best solubilizing agent, allowed keeping up high concentrations of vitamin K3 in the dark (97 ± 2 %) and exposed to the sun (84 ± 4 %) for 27 days. However, for longtime storage, the samples should be stored in the dark. Regarding the omnipresence of polyphenolic acids, sodium ferulate and Na-3,4-

DiOMe-Cinn constitute potential solubilizers for vitamin K3 for the preparation of aqueous husbandry supplements. Moreover, such as nicotinamide, aromatic sodium carboxylates might also improve the solubility of menadione bisulfite further due to complexation.[185] Due to their antioxidant properties and because of their positive effect on the quality and shelf-life of milk and meat, polyphenolates might be useful multifunctional solubilizers for aromatic additives in animal husbandry in general.[73,74,108]

Nevertheless, polyphenolic acids are well-known for their antithrombic properties. Thus, the π-complexation of vitamin K3 might counteract the coagluative properties of vitamin K3.[16,186] Consequently, further studies on the interaction of vitamin K3 with polyphenolates in the organism should be performed.

4.1.2.4 Folic acid

Folic acid – the synthetic form of folate – belongs to the B vitamins and is also known under the names vitamin B9, pteroil (mono)-glutamic acid, see Figure 97. The photosensitive and very slightly water-soluble vitamin is involved in the synthesis and methylation of DNA, in homocysteine metabolism and in several biochemical reactions, such as the production of red globules in children.[305,306] The sparing water-solubility of folic acid (1.6 mg·kg^{-1} at 25 °C) seems contradicting regarding the molecular structure of folic acid, which comprises many potential hydrogen bonding sites.[307,308] The reason for the sparing solubility of the aromatic vitamin might be the strong hydrogen bonding network between neighbored folic acid molecules in the crystal, but also the intermolecular π-stacking of the pteridine ring and phenyl ring of folic acid at a distance of 3.28 Å.[307,309] As the sparing water-solubility of the aromatic vitamins RF and vitamin K3, which also perform π-stacking in their crystalline state, was overcome using aromatic sodium carboxylates, folic acid's sparingly low solubility in water might be improved by sodium polyphenolates, too, see sections 4.2.1 and 4.1.2.3.[198]

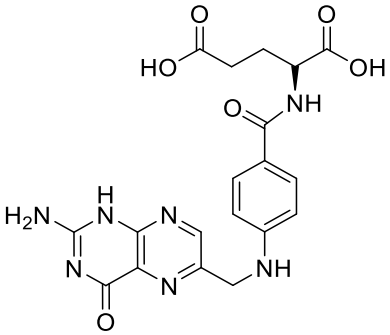

Figure 97: Molecular structure of folic acid

Therefore, the water-solubility of folic acid was determined in presence of three sodium polyphenolates comprising medium, good and very good solubilizing properties regarding the solubilization of RF from section 4.1.2.1.1 and in presence of sodium carboxylates with distinct chain length and conjugation using saturation experiments.

First, the solubility of folic acid in water was determined to be 0.025 ± 0.004 mmol·kg^{-1} (11 ± 2 mg·kg^{-1}). This is in line with the solubility provided by Sigma Aldrich (10 mg·L^{-1} at 0 °C). Comprising pK_a values below 8.38, the deprotonation of the exchangeable groups leads to a high solubility of folic acid in aqueous alkaline solution (50 g·L^{-1} in 1 mol·kg^{-1} NaOH solution).[308,310] To prevent a pH effect on the solubility, the pH value of all solutions before saturation with folic acid was tested with indicator paper to be constantly neutral.

While the samples comprising folic acid in pure water was colorless, saturation of 0.37 mol·kg^{-1} aqueous Na-4-OH-3-OMe-Benz, Na-4-OH-3-OMe-Cinn and Na-3,4-DiOMe-Cinn solutions with folic acid resulted in copigmentation leading to yellow solutions, see Figure 98. Hence, the interactions of sodium polyphenolates with folic acid should be similar to the ones between polyphenolates and RF, RF-PO_4, LC and vitamin K3, see sections 4.1.2.1.1, 4.1.2.2 and 4.1.2.3.

As in the case of RF from section 4.1.2.1.1, only the sodium salt of the polyphenolic acids induced copigmentation, while the polyphenolic acid did neither induce copigmentation nor improve the water-solubility of folic acid, see Figure 98 on the right. Thus, saturation of water comprising 0.37 mol·kg^{-1} ferulic acid – being largely over the solubility of ferulic acid and hoping for mutual solubilization – with folic acid resulted in a colorless solution after filtration. Hence, the sodium salt of polyphenolic acids was required to observe a significant change in the color and increase of the vitamin's solubility.

As in the case of RF-PO_4, 0.37 mol·kg^{-1} solutions of Na-4-OH-3-OMe-Cinn (50 ± 4 mmol·kg^{-1}; molar ratio 7.2) solubilized more folic acid than Na-3,4-DiOMe-Cinn (22 ± 4 mmol·kg^{-1}, molar ratio 17). Na-4-OH-3-OMe-Benz solution solubilized 13.9± 0.3 mmol·kg^{-1} (molar ratio of 26.6). Thus, an elongation of the hydrophobic chain length to Na-4-OH-3-OMe-Cinn increased the solubility further by a factor of 3.6.

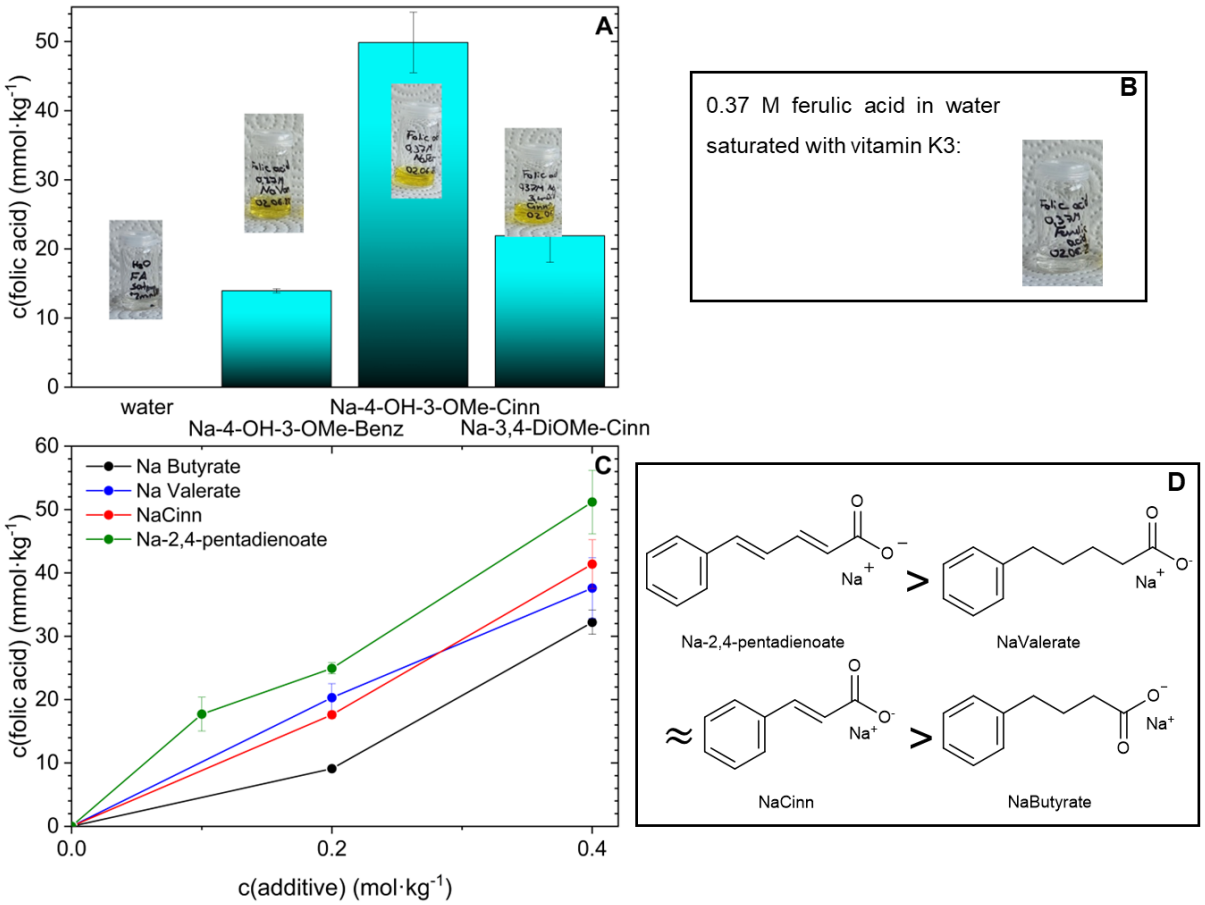

Figure 98: A) Solubility of folic acid in pure water and in aqueous 0.37 mol·kg^{-1} sodium vanillate, ferulate and Na-3,4-DiOMe-Cinn (from left to right) solutions. The solubility in pure water was too low (0.025 ± 0.004 mmol·kg^{-1}), so that the column is not visible. B) Attempt to solubilize folic acid in water comprising 0.37 mol·kg^{-1} ferulic acid. C) Solubility of folic acid in pure water and in aqueous NaButyrate, NaValerate, NaCinn and Na-2,4-Pentaidenoate solutions. D) Solubilization power

To clarify if the solubilization mechanism of folic acid was also strongly dependent on the electronic system of the sodium polyphenolates as in the case of RF, LC and vitamin K3 or if it followed classical solubilization processes from section 4.1.1, the solubility of folic acid was determined in presence of four sodium polyphenolate-related compounds comprising distinct hydrophobic chain lengths and electronic systems, see Figure 98 C. In line with the solubilization curves regarding RF and vitamin K3, the solubility of folic acid increased with increasing concentration of the solubilizer, see section 4.1.2.1.1 and 4.1.2.3.1. Despite of a shorter hydrophobic side chain, NaCinn solubilized significantly more folic acid than NaButyrate. Hence, the more developed conjugation of NaCinn contributed more to the solubilization of folic acid than the increased amphiphilicity of NaButyrate. The importance of the solubilizer's aromatic systems is even more obvious when regarding Na-2,4-Pentadienoate in relation to NaValerate, see Figure 98 C. Though having the same backbone, Na-2,4-Pentadienoate solubilized 23-36 % more folic acid than NaValerate when regarding additive concentrations from 0.2 to 0.4 mol·kg^{-1}.

Nevertheless, the solubility of folic acid increased even more when increasing the hydrophobic chain length from NaButyrate to NaValerate (17-120 %) when regarding additive

concentrations from 0.2 to 0.4 mol·kg^{-1}. Hence, the solubilization process of folic acid depends more on the hydrophobic chain length. NOESY measurements of an aqueous 3 mol·kg^{-1} Na-3,4-DiOMe-Cinn solution saturated with folic acid, revealed several cross-peaks between the protons of folic acid and the polyphenolates, see Figure 99. Hence, folic acid and aromatic sodium carboxylates are at least intermittently maximum 5 Å away from each other in solution, which is the reason for the observation of copigmentation.[249,277–280] However, upon dilution with water, the samples became colorless. Thus, the π-complexation of sodium polyphenolates with folic acid is reversible and only strongly developed at high polyphenolate concentrations.

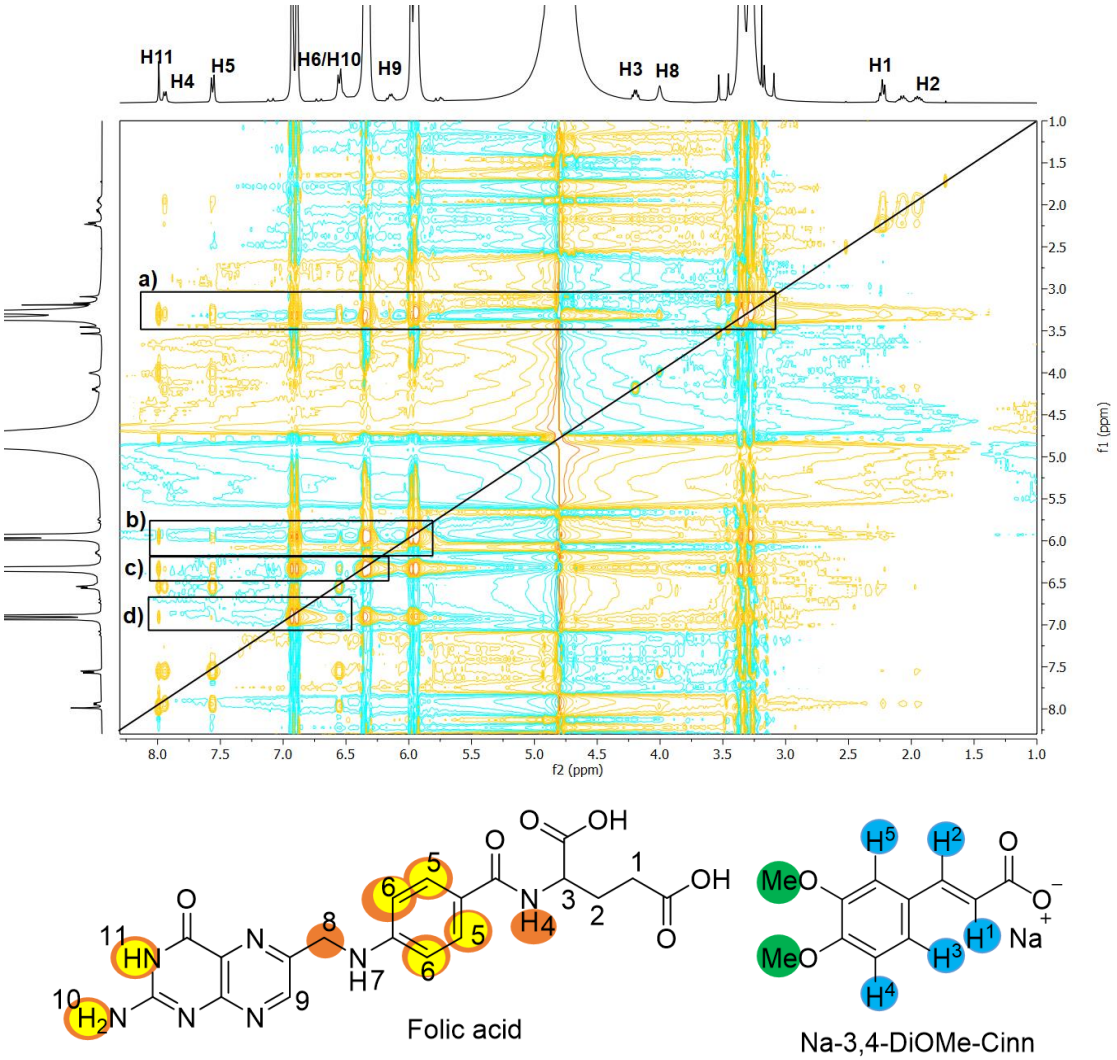

Figure 99: Top: NOESY spectrum of an aqueous 3 mol·kg^{-1} Na-3,4-DiOMe-Cinn solution saturated with folic acid. a) Cross-peaks of methoxy groups of Na-3,4-DiOMe-Cinn with the protons H4, H5, H6, H8, H10 and H11 of folic acid; b) cross-peaks of H1 and H4 of Na-3,4-DiOMe-Cinn with H5, H6, H10 and H11 of folic acid; c) cross-peaks of H3 and H5 of Na-3,4-DiOMe-Cinn with H5, H6, H10 and H11 of folic acid; d) cross-peaks of H2 of Na-3,4-DiOMe-Cinn with H5, H6, H10 and H11 of folic acid. Bottom: The blue marked protons gave rise to cross-peak with yellow marked ones and the green marked protons gave rise to cross-peaks with the orange marked protons. For the ^{1}H-NMR spectrum see Figure A 78 in the Appendix.

Finally, reaching a molar solubilizer to folic acid ratio of 7.2 corresponding to a weight ratio of 3.5, sodium ferulate was the best solubilizing agent for folic acid tested and increased the water-solubility of folic acid by almost 2000 times. Taking into account the photoprotective

effect of caffeic acid, ferulic and p-coumaric acid reported by Wusigale et al., other polyphenolic acids and sodium polyphenolates might constitute not only valuable solubilizing but also photostabilizing antioxidants for folic acid.[306,311]

4.1.2.5 Evaluation of the solubilization of aromatic natural compounds by means of polyphenolates in water

Sodium polyphenolates were revealed as efficient hydrotropes for RF, LC, RF-PO_4, vitamin K3 and folic acid. Solubility curves with RF, vitamin K3 and folic acid revealed an exponential increase of RF's, vitamin K3's and folic acids' water-solubility with the concentration of aromatic sodium carboxylates. Thereby, the solubilization of RF, LC, RF-PO_4, vitamin K3 and folic acid was strongly influenced by the size and type of the electronic π-system of the solubilizer.

Despite a similar order of the solubilization power of sodium polyphenolates for the solubilization of RF, LC, vitamin K3 and folic acid in water, the extent to which the bio-compounds' solubilization depended on the electronic configuration of the solubilizer differed. Thus, the introduction of a complete conjugation on NaValerate (NaValerate →Na-2,4-Pentadienoate) increased RF's solubility by 936-1852 %, vitamin K3's solubility by 210 % and the solubility of folic acid only by 23-36 %. Still, polyphenolates increased the water-solubility of folic acid ca. 10 times more than the one of RF and vitamin K3, although folic acid was the least soluble compound out of the three vitamins, see Figure 100. Thus, sodium ferulate applied at 0.37 $mol \cdot kg^{-1}$ increased the solubility of vitamin K3 28-fold, the one of RF 220-fold and the one of folic acid 2000-fold.

An elongation of the hydrophobic chain from sodium 4-phenylbutyrate to sodium 5-phenylvalerate improved the solubility of vitamin K3 by 70-160 % and the one of folic acid by 17-120 %, while RF was least affected by the elongation (28-29 %). Thus, the solubility of folic acid can be modified more when increasing the hydrophobic chain length, while the solubility of RF and vitamin K3 was increased more with increasing size of the conjugated electronic system of the solubilizer, see Figure 100. As sodium polyphenolates exerted salting-in properties on the basis of their amphiphilicity (section 4.1.1), aggregation of polyphenolates around folic acid was assumed at first. However, often more amphiphilic compounds turned out as worse solubilizers, see section 4.1.2.1.1. Sterics could not be either the reason for the huge effect of polyphenolates on folic acid's water-solubility, as folic acid is bulkier than RF and vitamin K3. Solubilization experiments with RF, LC and RF-PO_4 showed that sterically more demanding substitutents weaken the solubilizing power of polyphenolates, see section 4.1.2.2. In the end, the reason for the stronger effect of aromatic solubilizers on folic acid than on RF or vitamin K3 could not be revealed.

In the case of RF, LC and RF-PO_4, the presence of larger aggregates was denied via DLS and surface tension measurements. Instead, reversible copigmentation upon dilution with water

was observed for RF, RF-PO_4, LC, vitamin K3 and folic acid when being dissolved in concentrated aqueous aromatic sodium carboxylate solutions. The copigmentation phenomenon might originate from HOMO-LUMO interactions of the sodium polyphenolates, constituting electron-rich π-donors, and RF, LC, RF-PO_4, vitamin K3 and folic acid, which would be then π-acceptors due to the presence of keto groups and/or a pyrimidine rings.[296,312] Researchers claim that HOMO-LUMO interactions are only important for the absorption of light and not for the stability of π-complexes in the ground state. Thus, the reason for the electron dependent solubilizing mechanism are rather optimized dispersion forces due to the enlarged interaction surface of the planar aromatic molecules and maybe an increase of the water entropy. Moreover, attractive electrostatic interactions between the aromatic rings due to a quadrupole moment on the aromatic rings might also contribute to the copigmentation and to the increase in solubility, see Figure 3 in section 2.5.[54] In any case, π-complexation of aromatic sodium carboxylates with RF, vitamin K3 and folic acid was confirmed via the strong dependence of the biocompounds' water-solubility on the size and type of the solubilizer's π-system and via NMR measurements, see sections 4.1.2.1.1, 4.1.2.1.7, 4.1.2.3 and 4.1.2.4. The (i) reversibility of the copigmentation upon dilution, (ii) the absence of copigmentation for low polyphenolate and vitamin concentrations, (iii) the absence of a change in surface tension of polyphenolate solutions upon saturation with RF, (iv) the weak shift of the chemical shift in NMR and (v) the failure to generate cocrystals of RF with sodium polyphenolates indicated weak and dynamic interaction between the aromatic solute and aromatic sodium carboxylates. Further, the photostabilization of RF by sodium polyphenolates in the diluted and even more in the concentrated aqueous polyphenolate solutions, proved that the strong hydrotropic solubilizing power of polyphenolates via complexation can coexist with their photostabilizing properties. Thus, the conversion of polyphenolic acids to the sodium salts did not prevent their action as radical scavengers. Consequently, more than 90 % of the absorbance at RF's absorption maximum and > 84 % of RF could be preserved for 8 weeks using concentrated ($\geq$ 370 mM) aqueous solutions of sodium 3,4-dimethoxycinnamate, vanillate and ferulate.

Regarding additionally the antioxidant properties of polyphenolic acids, sodium polyphenolates can be seen as multifunctional hydrotropic solubilizing agents.[84]

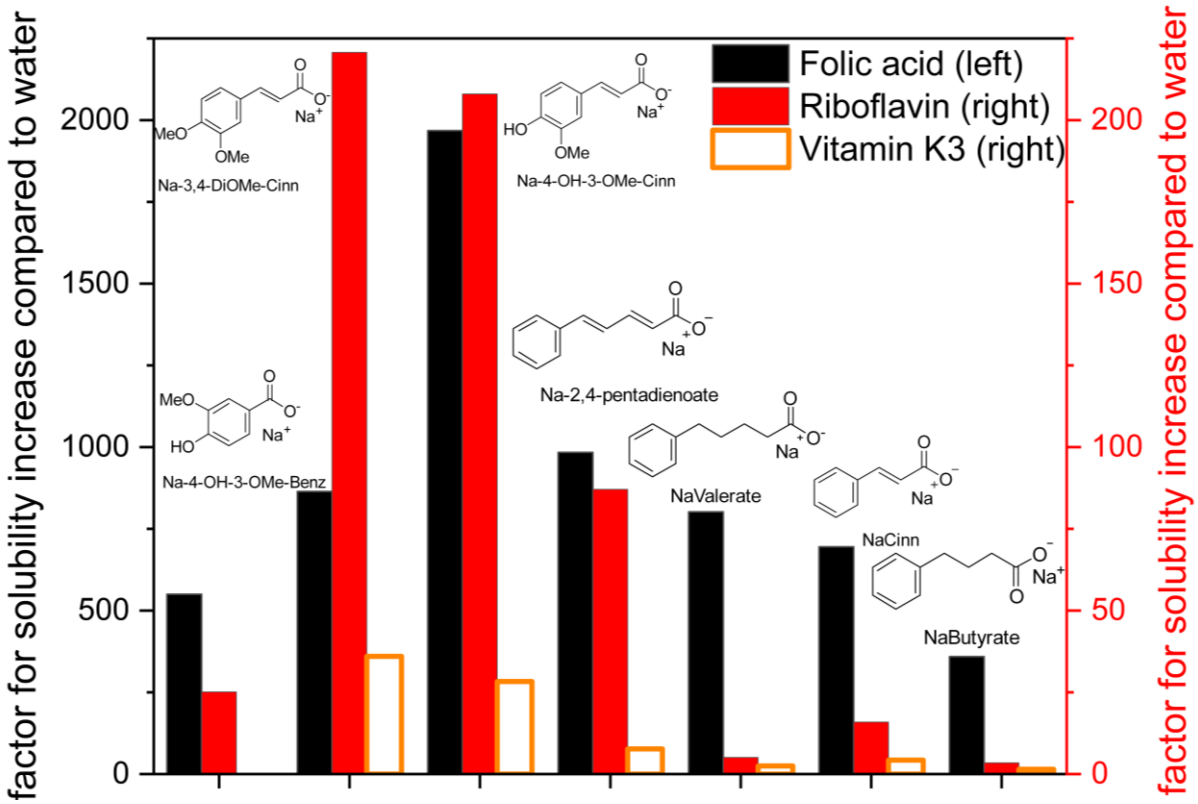

Figure 100: Factor for the increase of the water-solubility of folic acid, riboflavin and vitamin K3 in presence of 0.37 mol·kg^{-1} of Na-4-OH-3-OMe-Benz, Na-3,4-DiOMe-Cinn and Na-4-OH-3-OMe-Cinn and in presence of 0.2 mol·kg^{-1} of the residual aromatic sodium carboxylate in the diagram.

Further, the aromatic drug caffeine is well known for π-stacked aggregation, see Figure 101. However, aggregation of this aromatic drug is supposed to limit its bioavailability and is therefore subject of current research.[313] An increased solubility of a drug might increase the probability for absorption. As aromatic sodium carboxylates managed to improve the water-solubility RF, RF-PO_4, LC, vitamin K3 and folic acid, which also stack in their crystalline form, they were thought to improve the solubility of caffeine, too. Thus, quantitative ^{1}H-NMR analysis was used to see, if sodium polyphenolates could be used as solubilizers for caffeine, too. Indeed, the water-solubility of caffeine (0.106 mol·kg^{-1}) could be enhanced to 0.551 mol·kg^{-1} and 741 ± 21 mmol·kg^{-1} using 0.37 mol·kg^{-1} Na-4-OH-3-OMe-Benz and Na-4-OH-3-OMe-Cinn, respectively, see section 7.11.12 for the NMR spectrum. Contrary to RF, RF-PO_4, LC, vitamin K3 and folic acid, copigmentation was not observed in the case of caffeine. This might be due to the smaller aromatic moiety. In any case, the shielding of caffeine's protons by sodium ferulate and vanillate proved a significant interaction, which is certainly the reason for the enhancement of caffein's water-solubility, see Figure A 79 in section 7.11.12.

As the water-solubility of partially water-soluble aromatic drugs was greatly enhanced by sodium polyphenolates, polyphenolates might also act on the solubility of the blue pigment indigo, which is widely known for its insolubility in water and in most common organic solvents due to π-stacked aggregation, see Figure 101.[314] However, the pigment could not be dissolved in aqueous sodium polyphenolate solutions (0.37 M Na-4-OH-3-OMe-Cinn; 3 M Na-3,4-

DiOMe-Cinn). Hence, even after stirring for several days, the solution did not exhibit even a minor blue touch. Probably, the large aromatic system of indigo was too large and thus the Van-der-Waals interactions between two indigo molecules are far beyond Van-der-Waals interactions of indigo and aromatic sodium polyphenolates. Moreover, the hydrophobicity of indigo might additionally contribute to the failure of sodium polyphenolates in its solubilization.

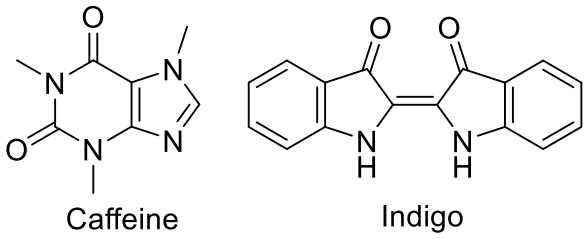

Figure 101: Molecular structure of caffeine and indigo

Therefore, a brief experiment was performed with the water-insoluble curcumin, which is a hydrophobic colorant and was supposed be less planar than indigo – at least in its keto-form. An aqueous solution comprising 3.00 $mol \cdot kg^{-1}$ Na-3,4-DiOMe-Cinn was saturated with curcumin. As curcumin is not soluble in water, the sample should be uncolored, if no curcumin was dissolved, while it should be orange in the case of a solubilization of curcumin by the polyphenolate. Na-3,4-DiOMe-Cinn managed the solubilization of the hydrophobic natural colorant curcumin in water, see Figure 102. Although curcumin was not quantified due to time reasons, the intensification of the sample's orange color upon longer stirring showed that curcumin's solubilization is apparently retarded compared to the solubilization of the more hydrophilic RF, vitamin K3, folic acid and caffeine, where the maximum solubility was reached already after one hour of stirring when using ultrasonication. Because the curcumin content was so low that a dilution of the samples with water by the factor >1:10 resulted in a very pale coloration, polyphenolates might rather be used a cosolubilizers for curcumin in aqueous food formulations, see section 4.1.3. As curcumin could be still dissolved in water using Na-3,4-DiOMe-Cinn, the reason for the failure in solubilizing indigo is probably its strong stacking with other indigo molecules and not its hydrophobicity.

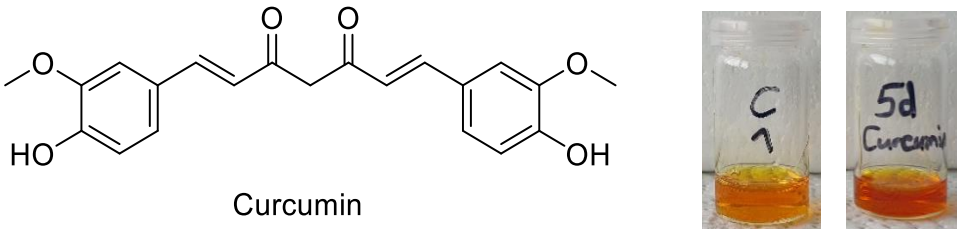

Figure 102: Molecular structure of curcumin and aqueous 3 M Na-3,4-DiOMe-Cinn solution saturated with curcumin. Left: 2 h; right: 5 days stirring.

Regarding Figure 100 above, sodium ferulate appears as the best solubilizing agent, if mixtures of RF, vitamin K3 and folic acid are desired. As this polyphenolate increased also the solubility of caffeine by a factor of 7, the compatibility of the four pharmaceutically important

drugs RF, vitamin K3, folic acid and caffeine was tested. It also was of interest to see, if polyphenolates can solubilize several solutes simultaneously via a similar mechanism. As all solutes are aromatic and because the solubilization of RF, vitamin K3 and folic acid was considerably influenced by the size and type of the solubilizer's conjugated π-system, a competition of the four drugs for sodium ferulate and thus a decrease of the drugs' solubility relatively to the pure sodium ferulate solution was expected. Therefore, a 0.37 mol·kg^{-1} aqueous sodium ferulate solution was saturated with caffeine, vitamin K3, folic acid and RF, whose solubility was then determined via quantitative NMR analysis, see Figure 103. The corresponding NMR spectra are given in section 7.11.13 in the Appendix.

As seen in the previous sections, 0.37 mol·kg^{-1} sodium ferulate improved the water-solubility of RF, caffeine, vitamin K3 and folic acid by a factor of 220, 7, 28 and 2000, respectively, see Figure 103. Matching up with the expectation, RF's solubility in the aqueous sodium ferulate solution was decreased by vitamin K3, folic acid and caffeine, Figure 103 A. Thereby, vitamin K3 reduced the solubility of RF least, while caffeine reduced RF's solubility most by a factor of 4. Moreover, all mixtures comprising caffeine exhibited the lowest RF content of 15-18 mmol·kg^{-1}.

Contrary to the expectation, the solubility of caffeine in the aqueous 0.37 mol·kg^{-1} sodium ferulate solution was not altered by the presence of RF and folic acid alone, see Figure 103 B. Yet, if vitamin K3 was added, the solubility of caffeine in the 0.37 mol·kg^{-1} sodium ferulate solution was increased, see Figure 103 B. The mixture comprising all four drugs resulted in the highest solubility of caffeine content (860 ± 10 mmol·kg^{-1}).

In line with the hydrotropic effect of vitamin K3 on caffeine, vitamin K3's solubility in the 0.37 mol·kg^{-1} sodium ferulate solution was only increased in the presence of caffeine, regardless of whether RF and folic acid were present in the mixture, see Figure 103 C. Thereby, in the absence of caffeine, RF and folic acid had no effect on the water-solubility of vitamin K3 in the sodium ferulate solution. Nevertheless, RF and folic acid promoted the solubility of vitamin K3 in the sodium ferulate solution further in the presence of caffeine. Thus, caffeine alone doubled the solubility of vitamin K3 (41 ± 3 mmol·kg^{-1}), while folic acid with caffeine, RF with caffeine, and folic acid together with RF and caffeine increased the solubility of vitamin K3 in the 0.37 mol·kg^{-1} sodium ferulate solution up to 50 mmol·kg^{-1}, see Figure 103 C.

Similar to caffeine, the solubility of folic acid in the 0.37 mol·kg^{-1} sodium ferulate solution was improved by the presence of vitamin K3, see Figure 103 D. Yet, although RF and caffeine alone had no effect on the solubility of folic acid, the presence of RF and/or caffeine reduced the solubility of folic acid in the sodium ferulate solution even in presence of vitamin K3. Nevertheless, 41.5 ± 5.5 mmol·kg^{-1} folic acid could be dissolved in a mixture comprising all four drugs, see Figure 103 D.

Although the solubility of RF and folic acid in an aqueous 0.37 mol·kg^{-1} sodium ferulate solution was reduced in the presence of caffeine, vitamin K3 and folic acid or RF, respectively, > 60 times RF and > 1660 times folic acid were dissolved in the aqueous sodium ferulate mixtures comprising RF, caffeine, vitamin K3 and folic acid than in pure water, see Figure 103 A-D. In the same sodium ferulate solution comprising the four drugs, the solubility of caffeine and vitamin K3 was 16 % (= 8 times water-solubility) and 179 % (= 78 times water-solubility) higher than in the sodium ferulate solution without other drugs, respectively.

As the total amount of the solubilized solutes (= total solute content in the 0.37 mol·kg^{-1} sodium ferulate solution comprising all four drugs subtracted by the solubility of all solutes in pure water) accounts for 865 mmol·kg^{-1}, less than 0.5 sodium ferulate molecules are required to solubilize one solute in the multi-drug solution. The low sodium ferulate content compared to the number of solute molecules indicates that sodium ferulate cannot surround the solutes, but must interact directly with the molecules. Further, summing up the solubility of each drug dissolved separately in the sodium ferulate solution, the combination of the four drugs in the sodium ferulate solution allowed solubilizing 100 mM more solutes in total. Thus, the combination of the drugs induced a synergistic effect on the total number of solute molecules in the 0.37 mol·kg^{-1} sodium ferulate solution.

Apparently, vitamin K3 was most compatible with other drugs, as it decreased the solubility of RF in an aqueous 0.37 mol·kg^{-1} sodium ferulate solution only by 15 %, and increased the solubility of folic acid and caffeine in an aqueous 0.37 mol·kg^{-1} sodium ferulate. In general, vitamin K3 and caffeine seemed to promote each other's solubility in the sodium ferulate solution. In the case of caffeine, this was not surprising, as caffeine was already postulated to have a hydrotropic potential.[315] However, this result goes further, as a mutual hydrotropy of vitamin K3 and caffeine was observed. The improvement of vitamin K3's and caffeine's water-solubility by the presence of caffeine and vitamin K3, respectively, can originate from facilitated hydrotropy or from a complexation of the two solutes. To know if sodium ferulate is required for the mutual increase of the water-solubility of caffeine and vitamin K3, the solubility of vitamin K3 and caffeine in pure water (saturation) was determined via ^{1}H-NMR analysis, see Figure A 91 in section 7.11.13. The water-solubility of caffeine was increased 1.2 times by the presence of vitamin K3 (pure water: 106 mmol·kg^{-1}; water + vitamin K3: 126 ± 3 mmol·kg^{-1}). Caffeine itself increased also the water-solubility of vitamin K3 by a factor of 10.5 (pure water: 0.68 ± 0.03 mmol·kg^{-1}; water + caffeine: 7.1 ± 0.1 mmol·kg^{-1}). Thus, in pure water, vitamin K3 and caffeine solubilized each other. Moreover, the solution exhibited a yellow coloration, while caffeine or vitamin K3 alone in pure water were colorless. Thus, complexation is probably the reason for the mutual increase of the two drugs' solubility in aqueous solution.

Yet, if 0.37 mol·kg^{-1} sodium ferulate was present in the solution, the solubility of caffeine and vitamin K3 was even further increased. Thus, caffeine and vitamin K3 promoted each other's water-solubility in the absence and in the presence of sodium ferulate, but sodium ferulate

enabled a better solubility of the two solutes, which acted as solubilizer for one another. Hence, vitamin K3 and caffeine did not promote the hydrotropic power of sodium ferulate. Instead, the two solutes dissolved each other in solution, each solute being the hydrotrope of the other and being dissolved additionally by sodium ferulate. This phenomenon, when the hydrotropic action is improved by an additive, is called facilitated hydrotropy. The origin of the effect here is that sodium ferulate solubilized vitamin K3 and caffeine, which then solubilized even more caffeine and vitamin K3, respectively.

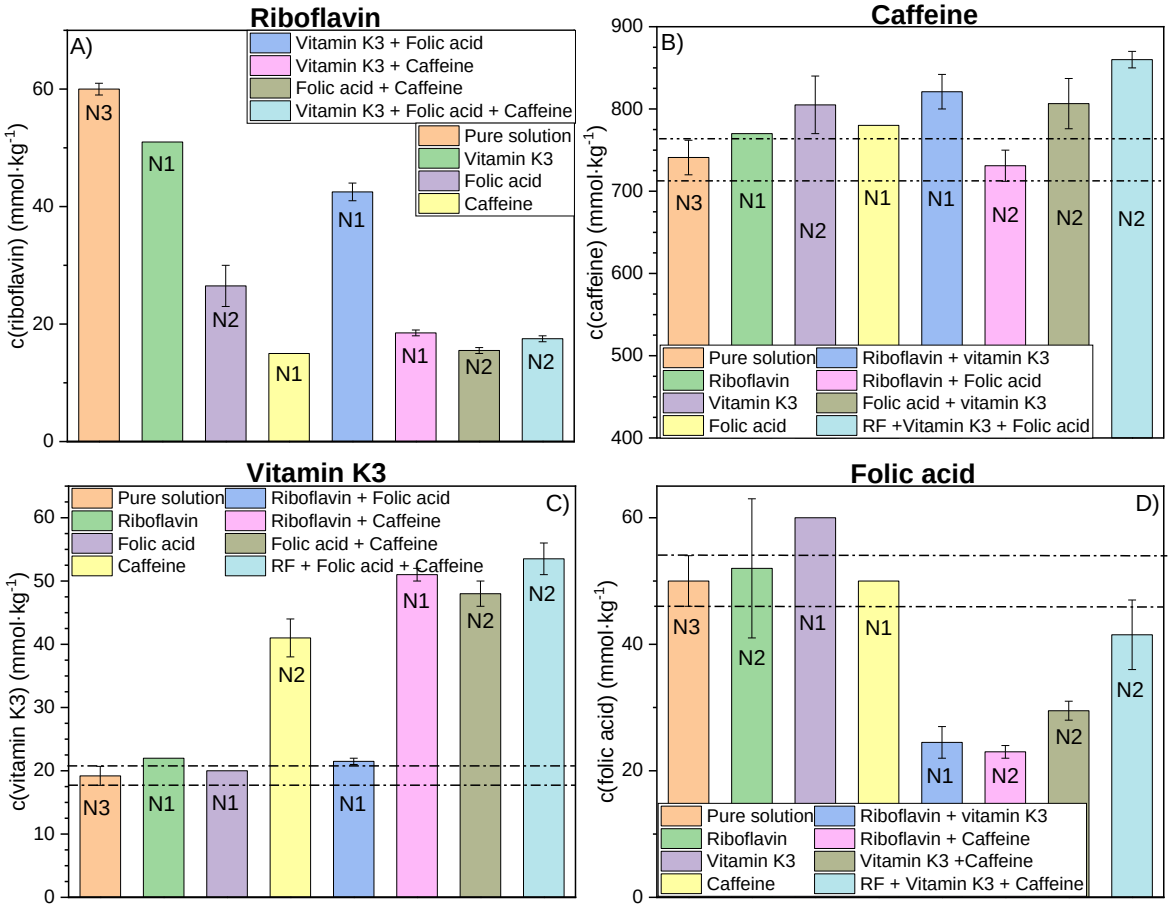

Figure 103: Water-solubility of riboflavin (A), caffeine (B), vitamin K3 (C) and folic acid (D) in a 0.37 mol·kg^{-1} sodium ferulate solution and in a 0.37 mol·kg^{-1} sodium ferulate solution saturated with other aromatic drugs. Solubility in pure water: riboflavin: 0.27 ± 0.02 mol·kg^{-1}; vitamin K3: 0.68 ± 0.03 mmol·kg^{-1}; folic acid: 0.025 ± 0.004 mmol·kg^{-1}; caffeine 106 mmol·kg^{-1}; N = number of experiments.

Further, reversible copigmentation was still present and thus stacking interactions between RF, folic acid and vitamin K3 with sodium ferulate still occurred, if applied in mixtures with other aromatic drugs, see Figure 104. The less intense coloration of the samples comprising RF in presence of the other drugs compared to the sample in absence of other drugs is in line with the decreased RF content from Figure 103 A. Hence, the interactions of sodium ferulate with RF, vitamin K3, folic acid and caffeine are probably similar to the ones in the sodium ferulate solution without other drugs.

Regardless the solubilizing mechanism, RF, vitamin K3, caffeine and folic acid could be solubilized in an aqueous 0.37 mol·kg^{-1} sodium ferulate solution alone and in combination with each other. As sodium polyphenolates were found to solubilize several aromatic biocompounds, they might constitute also an important role as biochemical solubilizers in animals and plants.

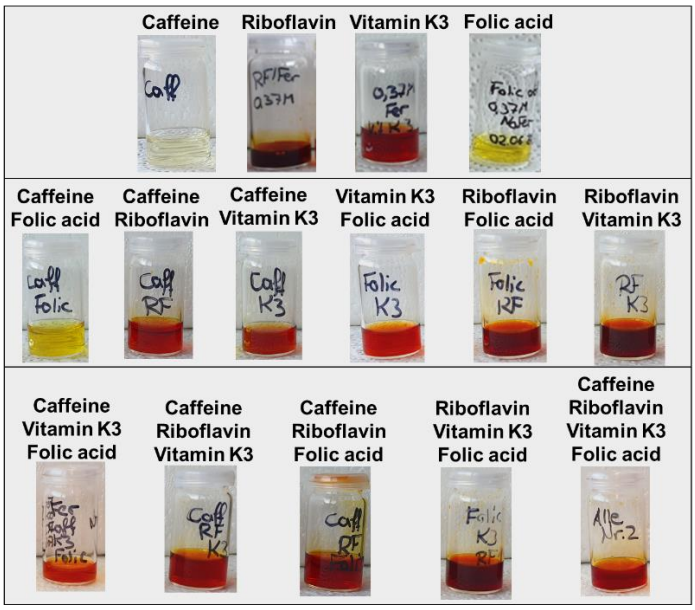

Figure 104: Color of a 0.37 mol·kg^{-1} sodium ferulate solution saturated with caffeine, riboflavin, vitamin K3 and folic acid alone or in combination. Upon dilution with water, the samples comprising RF became yellow and the residual ones became colorless.

4.1.3 Sodium ferulate as potential cosurfactant and π-complexer

In the previous two sections, aromatic sodium carboxylates were exposed to act as hydrotropic solubilizers based on their amphiphilicity or based on their conjugated electronic π-system. As even the hydrophobic curcumin could be dragged into an aqueous solution, a cosurfactive behavior of polyphenolates was assumed. To test, if polyphenolates may also act as cosurfactants, aqueous solutions comprising sodium ferulate and the standard surfactant SDS or the biological dispersant sodium cholate were saturated with a hydrophobic solute. Sodium ferulate was chosen, because this polyphenolate turned out as the best compromise, regarding the increase in solubility of RF, vitamin K3 and folic acid in Figure 100 above. To simplify the detection, the hydrophobic solute was chosen to be Sudan blue II, so that UV-Vis absorbance of the dye could be used for quantification. Further, the compatibility of the hydrophobic and water-insoluble Sudan blue II with RF, which underwent a distinct solubilization mechanism, in surfactant/sodium ferulate systems was tested to know if two solutes of a distinct polarity are compatible.

4.1.3.1 Cosurfactive promotion of the micellization of sodium dodecyl sulfate by sodium ferulate

While Sudan blue II was not water-soluble at all, the solubility of this hydrophobic dye increased with the concentration of SDS, see Figure 105 left and on the right A. When regarding Figure 105 on the right C, the CMC of SDS can be seen as the onset of the solubilization, because a very subtle blue coloration could be observed. Consequently, micellization of SDS is required to solubilize Sudan blue II. As DLS and surface tension measurements did not reveal significant structuring affinity of aromatic sodium carboxylates in aqueous solutions (section 4.1.1.2), the hydrophobicity of the Sudan blue II was presumably the reason why sodium ferulate alone could not solubilize Sudan blue II, see Figure 105 on the right B. However, the observation of a more intense blue coloration in the aqueous sample comprising SDS at its CMC and 0.37 mol·kg^{-1} sodium ferulate, indicated a decrease of the surfactant's CMC by sodium ferulate and hence cosurfactive action of ferulate.

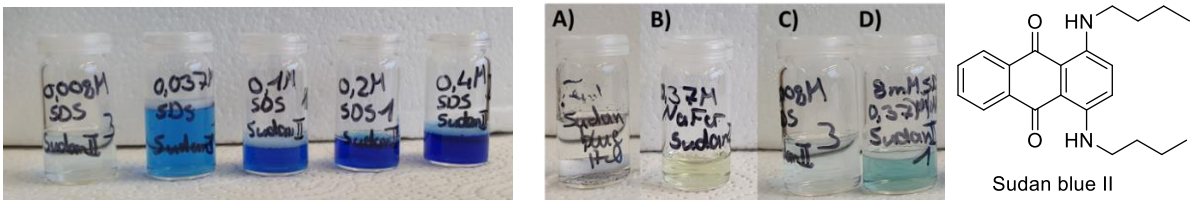

Figure 105: ***Left:*** *SDS solutions saturated with Sudan blue II (from left to right: 8 mmol·kg^{-1}, 37 mmol·kg^{-1}, 0.1 mmol·kg^{-1}, 0.2 mmol·kg^{-1} and 0.4 mmol·kg^{-1});* ***Middle:*** *Solutions saturated with Sudan blue II: A) pure water, B) aqueous 0.37 mmol·kg^{-1} sodium ferulate solution, C) aqueous 8 mmol·kg^{-1} SDS solution. D) aqueous sample containing 8 mmol·kg^{-1}SDS and 0.37 mmol·kg^{-1} sodium ferulate.* ***Right:*** *Molecular structure of Sudan blue II.*

On account of this, one might wonder if the π-system driven solubilization of aromatic solutes from section 4.1.2, competes with the cosurfactive action of sodium ferulate. Therefore, in the following, the solubility of Sudan blue II was measured in aqueous solutions comprising SDS, and SDS/sodium ferulate mixtures in absence and presence of RF via UV-Vis-spectroscopy. Simultaneously, the solubility of RF in these solutions was determined. The concentration of sodium ferulate was kept at 0.37 mol·kg^{-1} in mixtures with SDS, see Figure 106.

As already known from section 4.1.2.1.1, SDS increased the water-solubility of RF in a non-linear way, see Figure 106 blue curve. Although Sudan blue II alone did not alter the water-solubility of RF due to Sudan's insolubility in water, the hydrophobic dye increased the solubility of RF in aqueous SDS solutions more strongly than SDS alone, see Figure 106 yellow and bright blue curve. A reason for this synergistic effect of Sudan blue II and SDS might be the aromaticity and thus planarity of Sudan blue II, which might lead to attractive interactions of Sudan blue II with RF and facilitate RF's enclosure into SDS micelles.

However, SDS lowered the water-solubility of RF in solutions comprising 0.37 mol·kg^{-1} sodium ferulate, see Figure 106 red and black curve. Interestingly, the reduction of RF's solubility in ferulate/SDS systems occurred between the CMC and 37 mmol·kg^{-1} of SDS and the solubility of RF was not further reduced for higher concentrations of SDS. Thus, in ferulate/SDS/RF

solutions, a certain number of ferulate molecules seems to support the micellization of SDS by filling up the empty places in the micelles.

Saturation with Sudan blue II in 0.37 mol·kg^{-1} sodium ferulate solutions reduced the solubility of RF more strongly with increasing SDS concentration than SDS alone in a sodium ferulate solution, see Figure 106 black curves. Consequently, Sudan blue II either competes with RF for sodium ferulate or it promotes the implementation of sodium ferulate in the micellization of SDS.

Regarding now Figure 106 B, SDS increased the solubility of Sudan blue II linearly. Sodium ferulate and/or RF alone were not able to solubilize Sudan blue II. Yet, in presence of SDS, sodium ferulate increased the solubility of Sudan. Interestingly, RF alone and RF in combination with sodium ferulate improved the solubility of Sudan blue II in SDS comprising solutions even further. As the curves “SDS + RF” and “SDS + 0.37 M NaFer + RF” are equal, RF – and not sodium ferulate – seems to dominate in the synergistic interaction with SDS, see Figure 106.

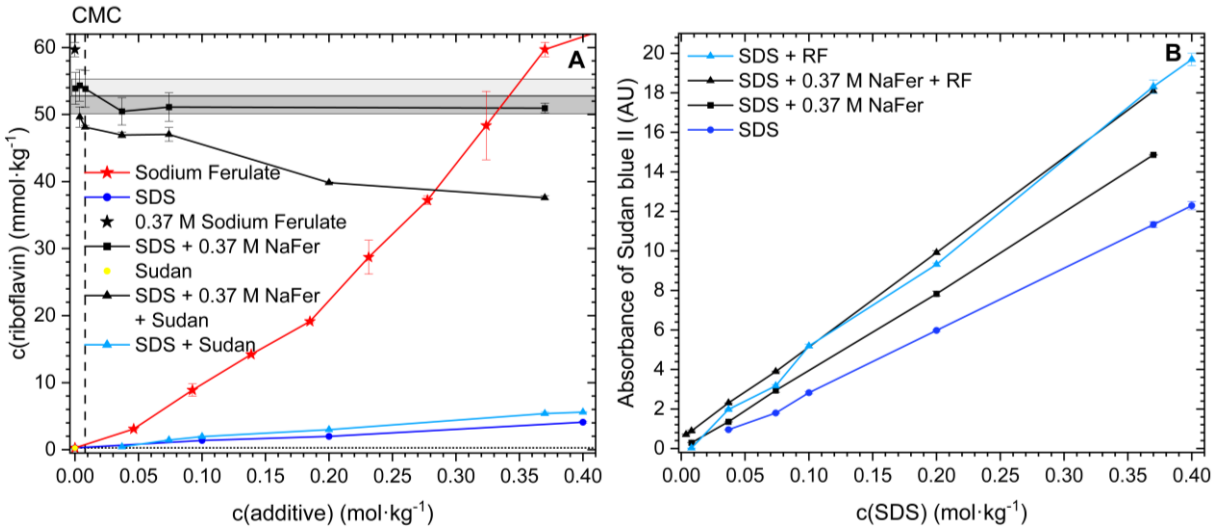

Figure 106: Solubility of A) RF and B) Sudan blue II in aqueous solutions of sodium dodecyl sulfate and sodium ferulate (NaFer) in absence and presence of Sudan blue II and RF, respectively. Yellow point: Water saturated with RF and Sudan blue II. All samples were saturated with RF and/or Sudan blue II.

To get further insight into the solubilization mechanism, DLS and conductivity measurements of aqueous 0.37 mol·kg^{-1} sodium ferulate solutions with or without SDS in the absence and presence of RF (saturation) were performed. Since Sudan blue II absorbs at the same wavelength, where the DLS laser operates, it was not possible to record DLS correlation functions in presence of Sudan blue II. DLS correlation functions of aqueous solutions comprising either 0.37 mol·kg^{-1} sodium ferulate and/or 0.37 mol·kg^{-1} SDS in absence and in presence of RF are displayed in Figure 107. At 0.37 mol·kg^{-1}, sodium ferulate did not exhibit a significant structuring potential, while SDS induced structuring. RF did not alter the correlation functions of pure sodium ferulate or pure SDS solutions. Yet, the presence of sodium ferulate in an aqueous SDS solution induced a doubling of the correlation compared to pure SDS in water, which is in line with the higher solubility of Sudan blue II in sodium ferulate/SDS mixtures

compared to pure SDS solutions. However, saturation of an aqueous solution comprising 0.37 M sodium ferulate and 0.37 M SDS with RF resulted in a regain of the correlation function as in the absence of sodium ferulate. Thus, RF acted as anti-structuring agent in aqueous sodium ferulate/SDS solutions. This is in agreement to the reduction of RF's water-solubility in presence of sodium ferulate by SDS and shows the competition of RF and SDS for sodium ferulate from Figure 106.

Also, in conformity to the structure reducing power of RF, sodium ferulate did not induce a better solubilization of Sudan blue II compared to the sample comprising only RF and SDS saturated with the Sudan blue II from Figure 106. Yet, the structure deteriorating effect and passivity of RF on the structuring potential of SDS and sodium ferulate contradicts the observation of an increased solubility of Sudan blue II in presence of RF in aqueous solutions comprising SDS, see the curves "SDS" and "SDS + RF" in Figure 106. As the hydrophobic dye is aromatic, π- and dispersive interactions of the dye with RF might be a reason for this effect.

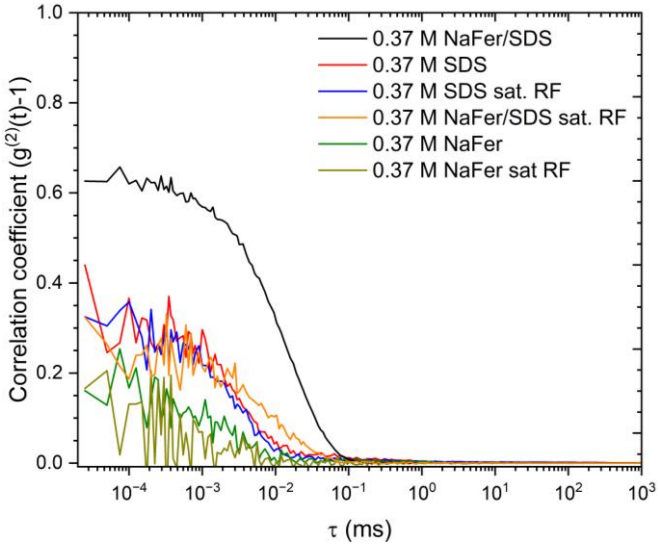

Figure 107: DLS correlation functions of aqueous sodium ferulate and sodium dodecyl sulfate solutions in absence and presence of RF (saturation).

Further, conductivity measurements showed that the presence of RF induced a slight decrease of the absolute conductivity of aqueous solutions comprising sodium ferulate (NaFer + RF, NaFer + SDS + RF, NaFer+ SDS + RF + Sudan), while RF did not alter the conductivity of solutions comprising SDS in absence of sodium ferulate, see Figure 108 A. It can be assumed that the complexation of RF and sodium ferulate retards the propagation of sodium ferulate through the solution. Thus, if RF has the choice between sodium ferulate and SDS, RF interacts rather with sodium ferulate than with SDS. Consequently, RF is associated with sodium ferulate, as seen in section 4.1.2.1. Moreover, the very weak decrease of the absolute conductivity of sodium ferulate by RF indicates the formation of very small aggregates, which is in line with the absence of larger structures of sodium ferulate and RF by DLS, surface tension and SAXS from section 4.1.2.1.5. Moreover, with decreasing concentration, the reduction of the conductivity of solutions comprising sodium ferulate by RF becomes smaller,

see Figure 108 A and B. This emphasizes once more the weak and reversible interactions of RF and sodium ferulate proposed in section 4.1.2.1.10.

In contrast to RF, Sudan blue II had no impact on the absolute conductivity at all, which originates probably also from the dye`s poor solubility in water even in presence of SDS and sodium ferulate.

The CAC of sodium ferulate and the CMC of SDS were determined via the intersect of the linear parts of the curves in Figure 108 A and B. As surfactants form more defined aggregates than hydrotropes, the CMC of SDS was clearly visible as a crinkle, while the CAC of sodium ferulate was indicated by a curved section in the conductivity curve. Consequently, the CMC of SDS could be determined more precisely than the CAC of sodium ferulate, see Figure 108 C and D.

While the CMC of SDS was significantly reduced by sodium ferulate, the CAC of ferulate seemed to be slightly elevated even though not significantly by SDS, see Figure 108 C and D. This originates most probably from the participation of sodium ferulate to the micellization of SDS and is in line with the increased solubility of Sudan blue II and with the increased structuring in sodium ferulate/SDS mixtures seen via DLS. As the participation of sodium ferulate in the micellization of SDS means a lower availability of sodium ferulate for RF, the presence of SDS caused a dropdown of RF’s solubility in aqueous sodium ferulate solutions.

Further, Sudan blue II and RF had no impact on the CMC of SDS, but increased the CMC of SDS in the SDS/sodium ferulate mixture slightly, see Figure 108 C and D. Simultaneously, the CAC of sodium ferulate in presence of SDS was significantly increased by RF, Sudan blue II, and by the combination of the two colorants. Regarding the complexation of RF and sodium ferulate and the absence of an aggregative solubilization of RF by ferulate, an increase of the CMC of SDS due to RF is not surprising. However, the hydrophobic dye, Sudan blue II, seems to prevent the interaction of SDS with sodium ferulate, too. As RF and Sudan blue II did not alter the CMC of SDS in the absence of sodium ferulate and because the copigmentation of sodium ferulate with RF was not influenced by SDS, the increased CAC of sodium ferulate originates probably from complexation of RF and/or Sudan with sodium ferulate. Nevertheless, because Sudan blue II was not solubilized in a pure sodium ferulate solution and because Sudan blue II was only soluble above the CMC in aqueous SDS in absence of ferulate, one can assume that the hydrophobic solute is primarily dissolved in micelles of SDS or in mixed SDS/ferulate micelles. Finally, a reddish color was observed for the samples comprising RF, sodium ferulate and SDS together. Thus, despite the competition of RF and SDS for sodium ferulate, RF and sodium ferulate interacted on a molecular scale via complexation. Consequently, sodium ferulate can act as cosurfactant and hydrotropic complexing agent simultaneously.

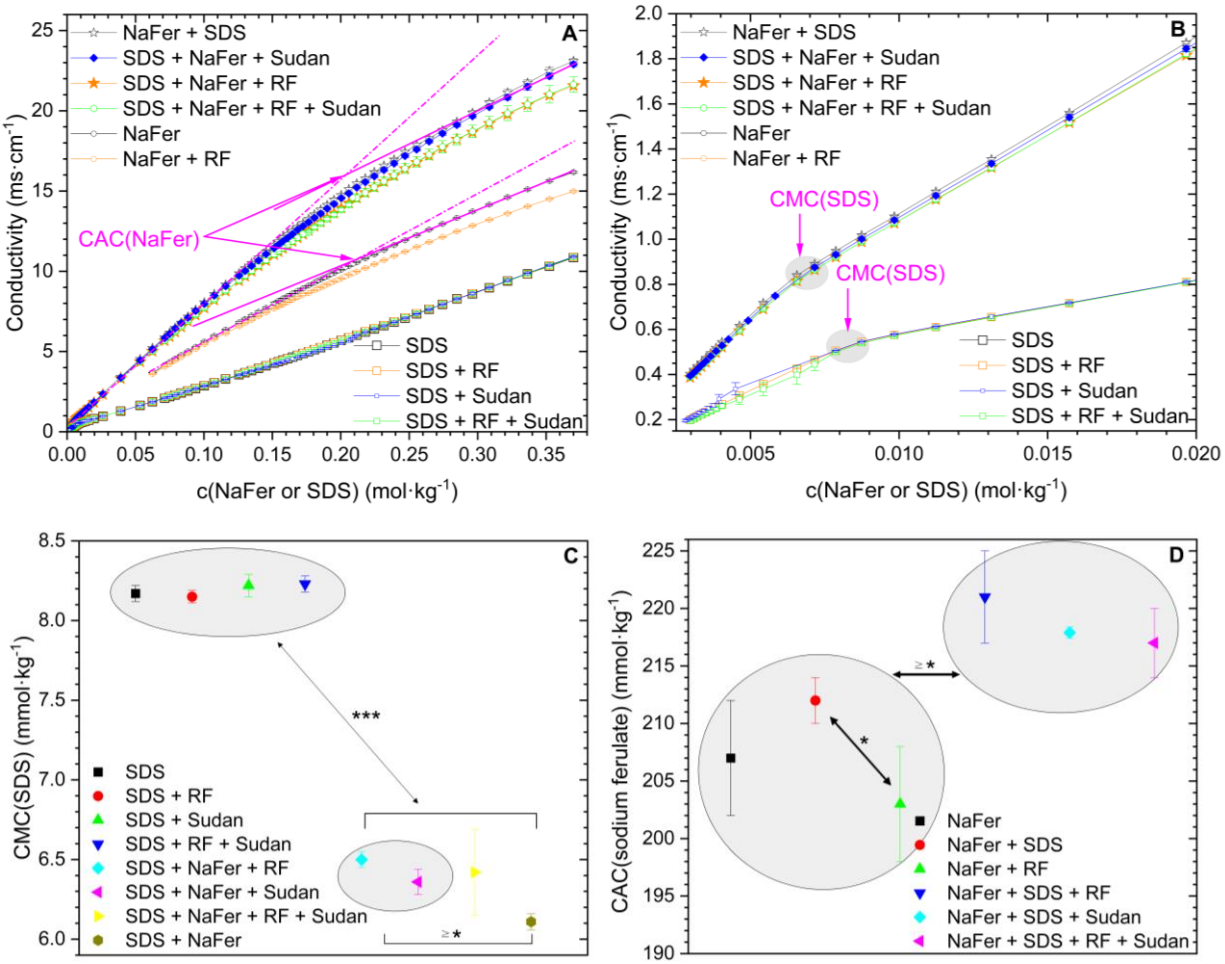

*Figure 108: A) and B) Entire and enlarged view of the conductivity, respectively; C) and D) Critical micellar concentration of SDS and critical aggregate concentration of sodium ferulate, respectively, in aqueous solutions comprising sodium ferulate and/or SDS in presence and absence of RF and/or Sudan blue II for a molar ratio of ferulate/SDS of one. The RF and Sudan blue II content is different for each sample, as the samples were saturated with the two colorants to see a maximum effect. The determination of the CAC and CMC is represented in pink in A and B. (pairwise t-test: * = $p \leq 0.05$; *** = $p \leq 0.001$; triplicates)*

4.1.3.2 Action of sodium ferulate on the solubilizing and structuring potential of sodium cholate

Food approved bile extracts consist of a mixture of so-called bile salts, which are classified as surfactants. Bile salts are crucial biological emulsifiers required for the dispersion of lipids. Due to cost reasons and because of an easier handling of a pure compound, this section dealt with the solubilizing properties of sodium cholate, which is a prominent representative of bile salts, see Figure 109 left. In contrast to common surfactants, bile salts consist of a cholesterol backbone with a weakly pronounced separation of a rather rigid unpolar steroid ring from the polar hydroxy and carboxylate functions on the concave side of the molecule, see Figure 109 right.

Despite of their indisputable self-assembling properties, bile salts do not have a clearly pronounced CMC, such as typical surfactants do, but rather several CMC-like and CAC-like

transitions, where the aggregation number and aggregate's structure change. This is reasoned in their rigidity and wide distribution of the polar unit, which prevents dense packing of the bile salts. As a consequence, the aggregation number of bile salts (4-8 molecules) is about ten times lower than the one of the typical surfactant SDS (50-80 molecules). Up to now, the aggregate structure and the micellar and aggregative transitions of bile salts depending on their concentration are intensively investigated.[316,317] Many researchers reported that cholate forms dimers close to its CMC at 13-18 mM, which then further aggregate at concentrations above 100 mM due to intermicellar interactions.[317–319]

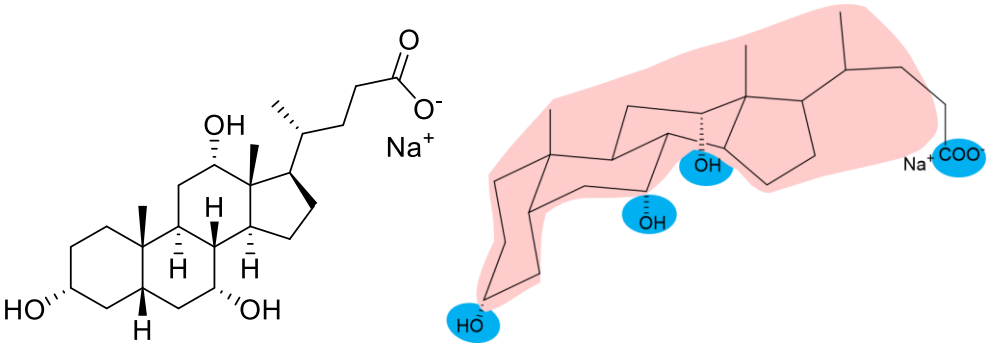

Figure 109: Molecular structure of sodium cholate with its polar (blue) and unpolar (red) moieties.[316]

Although also not allowed as food additive in the European Union, bile salts and extracts are common dispersants in the US.[320] Moreover, due to the association of bile salts with drugs, bile salts and derivatives are widely used in pharmaceutical formulations. Thus, for the preparation of Valium® MM, glycocholic acid is applied to solubilize the tranquilizer diazepam in mixed micelles of this bile acid derivative with soy lecithin. Analogously, the formulation of the multivitamin supplement Cernevit® was based on the dispersion by bile salt derivatives.[14] As sodium ferulate promoted increased solubility of a hydrophobic compound further due to its cosurfactive effect on SDS, and because bile salts are known to form mixed micelles with surfactants, sodium ferulate and cholate might undergo a synergistic aggregation too. Cholate is in particular of interest due to its green origin and its weaker toxicity. Moreover, it is important to know, if sodium ferulate exhibits cosurfactive properties in presence of a less amphiphilic and more rigid surfactant forming unconventional "micelles".

Therefore, the solubility of Sudan blue II and/or of RF was determined in aqueous systems consisting of either sodium cholate or sodium ferulate/cholate (molar ratio 1:1) mixtures, see Figure 110. As in the sodium ferulate/SDS system, RF was solubilized by sodium cholate, but RF's solubility in aqueous sodium ferulate solutions was reduced by the bio-dispersant. In contrast to the sodium ferulate/SDS system, where the reduction of RF's solubility stopped for SDS concentrations above its CMC, the solubility of RF was decreased continuously with the concentration of sodium cholate. Thus, sodium cholate has a higher affinity to sodium ferulate than SDS.

Further, congruent to the sodium ferulate/SDS system, Sudan blue II improved RF's solubility in aqueous cholate solutions, but reduced it further in aqueous sodium ferulate solutions

comprising sodium cholate, see Figure 110 A and B. Yet, RF was solubilized more than 10 times worse by sodium cholate than by SDS if Sudan blue II was present, see Figure 106 B and Figure 110 B.

In contrast to the sodium ferulate/SDS system, RF had no influence on the water-solubility of Sudan blue II in presence of sodium cholate and the combination of sodium ferulate with sodium cholate reduced the solubility of the hydrophobic dye. Saturation of sodium ferulate/cholate solutions with RF allowed increasing the solubility of Sudan blue II slightly, but the solubility of the hydrophobic solute was still beneath the one in absence of sodium ferulate. Thus, sodium ferulate exerts an anti-solubilizing effect on the hydrophobic dye in sodium cholate solutions and sodium cholate simultaneously decreases the solubility of RF in sodium ferulate solutions.

DLS measurements should reveal the reason for the reduction of RF's and Sudan blue II's water-solubility in the sodium ferulate/cholate system, see Figure 110 D. Although sodium ferulate improved the structuring of sodium cholate, such as in the sodium/ferulate/SDS system, the resulting correlation function was strongly fluctuating and about half as high as the one in the sodium ferulate/SDS system, see Figure 110 D. Hence, if Sudan blue II is embedded into sodium cholate aggregates, the solubility of this hydrophobic dye should either be maintained or increased in presence of sodium ferulate. Yet, UV-Vis-measurements showed a decrease of its solubility.

Further, RF reduced the structuring in the system comprising sodium cholate and sodium ferulate strongly, see Figure 110 D, but increased the solubility of Sudan blue II relatively to the sodium ferulate/sodium cholate system. Consequently, the correlation function of the DLS signal did not correlate to the solubility of Sudan blue II. Analogously, the weak increase of the correlation function of sodium cholate by the presence of sodium ferulate, does not correlate to the strong decrease of RF's solubility compared to pure aqueous sodium ferulate solutions, see Figure 106 A and Figure 110 A and D. Thus, sodium cholate seems to form less defined self-assemblies than SDS, while it reduces the solubility of RF in presence of sodium ferulate to the same extent as SDS.

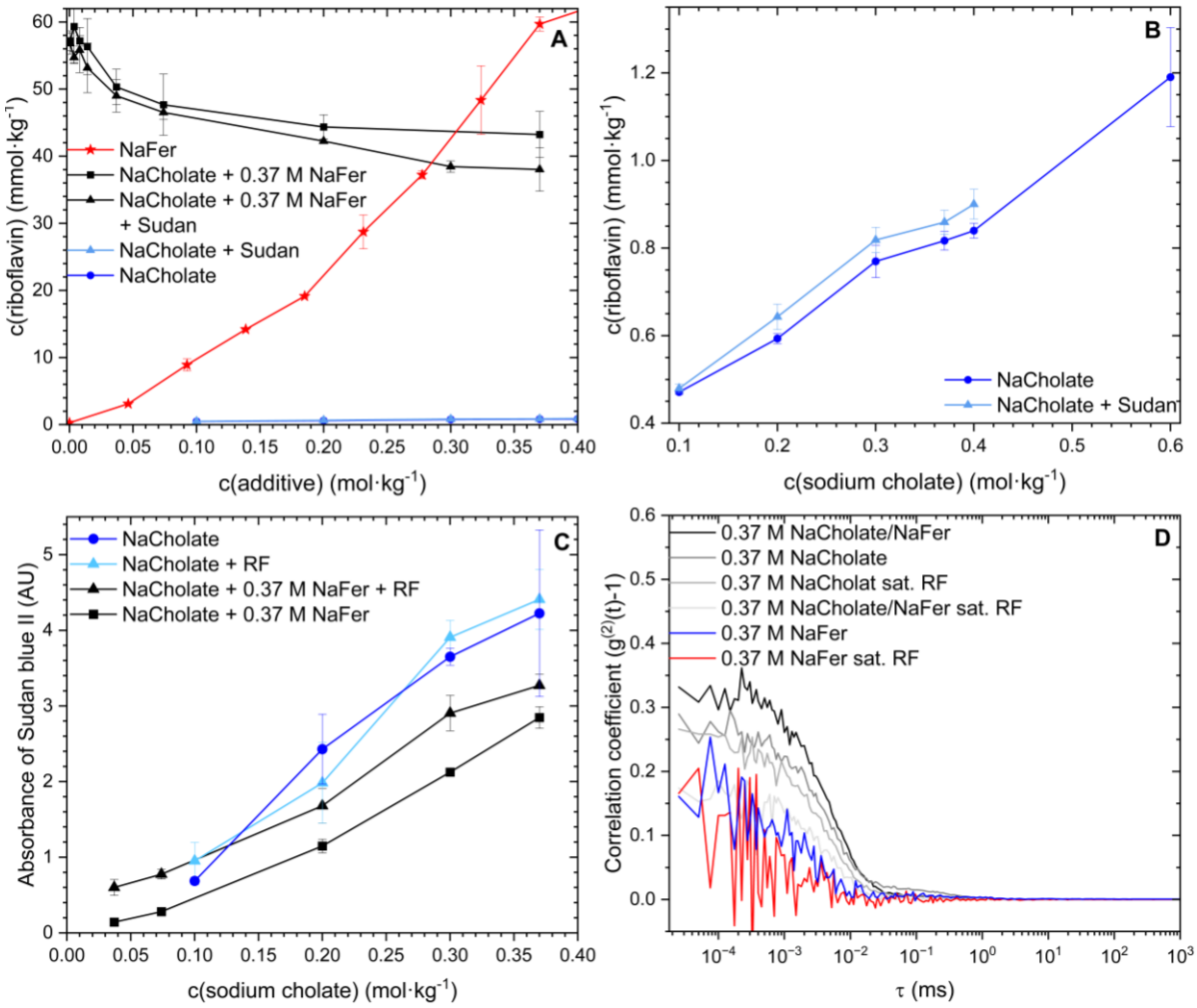

Figure 110: A) Water-solubility of riboflavin depending on the concentration of sodium cholate or ferulate; B) Enlarged view of A); C) Water-solubility of Sudan blue II represented by the absorbance depending on the concentration of sodium cholate; D) DLS correlation function of aqueous solutions comprising sodium ferulate and/or cholate in pure water and saturated with RF and/or Sudan blue II. If cholate and ferulate were present in the solutions together, the sodium ferulate concentration was kept constant at 0.37 mol·kg^{-1}.

To check, if the reduction of RF's and Sudan blue II's water-solubility by sodium cholate and ferulate, respectively, interrelates to the strong interaction of sodium cholate and ferulate, which could prevent their action as solubilizers, conductivity measurements were performed, see Figure 111. First, as in the sodium ferulate/SDS system, RF decreased the absolute conductivity of solutions comprising sodium ferulate. As copigmentation of RF and sodium ferulate was also observed in presence of SDS and sodium cholate, neither SDS nor sodium cholate cut the interaction of sodium ferulate and RF entirely.

Further, a CMC was not observed for sodium cholate. Instead, all samples comprising sodium cholate exhibited a broad curve, which is typical for aggregates showing a CAC. Although sodium cholate is often referred to be a biosurfactant, its low aggregation numbers are indeed rather comparable to the ones of a hydrotrope. Thus, many contradicting data on the CMC and CAC of sodium cholate are reported showing the complex action of cholate.[316,317] Nevertheless, because the propagation velocity in an electric field decreases only by ca. 30 % in the case of self-assembly to dimers, while it decreases by 86 % in the case of an aggregation

number of 50, conductivity is a precise technique for the determination of a CMC induced by of larger aggregates and not for the determination of dimers as in the case of sodium cholate. Moreover, due to sodium cholates secondary aggregation, it was not possible to distinguish between the CAC of sodium ferulate and cholate. Hence, a common CAC was determined using the intersect between the two linear part of the conductivity curves, see Figure 111.

The CAC of sodium cholate was not altered by the presence of RF, which is congruent to the absence of an alternation of the CMC of SDS by RF. Yet, in absence of RF, Sudan blue II reduced the CAC of sodium cholate significantly by ca. 15 $mmol \cdot kg^{-1}$. This was not the case for SDS. The reason therefore is probably the stronger structuring affinity of SDS in absence of the hydrophobic dye due to SDS's stronger developed amphiphilicity, while sodium cholate forms rather small assemblies. Apparently, RF acts as structure breaker, as the CAC of sodium cholate samples comprising Sudan blue II and RF was the same as of cholate in pure water.

The CAC of sodium ferulate and sodium cholate was significantly decreased by sodium cholate and ferulate, respectively. The CAC of 121±2 $mmol \cdot kg^{-1}$ in the sodium cholate/ferulate system was more in the region of sodium cholate. Thus, the reason for the reduced solubility of RF and Sudan blue II due to the presence of cholate and ferulate, respectively, is certainly the formation of small mixed aggregates of sodium ferulate and sodium cholate, which prevents the interaction of ferulate with RF and of cholate with Sudan blue II. The increase of the CAC in the sodium ferulate/cholate system upon saturation with RF and/or Sudan blue II shows the competition of RF and sodium cholate for sodium ferulate and the competition of Sudan blue II and sodium ferulate for sodium cholate. As the CAC of all sodium ferulate/cholate systems is beneath the CAC of sodium cholate in pure water, the attractive interactions of RF and Sudan blue II are apparently not sufficient to separate sodium ferulate and cholate, as it was already indicated by the reduction of RF's and Sudan blue II's water-solubility by cholate and sodium ferulate, respectively, in Figure 110 A and C. The continuous decrease of RF's solubility in aqueous sodium ferulate solutions with increasing concentration of sodium cholate compared to the constant solubility of RF in aqueous sodium ferulate solutions above a certain SDS concentration indicates also that sodium ferulate is more involved in the interaction with sodium cholate than in the one with SDS.

Consequently, mixed aggregation of sodium ferulate and sodium cholate deteriorates their solubilizing power as complexing agent and emulsifier, respectively. Therefore, sodium ferulate should be prevented in formulations of sodium cholate.

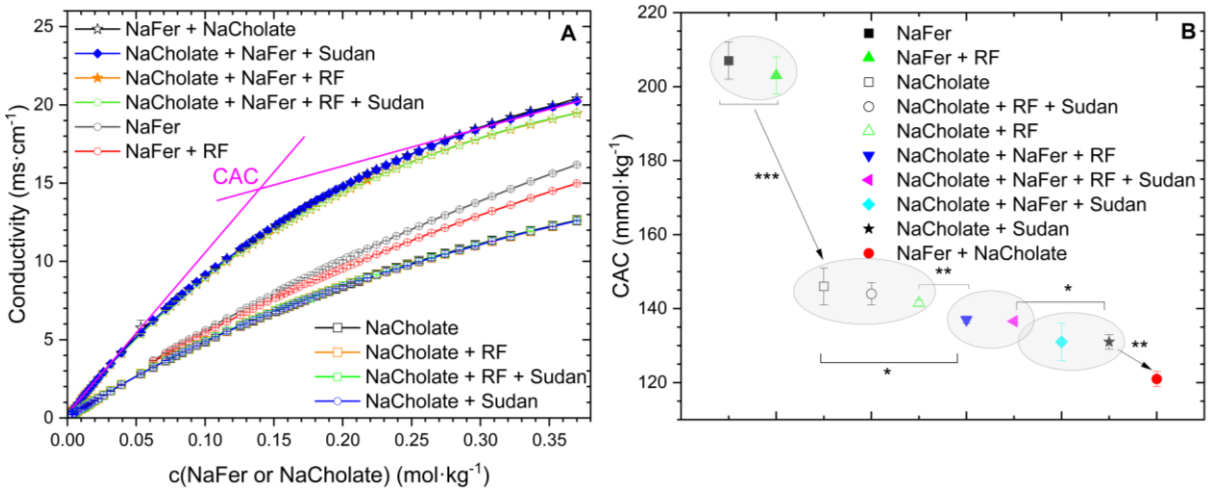

*Figure 111: A) Conductivity and B) Critical aggregate concentration of sodium cholate and sodium ferulate in aqueous solutions comprising sodium ferulate and/or sodium cholate in presence and absence of RF and/or Sudan blue II for a molar ratio of ferulate/cholate of one. The RF and Sudan blue II content was different for each sample, as the samples were saturated with the two colorants to see a maximum effect. The determination of the CACs represented in pink. (pairwise t-test: * = $p \leq 0.05$; ** = $p \leq 0.01$; *** = $p \leq 0.001$; triplicates)*

4.1.3.3 Conclusion

As expected, Sudan blue II was primarily solubilized via micellization, because the onset of its solubilization in aqueous SDS solutions is the CMC of SDS. Because sodium ferulate (i) decreased the CMC of SDS, (ii) increased the structuring of SDS, (iii) lowered thereby the onset of Sudan blue II's solubilization and (iv) increased the solubility of Sudan blue II further, the polyphenolate exhibits cosurfactive properties promoting the micellization of SDS, see Figure 112. As the CAC of sodium ferulate/SDS samples was increased by Sudan blue II, one part of sodium ferulate is supposed to interact with Sudan blue II on a molecular scale. However, sodium ferulate did not solubilize the dye in the absence of SDS. Thus, the increase of sodium ferulate's CAC might be explained by associations of sodium ferulate and Sudan blue II, which are embedded into the SDS micelles. In any case, the interaction of SDS and Sudan blue II with sodium ferulate competes with the interaction of RF with sodium ferulate and leads to a considerable reduction of RF's solubility in aqueous sodium ferulate solutions. On the contrary, RF improved the solubility of Sudan blue II in aqueous solutions comprising SDS or SDS and sodium ferulate. A reason for the latter case might be a reduction of the attractive interactions between sodium ferulate and SDS, which could enable a better contact of Sudan blue II to the hydrophobic moiety of SDS. However, this was not further investigated. In any case, sodium ferulate's cosurfactive action on SDS increased the solubility of a hydrophobic solute while RF's water-solubility was partially deteriorated. As RF's solubility still exceeded >100 times RF's solubility in pure water, the sodium ferulate/SDS system can be considered as a powerful formulation to solubilize hydrophobic and π-stacked compounds simultaneously, see Figure 112.

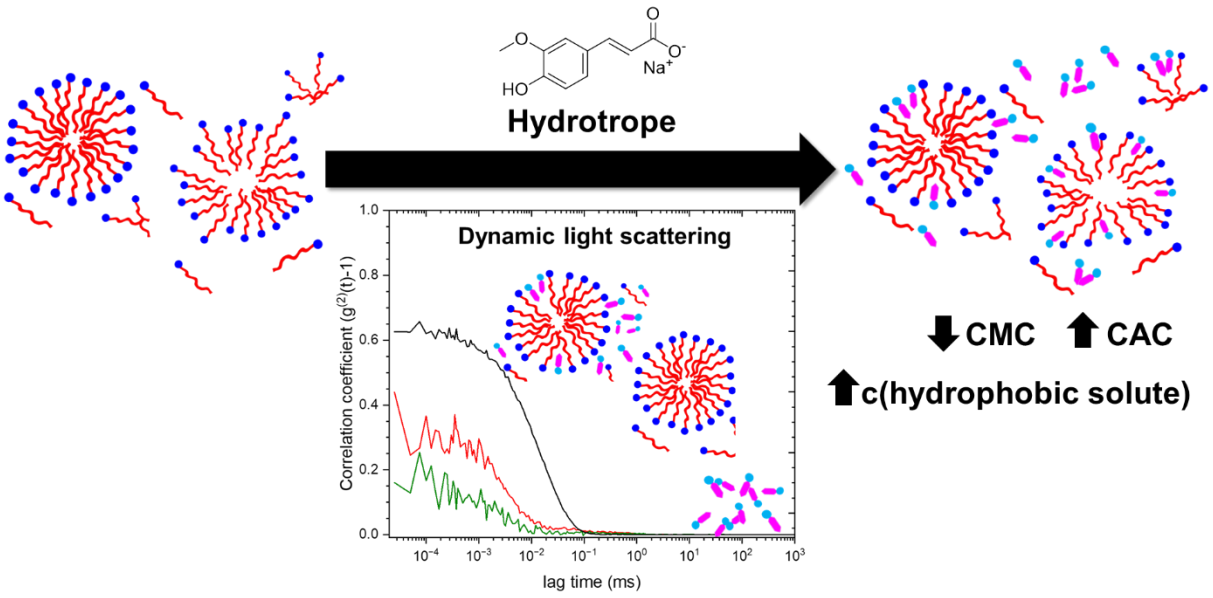

Figure 112: Cosurfactive support of sodium dodecyl sulfate by sodium ferulate

El-Khordagui reported that the polyphenolate sodium salicylate exhibits also cosurfactive properties on the self-aggregation of SDS in aqueous solution. He studied the influence on the surface tension, on the Krafft point, and on the CMC of SDS depending on the concentration of sodium salicylate. The cosurfactive power of sodium salicylate was more developed for concentrations below the polyphenolate's CAC. Thus, the surface tension and the CMC were decreased in the case of salicylate concentrations <0.5 M, while the trend was inverted for salicylate concentrations >0.5 M.[321] Consequently, salicylate's self-aggregation inhibited the micellization of SDS. If sodium ferulate behaves similar to sodium salicylate, sodium ferulate may exert even stronger cosurfactive action on SDS when applying lower ferulate concentrations. However, RF's water-solubility in such a system might be further decreased compared to the sodium ferulate solution without surfactant.

As sodium ferulate and Sudan blue II might undergo complexation such as it was shown for aromatic sodium carboxylates with RF, LC, RF-PO_4, vitamin K3 and folic acid, the reduction of RF's water-solubility in aqueous ferulate/SDS solutions might be less pronounced when using a non-aromatic hydrophobic solute instead of Sudan blue II. Imagining Sudan blue II being a hydrophobic drug or vitamin, such as vitamin E or D, the cosurfactive action of sodium ferulate coupled with its complexation of aromatic solutes might help to formulate multi-vitamin preparations. Although SDS is food approved by the US Food & Drug Administration, in the European Union, the surfactant is allowed only for medicinal purpose or for exterior applications as E487, such in ointments, cosmetics or toothpaste.[320,322] Thus, sodium ferulate/SDS formulations constitute a rather green option for drugs, cleaning agents and for the removal of cosmetic products than for food and beverage formulations.

The slight increase of sodium cholate's structuring and the significant decrease of its CAC by sodium ferulate proofed interactions between the two bio-molecules, too. However, the interaction between the two molecules was obstructive for their solubilizing power. While, upon saturation with Sudan blue II, RF's solubility was decreased similarly to the sodium ferulate/SDS system, contrary to the sodium ferulate/SDS system, the solubility of Sudan blue II was reduced by the presence of RF in the sodium ferulate/cholate system. Probably, the larger interaction surface between the rigid cholesterol backbone of sodium cholate and the planar benzyl ring of sodium ferulate resulted in too strong attractive interactions between the two bio-compounds. Although the sodium ferulate/sodium cholate system turned out as worse formulation to dissolve Sudan blue II and RF, the two solutes were still dissolved in higher quantities than in pure water. Thus, sodium cholate/sodium ferulate mixtures might still be used to dissolve slightly hydrophobic compounds together with aromatic ones. This might be especially useful for the preparation of surfactant-free drug formulations.

4.2 Further solubilization techniques for riboflavin

4.2.1 Solubility limiting factors of riboflavin

In general, solubilization can be limited by several factors. On the one hand, a molecule might be too hydrophobic and possess to less hydrogen bonding sites in order to interact with a solvent. However, the poor solubility of riboflavin cannot be increased significantly by only adjusting the solvent's polarity and hydrogen bonding capacity, although RF is quite polar and offers several hydroxy groups and two keto groups as potential hydrogen bonding partners, see Table 3 and Figure 113. Hence, this was not valid for RF.

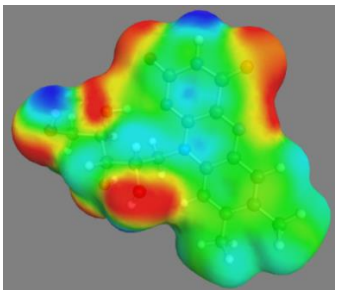

Figure 113: Sigma profile of riboflavin obtained from COSMOthermX.[323]

Further, being a medium sized molecule, the conformation of the ribityl chain might be decisive for RF's solubility, as the entropy of the surrounding solvent may be affected differently if the ribityl chain is stretched or bent. Yet, solubility starts actually already from the solid state of a potential solute. If the interactions of the solute with itself in the crystal are too strong, the crystal structure will not be disrupted and the compound may be insoluble though the interactions of the solute and solvent may be actually favorable. Hence, first the water-solubility of RF from distinct distributors was determined followed by an analysis of riboflavin's arrangement in the crystal, which was followed by a short analysis of the impact of the ribityl chain on RF's water-solubility.

Although the solubility of riboflavin in water is essential for the life of animals, plant and mushrooms, the water-solubility of riboflavin is reported to depend on its crystal morphologies by Sigma Aldrich.[180] Therefore, the water-solubility of RF from two batches from Carl Roth (97 %), two batches from BASF (> 97 %) and one batch from TCI(Lot. 35FLH) was analyzed, see Figure 114 and Table 20. The solubility of the distinct RF-types ranged from 0.192 to 0.287 mmol·kg^{-1} and thus differed by almost 50 %. The determined solubilities correlate with the ones provided in Table 3 and by Sigma Aldrich.[180] This shows that the solubilization of RF cannot only dependent on the solvent, but depends apparently on the crystalline morphology of RF.

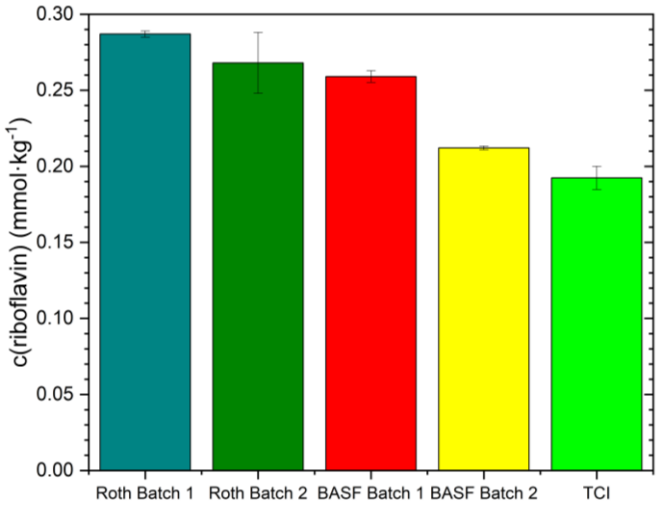

Figure 114: Water-solubility of RF from TCI and two batches from Carl Roth and from BASF. T = 23 °C.

Table 20: Water-solubility of RF from TCI and two batches from Carl Roth and from BASF. T = 23 °C. The first batch from Carl Roth was prepared in duplicate. The other samples were prepared in triplicate.

Compound	c(RF) (mmol·kg^{-1})
Roth Batch 1	0.287 ± 0.002
Roth Batch 2	0.27 ± 0.02
BASF-Batch 1	0.259 ± 0.004
BASF-Batch 2	0.212 ± 0.001
TCI	0.192 ± 0.008

Hence, RF crystals were synthesized from the liquid diffusion (or anti-solvent) method from a water/acetonitrile solution (50/50 (w/w)) saturated with either cinnamic or 3,4-dimethoxycinnamic acid and RF. This solution was overlayed with acetonitrile as antisolvent. Cinnamic and 3,4-dimethoxycinnamatic acid were supposed to act as weak hydrotropes for riboflavin due to the salting-in power of their corresponding sodium salts, see section 4.1.1. A hydrotrope was required, as otherwise riboflavin would precipitate too fast with increasing acetonitrile concentration, which would cause opaque and too tiny orange crystals. However, Single Crystal X-Ray analysis required transparent crystals of an appropriate size. On the other side, the acid and not the sodium salts of cinnamic and 3,4-dimethoxycinnamic acid were used, because of their low aqueous (< 1% (w/w)) solubility, which should prevent too high solubilization of RF in water that could hinder the precipitation and thus crystallization of RF.
Both samples resulted in transparent yellow needles, see Figure 115 A and B. Using this method, separate single crystals of RF were still rare. Instead, most RF crystals were attached to each other radially, as it was already reported by Sakate.[127,324] Cinnamic acid and 3,4-dimethoxycinnamic acid crystallized apart from RF upon evaporation of acetonitrile as unformed colorless plates and transparent needles, respectively.

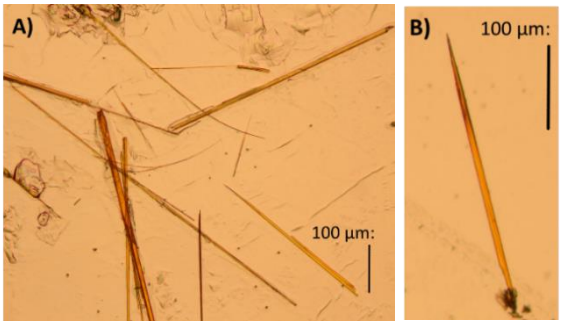

Figure 115: A) Riboflavin crystal needles in presence of cinnamic acid. B) Riboflavin crystal (size: 660 µm x 20 µm) in presence of 3,4-dimethoxycinnamic acid. The crystals were obtained by the liquid diffusion method (saturation of water/acetonitrile (50/50 (w/w)) with cinnamic or 3,4-dimethoxycinnamic acid and riboflavin followed by an overlay with acetonitrile).

The crystal structures of RF obtained in presence of cinnamic and 3,4-dimethoxycinnamic acid were similar. The RF molecules were arranged parallelly to each other, see Figure 116 and Figure 117. The aromatic isoalloxazine rings of two adjacent RFs were slightly displaced relatively to each other, so that the pyrimidine ring of one RF overlapped with the benzene ring of another RF. The shortest distance between two RF molecules (center of pyrimidine ring – benzene ring) was 3.643 Å if crystallized from the cinnamic acid sample and 3.313 Å if crystallized from the 3,4-dimethoxycinnamic acid sample, see Figure 116. This is in agreement with the postulation of Guerain et al. Guerain et al., who proposed a stacked arrangement of RF in the crystal at an intermolecular distance of 3.591 Å via powder diffraction images, which were interpreted with DFT calculations.[219] Thus their simulation matches with this primary experimental data. Additionally, the distance between two RF molecules is in line with the stacking distance of other flavin derivatives (3.3 Å to 3.6 Å).[325] Due to the displaced arrangement of the isoalloxazine rings, the distance of the plane formed by the middle aromatic ring of RF in the crystal obtained in presence of cinnamic acid is slightly longer (5.309 Å), see Figure 116.

Moreover, the ribityl chain of each RF molecule in the crystals was stretched and syn-oriented to the neighbored ribityl chain. Despite a potential uncertainty regarding the position of the hydrogen atoms due to their low electron density, in both RF crystals, two potential hydrogen bonds are supposed to be formed between the hydroxy groups (OH^7–OH^6 = 1.84(3) Å, OH^9–OH^4 = 2.11(3) Å in the RF crystal synthesized in presence of cinnamic acid and OH^7–OH^6 = 1.82(4) Å, OH^9–OH^4= 2.19(3) Å) in the RF crystal synthesized in presence of 3,4-dimethoxycinnamic acid, see Figure 116. Comparing the two crystals, the hydrogen bonding distance deviated by only 1.1 % for OH^7 – OH^6 and 3.7 % for OH^9 – OH^4, respectively. Another hydrogen bond might be formed between OH^6 and OH^9 (2.129 Å). Additionally, the amine group on the pyrimidine ring forms a hydrogen bond with at least one hydroxy group on the ribityl chain (OH^4 – NH^1 = 2.099 Å), see Figure 116. All of potential hydrogen bonds are in the magnitude of typical OH···H-bonds.[326]

Thus, hydrogen bonding of RF with other RF molecules in the crystal might contribute at least partially to the low solubility of RF in various solvents. However, hydrogen bonding of the ribityl chain as main solubility limiting factor seems absurd regarding the low solubility of RF in polar protic solvents due to RF's many hydrogen bonding sites.

Probably, π-stacking and thus dispersive interactions are mainly responsible for the low affinity of RF for solubilization. In particular, stacking of synthetic flavins was already reported by R. Cibulka et al.. Although stacking could be reduced by a modification of flavins with a space demanding group, the crystal images of the flavin derivatives pointed still an aggregation of them.[325] Consequently, π-stacking due to dispersive interactions of RF with other RF molecules appears as a reasonable explanation for the all-embracing poor solubility of RF.

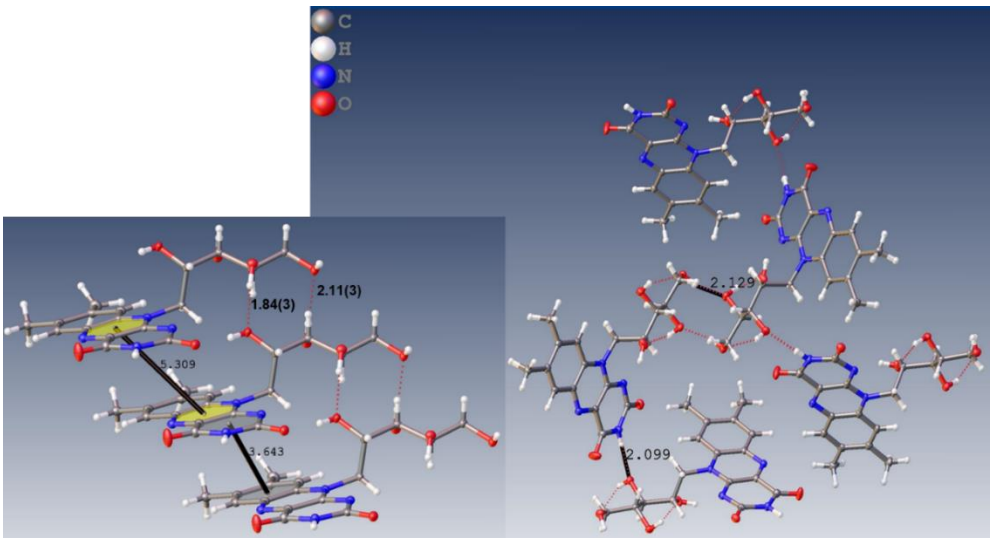

Figure 116: Crystal structure of pure RF needles obtained via the liquid diffusion method from a water/acetonitrile (50/50 (w/w)) solution in presence of cinnamic acid with distances given in Å.

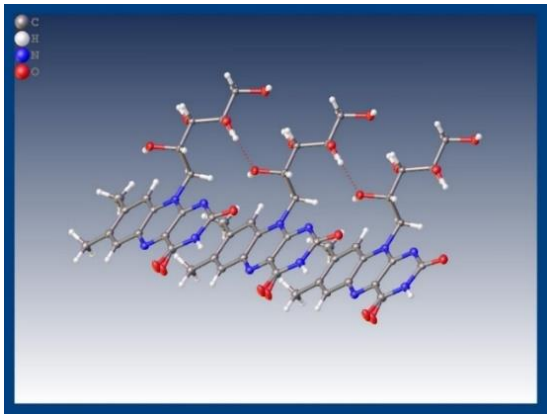

Figure 117: Crystal structure of pure RF needles obtained via the liquid diffusion method from a water/acetonitrile (50/50 (w/w)) solution in presence of 3,4-dimethoxycinnamic acid.

Although the ribityl chain of riboflavin states certainly not the major solubility determining factor, it may still influence the water-solubility of the vitamin. Thus, the solubility of LC corresponding more or less to RF without a ribityl chain and the solubility of ribose was compared to the one of RF, see Figure 118.

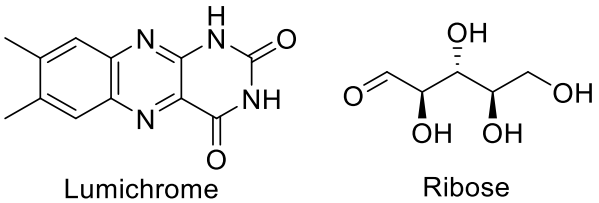

Figure 118: Molecular structure of ribose.

The aqueous solubility of LC was found to be approximately 8 times lower than the one of RF, see Table 21. The reason for the lower solubility of LC is the ribityl chain offering 4 hydroxy groups as hydrogen bonding partners. In water, the movement of the ribityl chain in water and its sterical demand might also weaken the aggregation of RF compared to LC. Although, hydrogen bonding of RF's ribityl chain observed in the crystal might be partially responsible for RF's poor water-solubility, the high solubility of ribose, which might also form hydrogen bonds

in its crystalline form, refutes that the potential hydrogen bonds found in the riboflavin crystal contribute significantly to the solubility limitation.

The change of the molar Gibbs enthalpy for solubilization $\Delta\Delta G$ upon introduction of a ribityl chain to LC and the addition of an isoalloxazine ring to ribose – both leading to RF – was estimated with equation 16 in section 3.2.2.6, see Table 21.[327] The modification of the isoalloxazine ring with a ribityl chain facilitates the solubilization only by 5.05 kJ·mol^{-1} corresponding to ca. twice the energetic amount of the thermal energy at room temperature. On the contrary, the introduction of a planar isoalloxazine ring to ribose disfavored the solubilization by 19.28 kJ·mol^{-1}. Thus, the isoalloxazine ring contributes approximately 4 times more to RF's solubility than the ribityl chain. Consequently, the hydration and hydrogen bonding of the ribose unit are not sufficient to influence the solubility problem of the isoalloxazine ring considerably.

Thus, (i) the low water-solubility of LC, (ii) the minor effect of the ribityl chain on RF's solubility and (iii) the strong loss in solubility upon induction of an isoalloxazine ring to ribose, confirm that dispersive interactions leading to π-stacking and not the hydrogen bonding in the ribityl chain are the main reason for the poor solubility of RF in water.

Table 21: Solubility of ribose, riboflavin and lumichrome in water. Last column: Change of the molar Gibbs energy of solubilization upon implementation of an isoalloxazine ring to ribose or a ribityl chain to lumichrome.

Compound	c(compound) (mmol·kg^{-1})	△△G(ribityl chain) (kJ·mol^{-1})
Ribose	679.2 [328]	Ribose → RF: 19.28
RF	0.27 ± 0.02	LC → RF: - 5.05
LC	0.035 ± 0.002	

To analyze the state of RF in water, Nuclear Overhauser Enhancement Spectroscopy (NOESY) was conducted. As the solubility of RF in deuterium oxide was not sufficient to have cross-peaks in the NOESY spectrum, the NOESY spectrum of RF was recorded in deuterated dimethyl sulfoxide (DMSO-d_6) after saturation. However, the NOESY spectrum did not reveal any hints for π-stacking of RF with itself in DMSO-d_6, see Figure A 13 and section 7.11.1.

Regarding the NOESY of RF in DMSO-d_6, the ribityl chain of RF is probably stretched in DMSO-d_6. Still, due to the too poor solubility of RF in DMSO-d_6 and water certain assumptions could not be retrieved.

Therefore, a NOESY spectrum of the better water-soluble RF-PO_4 (103 ± 8 mmol·kg^{-1}) – comprising the same aromatic backbone – in deuterium oxide was recorded, see Figure 119 and section 7.11.2. The cross-peak of H2 with H11 and H2 with H12 of RF-PO_4 indicated a bent conformation of the ribityl chain in deuterium oxide, see Figure 119 A.

Additionally, cross-peaks between H3 and H10, H8, H5 and H13 of RF-PO_4 in deuterium oxide suggested at least an intermittent anti-stacked orientation of RF-PO_4 in deuterium oxide, as H10 is an interior sugar chain proton and thus hardly accessible unless the molecule undergoes stacking. Note, the cross-peak of H3 with H13 might also arise from strong coupling

due to the aromaticity. In case of antiparallel stacking of RF-PO_4 in deuterium oxide, the cross-peaks of H3 with H11 and H12 points again to a curved conformation of the ribityl chain, see Figure 119 B. Comprising the same aromatic backbone and a similar ribityl chain to RF-PO_4, one can expect that RF performs π-stacking in aqueous solution. This is confirmed by the fact that the strongly hydrated phosphate group of RF-PO_4 should normally improve the contact of the RF-PO_4 with water and thus to rather weaken the stacking interactions of RF-PO_4 with itself.[329,330] On the other hand, the hydration of the phosphate group might influence the conformation of the ribityl chain of RF-PO_4. Hence, conclusions on the ribityl chain conformation of RF from the one of RF-PO_4 were not possible.

To summarize, Single Crystal X-Ray Analysis of a RF crystal and NOESY measurements revealed a π-stacking of riboflavin with other riboflavin molecules in its solid state and in water as the main solubility limiting factor.

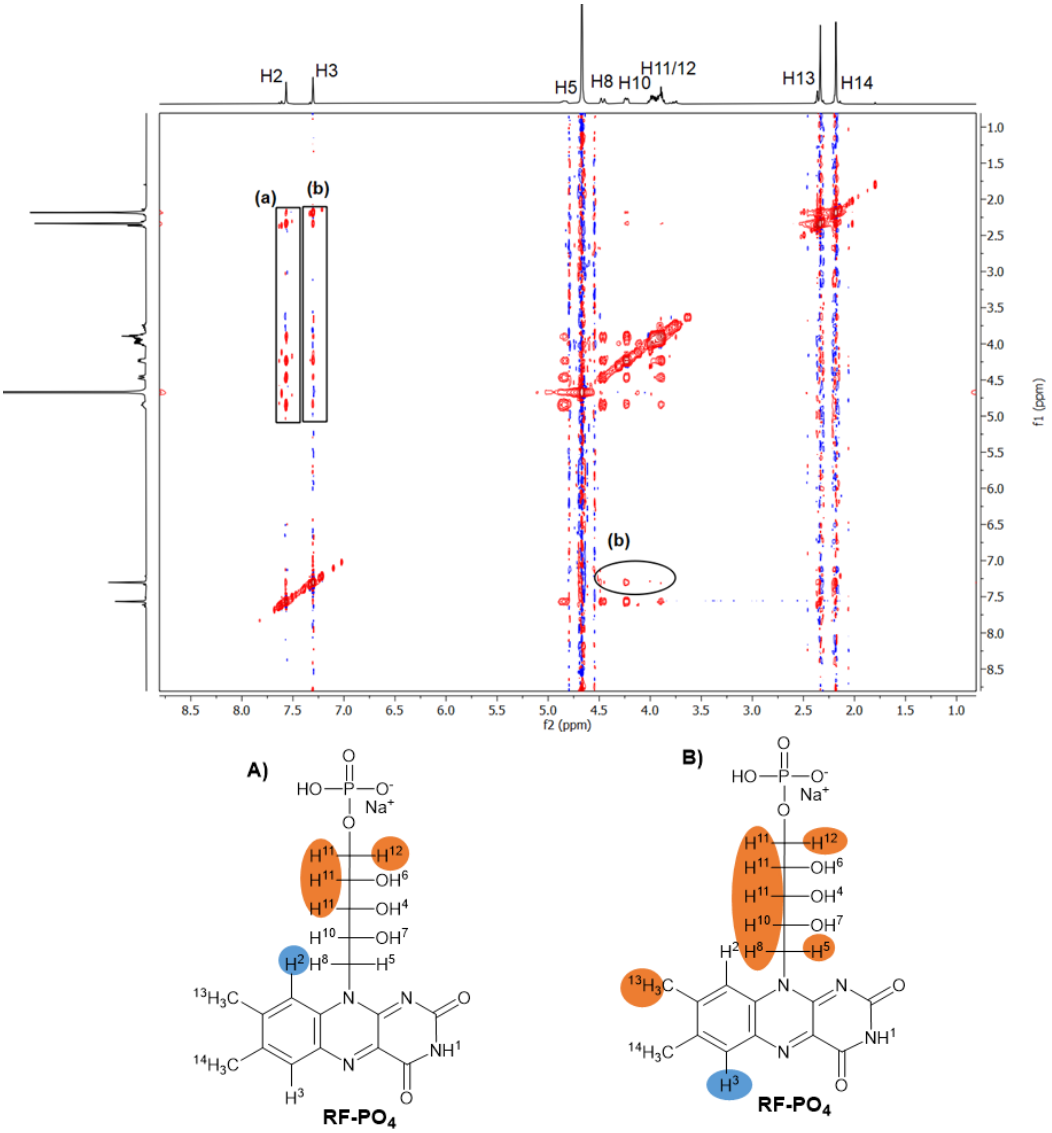

Figure 119: Top: NOESY NMR spectrum of RF-PO_4 in deuterium oxide (saturation): (a) Cross peak of H2 with H11, H12, H10, H13, H14, H8 and H5. (b) Cross-peak of H3 with H13, H14, H10, H8, H5, H11, H12. Bottom: A) Proton interaction indicating a curved ribityl chain in deuterium oxide; B) Proton interaction indicating anti-stacking arrangement of two RF-PO_4 molecules to each other and a bent ribityl chain.

4.2.2 Solubilization of riboflavin in presence of riboflavin 5'-monophosphate sodium salt in water

The results in section 4.2.1 showed that RF stacks with other RF molecules in aqueous solution. Comprising the same aromatic backbone, RF was supposed to stack with RF-PO_4 in water, too. Due to a strongly hydrated phosphate group, RF-PO_4 possesses a good water-solubility despite of stacking.[44] If RF-PO_4 stacks with RF, the strongly hydrated sodium phosphate group of RF-PO_4 might lead to a solubilization of potential RF-RF-PO_4 aggregates and thus increase the solubility of RF while keeping the one of RF-PO_4 constant. Therefore, the solubility of RF was determined in an aqueous sample, which was prior saturated with RF-PO_4. If the solubility of RF would be increased by the presence of RF-PO_4, it would mean that the solubility of RF-PO_4 should be higher than its solubility in pure water (103 ± 8 mmol·kg^{-1}). However, the saturation of water with RF-PO_4 and RF did not change the total content of RF-PO_4 (98 ± 6 mmol·kg^{-1}). Thus, RF-PO_4 did not change the solubility of RF in water. One reason therefore might be that the increase of RF's solubility is so low that it is covered by the high amount of RF-PO_4 in solution. Another reason therefore is probably the weaker hydration of potential RF-PO_4-RF stacking complexes. Thus, RF-PO_4 was found to perform stacking with an anti-orientation of the ribityl chain in water. Hence a loss of an anti-oriented ribityl phosphate group of RF-PO_4 of potential RF-PO_4 aggregates due to an aggregation with RF might be the reason, why RF-PO_4 cannot solubilize RF, as then the aggregate could not be hydrated strongly from two sides.

4.2.3 Attempt for the disruption of RF-RF-stacking via thermal energy

RF was found to perform stacking with other RF molecules but also with sodium polyphenolates, see sections 4.2.1 and 4.1.2.1.1. Sodium polyphenolates increased RF's water-solubility exponentially with the solubilization being strongly dependent on the electronic system of sodium polyphenolates. Thus, the higher the sodium polyphenolates concentration prior to saturation with RF was, the less sodium polyphenolate molecules were required to dissolve RF in water. Logically, RF should have been precipitated upon dilution with water, as, for saturation of solutions with lower sodium polyphenolate concentrations, more polyphenolates per RF were required for RF's solubilization. However, this was not the case, as the solution were stable in the dark for several months without precipitation of RF. As described in section 4.2.1, the attractive interactions between two RF molecules might be very high due to dispersive interactions and prevent the solubilization of RF in water. However, once RF was solubilized by polyphenolates, it did not aggregate again. Because stacking interactions are rather weak (2 kJ·mol^{-1} to 8 kJ·mol^{-1})[331,332], RF might not aggregate or precipitate again after a thermal disruption of the RF molecules, too.

Thus, stacking of RF with other RF molecules might be weakened with increasing temperature enabling a better access for solubilizers to separate the RF molecules completely from each other. Hence, aqueous sodium polyphenolate solutions were saturated with RF at a high temperature (90 °C), cooled down to room temperature (23 °C) and filtered, to see if the saturation temperature influenced the solubility of RF. As not all sodium polyphenolates are heat stable, one top candidate for RF solubilization - sodium ferulate - was not tested due to fast oxidation. Solubilizers comprising distinct solubilizing power were tested and compared to the surfactant SDS. To achieve maximum accuracy, the solubilizers were tested at their solubility limit or at a concentration, where the solubilizer did not precipitate upon heating. SDS was applied at two distinct concentrations, to be comparable to NaButyrate and Valerate and to know if a change of the concentration has an effect on the result. Consequently, aqueous solutions of 3 $mol \cdot kg^{-1}$ Na-3,4-DiOMe-Cinn and NaBenz, 0.858 $mol \cdot kg^{-1}$ Na-4-OH-3-OMe-Benz, 0.1 $mol \cdot kg^{-1}$ Na-2,4-Pentadienoate, 0.2 $mol \cdot kg^{-1}$ SDS and 0.4 $mol \cdot kg^{-1}$ NaButyrate, NaValerate and SDS were saturated with RF at 90 °C via stirring at 450 rpm in the dark for 1 h.

At 90 °C, the solubility of RF did not change in presence of medium and good solubilizers [Na-2-OH-Benz (medium), Na-4-OH-3-OMe-Benz (medium) and Na-3,4-DiOMe-Cinn (best)] compared to the sample preparation at 23 °C, see Figure 120 A. In the case of Na-2,4-Pentadienoate less RF was solubilized via saturation at 90 °C compared to 23 °C, see Figure 120 B. The reason was, the decrease of Na-2,4-Pentadienoate's water-solubility with increasing temperature leading to a loss of the solubilizer at high saturation temperatures. In presence of "bad" RF solubilizers comprising a lower conjugation and flawless amphiphilicity, the saturation at 90 °C (SDS, NaBenz, NaValerate, NaButyrate) resulted in a significant increase of the RF's water-solubility compared to the samples prepared via saturation at 23 °C, see Figure 120 A and B.

An explanation for this result might be a weakening of the stacking between the RF molecules by means of the thermal energy, which could facilitate an interaction with RF or an embracement of RF by solubilizer molecules. In presence of sodium polyphenolates being medium to good solubilizers, all polyphenolate molecules might be occupied by RF already, whereas in presence of weak solubilizers, free solubilizer molecules might still be available. This was reinforced by the observation of the same solubility of RF in presence of 0.2 $mol \cdot kg^{-1}$ and 0.4 $mol \cdot kg^{-1}$ SDS at saturation at 90 °C, whereas different concentrations of SDS led to different solubilities of RF at 23 °C, see Figure 120 B. As the solubility of RF in presence of good and medium RF solubilizers after saturation at 23 °C was still far beyond the solubility in presence of weak solubilizers after thermal treatment, further investigations of the thermal influence on the interactions between RF, polyphenolates and water were not attempted.

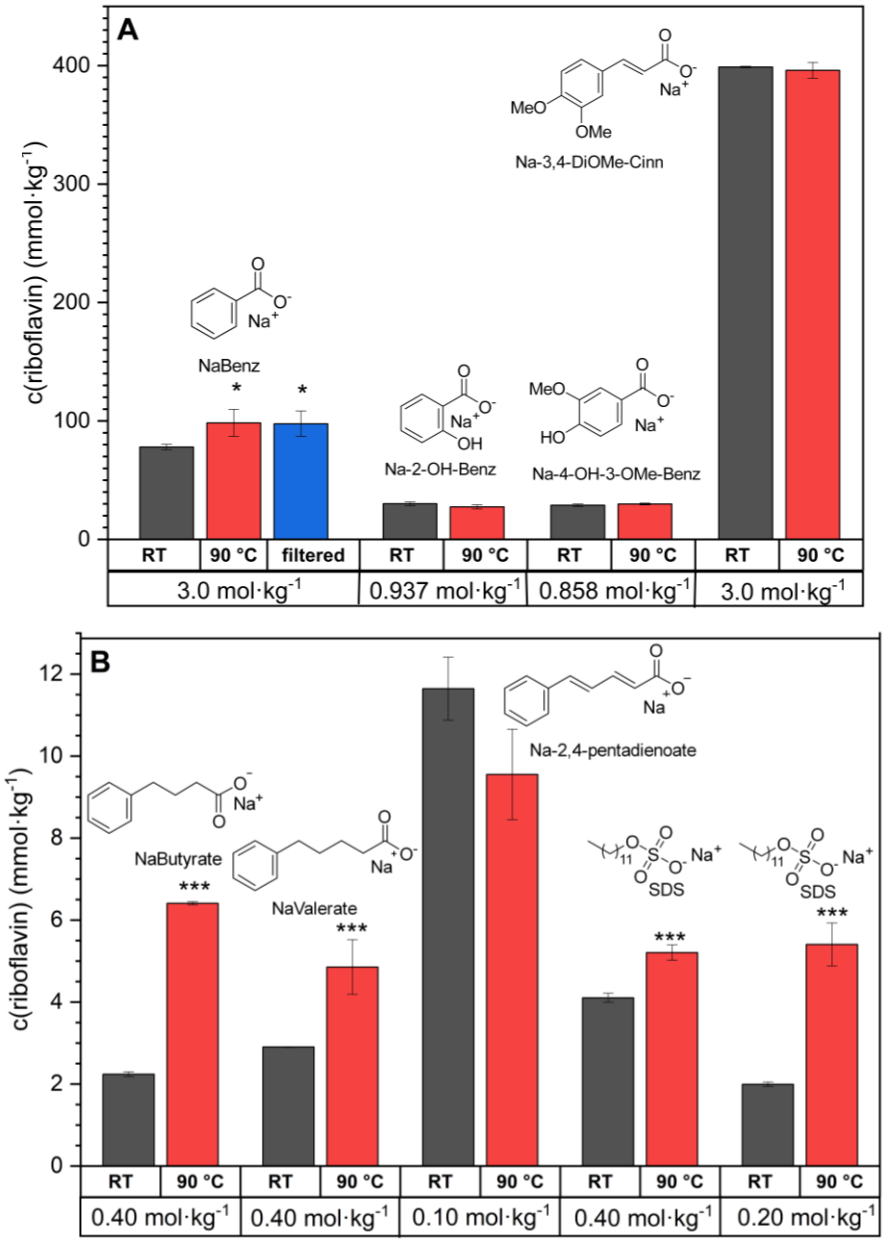

*Figure 120: A) Water-solubility of riboflavin at 23 °C (RT) and 90 °C in presence of 3.0 mol·kg^{-1} NaBenz, Na-3,4-DiOMe-Cinn, 0.858 mol·kg^{-1} Na-4-OH-3-OMe-Benz and 0.937 mol·kg^{-1} Na-2-OH-Benz. B) Water-solubility of riboflavin at 23 °C (RT) and 90 °C in presence of 0.4 mol·kg^{-1} NaButyrate, NaValerate, SDS, 0.2 mol·kg^{-1} SDS and 0.1 mol·kg^{-1} Na-2,4-Pentadienoate; (pairwise t-test: *** p = 0.001; * p = 0.05); Number of measurements = 3.*

4.2.4 Solubilization of RF by means of other natural additives

As the mechanism of cofactor binding of flavins by flavoenzymes involves stacking interactions between the aromatic residues of tyrosine, tryptophan or histidine at the cofactor binding site and the isoalloxazine ring of the flavin[60], and because aromatic sodium carboxylates, tyrosol, phloroglucinol, the salting-in agent NaSCN and the surfactant SDS improved the solubility of RF in water, other aromatic or hydrotrope-like compounds might also increase RF's water-solubility. Hence, natural aromatic and non-aromatic hydrotropic compounds were tested regarding the aqueous solubilization of RF. If the additive was sufficiently soluble, an additive

concentration of 0.37 mol·kg^{-1} (solubility limit of sodium ferulate in water) was used. Otherwise, lower concentrations were applied, see Table 10 in section 3.3.1.3. However, not all additives were completely dissolved at the applied concentrations. In such cases, the samples were still saturated with RF hoping for a mutual solubilization as it was observed in the case of RF and aromatic sodium carboxylates in section 4.1.2.1.

As reported in section 4.1.2.3 and 4.1.2.4, vitamin K3 and folic acid were also solubilized via an π-system driven solubilization mechanism by sodium polyphenolates. Moreover, as explained in section 4.1.2.1.1, RF and sodium polyphenolates solubilized each other. Hence, these two poorly water-soluble vitamins, as well as the slightly soluble aromatic hesperidin, L-tyrosine and ellagic acid were thought to potentially undergo a mutual increase of the water-solubility with RF. However, saturation of water with RF and these five compounds did not result in any change RF's water-solubility.

Moreover, the sparing water-soluble biotin was supposed to have slight aggregative potential and the possibility for hydrogen bonding with RF. Yet, saturation of water with biotin and RF did not alter RF's solubility, too.

The next aromatic and non-aromatic but hydrotropic compounds increased RF's water-solubility by less than 2 times: ATP, pyroglutamic acid and its sodium salt, adenine, adenosine, thiamine hydrochloride and thiamine, L-proline, γ-valerolactone, rutin, saccharine, and L-histidine, see Table A 74 in the Appendix. However, this increase of RF's solubility is not at all comparable to the one in the presence of polyphenolates from sections 4.1.2.1.1 and 4.1.2.1.4. On this account it is worth to mention that pyroglutamic acid solubilized RF more efficiently at pH 1 than at pH 3. Investigating the hydrotropic potential of pyroglutamic acid, A. Fusina also reported pyroglutamic acid to act more strongly on the solubility of the aromatic solutes, disperse red 13 and quercetin, at lower pH values. He supposed the formation of a salt of pyroglutamic acid with the solutes at low pH values to be the reason for the improved water-solubility of disperse red 13 and quercetin.[265] However, RF's amine group is not likely to be protonated due to its participation in the flavin's overall conjugation. Instead, the low pH might lead to a protonation of the hydroxy groups of the ribityl chain and thereby increase RF's solubility. This, would explain the weak influence of pyroglutamic acid on RF's water-solubility comparable to the one of the salting-in agent sodium thiocyanate or to the water/ethanol system, which enabled to alter the hydrogen bond network of water to improve RF's solubility.

Further the aromatic compounds, ethyl vanillin, caffeine, pyridoxine, Tetra-Na-NADPH, vanillyl alcohol, L-tryptophan, sodium saccharine, 3-indolsulfonic acid, fulvic acid, 3-indolepropionic acid, and resveratrol triphosphate trisodium salt were compared to the surfactant SDS, to NaBenz, NaCHC, as well as to the polyphenolates Na-3,4,5-TriOH-Benz and Na-4-OH-3-OMe-Cinn, see Figure 123 or Table A 74 in the Appendix. All of the latter aromatic compounds

increased the solubility of RF and copigmented with RF leading to an orange to reddish sample color, see Table A 74 in the Appendix.

Out of these compounds, resveratrol triphosphate trisodium salt, solubilizing 47.6 ± 0.5 mmol·kg^{-1} RF, was mostly comparable to the best sodium polyphenolates from section 4.1.2.1.1, see Table A 74 in the Appendix. However, the sample comprising resveratrol was basic. Due to the fast degradation of RF in alkaline medium, resveratrol triphosphate is not recommended as solubilizing agent and the increase of RF's solubility might originate from the deprotonation of the ribityl chain's hydroxy groups.[8]

Further, the weak performance of vanillyl alcohol and ethyl vanillin compared to sodium vanillate, showed once more the importance of the carboxylate group for a good solubilizing efficiency, as it was observed in section 4.1.2.1.1, see Figure 121 and Table A 74 in the Appendix

Tetra-Na-NADPH and pyridoxine solubilized considerable amounts of RF, while fulvic acid was even worse than NaBenz, see Figure 121, Figure 123 and Table A 74 in the Appendix. Caffeine solubilized RF considerably, too. Believing the molecular dynamic simulation of Cui Y., caffeine dissolves RF via stacked aggregation to reduce the contact with water, which enables to restore the native water-structure.[315] The interaction of RF with caffeine might correlate with the reduction of riboflavin in the plasma when drinking coffee.[333]

Nevertheless, Tetra-Na-NADPH, pyridoxine and caffeine solubilized RF comparable to the surfactant SDS and thus were worse than Na-3,4,5-TriOH-Benz and were therefore not further investigated.

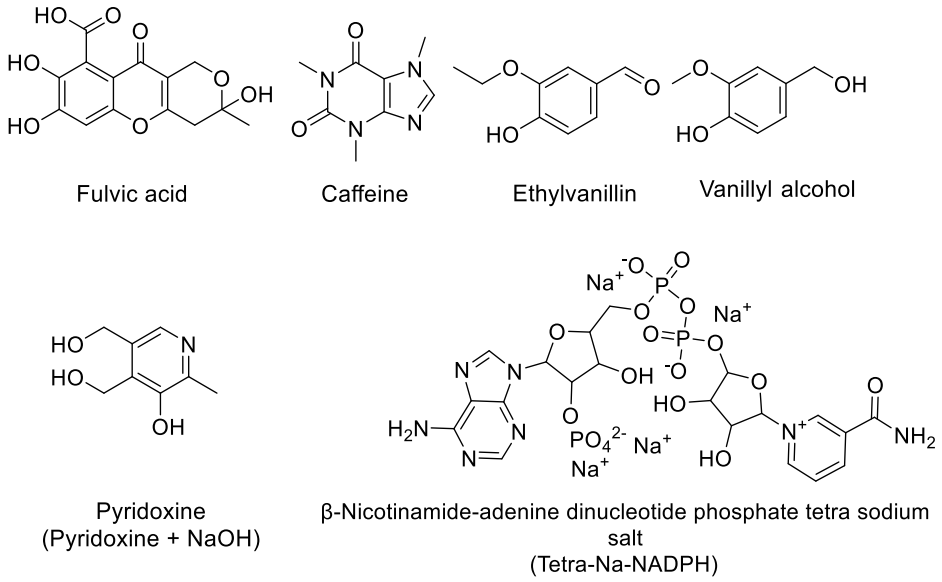

Figure 121: Molecular structures of natural aromatic compounds increasing the solubility of riboflavin.

Interestingly, indole derivatives ranged from bad to good solubilizers, see Figure 123. They are ordered according to their solubilizing power for RF in water in Figure 122. Out of the tested indole derivatives, L-tryptophan and indoxyl sulfate were the best solubilizers, being better than Na-3,4,5-TriOH-Benz and even almost on the level of Na-4-OH-3-OMe-Cinn. Saccharine

was worse than the two, but still almost as good as SDS. Although, except of the alpha amino group, 3-Indolepropionic acid had almost the same molecular structure as L-tryptophan, this compound was tremendously worse than L-tryptophan, solubilizing just as much RF as the non-aromatic hydrotrope NaCHC. On the contrary, the alpha amino group of L-tyrosine, led to a weaker solubilizing power of this amino acid compared to Na-4-OH-Prop, see Figure 123 and Figure 28 A. The reason for this opposite effect of the amino group on the solubilizing power of indole and benzoate derivatives was not clear. According to A. Fusina, tryptophan was not able to improve the water-solubility of quercetin and disperse red although these two compounds are certainly limited in their water-solubility not only by their hydrophobicity but also due to their π-stacking interactions.[265] Thus, the reason for the opposite effect of the amino group on the solubilizing power of indole and benzoate derivatives are most probably specific dispersive or hydrogen bonding interactions. This effect was not further investigated, because sodium polyphenolates were still more promising solubilizing agents for RF than indole derivatives.

Finally, L-tryptophan and indoxyl sulfate were the only RF solubilizing agents, which reached solubilizing power comparable to good sodium polyphenolates, such as Na-4-OH-3-OMe-Cinn. Yet, due to their toxicity these latter two indoles could be used for pharmaceutical, but not for food applications.[334]

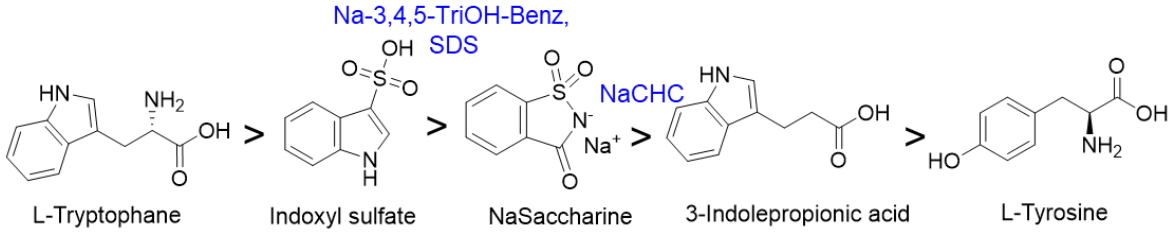

Figure 122: Riboflavin solubilizing power of indole derivatives and tyrosine. Indoxyl sulfate: indoxyl sulfuric acid was obtained by neutralization of the potassium salt with hydrochloric acid.

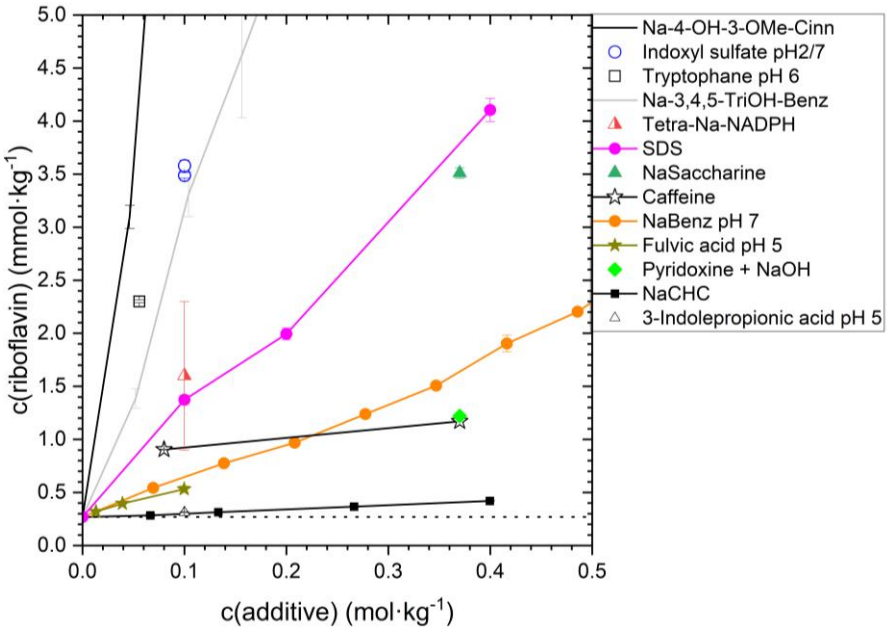

Figure 123: Water-solubility of riboflavin in the presence of natural additives.

Sugars were also supposed to have an impact on RF's water-solubility. Although Grundl et al. revealed sugars as salting-out agents in phase transition temperature measurements of binary water/DPnP systems, the hydroxy groups on RF's ribityl chain might undergo hydrogen bonding with the ones of sugars leading to a potential dissolution of RF due to the strong hydration of sugars.[51] Therefore, the influence of the two most common mono-sugars, glucose and fructose was briefly investigated for sugar concentrations up to 0.40 mol·kg^{-1}, see Figure 124. Interestingly, concentrations <0.2 mol·kg^{-1} led to a salting-out of RF, while higher concentrations of both sugars increased RF's water-solubility. A reason for this concentration dependent salting-in and -out effect of glucose and fructose might be that RF is occupied by sugar molecules leading to a salting-out at low concentrations, while high sugar concentrations enable enough possibilities for hydrogen bonding of the sugar molecules with RF and solubilize RF due to their strong hydration. Glucose did not increase the solubility of RF compared to pure water even when applied at 0.4 mol·kg^{-1}. On the contrary, using 0.4 mol·kg^{-1} fructose – corresponding to ca. 7 wt.% fructose – the water-solubility of RF could be raised by 24 %. Consequently, fructose is an elegant option to prevent the precipitation of RF from juices dyed with RF, as juices can comprise a fructose content up to 65.35 g·L^{-1}.[335] Nevertheless, the solubilizing power of fructose was not at all in the range of sodium polyphenolates and, contrary to polyphenolates, fructose exerts probably no photostabilizing properties on RF. Thus, sugars were not further investigated.

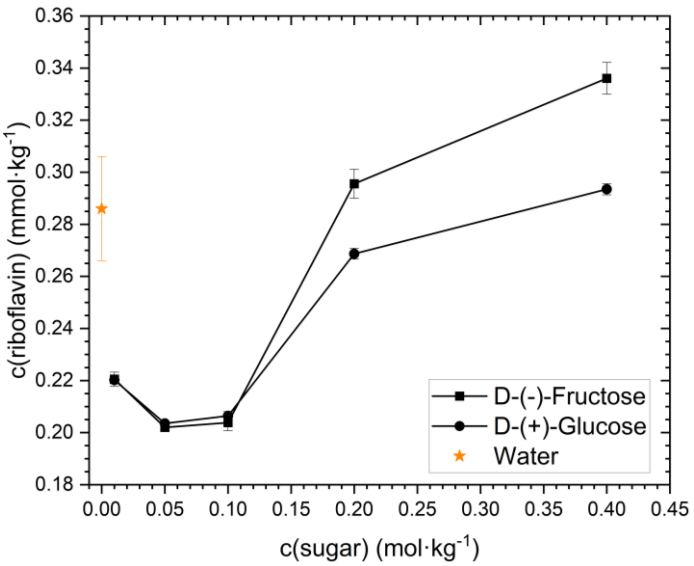

Figure 124: Solubilization of riboflavin with sugars in water

As aromatic charged molecules, anthocyanins were supposed to solubilize RF, too. Solubilization of RF with anthocyanins or proanthocyanidins would be interesting for the preparation of multivitamin supplements and colored juices. Supposing that the grape extract and OPC complex consist only of cyanin chloride, approximately 10 mmol·kg^{-1} solutions of an anthocyanin-rich grape extract and of an OPC complex 200 from Greenline products were prepared. All anthocyanin/proanthocyanidins were not water-soluble. The samples were still

saturated with RF hoping for a mutual solubilization of RF and of the anthocyanins. While the pure cyanin chloride showed almost no effect of RF's water-solubility, the grape extract and OPC complex increased RF's solubility 3.7 times, see Figure 125. Consequently, an anthocyanin mixtures are required to see a significant increase of RF's water-solubility. The poor solubility of anthocyanins in water was probably the reason, why these compounds did not increase the water-solubility of RF over 1 mmol·kg^{-1}. Based on the assumption of having maximum 10 mmol·kg^{-1} anthocyanin, the grape extract and OPC complex samples from Figure 125 exhibit a maximum molar anthocyanin/RF ratio of 13. Although, the grape extract and OPC complex increased the solubility of RF less than sodium polyphenolates, they constitute healthy antioxidant solubilizing agents for RF. The only disadvantage of anthocyanins/proanthocyanidins is that they might be photosensitized and thus degraded by RF.[10] As sodium polyphenolates quench RF's excited singlet and triplet state on diffusion scale, photosensitization of anthocyanin/proanthocyanidins could be probably avoided using anthocyanin/proanthocyanidins in combination with sodium polyphenolates.[10] However, in this research, the combination of anthocyanins/proanthocyanidins and sodium polyphenolates to solubilize RF was not tested in this research.

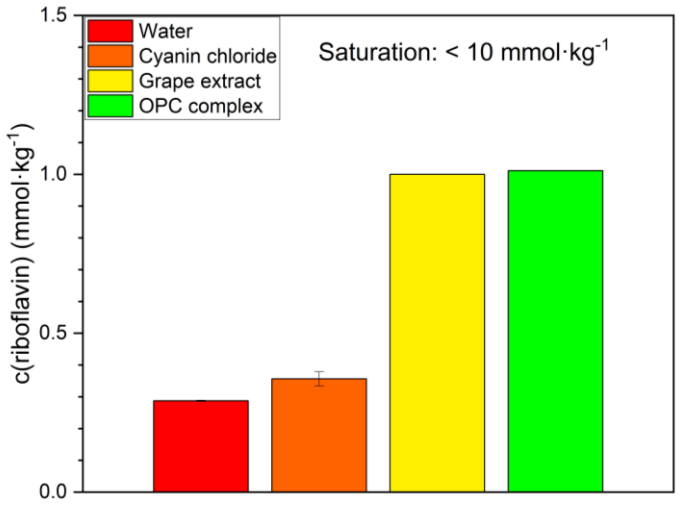

Figure 125: Solubilization of riboflavin in aqueous solutions of anthocyanins

Finally, the aromatic natural compounds L-tryptophan, indoxyl sulfate, sodium saccharine, caffeine, pyridoxine, fulvic acid Tetra-Na-NADPH as well as extracts of anthocyanin/ proanthocyanidins increase the solubility of RF significantly. The sugars glucose and fructose were seen to induce a salting-out of RF at low concentrations and fructose induced a salting-in of RF at higher sugar concentrations >0.20 mol·kg^{-1}. Nevertheless, sodium and choline polyphenolates are largely more efficient solubilizer for RF in aqueous medium, see section 4.1.2.1.1.

4.2.5 Solubility and photostability of riboflavin in water/ethanol/triacetin systems

RF comprises keto and hydroxy groups as potential hydrogen bonding sites, see Figure 113 in section 4.2.1. Thus, NaSCN and NaH_2PO_4 induced salting-in and -out of RF, respectively, see section 4.1.2.1.1.

Degot P. managed to solubilize the hydrophobic curcumin sufficiently so that it could be extracted from *Curcuma Longa* using the green, sustainable, bio-degradable and food-approved surfactant-free microemulsion of water/ethanol/triacetin. By changing the ratio between the three bio-solvents, the polarity and hydrogen bonding capacity of the resulting binary or ternary mixture can be adjusted. Triacetin was thought to be an appropriate oily phase, because RF is rather polar and a too hydrophobic oil was supposed to have a counter effect on RF's solubility. Ethanol should serve as cosolvent to improve the miscibility of triacetin and water.[13] Thus, in this edible system, the solubility of RF was supposed to be potentially increased more than with simple salting-in agent NaSCN.[13] If it would be possible to solubilize enough RF in the mixture and to dilute the final mixture to reach an ethanol content < 0.05%, the resulting edible/drinkable formulation would be even alcohol-free according to the European Union. Hence the solubility of RF was determined in the binary water/ethanol and ethanol/triacetin systems and then in the ternary water/ethanol/triacetin system. As RF is known to degrade faster in non-polar solvents, the decreased solvent polarity due to ethanol and triacetin might induce a destabilization of RF under light relatively to pure water.[8] Thus, the photodegradation of RF was additionally monitored in the binary water/ethanol and ethanol/triacetin systems with a plant LED lamp.

In the binary water/ethanol system, the solubility of RF increased synergistically with increasing ethanol content reaching a maximum solubility of RF at 50 wt.% ethanol and decreased again with further increasing ethanol content, see Figure 126. At the maximum, 0.919 ± 0.002 $mmol \cdot kg^{-1}$ RF, corresponding to 3.4 times the solubility of RF in pure water, were dissolved.

At 50 wt.%, which corresponds to a molar water/ethanol ratio of 2.5, ethanol lost its ability as hydrotrope for RF, although water was still the main phase. pH measurements revealed a point of inversion and thus the equivalence point of the acid-base equilibrium at 50 wt.% ethanol, see Figure 126. Consequently, the binary water/ethanol structure undergoes a strong structural change at 50 wt.% ethanol. The reason for the synergistic solubilization of RF might be that water and ethanol interactions reach their maximum at ca. 60 wt.% ethanol resulting in an "ideal" mixture.[336] At ca. 60 wt.% ethanol, water-water and ethanol-ethanol interactions should be as strong as water-ethanol interactions. Due to the absence of significant structuring of binary water/ethanol mixtures, ethanol can be regarded as cosolvent for < 50 wt.% ethanol.[250,337] For concentrations ≥ 60 wt.% ethanol, ethanol can be regarded as solvent.

As RF is known to degrade faster in organic solutions than in water, which might disfavor the usage of ethanol/water mixtures for the solubilization of RF, binary mixtures of water/ethanol were illuminated with a LED plant lamp to see the impact of the solvent constitution on RF's photodegradation speed.[8] For concentrations < 50 wt.% ethanol, RF's photodegradation followed zero order kinetics. Right at RF's maximum solubility in the binary water/ethanol mixtures (50 wt.% ethanol), the photodegradation kinetics of RF increased from zero order to two first order. A further change into second order degradation happened ≥ 90 wt.% ethanol. Thus, the structural change in the binary water/ethanol solutions at 50/50 (w/w) influenced also the photodegradation kinetics. Consequently, the 60/40 (w/w) water/ethanol mixture appears as most reasonable solvent mixture to keep the photodegradation of RF at zero order and the solubility of RF near its maximum in the binary water/ethanol system. The corresponding rate constants and plot of RF's photodegradation are reported in Figure A 102 A-C and Table A 123 in section 7.12 in the Appendix.

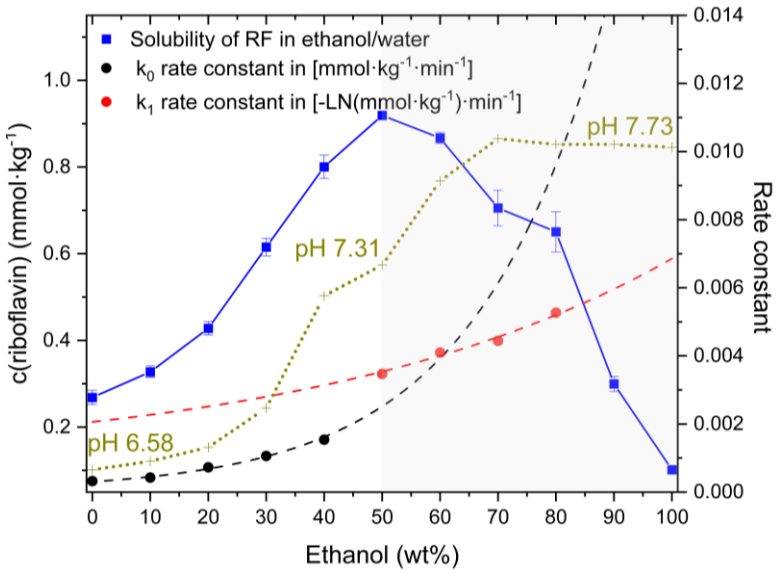

Figure 126: Solubility of riboflavin in the binary water/ethanol system, pH-value of the binary solvent mixture and first/second order rate constants for the photodegradation of riboflavin in the binary mixtures.

Owing to its poor solubility in hydrophobic solvents, RF's solubility in pure ethanol and binary ethanol/triacetin mixtures was below the solubility of RF in pure water, see Figure 126 and Figure 127. Above 60 wt.% triacetin, RF's solubility was beneath the detection limit of UV-Vis-spectroscopy. Thus, these points were not investigated. Nevertheless, a synergistic increase of RF's solubility was observed resulting in a maximum at 60-80 wt.% ethanol, see Figure 127. A minimum of the second order rate constant was also observed near 60-80 wt.% ethanol. A plot of the binary solvent's hydrogen bond donor/acceptor ratio shows that the ratio is 1-2 at this minimum, see Figure 127. Hence, a structural change of the hydrogen bonding network is probably the reason for the maximum solubility and minimum of the second order rate constant near 70 wt.% ethanol.

Thus, the optimum of RF's solubility in the binary ethanol-water system and in the ethanol/triacetin system coincides with an acceleration of RF's photodegradation. LC-MS analysis at the Central analytical department and UV-Vis-spectra revealed lumichrome as main photoproduct of RF in water, ethanol, in the binary water/ethanol mixtures, and in the binary ethanol/triacetin mixtures. The only difference was that CDRF was formed in pure water, while it was not detected via LC-MS in systems comprising ethanol. CDRF is formed via cycloaddition of RF's ribityl chain to the phenyl ring. As the orientation of the ribityl chain is decisive for the formation of CDRF, ethanol and triacetin certainly alter the hydrogen bonding network compared to pure water. Thus, the synergistic increase of RF's solubility and its destabilization are most probably both due to the alternation of the water's activity and of its hydrogen bond network.

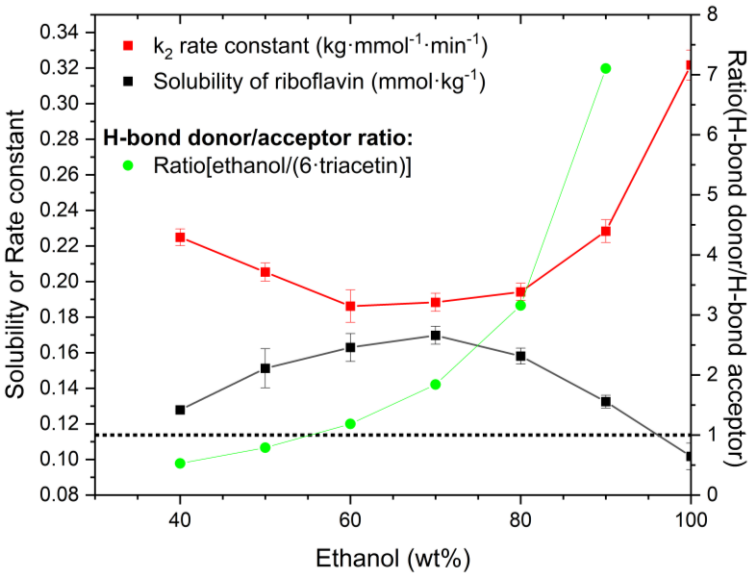

Figure 127: Solubility of riboflavin in binary ethanol/triacetin mixtures, second order rate constants for the photodegradation of riboflavin in the binary mixtures and molar ratio of ethanol triacetin, assuming 6 hydrogen bond acceptor possibilities on triacetin.

Because RF's solubility exhibited a synergistic increase in both binary systems, the solubility of RF was quantified in ternary mixtures along a constant water/ethanol ratio 50/50 (w/w) and then along a constant ethanol/triacetin ratio 60/40 (w/w), see Figure 128. As expected, judging from RF's rather polar structure, the solubility of this vitamin reached its maximum at high water content and ethanol content. Using the ternary water/ethanol/triacetin mixture of the composition 40/36/24 (w/w/w), a maximum solubility of RF 1.18 mmol·kg^{-1} (fractional solubility: 0.038 mol·mol^{-1}) was reached, corresponding to ca. 4.3 times (7.8 times higher regarding molar fractional solubility) water-solubility of RF. Although the ternary water/ethanol/triacetin solutions are completely food permitted, RF's solubility was increased only minorly. For a sufficiently yellow coloration of the final formulation, an increase of RF's solubility by the factor 50 would be required so that a 1:100 dilution with an aqueous solution would result in a beverage counting as alcohol-free in the European Union (≤ 0.5 vol.%). Hence, water/ethanol/triacetin systems can be used only for alcoholic formulations.

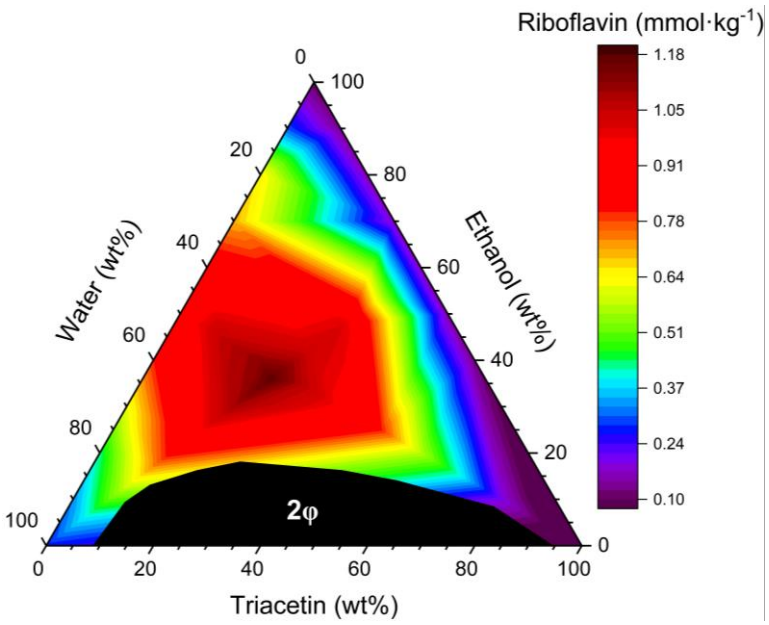

Figure 128: Solubility of riboflavin in the ternary water/ethanol/triacetin system.

5 Conclusion and Outlook

In this research, sodium salts of aromatic carboxylic acids were introduced as versatile natural solubilizers. Aromatic sodium carboxylates can act as salting-in and -out agents in the (anti)hydrotrope range, which can be adjusted via modification of the aryl ring with methoxy and hydroxy groups. The salting-in/-out properties of aromatic sodium carboxylates were in agreement with the classical hydrotrope theory and independent of the hydrotrope's tendency to form self-assemblies.[33,233,250]

On top of that, polyphenolates constitute multifunctional solubilizers for aromatic, poorly water-soluble and partially lipophilic vitamins. Thus, polyphenolates accelerated the dissolution and increased the water-solubility of riboflavin, vitamin K3, and folic acid exponentially with the polyphenolate concentration. Especially in the case of RF, but also in the case of vitamin K3 and folic acid, the solubilization was strongly promoted by the type (mesomeric effect) and size of the conjugated electronic π-system of aromatic sodium carboxylates. Moreover, the aromatic bio-compounds RF, lumichrome, RF-PO_4, vitamin K3 and folic acid underwent copigmentation with aromatic sodium carboxylates. The more electron-rich the solubilizer was, the stronger was the bathochromic shift of the absorption spectrum of the solutes, suggesting HOMO-LUMO interactions of sodium polyphenolates with the latter aromatic solutes. As the copigmentation was reversible upon simple dilution with water, the interactions of aromatic sodium carboxylates and the tested aromatic solutes can be considered as rather weak.
Further investigations with DLS and surface tension measurements on the solubilizing mechanism of RF ruled out the presence of larger aggregates and structuring. NMR analysis pointed to direct proximity of the solutes to the aromatic sodium carboxylates in aqueous solution suggesting π-complexation of RF, vitamin K3 and folic acid with aromatic sodium carboxylates. According to solubility and NMR measurements, the complexation of RF/RF-PO_4 and aromatic sodium carboxylates induced a mutual hydration. Additionally, NMR results suggested also a curved ribityl side chain of RF and RF-PO_4 in the presence of aromatic sodium carboxylates. Indications for a curved ribityl side chain of RF in pure water were not found. Solubilization experiments with RF, RF-PO_4 and LC proofed that sterics influence the solubilizing power of aromatic sodium carboxylates. Thus, a π-stacking induced change of the ribityl chain's conformation might also contribute to the strong influence of the solubilizer's efficiency on the water-solubility of RF. An alternation of the ribityl side chain conformation upon π-stacking of RF and aromatic sodium carboxylates could be also one reason for the mutual solubilization and for the improved hydration of RF and its solubilizers, when being dissolved together.

Sodium ferulate and 3,4-dimethoxycinnamate turned out to be the best and most efficient solubilizers for RF, vitamin K3 and folic acid. Using 0.37 $mol \cdot kg^{-1}$ sodium ferulate and

1.30 mol·kg^{-1} 3,4-dimethoxycinnamate, a water-solubility of RF of 60 ± 1 mmol·kg^{-1} and 225 ± 7 mmol·kg^{-1} at a molar solubilizer/RF ratio of 6.2 and 5.8, respectively, could be maintained stable against precipitation for several months. Accepting a minorly worse molar solubilizer/RF ratio, the solubility of RF could be increased by more than 2000 times (560 ± 20 mmol·kg^{-1}, ratio 7.8) using 4.34 mol·kg^{-1} sodium 3,4-dimethoxycinnamate.

The water-solubility of vitamin K3 rose from 0.68 ± 0.03 mmol·kg^{-1} to 19.2 ± 1.5 mmol·kg^{-1} and 263 ± 23 mmol·kg^{-1} using 0.37 mol·kg^{-1} sodium ferulate and 3.00 mol·kg^{-1} 3,4-dimethoxy-cinnamate, respectively. The water-solubility of folic acid could be increased 2000 times (50 ± 4 mmol·kg^{-1}, molar ferulate/folic acid ratio of 7.2) using 0.37 mol·kg^{-1} sodium ferulate. However, probably due to steric hindrance, 3,4-dimethoxycinnamate solubilized folic acid only half as efficiently as ferulate.

Thus, the size of the solubilizer's hydrophobic moiety was less important than the conjugated electronic system for the solubilization of RF. In contrast, the solubilizer's amphiphilicity was more significant for the solubilization of vitamin K3 and even more in the case of folic acid. Nevertheless, sodium ferulate was one of the best solubilizers for all three vitamins.

RF undergoes fast photodegradation, whereby 0.27 ± 0.02 mmol·kg^{-1} RF can be destroyed within 1 day in pure water. Thus, aromatic sodium carboxylates as well-known radical scavengers were tested as potential photostabilizing agents for RF. In diluted solutions of aromatic sodium carboxylates comprising 48 mg·kg^{-1} RF near the limitation for non-alcoholic beverages, RF's photodegradation was retarded by OH-and OMe-substituted benzoates and cinnamates (molar stabilizer/RF ratio 6 < 25 < 50). Cinnamate derivatives retarded RF's photodegradation up to 3-4 times relatively to RF in pure water. Substituted benzoates retarded the degradation only up to 2-2.7 times. RF's photodegradation in the diluted polyphenolate samples was consistent with the antioxidant and radical scavenging properties of polyphenolic acids.[84] At comparable molar stabilizer/RF ratios as in the diluted systems, high concentrations of polyphenolates (>0.3 mol·kg^{-1}) stabilized RF against photodegradation for several weeks. Counterintuitively, sodium and choline cinnamate stabilized RF in water when applied at high concentrations but destabilized RF in diluted cinnamate solutions. Thus, the photostabilizing mechanism in the concentrated polyphenolate/RF solutions cannot be the same as the one in the diluted ones. Nevertheless, the oxygen content in the samples comprising aromatic sodium carboxylates was independent of their photostabilization of RF in the diluted as well as in the concentrated regime. Additionally, sodium cinnamate possesses neither antioxidant nor radical scavenging properties. Therefore, a reason for the unexpectedly strong photostabilizing effect of cinnamate and for the stronger photostabilizing effect of polyphenolates in the concentrated samples might be π-stacking.

Regarding this concentration dependent solubilization and stabilization of RF and the π-interactions with aromatic sodium carboxylates, the action of polyphenolates might even go

beyond their potential competitive action to apoproteins of enzyme, which originates from the interaction of the phenolic OH-groups with flavin adenine dinucleotide.[127,174] As the redox potential of flavins depends strongly on the intermolecular interactions with other molecules, such as stacking, hydrophobic effects, hydrogen bonding and other electrostatic interactions, aromatic sodium carboxylates might be crucial participants in the regulation of RF's redox potential and thus help to control RF's reactivity in biological systems.[62]
Moreover, the concentration dependent photostabilization of RF might be advantageous for the stabilization of RF during storage as RF's degradability could be reactivated simply via dilution after digestion or injection in the blood.
The photostabilization of RF may be also used to prevent the photosensitization of other compounds by RF, which might cause an off-flavor or alter the color of products.[10] As RF is also used commonly as coloring agent, most sodium polyphenolates constitute a non-toxic, natural, green and cheap alternative to stabilize RF against precipitation and to preserve its color and vitamin function for a longer period of time.
However, in the case of vitamin K3, polyphenolates can be only used for the stabilization of higher concentrations of the vitamin and not for its photostabilization.

As counterpart to the inorganic sodium, the solubility enhancement of RF by polyphenolates was also monitored in presence of the strongly hydrated choline as counterion. As a nutraceutical, choline could upgrade food, dietary supplement and pharmaceutical formulations. Being hygroscopic, choline polyphenolates exhibited a considerably higher water-solubility enabling a stronger absolute increase of RF's water-solubility. Choline polyphenolates solubilized RF following an almost identical electron-driven mechanism as sodium polyphenolates and were only minorly less efficient than the corresponding sodium salts. Thus, choline polyphenolates may constitute valuable solubilizers or dispersers for drugs.[267]

Moreover, RF, lumichrome, vitamin K3, and folic acid did not precipitate upon dilution of concentrated polyphenolate solutions saturated with these solutes, although the solubilizing power of polyphenolates decreased with decreasing polyphenolate concentration. Thus, polyphenolates might be used to accelerate the dissolution process of drugs by the dilution of pre-solubilized high concentrated polyphenolate/drug solutions.

Aside of sodium polyphenolates, other solubilizing techniques for RF were approached. Thus, π-stacking of RF with other RF molecules was attempted to be overcome using thermal disruption of the dispersive interactions. RF was solubilized in aqueous solutions of aromatic sodium carboxylates or SDS at 90 °C, in the hope that the high temperature would separate the RF molecules and that slow cooling to room temperature would result in a kinetic stabilization. In the presence of medium to well performing aromatic solubilizers, the solubility

of RF was not further increased by this thermal method. Yet, in presence of weak solubilizers (sodium 4-phenylbutyrate, 5-phenylvalerate and sodium dodecyl sulfate), RF's solubility could be increased by 2-3 times being stable against precipitation for at least 1 week. Still, medium and well performing aromatic sodium carboxylates solubilized several times more RF when saturating at 23 °C than when applying the thermal solubilization in the presence of weak RF solubilizers. Thus, from an applicative view thermal disruption of the attractive interactions between RF molecules was too inefficient and not further investigated.

Moreover, other natural aromatic and hydrotropic non-aromatic compounds were found to improve riboflavin's water-solubility. However, except for L-tryptophan and indoxyl sulfate, none of the potential solubilizers could keep up with the strong solubilizing power of sodium polyphenolates. Nevertheless, the commonly used food additives saccharine, caffeine, L-proline, L-histidine and fructose can be used to solubilize riboflavin in beverages and food. Especially, fructose constitutes a great alternative solubilizer for RF, as fructose concentrations similar to the ones in juices improved RF's water-solubility by 24 %.

Although π-stacking of RF with other RF molecules in its crystalline form was revealed to be the main solubility determining factor, the salting-in and -out effect of sodium thiocyanate and sodium dihydrogen phosphate, respectively, indicated that hydrogen bonding can influence RF's water-solubility. A possibility to act on the ribityl chain conformation is the alternation of the solvent's hydrogen bond network. Therefore, the solubility of riboflavin in the ternary water/ethanol/triacetin mixture was measured to see, if only simple changes in the hydrogen bonding capacity and polarity of the solvent can improve riboflavin's solubility comparably to polyphenolates. However, RF's solubility was increased only by 4.3 times in a water/ethanol/triacetin 40/36/24 (w/w/w) solution. In consideration of the limitation of riboflavin for non-alcoholic beverages and its color intensity, even upon dilution, this RF concentrate cannot be categorized as alcohol-free. Although this formulation would be applicable for the stabilization of yellow coloration in alcoholic beverages, riboflavin's photodegradation kinetics is increased by one or two orders in ethanol/triacetin formulations compared to pure water.

Consequently, currently, polyphenolates are undisputedly the best solubilizers for riboflavin in aqueous solutions.

As sodium polyphenolates solubilized also caffeine and even minor amounts of the water-insoluble curcumin, they can be seen as general solubilizers for aromatic compounds. Hence, the compatibility of the widely applied drugs RF, vitamin K3, folic acid caffeine in a 0.37 $mol \cdot kg^{-1}$ sodium ferulate solution was tested to see if the aromatic drugs compete for the solubilizer. Indeed, the solubility of RF and folic acid in an aqueous 0.37 $mol \cdot kg^{-1}$ sodium ferulate solution was reduced in the presence of caffeine, vitamin K3, and folic acid or RF, respectively. On the contrary, 16 % more vitamin K3 and 179 % more caffeine were soluble in the sodium ferulate solution comprising RF, folic acid, caffeine, and vitamin K3 than in absence

of other drugs. Saturation of a 0.37 mol·kg^{-1} sodium ferulate solution with the four drugs simultaneously enabled to dissolve > 50 times more RF, > 1660 times more folic acid, 8 times more caffeine, and 78 times more vitamin K3 than in pure water. Thus, despite a similar solubilizing mechanism of sodium ferulate in the solubilization of the four drugs, RF, vitamin K3, folic acid, and caffeine could be solubilized in the aqueous sodium ferulate solution largely over their solubility in pure water. Consequently, sodium polyphenolates might be even applied to prepare solutions composed of several poorly aromatic solutes, which are dissolved via complexation with the polyphenolate. Thereby, the observation of facilitated hydrotropy of sodium ferulate with vitamin K3 and caffeine, showed that the two solutes might even act as each other's co-solubilizer – presumably also due to complexation. This might be useful for pharmaceutical medication and for multivitamin supplements, where a low solubilizer content is desired.

Additionally, the polyphenolate, sodium ferulate, turned out to have cosurfactive properties enhancing the structuring in an aqueous SDS solution, decreasing the CMC of SDS, reducing the onset of the solubilization of the hydrophobic aromatic dye Sudan blue II and increasing the water-solubility of the dye. Moreover, sodium ferulate's cosurfactive action was found to be compatible with its action as complexation agent for the aromatic solute RF. Although the presence of SDS and of the hydrophobic dye reduced the solubility of RF in aqueous ferulate solutions, RF's water-solubility was still more than 100 times surpassed. According to El-Khordagui, sodium salicylate exhibited a similar effect on SDS as sodium ferulate, which showed a dependence of the self-association of SDS on the concentration of the aromatic cosurfactant.[321] Thus, the synergy of sodium ferulate and SDS might be even stronger for distinct molar ratios of the two solubilizers.
The biological emulsifier sodium cholate, which is less amphiphilic and more rigid than SDS, was less compatible with sodium ferulate, as sodium ferulate and sodium cholate deteriorated each other's solubilizing power on Sudan blue II and RF, respectively. Nevertheless, sodium ferulate reduced the CAC of cholate and increased the structuring slightly. Hence, future studies should also investigate the cosurfactive action of aromatic sodium carboxylates on the self-aggregation of surfactants depending on their amphiphilicity and rigidity.

Undisputedly, sodium polyphenolates are green, natural, non-toxic, potentially edible, photostabilizing and cheap solubilizers offering the action as salting-in/-out agents in the (anti-)hydrotrope range, the action as π-complexation-driven solubilizers and the action as cosurfactive supporters of other solubilizers. The broad (co)solubilizing modes of aromatic carboxylic acids might be the reason for the widespread of these biological compounds in the plant kingdom, where they constitute an important role in allelopathy and plant defense.[68–70] Their versatile solubilizing properties might also be the reason for their sundry nutraceutical

effects.[19,79,80] Thus, such as salting-in acting superchaotropic boron clusters were proofed to act as membrane carriers, due to their salting-in/-out properties, sodium polyphenolates might support the transport of target molecules through membranes.[251] Moreover, the similar salting-in power of sodium cinnamate, salicylate and o-coumarate to the biological emulsifier cholate, indicates a function of these three carboxylate salts as biological dispersants.[252] Regarding additionally the effect of aromatic sodium carboxylates on the cloud point of water/DPnP mixtures and the potential importance of polyphenolates and other aromatic sodium carboxylates as bio-solubilizers, a change of the environmental temperature might have a considerable influence on the solution chemistry in biological systems.[233]

Further, the strong effect of aromatic carboxylates on the water-solubility of RF, RF-PO_4, LC, vitamin K3, folic acid, and caffeine and the acceleration of the aromatic solute's dissolution by aromatic carboxylates indicate that aromatic carboxylates might influence the bioavailability of other biological aromatic compounds, too. Their solubilizing power could be altered via changes in the pH value or by the transformation of polyphenolates into other metabolites.[65,100–102] Future research should focus on the importance of the salting-in and -out actions of aromatic carboxylate in biological systems near to membranes, on the interaction of aromatic solutes with sodium carboxylates in cells and on the effect of aromatic sodium carboxylates on the surfactive and hydrotropic action of biological surfactants and hydrotropes.

Major outcome:

- Aromatic sodium carboxylates were found to have salting-in/-out, hydrotropic, and cosurfactive properties in aqueous solution.
- Although the salting-in/-out properties on DPnP are dominated by the polyphenolate's amphiphilic character, aggregation was refuted. Specific molecular interactions are responsible for the salting-in/-out effect of polyphenolates on DPnP. Two polyphenolates were even comparable to a biological emulsifier.
- The hydrotropic properties of polyphenolates enabled to increase the water-solubility of aromatic solutes (riboflavin, RF-PO_4, lumichrome, vitamin K3, folic acid, caffeine, curcumin) considerably due to π-complexation. Facilitated hydrotropy was observed when solubilizing vitamin K3 and caffeine together in presence of one polyphenolate. Still, in mixtures of several aromatic solutes, some solutes compete for the polyphenolate.
- In the particular case of riboflavin, polyphenolate-riboflavin complexes were found to be more hydrophilic than the biocompounds alone. Aside of the complexation, a reason therefore might be the observed alternation of the average ribityl chain conformation by polyphenolates.

  Simultaneously, polyphenolates photostabilized riboflavin at low as well as high concentrations of both polyphenolates and riboflavin. Riboflavin's photostabilization was found to underly a distinct mechanism in the "diluted" and "concentrated" regime and did not considerably depend on the antioxidant properties of polyphenolates. In the diluted regime the photostabilization was provided by radical scavenging. In the concentrated regime the photostabilization might originate from the π-stacking and change of the ribityl chain conformation.
- The common polyphenolate – sodium ferulate – was exposed as cosurfactant for sodium dodecyl sulfate solution as ferulate promoted the structuring of the surfactant in aqueous solution, decreased its CMC, and increased the water-solubility of a hydrophobic solute. Although sodium cholate's CAC was reduced by sodium ferulate, too, the low effect on its structuring and reduction of the water-solubility of the hydrophobic dye refuted a significant cosurfactive action of the polyphenolate in presence of the bio-solubilizer.
- Moreover, sodium polyphenolates can act as cosurfactant and π-complexing hydrotrope simultaneously but the mechanisms are competitive.
- Besides this, several other hydrotropes and techniques were tested to improve riboflavin's water-solubility. The major solubility limiting factor of riboflavin was exposed to be its aggregation. Nevertheless, modification of the hydrogen bond possibilities can slightly improve riboflavin's water-solubility.

6 References

(1) Bitsch, I.; Bitsch, R. Riboflavin: Properties and Determination. In *Encyclopedia of Food and Health*; Elsevier, 2016; pp 633–640. https://doi.org/10.1016/B978-0-12-384947-2.00593-6.

(2) Boehnke, C.; Reuter, U.; Flach, U.; Schuh-Hofer, S.; Einhaupl, K. M.; Arnold, G. High-Dose Riboflavin Treatment Is Efficacious in Migraine Prophylaxis: An Open Study in a Tertiary Care Centre. *Eur. J. Neurol.* **2004**, *11* (7), 475–477. https://doi.org/10.1111/j.1468-1331.2004.00813.x.

(3) Organisation Mondiale de la Santé. Codex Alimentarius; 2015; pp 216–218.

(4) Suwannasom, N.; Kao, I.; Pruß, A.; Georgieva, R.; Bäumler, H. Riboflavin: The Health Benefits of a Forgotten Natural Vitamin. *Int. J. Mol. Sci.* **2020**, *21* (3), 950. https://doi.org/10.3390/ijms21030950.

(5) Marashly, E. T.; Bohlega, S. A. Riboflavin Has Neuroprotective Potential: Focus on Parkinson's Disease and Migraine. *Front. Neurol.* **2017**, *8*. https://doi.org/10.3389/fneur.2017.00333.

(6) Averianova, L. A.; Balabanova, L. A.; Son, O. M.; Podvolotskaya, A. B.; Tekutyeva, L. A. Production of Vitamin B2 (Riboflavin) by Microorganisms: An Overview. *Front. Bioeng. Biotechnol.* **2020**, *8*. https://doi.org/10.3389/fbioe.2020.570828.

(7) Berry Ottaway, P. Chemical and Physical Characteristics of Vitamins. *Technol. Vitam. food* **1993**, 246–260.

(8) Sheraz, M. A.; Kazi, S. H.; Ahmed, S.; Anwar, Z.; Ahmad, I. Photo, Thermal and Chemical Degradation of Riboflavin. *Beilstein J. Org. Chem.* **2014**, *10*, 1999–2012. https://doi.org/10.3762/bjoc.10.208.

(9) Lu, C.; Lin, W.; Wang, W.; Han, Z.; Yao, S.; Lin, N. Riboflavin (VB2) Photosensitized Oxidation of 2′-Deoxyguanosine-5′-Monophosphate (DGMP) in Aqueous Solution: A Transient Intermediates Study. *Phys. Chem. Chem. Phys.* **2000**, *2* (3), 329–334. https://doi.org/10.1039/a908492d.

(10) Cardoso, D. R.; Olsen, K.; Møller, J. K. S.; Skibsted, L. H. Phenol and Terpene Quenching of Singlet- and Triplet-Excited States of Riboflavin in Relation to Light-Struck Flavor Formation in Beer. *J. Agric. Food Chem.* **2006**, *54* (15), 5630–5636. https://doi.org/10.1021/jf060750d.

(11) Rao, J.; McClements, D. J. Food-Grade Microemulsions, Nanoemulsions and Emulsions: Fabrication from Sucrose Monopalmitate & Lemon Oil. *Food Hydrocoll.* **2011**, *25* (6), 1413–1423. https://doi.org/10.1016/j.foodhyd.2011.02.004.

(12) Rao, J.; McClements, D. J. Food-Grade Microemulsions and Nanoemulsions: Role of Oil Phase Composition on Formation and Stability. *Food Hydrocoll.* **2012**, *29* (2), 326–

334. https://doi.org/10.1016/j.foodhyd.2012.04.008.

(13) Degot, P.; Huber, V.; Hofmann, E.; Hahn, M.; Touraud, D.; Kunz, W. Solubilization and Extraction of Curcumin from Curcuma Longa Using Green, Sustainable, and Food-Approved Surfactant-Free Microemulsions. *Food Chem.* **2021**, *336*, 127660. https://doi.org/10.1016/j.foodchem.2020.127660.

(14) Rupp, C. Neue Mischmizellare Systeme Auf Basis von Phospholipiden Zur Solubilisierung Schlecht Wasserlöslicher Arzneistoffe, Christian-Albrechts-Universität, 2010.

(15) Aarabi, A.; Mizani, M.; Honarvar, M.; Faghihian, H.; Gerami, A. Extraction of Ferulic Acid from Sugar Beet Pulp by Alkaline Hydrolysis and Organic Solvent Methods. *J. Food Meas. Charact.* **2016**, *10* (1), 42–47. https://doi.org/10.1007/s11694-015-9274-z.

(16) Shahidi, F.; Ambigaipalan, P. Phenolics and Polyphenolics in Foods, Beverages and Spices: Antioxidant Activity and Health Effects – A Review. *J. Funct. Foods* **2015**, *18*, 820–897. https://doi.org/10.1016/j.jff.2015.06.018.

(17) Clifford, M. N. Chlorogenic Acids and Other Cinnamates - Nature, Occurrence and Dietary Burden. *J. Sci. Food Agric.* **1999**, *79* (3), 362–372. https://doi.org/10.1002/(SICI)1097-0010(19990301)79:3<362::AID-JSFA256>3.0.CO;2-D.

(18) Xu, G.; Ye, X.; Liu, D.; Ma, Y.; Chen, J. Composition and Distribution of Phenolic Acids in Ponkan (Citrus Poonensis Hort. Ex Tanaka) and Huyou (Citrus Paradisi Macf. Changshanhuyou) during Maturity. *J. Food Compos. Anal.* **2008**, *21* (5), 382–389. https://doi.org/10.1016/j.jfca.2008.03.003.

(19) Kumar, N.; Goel, N. Phenolic Acids: Natural Versatile Molecules with Promising Therapeutic Applications. *Biotechnol. Reports* **2019**, *24*. https://doi.org/10.1016/j.btre.2019.e00370.

(20) Authority, E. F. S. Scientific Opinion on Flavouring Group Evaluation 20, Revision 4 (FGE.20Rev4): Benzyl Alcohols, Benzaldehydes, a Related Acetal, Benzoic Acids, and Related Esters from Chemical Groups 23 and 30. *EFSA J.* **2012**, *10* (12), 1–140. https://doi.org/10.2903/j.efsa.2012.2994.

(21) TCI. *trans-Ferulic Acid*. https://www.tcichemicals.com/DE/de/p/H0267 (accessed 2022-08-04).

(22) TCI. *3,4-Dimethoxycinnamic Acid*. https://www.tcichemicals.com/DE/de/p/D1728 (accessed 2022-08-04).

(23) TCI. *trans-Cinnamic Acid*. https://www.tcichemicals.com/DE/de/p/C3412 (accessed 2022-08-04).

(24) Anastas, P. T.; Warner, J. C. *Green Chemistry: Theory and Practice*, 1st ed.; Oxford University Press: Oxford, 1998.

(25) Tanaka, K.; Kaupp, G. *Solvent-Free Organic Synthesis*; Wiley-VCH: Weinheim, 2009.

(26) Moity, L.; Durand, M.; Benazzouz, A.; Pierlot, C.; Molinier, V.; Aubry, J. M. Panorama of Sustainable Solvents Using the COSMO-RS Approach. *Green Chem.* **2012**, *14* (4), 1132–1145. https://doi.org/10.1039/c2gc16515e.

(27) Cox, S.; Sandall, A.; Smith, L.; Rossi, M.; Whelan, K. Food Additive Emulsifiers: A Review of Their Role in Foods, Legislation and Classifications, Presence in Food Supply, Dietary Exposure, and Safety Assessment. *Nutr. Rev.* **2021**, *79* (6), 726–741. https://doi.org/10.1093/nutrit/nuaa038.

(28) World Health Organization. Codex Alimentarius. In *General Standard for Food Additives*; 2021; pp 216–219.

(29) Kunz, W.; Holmberg, K.; Zemb, T. Hydrotropes. *Curr. Opin. Colloid Interface Sci.* **2016**, *22*, 99–107. https://doi.org/10.1016/j.cocis.2016.03.005.

(30) Larcinese-Hafner, V.; Tchakalova, V. Co-Surfactant, Co-Solvent, and Hydrotropic Properties of Some Common Cooling Agents. *Flavour Fragr. J.* **2018**, *33* (4), 303–312. https://doi.org/10.1002/ffj.3449.

(31) Ivanković, T.; Hrenović, J. Surfactants in the Environment. *Arch. Ind. Hyg. Toxicol.* **2010**, *61* (1), 95–110. https://doi.org/10.2478/10004-1254-61-2010-1943.

(32) Kapadiya, N.; Indrajeet, S.; Kushboo, M.; Gauri, K.; Sen, D. Hydrotropy: A Promising Tool for Solubility Enhancement: A Review. *Int. J. Drug Dev. Res.* **2011**, *3* (2), 26–33.

(33) Shimizu, S.; Matubayasi, N. Hydrotropy: Monomer-Micelle Equilibrium and Minimum Hydrotrope Concentration. *J. Phys. Chem. B* **2014**, *118* (35), 10515–10524. https://doi.org/10.1021/jp505869m.

(34) Hopkins Hatzopoulos, M.; Eastoe, J.; Dowding, P. J.; Rogers, S. E.; Heenan, R.; Dyer, R. Are Hydrotropes Distinct from Surfactants? *Langmuir* **2011**, *27* (20), 12346–12353. https://doi.org/10.1021/la2025846.

(35) Das, S.; Paul, S. Hydrotropic Solubilization of Sparingly Soluble Riboflavin Drug Molecule in Aqueous Nicotinamide Solution. *J. Phys. Chem. B* **2017**, *121* (37), 8774–8785. https://doi.org/10.1021/acs.jpcb.7b05774.

(36) Casey, D.; Charalambous, K.; Gee, A.; Law, R. V.; Ces, O. Amphiphilic Drug Interactions with Model Cellular Membranes Are Influenced by Lipid Chain-Melting Temperature. *J. R. Soc. Interface* **2014**, *11* (94), 20131062. https://doi.org/10.1098/rsif.2013.1062.

(37) Subbarao, C. V.; Chakravarthy, I. P. K.; Sai Bharadwaj, A. V. S. L.; Prasad, K. M. M. Functions of Hydrotropes in Solutions. *Chem. Eng. Technol.* **2012**, *35* (2), 225–237. https://doi.org/10.1002/ceat.201100484.

(38) Abranches, D. O.; Benfica, J.; Soares, B. P.; Leal-Duaso, A.; Sintra, T. E.; Pires, E.; Pinho, S. P.; Shimizu, S.; Coutinho, J. A. P. Unveiling the Mechanism of Hydrotropy: Evidence for Water-Mediated Aggregation of Hydrotropes around the Solute. *Chem. Commun.* **2020**, *56* (52), 7143–7146. https://doi.org/10.1039/D0CC03217D.

(39) Klossek, M. L.; Touraud, D.; Kunz, W. Eco-Solvents – Cluster-Formation, Surfactantless Microemulsions and Facilitated Hydrotropy. *Phys. Chem. Chem. Phys.* **2013**, *15* (26), 10971. https://doi.org/10.1039/c3cp50636c.

(40) Hofmeister, F. Arbeiten Aus Dem Pharmakologisehen Institut Der Deutschen Universität Zu Prag. 12. Zur Lehre von Der Wirkung Der Salze. *Arch Exp Pathol Pharmakol* **1888**, *25* (Dritte Mitteilung), 1–30.

(41) Assaf, K. I.; Nau, W. M. Der Chaotrope Effekt Als Aufbaumotiv in Der Chemie. *Angew. Chemie* **2018**, *130* (43), 14164–14177. https://doi.org/10.1002/ange.201804597.

(42) Mehringer, J.; Hofmann, E.; Touraud, D.; Koltzenburg, S.; Kellermeier, M.; Kunz, W. Salting-in and Salting-out Effects of Short Amphiphilic Molecules: A Balance between Specific Ion Effects and Hydrophobicity. *Phys. Chem. Chem. Phys.* **2021**, *23* (2), 1381–1391. https://doi.org/10.1039/D0CP05491G.

(43) Gibb, B. C. Hofmeister's Curse. *Nat. Chem.* **2019**, *11* (11), 963–965. https://doi.org/10.1038/s41557-019-0355-1.

(44) Collins, K. Ions from the Hofmeister Series and Osmolytes: Effects on Proteins in Solution and in the Crystallization Process. *Methods* **2004**, *34* (3), 300–311. https://doi.org/10.1016/j.ymeth.2004.03.021.

(45) Ball, P.; Hallsworth, J. E. Water Structure and Chaotropicity: Their Uses, Abuses and Biological Implications. *Phys. Chem. Chem. Phys.* **2015**, *17* (13), 8297–8305. https://doi.org/10.1039/C4CP04564E.

(46) Buchecker, T.; Schmid, P.; Renaudineau, S.; Diat, O.; Proust, A.; Pfitzner, A.; Bauduin, P. Polyoxometalates in the Hofmeister Series. *Chem. Commun.* **2018**, *54*, 1833–1836. https://doi.org/10.1039/C7CC09113C.

(47) Marcus, Y. Effect of Ions on the Structure of Water: Structure Making and Breaking. *Chem. Rev.* **2009**, *109* (3), 1346–1370. https://doi.org/10.1021/cr8003828.

(48) Okur, H. I.; Hladílková, J.; Rembert, K. B.; Cho, Y.; Heyda, J.; Dzubiella, J.; Cremer, P. S.; Jungwirth, P. Beyond the Hofmeister Series: Ion-Specific Effects on Proteins and Their Biological Functions. *J. Phys. Chem. B* **2017**, *121* (9), 1997–2014. https://doi.org/10.1021/acs.jpcb.6b10797.

(49) Kang, B.; Tang, H.; Zhao, Z.; Song, S. Hofmeister Series: Insights of Ion Specificity from Amphiphilic Assembly and Interface Property. *ACS Omega* **2020**, *5* (12), 6229–6239. https://doi.org/10.1021/acsomega.0c00237.

(50) Zhang, Y.; Cremer, P. Interactions between Macromolecules and Ions: The Hofmeister Series. *Curr. Opin. Chem. Biol.* **2006**, *10* (6), 658–663. https://doi.org/10.1016/j.cbpa.2006.09.020.

(51) Grundl, G.; Müller, M.; Touraud, D.; Kunz, W. Salting-out and Salting-in Effects of Organic Compounds and Applications of the Salting-out Effect of Pentasodium Phytate in Different Extraction Processes. *J. Mol. Liq.* **2017**, *236*, 368–375.

https://doi.org/10.1016/j.molliq.2017.03.091.

(52) Bauduin, P.; Wattebled, L.; Schrödle, S.; Touraud, D.; Kunz, W. Temperature Dependence of Industrial Propylene Glycol Alkyl Ether/Water Mixtures. *J. Mol. Liq.* **2004**, *115* (1), 23–28. https://doi.org/10.1016/j.molliq.2004.01.001.

(53) McGaughey, G. B.; Gagné, M.; Rappé, A. K. π-Stacking Interactions. *J. Biol. Chem.* **1998**, *273* (25), 15458–15463. https://doi.org/10.1074/jbc.273.25.15458.

(54) Hunter, C. A.; Sanders, J. K. M. The Nature of Pi-Pi Interactions. *J. Am. Chem. Soc.* **1990**, *112* (14), 5525–5534. https://doi.org/10.1021/ja00170a016.

(55) Sinnokrot, M. O.; Sherrill, C. D. Unexpected Substituent Effects in Face-to-Face π-Stacking Interactions. *J. Phys. Chem. A* **2003**, *107* (41), 8377–8379. https://doi.org/10.1021/jp030880e.

(56) Hohenstein, E. G.; Duan, J.; Sherrill, C. D. Origin of the Surprising Enhancement of Electrostatic Energies by Electron-Donating Substituents in Substituted Sandwich Benzene Dimers. *J. Am. Chem. Soc.* **2011**, *133* (34), 13244–13247. https://doi.org/10.1021/ja204294q.

(57) Wheeler, S. E.; Houk, K. N. Substituent Effects in the Benzene Dimer Are Due to Direct Interactions of the Substituents with the Unsubstituted Benzene. *J. Am. Chem. Soc.* **2008**, *130* (33), 10854–10855. https://doi.org/10.1021/ja802849j.

(58) Chen, T.; Li, M.; Liu, J. π–π Stacking Interaction: A Nondestructive and Facile Means in Material Engineering for Bioapplications. *Cryst. Growth Des.* **2018**, *18* (5), 2765–2783. https://doi.org/10.1021/acs.cgd.7b01503.

(59) Martinez, C. R.; Iverson, B. L. Rethinking the Term “Pi-Stacking.” *Chem. Sci.* **2012**, *3* (7), 2191. https://doi.org/10.1039/c2sc20045g.

(60) Datta, S.; Mukhopadhyay, C.; Bose, S. K. Molecular Complex Formation between Riboflavin and Salicylate in an Aqueous Medium. *Bull. Chem. Soc. Jpn.* **2003**, *76* (9), 1729–1734. https://doi.org/10.1246/bcsj.76.1729.

(61) Xiaoxiao, F.; Li, J.-F.; Zhang, R.-Q. Strong Orbital Interaction in Pi-Pi Stacking System. **2016**.

(62) Henriques, B. Riboflavin and β-Oxidation Flavoenzymes. In *B Vitamins and Folate: Chemistry, Analysis, Function and Effects*; Preedy, V. R., Ed.; Royal Society of Chemistry, 2012; pp 611–632. https://doi.org/10.1039/9781849734714.

(63) Schefer, S.; Oest, M.; Rohn, S. Interactions between Phenolic Acids, Proteins, and Carbohydrates—Influence on Dough and Bread Properties. *Foods* **2021**, *10* (11), 2798. https://doi.org/10.3390/foods10112798.

(64) Strack, D. *Plant Biochemistry, Phenolic Metabolism*, Harborne.; Academic: London, 1997.

(65) Anantharaju, P. G.; Gowda, P. C.; Vimalambike, M. G.; Madhunapantula, S. V. An Overview on the Role of Dietary Phenolics for the Treatment of Cancers. *Nutr. J.*

2016, *15* (1), 99. https://doi.org/10.1186/s12937-016-0217-2.

(66) *Plant Physiological Aspects of Phenolic Compounds*; Soto-Hernández, M., García-Mateos, R., Palma-Tenango, M., Eds.; IntechOpen, 2019. https://doi.org/10.5772/intechopen.77494.

(67) Grzegorczyk, I.; Królicka, A.; Wysokińska, H. Establishment of Salvia Officinalis L. Hairy Root Cultures for the Production of Rosmarinic Acid. *Zeitschrift für Naturforsch. C* **2006**, *61* (5–6), 351–356. https://doi.org/10.1515/znc-2006-5-609.

(68) Lyu, S.-W.; Blum, U.; Gerig, T. M.; O'Brien, T. E. Effects of Mixtures of Phenolic Acids on Phosphorus Uptake by Cucumber Seedlings. *J. Chem. Ecol.* **1990**, *16* (8), 2559–2567. https://doi.org/10.1007/BF01017478.

(69) Hättenschwiler, S.; Vitousek, P. M. The Role of Polyphenols in Terrestrial Ecosystem Nutrient Cycling. *Trends Ecol. Evol.* **2000**, *15* (6), 238–243. https://doi.org/10.1016/S0169-5347(00)01861-9.

(70) Chan, Y.-K. Utilization of Simple Phenolics for Dinitrogen Fixation by Soil Diazotrophic Bacteria. *Plant Soil* **1986**, *90* (1–3), 141–150. https://doi.org/10.1007/BF02277393.

(71) Brenes-Balbuena, M.; Garcia-Garcia, P.; Garrido-Fernandez, A. Phenolic Compounds Related to the Black Color Formed during the Processing of Ripe Olives. *J. Agric. Food Chem.* **1992**, *40* (7), 1192–1196. https://doi.org/10.1021/jf00019a023.

(72) Tan, S. C. Determinants of Eating Quality in Fruit and Vegetables; Nutrition Society of Australia: Kent Town, Australia, 2000; Vol. 24, pp 183–190.

(73) Bonanno, A.; Di Grigoli, A.; Todaro, M.; Alabiso, M.; Vitale, F.; Di Trana, A.; Giorgio, D.; Settanni, L.; Gaglio, R.; Laddomada, B.; Di Miceli, G. Improvement of Oxidative Status, Milk and Cheese Production, and Food Sustainability Indexes by Addition of Durum Wheat Bran to Dairy Cows' Diet. *Animals* **2019**, *9* (9), 698. https://doi.org/10.3390/ani9090698.

(74) Zhang, S.; Li, Y.; Li, L.; Wei, C.; You, J. Study of the Inhibitory Effect of Ferulic Acid on Short-Chain Fatty Acids in Milk Samples by Dispersive Liquid–Liquid Micro-Extraction in Combination with Fluorescence Derivatization. *J. Liq. Chromatogr. Relat. Technol.* **2017**, *40* (4), 184–189. https://doi.org/10.1080/10826076.2017.1296460.

(75) Hanhineva, K.; Törrönen, R.; Bondia-Pons, I.; Pekkinen, J.; Kolehmainen, M.; Mykkänen, H.; Poutanen, K. Impact of Dietary Polyphenols on Carbohydrate Metabolism. *Int. J. Mol. Sci.* **2010**, *11* (4), 1365–1402. https://doi.org/10.3390/ijms11041365.

(76) Vishnu Prasad, C. N.; Anjana, T.; Banerji, A.; Gopalakrishnapillai, A. Gallic Acid Induces GLUT4 Translocation and Glucose Uptake Activity in 3T3-L1 Cells. *FEBS Lett.* **2010**, *584* (3), 531–536. https://doi.org/10.1016/j.febslet.2009.11.092.

(77) Adisakwattana, S.; Sookkongwaree, K.; Roengsumran, S.; Petsom, A.; Ngamrojnavanich, N.; Chavasiri, W.; Deesamer, S.; Yibchok-anun, S. Structure–

Activity Relationships of Trans-Cinnamic Acid Derivatives on α-Glucosidase Inhibition. *Bioorg. Med. Chem. Lett.* **2004**, *14* (11), 2893–2896. https://doi.org/10.1016/j.bmcl.2004.03.037.

(78) Jed A. Riemer, Scarsdale, N. Y. Bitterness Inhibitors. 5,336,513, 1994.

(79) Kumar, N.; Pruthi, V.; Goel, N. Structural, Thermal and Quantum Chemical Studies of p-Coumaric and Caffeic Acids. *J. Mol. Struct.* **2015**, *1085*, 242–248. https://doi.org/10.1016/j.molstruc.2014.12.064.

(80) Saravanakumar, M.; Raja, B. Veratric Acid, a Phenolic Acid Attenuates Blood Pressure and Oxidative Stress in l-NAME Induced Hypertensive Rats. *Eur. J. Pharmacol.* **2011**, *671* (1–3), 87–94. https://doi.org/10.1016/j.ejphar.2011.08.052.

(81) Wang, H.; Cao, G.; Prior, R. L. Total Antioxidant Capacity of Fruits. *J. Agric. Food Chem.* **1996**, *44* (3), 701–705. https://doi.org/10.1021/jf950579y.

(82) Tsao, R.; Deng, Z. Separation Procedures for Naturally Occurring Antioxidant Phytochemicals. *J. Chromatogr. B* **2004**, *812* (1–2), 85–99. https://doi.org/10.1016/j.jchromb.2004.09.028.

(83) Giacomelli, C.; Miranda, F. da S.; Gonçalves, N. S.; Spinelli, A. Antioxidant Activity of Phenolic and Related Compounds: A Density Functional Theory Study on the O–H Bond Dissociation Enthalpy. *Redox Rep.* **2004**, *9* (5), 263–269. https://doi.org/10.1179/135100004225006038.

(84) Chen, J.; Yang, J.; Ma, L.; Li, J.; Shahzad, N.; Kim, C. K. Structure-Antioxidant Activity Relationship of Methoxy, Phenolic Hydroxyl, and Carboxylic Acid Groups of Phenolic Acids. *Sci. Rep.* **2020**, *10* (1), 2611. https://doi.org/10.1038/s41598-020-59451-z.

(85) Alcalde, B.; Granados, M.; Saurina, J. Exploring the Antioxidant Features of Polyphenols by Spectroscopic and Electrochemical Methods. *Antioxidants* **2019**, *8* (11), 523. https://doi.org/10.3390/antiox8110523.

(86) Aitipamula, S.; Das, S. Cocrystal Formulations: A Case Study of Topical Formulations Consisting of Ferulic Acid Cocrystals. *Eur. J. Pharm. Biopharm.* **2020**, *149*, 95–104. https://doi.org/10.1016/j.ejpb.2020.01.021.

(87) Friedman, M. Food Browning and Its Prevention: An Overview. *J. Agric. Food Chem.* **1996**, *44* (3), 631–653. https://doi.org/10.1021/jf950394r.

(88) Jilek, M. L.; Bunzel, M. Dehydrotriferulic and Dehydrodiferulic Acid Profiles of Cereal and Pseudocereal Flours. *Cereal Chem. J.* **2013**, *90* (5), 507–514. https://doi.org/10.1094/CCHEM-11-12-0144-R.

(89) Garcia-Conesa, M. T.; Plumb, G. W.; Kroon, P. A.; Wallace, G.; Williamson, G. Antioxidant Properties of Ferulic Acid Dimers. *Redox Rep.* **1997**, *3* (4), 239–244. https://doi.org/10.1080/13510002.1997.11747116.

(90) Shahidi, F.; Janitha, P. K.; Wanasundara, P. D. Phenolic Antioxidants. *Crit. Rev. Food Sci. Nutr.* **1992**, *32* (1), 67–103. https://doi.org/10.1080/10408399209527581.

(91) Riemer, J. A.; Scarsdale, N. Y. Bitterness Inhibitors. 5,336,513, 1994.

(92) Sathya, S.; Pandima Devi, K. The Use of Polyphenols for the Treatment of Alzheimer's Disease. In *Role of the Mediterranean Diet in the Brain and Neurodegenerative Diseases*; Elsevier, 2018; pp 239–252. https://doi.org/10.1016/B978-0-12-811959-4.00015-8.

(93) Sgarbossa, A.; Giacomazza, D.; Di Carlo, M. Ferulic Acid: A Hope for Alzheimer's Disease Therapy from Plants. *Nutrients* **2015**, *7* (7), 5764–5782. https://doi.org/10.3390/nu7075246.

(94) Kumar, N.; Pruthi, V. Potential Applications of Ferulic Acid from Natural Sources. *Biotechnol. Reports* **2014**, *4*, 86–93. https://doi.org/10.1016/j.btre.2014.09.002.

(95) Zduńska, K.; Dana, A.; Kolodziejczak, A.; Rotsztejn, H. Antioxidant Properties of Ferulic Acid and Its Possible Application. *Skin Pharmacol. Physiol.* **2018**, *31* (6), 332–336. https://doi.org/10.1159/000491755.

(96) Bezerra, G. S. N.; Pereira, M. A. V.; Ostrosky, E. A.; Barbosa, E. G.; de Moura, M. de F. V.; Ferrari, M.; Aragão, C. F. S.; Gomes, A. P. B. Compatibility Study between Ferulic Acid and Excipients Used in Cosmetic Formulations by TG/DTG, DSC and FTIR. *J. Therm. Anal. Calorim.* **2017**, *127* (2), 1683–1691. https://doi.org/10.1007/s10973-016-5654-9.

(97) Zheng, Y.; You, X.; Guan, S.; Huang, J.; Wang, L.; Zhang, J.; Wu, J. Poly(Ferulic Acid) with an Anticancer Effect as a Drug Nanocarrier for Enhanced Colon Cancer Therapy. *Adv. Funct. Mater.* **2019**, *29* (15), 1808646. https://doi.org/10.1002/adfm.201808646.

(98) Grosso, G.; Stepaniak, U.; Micek, A.; Kozela, M.; Stefler, D.; Bobak, M.; Pajak, A. Dietary Polyphenol Intake and Risk of Hypertension in the Polish Arm of the HAPIEE Study. *Eur. J. Nutr.* **2018**, *57* (4), 1535–1544. https://doi.org/10.1007/s00394-017-1438-7.

(99) Radtke, J.; Linseisen, J.; Wolfram, G. Phenolsäurezufuhr Erwachsener in Einem Bayerischen Teilkollektiv Der Nationalen Verzehrsstudie. *Eur. J. Nutr.* **1998**, *37* (2), 190–197. https://doi.org/10.1007/s003940050016.

(100) Wen, X.; Walle, T. Methylated Flavonoids Have Greatly Improved Intestinal Absorption and Metabolic Stability. *Drug Metab. Dispos.* **2006**, *34* (10), 1786–1792. https://doi.org/10.1124/dmd.106.011122.

(101) Rook, M. P-Methoxycinnamate and Its Metabolite. *J. Pharm. Sci.* **1968**, *57*, 6–9.

(102) Rychlicka, M.; Rot, A.; Gliszczyńska, A. Biological Properties, Health Benefits and Enzymatic Modifications of Dietary Methoxylated Derivatives of Cinnamic Acid. *Foods* **2021**, *10* (6), 1417. https://doi.org/10.3390/foods10061417.

(103) Zhao, Z.; Egashira, Y.; Sanada, H. Ferulic Acid Is Quickly Absorbed from Rat Stomach as the Free Form and Then Conjugated Mainly in Liver. *J. Nutr.* **2004**, *134* (11), 3083–3088. https://doi.org/10.1093/jn/134.11.3083.

(104) Yang, C.; Tian, Y.; Zhang, Z.; Xu, F.; Chen, Y. High-Performance Liquid Chromatography–Electrospray Ionization Mass Spectrometry Determination of Sodium Ferulate in Human Plasma. *J. Pharm. Biomed. Anal.* **2007**, *43* (3), 945–950. https://doi.org/10.1016/j.jpba.2006.09.027.

(105) Nagy, K.; Redeuil, K.; Williamson, G.; Rezzi, S.; Dionisi, F.; Longet, K.; Destaillats, F.; Renouf, M. First Identification of Dimethoxycinnamic Acids in Human Plasma after Coffee Intake by Liquid Chromatography-Mass Spectrometry. *J. Chromatogr. A* **2011**, *1218* (3), 491–497. https://doi.org/10.1016/j.chroma.2010.11.076.

(106) Bourne, L. C.; Rice-Evans, C. Bioavailability of Ferulic Acid. *Biochem. Biophys. Res. Commun.* **1998**, *253* (2), 222–227. https://doi.org/10.1006/bbrc.1998.9681.

(107) Sinha, A. S.; Maguire, A. R.; Lawrence, S. E. Cocrystallization of Nutraceuticals. *Cryst. Growth Des.* **2015**, *15* (2), 984–1009. https://doi.org/10.1021/cg501009c.

(108) Rios, H. G.; Lozano, D. A. G.; Berrondo, A.; Mir. Ferulic Acid as Feed Supplement in Beef Cattle to Promote Animal Growth and Improve the Meat Quality of the Carcass and the Meat. US 2013/0041036A1, 2013.

(109) ECHA. *Benzoic acid Endpoint summary Administrative data Description of key information Acute toxicity : via oral route*. https://echa.europa.eu/de/registration-dossier/-/registered-dossier/13124/7/3/1 (accessed 2023-08-23).

(110) ECHA. *Sodium benzoate*. https://echa.europa.eu/de/registration-dossier/-/registered-dossier/14966/7/3/1#:~:text=The LD50 was %3E2000 mg,was %3E12200 mg%2Fm3. (accessed 2023-01-09).

(111) Hoskins, J. A. The Occurrence, Metabolism and Toxicity of Cinnamic Acid and Related Compounds. *J. Appl. Toxicol.* **1984**, *4* (6), 283–292. https://doi.org/10.1002/jat.2550040602.

(112) Kakkar, S.; Bais, S. A Review on Protocatechuic Acid and Its Pharmacological Potential. *ISRN Pharmacol.* **2014**, *2014*, 1–9. https://doi.org/10.1155/2014/952943.

(113) Johnson, W.; Zhu, J. *Amended Safety Assessment of Malic Acid and Sodium Malate as Used in Cosmetics*; Washington, 2019.

(114) Safety Assessment of Salicylic Acid, Butyloctyl Salicylate, Calcium Salicylate, C12–15 Alkyl Salicylate, Capryloyl Salicylic Acid, Hexyldodecyl Salicylate, Isocetyl Salicylate, Isodecyl Salicylate, Magnesium Salicylate, MEA-Salicylate, Ethylhexyl Salicyla. *Int. J. Toxicol.* **2003**, *22* (3), 1–108. https://doi.org/10.1177/1091581803022S303.

(115) Edom. *Ferulic acid - Safety Data Sheet*. https://sds.edqm.eu/pdf/SDS/EDQM_201700215_1.0_SDS_DE.pdf?ref=1647962903 (accessed 2023-05-23).

(116) Wang, B.-H.; Ou-Yang, J.-P. Pharmacological Actions of Sodium Ferulate in Cardiovascular System. *Cardiovasc. Drug Rev.* **2005**, *23* (2), 161–172. https://doi.org/10.1111/j.1527-3466.2005.tb00163.x.

(117) Mirza, A. C.; Panchal, S. S. Safety Assessment of Vanillic Acid: Subacute Oral Toxicity Studies in Wistar Rats. *Turkish J. Pharm. Sci.* **2020**, *17* (4), 432–439. https://doi.org/10.4274/tjps.galenos.2019.92678.

(118) Mirza, A. C.; Panchal, S. S. Safety Evaluation of Syringic Acid: Subacute Oral Toxicity Studies in Wistar Rats. *Heliyon* **2019**, *5* (8), e02129. https://doi.org/10.1016/j.heliyon.2019.e02129.

(119) CDH fine chemicals. *Veratric acid - Material safety data sheet*. https://www.cdhfinechemical.com/images/product/msds/37_1303637273_VERATRIC ACIDCASNO93-07-2MSDS.pdf (accessed 2023-08-21).

(120) Konishi, Y.; Shimizu, M. Transepithelial Transport of Ferulic Acid by Monocarboxylic Acid Transporter in Caco-2 Cell Monolayers. *Biosci. Biotechnol. Biochem.* **2003**, *67* (4), 856–862. https://doi.org/10.1271/bbb.67.856.

(121) Sullivan, D. *pH of blood: What to know*. Medical News Today. https://www.medicalnewstoday.com/articles/ph-of-blood (accessed 2022-10-07).

(122) Faraji, M.; Farajtabar, A.; Gharib, F.; Ghasemnejad-Borsa, H. Deprotonation of Salicylic Acid and 5-Nitrosalicylic Acid in Aqueous Solutions of Ethanol. *J. Serbian Chem. Soc.* **2011**, *76* (11), 1455–1463. https://doi.org/10.2298/JSC100506129F.

(123) Genaro-Mattos, T. C.; Maurício, Â. Q.; Rettori, D.; Alonso, A.; Hermes-Lima, M. Antioxidant Activity of Caffeic Acid against Iron-Induced Free Radical Generation—A Chemical Approach. *PLoS One* **2015**, *10* (6), e0129963. https://doi.org/10.1371/journal.pone.0129963.

(124) Clutton, R. E. Blood Gas Analysis. In *Equine Respiratory Medicine and Surgery*; Elsevier, 2004; pp 201–209. https://doi.org/10.1016/B978-0-7020-2759-8.50019-2.

(125) Karmazyn, M.; Gan, X. T.; Humphreys, R. A.; Yoshida, H.; Kusumoto, K. The Myocardial Na + -H + Exchange. *Circ. Res.* **1999**, *85* (9), 777–786. https://doi.org/10.1161/01.RES.85.9.777.

(126) Shi, L.; Quick, M.; Zhao, Y.; Weinstein, H.; Javitch, J. A. The Mechanism of a Neurotransmitter:Sodium Symporter—Inward Release of Na+ and Substrate Is Triggered by Substrate in a Second Binding Site. *Mol. Cell* **2008**, *30* (6), 667–677. https://doi.org/10.1016/j.molcel.2008.05.008.

(127) Sebrell. RIBOFLAVIN. In *The Vitamins*; Sebrell, W. H., Harris, R. S., Eds.; Elsevier, 1972; pp 1–96. https://doi.org/10.1016/B978-0-12-633765-5.50008-3.

(128) Lienhart, W.-D.; Gudipati, V.; Macheroux, P. The Human Flavoproteome. *Arch. Biochem. Biophys.* **2013**, *535* (2), 150–162. https://doi.org/10.1016/j.abb.2013.02.015.

(129) Pinto, J. T.; Cooper, A. J. L. From Cholesterogenesis to Steroidogenesis: Role of Riboflavin and Flavoenzymes in the Biosynthesis of Vitamin D. *Adv. Nutr.* **2014**, *5* (2), 144–163. https://doi.org/10.3945/an.113.005181.

(130) Sepúlveda Cisternas, I.; Salazar, J. C.; García-Angulo, V. A. Overview on the Bacterial

Iron-Riboflavin Metabolic Axis. *Front. Microbiol.* **2018**, *9*. https://doi.org/10.3389/fmicb.2018.01478.

(131) Balasubramaniam, S.; Yaplito-Lee, J. Riboflavin Metabolism: Role in Mitochondrial Function. *J. Transl. Genet. Genomics* **2020**. https://doi.org/10.20517/jtgg.2020.34.

(132) Revuelta, J. L.; Ledesma-Amaro, R.; Jiménez, A. Industrial Production of Vitamin B2 by Microbial Fermentation. In *Industrial Biotechnology of Vitamins, Biopigments, and Antioxidants*; Vandamme, E. J., Revuelta, J. L., Eds.; Wiley-VCH Verlag GmbH & Co. KGaA: Weinheim, Germany, 2016; pp 15–40. https://doi.org/10.1002/9783527681754.

(133) AI, M.-B.; E, P.; B., P. Immunomodulatory Effect of Riboflavin Deficiency and Enrichment - Reversible Pathological Response versus Silencing of Inflammatory Activation. *J Physiol Pharmacol* **2015**, *66* (6), 793–802.

(134) Mosegaard, S.; Dipace, G.; Bross, P.; Carlsen, J.; Gregersen, N.; Olsen, R. K. J. Riboflavin Deficiency—Implications for General Human Health and Inborn Errors of Metabolism. *Int. J. Mol. Sci.* **2020**, *21* (11), 3847. https://doi.org/10.3390/ijms21113847.

(135) O'Brien, M.; Kiely, M.; Harrington, K.; Robson, P.; Strain, J.; Flynn, A. The North/South Ireland Food Consumption Survey: Vitamin Intakes in 18–64-Year-Old Adults. *Public Health Nutr.* **2001**, *4* (5a), 1069–1079. https://doi.org/10.1079/PHN2001188.

(136) Powers, H. J.; Hill, M. H.; Mushtaq, S.; Dainty, J. R.; Majsak-Newman, G.; Williams, E. A. Correcting a Marginal Riboflavin Deficiency Improves Hematologic Status in Young Women in the United Kingdom (RIBOFEM). *Am. J. Clin. Nutr.* **2011**, *93* (6), 1274–1284. https://doi.org/10.3945/ajcn.110.008409.

(137) Preziosi, P.; Galan, P.; Deheeger, M.; Yacoub, N.; Drewnowski, A.; Hercberg, S. Breakfast Type, Daily Nutrient Intakes and Vitamin and Mineral Status of French Children, Adolescents and Adults. *J. Am. Coll. Nutr.* **1999**, *18* (2), 171–178. https://doi.org/10.1080/07315724.1999.10718846.

(138) Anderson, J. J. B.; Suchindran, C. M.; Roggenkamp, K. J. Micronutrient Intakes in Two Us Populations of Older Adults: Lipid Research Clinics Program Prevalence Study Findings. *J. Nutr. Heal. Aging* **2009**, *13* (7), 595–600. https://doi.org/10.1007/s12603-009-0169-8.

(139) Van Houten, B.; Woshner, V.; Santos, J. H. Role of Mitochondrial DNA in Toxic Responses to Oxidative Stress. *DNA Repair (Amst).* **2006**, *5* (2), 145–152. https://doi.org/10.1016/j.dnarep.2005.03.002.

(140) Hoppel, C. L.; Tandler, B. Riboflavin and Mouse Hepatic Cell Structure and Function. Mitochondrial Oxidative Metabolism in Severe Deficiency States. *J. Nutr.* **1975**, *105* (5), 562–570. https://doi.org/10.1093/jn/105.5.562.

(141) Ross, W. N. Understanding Calcium Waves and Sparks in Central Neurons. *Nat. Rev. Neurosci.* **2012**, *13* (3), 157–168. https://doi.org/10.1038/nrn3168.

(142) Cardoso, D. R.; Libardi, S. H.; Skibsted, L. H. Riboflavin as a Photosensitizer. Effects on Human Health and Food Quality. *Food Funct.* **2012**, *3* (5), 487. https://doi.org/10.1039/c2fo10246c.

(143) Ashoor, S. H.; Seperich, G. J.; Monte, W. C.; Welty, J. HPLC Determination of Riboflavin in Eggs and Dairy Products. *J. Food Sci.* **1983**, *48* (1), 92–94. https://doi.org/10.1111/j.1365-2621.1983.tb14796.x.

(144) McCormick, D. B. Two Interconnected B Vitamins: Riboflavin and Pyridoxine. *Physiol. Rev.* **1989**, *69* (4), 1170–1198. https://doi.org/10.1152/physrev.1989.69.4.1170.

(145) Future Market Insights. *In Global Riboflavin Pigment Market, Developing Countries Will Offer the Best Growth Opportunities – Future Market Insights, Inc.* GlobeNewswire. https://ca.sports.yahoo.com/news/global-riboflavin-pigment-market-developing-133000210.html?guccounter=1&guce_referrer=aHR0cHM6Ly93d3cuZ29vZ2xlLmNvbS8&guce_referrer_sig=AQAAAFxTm8j06RUwdIBbf8IOpW2okdXMYXhV-f56iOrvBkaFHLGqQlKknLN778BegWGgbkjqGPsuXgpAoyGHUd (accessed 2022-10-08).

(146) Mordor Intelligence. *RIBOFLAVIN MARKET - GROWTH, TRENDS, COVID-19 IMPACT, AND FORECASTS (2022-2027)*. https://www.mordorintelligence.com/industry-reports/riboflavin-market (accessed 2022-10-08).

(147) Watch, M. *Vitamin B2 (Riboflavin) Market Share 2022 Global Trends, Industry Analysis, Key Players and Forecast to 2028*. https://www.marketwatch.com/press-release/vitamin-b2-riboflavin-market-share-2022-global-trends-industry-analysis-key-players-and-forecast-to-2028-2022-09-19 (accessed 2022-10-08).

(148) Abbas, C. A.; Sibirny, A. A. Genetic Control of Biosynthesis and Transport of Riboflavin and Flavin Nucleotides and Construction of Robust Biotechnological Producers. *Microbiol. Mol. Biol. Rev.* **2011**, *75* (2), 321–360. https://doi.org/10.1128/MMBR.00030-10.

(149) Kato, T.; Park, E. Y. Riboflavin Production by Ashbya Gossypii. *Biotechnol. Lett.* **2012**, *34* (4), 611–618. https://doi.org/10.1007/s10529-011-0833-z.

(150) Stahmann, K.-P.; Revuelta, J. L.; Seulberger, H. Three Biotechnical Processes Using Ashbya Gossypii, Candida Famata, or Bacillus Subtilis Compete with Chemical Riboflavin Production. *Appl. Microbiol. Biotechnol.* **2000**, *53* (5), 509–516. https://doi.org/10.1007/s002530051649.

(151) Schwechheimer, S. K.; Park, E. Y.; Revuelta, J. L.; Becker, J.; Wittmann, C. Biotechnology of Riboflavin. *Appl. Microbiol. Biotechnol.* **2016**, *100* (5), 2107–2119. https://doi.org/10.1007/s00253-015-7256-z.

(152) Masłowska, J.; Malicka, M. Thermal Behaviour of Riboflavin. *J. Therm. Anal.* **1988**, *34*

(1), 3–9. https://doi.org/10.1007/BF01913365.

(153) Cardoso, D. R.; Homem-de-Mello, P.; Olsen, K.; da Silva, A. B. F.; Franco, D. W.; Skibsted, L. H. Deactivation of Triplet-Excited Riboflavin by Purine Derivatives: Important Role of Uric Acid in Light-Induced Oxidation of Milk Sensitized by Riboflavin. *J. Agric. Food Chem.* **2005**, *53* (9), 3679–3684. https://doi.org/10.1021/jf048347z.

(154) Jung, M. Y.; Oh, Y. S.; Kim, D. K.; Kim, H. J.; Min, D. B. Photoinduced Generation of 2,3-Butanedione from Riboflavin. *J. Agric. Food Chem.* **2007**, *55* (1), 170–174. https://doi.org/10.1021/jf061999y.

(155) Huang, R.; Kim, H. J.; Min, D. B. Photosensitizing Effect of Riboflavin, Lumiflavin, and Lumichrome on the Generation of Volatiles in Soy Milk. *J. Agric. Food Chem.* **2006**, *54* (6), 2359–2364. https://doi.org/10.1021/jf052448v.

(156) Wahl, P.; Auchet, J. C. Time Resolved Fluorescence of Flavin Adenine Dinucleotide. *FEBS Lett.* **1974**, *44* (1), 67–70. https://doi.org/10.1016/0014-5793(74)80307-8.

(157) Naman, S. A.; Tegnér, L. DECAY KINETICS OF THE TRIPLET EXCITED STATE OF LUMIFLAVIN. *Photochem. Photobiol.* **1986**, *43* (3), 331–333. https://doi.org/10.1111/j.1751-1097.1986.tb05612.x.

(158) Ahmad, I.; Fasihullah, Q.; Noor, A.; Ansari, I. A.; Ali, Q. N. M. Photolysis of Riboflavin in Aqueous Solution: A Kinetic Study. *Int. J. Pharm.* **2004**, *280* (1–2), 199–208. https://doi.org/10.1016/j.ijpharm.2004.05.020.

(159) Sheraz, M. A.; Kazi, S. H.; Ahmed, S.; Mirza, T.; Ahmad, I.; Evstigneev, M. P. Effect of Phosphate Buffer on the Complexation and Photochemical Interaction of Riboflavin and Caffeine in Aqueous Solution: A Kinetic Study. *J. Photochem. Photobiol. A Chem.* **2014**, *273*, 17–22. https://doi.org/10.1016/j.jphotochem.2013.09.007.

(160) Metzler, D. E.; Cairns, W. L. Photochemical Degradation of Flavines. VI. New Photoproduct and Its Use in Studying the Photolytic Mechanism. *J. Am. Chem. Soc.* **1971**, *93* (11), 2772–2777. https://doi.org/10.1021/ja00740a031.

(161) Rivlin, R. S. Riboflavin (Vitamin B2). In *Handbook of Vitamins*; Zempleni, J., Rucker, R. B., McCormick, D. B., Suttie, J. W., Eds.; CRC Press: Boca Raton: USA, 2007; pp 233–251.

(162) Ball, G. F. M. Bioavailability and Stability. In *Vitamins in Foods Analysis*; CRC Press: Boca Raton: USA, 2006; pp 165–176.

(163) Smith, E. C.; Metzler, D. E. The Photochemical Degradation of Riboflavin. *J. Am. Chem. Soc.* **1963**, *85* (20), 3285–3288. https://doi.org/10.1021/ja00903a051.

(164) McBride, M. M.; Metzler, D. E. PHOTCHEMICAL DEGRADATION OF FLAVINS—III. HYDROXYETHYL AND FORMYLMETHYL ANALOGS OF RIBOFLAVIN. *Photochem. Photobiol.* **1967**, *6* (2), 113–123. https://doi.org/10.1111/j.1751-1097.1967.tb08796.x.

(165) Ahmad, I.; Fasihullah, Q.; Vaid, F. H. M. Photolysis of Formylmethylflavin in Aqueous and Organic Solvents. *Photochem. Photobiol. Sci.* **2006**, *5* (7), 680.

https://doi.org/10.1039/b602917e.

(166) Ahmad, I.; Mirza, T.; Iqbal, K.; Ahmed, S.; Sheraz, M. A.; Vaid, F. H. M. Effect of PH, Buffer, and Viscosity on the Photolysis of Formylmethylflavin: A Kinetic Study. *Aust. J. Chem.* **2013**, *66* (5), 579. https://doi.org/10.1071/CH12457.

(167) Ahmad, I.; Qadeer, K.; Iqbal, K.; Ahmed, S.; Sheraz, M. A.; Ali, S. A.; Mirza, T.; Hafeez, A. Correction for Irrelevant Absorption in Multicomponent Spectrophotometric Assay of Riboflavin, Formylmethylflavin, and Degradation Products: Kinetic Applications. *AAPS PharmSciTech* **2013**, *14* (3), 1101–1107. https://doi.org/10.1208/s12249-013-9998-1.

(168) Ahmad, I.; Vaid, F. H. M. Photochemistry of Flavins in Aqueous and Organic Solvents. In *Flavins Photochemistry and Photobiology*; Silva, E.; Edwards, A. M., Ed.; The Royal Society of Chemistry: Cambridge, 2006; pp 13–40. https://doi.org/10.1039/9781847555397-00013.

(169) Ahmad, I.; Rapson, H. D. C.; Heelis, P. F.; Phillips, G. O. Alkaline Hydrolysis of 7,8-Dimethyl-10-(Formylmethyl)Isoalloxazine. A Kinetic Study. *J. Org. Chem.* **1980**, *45* (4), 731–733. https://doi.org/10.1021/jo01292a040.

(170) Ahmad, I.; Fasihullah, Q.; Vaid, F. H. M. A Study of Simultaneous Photolysis and Photoaddition Reactions of Riboflavin in Aqueous Solution. *J. Photochem. Photobiol. B Biol.* **2004**, *75* (1–2), 13–20. https://doi.org/10.1016/j.jphotobiol.2004.04.001.

(171) Ahmad, I.; Fasihullah, Q.; Vaid, F. H. M. Effect of Phosphate Buffer on Photodegradation Reactions of Riboflavin in Aqueous Solution. *J. Photochem. Photobiol. B Biol.* **2005**, *78* (3), 229–234. https://doi.org/10.1016/j.jphotobiol.2004.11.010.

(172) Ahmad, I.; Fasihullah, Q.; Vaid, F. H. M. Effect of Light Intensity and Wavelengths on Photodegradation Reactions of Riboflavin in Aqueous Solution. *J. Photochem. Photobiol. B Biol.* **2006**, *82* (1), 21–27. https://doi.org/10.1016/j.jphotobiol.2005.08.004.

(173) Ahmad, I.; Ahmed, S.; Sheraz, M. A.; Vaid, F. H. M. Effect of Borate Buffer on the Photolysis of Riboflavin in Aqueous Solution. *J. Photochem. Photobiol. B Biol.* **2008**, *93* (2), 82–87. https://doi.org/10.1016/j.jphotobiol.2008.07.005.

(174) Ahmad, I.; Ahmed, S.; Sheraz, M. A.; Aminuddin, M.; Vaid, F. H. M. Effect of Caffeine Complexation on the Photolysis of Riboflavin in Aqueous Solution: A Kinetic Study. *Chem. Pharm. Bull.* **2009**, *57* (12), 1363–1370. https://doi.org/10.1248/cpb.57.1363.

(175) Moore, W. M.; Ireton, R. C. The Photochemistry of Riboflavin--V. The Photodegradation of Isoalloxazines in Alcoholic Solvents. *Photochem. Photobiol.* **1977**, *25* (4), 347–356. https://doi.org/10.1111/j.1751-1097.1977.tb07354.x.

(176) Koziol, J. Absorption Spectra of Riboflavin, Lumiflavin, and Lumichrome in Organic Solvents. *Experientia* **1965**, *21* (4), 189–190. https://doi.org/10.1007/BF02141876.

(177) Kozioł, J.; Knobloch, E. The Solvent Effect on the Fluorescence and Light Absorption

of Riboflavin and Lumiflavin. *Biochim. Biophys. Acta - Biophys. Incl. Photosynth.* **1965**, *102* (1), 289–300. https://doi.org/10.1016/0926-6585(65)90221-9.

(178) Ahmad, I.; Anwar, Z.; Ali, S. A.; Hasan, K. A.; Sheraz, M. A.; Ahmed, S. Ionic Strength Effects on the Photodegradation Reactions of Riboflavin in Aqueous Solution. *J. Photochem. Photobiol. B Biol.* **2016**, *157*, 113–119. https://doi.org/10.1016/j.jphotobiol.2016.02.010.

(179) Goldsmith, M. R.; Rogers, P. J.; Cabral, N. M.; Ghiggino, K. P.; Roddick, F. A. Riboflavin Triplet Quenchers Inhibit Lightstruck Flavor Formation in Beer. *J. Am. Soc. Brew. Chem.* **2005**, *63* (4), 177–184. https://doi.org/10.1094/ASBCJ-63-0177.

(180) Sigma Aldrich. *(-)-Riboflavin Product information*. https://www.sigmaaldrich.com/deepweb/assets/sigmaaldrich/product/documents/500/065/r9881pis.pdf (accessed 2022-08-04).

(181) Selleckchem.com. *Riboflavin*. https://www.selleckchem.com/products/Riboflavin-Vitamin-B2.html (accessed 2022-10-14).

(182) Coffman, R. E.; Kildsig, D. O. Effect of Nicotinamide and Urea on the Solubility of Riboflavin in Various Solvents. *J. Pharm. Sci.* **1996**, *85* (9), 951–954. https://doi.org/10.1021/js960012b.

(183) Ahmad, I. Effect of Nicotinamide on the Photolysis of Riboflavin in Aqueous Solution. *Sci. Pharm.* **2016**, *84* (2), 289–303. https://doi.org/10.3797/scipharm.1507-04.

(184) Datta, S.; Mukhopadhyay, C.; Bhattacharya, S.; Bose, S. K. Stability and Conformation of the Complexes of Riboflavin with Aromatic Hydroxy Compounds in an Aqueous Medium. *Spectrochim. Acta Part A Mol. Biomol. Spectrosc.* **2005**, *64* (1), 116–126. https://doi.org/10.1016/j.saa.2005.07.019.

(185) EFSA. Scientific Opinion on the Safety and Efficacy of Vitamin K3 (Menadione Sodium Bisulphite and Menadione Nicotinamide Bisulphite) as a Feed Additive for All Animal Species. *EFSA J.* **2014**, *12* (1). https://doi.org/10.2903/j.efsa.2014.3532.

(186) Myneni, V.; Mezey, E. Regulation of Bone Remodeling by Vitamin K2. *Oral Dis.* **2017**, *23* (8), 1021–1028. https://doi.org/10.1111/odi.12624.

(187) Booth, S. L.; Suttie, J. W. Dietary Intake and Adequacy of Vitamin K. *J. Nutr.* **1998**, *128* (5), 785–788. https://doi.org/10.1093/jn/128.5.785.

(188) Indyk, H. E.; Shearer, M. J.; Woollard, D. C. Vitamin K: Properties and Determination. In *Encyclopedia of Food and Health*; Elsevier, 2016; pp 430–435. https://doi.org/10.1016/B978-0-12-384947-2.00728-5.

(189) Hirota, Y.; Tsugawa, N.; Nakagawa, K.; Suhara, Y.; Tanaka, K.; Uchino, Y.; Takeuchi, A.; Sawada, N.; Kamao, M.; Wada, A.; Okitsu, T.; Okano, T. Menadione (Vitamin K3) Is a Catabolic Product of Oral Phylloquinone (Vitamin K1) in the Intestine and a Circulating Precursor of Tissue Menaquinone-4 (Vitamin K2) in Rats. *J. Biol. Chem.* **2013**, *288* (46), 33071–33080. https://doi.org/10.1074/jbc.M113.477356.

(190) Akbari, S.; Rasouli-Ghahroudi, A. A. Vitamin K and Bone Metabolism: A Review of the Latest Evidence in Preclinical Studies. *Biomed Res. Int.* **2018**, *2018*, 1–8. https://doi.org/10.1155/2018/4629383.

(191) Wang, H.; Yang, P.; Li, L.; Zhang, N.; Ma, Y. Effects of Sources or Formulations of Vitamin K3 on Its Stability during Extrusion or Pelleting in Swine Feed. *Animals* **2021**, *11* (3), 633. https://doi.org/10.3390/ani11030633.

(192) Wei, X.; Hang, Y.; Li, X.; Hua, X.; Cong, X.; Yi, W.; Guo, X. Effects of Dietary Vitamin K3 Levels on Growth, Coagulation, Calcium Content, and Antioxidant Capacity in Largemouth Bass, Micropterus Salmoides. *Aquac. Fish.* **2023**, *8* (2), 159–165. https://doi.org/10.1016/j.aaf.2021.08.004.

(193) Dubbs, M. D.; Gupta, R. B. Solubility of Vitamin E (α-Tocopherol) and Vitamin K 3 (Menadione) in Ethanol−Water Mixture. *J. Chem. Eng. Data* **1998**, *43* (4), 590–591. https://doi.org/10.1021/je980017l.

(194) DSM. *Vitamin K3*. https://www.dsm.com/anh/products-and-services/products/vitamins/vitamin-k3.html#aquaculture (accessed 2023-09-05).

(195) Reports and Data. *Pharma and Healthcare - Vitamin K3 Market*. https://www.reportsanddata.com/report-detail/vitamin-k3-market (accessed 2023-08-23). https://doi.org/Report ID: RND_005878.

(196) Zhu, B.; Wang, J. R.; Zhang, Q.; Mei, X. Improving Dissolution and Photostability of Vitamin K3 via Cocrystallization with Naphthoic Acids and Sulfamerazine. *Cryst. Growth Des.* **2016**, *16* (1), 483–492. https://doi.org/10.1021/acs.cgd.5b01491.

(197) Yu, Y.; Li, F.; Long, S.; Xu, L.; Liu, G. Solubility, Thermodynamic Properties, HSP, and Molecular Interactions of Vitamin K3 in Pure Solvents. *J. Mol. Liq.* **2020**, *317*, 113945. https://doi.org/10.1016/j.molliq.2020.113945.

(198) Rane, S.; Ahmed, K.; Salunke-Gawali, S.; Zaware, S. B.; Srinivas, D.; Gonnade, R.; Bhadbhade, M. Vitamin K3 Family Members – Part II: Single Crystal X-Ray Structures, Temperature-Induced Packing Polymorphism, Magneto-Structural Correlations and Probable Anti-Oncogenic Candidature. *J. Mol. Struct.* **2008**, *892* (1–3), 74–83. https://doi.org/10.1016/j.molstruc.2008.05.015.

(199) Kremer, F. *Vorlesung "Molekülphysik/Festkörperphysik."* https://research.uni-leipzig.de/mop/lectures/Vorlesung_WS2014_2015/25. Vorlesung 13.1.2015.pdf (accessed 2023-11-16).

(200) Picollo, M.; Aceto, M.; Vitorino, T. UV-Vis Spectroscopy. *Phys. Sci. Rev.* **2019**, *4*. https://doi.org/https://doi.org/10.1515/psr-2018-0008.

(201) Akash, M. S. H.; Rehman, K. *Essentials of Pharmaceutical Analysis*; Springer Nature Singapore Pte Ltd: Singapore, 2022. https://doi.org/10.1007/978-981-15-1547-7.

(202) Latscha, H. P.; Linti, G. W.; Klein, H. A. *Analytische Chemie*, III.; Springer-Verlag, Ed.; Springer-Lehrbuch; Springer Berlin Heidelberg: Berlin, Heidelberg, 2004.

https://doi.org/10.1007/978-3-642-18493-2.

(203) Kromidas, S.; Kuss, H. *Chromatogramme Richtig Integrieren Und Bewerten*; 2008. https://doi.org/10.1002/9783527622221.

(204) Kaczmarski, K.; Kowalska, T.; Prus, W. Theory and Mechanism of Thin-Layer Chromatography. *Handb. Thin-Layer Chromatogr.* **2003**, No. January. https://doi.org/10.1201/9780203912430.ch2.

(205) Reuhs, B. L. High-Performance Liquid Chromatography. In *Food Analysis*; Nielsen, S. S., Ed.; Springer International Publishing: Cham, 2017; pp 213–226. https://doi.org/10.1007/978-3-319-45776-5_13.

(206) Hatada, K.; Kitayama, T. Introduction to NMR Spectroscopy. In *NMR Spectroscopy of Polymers*; Springer Berlin Heidelberg: Berlin, Heidelberg, 2004; pp 1–42. https://doi.org/10.1007/978-3-662-08982-8_1.

(207) Frydman, L.; Lupulescu, A.; Scherf, T. Principles and Features of Single-Scan Two-Dimensional NMR Spectroscopy. *J. Am. Chem. Soc.* **2003**, *125* (30), 9204–9217. https://doi.org/10.1021/ja030055b.

(208) Fattori, J.; Rodrigues, F. H. S.; Pontes, J. G. M.; Paula Espíndola, A.; Tasic, L. Monitoring Intermolecular and Intramolecular Interactions by NMR Spectroscopy. In *Applications of NMR Spectroscopy: Volume 3*; ur-Rahman, A., Choudhary, M. I., Eds.; Bentham Science Publishers, 2015; pp 180–266. https://doi.org/https://doi.org/10.1016/B978-1-68108-063-5.50006-0.

(209) Lindon, J. C. Multidimensional NMR Spectroscopy. In *Reference Module in Chemistry, Molecular Sciences and Chemical Engineering*; Elsevier, 2016. https://doi.org/10.1016/B978-0-12-409547-2.12670-8.

(210) Finsy, R. Particle Sizing by Quasi-Elastic Light Scattering. *Adv. Colloid Interface Sci.* **1994**, *52*, 79–143. https://doi.org/10.1016/0001-8686(94)80041-3.

(211) Picton Drake, S.; Purvis, A. Everyday Relativity and the Doppler Effect. *Am. J. Phys.* **2014**, *82* (1), 52–59. https://doi.org/10.1119/1.4830887.

(212) Almeida, L. B. The Fractional Fourier Transform and Time-Frequency Representations. *IEEE Trans. Signal Process.* **1994**, *42* (11), 3084–3091. https://doi.org/10.1109/78.330368.

(213) Berne, B. J.; Pecora, R. *Dynamic Light Scattering. With Applications to Chemistry, Biology, and Physics*, 1st ed.; Inc, Ed.; Dover Publications: New York.

(214) Stetefeld, J.; McKenna, S. A.; Patel, T. R. Dynamic Light Scattering: A Practical Guide and Applications in Biomedical Sciences. *Biophys. Rev.* **2016**, *8* (4), 409–427. https://doi.org/10.1007/s12551-016-0218-6.

(215) Einstein, A. *Über Die von Der Molekularkinetischen Theorie Der Wärme Geforderte Bewegung von in Ruhenden Flüssigkeiten Suspendierten Teilchen*; 1905; Vol. 17.

(216) Dolomanov, O. V.; Bourhis, L. J.; Gildea, R. J.; Howard, J. A. K.; Puschmann, H.

OLEX2 : A Complete Structure Solution, Refinement and Analysis Program. *J. Appl. Crystallogr.* **2009**, *42* (2), 339–341. https://doi.org/10.1107/S0021889808042726.

(217) Sheldrick, G. M. Crystal Structure Refinement with SHELXL. *Acta Crystallogr. Sect. C Struct. Chem.* **2015**, *71* (1), 3–8. https://doi.org/10.1107/S2053229614024218.

(218) Sheldrick, G. M. SHELXT – Integrated Space-Group and Crystal-Structure Determination. *Acta Crystallogr. Sect. A Found. Adv.* **2015**, *71* (1), 3–8. https://doi.org/10.1107/S2053273314026370.

(219) Guerain, M.; Affouard, F.; Henaff, C.; Dejoie, C.; Danède, F.; Siepmann, J.; Siepmann, F.; Willart, J.-F. Structure Determination of Riboflavin by Synchrotron High-Resolution Powder X-Ray Diffraction. *Acta Crystallogr. Sect. C Struct. Chem.* **2021**, *77* (12), 800–806. https://doi.org/10.1107/S2053229621012171.

(220) Rigaku. CrysAlisPro. Rigaku 2021.

(221) Rigaku. CrysAlisPro (ROD). Oxford: Poland.

(222) Jones, P. G. Crystal Growing. *Chem. Br.* **1981**, *17* (5).

(223) Selleckchem. *Riboflavin phosphate sodium*. https://www.selleckchem.com/products/flavin-mononucleotide.html (accessed 2022-08-06).

(224) Tsurko, J.; Kunz, W. Salting-in and Salting-out Effects of Polyphenols,Aromatic Compounds and Amino Acids on Poly (N-Isopropylacrylamide) and Egg White Aqueous Solutions. *Sci. Innov.* **2021**, *17* (4), 72–78. https://doi.org/10.15407/scine17.04.072.

(225) Bauduin, P.; Renoncourt, A.; Kopf, A.; Touraud, D.; Kunz, W. Unified Concept of Solubilization in Water by Hydrotropes and Cosolvents. *Langmuir* **2005**, *21* (15), 6769–6775. https://doi.org/10.1021/la050554l.

(226) Lin, S.; Blankschtein, D. Role of the Bile Salt Surfactant Sodium Cholate in Enhancing the Aqueous Dispersion Stability of Single-Walled Carbon Nanotubes: A Molecular Dynamics Simulation Study. *J. Phys. Chem. B* **2010**, *114* (47), 15616–15625. https://doi.org/10.1021/jp1076406.

(227) Saleh, A. M.; Ebian, A. R.; Etman, M. A. Solubilization of Water by Hydrotropic Salts. *J. Pharm. Sci.* **1986**, *75* (7), 644–647. https://doi.org/10.1002/jps.2600750705.

(228) Shukla, T.; Khare, P.; Thakur, N.; Dhote, V.; Chandel, H. S.; Pandey, S. P. Exploring the Use of Sodium Benzoate as Hydrotrope for the Estimation of Lornoxicam in Their Marketed Formulation. *Pharm. Methods* **2014**, *5* (1), 14–19. https://doi.org/10.5530/phm.2014.1.3.

(229) Cho, Y. W.; Lee, J.; Lee, S. C.; Huh, K. M.; Park, K. Hydrotropic Agents for Study of in Vitro Paclitaxel Release from Polymeric Micelles. *J. Control. Release* **2004**, *97* (2), 249–257. https://doi.org/10.1016/j.jconrel.2004.03.013.

(230) Kwon, Y. Theoretical Study on Salicylic Acid and Its Analogues: Intramolecular

Hydrogen Bonding. *J. Mol. Struct. THEOCHEM* **2000**, *532* (1–3), 227–237. https://doi.org/10.1016/S0166-1280(00)00555-8.

(231) Raschke, T. M.; Levitt, M. Detailed Hydration Maps of Benzene and Cyclohexane Reveal Distinct Water Structures. *J. Phys. Chem. B* **2004**, *108* (35), 13492–13500. https://doi.org/10.1021/jp049481p.

(232) Häckl, K. Synthesis and Evaluation of Novel Bio-Based Solvents and Solubilizers, University of Regensburg, 2019.

(233) Ulmann, N.; Häckl, K.; Touraud, D.; Kunz, W. Investigation of the Salting-in/-out, Hydrotropic and Surface-Active Behavior of Plant-Based Hormone and Phenolic Acid Salts. *J. Colloid Interface Sci.* **2023**, *641*, 631–642. https://doi.org/10.1016/j.jcis.2023.03.077.

(234) Mehringer, J.; Do, T.-M.; Touraud, D.; Hohenschutz, M.; Khoshsima, A.; Horinek, D.; Kunz, W. Hofmeister versus Neuberg: Is ATP Really a Biological Hydrotrope? *Cell Reports Phys. Sci.* **2021**, *2* (2), 100343. https://doi.org/10.1016/j.xcrp.2021.100343.

(235) Witkowska, A.; Haucke, V. Liquid-like Protein Assemblies Initiate Endocytosis. *Nat. Cell Biol.* **2021**, *23* (4), 301–302. https://doi.org/10.1038/s41556-021-00665-2.

(236) Day, K. J.; Kago, G.; Wang, L.; Richter, J. B.; Hayden, C. C.; Lafer, E. M.; Stachowiak, J. C. Liquid-like Protein Interactions Catalyse Assembly of Endocytic Vesicles. *Nat. Cell Biol.* **2021**, *23* (4), 366–376. https://doi.org/10.1038/s41556-021-00646-5.

(237) Martin, E. W.; Mittag, T. Relationship of Sequence and Phase Separation in Protein Low-Complexity Regions. *Biochemistry* **2018**, *57* (17), 2478–2487. https://doi.org/10.1021/acs.biochem.8b00008.

(238) Hyman, A. A.; Weber, C. A.; Jülicher, F. Liquid-Liquid Phase Separation in Biology. *Annu. Rev. Cell Dev. Biol.* **2014**, *30* (1), 39–58. https://doi.org/10.1146/annurev-cellbio-100913-013325.

(239) Lu, Y.; Li, S.; Xu, H.; Zhang, T.; Lin, X.; Wu, X. Effect of Covalent Interaction with Chlorogenic Acid on the Allergenic Capacity of Ovalbumin. *J. Agric. Food Chem.* **2018**, *66* (37), 9794–9800. https://doi.org/10.1021/acs.jafc.8b03410.

(240) Friberg, S. E.; Fei, L.; Campbell, S.; Yang, H.; Lu, Y. Vapor Pressure of Phenethyl Alcohol in an Aqueous Hydrotrope Solution. *Colloids Surfaces A Physicochem. Eng. Asp.* **1997**, *127* (1–3), 233–239. https://doi.org/10.1016/S0927-7757(97)00068-X.

(241) Horváth-Szabó, G.; Yin, Q.; Friberg, S. E. The Hydrotrope Action of Sodium Xylenesulfonate on the Solubility of Lecithin. *J. Colloid Interface Sci.* **2001**, *236* (1), 52–59. https://doi.org/10.1006/jcis.2000.7391.

(242) Winkler, R.; Buchecker, T.; Hastreiter, F.; Touraud, D.; Kunz, W. PPh4Cl in Aqueous Solution – the Aggregation Behavior of an Antagonistic Salt. *Phys. Chem. Chem. Phys.* **2017**, *19* (37), 25463–25470. https://doi.org/10.1039/C7CP02677C.

(243) Ali, B. A.; Zughul, M. B.; Badwan, A. A. Surface Activity and Energetics of Aggregate

Formation in Aqueous Sodium Benzoate and Salicylate Solutions. *J. Dispers. Sci. Technol.* **1995**, *16* (6), 451–468. https://doi.org/10.1080/01932699508943699.

(244) Moroi, Y.; Motomura, K.; Matuura, R. The Critical Micelle Concentration of Sodium Dodecyl Sulfate-Bivalent Metal Dodecyl Sulfate Mixtures in Aqueous Solutions. *J. Colloid Interface Sci.* **1974**, *46* (1), 111–117. https://doi.org/10.1016/0021-9797(74)90030-7.

(245) Khoshsima, A.; Dehghani, M. R.; Touraud, D.; Kunz, W. An Investigation of the Fish Diagrams of Water or Brine/Decane or Dodecane/Propylene Glycol Ether (C3P1 or C3P2) Systems. *J. Mol. Liq.* **2015**, *206*, 170–175. https://doi.org/10.1016/j.molliq.2015.02.016.

(246) Lunkenheimer, K.; Schrödle, S.; Kunz, W. Dowanol DPnB in Water as an Example of a Solvo-Surfactant System: Adsorption and Foam Properties. In *Trends in Colloid and Interface Science XVII*; Springer Berlin Heidelberg: Berlin, Heidelberg, 2004; pp 14–20. https://doi.org/10.1007/b93970.

(247) Zemb, T. N.; Klossek, M.; Lopian, T.; Marcus, J.; Schöettl, S.; Horinek, D.; Prevost, S. F.; Touraud, D.; Diat, O.; Marčelja, S.; Kunz, W. How to Explain Microemulsions Formed by Solvent Mixtures without Conventional Surfactants. *Proc. Natl. Acad. Sci.* **2016**, *113* (16), 4260–4265. https://doi.org/10.1073/pnas.1515708113.

(248) Das, S.; Wong, A. B. H. Stabilization of Ferulic Acid in Topical Gel Formulation via Nanoencapsulation and PH Optimization. *Sci. Rep.* **2020**, *10* (1), 12288. https://doi.org/10.1038/s41598-020-68732-6.

(249) Agarwal, N.; Nair, M. S.; Mazumder, A.; Poluri, K. M. *Characterization of Nanomaterials Using Nuclear Magnetic Resonance Spectroscopy*; Elsevier Ltd., 2018. https://doi.org/10.1016/B978-0-08-101973-3.00003-1.

(250) Buchecker, T.; Krickl, S.; Winkler, R.; Grillo, I.; Bauduin, P.; Touraud, D.; Pfitzner, A.; Kunz, W. The Impact of the Structuring of Hydrotropes in Water on the Mesoscale Solubilisation of a Third Hydrophobic Component. *Phys. Chem. Chem. Phys.* **2017**, *19* (3), 1806–1816. https://doi.org/10.1039/C6CP06696H.

(251) Barba-Bon, A.; Salluce, G.; Lostalé-Seijo, I.; Assaf, K. I.; Hennig, A.; Montenegro, J.; Nau, W. M. Boron Clusters as Broadband Membrane Carriers. *Nature* **2022**, *603* (7902), 637–642. https://doi.org/10.1038/s41586-022-04413-w.

(252) Salcedo, J.; Delgado, A.; González-Caballero, F. Electrokinetic and Stability Properties of Cholesterol in Aqueous NaCl and NaCl + Bile Salt Solutions. In *Trends in Colloid and Interface Science III*; Steinkopff: Darmstadt, 1989; Vol. 69, pp 64–69. https://doi.org/10.1007/BFb0116188.

(253) Product Information, S. *(-) Riboflavin Cell Culture Tested*. https://www.sigmaaldrich.com/deepweb/assets/sigmaaldrich/product/documents/191/415/r9504pis.pdf.

(254) Bird, J. C.; Kuna, A. Aqueous Solution of Riboflavin. 534,826, 1946.
(255) Mishra, M. K.; Mukherjee, A.; Ramamurty, U.; Desiraju, G. R. Crystal Chemistry and Photomechanical Behavior of 3,4-Dimethoxycinnamic Acid: Correlation between Maximum Yield in the Solid-State Topochemical Reaction and Cooperative Molecular Motion. *IUCrJ* **2015**, *2* (6), 653–660. https://doi.org/10.1107/S2052252515017297.
(256) Nishijo, J.; Yonetani, I. Interaction of Theobromine with Sodium Benzoate. *J. Pharm. Sci.* **1982**, *71* (3), 354–356. https://doi.org/10.1002/jps.2600710324.
(257) Vraneš, M.; Borović, T. T.; Drid, P.; Trivić, T.; Tomaš, R.; Janković, N. Influence of Sodium Salicylate on Self-Aggregation and Caffeine Solubility in Water—A New Hypothesis from Experimental and Computational Data. *Pharmaceutics* **2022**, *14* (11), 2304. https://doi.org/10.3390/pharmaceutics14112304.
(258) EFSA. Scientific Opinion on Flavouring Group Evaluation 20, Revision 4 (FGE.20Rev4): Benzyl Alcohols, Benzaldehydes, a Related Acetal, Benzoic Acids, and Related Esters from Chemical Groups 23 and 30. *EFSA J.* **2012**, *10* (12). https://doi.org/10.2903/j.efsa.2012.2994.
(259) Dhapte, V.; Mehta, P. Advances in Hydrotropic Solutions: An Updated Review. *St. Petersbg. Polytech. Univ. J. Phys. Math.* **2015**, *1* (4), 424–435. https://doi.org/10.1016/j.spjpm.2015.12.006.
(260) Undheim, K.; Benneche, T. Pyrimidines and Their Benzo Derivatives. In *Comprehensive Heterocyclic Chemistry II*; Elsevier, 1996; p 97. https://doi.org/10.1016/B978-008096518-5.00118-0.
(261) Kammerer, D. R. Anthocyanins. In *Handbook on Natural Pigments in Food and Beverages*; Elsevier, 2016; pp 61–80. https://doi.org/10.1016/B978-0-08-100371-8.00003-8.
(262) Morata, A.; López, C.; Tesfaye, W.; González, C.; Escott, C. Anthocyanins as Natural Pigments in Beverages. In *Value-Added Ingredients and Enrichments of Beverages*; Elsevier, 2019; pp 383–428. https://doi.org/10.1016/B978-0-12-816687-1.00012-6.
(263) Trouillas, P.; Sancho-García, J. C.; De Freitas, V.; Gierschner, J.; Otyepka, M.; Dangles, O. Stabilizing and Modulating Color by Copigmentation: Insights from Theory and Experiment. *Chem. Rev.* **2016**, *116* (9), 4937–4982. https://doi.org/10.1021/acs.chemrev.5b00507.
(264) Wang, W.; Han, J. J.; Wang, L. Q.; Li, L. S.; Shaw, W. J.; Li, A. D. Q. Dynamic π-π Stacked Molecular Assemblies Emit from Green to Red Colors. *Nano Lett.* **2003**, *3* (4), 455–458. https://doi.org/10.1021/nl025976j.
(265) Fusina, A. Hydrotropic Concepts Applied to the Water-Solubilization of Polyphenols : Example of Meglumine, Modeling, Physicochemical Study and Applications, Universität Regensburg and Centrale Lille, 2023.
(266) Booth, J. J.; Abbott, S.; Shimizu, S. Mechanism of Hydrophobic Drug Solubilization by

Small Molecule Hydrotropes. *J. Phys. Chem. B* **2012**, *116* (51), 14915–14921. https://doi.org/10.1021/jp309819r.

(267) Zeisel, S. H.; da Costa, K.-A. Choline: An Essential Nutrient for Public Health. *Nutr. Rev.* **2009**, *67* (11), 615–623. https://doi.org/10.1111/j.1753-4887.2009.00246.x.

(268) Sintra, T. E.; Luís, A.; Rocha, S. N.; Lobo Ferreira, A. I. M. C.; Gonçalves, F.; Santos, L. M. N. B. F.; Neves, B. M.; Freire, M. G.; Ventura, S. P. M.; Coutinho, J. A. P. Enhancing the Antioxidant Characteristics of Phenolic Acids by Their Conversion into Cholinium Salts. *ACS Sustain. Chem. Eng.* **2015**, *3* (10), 2558–2565. https://doi.org/10.1021/acssuschemeng.5b00751.

(269) Oh, K.-I.; Rajesh, K.; Stanton, J. F.; Baiz, C. R. Quantifying Hydrogen-Bond Populations in Dimethyl Sulfoxide/Water Mixtures. *Angew. Chemie Int. Ed.* **2017**, *56* (38), 11375–11379. https://doi.org/10.1002/anie.201704162.

(270) Römisch, W.; Eisenreich, W.; Richter, G.; Bacher, A. Rapid One-Pot Synthesis of Riboflavin Isotopomers. *J. Org. Chem.* **2002**, *67* (25), 8890–8894. https://doi.org/10.1021/jo026105x.

(271) Edwards, A. M.; Saldaño, A.; Bueno, C.; Silva, E.; Alegría, S. SPECTROSCOPIC PROPERTIES OF HYDROPHOBIC FLAVIN ESTERS.: A ONE AND TWO-DIMENSIONAL ^{1}H-NMR AND 13C-NMR STUDY. *Boletín la Soc. Chil. Química* **2000**, *45* (3). https://doi.org/10.4067/S0366-16442000000300013.

(272) Kim, T.; Park, S. Y.; Lee, M.-H.; Kim, D.-H.; Chung, I. Syntheses of Polyrotaxane Conjugated with 5-Fluorouracil and Vitamins with Improved Antitumor Activities. *J. Bioact. Compat. Polym.* **2019**, *34* (1), 25–38. https://doi.org/10.1177/0883911518813617.

(273) Bienz, S. Vorlesungsskript Zu Anwendung Spektroskopischer Methoden Teil : Kernmagnetische Resonanz. **2002**.

(274) R. Ellson; R. Stearns; M. Mutz; C. Brown; B. Browning; D. Harris; S. Qureshi; J. Shieh; D. Wold. In Situ DMSO Hydration Measurements of HTS Compound Libraries. *Comb. Chem. High Throughput Screen.* **2005**, *8* (6), 489–498. https://doi.org/10.2174/1386207054867382.

(275) Riwar, L.-J.; Trapp, N.; Kuhn, B.; Diederich, F. Substituent Effects in Parallel-Displaced π-π Stacking Interactions: Distance Matters. *Angew. Chemie Int. Ed.* **2017**, *56* (37), 11252–11257. https://doi.org/10.1002/anie.201703744.

(276) Majumder, M.; Sathyamurthy, N. A Theoretical Investigation on the Effect of π–π Stacking Interaction on 1H Isotropic Chemical Shielding in Certain Homo- and Hetero-Nuclear Aromatic Systems. *Theor. Chem. Acc.* **2012**, *131* (2), 1092. https://doi.org/10.1007/s00214-012-1092-3.

(277) Yusa, S. I. Polymer Characterization. *Polym. Sci. Nanotechnol. Fundam. Appl.* **2020**, 105–124. https://doi.org/10.1016/B978-0-12-816806-6.00006-6.

(278) Chen, L.; Wang, H.; Liu, J.; Xing, R.; Yu, X.; Han, Y. Tuning the π-π Stacking Distance and J-Aggregation of DPP-Based Conjugated Polymer via Introducing Insulating Polymer. *J. Polym. Sci. Part B Polym. Phys.* **2016**, *54* (8), 838–847. https://doi.org/10.1002/polb.23984.

(279) Zhao, Y.; Sarnello, E. S.; Robertson, L. A.; Zhang, J.; Shi, Z.; Yu, Z.; Bheemireddy, S. R.; Z, Y.; Li, T.; Assary, R. S.; Cheng, L.; Zhang, Z.; Zhang, L.; Shkrob, I. A. Competitive Pi-Stacking and H-Bond Piling Increase Solubility of Heterocyclic Redoxmers. *J. Phys. Chem. B* **2020**, *124* (46), 10409–10418. https://doi.org/10.1021/acs.jpcb.0c07647.

(280) Deng, J.-H.; Luo, J.; Mao, Y.-L.; Lai, S.; Gong, Y.-N.; Zhong, D.-C.; Lu, T.-B. π-π Stacking Interactions: Non-Negligible Forces for Stabilizing Porous Supramolecular Frameworks. *Sci. Adv.* **2020**, *6* (2). https://doi.org/10.1126/sciadv.aax9976.

(281) Xu, Y.; Szép, S.; Lu, Z. The Antioxidant Role of Thiocyanate in the Pathogenesis of Cystic Fibrosis and Other Inflammation-Related Diseases. *Proc. Natl. Acad. Sci.* **2009**, *106* (48), 20515–20519. https://doi.org/10.1073/pnas.0911412106.

(282) Arakawa, R.; Yamaguchi, M.; Hotta, H.; Osakai, T.; Kimoto, T. Product Analysis of Caffeic Acid Oxidation by On-Line Electrochemistry/ Electrospray Ionization Mass Spectrometry. *J. Am. Soc. Mass Spectrom.* **2004**, *15* (8), 1228–1236. https://doi.org/10.1016/j.jasms.2004.05.007.

(283) Singleton, V. L.; Cilliers, J. J. L. Characterization of the Products of Nonenzymic Autoxidative Phenolic Reactions in a Caffeic Acid Model System. *J. Agric. Food Chem.* **1991**, *39* (7), 1298–1303. https://doi.org/10.1021/jf00007a021.

(284) Schuman Jorns, M.; Schollnhammer, G.; Hemmerich, P. Intramolecular Addition of the Riboflavin Side Chain. Anion-Catalyzed Neutral Photochemistry. *Eur. J. Biochem.* **1975**, *57* (1), 35–48. https://doi.org/10.1111/j.1432-1033.1975.tb02274.x.

(285) Sheraz, M.; Kazi, S.; Ahmed, S.; Qadeer, K.; Khan, M.; Ahmad, I. Multicomponent Spectrometric Analysis of Riboflavin and Photoproducts and Their Kinetic Applications. *Open Chem.* **2014**, *12* (6), 635–642. https://doi.org/10.2478/s11532-014-0527-1.

(286) Tazaki, H.; Kawabata, J.; Fujita, T. Novel Oxidative Dimer from Caffeic Acid. *Biosci. Biotechnol. Biochem.* **2003**, *67* (5), 1185–1187. https://doi.org/10.1271/bbb.67.1185.

(287) Le Person, A.; Lacoste, A.-S.; Cornard, J.-P. Photo-Degradation of Trans-Caffeic Acid in Aqueous Solution and Influence of Complexation by Metal Ions. *J. Photochem. Photobiol. A Chem.* **2013**, *265*, 10–19. https://doi.org/10.1016/j.jphotochem.2013.05.004.

(288) Ford, C. W.; HARTLEY, R. D. Identification of Phenols, Phenolic Acid Dimers, and Monosaccharides by Gas-Liquid Chromatography on a Capillary Column. *J. Chromatogr.* **1988**, *436*, 484–489.

(289) Agata, I.; Kusakabe, H.; Hatano, T.; Nishibe, S.; Okuda, T. Melitric Acids A and B, New Trimeric Caffeic Acid Derivatives from Melissa Officinalis. *Chem. Pharm. Bull.* **1993**, *41* (9), 1608–1611. https://doi.org/10.1248/cpb.41.1608.

(290) Rondini, L.; Peyrat-Maillard, M.-N.; Marsset-Baglieri, A.; Fromentin, G.; Durand, P.; Tomé, D.; Prost, M.; Berset, C. Bound Ferulic Acid from Bran Is More Bioavailable than the Free Compound in Rat. *J. Agric. Food Chem.* **2004**, *52* (13), 4338–4343. https://doi.org/10.1021/jf0348323.

(291) He, Y.; Jia, Y.; Lu, F. New Products Generated from the Transformations of Ferulic Acid Dilactone. *Biomolecules* **2020**, *10* (2), 175. https://doi.org/10.3390/biom10020175.

(292) Braune, A.; Bunzel, M.; Yonekura, R.; Blaut, M. Conversion of Dehydrodiferulic Acids by Human Intestinal Microbiota. *J. Agric. Food Chem.* **2009**, *57* (8), 3356–3362. https://doi.org/10.1021/jf900159h.

(293) Bunzel, M.; Ralph, J.; Brüning, P.; Steinhart, H. Structural Identification of Dehydrotriferulic and Dehydrotetraferulic Acids Isolated from Insoluble Maize Bran Fiber. *J. Agric. Food Chem.* **2006**, *54* (17), 6409–6418. https://doi.org/10.1021/jf061196a.

(294) Choe, E.; Huang, R.; Min, D. B. Chemical Reactions and Stability of Riboflavin in Foods. *J. Food Sci.* **2005**, *70* (1), 28–36.

(295) Lang, W.; Zander, R. Salting-out of Oxygen from Aqueous Electrolyte Solutions: Prediction and Measurement. *Ind. Eng. Chem. Fundam.* **1986**, *25* (4), 775–782. https://doi.org/10.1021/i100024a050.

(296) Bender, C. J. Theoretical Models of Charge-Transfer Complexes. *Chem. Soc. Rev.* **1986**, *15* (4), 475–502. https://doi.org/10.1039/CS9861500475.

(297) Zhao, Z.; Vavrusova, M.; Skibsted, L. H. Antioxidant Activity and Calcium Binding of Isomeric Hydroxybenzoates. *J. Food Drug Anal.* **2018**, *26* (2), 591–598. https://doi.org/10.1016/j.jfda.2017.07.001.

(298) Gerstner, G. How to Fortify Beverages With Calcium. *Food Mark. Technol.* **2003**, 16–19.

(299) Jungbunzlauer. *Mineral Fortification in Dairy Alternatives*. Wellness Foods Europe. https://www.jungbunzlauer.com/fileadmin/content/_PDF/PRINT_PROJECTS/Article_facts/JBL_AR_Mineral_fortification_in_dairy_alternatives_2020-095.pdf (accessed 2022-08-08).

(300) Jungbunzlauer. *Solutions for food and beverage fortification*. https://www.jungbunzlauer.com/fileadmin/content/_PDF/PRINT_PROJECTS/Flyer/JBL_FL_Solutions_for_food_and_beverage_fortification_2020-144.pdf (accessed 2022-08-08).

(301) Buglass, A. J. Chemical Composition of Beverages and Drinks. In *Handbook of Food*

Chemistry; Cheung, P. C. K., Ed.; Springer Berlin Heidelberg: Berlin, Heidelberg, 2014; pp 1–62. https://doi.org/10.1007/978-3-642-41609-5_29-1.

(302) Scientific Opinion of the Panel on Food Additives and Nutrient Sources Added to Food on a Request from the Commission on Magnesium Ascorbate, Zinc Ascorbate and Calcium Ascorbate Added for Nutritional Purposes in Food Supplements. *EFSA J.* **2009**, *995*, 1–22.

(303) Boulton, R. The Copigmentation of Anthocyanins and Its Role in the Color of Red Wine: A Critical Review. *Am. J. Enol. Vitic.* **2001**, *52* (2), 67–87. https://doi.org/10.5344/ajev.2001.52.2.67.

(304) Selleckchem. *Menadione bisulfite sodium*. https://www.selleckchem.com/datasheet/menadione-bisulfite-sodium-S595300-DataSheet.html (accessed 2023-08-08).

(305) Bottari, E.; D'Ambrosio, A.; De Tommaso, G.; Festa, M. R.; Iuliano, M.; Meschino, M. Solubility of Folic Acid and Protonation of Folate in NaCl at Different Concentrations, Even in Physiological Solution. *Analyst* **2021**, *146* (7), 2339–2347. https://doi.org/10.1039/D1AN00013F.

(306) Wusigale; Hu, L.; Cheng, H.; Gao, Y.; Liang, L. Mechanism for Inhibition of Folic Acid Photodecomposition by Various Antioxidants. *J. Agric. Food Chem.* **2020**, *68* (1), 340–350. https://doi.org/10.1021/acs.jafc.9b06263.

(307) Kaduk, J. A.; Crowder, C. E.; Zhong, K. Crystal Structure of Folic Acid Dihydrate, C29H29N2O6(H2O)2. *Powder Diffr.* **2015**, *30* (1), 52–56. https://doi.org/10.1017/S0885715614000815.

(308) Wu, Z.; Li, X.; Hou, C.; Qian, Y. Solubility of Folic Acid in Water at PH Values between 0 and 7 at Temperatures (298.15, 303.15, and 313.15) K. *J. Chem. Eng. Data* **2010**, *55* (9), 3958–3961. https://doi.org/10.1021/je1000268.

(309) Mastropaolo, D.; Camerman, A.; Camerman, N. Folic Acid: Crystal Structure and Implications for Enzyme Binding. *Science (80-.).* **1980**, *210* (4467), 334–336. https://doi.org/10.1126/science.7423195.

(310) Sigma Aldrich. *Folic Acid Cell Culture Tested Product Information*. https://www.sigmaaldrich.com/deepweb/assets/sigmaaldrich/product/documents/102/092/f8758pis.pdf (accessed 2022-09-29).

(311) Wusigale; Fu, X.; Yin, X.; Ji, C.; Cheng, H.; Liang, L. Effects of Folic Acid and Caffeic Acid on Indirect Photo-Oxidation of Proteins and Their Costabilization under Irradiation. *J. Agric. Food Chem.* **2021**, *69* (42), 12505–12516. https://doi.org/10.1021/acs.jafc.1c02209.

(312) Zhu, B.; Wang, J.-R.; Zhang, Q.; Mei, X. Improving Dissolution and Photostability of Vitamin K3 via Cocrystallization with Naphthoic Acids and Sulfamerazine. *Cryst. Growth Des.* **2016**, *16* (1), 483–492. https://doi.org/10.1021/acs.cgd.5b01491.

(313) Shumilin, I.; Allolio, C.; Harries, D. How Sugars Modify Caffeine Self-Association and Solubility: Resolving a Mechanism of Selective Hydrotropy. *J. Am. Chem. Soc.* **2019**, *141* (45), 18056–18063. https://doi.org/10.1021/jacs.9b07056.

(314) Kettner, F.; Hüter, L.; Schäfer, J.; Röder, K.; Purgahn, U.; Krautscheid, H. Selective Crystallization of Indigo B by a Modified Sublimation Method and Its Redetermined Structure. *Acta Crystallogr. Sect. E Struct. Reports Online* **2011**, *67* (11), o2867–o2867. https://doi.org/10.1107/S1600536811040220.

(315) Cui, Y. Parallel Stacking of Caffeine with Riboflavin in Aqueous Solutions: The Potential Mechanism for Hydrotropic Solubilization of Riboflavin. *Int. J. Pharm.* **2010**, *397* (1–2), 36–43. https://doi.org/10.1016/j.ijpharm.2010.06.043.

(316) Garidel, P.; Hildebrand, A.; Knauf, K.; Blume, A. Membranolytic Activity of Bile Salts: Influence of Biological Membrane Properties and Composition. *Molecules* **2007**, *12* (10), 2292–2326. https://doi.org/10.3390/12102292.

(317) Maslova, V. A.; Kiselev, M. A. Structure of Sodium Cholate Micelles. *Crystallogr. Reports* **2018**, *63* (3), 472–475. https://doi.org/10.1134/S1063774518030173.

(318) Coello, A.; Meijide, F.; Núñez, E. R.; Tato, J. V. Aggregation Behavior of Bile Salts in Aqueous Solution. *J. Pharm. Sci.* **1996**, *85* (1), 9–15. https://doi.org/10.1021/js950326j.

(319) Hebling, C. M.; Thompson, L. E.; Eckenroad, K. W.; Manley, G. A.; Fry, R. A.; Mueller, K. T.; Strein, T. G.; Rovnyak, D. Sodium Cholate Aggregation and Chiral Recognition of the Probe Molecule (R , S)-1,1′-Binaphthyl-2,2′-Diylhydrogenphosphate (BNDHP) Observed by 1 H and 31 P NMR Spectroscopy. *Langmuir* **2008**, *24* (24), 13866–13874. https://doi.org/10.1021/la802000x.

(320) U.S. Food & Drug Administration. *Food Additive Status List*. https://www.fda.gov/food/food-additives-petitions/food-additive-status-list#ftnS (accessed 2023-08-08).

(321) El-Khordagui, L. K. Effect of Sodium Salicylate on the Solution Properties of Sodium Dodecyl Sulphate. *Int. J. Pharm.* **1992**, *83* (1–3), 53–58. https://doi.org/10.1016/0378-5173(82)90007-2.

(322) European Medicines Agency; Committee for Human Medicinal Products. Questions and Answers on Sodium Laurilsulfate in the Context of the Revision of the Guideline on ‘Excipients in the Label and Package Leaflet of Medicinal Products for Human Use’ (CPMP/463/00 Rev.1); 2015; pp 1–6.

(323) Klamt, A. COSMOthermX. COSMOlogic GmbH & Co. KG.

(324) Sakate, H. *The crystallographic study of riboflavin*. https://www.med.nagoya-u.ac.jp/medlib/nagoya_j_med_sci/pdf/v18n56p203_214.pdf (accessed 2022-01-21).

(325) Daďová, J.; Kümmel, S.; Feldmeier, C.; Cibulková, J.; Pažout, R.; Maixner, J.; Gschwind, R. M.; König, B.; Cibulka, R. Aggregation Effects in Visible-Light Flavin

Photocatalysts: Synthesis, Structure, and Catalytic Activity of 10-Arylflavins. *Chem. - A Eur. J.* **2013**, *19* (3), 1066–1075. https://doi.org/10.1002/chem.201202488.

(326) Grabowski, S. J. Chapter 1. Hydrogen Bond – Definitions, Criteria of Existence and Various Types. In *Understanding Hydrogen Bonds: Theoretical and Experimental Views*; 2020; Vol. 1, pp 1–40. https://doi.org/10.1039/9781839160400-00001.

(327) Queimada, A. J.; Mota, F. L.; Pinho, S. P.; Macedo, E. A. Solubilities of Biologically Active Phenolic Compounds: Measurements and Modeling. *J. Phys. Chem. B* **2009**, *113* (11), 3469–3476. https://doi.org/10.1021/jp808683y.

(328) Hu, S.; Han, J.; Liu, H.; Qiu, J.; Yi, D.; An, M.; Guo, Y.; Huang, H.; He, H.; Wang, P. Determination and Correlation of d -Ribose Solubility in Twelve Pure and Four Binary Solvent Systems. *J. Chem. Eng. Data* **2020**, *65* (4), 2144–2155. https://doi.org/10.1021/acs.jced.0c00009.

(329) Eiberweiser, A.; Nazet, A.; Hefter, G.; Buchner, R. Ion Hydration and Association in Aqueous Potassium Phosphate Solutions. *J. Phys. Chem. B* **2015**, *119* (16), 5270–5281. https://doi.org/10.1021/acs.jpcb.5b01417.

(330) Pribil, A. B.; Hofer, T. S.; Randolf, B. R.; Rode, B. M. Structure and Dynamics of Phosphate Ion in Aqueous Solution: An Ab Initio QMCF MD Study. *J. Comput. Chem.* **2008**, *29* (14), 2330–2334. https://doi.org/10.1002/jcc.20968.

(331) Tsuzuki, S.; Honda, K.; Uchimaru, T.; Mikami, M.; Tanabe, K. Origin of Attraction and Directionality of the π/π Interaction: Model Chemistry Calculations of Benzene Dimer Interaction. *J. Am. Chem. Soc.* **2002**, *124* (1), 104–112. https://doi.org/10.1021/ja0105212.

(332) Hunter, C. A.; Sanders, J. K. M. The Nature of .Pi.-.Pi. Interactions. *J. Am. Chem. Soc.* **1990**, *112* (14), 5525–5534. https://doi.org/10.1021/ja00170a016.

(333) Ulvik, A.; Vollset, S. E.; Hoff, G.; Ueland, P. M. Coffee Consumption and Circulating B-Vitamins in Healthy Middle-Aged Men and Women. *Clin. Chem.* **2008**, *54* (9), 1489–1496. https://doi.org/10.1373/clinchem.2008.103465.

(334) Kim, J.; Hong, H.; Heo, A.; Park, W. Indole Toxicity Involves the Inhibition of Adenosine Triphosphate Production and Protein Folding in Pseudomonas Putida. *FEMS Microbiol. Lett.* **2013**, *343* (1), 89–99. https://doi.org/10.1111/1574-6968.12135.

(335) Walker, R. W.; Dumke, K. A.; Goran, M. I. Fructose Content in Popular Beverages Made with and without High-Fructose Corn Syrup. *Nutrition* **2014**, *30* (7–8), 928–935. https://doi.org/10.1016/j.nut.2014.04.003.

(336) Atamas, N. A.; Atamas, A. A. The Investigations of Water-Ethanol Mixture by Monte Carlo Method. *Int. J. Chem. Mol. Eng.* **2009**, *3* (2009), 1–4.

(337) Rubino, J. T. Cosolvents and Cosolvency. In *Encyclopedia of Pharmaceutical Science and Technology*; CRC Press: New York, 2007; pp 806–808. https://doi.org/10.1081/E-EPT-100000466.

7 Appendix

7.1 Calibration curves for UV-Vis-absorbance measurements

Table A 1: Calibration curve for riboflavin in water at the UV-Vis-spectrophotometer at 449 nm.

Slope (AU·kg·mmol^{-1})	Intercept (AU)	Correlation coefficient R^2
12.353	0.0028	0.9999
12.394	0.0057	0.9999
12.133	0.0025	0.9998
averaged	**averaged**	
12.3 ± 0.1	0.004 ± 0.001	

Table A 2: Calibration curve for lumichrome in water at the UV-Vis-spectrophotometer at 386 nm.

Slope (AU·kg·mmol^{-1})	Intercept (AU)	Correlation coefficient R^2
12.5	0.019	0.9784
11.6	0.068	0.9937
11.0	0.081	0.9957
averaged	**averaged**	-
11.7 ± 0.6	0.05 ± 0.03	-

Table A 3: Calibration curve for RF-PO_4 in water at the UV-Vis-spectrophotometer at 445 nm.

Slope (AU·kg·mmol^{-1})	Intercept (AU)	Correlation coefficient R^2
11.02	0.003	0.9998
11.01	0.005	0.9999
11.21	0.002	0.9998
averaged	**averaged**	-
11.08 ± 0.003	0.09 ± 0.001	-

Table A 4: Calibration curve for vitamin K3 in water at the UV-Vis-spectrophotometer at 336 nm.

Slope (AU·kg·mmol^{-1})	Intercept (AU)	Correlation coefficient R^2
2.5867	0.0109	0.9995
2.6391	0.0060	0.9999
2.6286	0.0100	0.9999
averaged	**averaged**	
2.62 ± 0.009	0.009 ± 0.002	

Table A 5: Calibration curves for riboflavin in the binary water/ethanol system at the UV-Vis-spectrophotometer at 449 nm.

Ethanol/water (w/w)	Slope/(AU·kg·mmol^{-1})	Intercept / AU
0	11.8 ± 0.2	0.006
10	12.3 ± 0.1	0.003
20	12.2 ± 0.5	0.007
30	11.9 ± 0.3	0.000
40	12.16 ± 0.04	0.016
50	11.0 ± 0.1	-0.001
60	10.8 ± 0.2	0.017
70	10.37 ± 0.05	0.007
80	10.26 ± 0.06	0.016
90	9.3 ± 0.5	0.011
100	8.84 ± 0.06	0.023

Table A 6: Calibration curves for riboflavin in the binary ethanol/triacetin system at the UV-Vis-spectrophotometer at 449 nm.

Ethanol/triacetin (w/w)	Slope/(AU·kg·mmol^{-1})	Intercept / AU
40/60	11.13 ± 0.04	0.010
50/50	10.62 ± 0.09	0.020
60/40	10.34 ± 0.08	0.009
70/30	10.00 ± 0.2	0.007
80/20	9.41 ± 0.05	0.020
90/10	9.3 ± 0.6	0.009

Table A 7: Calibration curves for riboflavin in the ternary water/ethanol/triacetin system at a fixed water/ethanol ratio 1:1 (w/w) at the UV-Vis-spectrophotometer at 449 nm.

Water/ethanol/triacetin (w/w)	Slope/(AU·kg·mmol^{-1})	Intercept / AU
45/45/10	11.6 ± 0.5	-0.006
40/40/20	11.3 ± 0.4	-0.006
35/35/30	11.68 ± 0.6	-0.006
30/30/40	12.1 ± 0.2	0.015
25/25/50	12.06 ± 0.06	-0.007
20/20/60	12.4 ± 0.3	-0.006
15/15/70	11.98 ± 0.05	-0.007
10/10/80	13.0 ± 0.1	0.016

Table A 8: Calibration curves for riboflavin in the ternary water/ethanol/triacetin system at a fixed ethanol/triacetin ratio of 6:4 (w/w) at the UV-Vis-spectrophotometer at 449 nm

Water/ethanol/triacetin (w/w)	Slope/(AU·kg·mmol^{-1})	Intercept / AU
0/60/40	10.34 ± 0.08	0.009
10/54/36	10.7 ± 0.1	-0.006
20/48/32	10.4 ± 0.2	-0.023
30/42/28	11.28 ± 0.03	-0.005
40/36/24	11.39 ± 0.2	0.004
50/30/20	12.33 ± 0.09	0.002
60/24/16	12.1 ± 0.2	-0.003

70/18/12	12.5 ± 0.1	0.017
80/12/8	12.78 ± 0.09	0.018
90/6/4	13.37 ± 0.05	0.017

7.2 Single Crystal X-ray analysis of riboflavin

7.2.1 Riboflavin crystal obtained in presence of 3,4-dimethoxy-cinnamic acid

$C_{17}H_{20}N_4O_6$, M_r = 376.37, orthorhombic, $P2_12_12_1$ (No. 19), a = 5.31333(5) Å, b = 15.11045(13) Å, c = 20.03449(17) Å, $\alpha = \beta = \gamma = 90^{\circ}$, V = 1608.51(2) Å^3, Z = 4, Z' = 1, μ(Cu K_α) = 1.009, 16921 reflections measured, 3236 unique (Rint = 0.0260), which were used in all calculations. The final wR2 was 0.0812 (all data) and R1 was 0.0292 (I≥2 σ(I)).

Table A 9: Compound characterization of the riboflavin crystal obtained from a water/acetonitrile (50/50 (w/w)) solution saturated with 3,4-dimethoxycinnamic acid and riboflavin.

Parameter	Obtained value	Parameter	Obtained value
Formula	C17H20N4O6	**Z**	4
$\rho_{calc.}$ (g·cm^{-3})	1.554	**Z'**	1
μ·mm^{-1}	1.009	**λ (Å)**	1.54184
Formula Weight	376.37	**Radiation type**	Cu K_α
Color	Clear yellow	**θ_{min} (°)**	3.664
Shape	Prism-shaped	**θ_{max} (°)**	75.054
Size (mm^3)	0.28×0.04×0.03	**Measured Refl's.**	16921
T (K)	123.01(10)	**Indep't Refl's**	3236
Crystal System	orthorhombic	**Refl's I≥2 σ(I)**	3105
Flack Parameter	0.2(2)	**R_{int}**	0.0260
Hooft Parameter	0.06(5)	**Parameters**	328
Space Group	P212121	**Restraints**	6
a (Å)	5.31333(5)	**Largest Peak**	0.424
b (Å)	15.11045(13)	**Deepest Hole**	-0.335
c (Å)	20.03449(17)	**GooF**	1.038
α (°)	90	**wR_2 (all data)**	0.0812
β (°)	90	**wR_2**	0.0801
γ (°)	90	**R_1(all data)**	0.0309
V (Å^3)	1608.51(2)	**R_1**	0.0292

Table A 10: Fractional Atomic Coordinates (×10^4) and Equivalent Isotropic Displacement Parameters (Å^2×10^3) for the riboflavin crystal obtained from a water/acetonitrile (50/50 (w/w)) solution saturated with 3,4-dimethoxycinnamic acid and riboflavin. U_{eq} is defined as 1/3 of the trace of the orthogonalized U_{ij}.

Atom	x	y	z	U_{eq}
O4	6079(3)	5757.2(9)	6020.6(7)	18.4(3)
O6	12784(3)	6098.0(10)	4901.2(7)	20.2(3)
O2	13984(3)	8843.7(10)	7656.8(7)	22.6(3)
O5	10762(3)	7489.1(9)	5706.8(7)	19.7(3)

O3	4133(3)	7269.8(11)	6725.0(7)	23.4(3)
O1	8930(90)	9300(30)	9390(20)	28(4)
N1	7216(3)	6998.0(11)	7856.4(8)	16.8(4)
N4	10559(3)	7959.7(11)	7710.7(8)	18.6(4)
N3	11227(4)	9133.6(11)	8492.9(9)	19.7(4)
N2	5906(3)	7867.2(11)	9041.9(8)	18.0(4)
C12	8595(4)	7708.8(13)	8064.6(10)	16.7(4)
C9	7771(4)	8132.0(13)	8674.9(10)	17.7(4)
C15	7070(4)	6632.5(13)	5964.2(10)	16.0(4)
C11	12002(4)	8644.7(13)	7936.7(10)	19.2(4)
C1	5224(4)	6680.3(13)	8238.5(9)	17.1(4)
C10	9159(4)	8943.7(14)	8881.4(10)	21.1(4)
C13	7891(4)	6592.2(13)	7207.8(10)	17.6(4)
C2	3839(4)	5919.3(14)	8072.8(10)	20.0(4)
C5	2621(4)	6828.0(14)	9240.0(10)	18.7(4)
C4	1265(4)	6087.0(13)	9078.2(10)	19.5(4)
C14	6757(4)	7129.3(13)	6628.7(10)	17.1(4)
C3	1934(4)	5617.0(13)	8485.2(10)	20.1(4)
C6	4618(4)	7135.4(13)	8838.8(10)	17.9(4)
C17	10153(4)	6181.6(14)	5052.9(10)	18.0(4)
C16	9821(4)	6600.1(13)	5739.8(10)	16.4(4)
C8	-828(4)	5762.0(14)	9519.2(11)	22.0(4)
C7	582(5)	4778.3(14)	8306.0(11)	25.6(5)
O1A	8430(40)	9426(13)	9339(8)	27(2)

Table A 11: Anisotropic displacement parameters (×10⁴) for the riboflavin crystal obtained from a water/acetonitrile (50/50 (w/w)) solution saturated with 3,4-dimethoxycinnamic acid and riboflavin. The anisotropic displacement factor exponent takes the form: $-2^2[h^2a^{*2} \times U_{11} + ... + 2hka^* \times b^* \times U_{12}]$

Atom	U_{11}	U_{22}	U_{33}	U_{23}	U_{13}	U_{12}
O4	16.7(7)	19.7(7)	18.7(7)	-0.8(5)	-1.8(6)	-2.0(6)
O6	17.5(7)	21.2(7)	21.7(7)	1.5(6)	4.6(6)	1.2(6)
O2	18.2(8)	27.6(7)	22.1(7)	2.4(6)	2.5(6)	1.8(6)
O5	19.3(7)	18.5(7)	21.3(7)	1.4(5)	-1.7(6)	-2.3(6)
O3	17.4(8)	33.8(8)	19.1(7)	-0.8(6)	0.5(6)	7.6(6)
O1	28(8)	27(7)	30(5)	-12(5)	12(6)	-1(6)
N1	18.7(8)	18.4(8)	13.4(7)	-1.8(6)	-1.2(7)	3.5(7)
N4	18.7(9)	20.6(8)	16.6(7)	0.2(6)	0.5(7)	3.3(7)
N3	19.4(9)	19.0(8)	20.8(8)	-1.9(7)	1.3(7)	-2.5(7)
N2	19.2(9)	18.6(8)	16.2(7)	-0.5(6)	-0.9(7)	1.3(7)
C12	17.6(10)	16.9(9)	15.7(9)	0.9(7)	-1.0(8)	5.5(8)
C9	19.5(10)	18.5(9)	15.1(8)	-0.6(7)	-1.2(8)	2.8(8)
C15	15.9(9)	17.4(9)	14.6(9)	0.0(7)	-1.9(8)	0.3(8)
C11	19.5(10)	21.0(9)	16.9(9)	3.6(7)	-0.5(8)	4.0(8)
C1	17.4(9)	18.8(9)	15.2(8)	1.5(7)	-1.8(8)	3.6(8)
C10	21.4(10)	20.9(9)	21.0(9)	-1.2(7)	1.0(9)	-1.5(8)
C13	19.3(10)	20.0(9)	13.4(9)	-2.1(7)	-0.1(8)	3.0(8)
C2	22.5(11)	19.6(9)	18.0(9)	-1.7(7)	-2.7(8)	2.9(9)
C5	21.6(10)	19.9(9)	14.6(9)	-0.8(7)	-0.7(8)	2.0(8)
C4	18.0(10)	21.9(9)	18.7(9)	3.6(7)	-4.0(8)	1.4(8)
C14	15.5(10)	19.7(8)	16.2(9)	-0.7(7)	-0.5(8)	3.0(8)
C3	21.3(11)	20.0(9)	18.9(9)	1.2(7)	-6.3(8)	1.8(8)
C6	19.7(10)	17.9(8)	16.2(9)	0.5(7)	-3.1(8)	2.4(8)
C17	15.6(10)	20.4(9)	18.2(9)	0.9(7)	0.7(8)	0.8(8)
C16	17.0(9)	15.9(8)	16.3(9)	2.5(7)	-1.1(8)	1.1(8)
C8	20.1(11)	23.2(10)	22.6(10)	3.1(8)	-1.1(9)	-1.4(9)
C7	28.6(13)	22.9(10)	25.3(10)	-2.7(8)	-3.2(10)	-2.9(9)
O1A	23(4)	25(4)	32(2)	-13(2)	11(3)	-6(3)

Table A 12: Bond lengths in Å for the riboflavin crystal obtained from a water/acetonitrile (50/50 (w/w)) solution saturated with 3,4-dimethoxycinnamic acid and riboflavin

Atom	Atom	Length (Å)	Atom	Atom	Length (Å)
O4	C15	1.428(2)	C12	C9	1.448(3)
O6	C17	1.436(3)	C9	C10	1.490(3)
O2	C11	1.230(3)	C15	C14	1.537(3)
O5	C16	1.435(2)	C15	C16	1.530(3)
O3	C14	1.423(3)	C1	C2	1.405(3)
O1	C10	1.16(4)	C1	C6	1.422(3)
N1	C12	1.366(3)	C10	O1A	1.234(16)
N1	C1	1.392(3)	C13	C14	1.539(3)
N1	C13	1.481(2)	C2	C3	1.384(3)
N4	C12	1.317(3)	C5	C4	1.370(3)
N4	C11	1.365(3)	C5	C6	1.410(3)
N3	C11	1.399(3)	C4	C3	1.429(3)
N3	C10	1.377(3)	C4	C8	1.503(3)
N2	C9	1.297(3)	C3	C7	1.500(3)
N2	C6	1.363(3)	C17	C16	1.525(3)

Table A 13: Bond angles for the riboflavin crystal obtained from a water/acetonitrile (50/50 (w/w)) solution saturated with 3,4-dimethoxycinnamic acid and riboflavin.

Atom	Atom	Atom	Angle (°)	Atom	Atom	Atom	Angle (°)
C12	N1	C1	120.76(16)	N3	C10	C9	114.19(17)
C12	N1	C13	117.62(17)	O1A	C10	N3	123.2(6)
C1	N1	C13	121.61(17)	O1A	C10	C9	122.5(6)
C12	N4	C11	118.97(17)	N1	C13	C14	110.38(17)
C10	N3	C11	125.10(18)	C3	C2	C1	120.80(18)
C9	N2	C6	117.70(17)	C4	C5	C6	122.01(19)
N1	C12	C9	116.30(18)	C5	C4	C3	118.16(19)
N4	C12	N1	119.15(17)	C5	C4	C8	121.14(19)
N4	C12	C9	124.55(19)	C3	C4	C8	120.69(19)
N2	C9	C12	125.00(19)	O3	C14	C15	107.23(16)
N2	C9	C10	118.35(18)	O3	C14	C13	111.11(17)
C12	C9	C10	116.64(18)	C15	C14	C13	110.66(16)
O4	C15	C14	110.10(15)	C2	C3	C4	120.94(19)
O4	C15	C16	110.25(16)	C2	C3	C7	119.08(19)
C16	C15	C14	111.93(16)	C4	C3	C7	120.0(2)
O2	C11	N4	120.96(19)	N2	C6	C1	122.09(19)
O2	C11	N3	119.1(2)	N2	C6	C5	118.38(18)
N4	C11	N3	119.97(19)	C5	C6	C1	119.54(19)
N1	C1	C2	123.41(18)	O6	C17	C16	109.88(16)
N1	C1	C6	118.06(18)	O5	C16	C15	108.45(15)
C2	C1	C6	118.50(19)	O5	C16	C17	107.85(15)
O1	C10	N3	119(2)	C17	C16	C15	112.88(16)
O1	C10	C9	125(2)				

Table A 14: Torsion angles for the riboflavin crystal obtained from a water/acetonitrile (50/50 (w/w)) solution saturated with 3,4-dimethoxycinnamic acid and riboflavin.

Atom	Atom	Atom	Atom	Angle (°)
O4	C15	C14	O3	-68.0(2)
O4	C15	C14	C13	53.3(2)
O4	C15	C16	O5	-178.47(15)
O4	C15	C16	C17	62.1(2)
O6	C17	C16	O5	65.5(2)
O6	C17	C16	C15	-174.68(16)
N1	C12	C9	N2	2.6(3)
N1	C12	C9	C10	-176.04(18)
N1	C1	C2	C3	177.67(19)
N1	C1	C6	N2	0.6(3)
N1	C1	C6	C5	-179.61(17)
N1	C13	C14	O3	-51.6(2)
N1	C13	C14	C15	-170.59(17)
N4	C12	C9	N2	-176.88(19)
N4	C12	C9	C10	4.5(3)
N2	C9	C10	O1	11(3)
N2	C9	C10	N3	175.07(19)
N2	C9	C10	O1A	-8.6(15)
C12	N1	C1	C2	-175.80(18)
C12	N1	C1	C6	2.1(3)
C12	N1	C13	C14	-80.6(2)
C12	N4	C11	O2	172.90(18)
C12	N4	C11	N3	-7.3(3)
C12	C9	C10	O1	-171(3)
C12	C9	C10	N3	-6.2(3)
C12	C9	C10	O1A	170.1(15)
C9	N2	C6	C1	-1.6(3)
C9	N2	C6	C5	178.65(18)
C11	N4	C12	N1	-177.01(17)
C11	N4	C12	C9	2.5(3)
C11	N3	C10	O1	167(3)
C11	N3	C10	C9	1.7(3)
C11	N3	C10	O1A	-174.5(15)
C1	N1	C12	N4	176.01(17)
C1	N1	C12	C9	-3.5(3)
C1	N1	C13	C14	98.4(2)
C1	C2	C3	C4	2.2(3)
C1	C2	C3	C7	-177.19(19)
C10	N3	C11	O2	-174.96(19)
C10	N3	C11	N4	5.3(3)
C13	N1	C12	N4	-5.0(3)
C13	N1	C12	C9	175.49(18)
C13	N1	C1	C2	5.3(3)
C13	N1	C1	C6	-176.86(17)
C2	C1	C6	N2	178.58(18)
C2	C1	C6	C5	-1.6(3)
C5	C4	C3	C2	-2.3(3)

C5	C4	C3	C7	177.09(19)
C4	C5	C6	N2	-178.67(19)
C4	C5	C6	C1	1.5(3)
C14	C15	C16	O5	-55.6(2)
C14	C15	C16	C17	-174.99(16)
C6	N2	C9	C12	-0.1(3)
C6	N2	C9	C10	178.55(18)
C6	C1	C2	C3	-0.2(3)
C6	C5	C4	C3	0.4(3)
C6	C5	C4	C8	178.93(19)
C16	C15	C14	O3	168.99(16)
C16	C15	C14	C13	-69.7(2)
C8	C4	C3	C2	179.19(19)
C8	C4	C3	C7	-1.4(3)

Table A 15: Hydrogen fractional atomic coordinates (×10⁴) and equivalent isotropic displacement parameters (Å²×10³) for the riboflavin crystal obtained from a water/acetonitrile (50/50 (w/w)) solution saturated with 3,4-dimethoxycinnamic acid and riboflavin. U_{eq} is defined as 1/3 of the trace of the orthogonalized U_{ij}.

Atom	x	y	z	U_{eq}
H3	3475.96	6808.06	6880.5	35
H14	7628.6	7714.53	6598.9	21
H17A	9480(40)	5600(16)	5020(11)	11(5)
H17B	9350(50)	6539(16)	4699(12)	19(6)
H13A	7210(50)	5974(17)	7200(11)	18(6)
H5A	2300(50)	7120(18)	9621(13)	20(6)
H7A	1370(60)	4520(20)	7921(15)	37(8)
H6	13400(60)	6600(20)	4765(16)	41(9)
H16	10720(50)	6301(15)	6040(12)	14(6)
H8A	-2430(60)	5700(20)	9279(14)	33(8)
H8B	-1160(60)	6150(20)	9876(15)	37(8)
H2	4230(50)	5581(16)	7656(12)	19(6)
H13B	9780(60)	6606(18)	7191(12)	25(6)
H5	11890(70)	7470(20)	6053(18)	51(10)
H3A	12160(60)	9550(20)	8626(14)	30(7)
H15	6130(40)	6962(15)	5633(11)	12(5)
H8C	-460(60)	5180(20)	9730(14)	36(8)
H7B	730(60)	4360(20)	8680(15)	36(8)
H7C	-1210(80)	4890(20)	8252(17)	50(9)
H4	5020(60)	5720(20)	5777(15)	31(8)

7.2.2 Riboflavin crystal obtained in presence of cinnamic acid

$C_{17}H_{20}N_4O_6$, M_r = 376.37, orthorhombic, $P2_12_12_1$ (No. 19), a = 5.30940(10) Å, b = 15.11770(10) Å, c = 20.0373(2) Å, $\alpha = \beta = \gamma = 90^{\circ}$, V = 1608.31(4) Å^3, Z = 4, Z' = 1, μ(Cu K_α) = 1.009, 14730 reflections measured, 3253 unique (R_{int} = 0.0222), which were used in all calculations. The final wR_2 was 0.0664 (all data) and R_1 was 0.0263 (I≥2 σ(I)).

Table A 16: Compound characterization for the riboflavin crystal obtained from a water/acetonitrile (50/50 (w/w)) solution saturated with cinnamic acid and riboflavin.

Parameter	Obtained value	Parameter	Obtained value
Formula	$C_{17}H_{20}N_4O_6$	**Z**	4
$\rho_{calc.}$ (g·cm^{-3})	1.554	**Z'**	1
μ·mm^{-1}	1.009	**λ (Å)**	1.54184
Formula Weight	376.37	**Radiation type**	Cu K_α
Color	clear yellow	**θ_{min} (°)**	3.663
Shape	needle-shaped	**θ_{max} (°)**	74.975
Size (mm^3)	0.22×0.03×0.02	**Measured Refl's.**	14730
T (K)	123.00(10)	**Indep't Refl's**	3253
Crystal System	orthorhombic	**Refl's I≥2 σ(I)**	3077
Flack Parameter	-0.22(7)	**R_{int}**	0.0222
Hooft Parameter	-0.25(6)	**Parameters**	324
Space Group	$P2_12_12_1$	**Restraints**	0
a (Å)	5.30940(10)	**Largest Peak**	0.191
b (Å)	15.11770(10)	**Deepest Hole**	-0.152
c (Å)	20.0373(2)	**GooF**	1.037
α (°)	90	**wR_2 (all data)**	0.0664
β (°)	90	**wR_2**	0.0652
γ (°)	90	**R_1(all data)**	0.0288
V (Å^3)	1608.31(4)	**R_1**	0.0263

Table A 17: Fractional Atomic Coordinates (×10⁴) and Equivalent Isotropic Displacement Parameters (Å²×10³) for the riboflavin crystal obtained from a water/acetonitrile (50/50 (w/w)) solution saturated with cinnamic acid and riboflavin. U_{eq} is defined as 1/3 of the trace of the orthogonalized U_{ij}.

Atom	x	y	z	U_{eq}
O4	6068(3)	5756.7(8)	6020.8(7)	15.0(3)
O6	12776(3)	6097.7(9)	4900.2(7)	16.5(3)
O2	13988(3)	8844.8(9)	7657.9(7)	18.6(3)
O5	10763(3)	7487.5(8)	5707.0(7)	15.6(3)
O3	4120(3)	7264.1(9)	6725.1(7)	19.8(3)
O1	8528(3)	9401.8(10)	9348.5(8)	30.2(4)
N1	7218(3)	6997.8(10)	7856.4(7)	13.7(3)
N4	10558(3)	7960.9(10)	7710.8(8)	15.0(3)
N3	11231(3)	9134.5(10)	8492.7(8)	16.2(3)
N2	5908(3)	7869.0(9)	9042.0(8)	14.2(3)
C12	8597(4)	7709.7(11)	8066.0(9)	13.3(4)
C9	7775(4)	8133.5(12)	8673.7(9)	14.5(4)
C15	7075(3)	6631.9(11)	5965.1(9)	12.4(3)
C13	7893(4)	6595.0(12)	7207.4(9)	13.9(4)
C11	11999(4)	8645.7(12)	7937.0(9)	15.7(4)
C1	5226(4)	6680.9(11)	8238.9(9)	13.7(4)
C2	3837(4)	5920.4(12)	8074.7(9)	15.9(4)
C4	1269(4)	6087.0(12)	9077.6(9)	15.6(4)
C10	9160(4)	8945.2(12)	8881.8(9)	17.2(4)
C6	4620(4)	7135.3(11)	8837.2(9)	14.3(4)
C14	6760(4)	7125.6(12)	6628.9(9)	13.6(4)
C3	1933(4)	5617.8(12)	8485.9(10)	16.3(4)
C5	2620(4)	6828.0(12)	9240.0(9)	15.3(4)
C17	10153(3)	6180.9(12)	5053.6(9)	14.3(4)
C16	9816(3)	6599.1(11)	5739.4(9)	12.9(3)
C8	-830(4)	5760.5(13)	9519.6(10)	17.6(4)
C7	585(4)	4777.8(12)	8304.6(10)	21.5(4)

Table A 18: Anisotropic Displacement Parameters (×10⁴) for the riboflavin crystal obtained from a water/acetonitrile (50/50 (w/w)) solution saturated with cinnamic acid and riboflavin. The anisotropic displacement factor exponent takes the form: $-2^2[h^2a^{*2} \times U_{11} + ... + 2hka^* \times b^* \times U_{12}]$.

Atom	U_{11}	U_{22}	U_{33}	U_{23}	U_{13}	U_{12}
O4	13.1(6)	16.1(6)	15.8(6)	-1.1(5)	-1.0(5)	-1.8(5)
O6	14.0(7)	16.6(6)	18.9(7)	1.6(5)	4.5(5)	1.4(5)
O2	14.9(7)	23.9(6)	17.0(6)	1.6(5)	2.0(5)	1.9(6)
O5	14.7(7)	14.8(6)	17.3(6)	1.9(5)	-1.3(6)	-2.6(5)
O3	14.8(7)	30.4(7)	14.1(6)	-3.2(5)	-0.4(6)	8.5(6)
O1	33.0(9)	28.1(7)	29.5(8)	-16.2(6)	14.7(7)	-12.3(7)
N1	15.8(8)	14.4(7)	11.0(7)	-1.3(5)	-0.7(6)	2.9(6)
N4	14.9(8)	16.7(7)	13.5(7)	0.1(6)	-0.2(6)	3.6(6)
N3	15.8(8)	16.0(7)	16.7(8)	-2.7(6)	2.0(6)	-1.9(7)
N2	14.5(8)	14.7(7)	13.4(7)	-0.9(5)	-1.4(6)	1.1(6)
C12	14.0(9)	13.0(8)	12.8(8)	0.2(6)	-1.3(7)	4.6(7)
C9	16.3(9)	15.3(8)	11.9(8)	-0.4(7)	-1.2(7)	2.2(7)
C15	13.4(8)	13.1(8)	10.6(8)	1.2(6)	-2.0(7)	0.4(7)
C13	16.0(9)	15.4(8)	10.3(8)	-2.0(6)	-1.0(7)	2.3(7)
C11	17.0(9)	17.3(9)	12.7(9)	2.7(6)	-1.0(7)	4.5(7)
C1	14.1(8)	16.0(8)	11.0(8)	1.6(6)	-2.2(7)	2.6(7)
C2	19.1(10)	15.0(8)	13.5(8)	-2.0(6)	-3.0(7)	1.6(8)
C4	14.5(9)	17.6(8)	14.7(9)	3.4(7)	-3.2(7)	1.7(7)
C10	17.7(9)	17.5(8)	16.5(9)	-1.6(7)	0.9(8)	-1.0(7)
C6	16.1(9)	14.6(8)	12.1(8)	-0.4(6)	-3.3(7)	1.9(7)
C14	11.0(9)	16.0(8)	13.9(9)	-0.3(6)	-0.6(7)	2.4(7)
C3	17.2(10)	15.5(8)	16.2(9)	0.9(7)	-5.7(8)	1.2(7)
C5	17.1(9)	16.2(8)	12.5(8)	-0.6(7)	-1.2(7)	2.2(7)
C17	12.4(9)	17.0(8)	13.4(8)	1.4(7)	0.6(7)	1.4(7)
C16	12.9(8)	12.1(8)	13.6(8)	2.3(7)	-1.1(7)	-0.1(7)
C8	16.0(10)	18.9(9)	17.9(9)	2.1(7)	-1.5(8)	-1.9(8)
C7	24.6(11)	18.5(9)	21.5(10)	-2.7(7)	-3.3(9)	-4.6(8)

Table A 19: Bond lengths for the riboflavin crystal obtained from a water/acetonitrile (50/50 (w/w)) solution saturated with cinnamic acid and riboflavin.

Atom	Atom	Length (Å)	Atom	Atom	Length (Å)
O4	C15	1.431(2)	C12	C9	1.444(2)
O6	C17	1.432(2)	C9	C10	1.490(3)
O2	C11	1.232(2)	C15	C14	1.534(2)
O5	C16	1.436(2)	C15	C16	1.525(2)
O3	C14	1.430(2)	C13	C14	1.533(3)
O1	C10	1.210(2)	C1	C2	1.405(3)
N1	C12	1.368(2)	C1	C6	1.419(2)
N1	C13	1.480(2)	C2	C3	1.382(3)
N1	C1	1.391(2)	C4	C3	1.426(3)
N4	C12	1.317(2)	C4	C5	1.369(3)
N4	C11	1.365(2)	C4	C8	1.507(3)
N3	C11	1.397(2)	C6	C5	1.412(3)
N3	C10	1.378(3)	C3	C7	1.502(3)
N2	C9	1.299(2)	C17	C16	1.523(2)
N2	C6	1.366(2)			

Table A 20: Bond Angles for the riboflavin crystal obtained from a water/acetonitrile (50/50 (w/w)) solution saturated with cinnamic acid and riboflavin.

Atom	Atom	Atom	Angle (°)	Atom	Atom	Atom	Angle (°)
C12	N1	C13	117.65(16)	C3	C2	C1	121.00(17)
C12	N1	C1	120.58(15)	C3	C4	C8	120.58(17)
C1	N1	C13	121.76(16)	C5	C4	C3	118.36(18)
C12	N4	C11	118.83(16)	C5	C4	C8	121.05(17)
C10	N3	C11	125.02(16)	O1	C10	N3	122.71(17)
C9	N2	C6	117.47(16)	O1	C10	C9	123.31(18)
N1	C12	C9	116.51(16)	N3	C10	C9	113.98(16)
N4	C12	N1	118.95(16)	N2	C6	C1	122.23(17)
N4	C12	C9	124.54(17)	N2	C6	C5	118.15(16)
N2	C9	C12	124.99(17)	C5	C6	C1	119.62(17)
N2	C9	C10	118.11(16)	O3	C14	C15	107.16(15)
C12	C9	C10	116.89(17)	O3	C14	C13	111.06(16)
O4	C15	C14	109.95(14)	C13	C14	C15	111.00(14)
O4	C15	C16	110.47(14)	C2	C3	C4	120.79(17)
C16	C15	C14	112.15(15)	C2	C3	C7	118.96(17)
N1	C13	C14	110.75(15)	C4	C3	C7	120.24(18)
O2	C11	N4	120.99(17)	C4	C5	C6	121.81(17)
O2	C11	N3	118.85(17)	O6	C17	C16	110.15(15)
N4	C11	N3	120.16(17)	O5	C16	C15	108.50(14)
N1	C1	C2	123.49(17)	O5	C16	C17	107.84(14)
N1	C1	C6	118.12(16)	C17	C16	C15	113.15(15)
C2	C1	C6	118.36(17)				
C3	C2	C1	121.00(17)				

Table A 21: Torsion Angles for the riboflavin crystal obtained from a water/acetonitrile (50/50 (w/w)) solution saturated with cinnamic acid and riboflavin.

Atom	Atom	Atom	Atom	Angle/°
O4	C15	C14	O3	-67.61(18)
O4	C15	C14	C13	53.8(2)
O4	C15	C16	O5	-178.56(14)
O4	C15	C16	C17	61.81(18)
O6	C17	C16	O5	65.28(18)
O6	C17	C16	C15	-174.71(14)
N1	C12	C9	N2	2.8(3)
N1	C12	C9	C10	-176.05(16)
N1	C13	C14	O3	-51.5(2)
N1	C13	C14	C15	-170.61(15)
N1	C1	C2	C3	177.66(17)
N1	C1	C6	N2	0.5(3)
N1	C1	C6	C5	-179.54(16)
N4	C12	C9	N2	-177.02(17)
N4	C12	C9	C10	4.2(3)
N2	C9	C10	O1	-5.2(3)
N2	C9	C10	N3	175.02(17)

N2	C6	C5	C4	-178.62(17)
C12	N1	C13	C14	-80.7(2)
C12	N1	C1	C2	-175.82(16)
C12	N1	C1	C6	2.1(2)
C12	N4	C11	O2	172.62(16)
C12	N4	C11	N3	-7.4(2)
C12	C9	C10	O1	173.67(19)
C12	C9	C10	N3	-6.1(2)
C9	N2	C6	C1	-1.4(3)
C9	N2	C6	C5	178.61(17)
C13	N1	C12	N4	-5.0(2)
C13	N1	C12	C9	175.21(16)
C13	N1	C1	C2	5.4(3)
C13	N1	C1	C6	-176.61(15)
C11	N4	C12	N1	-177.03(16)
C11	N4	C12	C9	2.7(3)
C11	N3	C10	O1	-177.96(19)
C11	N3	C10	C9	1.8(3)
C1	N1	C12	N4	176.18(16)
C1	N1	C12	C9	-3.6(2)
C1	N1	C13	C14	98.09(19)
C1	C2	C3	C4	2.1(3)
C1	C2	C3	C7	-177.16(17)
C1	C6	C5	C4	1.4(3)
C2	C1	C6	N2	178.59(16)
C2	C1	C6	C5	-1.5(3)
C10	N3	C11	O2	-174.86(17)
C10	N3	C11	N4	5.2(3)
C6	N2	C9	C12	-0.2(3)
C6	N2	C9	C10	178.57(16)
C6	C1	C2	C3	-0.3(3)
C14	C15	C16	O5	-55.52(18)
C14	C15	C16	C17	-175.15(14)
C3	C4	C5	C6	0.4(3)
C5	C4	C3	C2	-2.2(3)
C5	C4	C3	C7	177.12(17)
C16	C15	C14	O3	169.05(15)
C16	C15	C14	C13	-69.53(19)
C8	C4	C3	C2	179.21(17)
C8	C4	C3	C7	-1.5(3)
C8	C4	C5	C6	178.99(17)

Table A 22: Hydrogen Fractional Atomic Coordinates (×10⁴) and Equivalent Isotropic Displacement Parameters (Å²×10³) for the riboflavin crystal obtained from a water/acetonitrile (50/50 (w/w)) solution saturated with cinnamic acid and riboflavin. U_{eq} is defined as 1/3 of the trace of the orthogonalized U_{ij}.

Atom	x	y	z	U_{eq}
H17A	9360(50)	6552(14)	4717(12)	21(6)
H5A	2300(40)	7174(14)	9646(12)	12(5)
H15	6140(40)	6960(14)	5646(10)	13(5)
H17B	9500(40)	5579(13)	5028(10)	6(5)
H13A	7270(50)	5980(16)	7202(11)	20(6)
H13B	9740(50)	6610(14)	7183(11)	14(5)
H14	7650(50)	7710(15)	6599(11)	18(6)
H8A	-1110(50)	6135(16)	9887(13)	29(6)
H16	10800(40)	6236(13)	6077(11)	18(5)
H2	4250(40)	5610(13)	7664(11)	14(5)
H6	13360(50)	6584(17)	4776(13)	28(7)
H8B	-2390(50)	5660(15)	9280(13)	27(6)
H3A	12200(50)	9597(18)	8631(13)	33(7)
H8C	-450(50)	5191(16)	9738(13)	29(6)
H3	4000(60)	7654(17)	7030(15)	38(8)
H7A	1410(50)	4485(15)	7898(13)	27(6)
H7B	-1230(60)	4889(17)	8224(13)	32(7)
H7C	800(50)	4333(17)	8691(14)	41(8)
H5	11920(60)	7515(18)	6042(16)	44(8)
H4	4960(60)	5699(17)	5728(14)	37(8)

7.3 DLS correlation functions of sodium polyphenolates in water at 10 °C

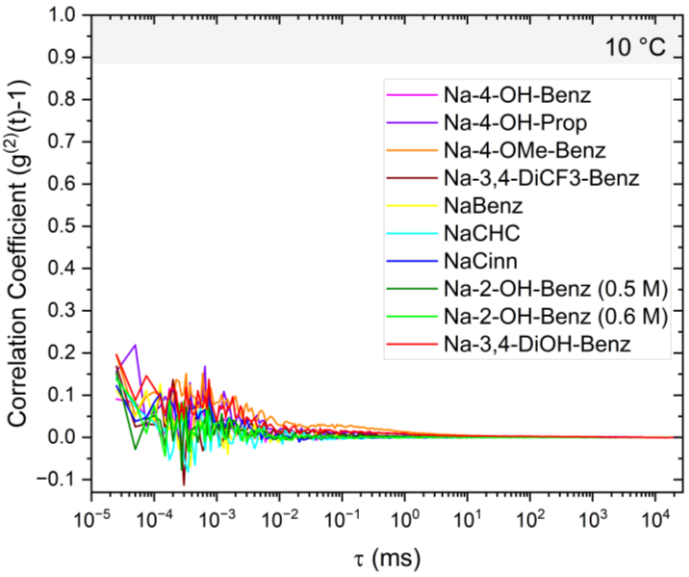

Figure A 1: DLS correlation functions of 0.5 mol·kg⁻¹ sodium polyphenolates and related compounds in water at 10 °C. Additionally, Na-2-OH-Benz was measured at 0.6 mol·kg⁻¹ in water and in the water/DPnP system. τ = lag time, time delay for the detection. The samples were prepared in duplicate.

7.4 NMR measurements of Na-4-OH-3-OMe-Cinn dissolved in the binary water/DPnP system

^{1}H-NMR measurements of Na-4-OH-3-OMe-Cinn – as representative for a medium salting-in behavior – in presence and absence of DPnP were conducted. Because DPnP is liquid, its ^{1}H-NMR spectrum was recorded without any solvent, see Figure A 2. For the reference, Na-4-OH-3-OMe-Cinn was dissolved in deuterium oxide instead of water to keep the water peak small, see Figure A 3. Additionally, ^{1}H-NMR, COSY and NOESY spectra of Na-4-OH-3-OMe-Cinn (0.2 mol·kg^{-1}) in the water/DPnP (45/55 (w/w)) mixture) were recorded, see Figure A 4 - Figure A 6. The numeration of the protons and the corresponding NMR spectra with the peak attribution are displayed in Figure 21. The peaks were assigned using the splitting, the integrals and cross-peaks in the COSY spectrum of the water/DPnP (45/55 (w/w)) mixture containing 0.2 mol·kg^{-1} Na-4-OH-3-OMe-Cinn from Figure A 6. The peak attribution is reported in Table A 23 - Table A 26.[233]

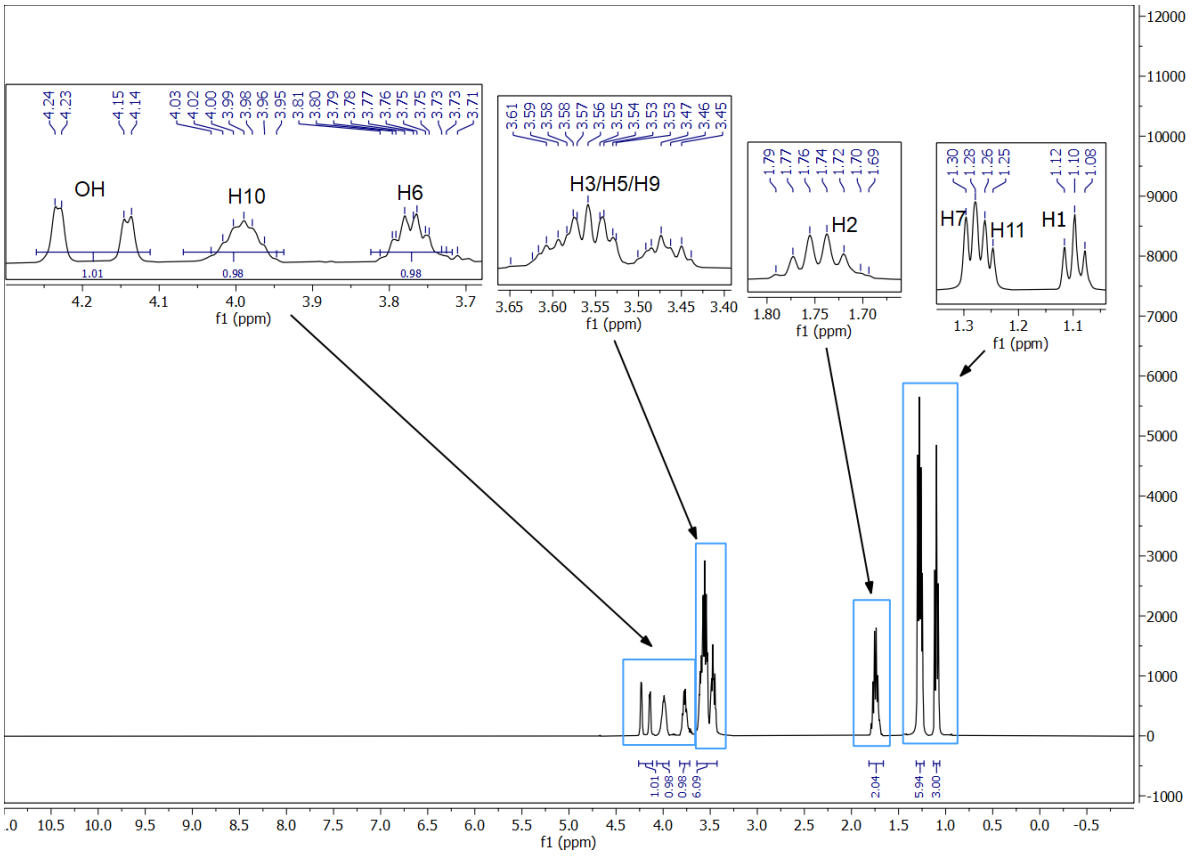

Figure A 2: ^{1}H-NMR spectrum of DPnP.[233]

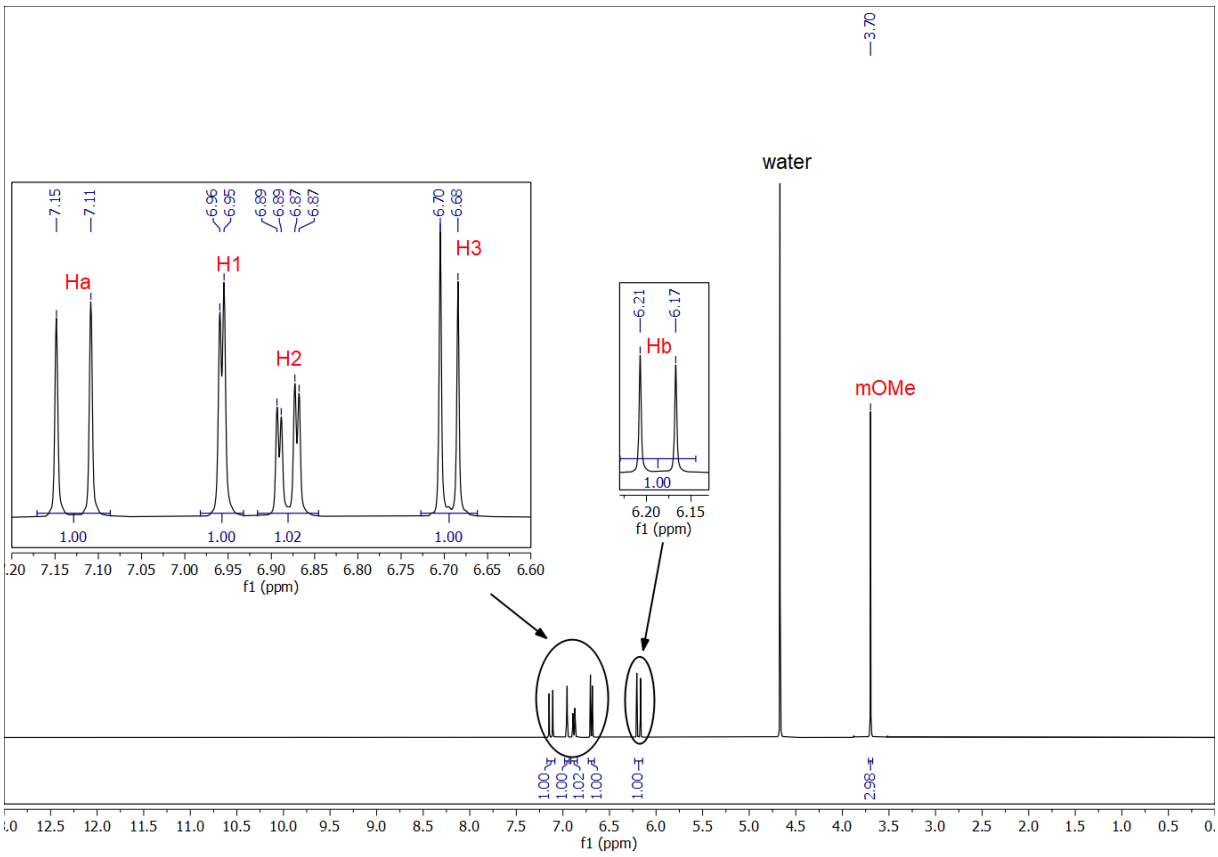

Figure A 3: *^{1}H-NMR spectrum of sodium ferulate (Na-4-OH-3-OMe-Cinn) in deuterium oxide (saturation).*[233]

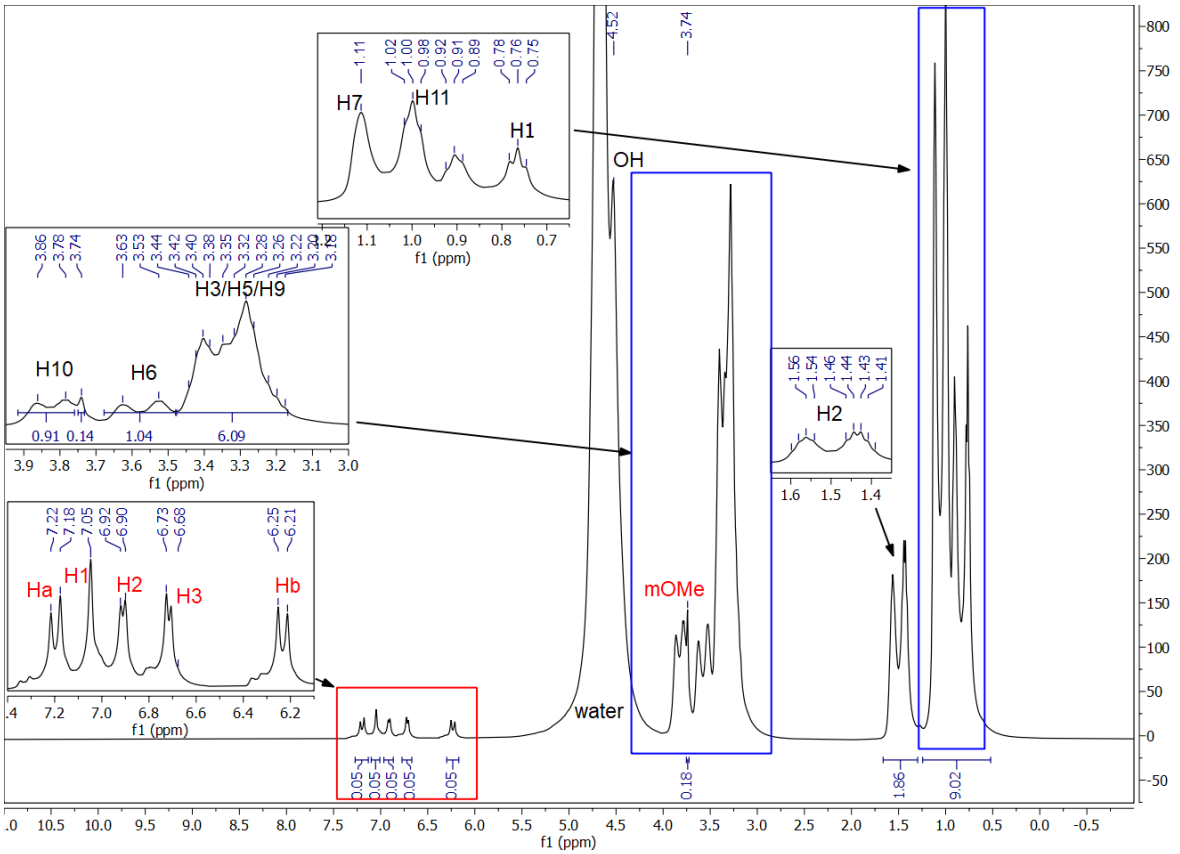

Figure A 4: ^{1}H-NMR spectrum of 0.2 mol·kg^{-1} Na-4-OH-3-OMe-Cinn in a water/DPnP mixture (45/55 (w/w)). Red: Protons of Na-4-OH-3-OMe-Cinn; black: Protons of DPnP.[233]

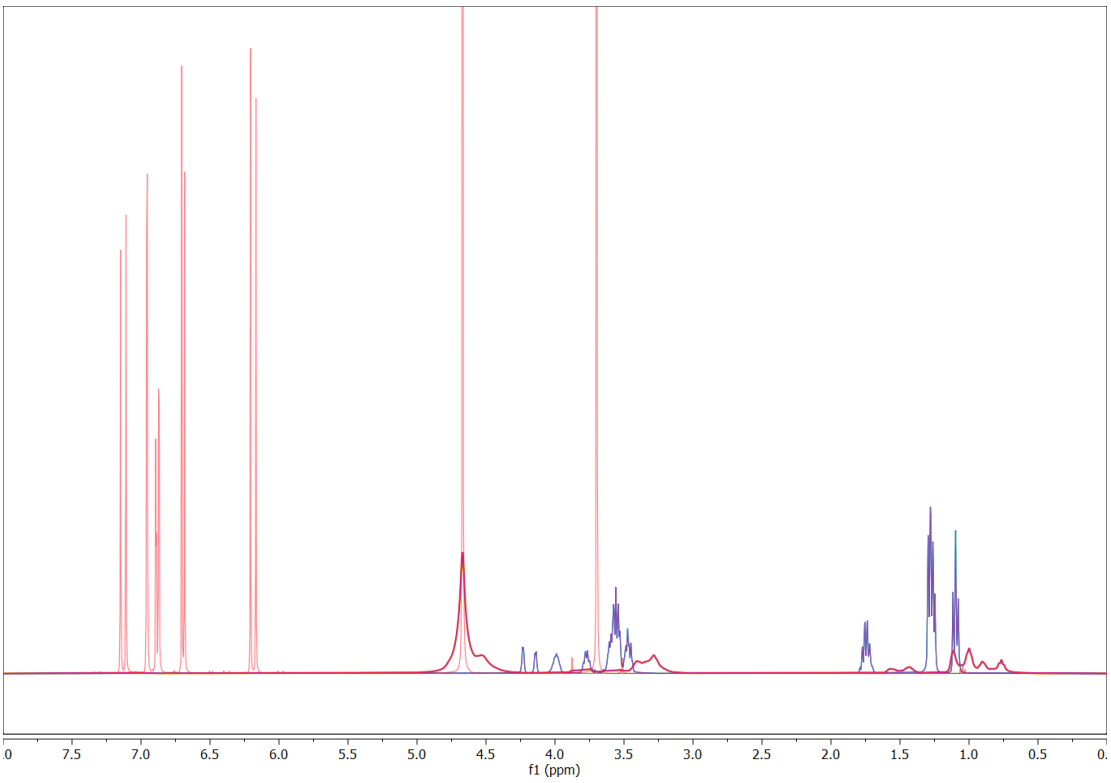

Figure A 5: Superimposed ^{1}H-NMR spectra of Na-4-OH-3-OMe-Cinn in deuterium oxide, of pure DPnP and of a water/DPnP (45/55 (w/w)) mixture containing 0.2 mol·kg^{-1} Na-4-OH-3-OMe-Cinn. Red: Spectrum of Na-4-OH-3-OMe-Cinn; blue: Spectrum of DPnP; dark red: Spectrum of Na-4-OH-3-OMe-Cinn in the water/DPnP mixture.[233]

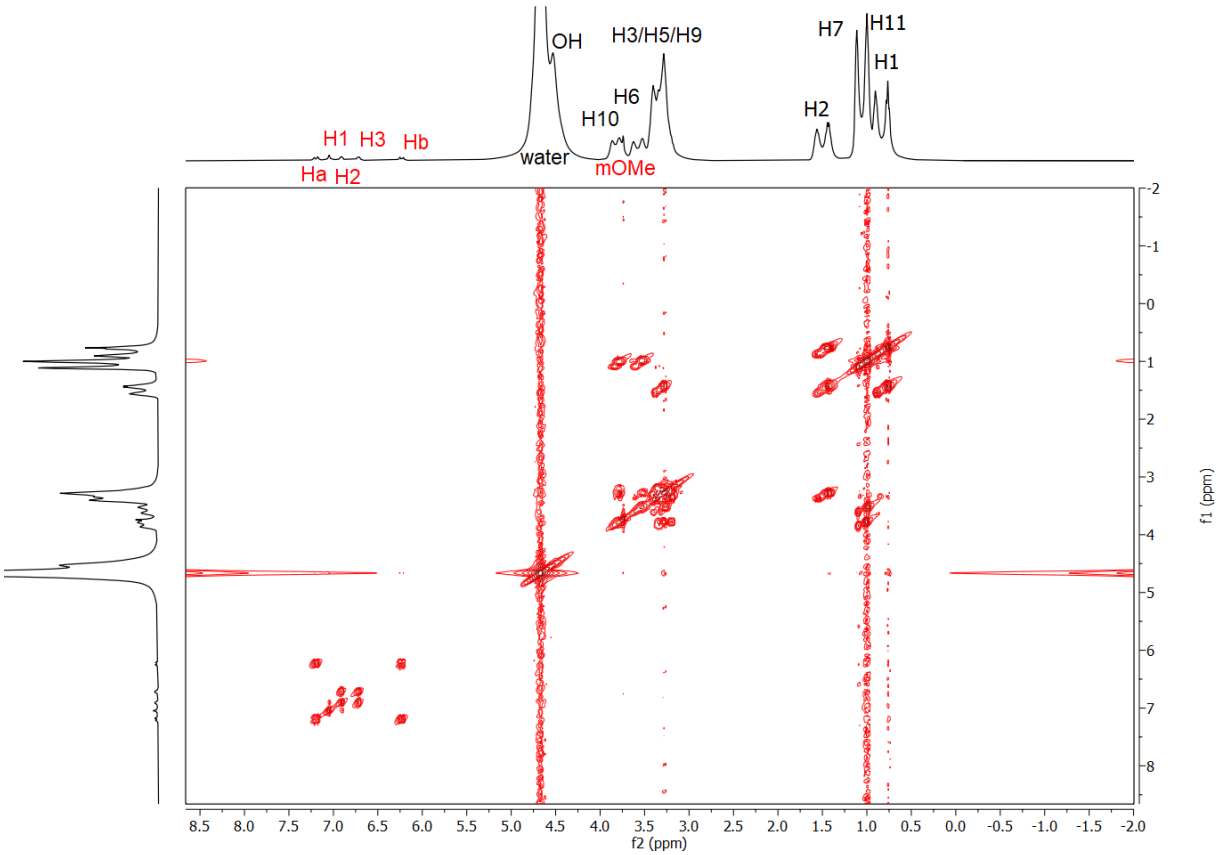

Figure A 6: COSY spectrum of a water/DPnP (45/55 (w/w)) mixture containing 0.2 mol·kg^{-1} sodium ferulate. Red: Protons of sodium ferulate; black: Protons of DPnP.[233]

Table A 23: Attribution of the protons of Na-4-OH-3-OMe-Cinn to the ^{1}H-NMR signals in deuterium oxide with the corresponding splitting and coupling constants J. dd = doublet of doublets.[233]

Proton	δ (ppm)	Number of protons	Splitting	J (Hz)
1	6.96	1	doublet	^{4}J(1-2) = 1.99
2	6.88	1	dd	^{3}J(2-3) = 8.26, ^{4}J(1-2) = 1.99
3	6.69	1	doublet	^{3}J(2-3) = 8.26
a	7.13	1	doublet	^{3}J(a-b) = 15.95
b	6.19	1	doublet	^{3}J(a-b) = 15.95
OMe	3.70	3	singlet	-

Table A 24: Attribution of the protons of 0.2 mol·kg^{-1} sodium Na-4-OH-3-OMe-Cinn in the water/DPnP (45/55 (w/w)) mixture to the ^{1}H-NMR signals with the corresponding splitting and coupling constants J. $\triangle\delta$ = change of the chemical shift relatively to Na-4-OH-3-OMe-Cinn dissolved in pure deuterium oxide from Table A 23. Left: deshielding.[233]

Proton	δ (ppm)	Number of protons	Splitting	J (Hz)	△δ (ppm)
1	7.05	1	singlet	-	Left: 0.09
2	6.91	1	doublet	^{3}J(2-3) = 8.25	Left: 0.03
3	6.72	1	doublet	^{3}J(2-3) = 8.25	Left: 0.03
a	7.20	1	doublet	^{3}J(a-b) = 15.96	Left: 0.07
b	6.23	1	doublet	^{3}J(a-b) = 15.96	Left: 0.04
OMe	3.74	3	singlet	-	Left: 0.04

Table A 25: Attribution of the protons of DPnP (no additional solvent) to the ^{1}H-NMR signals with the corresponding splitting and coupling constants J. dd = doublet of doublets.[233]

Proton	δ (ppm)	Number of protons	Splitting	J (Hz)
1	1.10	3	triplet	^{3}J(1-2) = 7.45
2	1.73	2	multiplet	-
3	3.53	2	multiplet	-
5	3.53	2	multiplet	-
6	3.77	1	multiplet	-
7	1.29	3	doublet	^{3}J(7-6) = 6.87
9	3.53	2	multiplet	-
10	3.99	1	septet	^{3}J(10-OH) = 15.34; ^{3}J(10-11) = 5.94; ^{3}J(10-9) = 6.61-10.87
11	1.26	3	doublet	^{3}J(11-10) = 5.94
OH	(4.19)	1	dd	^{4}J(OH-11;9) = 3.53; (J = 36.40)

Table A 26: Attribution of the protons of DPnP in the water/DPnP (45/55 (w/w)) mixture with 0.2 mol·kg^{-1} Na-4-OH-3-OMe-Cinn to the ^{1}H-NMR signals with the corresponding splitting and coupling constants J. td = triplet of doublets; "d" = pseudo-doublet; For H6 and H10 a high coupling constant was obtained, which is typical for a geminal coupling, though no geminal proton is present for both. $\triangle\delta$ = change of the chemical shift relatively to pure DPnP from Table A8. Left: deshielding; right: shielding.[233]

Proton	δ (ppm)	Number of protons	Splitting	J (Hz)	△δ (ppm)
1	0.84	3	td	^{3}J(1-2) = 7.65	Right: 0.26
2	1.50	2	td	^{3}J(2-1) = 7.65	Right: 0.23
3	3.34	2	multiplet	-	Right: 0.19
5	3.34	2	multiplet	-	Right: 0.19

6	3.58	1	“d”	J = 40.94	Left: 0.33
7	1.11	3	singlet	-	Right: 0.18
9	3.34	2	multiplet	-	Right: 0.19
10	3.83	1	“d”	J = 31.16	Right: 0.16
11	1.00	3	triplet	^{3}J(11-10) = 7.73	Right: 0.26
OH	(4.52)	1	singlet	-	

7.5 Tables on the aqueous solubilization curves of riboflavin in presence of different additives

Table A 27: Solubilization of RF in water by means of sodium cyclohexane carboxylate (NaCHC). After subtraction of the aqueous solubility of RF, the molar ratio was calculated from the molar concentration of the additive and RF. ∆c(RF) = standard deviation.

c(additive) (mol·kg^{-1})	c(RF) (mmol·kg^{-1})	Δc(RF) (mmol·kg^{-1})	c(RF) (g·kg^{-1})	Δc(RF) (g·kg^{-1})	Molar ratio (additive/RF)
0.799	0.61	0.02	0.230	0.009	2317.2
0.666	0.59	0.06	0.22	0.02	2057.4
0.400	0.421	0.006	0.158	0.002	2649.3
0.266	0.367	0.008	0.138	0.003	2756.9
0.133	0.31461	0.00002	0.118408	0.000009	2985.8
0.067	0.28	0.01	0.105	0.004	4547.0

Table A 28: Solubilization of RF in water by means of sodium benzoate (NaBenz). After subtraction of the aqueous solubility of RF, the molar ratio was calculated from the molar concentration of the additive and RF. ∆c(RF) = standard deviation.

c(additive) (mol·kg^{-1})	c(RF) (mmol·kg^{-1})	Δc(RF) (mmol·kg^{-1})	c(RF) (g·kg^{-1})	Δc(RF) (g·kg^{-1})	Molar ratio (additive/RF)
2.997	121	-	45.5	-	24.9
1.041	7.3	0.2	2.75	0.06	148.1
0.971	6.27	0.05	2.36	0.02	162.0
0.902	5.51	0.07	2.07	0.02	172.2
0.833	4.80	0.09	1.81	0.03	183.8
0.763	4.128	0.009	1.554	0.003	197.9
0.694	3.669	0.006	1.381	0.002	204.2
0.625	3.11	0.04	1.17	0.01	219.8
0.555	2.65	0.02	0.998	0.006	233.1
0.486	2.20	0.01	0.829	0.005	251.2
0.416	1.90	0.08	0.72	0.03	254.8
0.347	1.508	0.005	0.567	0.002	280.4
0.278	1.239	0.008	0.466	0.003	286.4
0.208	0.969	0.008	0.365	0.003	297.7
0.139	0.775	0.006	0.292	0.002	274.9
0.069	0.544	0.006	0.205	0.002	253.3

Table A 29: Solubilization of RF in water by means of sodium terephthalate. After subtraction of the aqueous solubility of RF, the molar ratio was calculated from the molar concentration of the additive and RF. ∆c(RF) = standard deviation.

c(additive) (mol·kg^{-1})	c(RF) (mmol·kg^{-1})	Δc(RF) (mmol·kg^{-1})	c(RF) (g·kg^{-1})	Δc(RF) (g·kg^{-1})	Molar ratio (additive/RF)
0.952	7.048	0.008	2.653	0.003	140.4
0.714	6.19	0.01	2.330	0.005	120.6
0.595	4.2	0.2	1.58	0.08	151.2
0.476	3.0740	0.0002	1.15696	0.00007	169.7
0.381	2.145	0.004	0.807	0.001	203.1
0.286	1.452	0.008	0.547	0.003	241.5
0.190	0.900	0.007	0.339	0.003	302.1
0.095	0.4	0.1	0.16	0.04	637.8

Table A 30: Solubilization of RF in water by means of sodium salicylate (Na-2-OH-Benz). After subtraction of the aqueous solubility of RF, the molar ratio was calculated from the molar concentration of the additive and RF. ∆c(RF) = standard deviation.

c(additive) (mol·kg^{-1})	c(RF) (mmol·kg^{-1})	Δc(RF) (mmol·kg^{-1})	c(RF) (g·kg^{-1})	Δc(RF) (g·kg^{-1})	Molar ratio (additive/RF)
0.937	30	1	11.3	0.6	31.4
0.874	27.7	0.3	10.4	0.1	31.9
0.812	22.8	0.2	8.57	0.08	36.1
0.749	19.4	0.1	7.31	0.03	39.1
0.687	16.3	0.2	6.15	0.08	42.8
0.625	13.8	0.2	5.18	0.09	46.3
0.562	11.6	0.1	4.35	0.03	49.8
0.500	8.5	1.1	3.2	0.4	61.0
0.437	7.4	0.1	2.80	0.03	61.0
0.375	5.7	0.1	2.13	0.03	69.6
0.312	4.7	0.3	1.75	0.11	71.1
0.250	3.20	0.03	1.20	0.01	85.3
0.187	2.25	0.01	0.847	0.002	94.6
0.125	1.41	0.02	0.53	0.01	109.5
0.062	0.9	0.4	0.3	0.1	105.7

Table A 31: Solubilization of RF in water by means of sodium 3-hydroxybenzoate (Na-3-OH-Benz). After subtraction of the aqueous solubility of RF, the molar ratio was calculated from the molar concentration of the additive and RF. ∆c(RF) = standard deviation.

c(additive) (mol·kg^{-1})	c(RF) (mmol·kg^{-1})	Δc(RF) (mmol·kg^{-1})	c(RF) (g·kg^{-1})	Δc(RF) (g·kg^{-1})	Molar ratio (additive/RF)
2.498	119	2	44.7	0.6	21.1
1.249	22.9	0.1	8.62	0.04	55.2
0.999	15.5	0.8	5.8	0.3	65.6
0.874	12.2	0.9	4.6	0.3	73.4
0.750	8.8	0.4	3.3	0.1	88.2
0.625	6.4	0.2	2.41	0.09	101.8
0.500	4.56	0.06	1.72	0.02	116.5
0.375	2.89	0.01	1.088	0.005	143.1
0.312	2.30	0.03	0.86	0.01	154.0

0.250	1.72	0.06	0.65	0.02	172.4
0.187	1.25	0.03	0.47	0.01	191.7
0.125	0.89	0.01	0.33	0.00	202.1
0.062	0.58	0.03	0.22	0.01	199.3

Table A 32: Solubilization of RF in water by means of sodium 4-hydroxybenzoate (Na-4-OH-Benz). After subtraction of the aqueous solubility of RF, the molar ratio was calculated from the molar concentration of the additive and RF. ∆c(RF) = standard deviation.

c(additive) (mol·kg^{-1})	c(RF) (mmol·kg^{-1})	Δc(RF) (mmol·kg^{-1})	c(RF) (g·kg^{-1})	Δc(RF) (g·kg^{-1})	Molar ratio (additive/RF)
0.937	19.4	0.8	7.3	0.3	49.0
0.874	18	1	6.6	0.4	50.6
0.812	14.4	0.1	5.42	0.04	57.4
0.749	12.1	0.2	4.6	0.1	63.4
0.687	10.7	0.2	4.0	0.1	66.0
0.625	8.6	0.3	3.2	0.1	74.9
0.562	7.3	0.4	2.8	0.1	79.4
0.500	5.79	0.05	2.18	0.02	90.6
0.437	4.87	0.04	1.83	0.02	95.0
0.375	3.67	0.03	1.38	0.01	110.2
0.312	2.949	0.003	1.11	0.00	116.6
0.250	2.19	0.04	0.82	0.01	130.4
0.187	1.604	0.005	0.604	0.002	140.4
0.125	1.06	0.03	0.40	0.01	157.3
0.062	0.63	0.01	0.237	0.004	173.9

Table A 33: Solubilization of RF in water by means of sodium 2-methoxybenzoate (Na-2-OMe-Benz). After subtraction of the aqueous solubility of RF, the molar ratio was calculated from the molar concentration of the additive and RF. Violet: Additive concentrations above its aqueous solubility, as the additive's solubility was increased by RF, too. ∆c(RF) = standard deviation.

c(additive) (mol·kg^{-1})	c(RF) (mmol·kg^{-1})	Δc(RF) (mmol·kg^{-1})	c(RF) (g·kg^{-1})	Δc(RF) (g·kg^{-1})	Molar ratio (additive/RF)
5.168	53.8	0.1	20.23	0.05	96.6
4.594	59.3	0.7	22.3	0.3	77.8
4.020	33	4	12	1	122.2
3.445	29.1	0.5	10.9	0.2	119.7
2.871	20.8	0.3	7.8	0.1	139.8
2.297	13.79	0.01	5.191	0.005	169.9
1.723	7.94	0.03	2.99	0.01	224.6
1.436	5.7	0.2	2.16	0.09	262.5
1.148	3.79	0.05	1.43	0.02	326.6
0.919	2.37	0.06	0.89	0.02	436.7
0.689	1.68	0.03	0.63	0.01	487.4
0.574	1.4	0.1	0.52	0.04	514.7
0.459	1.05	0.02	0.40	0.01	586.0
0.287	0.74	0.03	0.28	0.01	606.8
0.230	0.70	0.04	0.27	0.01	528.8
0.172	0.546	0.004	0.206	0.002	623.4
0.115	0.429	0.002	0.161	0.001	723.5
0.057	0.375	0.002	0.141	0.001	547.3

Table A 34: Solubilization of RF in water by means of sodium 3-methoxybenzoate (Na-3-OMe-Benz). After subtraction of the aqueous solubility of RF, the molar ratio was calculated from the molar concentration of the additive and RF. Violet: Additive concentrations above its aqueous solubility, as the additive's solubility was increased by RF, too. ∆c(RF) = standard deviation.

c(additive) (mol·kg^{-1})	c(RF) (mmol·kg^{-1})	Δc(RF) (mmol·kg^{-1})	c(RF) (g·kg^{-1})	Δc(RF) (g·kg^{-1})	Molar ratio (additive/RF)
5.168	321.7	0.9	121.1	0.4	16.1
4.594	366	7	138	3	12.5
4.020	214	1	80.5	0.4	18.8
3.445	154.20	0.05	58.04	0.02	22.4
2.871	119	1	44.8	0.5	24.1
2.297	78.6	0.5	29.6	0.2	29.3
1.723	47.64	0.03	17.93	0.01	36.4
1.148	23.3	0.5	8.8	0.2	49.9
0.919	14.5	0.1	5.45	0.05	64.6
0.689	9.42	0.03	3.54	0.01	75.3
0.574	7.08	0.03	2.66	0.01	84.3
0.459	4.91	0.04	1.85	0.01	99.0
0.287	3.0	0.1	1.12	0.06	106.0
0.230	1.936	0.003	0.729	0.001	137.9
0.172	1.452	0.004	0.547	0.002	145.7
0.115	1.05	0.03	0.40	0.01	147.0
0.057	0.68	0.02	0.25	0.01	141.3

Table A 35: Solubilization of RF in water by means of sodium 4-methoxybenzoate (Na-4-OMe-Benz). After subtraction of the aqueous solubility of RF, the molar ratio was calculated from the molar concentration of the additive and RF. Violet: Additive concentrations above the additive's aqueous solubility, as its solubility was increased by RF, too. ∆c(RF) = standard deviation.

c(additive) (mol·kg^{-1})	c(RF) (mmol·kg^{-1})	Δc(RF) (mmol·kg^{-1})	c(RF) (g·kg^{-1})	Δc(RF) (g·kg^{-1})	Molar ratio (additive/RF)
2.871	30.3	0.2	11.42	0.07	95.5
2.297	29.92	0.06	11.26	0.02	77.5
1.723	26.57	0.04	10.00	0.01	65.5
1.436	24.2	0.4	9.1	0.2	60.0
1.148	20	1	7.7	0.5	57.1
0.919	15.96	0.03	6.01	0.01	58.6
0.689	10.1866	0.0002	3.8339	0.0001	69.5
0.574	7.72	0.05	2.91	0.02	77.1
0.459	5.45	0.03	2.05	0.01	88.7
0.287	2.90	0.01	1.092	0.003	109.1
0.230	2.18	0.003	0.821	0.001	120.1
0.172	1.61	0.004	0.607	0.002	128.3
0.115	1.14	0.02	0.43	0.01	131.6
0.057	0.68	0.01	0.254	0.002	141.7

Table A 36: Solubilization of RF in water by means of sodium 2,3-dihydroxybenzoate (Na-2,3-DiOH-Benz). After subtraction of the aqueous solubility of RF, the molar ratio was calculated from the molar concentration of the additive and RF. Violet: Additive concentrations above the additive's aqueous solubility, as its solubility was increased by RF, too. ∆c(RF) = standard deviation.

c(additive) (mol·kg^{-1})	c(RF) (mmol·kg^{-1})	Δc(RF) (mmol·kg^{-1})	c(RF) (g·kg^{-1})	Δc(RF) (g·kg^{-1})	Molar ratio (additive/RF)
2.271	10.0	0.3	3.8	0.1	233.1
1.704	7.57	0.04	2.85	0.01	233.5
1.136	6.1	0.2	2.29	0.06	195.7
0.909	5.7	0.3	2.1	0.1	167.2
0.681	4.92	0.01	1.852	0.005	146.6
0.568	5.02	0.04	1.89	0.01	119.4
0.454	4.576	0.007	1.722	0.003	105.5
0.341	4.79	0.02	1.802	0.006	75.4
0.227	5.08	0.02	1.911	0.008	47.2
0.114	2.3	0.1	0.85	0.05	57.3
0.057	0.970	0.002	0.365	0.001	81.1

Table A 37: Solubilization of RF in water by means of sodium 2,4-dihydroxybenzoate (Na-2,4-DiOH-Benz). After subtraction of the aqueous solubility of RF, the molar ratio was calculated from the molar concentration of the additive and RF. ∆c(RF) = standard deviation.

c(additive) (mol·kg^{-1})	c(RF) (mmol·kg^{-1})	Δc(RF) (mmol·kg^{-1})	c(RF) (g·kg^{-1})	Δc(RF) (g·kg^{-1})	Molar ratio (additive/RF)
2.271	48.3	0.9	18.2	0.4	47.3
1.704	48.4	1.4	18.2	0.5	35.4
1.136	41.4	0.3	15.6	0.1	27.6
0.909	41.6	0.2	15.7	0.1	22.0
0.681	55.3	0.5	20.8	0.2	12.4
0.568	38.4	0.5	14.5	0.2	14.9
0.454	25.7	0.4	9.7	0.2	17.9
0.341	15.6	0.1	5.86	0.05	22.3
0.227	7.96	0.08	2.99	0.03	29.6
0.114	3.08	0.01	1.159	0.005	40.4
0.057	1.49	0.01	0.560	0.003	46.6

Table A 38: Solubilization of RF in water by means of sodium 3,4-dihydroxybenzoate (Na-3,4-DiOH-Benz). After subtraction of the aqueous solubility of RF, the molar ratio was calculated from the molar concentration of the additive and RF. ∆c(RF) = standard deviation.

c(additive) (mol·kg^{-1})	c(RF) (mmol·kg^{-1})	Δc(RF) (mmol·kg^{-1})	c(RF) (g·kg^{-1})	Δc(RF) (g·kg^{-1})	Molar ratio (additive/RF)
0.852	31	3	12	1	27.4
0.795	26.2	0.9	9.8	0.4	30.7
0.738	22.5	0.6	8.5	0.2	33.2
0.681	19.2	0.7	7.2	0.3	36.0
0.625	15.1	0.5	5.7	0.2	42.2
0.568	12.4	0.3	4.7	0.1	46.7
0.511	10.5	0.1	4.0	0.1	49.8
0.454	8.7	0.2	3.3	0.1	53.8
0.398	7.022	0.005	2.643	0.002	58.9

0.341	5.407	0.008	2.035	0.003	66.3
0.284	4.16	0.03	1.57	0.01	72.9
0.227	3.0	0.2	1.1	0.1	81.7
0.170	2.20	0.07	0.83	0.03	88.1
0.114	1.45	0.01	0.548	0.003	95.9
0.057	0.82	0.01	0.308	0.004	103.3

Table A 39: Solubilization of RF in water by means of sodium 3,5-dihydroxybenzoate (Na-3,5-DiOH-Benz). After subtraction of the aqueous solubility of RF, the molar ratio was calculated from the molar concentration of the additive and RF. ∆c(RF) = standard deviation.

c(additive) (mol·kg^{-1})	c(RF) (mmol·kg^{-1})	Δc(RF) (mmol·kg^{-1})	c(RF) (g·kg^{-1})	Δc(RF) (g·kg^{-1})	Molar ratio (additive/RF)
0.852	40.4	0.3	15.2	0.1	21.2
0.795	36	1	13.5	0.4	22.3
0.738	31	1	11.7	0.6	23.9
0.681	25.6	0.4	9.6	0.1	26.9
0.625	21.5	0.3	8.1	0.1	29.4
0.568	18.2	0.7	6.9	0.3	31.7
0.511	14.39	0.08	5.41	0.03	36.2
0.454	12.5	0.4	4.7	0.1	37.2
0.398	9.71	0.09	3.65	0.03	42.1
0.341	7.58	0.09	2.85	0.03	46.6
0.284	6.10	0.05	2.30	0.02	48.7
0.227	4.39	0.09	1.65	0.03	55.1
0.170	2.86	0.02	1.08	0.01	65.8
0.114	1.86	0.07	0.70	0.02	71.5
0.057	0.99	0.03	0.37	0.01	78.3

Table A 40: Solubilization of RF in water by means of sodium 3,4-dimethoxybenzoate (Na-3,4-DiOMe-Benz). After subtraction of the aqueous solubility of RF, the molar ratio was calculated from the molar concentration of the additive and RF. Violet: Additive concentrations above additive's aqueous solubility, as its solubility was increased by RF, too. ∆c(RF) = standard deviation.

c(additive) (mol·kg^{-1})	c(RF) (mmol·kg^{-1})	Δc(RF) (mmol·kg^{-1})	c(RF) (g·kg^{-1})	Δc(RF) (g·kg^{-1})	Molar ratio (additive/RF)
0.882	31.42	0.03	11.82	0.01	28.3
0.784	30.1	0.6	11.3	0.2	26.3
0.588	19.57	0.03	7.36	0.01	30.5
0.490	13.4	0.4	5.1	0.1	37.2
0.392	10.13	0.09	3.81	0.04	39.7
0.294	6.77	0.04	2.55	0.02	45.2
0.245	6.2	0.1	2.32	0.04	41.6
0.196	5.0	0.4	1.9	0.1	41.2
0.147	3.49	0.08	1.31	0.03	45.6
0.098	2.08	0.01	0.782	0.005	54.2
0.049	1.33	0.04	0.50	0.02	46.1

Table A 41: Solubilization of RF in water by means of sodium 2,3-dimethoxybenzoate (Na-2,3-DiOMe-Benz). After subtraction of the aqueous solubility of RF, the molar ratio was calculated from the molar concentration of the additive and RF. ∆c(RF) = standard deviation.

c(additive) (mol·kg^{-1})	c(RF) (mmol·kg^{-1})	Δc(RF) (mmol·kg^{-1})	c(RF) (g·kg^{-1})	Δc(RF) (g·kg^{-1})	Molar ratio (additive/RF)
4.898	60	5	23	2	82.0
3.918	30	13	11	5	134.0
2.939	22	1	8.3	0.4	135.2
2.449	11.396	0.005	4.289	0.002	220.1
0.980	2.5	0.3	1.0	0.1	430.0
0.784	1.70	0.02	0.64	0.01	548.6
0.686	1.45	0.02	0.54	0.01	582.5
0.588	1.301	0.002	0.490	0.001	569.8
0.490	1.09	0.02	0.41	0.01	593.9
0.392	0.85	0.02	0.32	0.01	676.5
0.294	0.69	0.01	0.260	0.004	699.3
0.245	0.62	0.01	0.234	0.004	696.9
0.196	0.51	0.01	0.192	0.003	817.9
0.147	0.48	0.02	0.18	0.01	702.4
0.098	0.43	0.08	0.16	0.03	594.9
0.049	0.426	0.002	0.160	0.001	313.7

Table A 42: Solubilization of RF in water by means of sodium 2,4-dimethoxybenzoate (Na-2,4-DiOMe-Benz). After subtraction of the aqueous solubility of RF, the molar ratio was calculated from the molar concentration of the additive and RF. ∆c(RF) = standard deviation.

c(additive) (mol·kg^{-1})	c(RF) (mmol·kg^{-1})	Δc(RF) (mmol·kg^{-1})	c(RF) (g·kg^{-1})	Δc(RF) (g·kg^{-1})	Molar ratio (additive/RF)
3.918	53.0	0.2	19.95	0.08	74.3
2.939	44.7	0.3	16.8	0.1	66.2
2.449	64	8	24.2	2.9	38.3
1.959	33.3	0.5	12.5	0.2	59.3
0.980	11.42	0.05	4.30	0.02	87.9
0.784	8.18	0.07	3.08	0.02	99.0
0.686	6.9	0.2	2.59	0.09	103.8
0.588	5.54	0.02	2.09	0.01	111.5
0.490	4.39	0.03	1.65	0.01	118.8
0.392	3.25	0.09	1.23	0.03	131.3
0.294	2.174	0.005	0.818	0.002	154.3
0.245	1.85	0.02	0.70	0.01	154.6
0.196	1.48	0.02	0.56	0.01	162.5

Table A 43: Solubilization of RF in water by means of sodium 3,5-dimethoxybenzoate (Na-3,5-DiOMe-Benz). After subtraction of the aqueous solubility of RF, the molar ratio was calculated from the molar concentration of the additive and RF. Violet: Additive concentrations above additive's aqueous solubility, as its solubility was increased by RF, too. The salt Na-3,5-DiOMe-Benz was never entirely solubilized. ∆c(RF) = standard deviation.

c(additive) (mol·kg^{-1})	c(RF) (mmol·kg^{-1})	Δc(RF) (mmol·kg^{-1})	c(RF) (g·kg^{-1})	Δc(RF) (g·kg^{-1})	Molar ratio (additive/RF)
3.918	214	30	80	10	18.3
2.939	261	5	98	2	11.3
2.449	195	1	73.3	0.4	12.6
1.959	139.9	0.9	52.7	0.3	14.0
1.469	86.2	0.5	32.5	0.2	17.1
0.980	46.2	0.3	17.4	0.1	21.3
0.784	36.2	0.7	13.6	0.3	21.8
0.588	23.4	0.1	8.80	0.04	25.4
0.490	17.4	0.3	6.5	0.1	28.7
0.392	12.36	0.05	4.65	0.02	32.4
0.294	8.4	0.1	3.18	0.05	36.0
0.196	6.0	0.5	2.3	0.2	34.1
0.098	2.30	0.02	0.866	0.009	48.2
0.049	1.127	0.010	0.424	0.004	57.1

Table A 44: Solubilization of RF in water by means of sodium vanillate (Na-4-OH-3-OMe-Benz). After subtraction of the aqueous solubility of RF, the molar ratio was calculated from the molar concentration of the additive and RF. Violet: Additive concentrations above the additive's aqueous solubility, as its solubility was increased by RF, too. After 2 days, vanillate might precipitate from the samples with > 1.105 mol·kg^{-1} vanillate saturated with RF. Thus, RF probably enlightens a kinetic solubilization of RF leading to a supersaturation of water with vanillate. ∆c(RF) = standard deviation.

c(additive) (mol·kg^{-1})	c(RF) (mmol·kg^{-1})	Δc(RF) (mmol·kg^{-1})	c(RF) (g·kg^{-1})	Δc(RF) (g·kg^{-1})	Molar ratio (additive/RF)
1.262	52	3	20	1	24.4
1.210	49	4	19	1	24.6
1.157	49	3	18	1	23.9
1.105	45	2	17.1	0.6	24.5
1.052	39	3	15	1	27.1
0.999	39	4	15	2	25.5
0.947	35	3	13	1	27.4
0.894	29.8	0.2	11.22	0.09	30.3
0.842	27.2	0.2	10.22	0.08	31.3
0.789	23.7	0.2	8.92	0.09	33.7
0.736	22.5	0.5	8.5	0.2	33.2
0.684	20.3	0.9	7.6	0.3	34.1
0.631	17.6	0.1	6.62	0.04	36.4
0.579	15.2	0.1	5.72	0.04	38.8
0.526	12.9	0.2	4.84	0.08	41.8
0.473	10.7	0.2	4.04	0.09	45.3
0.421	9.07	0.08	3.41	0.03	47.8
0.368	7.2	0.1	2.71	0.05	53.0
0.316	5.89	0.01	2.215	0.005	56.2
0.263	4.59	0.01	1.727	0.005	60.9

0.210	3.47	0.02	1.305	0.006	65.8
0.158	2.475	0.003	0.931	0.001	71.6
0.105	1.564	0.007	0.589	0.003	81.3
0.053	0.808	0.008	0.304	0.003	97.7
0.028	0.539	0.004	0.203	0.002	103.3
0.006	0.341	0.004	0.128	0.001	78.1
0.003	0.308	0.001	0.1160	0.0006	73.0

Table A 45: Solubilization of RF in water by means of sodium syringate (Na-4-OH-3,5-DiOMe-Benz). After subtraction of the aqueous solubility of RF, the molar ratio was calculated from the molar concentration of the additive and RF. Violet: Additive concentrations above the additive's aqueous solubility, as its solubility was increased by RF, too. ∆c(RF) = standard deviation.

c(additive) (mol·kg^{-1})	c(RF) (mmol·kg^{-1})	Δc(RF) (mmol·kg^{-1})	c(RF) (g·kg^{-1})	Δc(RF) (g·kg^{-1})	Molar ratio (additive/RF)
2.726	300	20	114	9	9.0
2.272	220	10	84	4	10.2
1.817	164	1	61.5	0.5	11.1
1.363	120	4	45	2	11.4
0.909	55	7	21	3	16.7
0.636	39	2	14.6	0.8	16.5
0.545	33.7	0.6	12.7	0.2	16.3
0.454	26.6	0.9	10.0	0.3	17.3
0.363	19.2	0.5	7.2	0.2	19.2
0.273	13.2	0.3	5.0	0.1	21.0
0.227	15	5	6	2	15.3
0.182	7.1	0.1	2.66	0.04	26.8
0.136	5.0	0.2	1.89	0.06	28.8
0.091	3.1	0.1	1.17	0.04	32.0
0.045	1.42	0.01	0.53	0.00	39.6

Table A 46: Solubilization of RF in water by means of sodium cinnamate (NaCinn). After subtraction of the aqueous solubility of RF, the molar ratio was calculated from the molar concentration of the additive and RF. ∆c(RF) = standard deviation.

c(additive) (mol·kg^{-1})	c(RF) (mmol·kg^{-1})	Δc(RF) (mmol·kg^{-1})	c(RF) (g·kg^{-1})	Δc(RF) (g·kg^{-1})	Molar ratio (additive/RF)
0.588	36	1	13.6	0.5	16.4
0.529	30	4	11	1	17.7
0.470	24	4	9	1	20.1
0.411	20	4	7	2	21.3
0.353	17.8	0.3	6.7	0.1	20.1
0.294	12	2	4.6	0.9	24.6
0.235	9.6	0.9	3.6	0.3	25.3
0.176	5.9	0.6	2.2	0.2	31.3
0.118	4.0	0.9	1.5	0.3	31.8
0.059	1.7	0.4	0.6	0.2	40.8
0.029	0.9	0.3	0.3	0.1	49.1

Table A 47: Solubilization of RF in water by means of sodium o-coumarate (Na-2-OH-Cinn). After subtraction of the aqueous solubility of RF, the molar ratio was calculated from the molar concentration of the additive and RF. ∆c(RF) = standard deviation.

c(additive) (mol·kg^{-1})	c(RF) (mmol·kg^{-1})	Δc(RF) (mmol·kg^{-1})	c(RF) (g·kg^{-1})	Δc(RF) (g·kg^{-1})	Molar ratio (additive/RF)
1.074	119.2	0.4	25.8	0.1	9.0
0.860	81	3.	17.4	0.6	10.7
0.752	69.4	0.9	15.0	0.2	10.9
0.645	53.3	0.1	11.53	0.02	12.1
0.537	39.4	0.4	8.52	0.08	13.7
0.430	27.9	0.7	6.0	0.1	15.6
0.322	19	1	4.1	0.3	17.1
0.269	13.05	0.08	2.82	0.02	21.0
0.215	9.5	0.5	2.1	0.1	23.3
0.161	6.3	0.1	1.36	0.02	26.8
0.107	3.59	0.01	0.777	0.002	32.3
0.054	1.58	0.03	0.34	0.01	40.9

Table A 48: Solubilization of RF in water by means of sodium m-coumarate (Na-3-OH-Cinn). After subtraction of the aqueous solubility of RF, the molar ratio was calculated from the molar concentration of the additive and RF. ∆c(RF) = standard deviation.

c(additive) (mol·kg^{-1})	c(RF) (mmol·kg^{-1})	Δc(RF) (mmol·kg^{-1})	c(RF) (g·kg^{-1})	Δc(RF) (g·kg^{-1})	Molar ratio (additive/RF)
2.149	438	8	164.8	2.9	4.9
1.074	157	1	59.1	0.4	6.9
0.860	113	2	42.5	0.8	7.6
0.752	92	2	34.6	0.7	8.2
0.645	73.2	0.7	27.5	0.3	8.8
0.537	53.0	0.8	19.9	0.3	10.2
0.430	38	1	14.4	0.4	11.3
0.322	23.4	0.2	8.81	0.07	13.9
0.269	17.49	0.01	6.583	0.004	15.6
0.215	12.7	0.2	4.80	0.07	17.2
0.161	7.93	0.08	2.99	0.03	21.0
0.107	4.84	0.09	1.82	0.04	23.5
0.054	1.958	0.005	0.737	0.002	31.8

Table A 49: Solubilization of RF in water by means of sodium p-coumarate (Na-4-OH-Cinn). After subtraction of the aqueous solubility of RF, the molar ratio was calculated from the molar concentration of the additive and RF. ∆c(RF) = standard deviation.

c(additive) (mol·kg^{-1})	c(RF) (mmol·kg^{-1})	Δc(RF) (mmol·kg^{-1})	c(RF) (g·kg^{-1})	Δc(RF) (g·kg^{-1})	Molar ratio (additive/RF)
0.806	124	15	47	5	6.5
0.752	114	6	43	2	6.6
0.698	98.9	0.8	37.2	0.3	7.1
0.645	88	5	33	2	7.3
0.591	70.8	0.7	26.6	0.3	8.4
0.537	66	1	24.7	0.4	8.2
0.484	54	5	20	2	8.9

0.430	42	1	15.8	0.5	10.3
0.376	38	1	14.4	0.6	9.9
0.322	29	2	10.9	0.6	11.2
0.269	24	2	9.1	0.7	11.2
0.215	16.1	0.1	6.07	0.05	13.5
0.161	10.7	0.7	4.0	0.3	15.5
0.107	6.7	0.1	2.52	0.05	16.7
0.054	1.8	0.3	0.66	0.10	36.0

Table A 50: Solubilization of RF in water by means of sodium 4-methoxycinnamate (Na-4-OMe-Cinn). After subtraction of the aqueous solubility of RF, the molar ratio was calculated from the molar concentration of the additive and RF. Violet: Additive concentrations above the additive's aqueous solubility, as its solubility was increased by RF, too. The salt Na-4-OMe-Cinn was never entirely solubilized. Yet, RF enabled a solubilization up to 0.6 mol·kg^{-1}. ∆c(RF) = standard deviation.

c(additive) (mol·kg^{-1})	c(RF) (mmol·kg^{-1})	Δc(RF) (mmol·kg^{-1})	c(RF) (g·kg^{-1})	Δc(RF) (g·kg^{-1})	Molar ratio (additive/RF)
0.599	31	5	12	2	19.2
0.500	29.9	0.4	11.3	0.1	16.8
0.400	36.9	0.9	13.9	0.4	10.9
0.250	26.0	0.2	9.77	0.07	9.7
0.200	22	2	8.3	0.6	9.2
0.150	12.16	0.04	4.58	0.01	12.6
0.100	6.85	0.01	2.58	0.01	15.2
0.050	3.0	0.1	1.13	0.04	18.3

Table A 51: Solubilization of RF in water by means of sodium ferulate (Na-4-OH-3-OMe-Cinn). After subtraction of the aqueous solubility of RF, the molar ratio was calculated from the molar concentration of the additive and RF. Violet: Additive concentrations above the additive's aqueous solubility, as its solubility was increased by RF, too. ∆c(RF) = standard deviation.

c(additive) (mol·kg^{-1})	c(RF) (mmol·kg^{-1})	Δc(RF) (mmol·kg^{-1})	c(RF) (g·kg^{-1})	Δc(RF) (g·kg^{-1})	Molar ratio (additive/RF)
1.388	44	2	16.4	0.8	32.1
0.925	51	5	19	2	18.2
0.740	54	1	20.2	0.5	13.9
0.555	67	2	25.1	0.6	8.3
0.463	66	2	24.7	0.8	7.1
0.370	60	1	22.5	0.4	6.2
0.324	48	5	18	2	6.7
0.278	37.2	0.6	14.0	0.2	7.5
0.231	29	3	10.8	0.9	8.1
0.185	19.1	0.2	7.20	0.06	9.8
0.139	14.21	0.08	5.35	0.03	10.0
0.093	8.9	0.9	3.4	0.3	10.7
0.046	3.1	0.1	1.17	0.04	16.4
0.028	1.86	0.06	0.70	0.02	17.5
0.011	0.86	0.03	0.32	0.01	18.7
0.006	0.57	0.03	0.21	0.01	18.6
0.003	0.43	0.03	0.16	0.01	17.6

Table A 52: Solubilization of RF in water by means of sodium caffeate (Na-3,4-DiOH-Cinn). After subtraction of the aqueous solubility of RF, the molar ratio was calculated from the molar concentration of the additive and RF. Violet: Additive concentrations above the additive's aqueous solubility, as its solubility was increased by RF, too. ∆c(RF) = standard deviation.

c(additive) (mol·kg^{-1})	c(RF) (mmol·kg^{-1})	Δc(RF) (mmol·kg^{-1})	c(RF) (g·kg^{-1})	Δc(RF) (g·kg^{-1})	Molar ratio (additive/RF)
0.597	109	1	41.1	0.4	5.5
0.547	96	5	36	2	5.7
0.497	86	6	32	2	5.8
0.447	71.6	0.6	26.9	0.2	6.3
0.398	56	4	21	2	7.2
0.348	46	4	17	2	7.6
0.298	30	3	11	1	9.9
0.249	24	4	9	2	10.3
0.199	17.2	0.3	6.5	0.1	11.7
0.149	14	3	5	1	10.9
0.099	5.9	0.4	2.2	0.2	17.5
0.050	3.0	0.3	1.1	0.1	17.9
0.028	1.5	0.1	0.56	0.04	22.7
0.006	0.63	0.09	0.24	0.03	15.4
0.003	0.34	0.08	0.13	0.03	42.5

Table A 53: Solubilization of RF in water by means of sodium 3,4-dimethoxycinnamate (Na-3,4-DiOMe-Cinn). After subtraction of the aqueous solubility of RF, the molar ratio was calculated from the molar concentration of the additive and RF. Violet: Additive concentrations above the additive's aqueous solubility, as its solubility was increased by RF, too. The salt Na-3,4-DiOMe-Cinn was never entirely solubilized. Yet, RF enabled a solubilization > 4 mol·kg^{-1}. The solubilization was not continued for higher additive concentrations due to the too high viscosity of the samples, which hindered the stirring and filtering process. ∆c(RF) = standard deviation.

c(additive) (mol·kg^{-1})	c(RF) (mmol·kg^{-1})	Δc(RF) (mmol·kg^{-1})	c(RF) (g·kg^{-1})	Δc(RF) (g·kg^{-1})	Molar ratio (additive/RF)
4.344	560	20	209	9	7.8
3.910	500	10	186	5	7.9
3.475	500	60	190	20	7.0
3.041	399	1	150.1	0.2	7.6
2.606	358	0	135	0	7.3
2.172	370	20	138	7	5.9
1.738	280	10	105	4	6.2
1.303	225	7	85	3	5.8
1.086	190	10	71	5	5.8
0.869	123	1	46.5	0.3	7.1
0.652	111	2	41.6	0.6	5.9
0.434	71	3	27	1	6.1
0.348	50	6	19	2	6.9
0.261	40	3	15	1	6.6
0.217	37	2	13.9	0.8	5.9
0.174	24	1	9.1	0.5	7.3
0.130	17.7	0.4	6.7	0.1	7.5
0.087	12	2	4.4	0.6	7.6
0.043	4.9	0.6	1.8	0.2	9.4

Table A 54: Solubilization of RF in water by means of sodium 4-hydroxy-3,5-dimethoxycinnamate (Na-4-OH-3,5-DiOMe-Cinn). After subtraction of the aqueous solubility of RF, the molar ratio was calculated from the molar concentration of the additive and RF. Violet: Additive concentrations above the additive's aqueous solubility, as its solubility was increased by RF, too. The salt (Na-4-OH-3,5-DiOMe-Cinn) was never entirely solubilized. Yet, RF enabled a solubilization > 1.6 mol·kg^{-1}. The solubilization was not continued for higher additive concentrations because the chemical was expensive. ∆c(RF) = standard deviation.

c(additive) (mol·kg^{-1})	c(RF) (mmol·kg^{-1})	Δc(RF) (mmol·kg^{-1})	c(RF) (g·kg^{-1})	Δc(RF) (g·kg^{-1})	Molar ratio (additive/RF)
1.625	381	-	143	-	4.3
1.218	276	-	104	-	4.4
1.015	243	-	92	-	4.2
0.812	179	-	67	-	4.5
0.609	135	-	51	-	4.5
0.406	74	-	28	-	5.5
0.325	62.8	0.7	23.6	0.3	5.2
0.162	27.5	1.3	10.4	0.5	6.0
0.081	13.0	0.5	4.9	0.2	6.4

Table A 55: Solubilization of RF in water by means of sodium gallate (Na-3,4,5-TriOH-Benz). After subtraction of the aqueous solubility of RF, the molar ratio was calculated from the molar concentration of the additive and RF. Violet: Additive concentrations above the additive's aqueous solubility, as its solubility was increased by RF, too. ∆c(RF) = standard deviation.

c(additive) (mol·kg^{-1})	c(RF) (mmol·kg^{-1})	Δc(RF) (mmol·kg^{-1})	c(RF) (g·kg^{-1})	Δc(RF) (g·kg^{-1})	Molar ratio (additive/RF)
0.677	38	2	14.2	0.6	18.0
0.625	30	2	11.3	0.9	21.1
0.573	27	2	10.2	0.9	21.3
0.521	22.7	0.5	8.5	0.2	23.2
0.469	18.7	0.6	7.0	0.2	25.5
0.416	15.9	0.4	6.0	0.2	26.6
0.364	12.7	0.2	4.8	0.1	29.2
0.312	10.1	0.4	3.8	0.2	31.7
0.260	8.2	0.1	3.10	0.04	32.7
0.208	6.0	0.5	2.2	0.2	36.6
0.156	4.6	0.6	1.7	0.2	35.9
0.104	3.3	0.2	1.25	0.08	34.2
0.052	1.4	0.1	0.52	0.03	46.7

Table A 56: Solubilization of RF in water by means of sodium 4-hydroxypropionate (Na-4-OH-Prop). After subtraction of the aqueous solubility of RF, the molar ratio was calculated from the molar concentration of the additive and RF. ∆c(RF) = standard deviation.

c(additive) (mol·kg^{-1})	c(RF) (mmol·kg^{-1})	Δc(RF) (mmol·kg^{-1})	c(RF) (g·kg^{-1})	Δc(RF) (g·kg^{-1})	Molar ratio (additive/RF)
3.189	124	2	46.7	0.6	25.8
2.657	106	5	40	2	25.0
2.126	70.8	0.1	26.66	0.05	30.1
1.594	42.5	0.1	16.0	0.0	37.7
1.063	36.1	0.5	13.6	0.2	29.7
0.850	12.63	0.03	4.75	0.01	68.8

0.638	7.98	0.03	3.00	0.01	82.7
0.531	5.93	0.02	2.23	0.01	93.9
0.425	4.140	0.006	1.558	0.002	109.9
0.319	2.89	0.04	1.09	0.01	121.9
0.213	1.65	0.01	0.620	0.005	154.4
0.106	0.87	0.01	0.326	0.005	177.9
0.053	0.5235	0.0002	0.1970	0.0001	209.7

Table A 57: Solubilization of RF in water by means of sodium xylene sulfonate (SXS). After subtraction of the aqueous solubility of RF, the molar ratio was calculated from the molar concentration of the additive and RF. ∆c(RF) = standard deviation.

c(additive) (mol·kg^{-1})	c(RF) (mmol·kg^{-1})	Δc(RF) (mmol·kg^{-1})	c(RF) (g·kg^{-1})	Δc(RF) (g·kg^{-1})	Molar ratio (additive/RF)
1.921	21.42	0.09	8.06	0.03	90.8
1.441	13.1	0.2	4.93	0.07	112.2
0.720	4.490	0.006	1.690	0.002	170.7
0.384	1.992	0.007	0.750	0.003	223.1
0.192	0.985	0.004	0.371	0.001	268.6
0.096	0.59	0.01	0.223	0.005	298.7
0.048	0.437	0.005	0.165	0.002	287.1

Table A 58: Solubilization of RF in water by means of sodium thiocyanate (NaSCN). After subtraction of the aqueous solubility of RF, the molar ratio was calculated from the molar concentration of the additive and RF. ∆c(RF) = standard deviation.

c(additive) (mol·kg^{-1})	c(RF) (mmol·kg^{-1})	Δc(RF) (mmol·kg^{-1})	c(RF) (g·kg^{-1})	Δc(RF) (g·kg^{-1})	Molar ratio (additive/RF)
4.000	15.6	0.9	5.9	0.3	261.6
3.500	9.75	0.09	3.67	0.03	369.2
3.000	6.6	0.1	2.48	0.04	473.8
2.500	4.59	0.06	1.73	0.02	578.1
2.000	2.95	0.05	1.11	0.02	746.9
1.500	1.81	0.01	0.681	0.005	974.8
1.000	1.0659	0.0003	0.4012	0.0001	1256.4
0.750	0.787	0.008	0.296	0.003	1449.6
0.500	0.578	0.004	0.218	0.001	1622.8
0.400	0.50494	0.00005	0.19005	0.00002	1702.5
0.300	0.457	0.002	0.1722	0.0009	1600.6
0.200	0.395	0.001	0.1486	0.0004	1603.5
0.100	0.310	0.001	0.1167	0.0005	2502.9

Table A 59: Solubilization of RF in water by means of sodium 5-phenylvalerate (NaValerate). After subtraction of the aqueous solubility of RF, the molar ratio was calculated from the molar concentration of the additive and RF. Violet: Additive concentrations above the additive's aqueous solubility, as its solubility was increased by RF, too. For additive concentrations > 0.2 mol·kg^{-1} a part of RF and the additive precipitated within 1-2 weeks. ∆c(RF) = standard deviation.

c(additive) (mol·kg^{-1})	c(RF) (mmol·kg^{-1})	Δc(RF) (mmol·kg^{-1})	c(RF) (g·kg^{-1})	Δc(RF) (g·kg^{-1})	Molar ratio (additive/RF)
0.400	2.903	0.008	1.093	0.003	151.9
0.200	1.3	0.1	0.48	0.04	200.8
0.100	0.8	0.2	0.30	0.09	194.6
0.050	0.6	0.1	0.21	0.05	171.9
0.025	0.38	0.04	0.14	0.01	234.7

Table A 60: Solubilization of RF in water by means of sodium 5-phenyl-2,4-pentadienoate (Na-2,4-Pentadienoate). After subtraction of the aqueous solubility of RF, the molar ratio was calculated from the molar concentration of the additive and RF. Violet: Additive concentrations above the additive's aqueous solubility, as its solubility was increased by RF, too. For additive concentrations > 0.1 mol·kg^{-1} a part of RF and the additive precipitated with 1-2 weeks. ∆c(RF) = standard deviation.

c(additive) (mol·kg^{-1})	c(RF) (mmol·kg^{-1})	Δc(RF) (mmol·kg^{-1})	c(RF) (g·kg^{-1})	Δc(RF) (g·kg^{-1})	Molar ratio (additive/RF)
0.400	30	1	11.3	0.4	13.4
0.200	25	4	9	2	8.2
0.100	11.6	0.8	4.4	0.3	8.8
0.050	3.3	0.7	1.2	0.2	16.5
0.025	2.7	0.6	1.0	0.2	10.3

Table A 61: Solubilization of RF in water by means of sodium 3,5-bis(trifluoromethyl)benzoate (Na-3,5-DiCF3-Benz). After subtraction of the aqueous solubility of RF, the molar ratio was calculated from the molar concentration of the additive and RF. ∆c(RF) = standard deviation.

c(additive) (mol·kg^{-1})	c(RF) (mmol·kg^{-1})	Δc(RF) (mmol·kg^{-1})	c(RF) (g·kg^{-1})	Δc(RF) (g·kg^{-1})	Molar ratio (additive/RF)
1.071	32.9	0.2	12.39	0.08	32.8
0.535	8	1	3.2	0.4	65.9
0.286	3	1	1.2	0.4	97.9
0.143	0.84	0.01	0.315	0.004	251.9

Table A 62: Solubilization of RF in water by means of sodium dihydrogen phosphate (NaH_2PO_4). ∆c(RF) = standard deviation.

c(additive) (mol·kg^{-1})	c(RF) (mmol·kg^{-1})	Δc(RF) (mmol·kg^{-1})	c(RF) (g·kg^{-1})	Δc(RF) (g·kg^{-1})
4.000	0.019	-	0.007	-
3.500	0.034	-	0.013	-
3.000	0.040	-	0.015	-
2.500	0.070	0.006	0.026	0.002
2.000	0.076	0.004	0.029	0.001
1.500	0.121	0.002	0.046	0.001
1.000	0.156	0.001	0.0585	0.0002
0.750	0.179	0.002	0.067	0.001
0.500	0.17	0.02	0.063	0.006
0.400	0.202	0.002	0.076	0.001

0.300	0.212	0.002	0.080	0.001
0.200	0.216	0.006	0.081	0.002
0.100	0.27	0.03	0.10	0.01

Table A 63: Solubilization of RF in water by means of sodium 4-phenylbutyrate (NaButyrate). After subtraction of the aqueous solubility of RF, the molar ratio was calculated from the molar concentration of the additive and RF. Violet: Additive concentrations above the additive's aqueous solubility, as its solubility was increased by RF, too. For additive concentrations > 0.2 mol·kg^{-1} a part of RF and the additive precipitated with 1-2 weeks. ∆c(RF) = standard deviation.

c(additive) (mol·kg^{-1})	c(RF) (mmol·kg^{-1})	Δc(RF) (mmol·kg^{-1})	c(RF) (g·kg^{-1})	Δc(RF) (g·kg^{-1})	Molar ratio (additive/RF)
0.400	2.24	0.06	0.84	0.02	203.0
0.200	0.99	0.02	0.372	0.007	278.5
0.100	0.58	0.01	0.218	0.005	323.1
0.050	0.415	0.007	0.156	0.003	343.7
0.025	0.329	0.002	0.1237	0.0009	426.5

Table A 64: Solubilization of RF in water by means of sodium dodecyl sulfate (SDS). After subtraction of the aqueous solubility of RF, the molar ratio was calculated from the molar concentration of the additive and RF. ∆c(RF) = standard deviation.

c(additive) (mol·kg^{-1})	c(RF) (mmol·kg^{-1})	Δc(RF) (mmol·kg^{-1})	c(RF) (g·kg^{-1})	Δc(RF) (g·kg^{-1})	Molar ratio (additive/RF)
0.400	4.1	0.1	1.54	0.04	104.3
0.200	1.99	0.05	0.75	0.02	116.0
0.100	1.37	0.04	0.52	0.02	90.7

Table A 65: Solubilization of RF in water by means of sodium 2,4,6-trihydroxybenzoate. After subtraction of the aqueous solubility of RF, the molar ratio was calculated from the molar concentration of the additive and RF. Violet: Additive not soluble, turbid solution. Thus, RF solubilized the additive, too. ∆c(RF) = standard deviation.

c(additive) (mol·kg^{-1})	c(RF) (mmol·kg^{-1})	Δc(RF) (mmol·kg^{-1})	c(RF) (g·kg^{-1})	Δc(RF) (g·kg^{-1})	Molar ratio (additive/RF)
0.08	18	1	6.8	0.4	4.5

Table A 66: Solubilization of RF in water by means of tannin. After subtraction of the aqueous solubility of RF, the molar ratio was calculated from the molar concentration of the additive and RF. ∆c(RF) = standard deviation.

c(additive) (mol·kg^{-1})	c(RF) (mmol·kg^{-1})	Δc(RF) (mmol·kg^{-1})	c(RF) (g·kg^{-1})	Δc(RF) (g·kg^{-1})	Molar ratio (additive/RF)
0.2	36.33005	2.39912	13.6735409	0.90295679	5.54630401
0.1	13.28533	1.9415	5.00019965	0.73072236	7.68324737
0.05	7.14973	1.27319	2.69094388	0.47919052	7.26772708
0.01	2.56348	0.29734	0.96481697	0.11190986	4.36018627
0	0.286	0.02	0.10764182	0.0075274	0

Table A 67: Solubilization of RF in water by means of choline cinnamate. After subtraction of the aqueous solubility of RF, the molar ratio was calculated from the molar concentration of the additive and RF. ∆c(RF) = standard deviation.

c(additive) (mol·kg^{-1})	c(RF) (mmol·kg^{-1})	Δc(RF) (mmol·kg^{-1})	c(RF) (g·kg^{-1})	Δc(RF) (g·kg^{-1})	Molar ratio (additive/RF)
5.97	150	4	57	1	39.8
4.97	103	6	39	2	48.3
3.98	77	3	29	1	52.1
3.58	75	2	28.2	0.9	48.0
3.18	69	4	26	1	46.6
2.79	63	1	23.7	0.5	44.4
2.39	56.8	0.9	21.4	0.3	42.2
1.99	53	4	20	1	38.1
1.59	43	1	16.3	0.4	36.9
1.19	33.9	0.4	12.8	0.2	35.5
0.99	31.8	0.3	12.0	0.1	31.5
0.80	23.8	0.3	9.0	0.1	33.8
0.72	21	1	7.9	0.5	34.5
0.64	19	2	7.0	0.6	34.7
0.56	18	1	6.70	0.41	31.8
0.48	13.8	0.1	5.18	0.04	35.4
0.40	11.3	0.6	4.2	0.2	36.2
0.32	8.0	0.1	3.02	0.04	41.0
0.24	6.1	0.1	2.31	0.04	40.6
0.20	5.4	0.7	2.0	0.3	39.0
0.16	4.2	0.3	1.6	0.1	40.6
0.12	3.3	0.2	1.25	0.07	39.2
0.08	3	1	1.2	0.4	28.4
0.04	1.9	0.3	0.7	0.1	24.2

Table A 68: Solubilization of RF in water by means of choline 4-OH-3-OMe-Cinn. After subtraction of the aqueous solubility of RF, the molar ratio was calculated from the molar concentration of the additive and RF. ∆c(RF) = standard deviation.

c(additive) (mol·kg^{-1})	c(RF) (mmol·kg^{-1})	Δc(RF) (mmol·kg^{-1})	c(RF) (g·kg^{-1})	Δc(RF) (g·kg^{-1})	Molar ratio (additive/RF)
5.05	227	14	85	5	22.3
4.04	180	4	68	1	22.4
3.37	160.4	0.8	60.4	0.3	21.0
3.03	156	6	58.8	2.2	19.4
2.69	155.54	0.07	58.54	0.02	17.3
2.36	150	4	57	1	15.7
2.02	141	2	52.9	0.6	14.4
1.68	129	0	48.422	0.001	13.1
1.35	115	2	43.3	0.7	11.7
1.01	102.3	0.1	38.49	0.05	9.9
0.84	94	3	35	1	9.0
0.67	70.8	0.8	26.6	0.3	9.5
0.64	80	7	30.2	2.8	8.0
0.61	68	1	25.6	0.5	8.9
0.57	65.7	0.2	24.71	0.08	8.7

0.54	59	2	22.4	0.6	9.1
0.50	52.8	0.9	19.9	0.4	9.6
0.47	51	2	19.3	0.9	9.2
0.44	52	3	20	1	8.4
0.40	45	1	17.1	0.4	8.9
0.37	44	1	16.5	0.5	8.5
0.34	42	3	16	1	8.0
0.30	37	3	14	1	8.3
0.27	29	4	11	1	9.3
0.24	26	5	10	2	9.0
0.20	20.8	0.3	7.8	0.1	9.8
0.17	15	1	5.8	0.5	11.1
0.13	11.6	0.2	4.37	0.08	11.9
0.10	8.3	0.9	3.1	0.3	12.6
0.07	5.1	0.2	1.92	0.08	13.9
0.03	2.54	0.06	0.96	0.02	14.8

Table A 69: Solubilization of RF in water by means of choline 3,4-dimethoxybenzoate. After subtraction of the aqueous solubility of RF, the molar ratio was calculated from the molar concentration of the additive and RF. ∆c(RF) = standard deviation.

c(additive) (mol·kg^{-1})	**c(RF) (mmol·kg^{-1})**	**Δc(RF) (mmol·kg^{-1})**	**c(RF) (g·kg^{-1})**	**Δc(RF) (g·kg^{-1})**	**Molar ratio (additive/RF)**
3.50	42	1	16.0	0.5	83.1
3.15	43.0	0.3	16.2	0.1	73.8
2.80	40	2	14.9	0.8	71.4
2.45	34.74	0.07	13.07	0.03	71.2
2.10	31	1	11.8	0.4	67.9
1.75	29	1	11.0	0.4	60.3
1.40	25.3	0.9	9.5	0.4	56.0
1.05	20.658	0.004	7.775	0.001	51.6
0.70	15.1	0.7	5.7	0.3	47.4
0.56	12.0	0.1	4.53	0.04	47.6
0.42	8.64	0.02	3.251	0.007	50.3
0.35	7.4	0.2	2.77	0.06	49.4
0.18	3.58	0.07	1.35	0.02	52.9
0.14	2.86	0.02	1.076	0.008	54.2
0.11	2.26	0.07	0.85	0.02	52.8
0.07	1.49	0.03	0.56	0.01	57.3
0.04	1.0	0.1	0.38	0.05	47.5

Table A 70: Solubilization of RF in water by means of choline 3,4,5-trihydroxybenzoate. After subtraction of the aqueous solubility of RF, the molar ratio was calculated from the molar concentration of the additive and RF. ∆c(RF) = standard deviation.

c(additive) (mol·kg^{-1})	**c(RF) (mmol·kg^{-1})**	**Δc(RF) (mmol·kg^{-1})**	**c(RF) (g·kg^{-1})**	**Δc(RF) (g·kg^{-1})**	**Molar ratio (additive/RF)**
3.66	55	2	20.8	0.6	66.7
3.29	52	1	19.7	0.5	63.1
2.93	51	2	19.2	0.8	57.7

2.56	49.6	0.9	18.7	0.3	51.9
2.20	41	3	15	1	54.4
1.83	38	1	14.3	0.4	48.7
1.46	31.8	0.5	12.0	0.2	46.4
1.10	21.8	0.7	8.2	0.3	51.0
0.73	16	1	5.9	0.5	47.6
0.59	12	2	4.7	0.7	48.3
0.44	8.8	0.7	3.3	0.3	51.6
0.37	7.1	0.4	2.7	0.2	53.7
0.18	3.5	0.6	1.3	0.2	57.1
0.15	2.7	0.4	1.0	0.1	60.7
0.11	2.10	0.09	0.79	0.03	59.9
0.07	1.54	0.09	0.58	0.04	57.5
0.04	0.90	0.09	0.34	0.03	57.6

Table A 71: Solubilization of RF in water by means of choline 3,5-dihydroxybenzoate. After subtraction of the aqueous solubility of RF, the molar ratio was calculated from the molar concentration of the additive and RF. ∆c(RF) = standard deviation.

c(additive) (mol·kg^{-1})	**c(RF) (mmol·kg^{-1})**	**Δc(RF) (mmol·kg^{-1})**	**c(RF) (g·kg^{-1})**	**Δc(RF) (g·kg^{-1})**	**Molar ratio (additive/RF)**
3.89	54	2	20.4	0.7	72.1
3.50	48.5	0.4	18.2	0.1	72.6
3.11	47.0	0.3	17.7	0.1	66.5
2.72	44	2	16.4	0.6	62.9
2.33	38.1	0.8	14.3	0.3	61.6
1.94	34	1	12.7	0.5	58.1
1.55	28.3	0.5	10.6	0.2	55.5
1.17	20.7	0.6	7.8	0.2	57.2
0.78	13.5	0.3	5.1	0.1	58.5
0.62	10.7	0.2	4.04	0.09	59.4
0.47	8.7	0.4	3.3	0.1	55.2
0.39	6.4	0.1	2.42	0.05	63.1
0.19	3.3	0.3	1.2	0.1	65.1
0.16	2.32	0.02	0.873	0.008	75.8
0.12	1.748	0.001	0.6580	0.0004	78.9
0.08	1.21	0.02	0.454	0.007	82.9
0.04	0.739	0.009	0.278	0.003	82.8

Table A 72: Solubilization of RF in water by means of choline 4-OH-3-OMe-Benz. After subtraction of the aqueous solubility of RF, the molar ratio was calculated from the molar concentration of the additive and RF. ∆c(RF) = standard deviation.

c(additive) (mol·kg^{-1})	**c(RF) (mmol·kg^{-1})**	**Δc(RF) (mmol·kg^{-1})**	**c(RF) (g·kg^{-1})**	**Δc(RF) (g·kg^{-1})**	**Molar ratio (additive/RF)**
5.53	41.1	0.2	15.47	0.09	135.3
3.69	41	6	16	2	90.0
3.32	44	2	16.4	0.9	76.6
2.95	42	1	15.8	0.4	70.9
2.58	37.0	0.2	13.91	0.09	70.3
2.21	33.89	0.02	12.756	0.008	65.8
1.84	34	1	12.7	0.5	55.0

1.47	24.4	0.3	9.2	0.1	61.0
1.11	19	2	7.2	0.8	58.8
0.92	14	0	5	0	66.6
0.74	12.4	0.5	4.7	0.2	60.6
0.55	10.9	1.0	4.1	0.4	51.9
0.52	10.3	0.5	3.9	0.2	51.4
0.48	9.3	0.9	3.5	0.4	53.1
0.44	9	1	3.3	0.5	52.4
0.41	7.6	0.2	2.86	0.09	55.3
0.37	7.0	0.2	2.62	0.09	55.0
0.33	6.4	0.8	2.4	0.3	54.3
0.29	5.0	0.2	1.89	0.09	62.1
0.26	4.3	0.2	1.63	0.06	63.4
0.22	3.59	0.08	1.35	0.03	66.6
0.18	3.2	0.1	1.20	0.05	62.9
0.15	2.50	0.09	0.94	0.03	66.2
0.11	1.86	0.01	0.699	0.004	69.6
0.07	1.31	0.02	0.492	0.008	71.1
0.04	0.873	0.001	0.3285	0.0005	61.1

7.6 Effect of polyphenolates with different cations

Table A 73: Aqueous solubilization of RF in the presence of 0.37 mol·kg^{-1} ferulate salts, see Figure 37. The first value (NaFer) represents the reference – the RF solubility with 0.37 mol·kg^{-1} sodium ferulate in water without other additives. In the first column the appearance of the ferulate solution prior to saturation with RF is given. In the last column the solubility of RF is given relative to the reference. ⧋c(RF) = standard deviation of RF's water-solubility; Fer = ferulate.

Additive	Appearance	c(RF) (mmol·kg^{-1})	⧋c(RF) (mmol·kg^{-1})	Molar ratio (additive/RF)	solubility rel. to NaFer (%)
NaFer	Clear	56	3	6.7	0.0
CholineFer	Clear	44	1	8	-21.4
KFer	Turbid	37	5	10	-34.2
ArginineFer	Turbid	24	2	15	-56.7
MeglumineFer	Turbid	20	2	19	-64.2

7.7 Solubilization with other additives

Table A 74: Water-solubility of riboflavin in the presence of 0.37 mol·kg^{-1} additives. If the additives were not soluble at a concentration of 0.37 mol·kg^{-1}, lower concentrations were used or water was saturated (sat.) with the additive. The appearance and approximate pH value of the solution were documented prior to saturation with riboflavin. ⧋c(RF) = standard deviation of RF's water-solubility.

Additive	Appearance	c(RF) (mmol·kg^{-1})	⧋c(RF) (mmol·kg^{-1})	Molar ratio (additive/RF)	pH
Riboflavin in pure water	Clear	0.27	0.02		6/7
Biotin (50 mM)	Turbid	0.277	0.003	5584	4
Vit. K3 sat.	Turbid	0.279	0.004	-	6
Folic acid sat.	Turbid	0.276	0.004	-	6
Ellagic acid sat.	Turbid	0.266	0.006	-	6
L-Tyrosine (80 mM)	Turbid	0.277	0.005	8630	6
Hesperidin (80 mM)	Turbid	0.281	0.005	5981	6
L-Proline	Clear	0.305	0.008	9905	6
L-Histidine (80 mM)	Clear	0.326	0.002	1377	7
NaPyroglutamate	Clear	0.343	0.002	4960	3
Saccharine	Turbid	0.347	0.001	4710	2
Rutin (80 mM)	Turbid	0.349	0.004	993	6
ATP (80 mM)	Clear	0.3664	0.0007	813	3
Thiamin x HCl (300 mM)	Clear	0.37	0.01	819	3/4
Adenine (80 mM)	Clear	0.391	0.007	648	6
γ-valerolactone	Clear	0.423	0.006	850	7
Pyroglutamic acid	Clear	0.43	0.01	2233	1
Thiamine + NaOH (80 mM)	Clear	0.491	0.009	358	8
Adenosine (80 mM)	Turbid	0.51	0.01	330	6
Pyridoxin x HCl	Clear	0.605	0.008	612	3
Ethyl vanillin sat.	Turbid	0.74	0.01	-	5
Caffeine (80 mM)	Clear	0.905	0.006	125	6
Caffeine (370 mM)	Clear	1.17	-	411	6
Pyridoxine + NaOH	Clear	1.22	0.02	387	8
Tetra-Na-NADPH (100 mM)	Clear	1.6	0.7	76	7/8
Vanillyl alcohol sat.	Turbid	1.64	0.06	-	6
L-Tryptophan (80 mM)	Turbid	2.30	0.01	39.4	6
Indoxyl sulfate (0.1 M)	Clear	3.49	0.03	31	2
Indoxyl sulfate (0.1 M)	Clear	3.58	0.06	31	7
3-Indolepropionic acid (0.1 M)	Clear	3.49	0.03	2174	5
NaSaccharine	Clear	0.313	0.005	114	7/8
Resveratrol-Tri-PO4 (185 mM)	Clear	47.6	0.5	3.9	>8

7.8 Solubilization of lumichrome

Table A 75: Water-solubility of lumichrome in the presence of sodium polyphenolates and related compounds and in pure water.

Additive	c(lumichrome) (mmol·kg^{-1})	Additive	c(lumichrome) (mmol·kg^{-1})
Water	0.035 ± 0.002	**Na-4-OH-3-OMe-Benz**	0.42 ± 0.01
NaBenz	0.08 ± 0.01	**NaCinn**	0.573 ± 0.006
NaCHC	0.19 ± 0.02	**Na-2,4-Pentadienoate**	4.41 ± 0.04
NaButyrate	0.186 ± 0.003	**Na-4-OH-3-OMe-Cinn**	4.5 ± 0.2
NaValerate	0.31 ± 0.05	**Na-3,4-DiOMe-Cinn**	7.1 ± 0.3

7.9 Solubilization of folic acid

Table A 76: Solubility of folic acid in water in the absence and presence of aromatic sodium carboxylates, molar additive/folic acid ratio and factor for the increase in the water-solubility compared to pure water.

Additive	c(folic acid) (mmol·kg^{-1})	Ratio	Factor
Pure water	0.025 ± 0.004		
0.2 M NaButyrate	9.1 ± 0.4	21± 1	364
0.37 M Na-4-OH-3-OMe-Benz	13.9 ± 0.3	26.6 ± 0.6	556
0.2 M NaCinn	17.6 ± 0.6	11.4 ± 0.4	704
0.2 M NaValerate	20 ± 2	10 ± 1	800
0.37 M Na-3,4-DiOMe-Cinn	22 ± 4	17 ± 3	880
0.2 M Na-2,4-Pentadienoate	24.9 ± 0.9	8.0 ± 0.3	996
0.37 M Na-4-OH-3-OMe-Cinn	50 ± 4	7.2 ± 0.5	2000

7.10 SAXS measurements

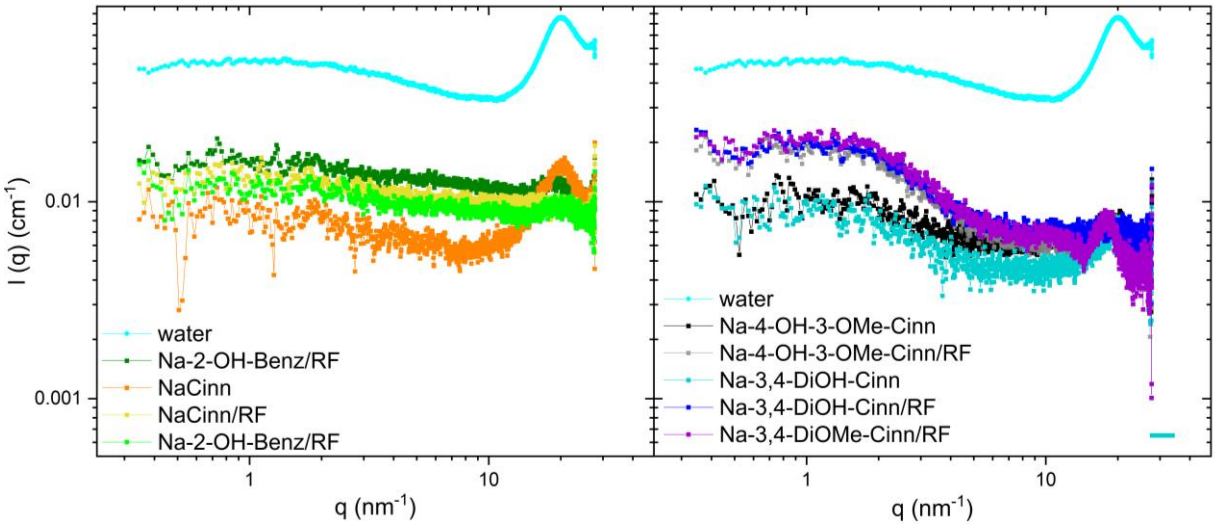

Figure A 7: SAXS measurements of 0.30 mol·kg^{-1} aqueous sodium polyphenolates solutions without riboflavin and saturated with riboflavin. The signal to noise ratio was low, thus aggregates could not be detected.

7.11 NMR Measurements

7.11.1 Riboflavin in $DMSO_6$

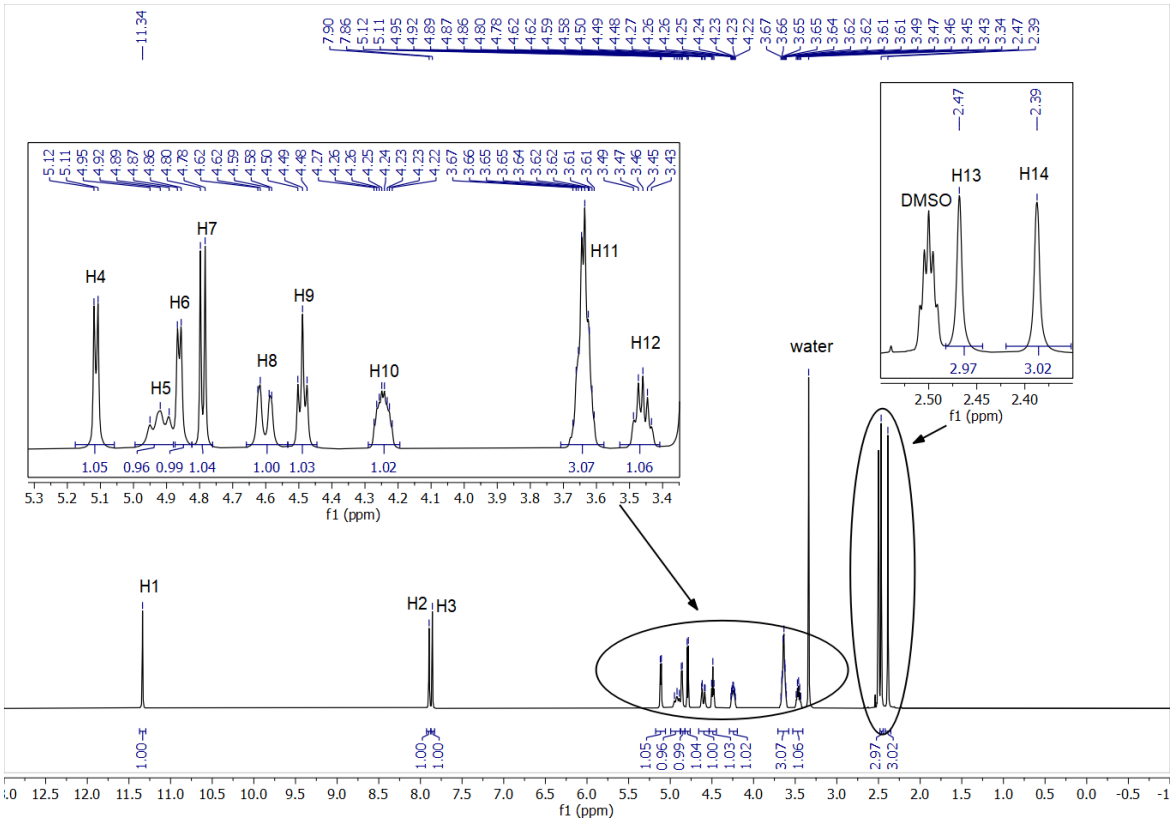

Figure A 8: ^{1}H-NMR spectrum of riboflavin in DMSO-d_6 (saturation).

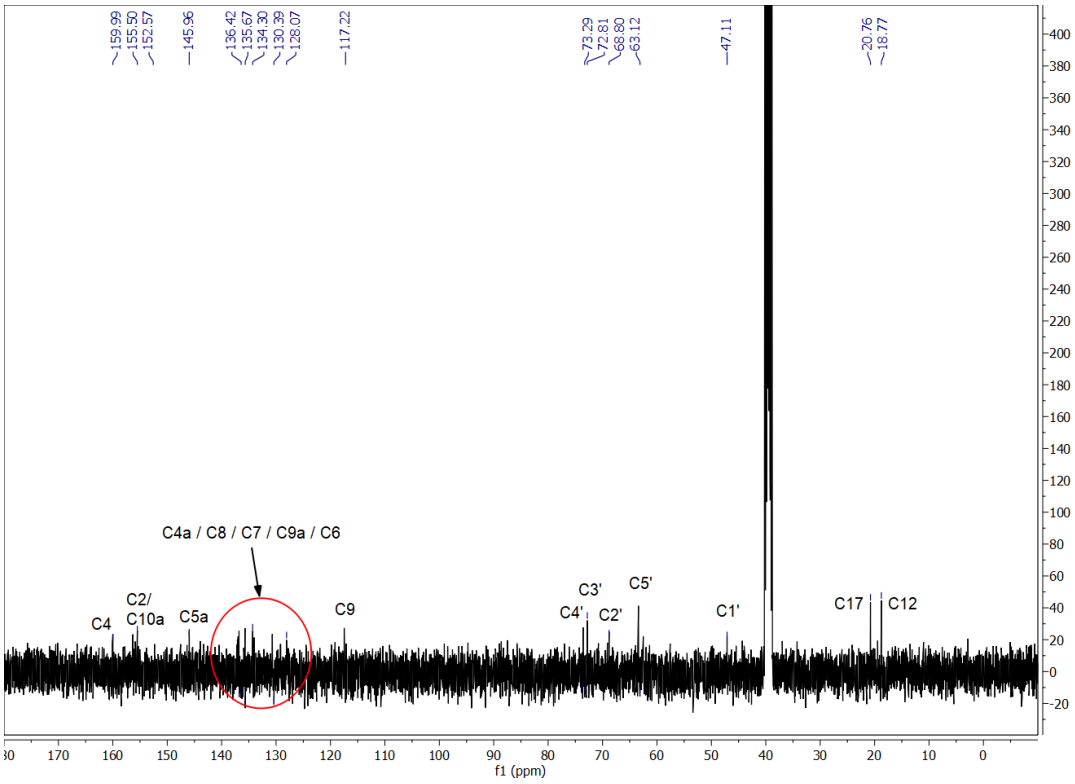

Figure A 9: ^{13}C-NMR spectrum of riboflavin in DMSO-d_6 (saturation).

Table A 77: Attribution of ^{1}H-NMR signals to RF atoms, see Figure A 8.The COSY, NOESY, HSQC and HMBC spectrum were used for validation of the attribution see Figure A 10-Figure A 13. s = singlet, d = doublet, t = triplet, m = multiplet.

Proton	δ (ppm)	Number of protons	Splitting	J (Hz)	Attribution via
1	11.34	1	s	-	Shift
2	7.90	1	s	-	HSQC
3	7.86	1	s	-	HSQC
4 (OH)	5.11	1	d	^{3}J(4-11) = 4.95	HMBC
5/8	4.92	1	t	^{2}J(5-8) = 10.51	HSQC, Integral, Shift
6 (OH)	4.86	1	d	^{3}J(6-11) = 4.68	HMBC
7 (OH)	4.79	1	d	^{3}J(7-10) = 5.84	HMBC
8/5	4.60	1	d	^{2}J(8-5) = 13.65	COSY
9 (OH)	4.49	1	t	^{2}J(9-11) = 5.68	Splitting/HMBC
10	4.25	1	m	Not resolved	COSY
11	3.64	3	m	Not resolved	COSY
12	3.46	1	m	Not resolved	COSY
13	2.47	3	s	-	HSQC
14	2.39	3	s	-	HSQC

Table A 78: Attribution of ^{13}C-NMR signals to RF carbon atoms from Figure A 9. The atoms attributed via HSQC are indicated in brackets, see Figure A 9. C9a was not certain, as the noise was too strong.

Carbon	δ (ppm)	Carbon	δ (ppm)
4	159.99	9	117.22 (HSQC)
10a	155.50	3‘	72.81 (HSQC)
2	152.57	4‘	73.29(HSQC)
5a	145.96	2‘	68.80 (HSQC)
4a	136.42	5‘	63.12 (HSQC)
8	135.67	1‘	47.11 (HSQC)
7	134.30	12	20.76 (HSQC)
9a*	134.01/128.07	17	18.77 (HSQC)
6	130.39 (HSQC)		

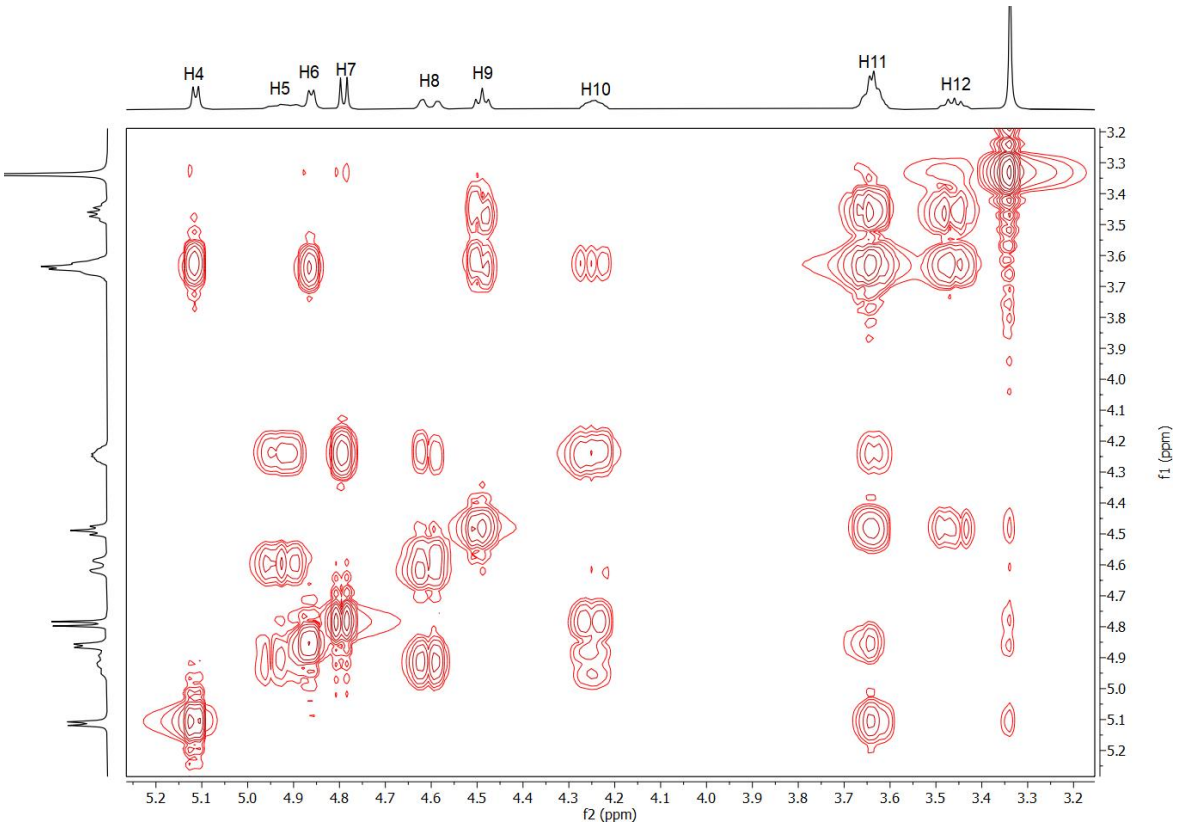

Figure A 10: COSY spectrum of riboflavin in DMSO-d_6 (saturation). The following interactions were visible: H12 with H9/11; H11 with H6/H4/H10/H12/H9; H10 with H8/H5/H11; H8 with H5/H10.

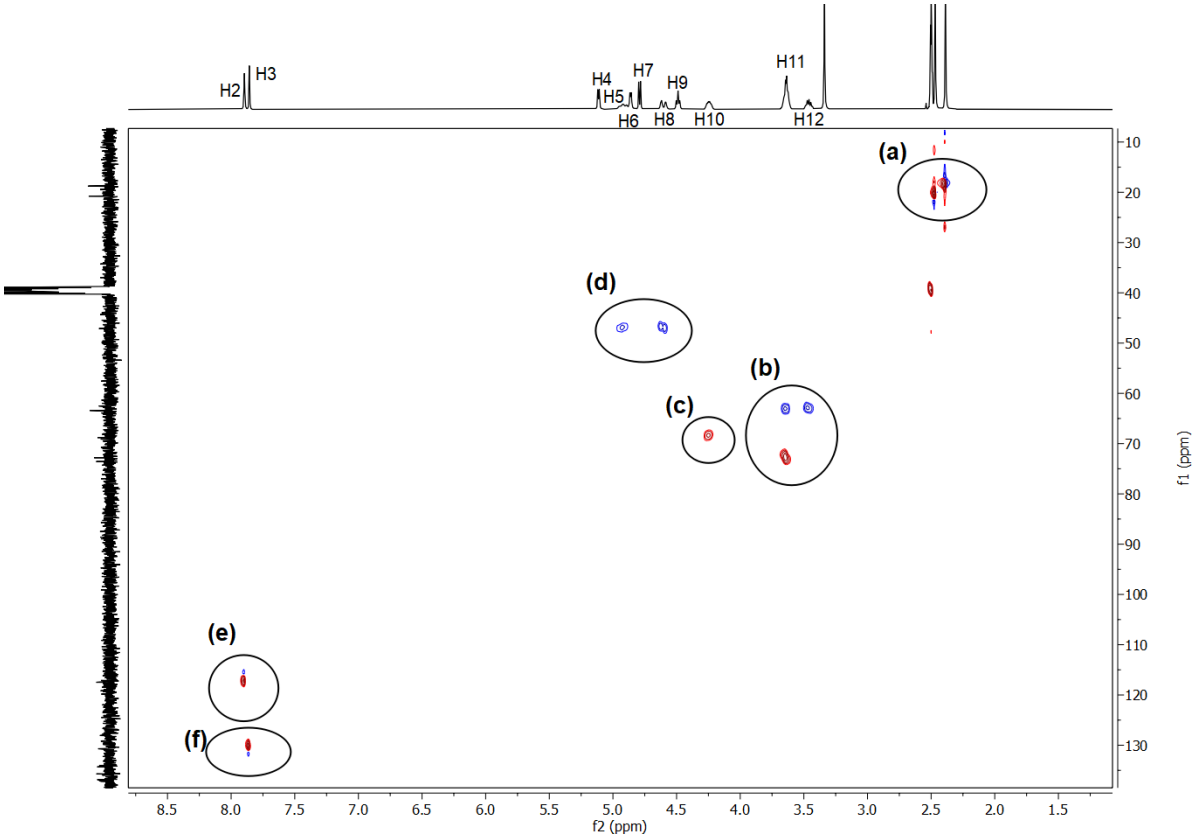

Figure A 11: HSQC spectrum of riboflavin in DMSO-d_6 (saturation). The protons could be attributed to the following carbons atoms: (a) C17 to H14 and C12 to H13 - (b) C5' to H12 and C5'/C3'/C4' to H11 - (c) C2' to H10 - (d) C1 to H8/5 - (e)C6 to H3 - (f)C9 to H2.

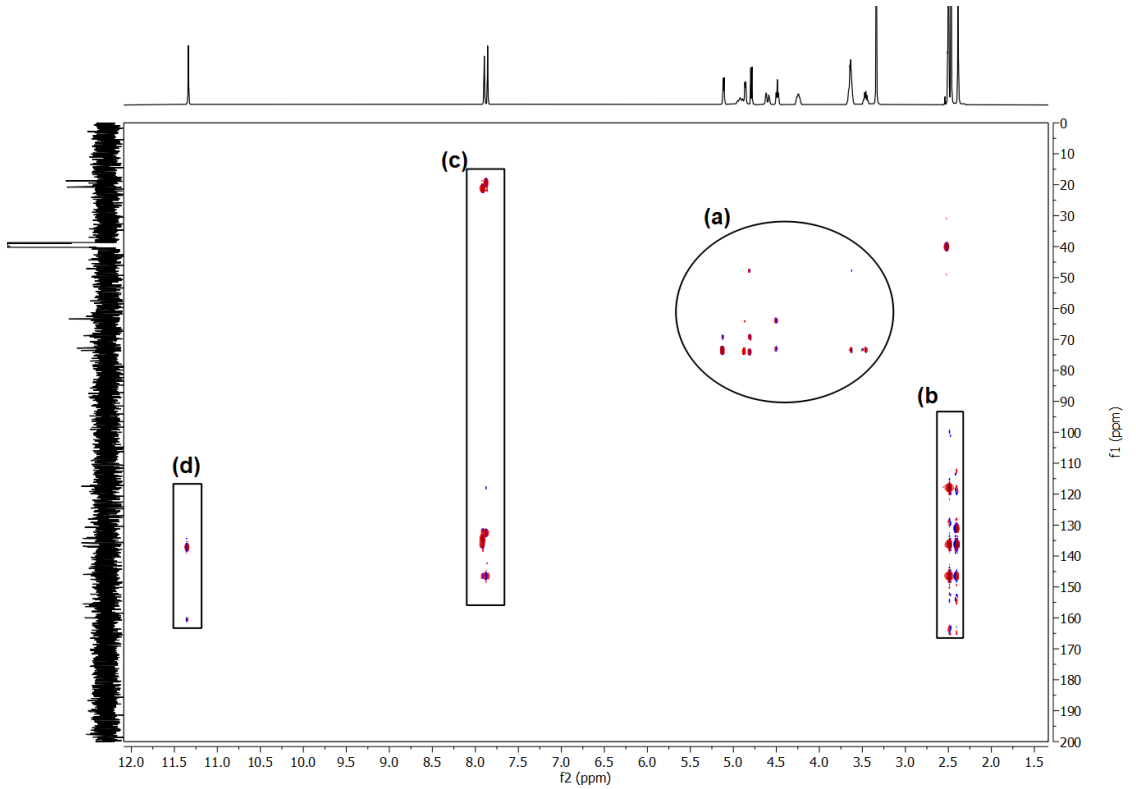

Figure A 12: HMBC spectrum of riboflavin in DMSO-d_6 (saturation). The following cross peaks are visible: (a) C3'/C4'-H12 and C3'/C4'-H11 and C5'/C3'/C4'-H9 and C4'/C2'/C1'-H7 and C4'-H6 and C4'/C2'/C3'-H4 – (b) C9/C6/C9a/C7/C8/C5a/C4a-H13/14 – (c) C12/C17/C6/C9a/C7/C8/C5a/C4a/C9-H2/3 – (d) C4a/C4-H1.

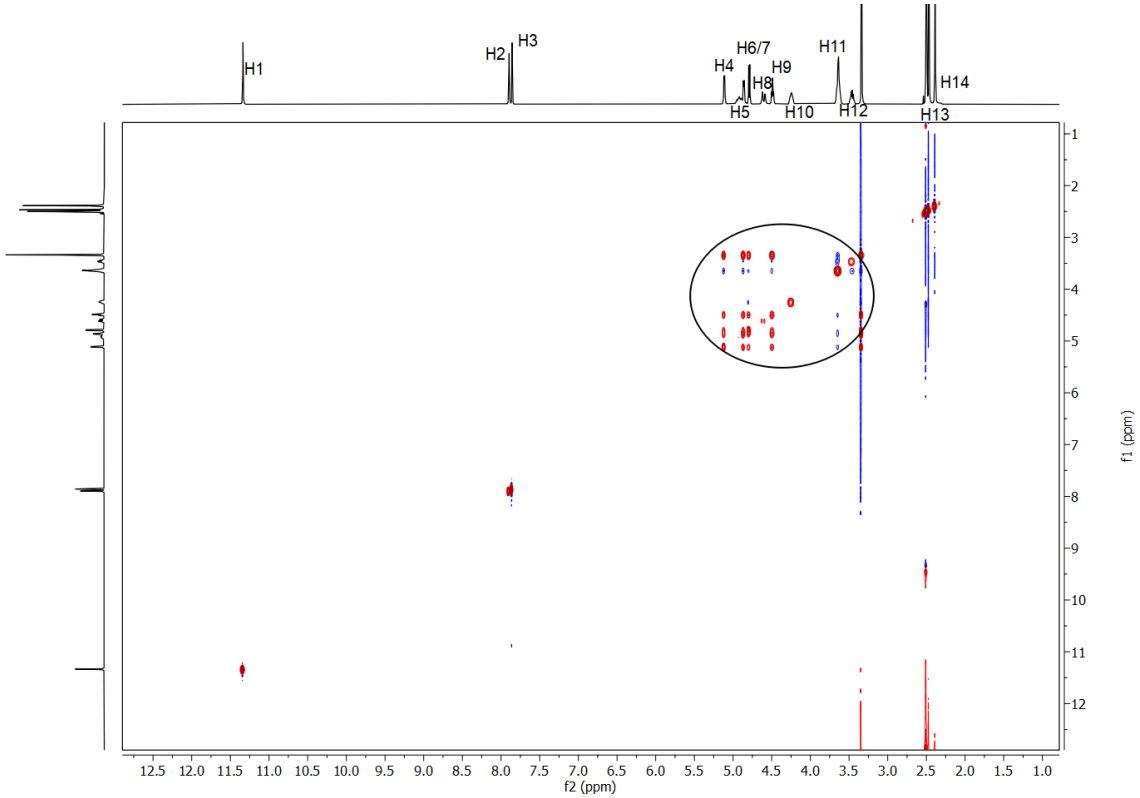

Figure A 13: NOESY spectrum of riboflavin in DMSO-d_6 (saturation). The interactions of the sugar chain were marked with a circle. The interactions, which were depicted in Figure A 10 above, are visible in the NOESY spectrum, too. Additionally, a cross-peak between H10 and H7 was found. Therefore, H7 belonged to the OH-group nearest to the isoalloxazine ring.

7.11.2 NMR experiments with riboflavin 5'-monophosphate sodium salt in deuterium oxide

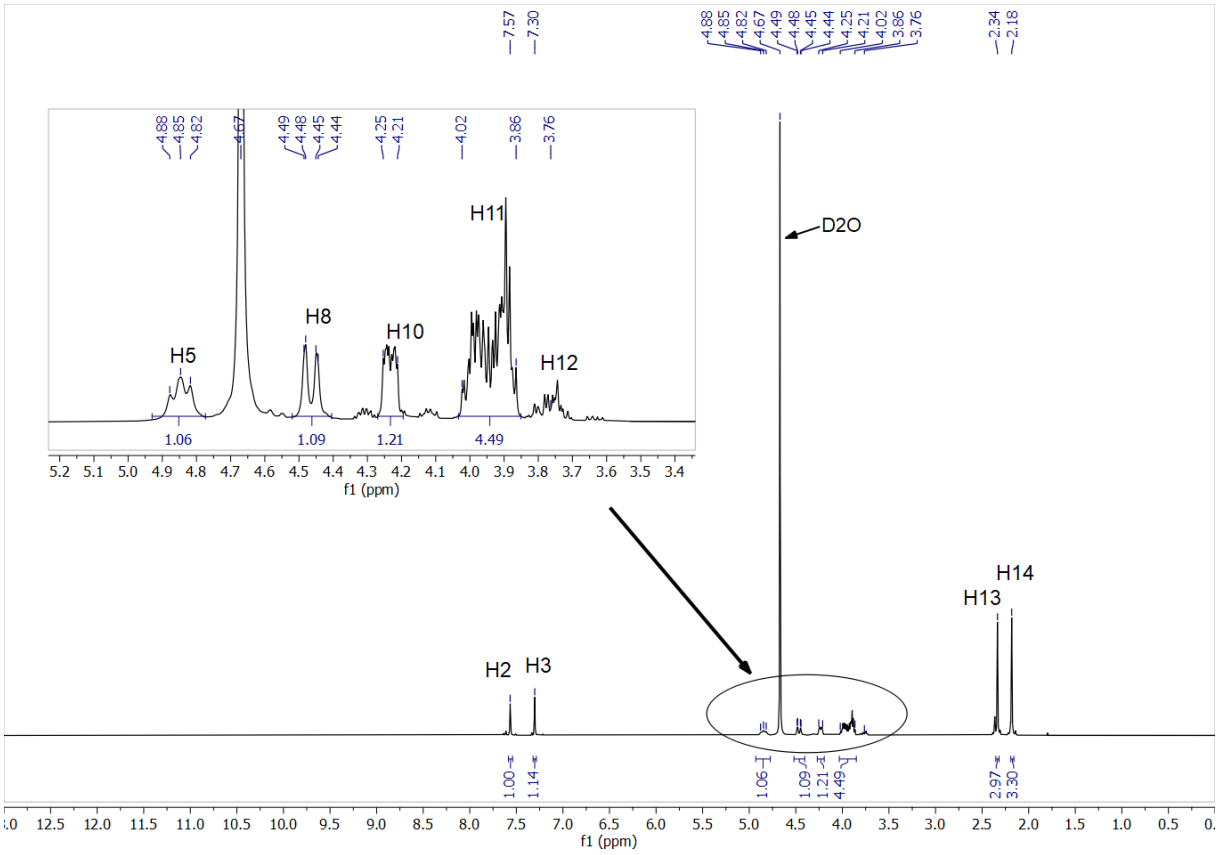

Figure A 14: ^{1}H-NMR spectrum of riboflavin 5'-monophoshpate sodium salt in deuterium oxide (saturation).

Table A 79: Attribution of ^{1}H-NMR signals from Figure A 14 to RF-PO$_4$ protons via the chemical shift δ, the integrals, the splitting and coupling constants. The right column shows the interactions observed from the NOESY spectrum in Figure 119. vis. = visible, s = singlet, d = doublet, t = triplet, m = multiplet.

Proton	δ (ppm)	Number of protons	Splitting	J (Hz)	NOESY
1	Not vis.	1	-	-	
2	7.57	1	s	-	H13, H10 H8, H5
3	7.30	1	s	-	H14
4 (OH)	Not vis		-	-	
5	4.85	1	t	^{2}J(5-8) = 12.72	H2
6 (OH)	Not vis	-	-	-	
7 (OH)	Not vis	-	-	-	
8	4.46	1	d	^{2}J(8-5) = 14.60	H2
10	4.23	1	m		H2
11	3.94	3	m		
12	3.76	1	m		
13	2.33	3	s	-	H2
14	2.18	3	s	-	H3

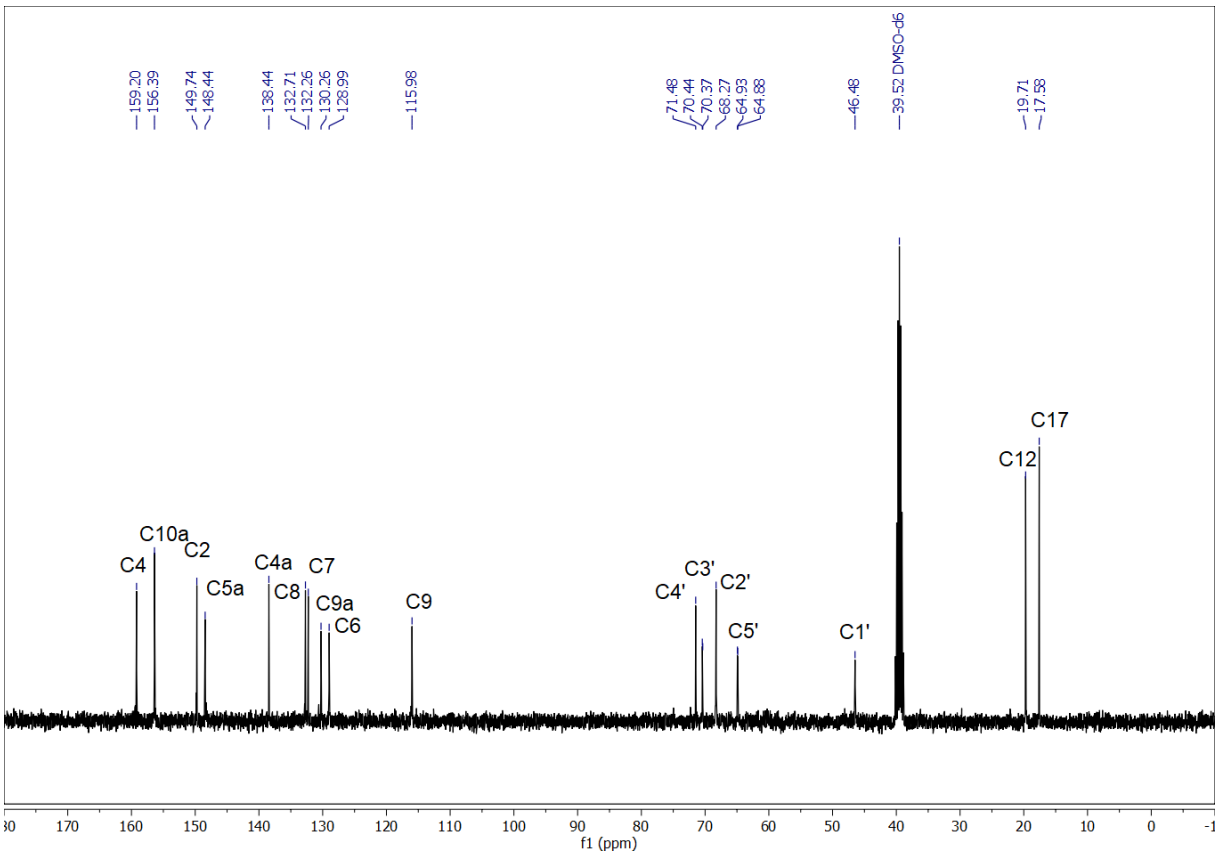

Figure A 15: ^{13}C-NMR spectrum of riboflavin 5'-monophosphate sodium salt in deuterium oxide (saturation). To have a reference an NMR tube with DMSO-d_6 was inserted.

Table A 80: Attribution of ^{13}C-NMR signals from Figure A 15 to RF-PO_4 carbons via the chemical shift δ, the HSQC and HMBC spectrum from Figure A 16 and Figure A 17. C3' and C5' gave rise to two signals probably due to different degrees of protonation and different conformations of the ribityl chain.

Carbon	δ (ppm)	HSQC	HMBC
4	159.20		
2	156.39		H3, H14, H13
10a	149.75		
4a	138.44		H2, H13, H14
5a	148.44		
8	132.70		H2, H13
7	132.26		H3, H14
9a	130.26		
6	128.99	H3	
9	115.98	H2	H13
4‘	71.48	H11/12	H11, H12
3‘	70.44/70.37	H11/12	
2‘	68.27	H10	
5‘	64.93/64.88	H11/12	H12
1‘	46.48	H8 / H5	
12	19.71	H13	H2, H14
17	17.58	H14	H3, H13

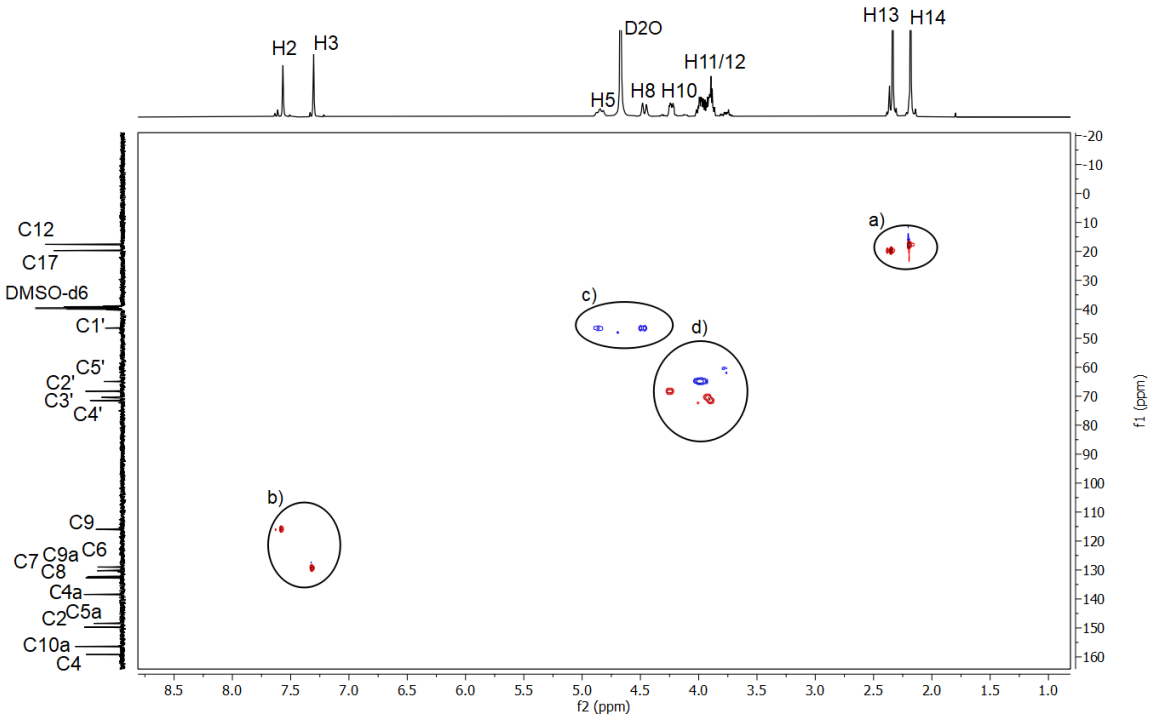

Figure A 16: HSQC NMR spectrum of riboflavin 5'-monophosphate in deuterium oxide (saturation). To have a reference in ^{13}C-NMR tube with DMSO-d_6 was inserted. ^{1}H-NMR was conducted in deuterium oxide only. The following cross peaks are present: a) H14/H13 with C17/C12, b) H2 with C9; H3 with C6, c) H5 and H8 with C1', d) H11 with C5', C3', C4' and H10 with C2'.

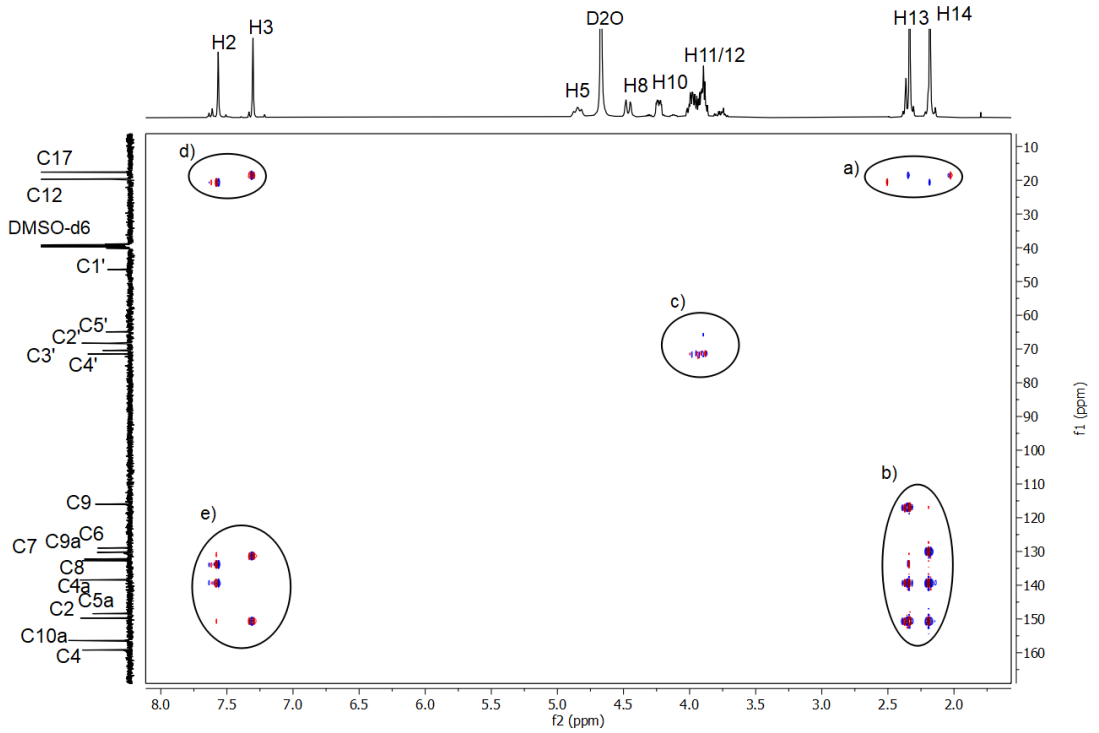

Figure A 17: HMBC NMR spectrum of riboflavin 5'-phosphate sodium salt in deuterium oxide (saturation). To have a reference in ^{13}C-NMR tube with DMSO-d_6 was inserted. ^{1}H-NMR was conducted in deuterium oxide only. The following cross peaks are present: a) H14 with C12 and H13 with C17, b) H13 with C9, C8, C4a, C2 and H14 with C7, C4a, C2, c) H12 with C5' and H11/H12 with C4', d) H3 with C17 and H2 with C12, e) H3 with C7, C2 and H2 with C8, C4a.

7.11.3 Riboflavin in presence of sodium benzoate in DMSO-d_6

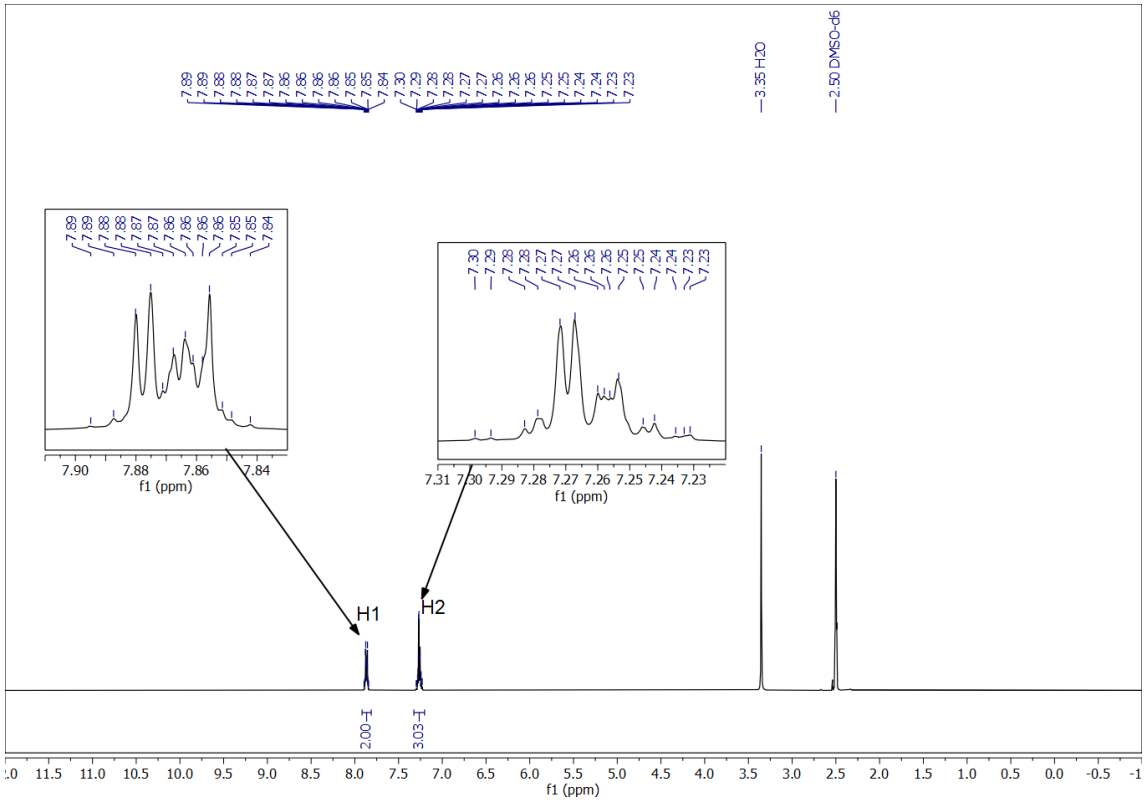

Figure A 18: ^{1}H-NMR of sodium benzoate in DMSO-d_6 (saturation).

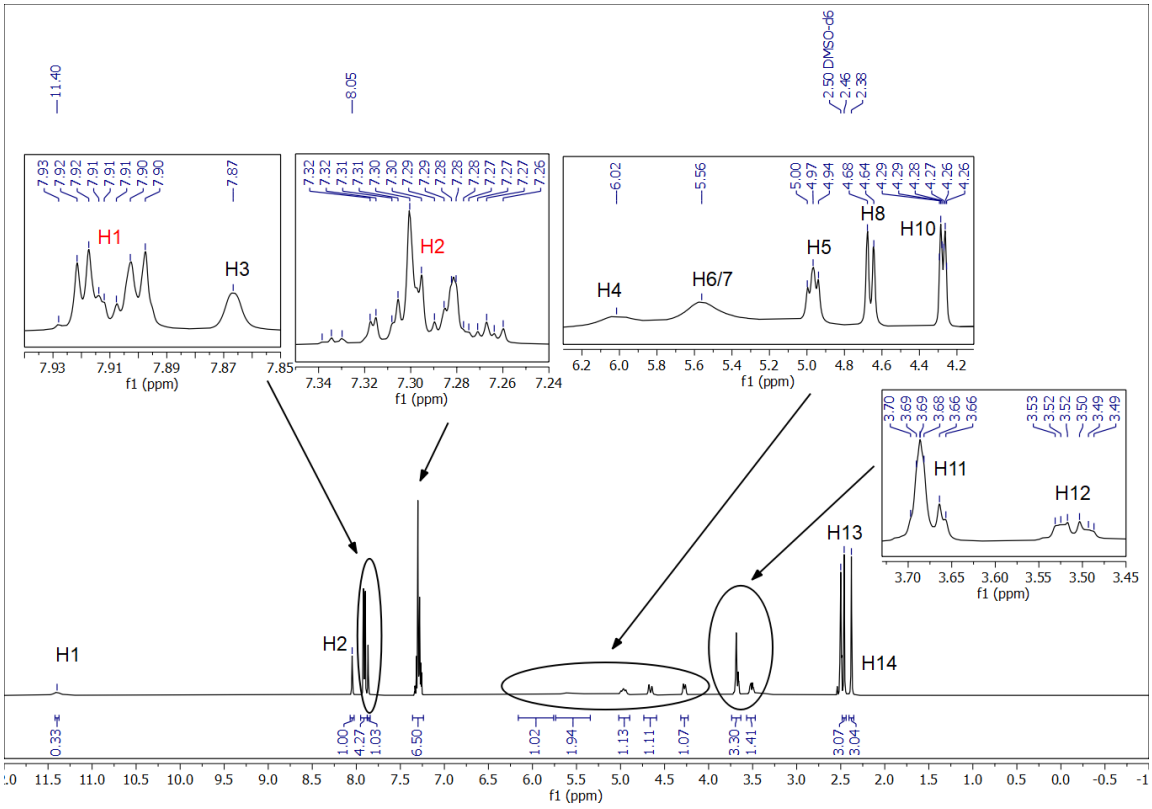

Figure A 19: ^{1}H-NMR spectrum of sodium benzoate and riboflavin (RF) in DMSO-d_6 (saturation) at a molar ratio of NaBenz/RF = 2. Red: Protons of NaBenz; Black: Protons of RF.

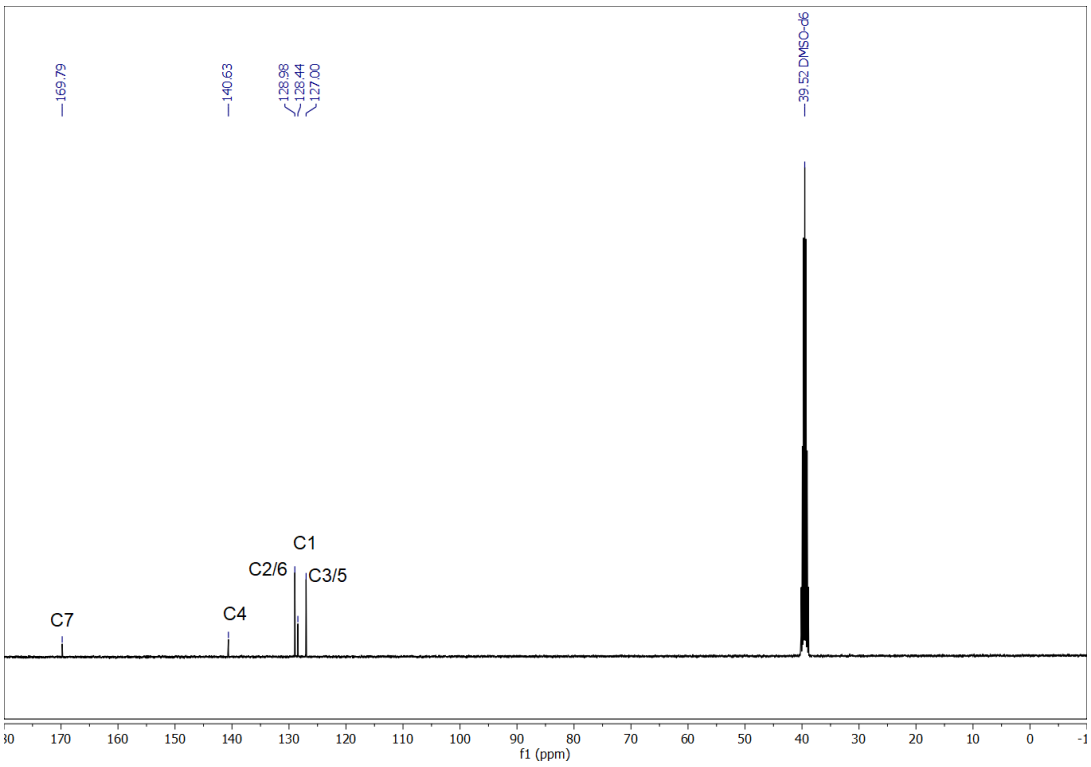

Figure A 20: ^{13}C-NMR spectrum of sodium benzoate in DMSO-d_6 (saturation).

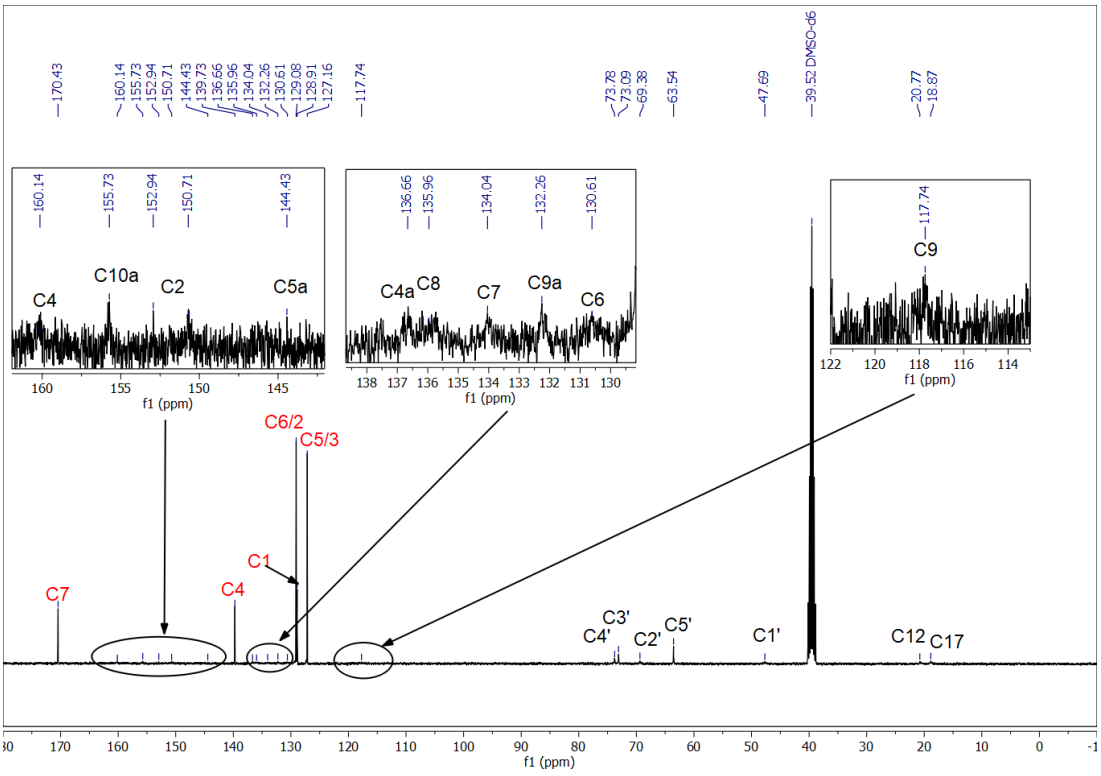

Figure A 21: ^{13}C-NMR spectrum of sodium benzoate and riboflavin (RF) at a molar ratio of NaBenz/RF = 2 in DMSO-d_6. Red: Carbons of NaBenz; Black: Carbons of RF.

Table A 81: δ_{exp}: Chemical shift of sodium benzoate's protons in DMSO-d_6 from Figure A 18 chemical shift of the protons of NaBenz in the presence of riboflavin at a molar ratio of 2 in DMSO-d_6 from Figure A 19. Δδ: Change of the chemical shift of the protons of NaBenz due to the presence of RF relatively to NaBenz in pure DMSO-d_6. Fifth column: Splitting for pure NaBenz and in presence of RF. The protons of NaBenz were assigned via the integrals. Left = deshielding/shift downfield; Right = shielding/ shift upfield.

	NaBenz	**NaBenz/RF = 2**		
Proton	**δ_{exp} (ppm)**	**δ_{exp} (ppm)**	**Δδ (ppm)**	**Splitting**
1	7.87	7.91	Left: 0.04	multiplet
2	7.26	7.29	Left: 0.03	multiplet

Table A 82: δ_{exp}: Chemical shift of the protons of riboflavin at a molar ratio of sodium benzoate/RF = 2 in DMSO-d_6 from Figure A 19. Δδ: Change of the chemical shift RF's protons due to the presence of NaBenz relatively to RF in pure DMSO-d_6 from Figure A 8. Fourth/fifth column: Splitting and coupling of RF's protons in presence of NaBenz. Left = deshielding/shift downfield; Right = shielding/ shift upfield, vis. = visible, s = singlet, d = doublet, t = triplet, m = multiplet.

Proton	**δ_{exp} (ppm)**	**Δδ (ppm)**	**Splitting**	**J (Hz)**
1	11.40	Left: 0.06	s	
2	8.05	Left: 0.15	s	
3	7.87	-	s	
4 (OH)	6.02	Left: 0.91	s	
5	4.97	Left: 0.05	t	^{2}J(5-8) = 11.44
6 (OH)	5.56	Left: 0.70	s	
7 (OH)	5.56	Left: 0.77	s	
8	4.66	Left: 0.06	d	^{2}J(8-5) = 13.41
9 (OH)	Not vis.	-	-	
10	4.27	Left: 0.02	td	^{3}J(10-7) = 9.50; ^{3}J(10-11/8/5) = 2.72
11	3.67	Left: 0.03	m	
12	3.51	Left: 0.05	m	
13	2.46	-	s	
14	2.38	-	s	

Table A 83: $\delta_{exp:}$ Chemical shift of sodium benzoate's carbon atoms in DMSO-d_6 from Figure A 20, chemical shift of NaBenz's carbon atoms at a molar ratio of NaBenz/riboflavin of 2 in DMSO-d_6 Figure A 21. $\delta_{calc:}$ Calculated chemical shift of NaBenz's carbon atoms in DMSO-d_6. Δδ. Change of the chemical shift of the carbon atoms of NaBenz due to the presence of RF relatively to NaBenz in pure DMSO-d_6. Left = deshielding/shift downfield; Right = shielding/ shift upfield.

		NaBenz	**NaBenz/RF = 2**	
Carbon	**δ_{calc} (ppm)**	**δ_{exp} (ppm)**	**δ_{exp} (ppm)**	**Δδ (ppm)**
7	-	169.79	170.44	Left: 0.65
4	133.3	140.63	139.73	Right: 0.90
6/2	130.1	128.98	129.08	Left: 0.10
1	130.9	128.44	128.91	Left: 0.47
5/3	128.4	127.00	127.16	Left: 0.16

Table A 84: Attribution of ^{13}C-NMR signals of riboflavin (RF) in the presence of sodium benzoate in DMSO-d_6 (δ_{exp}) from Figure A 21 and change of the chemical shift Δδ due to the presence of NaBenz at a molar ratio of NaBenz/RF = 2 relatively to RF in pure DMSO-d_6 from Table A 78 in section 7.11.1. Left = deshielding/shift downfield; Right = shielding/ shift upfield. All RF signals were very weak and hardly observable. If signals were hardly visible, they were set in brackets. For C2 two signals were observed.

Carbon	δ_{exp} (ppm)	Δδ (ppm)	Carbon	δ_{exp} (ppm)	Δδ (ppm)
4	160.14	Left: 0.15	**9**	117.74	Left: 0.52
10a	155.73	Left: 0.23	**4‘**	73.78	Left: 0.49
2	152.94/150.71	Left: 0.37 (Right: 1.86)	**3‘**	73.09	Left: 0.28
5a	144.43	(Right: 1.53)	**2‘**	69.38	Left: 0.58
4a	136.66	Left: 0.24	**5‘**	63.54	Left: 0.42
8	135.96	Left: 0.29	**1‘**	47.69	Left: 0.58
7	134.04	Right: 0.26	**12/17**	20.77	-
9a	132.26	(Right: 1.75)	**17 /12**	18.87	Left: 0.10
6	130.61	Left: 0.22			

7.11.4 Riboflavin in presence of sodium salicylate in DMSO-d_6

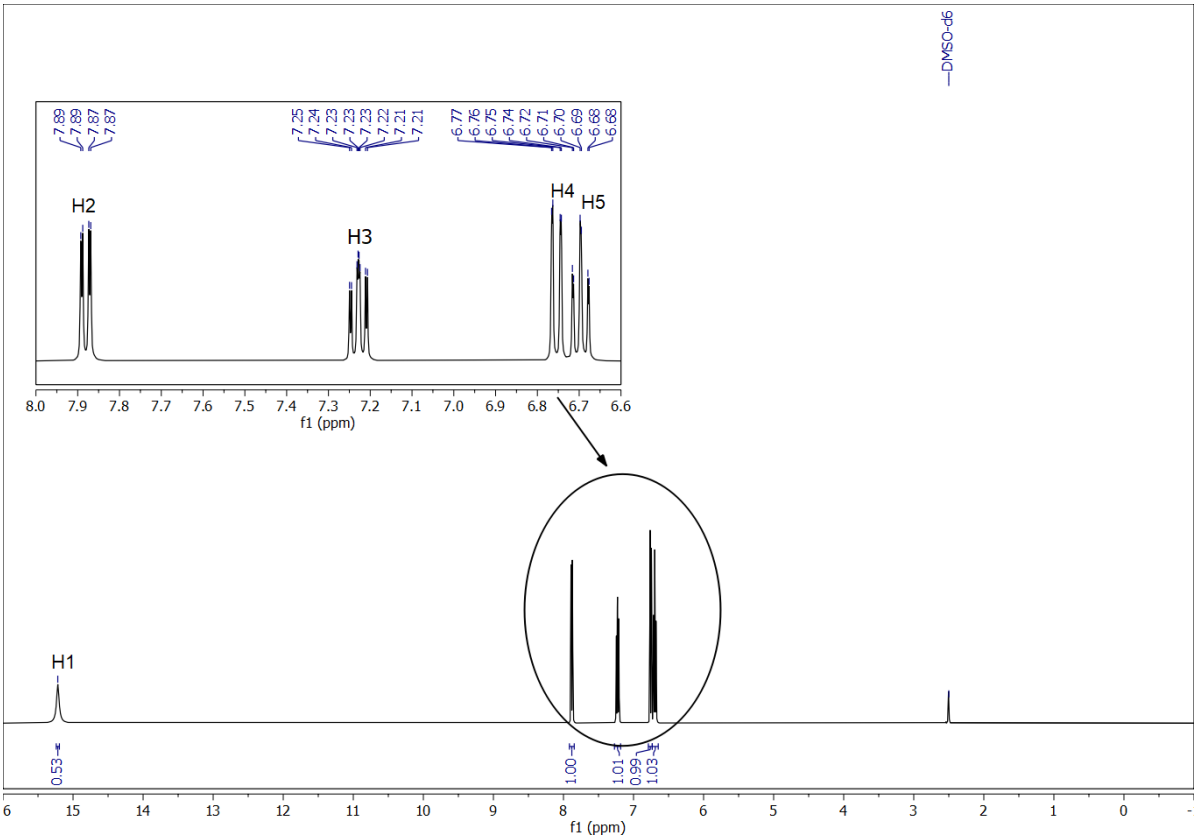

Figure A 22: ^{1}H-NMR spectrum of Na-2-OH-Benz in DMSO-d_6 (saturation).

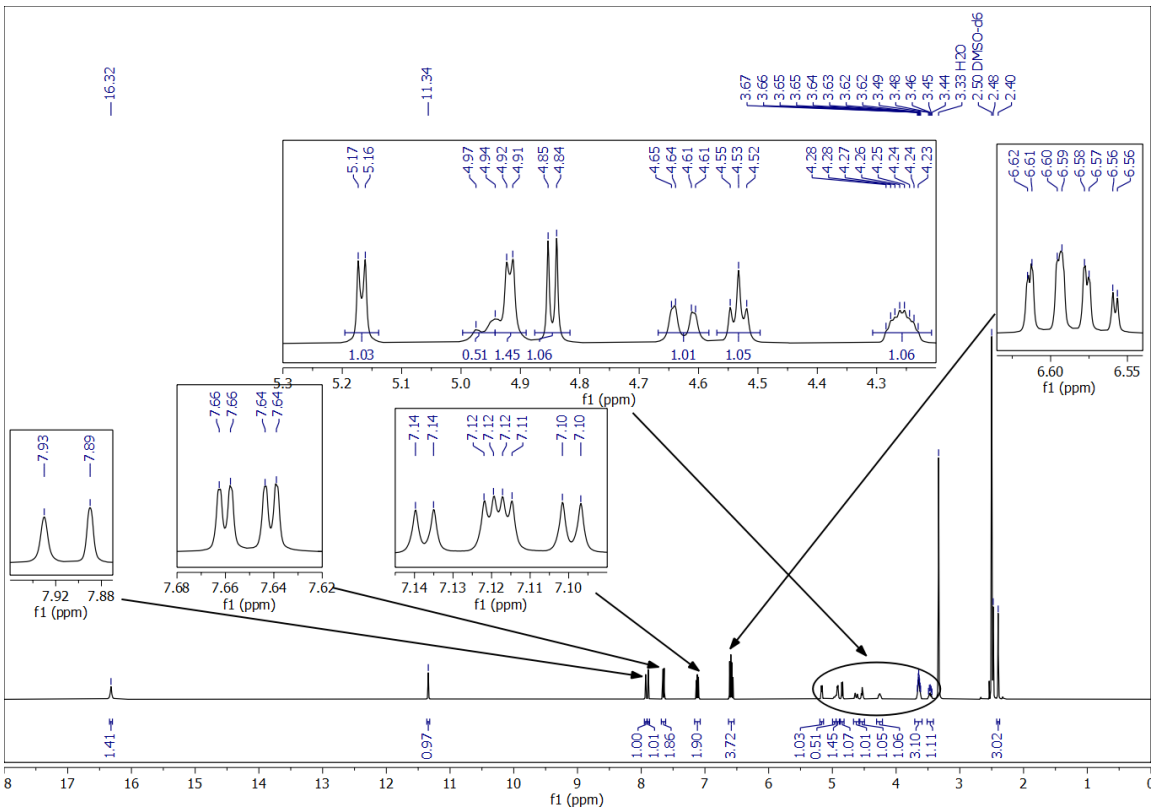

Figure A 23: ^{1}H-NMR spectrum of Na-2-OH-Benz with riboflavin in DMSO-d_6 at a molar ratio of Na-2-OH-Benz/RF = 2.

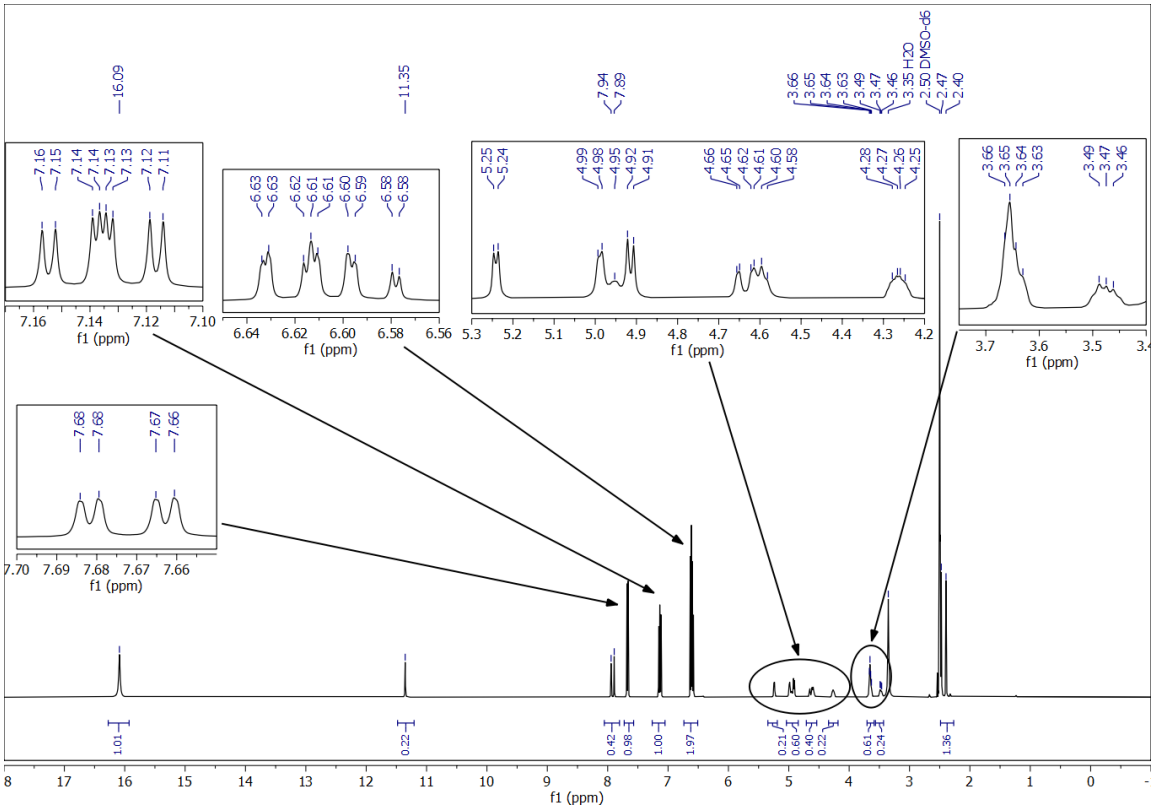

Figure A 24: ^{1}H-NMR spectrum of Na-2-OH-Benz with riboflavin in DMSO-d_6 at a molar ratio of Na-2-OH-Benz/RF = 5.

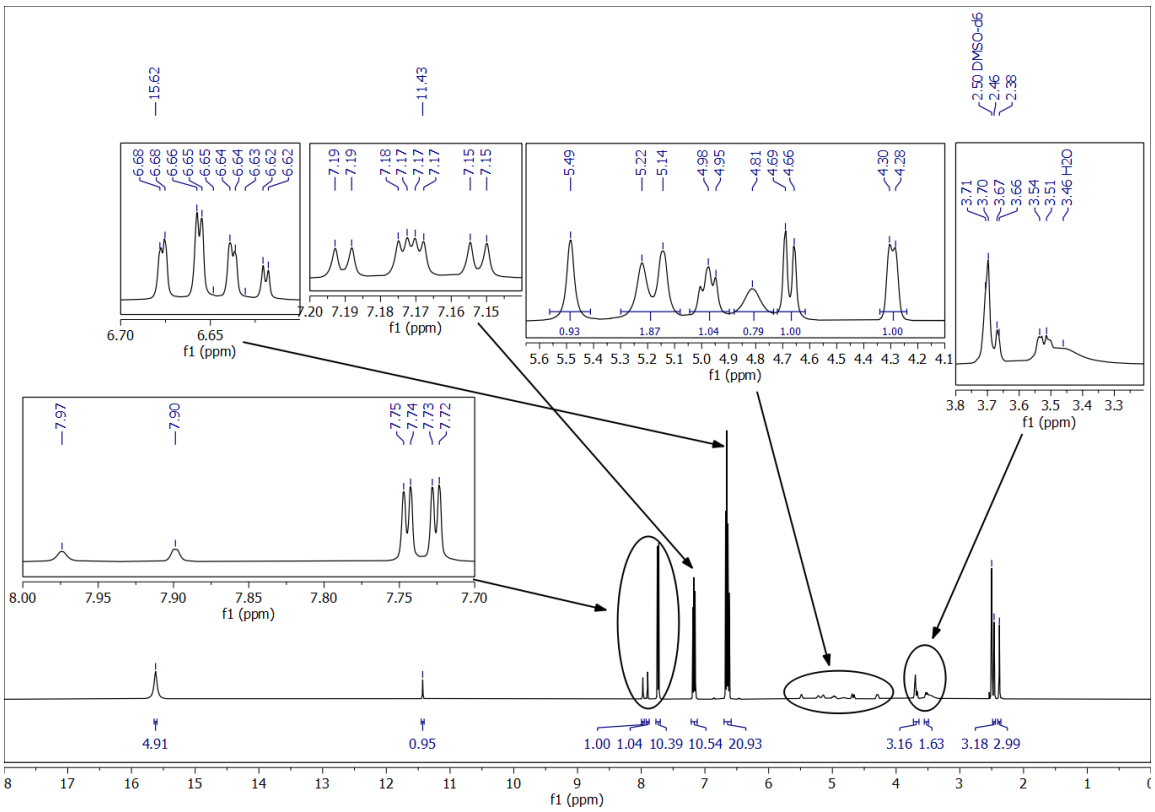

Figure A 25: ^{1}H-NMR spectrum of Na-2-OH-Benz with riboflavin in DMSO-d_6 at a molar ratio of Na-2-OH-Benz/RF = 10.

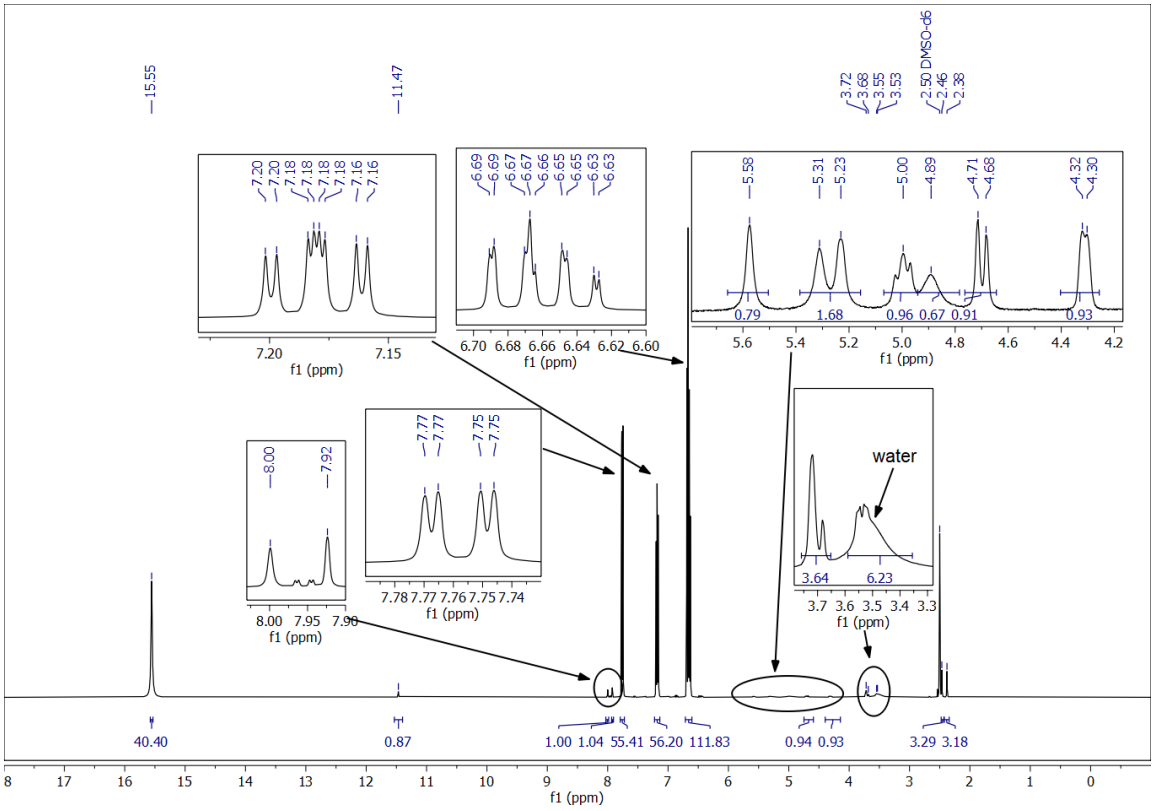

Figure A 26: ^{1}H-NMR spectrum of Na-2-OH-Benz with riboflavin in DMSO-d_6 at a molar ratio of Na-2-OH-Benz/RF = 50.

Table A 85: Chemical shift δ_{exp} (ppm) of sodium salicylate's protons in DMSO-d_6 and at the molar ratios of Na-2-OH-Benz/riboflavin of 2, 5, 10 and 50 in DMSO-d_6, see Figure A 22 - Figure A 26.

Proton	Na-2-OH-Benz	Ratio 50	Ratio 10	Ratio 5	Ratio 2
1	15.22	15.55	15.62	16.09	16.32
2	7.88	7.76	7.73	7.67	7.65
3	7.23	7.18	7.17	7.14	7.12
4	6.75	6.68	6.67	6.62	6.57
5	6.70	6.64	6.63	6.60	6.60

Table A 86: Splitting and coupling constants (Hz) of sodium salicylate's protons in absence and presence of riboflavin at different molar ratios of Na-2-OH-Benz to RF in DMSO-d_6 retrieved from Figure A 22 - Figure A 26. s = singlet, dd = doublet of doublets, ddd = doublet of doublets of doublets.

	Splitting	Na-2-OH-Benz	Ratio 50	Ratio 10	Ratio 5	Ratio 2
H1	s	-	-	-	-	-
H2	dd	^{3}J(2-5) = 7.70 ^{4}J(2-3) = 1.82	^{3}J(2-5) = 7.60 ^{4}J(2-3) = 1.81	^{3}J(2-5) = 7.62 ^{4}J(2-3) = 1.85	^{3}J(2-5) = 7.57 ^{4}J(2-3) = 1.85	^{3}J(2-5) = 7.58 ^{4}J(2-3) = 1.85
H3	ddd	^{3}J(3-5) = 9.01 ^{3}J(3-4) = 7.15 ^{4}J(3-2) = 1.82	^{3}J(3-5) = 9.03 ^{3}J(3-4) = 7.20 ^{4}J(3-2) = 1.85	^{3}J(3-5) = 9.08 ^{3}J(3-4) = 7.14 ^{4}J(3-2) = 1.85	^{3}J(3-5) = 9.08 ^{3}J(3-4) = 7.26 ^{4}J(3-2) = 1.85	^{3}J(3-5) = 9.07 ^{3}J(3-4) = 7.06 ^{4}J(3-2) = 1.85
H4	dd	^{3}J(4-3) = 7.15 ^{4}J(4-5) = 0.98	^{3}J(4-3) = 7.20 ^{4}J(4-5) = 1.11	^{3}J(4-3) = 7.14 ^{4}J(4-5) = 1.09	^{3}J(4-3) = 7.26 ^{4}J(4-5) = 1.09	^{3}J(4-3) = 7.06 ^{4}J(4-5) = 1.12
H5	ddd	^{3}J(5-3) = 9.01 ^{3}J(5-2) = 7.70 ^{4}J(5-4) = 0.98	^{3}J(5-3) = 9.03 ^{3}J(5-2) = 7.60 ^{4}J(5-4) = 1.11	^{3}J(5-3) = 9.08 ^{3}J(5-2) = 7.62 ^{4}J(5-4) = 1.09	^{3}J(5-3) = 9.08 ^{3}J(5-2) = 7.57 ^{4}J(5-4) = 1.09	^{3}J(5-3) = 9.07 ^{3}J(5-2) = 7.58 ^{4}J(5-4) = 1.12

Table A 87: Change of the chemical shift Δδ (ppm)of Na-2-OH-Benz protons due to the presence of riboflavin at different mole ratios of Na-2-OH-Benz to RF in DMSO-d_6 relatively to Na-2-OH-Benz in pure DMSO-d_6, see Table A 85. Left = deshielding/shift downfield; Right = shielding/ shift upfield.

Proton	Ratio 2	Ratio 5	Ratio 10	Ratio 50
1	Left: 1.10	Left: 0.87	Left: 0.40	Left: 0.33
2	Right: 0.23	Right: 0.21	Right: 0.15	Right: 0.12
3	Right: 0.11	Right: 0.09	Right: 0.06	Right: 0.05
4	Right: 0.18	Right: 0.13	Right: 0.08	Right: 0.07
5	Right: 0.10	Right: 0.10	Right: 0.07	Right: 0.06

Table A 88: Attribution of riboflavin protons in presence of sodium salicylate in DMSO-d_6 (δ_{exp}) at a molar ratio of Na-2-OH-Benz/RF = 2 from the ^{1}H-NMR spectrum, see Figure A 23. J = coupling constants; s = singlet, d = doublet, t = triplet, m = multiplet.

Riboflavin with Na-2-OH-Benz in DMSO-d_6 at ratio 2				
Proton	**δ_{exp} (ppm)**	**Number of protons**	**Splitting**	**J (Hz)**
1	11.34	1	s	-
2	7.93	1	s	-
3	7.89	1	s	-
4 (OH)	5.17	1	d	^{3}J(4-11) = 4.81
5	4.94	1	t	^{2}J(5-8) = 13.00
6 (OH)	4.91	1	d	^{3}J(6-11) = 4.17
7 (OH)	4.85	1	d	^{3}J(7-10) = 5.82
8	4.53	1	d	^{2}J(8-5) = 13.33

9 (OH)	4.53	1	t	^{2}J(9-11) = 5.50
10	4.26	1	m	Not resolved
11	3.65	3	m	Not resolved
12	3.46	1	m	Not resolved
13	2.48	3	s	-
14	2.40	3	s	-

Table A 89: Attribution of riboflavin protons in presence of sodium salicylate in DMSO-d_6 (δ_{exp}) at a molar ratio of Na-2-OH-Benz/RF = 5 from the ^{1}H-NMR spectrum, see Figure A 24. J = coupling constants; s = singlet, d = doublet, t = triplet, m = multiplet.

Riboflavin with Na-2-OH-Benz in DMSO-d_6 at ratio 5				
Proton	**δ_{exp} (ppm)**	**Number of protons**	**Splitting**	**J (Hz)**
1	11.35	1	s	-
2	7.94	1	s	-
3	7.89	1	s	-
4 (OH)	5.24	1	d	^{3}J(4-11) = 4.37
5	4.95	1	t	Overlap with other peak
6 (OH)	4.99	1	d	^{3}J(6-11) = 3.95
7 (OH)	4.91	1	d	^{3}J(7-10) = 5.77
8	4.64	1	d	^{2}J(8-5) = 13.88
9 (OH)	4.60	1	t	^{2}J(9-11) = 5.74
10	4.26	1	m	Not resolved
11	3.65	3	m	Not resolved
12	3.47	1	m	Not resolved
13	2.47	3	s	-
14	2.40	3	s	-

Table A 90: Attribution of riboflavin's protons in presence of sodium salicylate in DMSO-d_6 (δ_{exp}) at a molar ratio of Na-2-OH-Benz/RF = 10 from the ^{1}H-NMR spectrum, see Figure A 25. J = coupling constants; s = singlet, d = doublet, t = triplet, m = multiplet.

Riboflavin with Na-2-OH-Benz in DMSO-d_6 at ratio 10				
Proton	**δ_{exp} (ppm)**	**Number of protons**	**Splitting**	**J (Hz)**
1	11.43	1	s	-
2	7.97	1	s	-
3	7.90	1	s	-
4 (OH)	5.49	1	s	-
5	4.98	1	t	^{2}J(5-8) = 13.13
6 (OH)	5.22	1	s	-
7 (OH)	5.14	1	s	-
8	4.67	1	d	^{2}J(8-5) = 13.13
9 (OH)	4.81	1	s	-
10	4.29	1	m	Not resolved
11	3.68	3	m	Not resolved
12	3.52	1	m	Not resolved
13	2.46	3	s	-
14	2.38	3	s	-

Table A 91: Attribution of riboflavin's protons in presence of sodium salicylate in DMSO-d_6 (δ_{exp}) at a molar ratio of Na-2-OH-Benz/RF = 50, see Figure A 26. J = coupling constants; s = singlet, d = doublet, t = triplet, m = multiplet.

Riboflavin with Na-2-OH-Benz in DMSO-d_6 at ratio 50				
Proton	**δ_{exp} (ppm)**	**Number of protons**	**Splitting**	**J (Hz)**
1	11.47	1	s	-
2	8.00	1	s	-
3	7.92	1	s	-
4 (OH)	5.58	1	s	-
5	4.99	1	t	^{2}J(5-8) = 12.15
6 (OH)	5.31	1	s	-
7 (OH)	5.23	1	s	-
8	4.70	1	d	^{2}J(8-5) = 12.15
9 (OH)	4.89	1	s	-
10	4.31	1	m	Not resolved
11	3.70	3	m	Not resolved
12	3.54	1	m	Not resolved
13	2.46	3	s	-
14	2.38	3	s	-

Table A 92: Change of the chemical shift $\Delta\delta$ of riboflavin protons in presence of sodium salicylate at different molar ratios of Na-2-OH-Benz to RF in DMSO-d_6. The change of the chemical shift was calculated from the data in Table A 88 - Table A 91 using the NMR spectrum of RF in pure DMSO-d_6 from Figure A 8 as reference. Left = deshielding/shift downfield; Right = shielding/ shift upfield.

Proton	**Ratio 2**	**Ratio 5**	**Ratio 10**	**Ratio 50**
1	Left: < 0.01	Left: 0.02	Left: 0.09	Left: 0.13
2	Left: 0.03	Left: 0.05	Left: 0.08	Left: 0.10
3	Left: 0.03	Left: 0.04	Left: 0.04	Left: 0.07
4 (OH)	Left: 0.05	Left: 0.13	Left: 0.37	Left: 0.46
5	Left: 0.02	Left: 0.03	Left: 0.06	Left: 0.08
6 (OH)	Left: 0.06	Left: 0.13	Left: 0.36	Left: 0.45
7 (OH)	Left: 0.06	Left: 0.12	Left: 0.35	Left: 0.44
8	Right: 0.07	Left: 0.04	Left: 0.07	Left: 0.10
9 (OH)	Left: 0.04	Left: 0.11	Left: 0.32	Left: 0.40
10	Left: 0.01	Left: 0.02	Left: 0.05	Left: 0.07
11	Left < 0.01	Left: 0.01	Left: 0.05	Left: 0.06
12	Left: < 0.01	Left: 0.02	Left: 0.06	Left: 0.08
13	Left: < 0.01	Left: 0.01	Left: 0.01	-
14	Left: < 0.01	Left: < 0.01	Left: 0.01	Right: 0.01

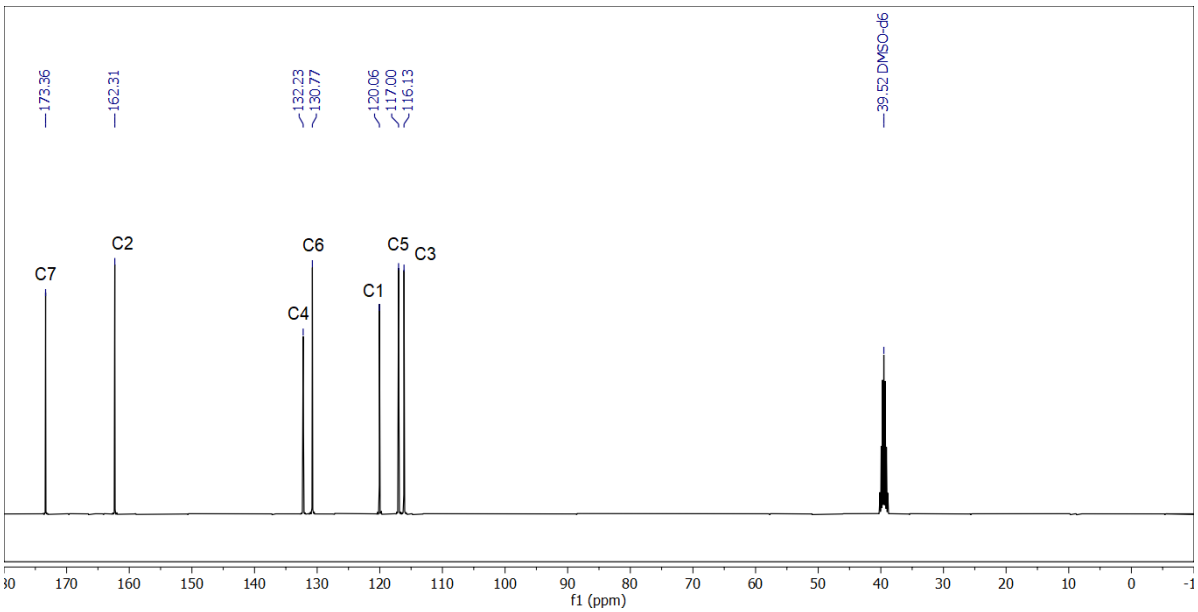

Figure A 27: ^{13}C-NMR spectrum with Na-2-OH-Benz in DMSO-d_6 (saturation).

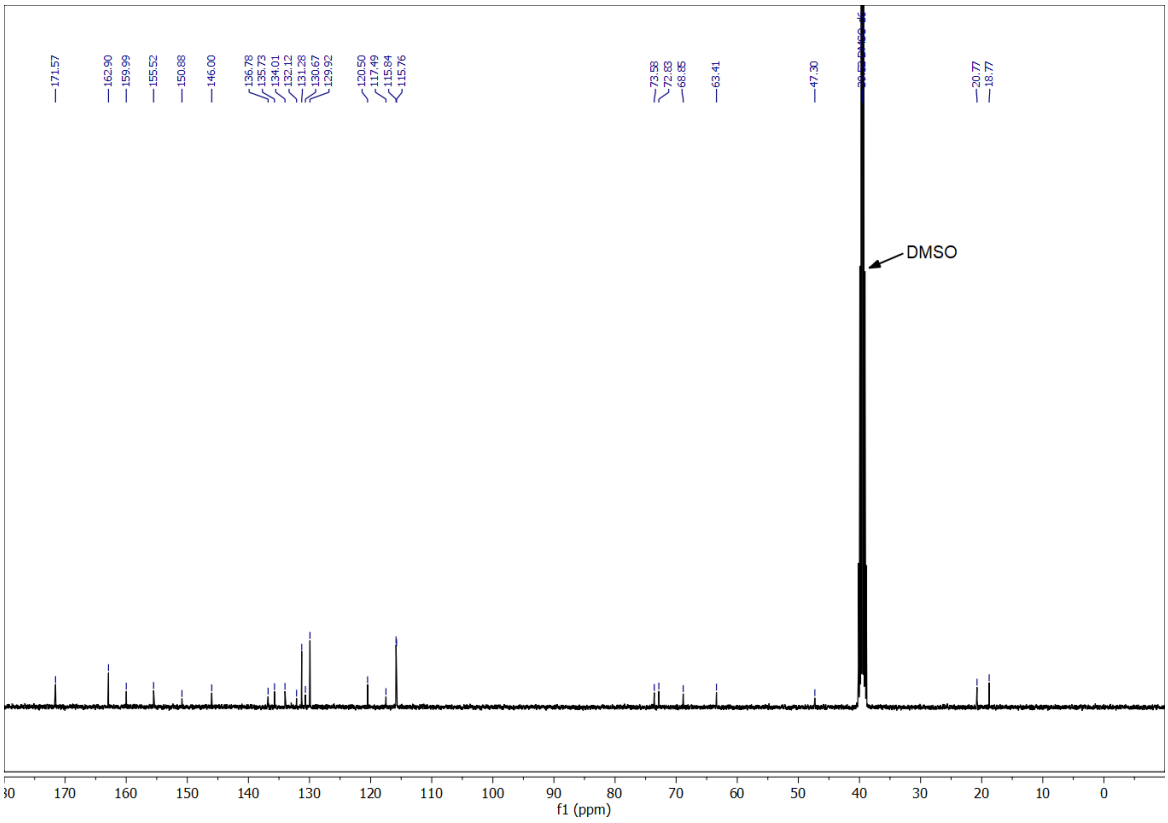

Figure A 28: ^{13}C-NMR spectrum of Na-2-OH-Benz/RF at the molar ratio 2 in DMSO-d_6.

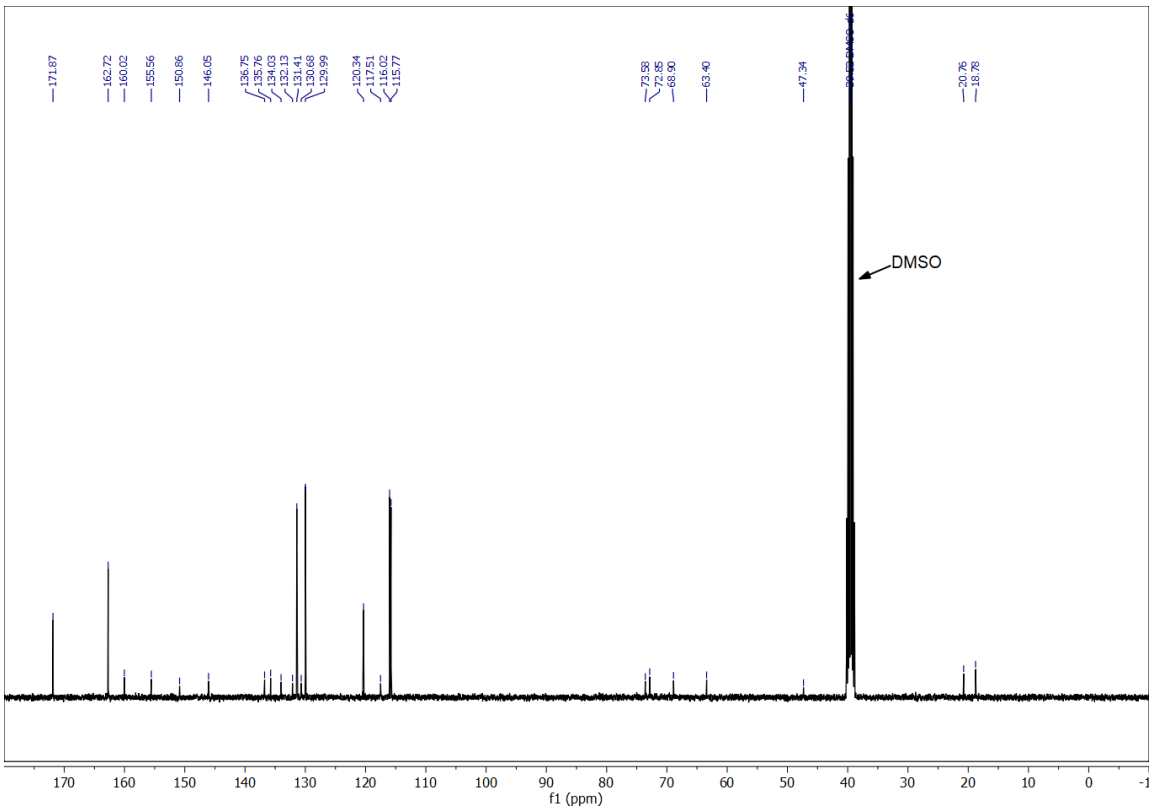

Figure A 29: ^{13}C-NMR spectrum of Na-2-OH-Benz/RF at the molar ratio 5 in DMSO-d_6.

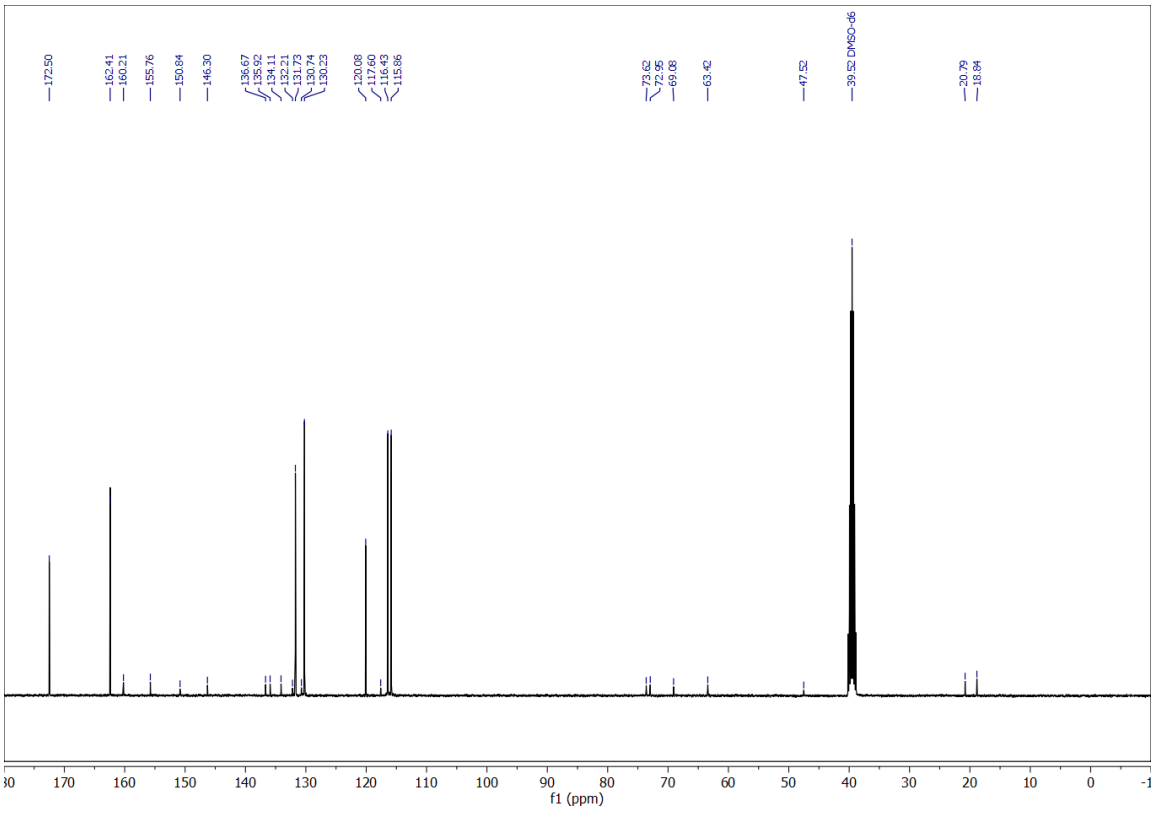

Figure A 30: ^{13}C-NMR spectrum of Na-2-OH-Benz/RF at the molar ratio 10 in DMSO-d_6.

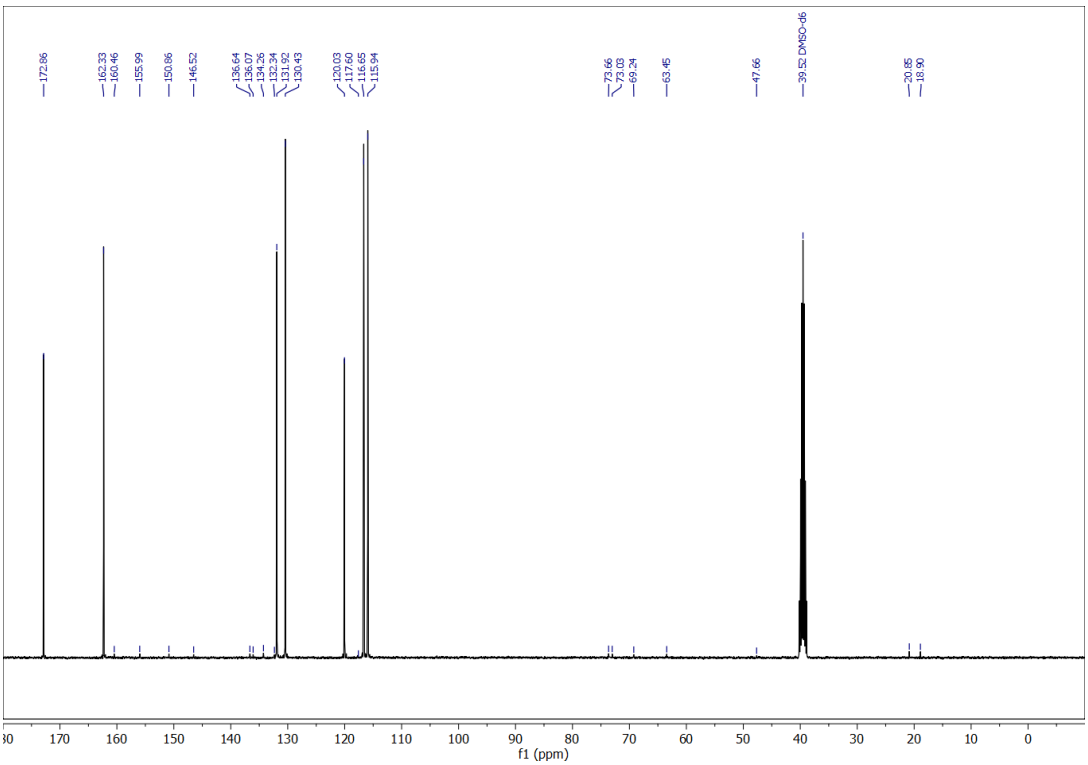

Figure A 31: ^{13}C-NMR spectrum of Na-2-OH-Benz/RF at the molar ratio 50 in DMSO-d_6.

Table A 93: Attribution of ^{13}C-NMR signals of Na-2-OH-Benz in DMSO-d_6 (δ_{exp}) from Figure A 27. The calculated chemical shift was determined with an increment table.[273]

Carbon	δ_{calc} (ppm)	δ_{exp} (ppm)
7	-	173.36
2	157.00	162.31
4	134.9	132.23
6	131.7	130.77
1	120.8	120.06
5	118.3	117.00
3	115.8	116.13

Table A 94: δ_{exp}: Attribution of sodium salicylate carbon atoms to ^{13}C-NMR signals in presence of riboflavin in DMSO-d_6 at the molar ratios of Na-2-OH-Benz/RF = 2, 5, 10 and 50. Δδ: Change of the chemical shift Δδ of Na-2-OH-Benz carbons due to the presence of RF at the different molar ratios relatively to Na-2-OH-Benz in pure DMSO-d_6. The corresponding NMR spectra are displayed in Figure A 28 - Figure A 31. Left = deshielding/shift downfield; Right = shielding/ shift upfield.

	δ_{exp} (ppm)				**Δδ *(ppm)***			
Carbon	**Ratio 2**	**Ratio 5**	**Ratio 10**	**Ratio 50**	**Ratio 50**	**Ratio 10**	**Ratio 5**	**Ratio 2**
7	171.57	171.87	172.50	172.86	Right: 0.50	Right: 0.86	Right: 1.49	Right: 1.79
2	162.90	162.72	162.41	162.33	Left: 0.02	Left: 0.10	Left: 0.41	Left: 0.59
4	131.28	131.41	131.73	131.92	Right:0.31	Right: 0.50	Right: 0.82	Right: 0.95
6	129.92	129.99	130.23	130.43	Right:0.34	Right: 0.54	Right: 0.78	Right: 0.85
1	120.50	120.34	120.08	120.03	Right: 0.03	Left: 0.02	Left: 0.28	Left: 0.44
5	115.84	116.02	116.43	116.65	Right: 0.35	Right: 0.57	Right: 0.98	Right: 1.16
3	115.76	115.77	115.86	115.94	Right: 0.19	Right: 0.27	Right: 0.36	Right: 0.37

Table A 95: Left: Attribution of riboflavin carbon atoms to ^{13}C-NMR signals in presence of sodium salicylate in DMSO-d_6 (δ_{exp}) at the molar ratios of Na-2-OH-Benz/RF = 2, 5, 10 and 50. Right: Change of the chemical shift Δδ of RF carbons due to the presence of Na-2-OH-Benz at different ratios relatively to RF in pure DMSO-d_6 from Figure A 9. The NMR spectra are displayed in Figure A 28 - Figure A 31. Left = deshielding/shift downfield; Right = shielding/ shift upfield.

	δ_{exp} (ppm)				**Δδ *(ppm)***			
Carbon	**Ratio 50**	**Ratio 10**	**Ratio 5**	**Ratio 2**	**Ratio 2**	**Ratio 5**	**Ratio 10**	**Ratio 50**
4	160.46	160.21	160.02	159.99	-	Left: 0.03	Left: 0.22	Left: 0.47
10a	155.99	155.76	155.56	155.52	Left: 0.02	Left: 0.06	Left: 0.26	Left: 0.49
2	150.86	150.84	150.86	150.88	Right: 1.70	Right: 1.72	Right: 1.70	Right: 1.68
5a	146.52	146.30	146.05	146.00	Left: 0.04	Left: 0.09	Left: 0.34	Left: 0.56
4a	136.64	136.67	136.75	136.78	Left: 0.36	Left: 0.33	Left: 0.25	Left:0.22
8	136.07	135.92	135.76	135.73	Left: 0.06	Left: 0.09	Left: 0.25	Left: 0.40
7	134.26	134.11	134.03	134.01	Right: 0.29	Right: 0.27	Right: 0.19	Right: 0.04
9a	132.34	132.21	132.13	132.12	Not determined, carbon of RF not certain			
6	131.28	130.73	130.69	130.67	Left: 0.28	Left: 0.30	Left:0.34	Left: 0.89
9	117.60	117.60	117.51	117.49	Left: 0.27	Left: 0.29	Left: 0.38	Left:0.38
4‘	73.66	73.62	73.58	73.58	Left: 0.29	Left:0.29	Left:0.33	Left: 0.37
3‘	73.03	72.95	72.85	72.83	Left: 0.02	Left 0.04	Left: 0.14	Left: 0.22
2‘	69.24	69.08	68.90	68.85	Left: 0.05	Left: 0.10	Left:0.28	Left:0.44
5‘	63.45	63.42	63.40	63.41	Left: 0.29	Left: 0.28	Left: 0.30	Left: 0.33
1‘	47.66	47.52	47.34	47.30	Left: 0.19	Left: 0.23	Left: 0.41	Left: 0.55
12	20.85	20.79	20.76	20.77	-	< 0.01	Left: 0.03	Left: 0.09
17	18.90	18.84	18.78	18.77	< 0.01	< 0.01	Left: 0.07	Left: 0.13

7.11.5 Riboflavin in presence of sodium 3-hydroxybenzoate in DMSO-d_6

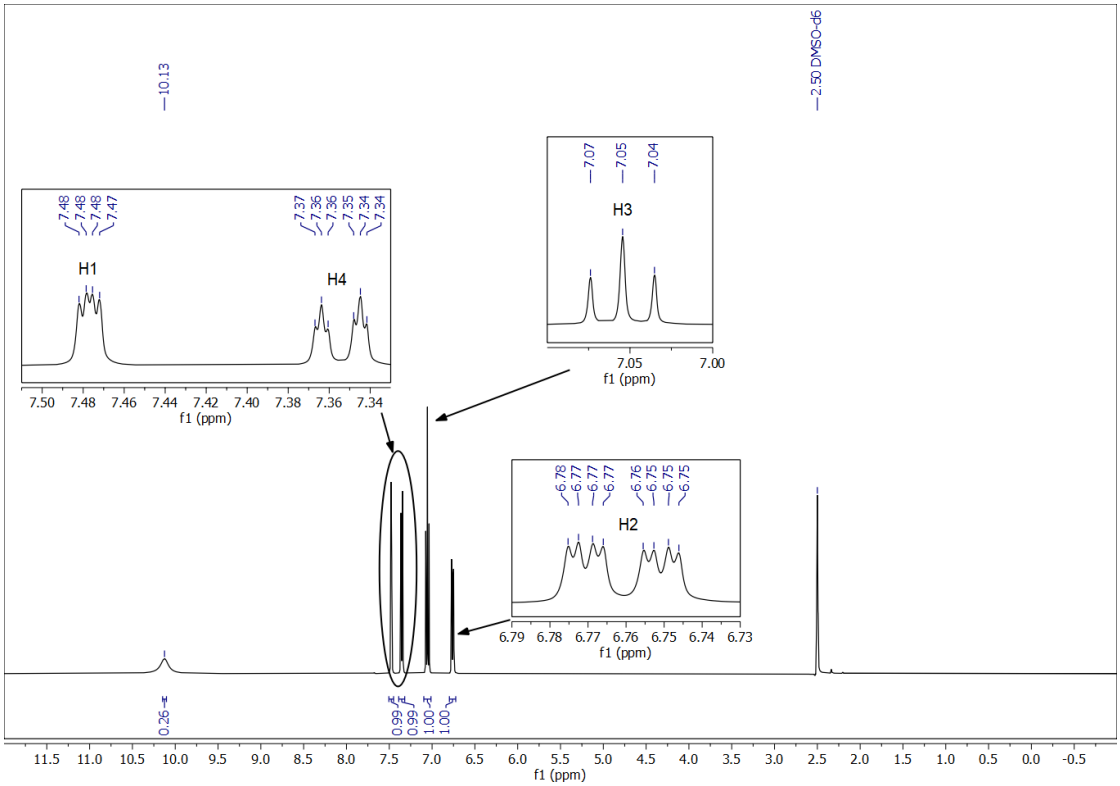

Figure A 32: ^{1}H-NMR spectrum of sodium 3-hydroxybenzoate in DMSO-d_6 (saturation).

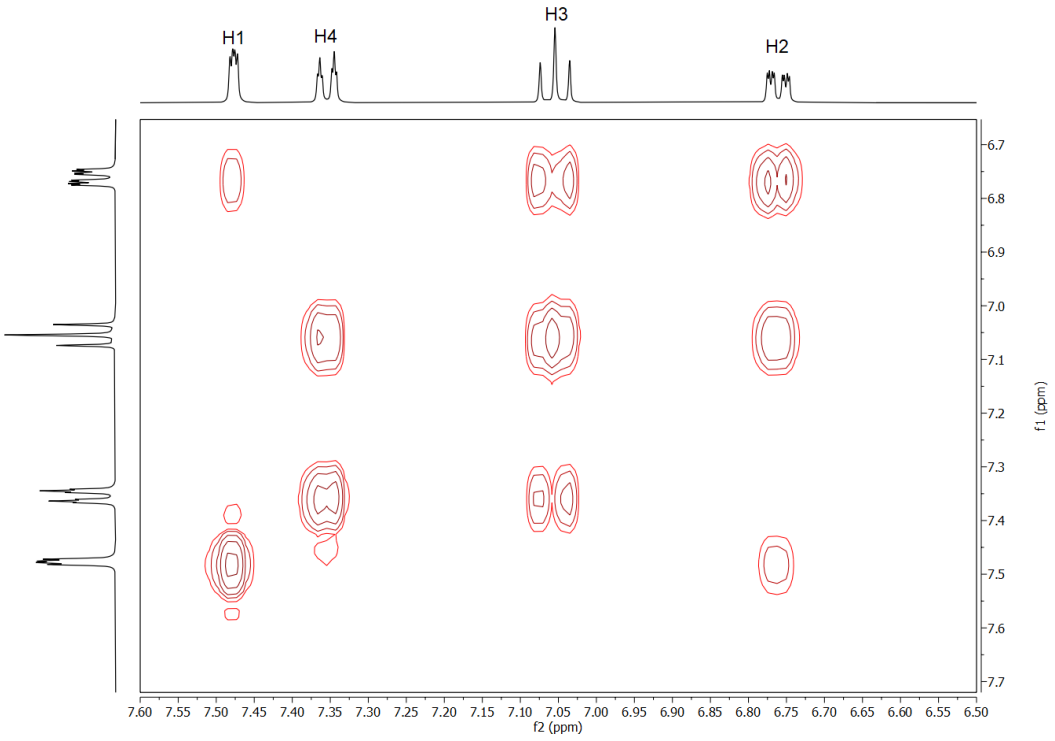

Figure A 33: COSY NMR spectrum sodium 3-hydroxybenzoate in DMSO-d_6 (saturation).

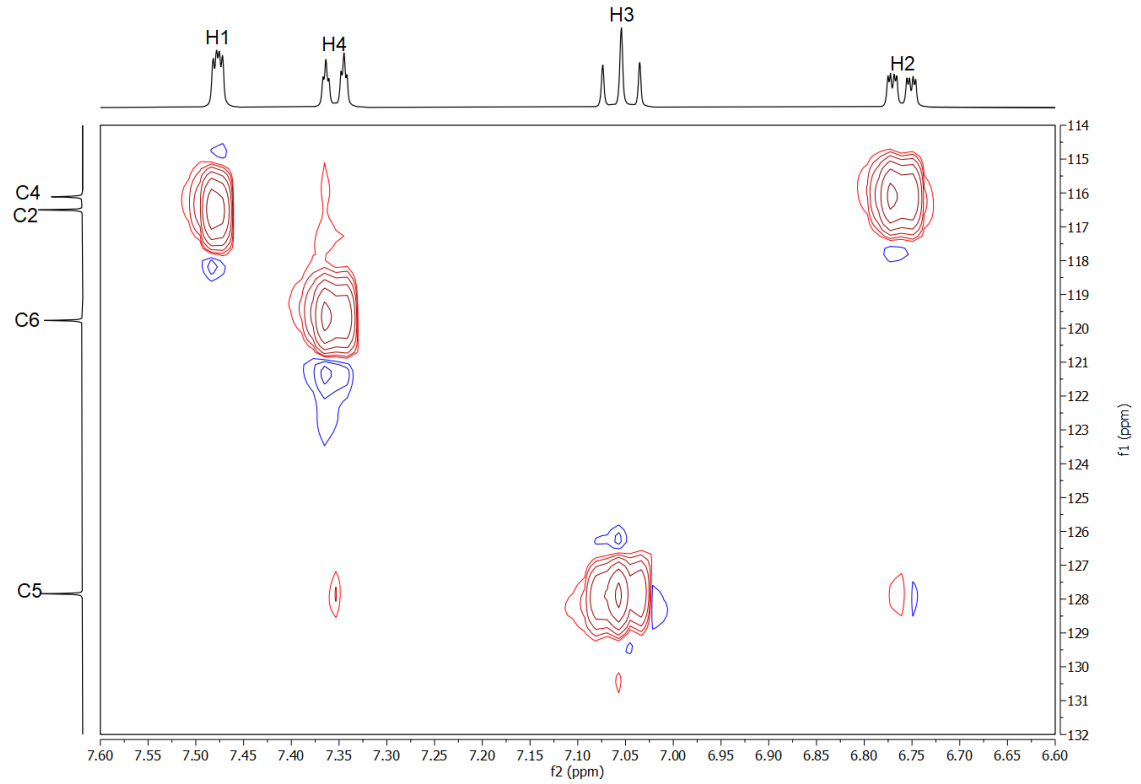

Figure A 34: HSQC NMR spectrum of sodium 3-hydroxybenzoate in DMSO-d_6 (saturation).

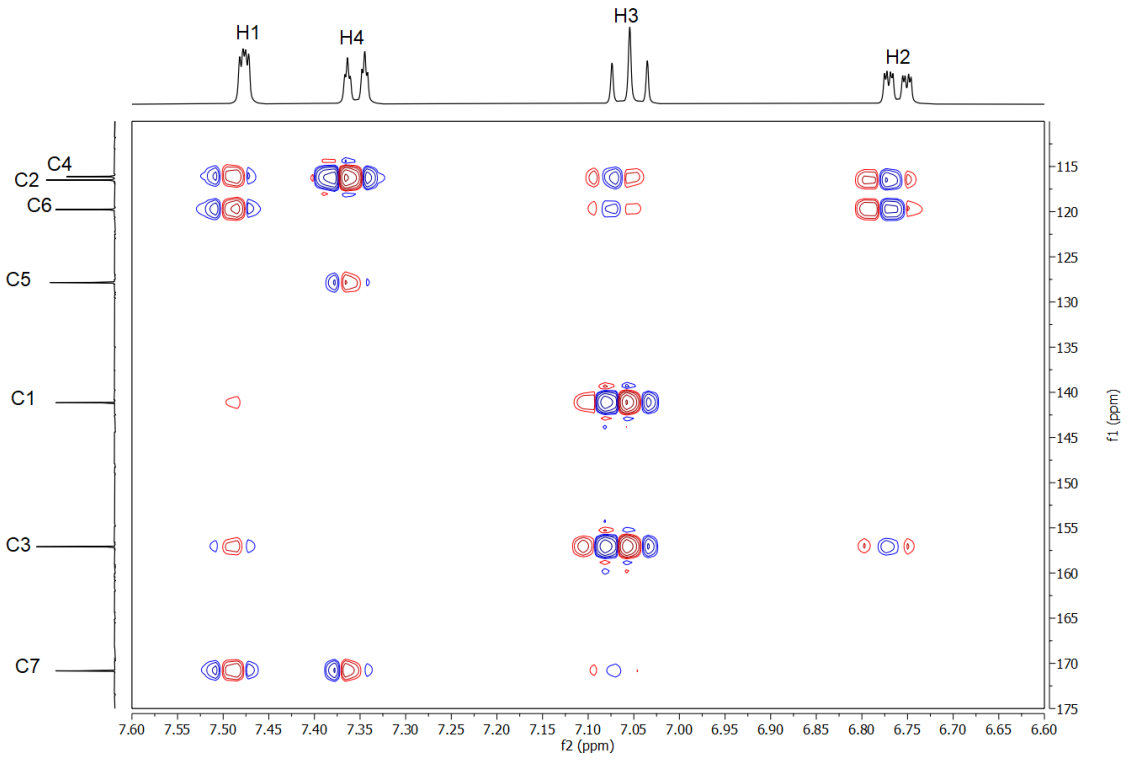

Figure A 35: HMBC NMR spectrum of sodium 3-hydroxybenzoate in DMSO-d_6 (saturation).

Table A 96: Attribution of ^{1}H-NMR signals of sodium 3-hydroxybenzoate in DMSO-d_6 (δ_{exp}) from Figure A 32. The signals were attributed via the splitting, coupling constants, COSY, HSQC and HMBC NMR spectra as well as by comparison with the calculated shift from an increment table.[273] (*) Coupling not visible due to similarity to coupling of H1 and H4. For COSY, HSQC and HMBC spectrum see Figure A 33 - Figure A 35. s = singlet, t = triplet, dd = doublet of doublets; ddd = doublet of doublets of doublets, dt = triplet of doublet.

Proton	δ_{calc} (ppm)	δ_{exp} (ppm)	Splitting	J (Hz)	COSY	HSQC	HMBC
OH	-	10.12	s	-			
1	7.55	7.48	dd	^{4}J(1-4) = 1.26 ^{4}J(1-2) = 2.63	H2	C2	C2/C6/C1/C3/C7
2	6.95	6.76	ddd	^{4}J(2-4) = 1.14 ^{4}J(1-2) = 2.59 ^{3}J(2-3) = 7.87	H3/H1	C4	C2/C6/C3
3	7.32	7.05	t	^{3}J(2-3) = 7.87 ^{3}J(3-4) = 7.61	H2/H4	C5	C3/C1/C2/C4/C7
4	7.66	7.35	dt	^{4}J(1-4) = 1.26 ^{3}J(3-4) = 7.61 ^{4}J(2-4) = *	H3	C6	C2/C5/C7

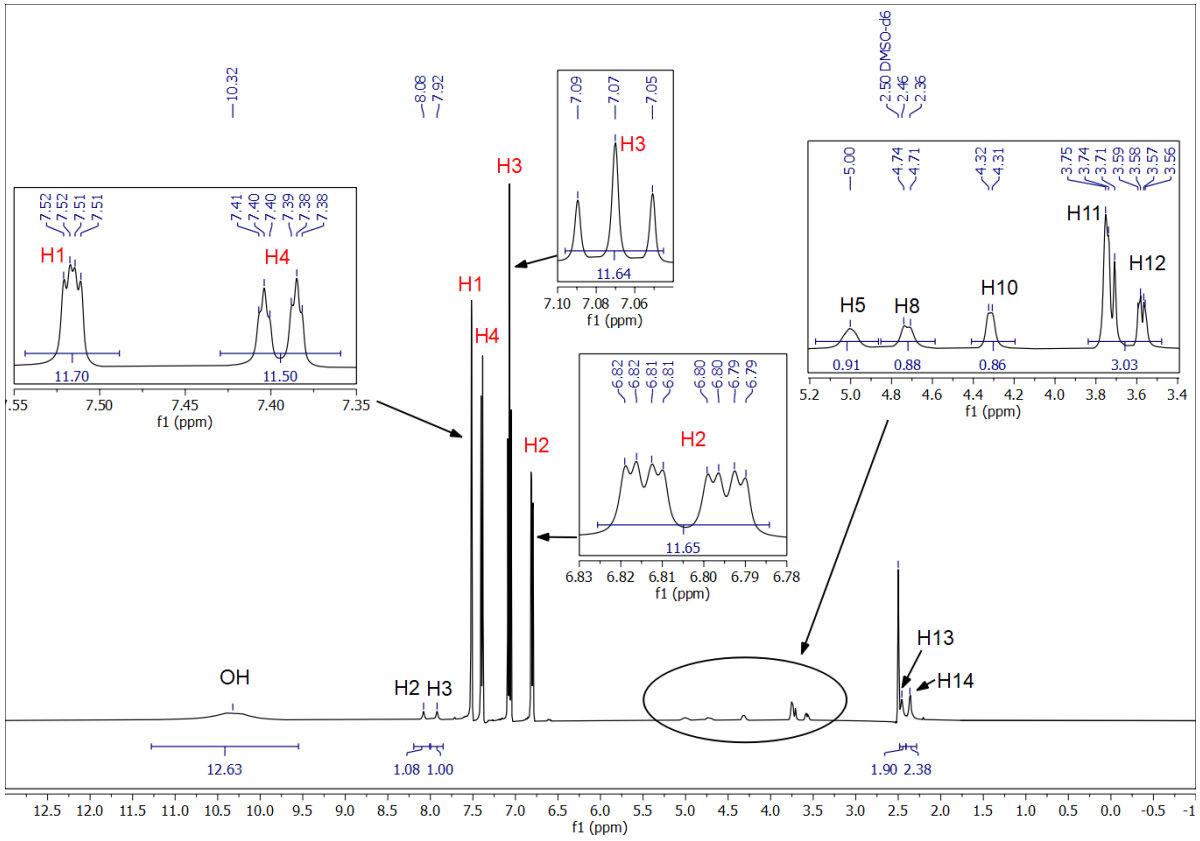

Figure A 36: ^{1}H-NMR spectrum of riboflavin and sodium 3-hydroxy benzoate in DMSO-d_6 at a molar ratio of Na-3-OH-Benz/RF = 11. Red: Protons of Na-3-OH-Benz; Black: Protons of RF.

Table A 97: Attribution of ^{1}H-NMR signals sodium 3-hydroxybenzoate in presence of riboflavin in DMSO-d_6 (δ_{exp}) at a molar ratio of 11 (Figure A 36) and change of the chemical shift Δδ of the protons of Na-3-OH-Benz due to the presence of RF relatively to Na-3-OH-Benz in pure DMSO-d_6 from Table A 96 Left = deshielding/shift downfield.

Proton	δ_{exp} (ppm)	Δδ (ppm)
OH	10.32	Left: 0.20
1	7.52	Left: 0.04
2	6.80	Left: 0.04
3	7.07	Left: 0.02
4	7.39	Left: 0.04

Table A 98: Attribution of ^{1}H-NMR signals riboflavin in the presence of sodium 3-hydroxybenzoate in DMSO-d_6 (δ_{exp}) at a molar ratio of Na-3-OH-Benz/RF = 11 from Figure A 36 and change of the chemical shift Δδ of riboflavin's protons due to the presence of RF relatively to RF in pure DMSO-d_6 from Figure A 8. The splitting and coupling of RF in DMSO-d_6 is given in the rightest two columns. Left = deshielding/shift downfield; Right = shielding/ shift upfield. s = singlet, d = doublet, t = triplet, m = multiplet, vis. = visible.

Proton	δ_{exp} (ppm)	Δδ (ppm)	Splitting	J (Hz)	Splitting pure RF	$J_{pure\ RF}$ (Hz)
1	Not vis.	-	-	-	s	-
2	8.08	Left: 0.18	s	-	s	-
3	7.92	Left: 0.06	s	-	s	-
4 (OH)	Not vis.	-	-	-	d	^{3}J(4-11) = 4.95
5	5.00	Left: 0.08	s	-	t	^{2}J(5-8) = 10.51
6 (OH)	Not vis.	-	-	-	d	^{3}J(6-11) = 4.68
7 (OH)	Not vis.	-	-	-	d	^{3}J(7-10) = 5.84
8	4.72	Left: 0.12	d	^{2}J(8-5) = 10.42	d	^{2}J(8-5) = 13.65
9 (OH)	Not vis.	-	-	-	t	^{2}J(9-11) = 5.68
10	4.32	Left: 0.07	d	^{3}J(10-7) = 5.89	m	m
11	3.73	Left: 0.09	m	-	m	m
12	3.57	Left: 0.09	m	-	m	m
13	2.46	-	-	-	s	-
14	2.36	Right: 0.03		-	s	-

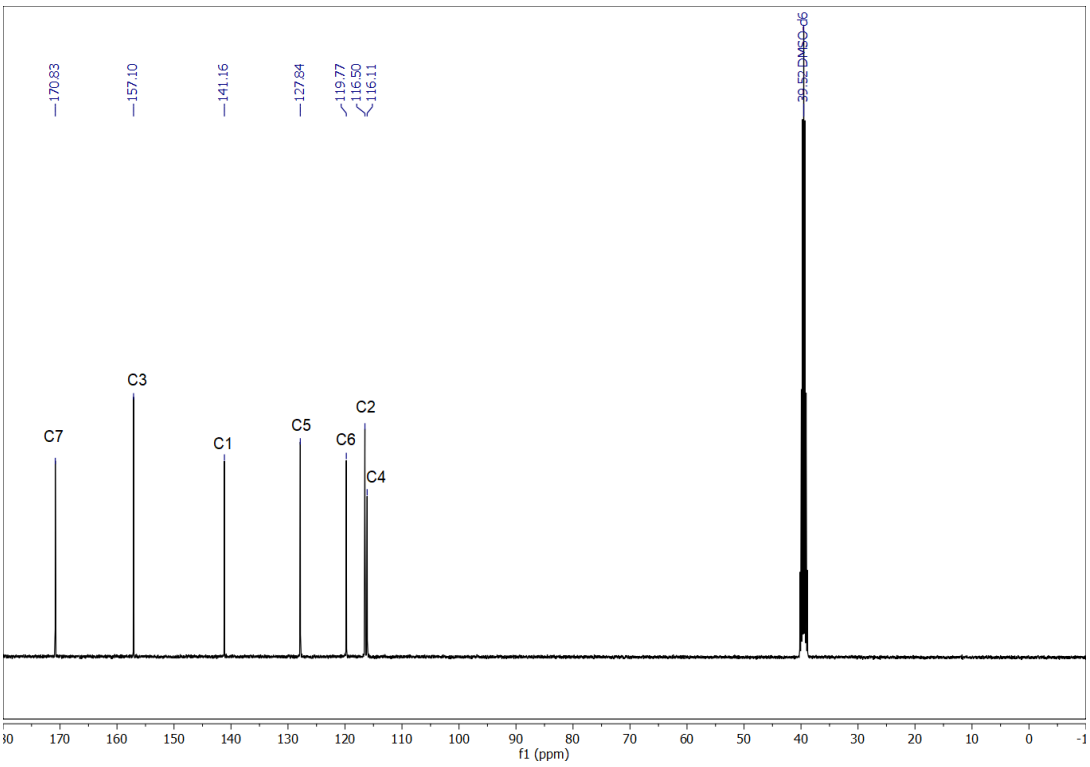

Figure A 37: ^{13}C-NMR spectrum of sodium 3-hydroxybenzoate in DMSO-d_6 (saturation).

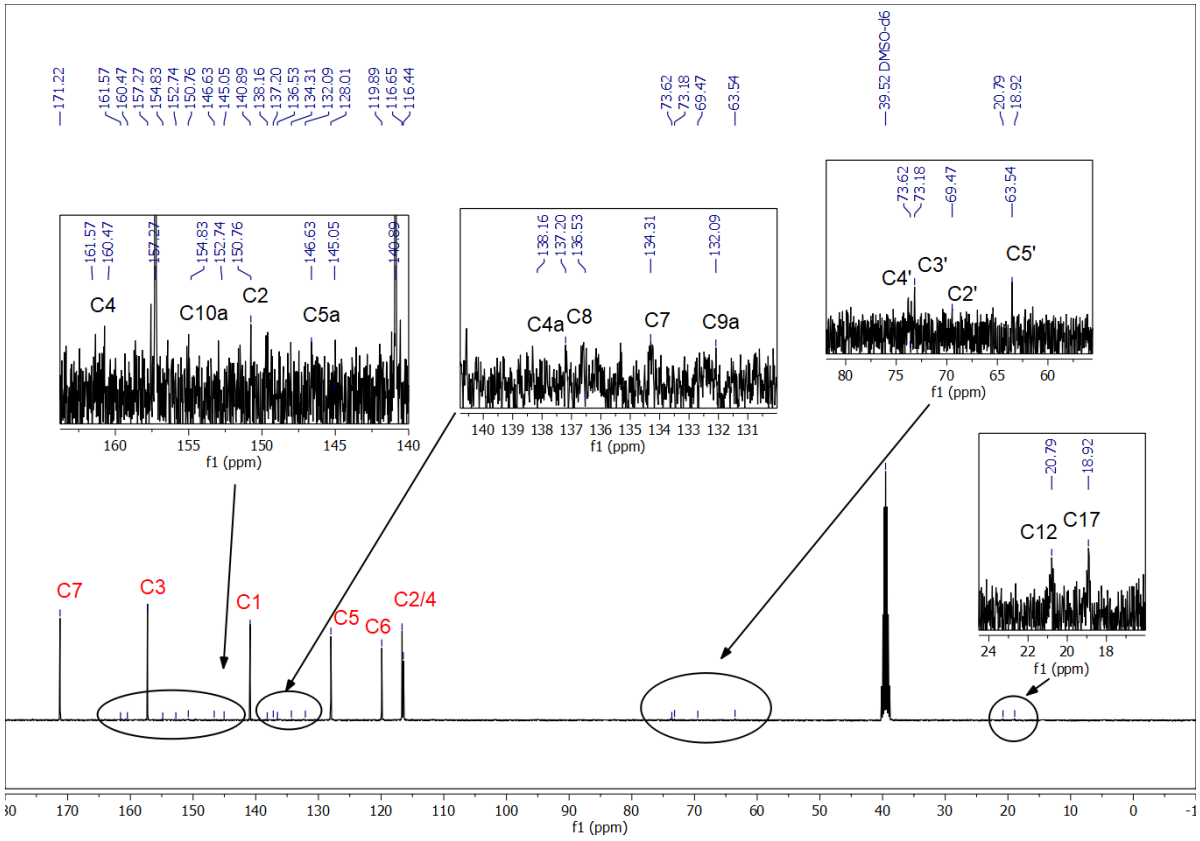

Figure A 38: ^{13}C-NMR spectrum of riboflavin in presence of sodium 3-hydroxybenzoate in DMSO-d_6 at a molar ratio of Na-3-OH-Benz/RF = 11. Red: Carbons of Na-3-OH-Benz; Black: Carbons of RF.

Table A 99: δ_{exp}: Chemical shift of the carbon atoms of sodium 3-hydroxybenzoate in DMSO-d_6 (saturation) from Figure A 37, chemical shift of the carbons of Na-3-OH-Benz in presence of RF in DMSO-d_6 at a molar ratio of Na-3-OH-Benz/RF = 11 from Figure A 38. The carbons were attributed via the HSQC/HMBC spectrum (Figure A 34, Figure A 35) and comparison with the theoretical shift δ_{calc}.[273] $\Delta\delta$: Change of the chemical shift in comparison to Na-3-OH-Benz in pure DMSO-d_6. Left = deshielding/shift downfield; Right = shielding/ shift upfield.

	Na-3-OH-Benz		Na-3-OH-Benz/RF = 11	
Carbon	**δ_{calc} (ppm)**	**δ_{exp} (ppm)**	**δ_{exp} (ppm**	**$\Delta\delta$ (ppm)**
7	-	170.82	171.22	Left: 0.40
3	155.3	157.10	157.27	Left: 0.17
1	132.5	141.16	140.89	Right: 0.27
5	130.0	127.84	128.01	Left: 0.17
6	122.5	119.77	119.89	Left: 0.12
2	117.5	116.50	116.65	Left: 0.15
4	120.7	116.11	116.44	Left: 0.33

*Table A 100: Attribution of ^{13}C-NMR signals of riboflavin in presence of sodium 3-hydroxybenzoate in DMSO-d_6 at a molar ratio of Na-3-OH-Benz/RF = 11 (δ_{exp}) from Figure A 38 and change of the chemical shift $\Delta\delta$ relatively to RF in pure DMSO-d_6 (saturation) from Figure A 9. For some carbons (C4, C2, C5a, C4a) two signals were found, hence two shifts are given. Left = deshielding/shift downfield; Right = shielding/ shift upfield, vis. = visible. *not certain signal in spectrum of pure RF in DSMO-d_6 hardly visible.*

Carbon	**δ_{exp} (ppm)**	**$\Delta\delta$ (ppm)**
4	161.57/160.47	Left: 1.58-0.48
2	150.76/152.74	Right: 1.80, Left: 0.17
10a	154.83	Right: 0.67
5a	146.63/145.50	Right: 0.46, Left: 0.67
4a	138.16/137.20	Left: 1.74-0.78
8	136.53	Left: 0.86
7	134.31	Left: 0.01
9a*	132.09	Right: 1.92
6	Not vis.	Not vis.
9	Not vis.	Not vis.
3‘	73.62	Right: 0.11
4‘	73.18	Left: 0.81
2‘	69.47	Left: 0.67
5‘	63.54	Left: 0.42
1‘	Not vis.	Not vis.
12	20.79	Left: 0.03
17	18.92	Left: 0.15

7.11.6 Riboflavin in presence of sodium 4-hydroxybenzoate in DMSO-d_6

Na-4-OH-Benz in presence of RF led to a distortion of the NMR signals. Only an additive/RF ratio of 2 led to reliable results. The corresponding ^{1}H-NMR spectrum and the attribution of the signals to the protons are given in Figure A 40 and Table A 101.

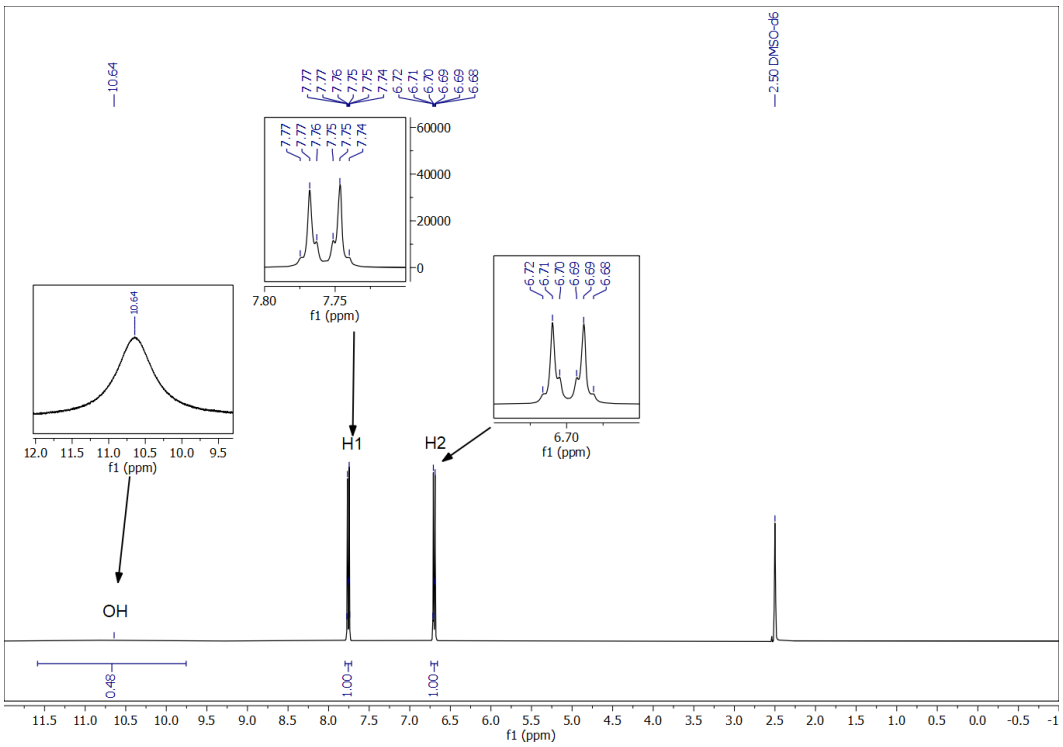

Figure A 39: ^{1}H-NMR spectrum of sodium 4-hydroxybenzoate in DMSO-d_6 (saturation).

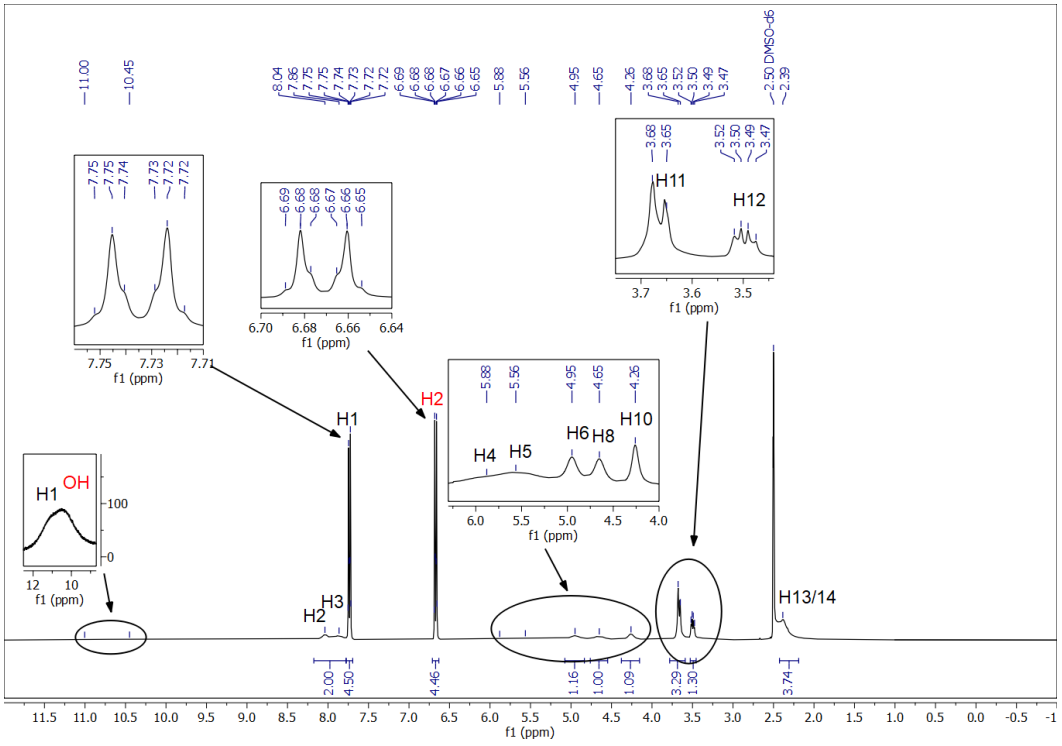

Figure A 40: ^{1}H-NMR spectrum of riboflavin in presence of sodium 4-hydroxybenzoate in DMSO-d_6 at the molar ratio of Na-4-OH-Benz/RF = 2. Red: Protons of Na-4-OH-Benz; Black: Protons of RF.

Table A 101: Attribution of ^{1}H-NMR signals from Figure A 39 to sodium 4-hydroxybenzoate protons in DMSO-d_6 (δ_{exp}) with the help of an increment table (δ_{calc}).[273] Attribution of the signals of Na-4-OH-Benz in presence of riboflavin at a molar ratio of 2 in DMSO-d_6 (δ_{exp}) from Figure A 40. The splitting and coupling constants were equal for Na-4-OH-Benz with and without RF. Δδ: Change of the chemical shift

of Na-4-OH-Benz due to the presence of RF in DMSO-d_6 (*) overlap with signal H1 of RF, see Table A 102. Right = shielding/ shift upfield, s = singlet, d = doublet.

	Na-4-OH-Benz		Na-4-OH-Benz/RF = 2	For pure Na-4-OH-Benz and with RF		
Proton	**δ_{calc} (ppm)**	**δ_{exp} (ppm)**	**δ_{exp} (ppm)**	**Splitting**	**J (Hz)**	**$\Delta\delta$ (ppm)**
OH	-	10.65	10.45*	s	-	Right: 0.20
1	7.99	7.76	7.73	d	^{3}J(1-2) = 8.50 ^{4}J(1-1) = 1.97	Right: 0.03
2	6.88	6.70	6.67	d	^{3}J(1-2) = 8.50 ^{4}J(2-2) = 2.00	Right: 0.03

Table A 102: Attribution of ^{1}H-NMR signals from Figure A 40 to riboflavin's protons (ratio of Na-4-OH-Benz/RF = 2) and change of the chemical shift Δδ of RF protons due to the presence of Na-4-OH-Benz in DMSO-d_6 relatively to RF in pure DMSO-d_6 from the Table A 77 in section 7.11.1 in the Appendix Last column: Splitting of the signals of RF signals in presence of Na-4-OH-Benz. (*) overlap with signal of OH-group of Na-4-OH-Benz, see Table A 101. Left = deshielding/shift downfield; Right = shielding/ shift upfield, vis. = visible, s = singlet; Quotation marks: pseudo-doublet/quartet, due to similar coupling constants.

Proton	**δ_{exp} (ppm)**	**$\Delta\delta$ (ppm)**	**Splitting**
1	11.00*	Right: 0.34	s (broad)
2	8.04	Left: 0.14	s (broad)
3	7.86	-	s (broad)
4 (OH)	5.88	Left: 0.77	s (broad)
5	4.95	Left: 0.03	s (broad)
6 (OH)	5.56	Left: 0.70	s (broad)
7 (OH)	Not vis.	Not vis.	-
8	4.65	Left: 0.05	s (broad)
9 (OH)	Not vis.	Not vis.	-
10	4.26	-	s (broad)
11	3.66	Left: 0.02	„d“
12	3.50	Left: 0.04	„q“
13	Not vis.	Not vis.	-
14	2.39	-	s (broad)

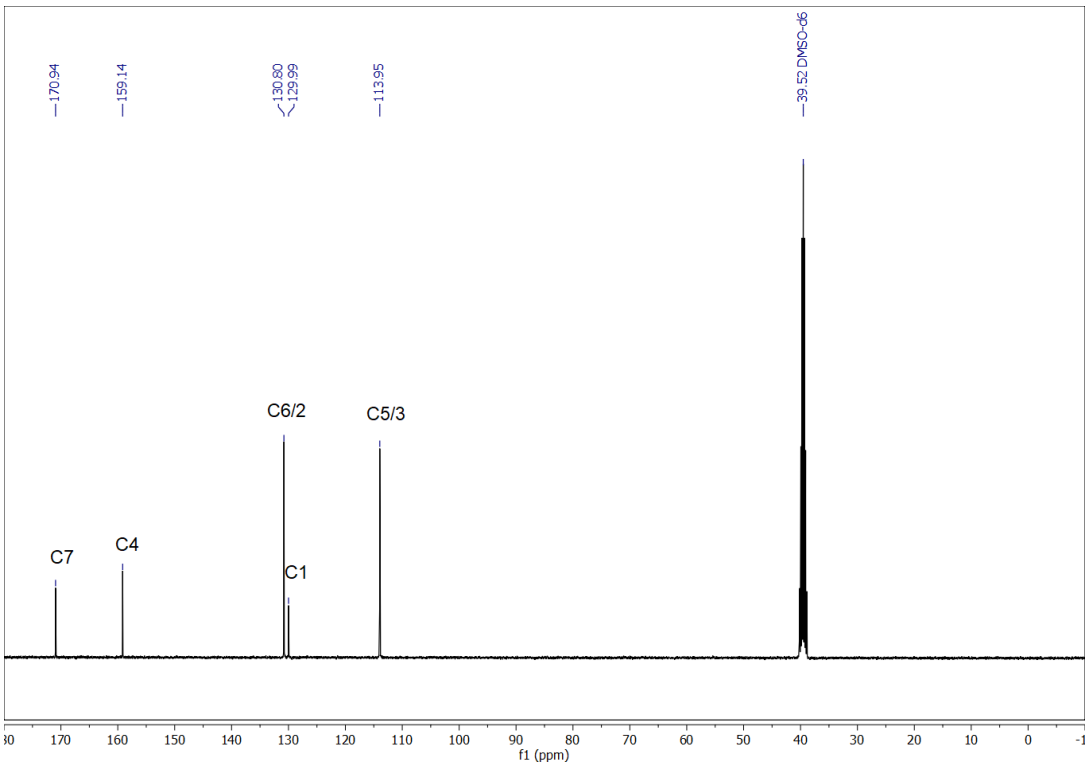

Figure A 41: ^{13}C-NMR of sodium 4-hydroxybenzoate in DMSO-d_6 (saturation).

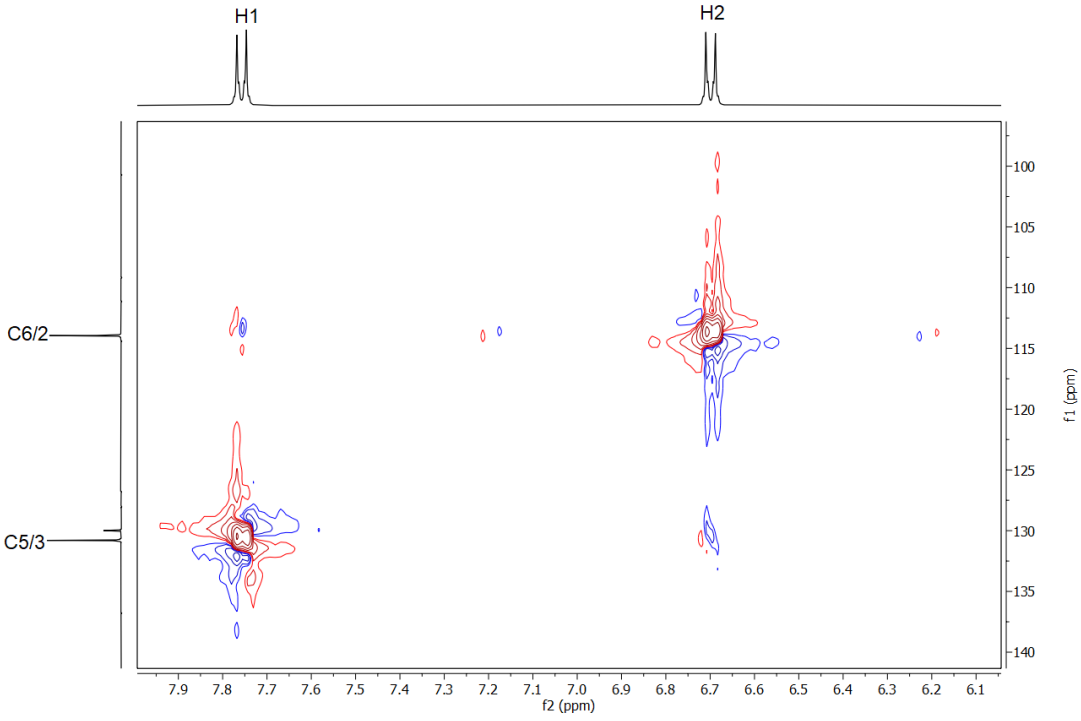

Figure A 42: HSQC spectrum of DMSO-d_6 saturated with Na-4-OH-Benz.

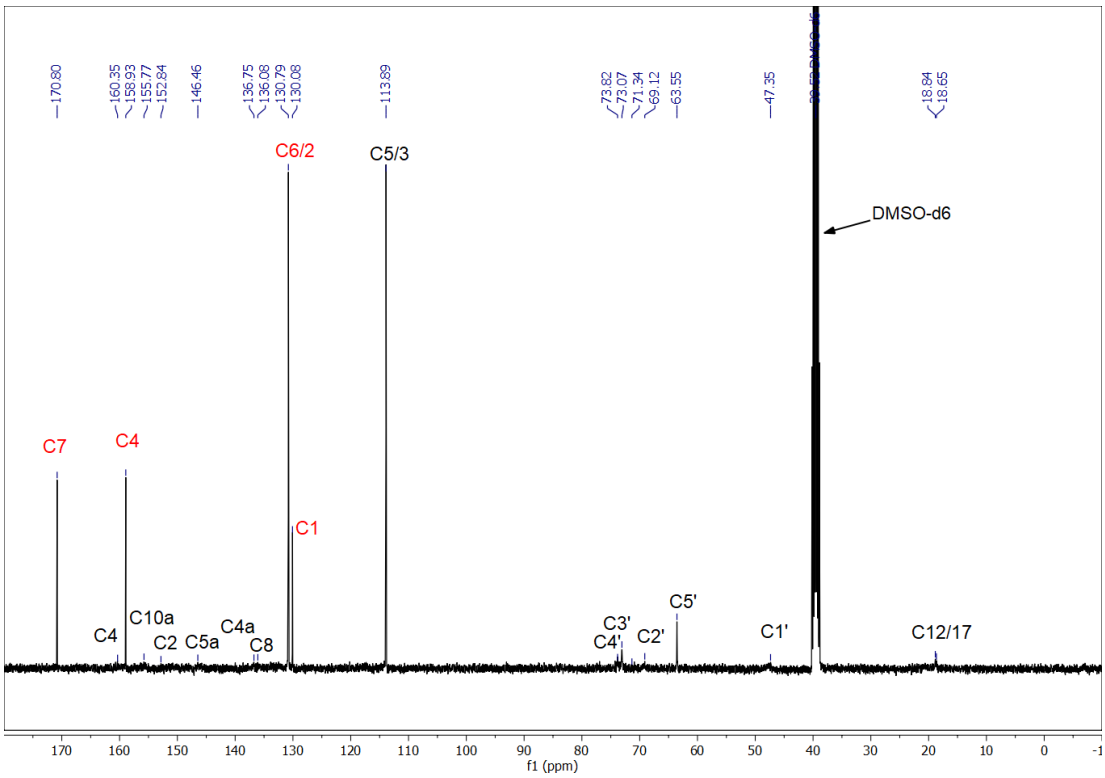

Figure A 43: ^{13}C-NMR of riboflavin in presence of sodium 4-hydroxybenzoate in DMSO-d_6 at a molar ratio of Na-4-OH-Benz/RF = 2. Red: Carbons of Na-4-OH-Benz; Black: Carbons of RF.

Table A 103: δ_{exp}: Chemical shift of sodium 4-hydroxybenzoate in DMSO-d_6 from Figure A 41, chemical shift of the protons of Na-4-OH-Benz in presence of riboflavin in DMSO-d_6 at a molar ratio of Na-4-OH-Benz/RF of 2 from Figure A 43.For the attribution of Na-4-OH-Benz carbons of Na-4-OH-Benz in DMSO-d_6, the HSQC spectrum (Figure A 42) and the theoretical shift δ_{calc} were used.[273] $\Delta\delta$: Change of the chemical shift of Na-4-OH-Benz carbons in presence of RF relatively to Na-4-OH-Benz in pure DMSO-d_6. Left = deshielding/shift downfield; Right = shielding/ shift upfield.

	Na-4-OH-Benz			**Na 4-OH-Benz/RF = 2**	
Carbon	**δ_{calc} (ppm)**	**δ_{exp} (ppm)**	**HSQC**	**δ_{exp} (ppm)**	**$\Delta\delta$ (ppm)**
7	-	170.94		170.80	Right: 0.14
1	123.3	129.99		130.08	Left: 0.09
5/3	115.8	113.95	H2	113.89	Right: 0.06
6/2	131.7	130.80	H1	130.79	-
4	160.2	159.14		158.93	Right:0.21

Table A 104: Chemical shift δ_{exp} of the carbon atoms of riboflavin in presence of sodium 4-hydroxybenzoate in DMSO-d_6 from Figure A 43 and change of the chemical shift $\Delta\delta$ at a molar ratio of Na-4-OH-Benz/RF = 2 compared to RF in pure DMSO-d_6 from Figure A 9. Left = deshielding/shift downfield; Right = shielding/ shift upfield. (*) overlap of C6 of RF with C6/2 or C1 of Na-4-OH-Benz, see Table A 103.

Carbon	δ_{exp} (ppm)	$\Delta\delta$ (ppm)	Carbon	δ_{exp} (ppm)	$\Delta\delta$ (ppm)
4	160.35	Left: 0.36	**9**	Not vis.	-
10a	152.84	Left: 0.27	**4‘**	73.82	Left: 0.53
2	155.77	Left: 0.27	**3‘**	73.07	Left:0.26
5a	(146.46)	Left: 0.50	**2‘**	69.12	Left: 0.32
4a	(136.75)	Left: 0.33	**5‘**	63.55	Left: 0.43
8	(136.07)	Left: 0.40	**1‘**	47.35	Left: 0.24
7	Not vis.	-	**12/17**	18.84	Right: 1.92
9a	Not vis.	-	**17 /12**	18.65	Right: 0.12
6	*	-			

7.11.7 Riboflavin in presence of sodium vanillate in DMSO-d_6

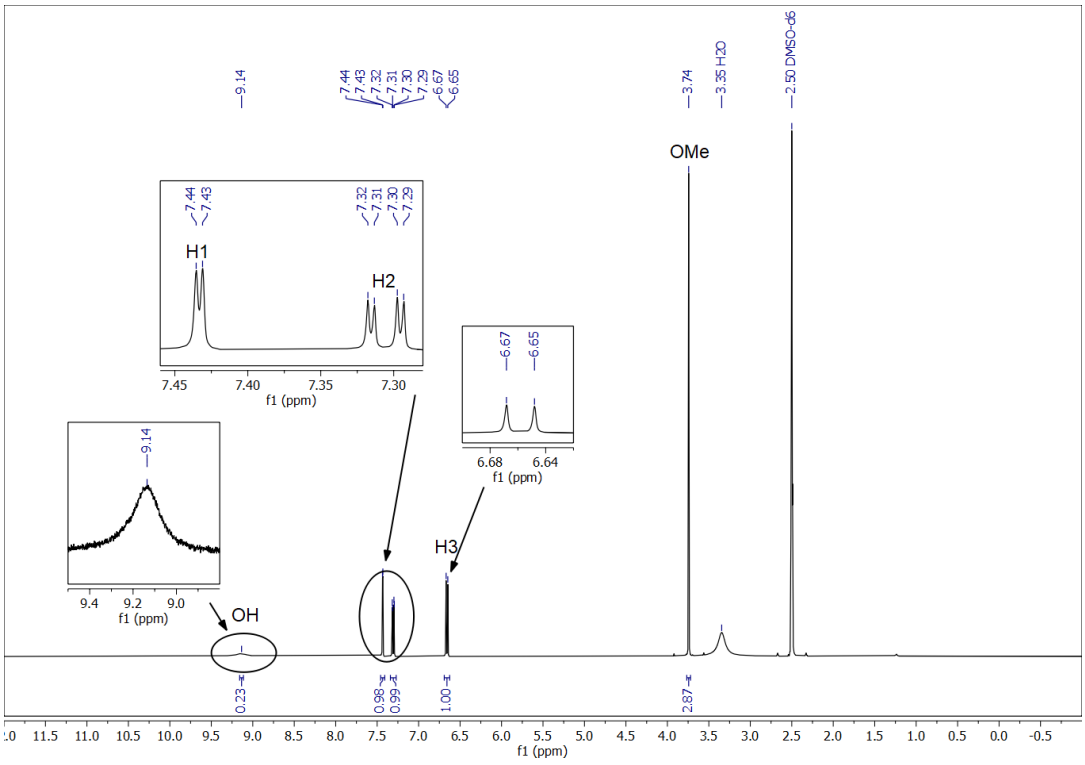

Figure A 44: ^{1}H-NMR spectrum of sodium vanillate in DMSO-d_6 (saturation).

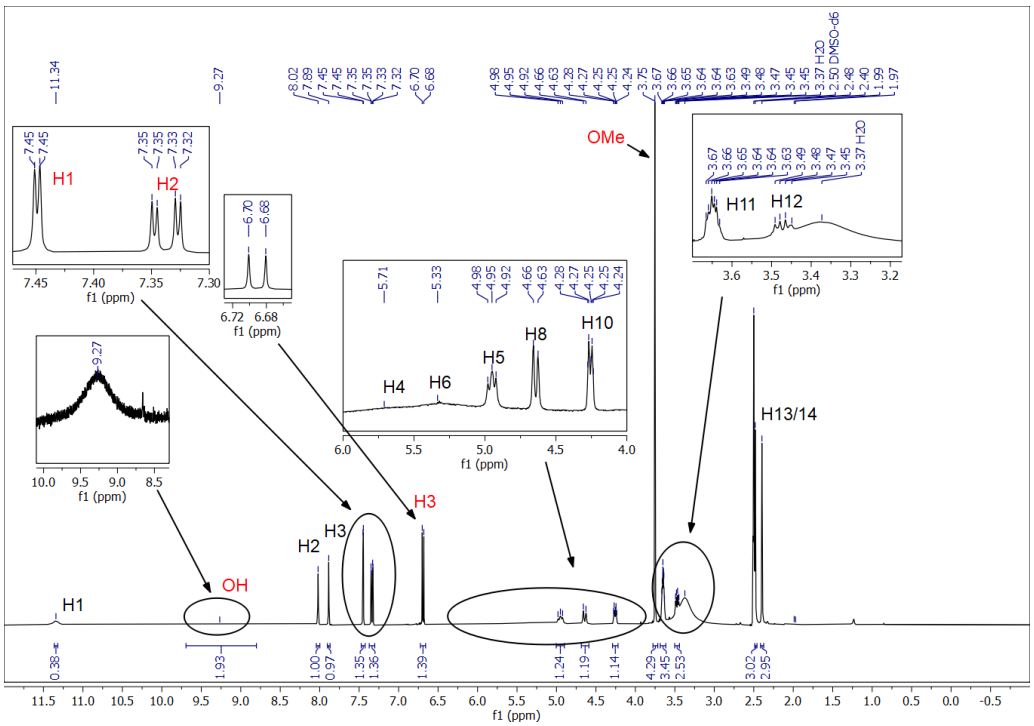

Figure A 45: ^{1}H-NMR spectrum of sodium vanillate and riboflavin in DMSO-d_6 (saturation) at a molar ratio of Na-4-OH-3-OMe-Benz/RF = 1.3. Red: Protons of sodium vanillate; Black: Protons of riboflavin.

Table A 105: δ_{exp}: Chemical shift of the protons of sodium vanillate in DMSO-d_6 from Figure A 44 with the corresponding coupling constant, chemical shift of the protons of sodium vanillate in DMSO-d_6 at a molar ratio of sodium vanillate/riboflavin = 1.3 from Figure A 45 with the corresponding coupling constants. The protons were attributed via the calculated chemical shift δ_{calc}. Splitting referring to both pure sodium vanillate and in presence of riboflavin, as the splitting was equal for both. Δδ: Change of the chemical shift of sodium vanillate protons due to the presence of RF relative to sodium vanillate in pure DMSO-d_6. Left = deshielding/shift downfield, s = singlet, d = doublet, dd = doublet of doublets.

	vanillate			vanillate/RF = 1.3			
Proton	**δ_{calc} (ppm)**	**δ_{exp} (ppm)**	**J (Hz)**	**δ_{exp} (ppm)**	**J (Hz)**	**Splitting**	**Δδ (ppm)**
OH	-	9.13	-	9.27	-	s	Left: 0.14
OMe	-	3.74	-	3.75	-	s	Left: 0.01
1	8.61	7.43	^{4}J(1-2) = 1.72	7.45	^{3}J(1-2) = 1.8	d	Left: 0.02
2	8.2	7.31	^{4}J(1-2) = 1.72 ^{3}J(2-3) = 8.12	7.34	^{3}J(1-2) = 1.8 ^{3}J(2-3) = 8.14	dd	Left: 0.03
3	7.02	6.66	^{3}J(2-3) = 8.12	6.69	^{3}J(2-3) = 8.14	d	Left: 0.03

Table A 106: δ_{exp}: Chemical shift of the protons of riboflavin in presence of sodium vanillate at a molar ratio of sodium vanillate/RF of 1.3 with the corresponding splitting and coupling from Figure A 45.$\Delta\delta$: Change of the chemical shift of RF protons in presence of vanillate in comparison to RF in pure DMSO-d_6 from Figure A 8. Left = deshielding/shift downfield, s = singlet, d = doublet, t =triplet, dd = doublet of doublet, m = multiplet, vis. = visible.

Proton	δ_{exp} (ppm)	Splitting	J (Hz)	$\Delta\delta$ (ppm)
1	11.34	s (broad)	-	-
2	8.02	s	-	Left: 0.12
3	7.89	s	-	Left: 0.03
4 (OH)	5.71	s (broad)	-	Left: 0.60
5	4.95	t	^{2}J(5-8) = 12.17	Left: 0.03
6 (OH)	5.33	s (broad)	-	Left: 0.47
7 (OH)	Not vis.	s (broad)	-	-
8	4.64	d	^{2}J(8-5) = 12.17	Left: 0.04
9 (OH)	Not vis.	-	-	-
10	4.26	dd	^{3}J(10-7) = 9.47, ^{3}J(10-5/8) = 3.09	-
11	3.65	m (but different)	-	-
12	3.47	m (but different)	-	-
13	2.48	s	-	-
14	2.40	s	-	-

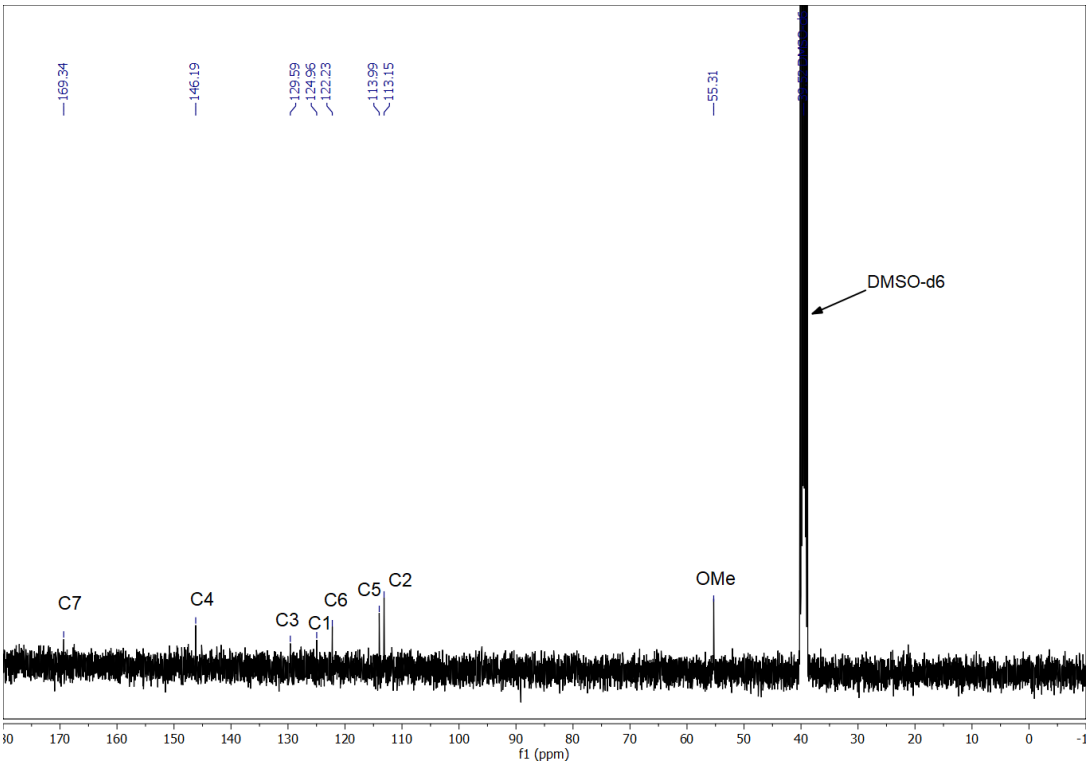

Figure A 46: ^{13}C-NMR spectrum of sodium vanillate in DMSO-d_6 (saturation).

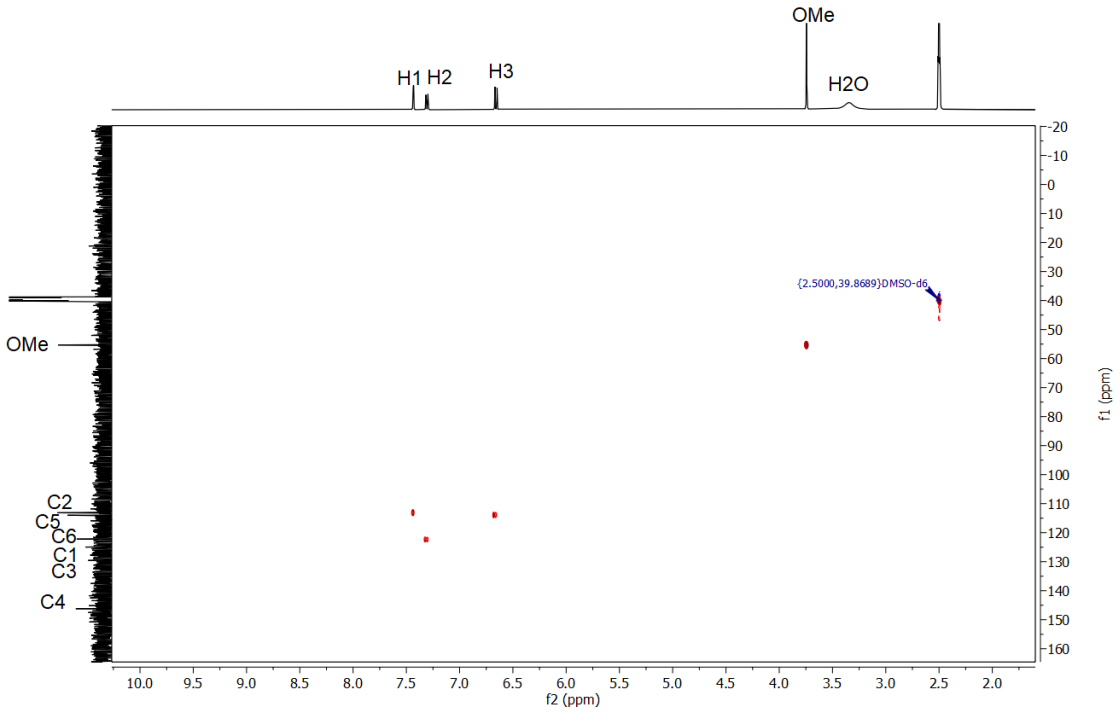

Figure A 47: HSQC NMR spectrum sodium vanillate in DMSO-d_6 (saturation). For the cross-peaks see Table A 107.

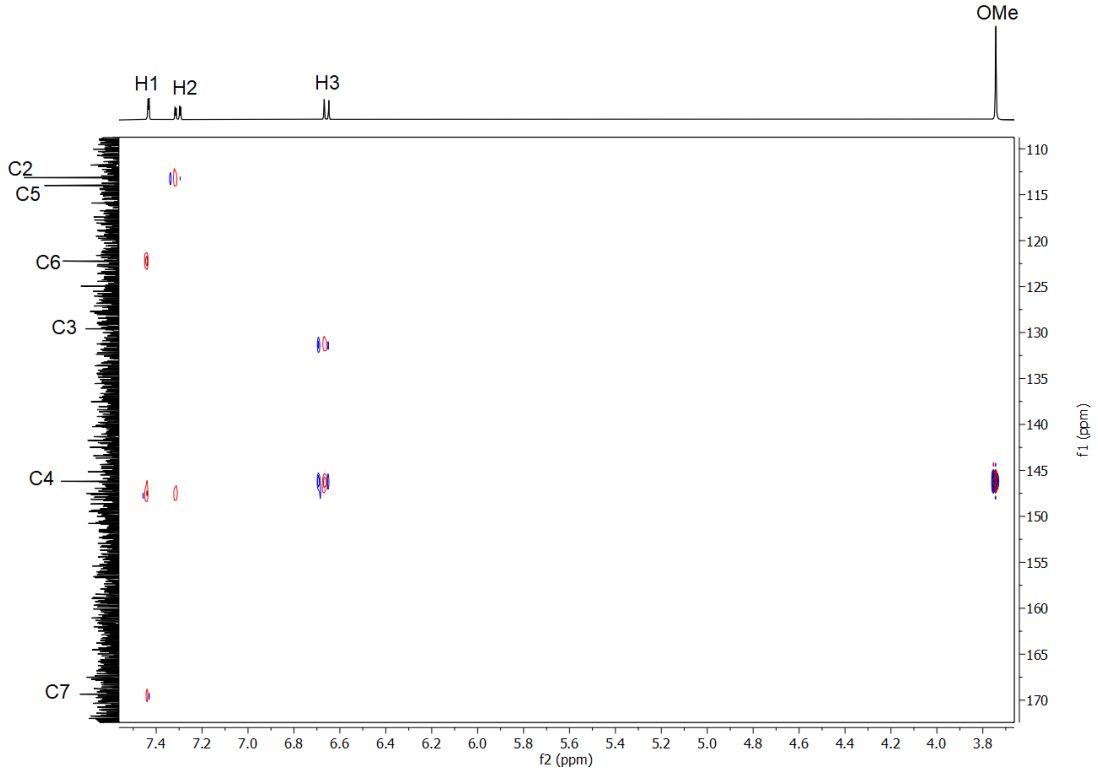

Figure A 48: HMBC NMR spectrum of sodium vanillate in DMSO-d_6 (saturation). For the cross peaks see Table A 107.

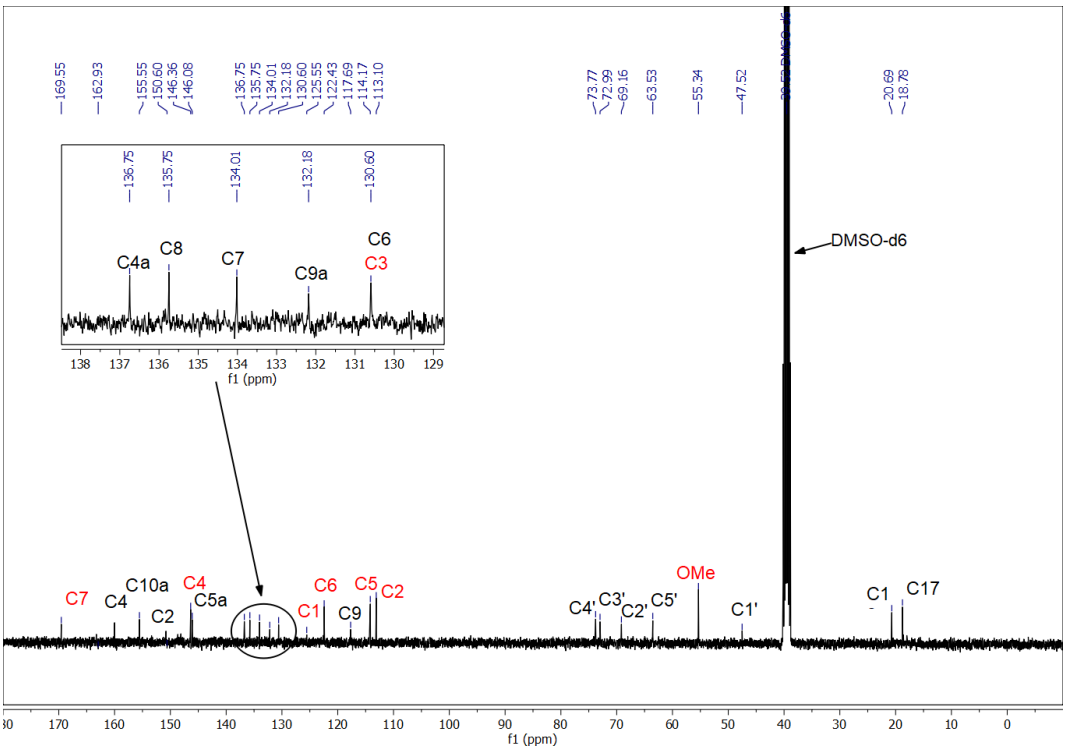

Figure A 49: ^{13}C-NMR spectrum of sodium vanillate and riboflavin in DMSO-d_6 (saturation) at a molar ratio of Na-4-OH-3-OMe-Benz/RF = 1.3. Red: Carbons of sodium vanillate; Black: Carbons of riboflavin.

Table A 107: δ_{exp}: Chemical shift of the carbon atoms of sodium vanillate in DMSO-d_6 from Figure A 46, chemical shift the carbon atoms of sodium vanillate in DMSO-d_6 in presence of riboflavin at a molar ratio of 1.3 from Figure A 49. Δδ: Change of the chemical shift of the carbons of sodium vanillate due to the presence of RF. The carbon atoms were attributed via cross peaks in the HSQC and HMBC NMR spectrum (Figure A 47, Figure A 48) and with the help of a theoretical shift δ_{calc}.[273]

	sodium vanillate				vanillate/RF = 1.3	
Carbon	**δ_{calc} (ppm)**	**δ_{exp} (ppm)**	**HMBC**	**HSQC**	**δ_{exp} (ppm)**	**$\Delta\delta$ (ppm)**
7	-	169.34	H1, H2	-	169.55	Left: 0.21
4	159.8	146.19	H1, H2, H3, OMe	-	146.36	Left: 0.17
6	135.9	122.23	H1	H2	122.43	Left: 0.20
3	125.1	129.59	H3	-	130.60	Right: 1.01
1	123.5	124.96	-	-	125.55	Left: 0.59
5	116.0	113.99	H2	H3	114.17	Left: 0.18
2	131.9	113.15	H2	H1	113.10	Right: 0.05
OMe	-	55.31	OMe	OMe	55.34	Left: 0.02

Table A 108: δ_{exp}: Chemical shift of the carbon atoms of riboflavin in presence of sodium vanillate in DMSO-d_6 from Figure A 49 at a molar ratio of vanillate/RF = 1.3. Δδ: Change of the chemical shift Δδ at a molar ratio of vanillate/RF = 1.3 compared to RF in pure DMSO-d_6 from Figure A 9. Left = deshielding/shift downfield; Right = shielding/ shift upfield.

Carbon	δ_{exp} (ppm)	Δδ (ppm)	Carbon	δ_{exp} (ppm)	Δδ (ppm)
4	162.93	Left: 2.94	**9**	117.69	Left: 0.47
10a	155.55	Left: 0.05	**4‘**	73.78	Left: 0.49
2	150.60	Right: 1.97	**3‘**	72.99	Left: 0.18
5a	146.07	Left 0.11	**2‘**	69.16	Left: 0.36
4a	136.75	Left: 0.33	**5‘**	63.53	Left: 0.41
8	135.75	Left: 0.08	**1‘**	47.52	Left: 0.41
7	134.01	Right: 0.29	**12/17**	20.69	Right:0.07
9a	132.18	Right: 1.83	**17/12**	18.78	-
6	130.60	Left: 0.21			

7.11.8 Riboflavin in presence of sodium cinnamate in DMSO-d_6

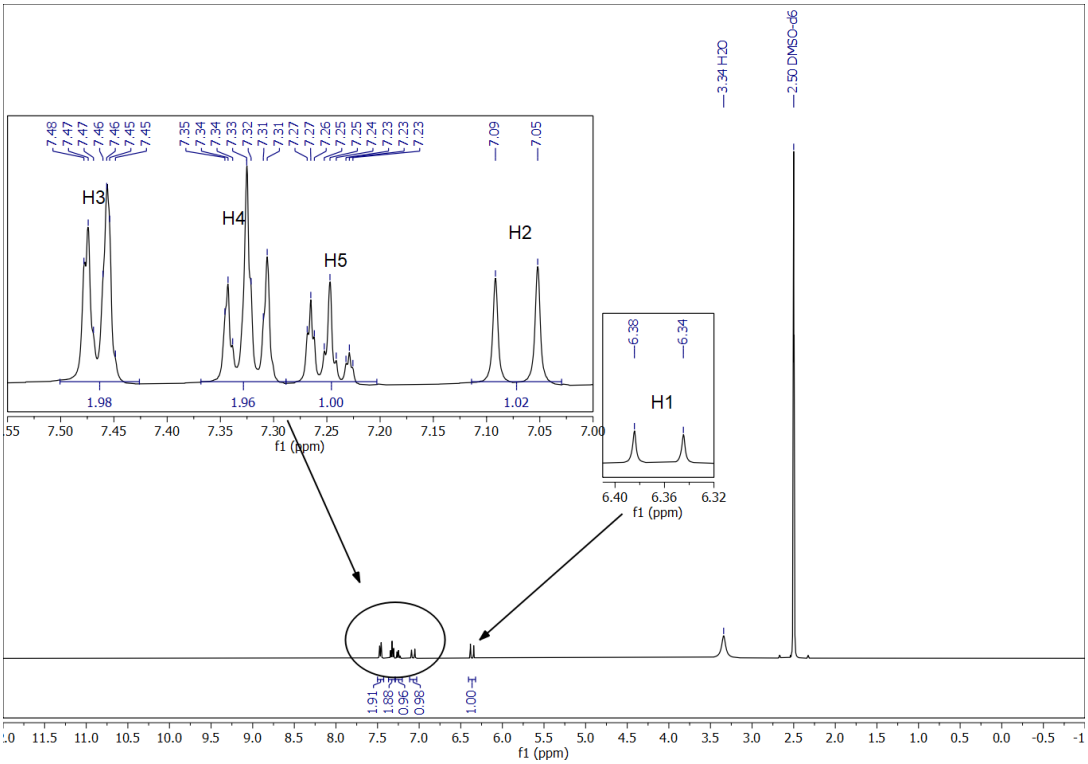

Figure A 50: ^{1}H-NMR spectrum of sodium cinnamate in DMSO-d_6 (saturation).

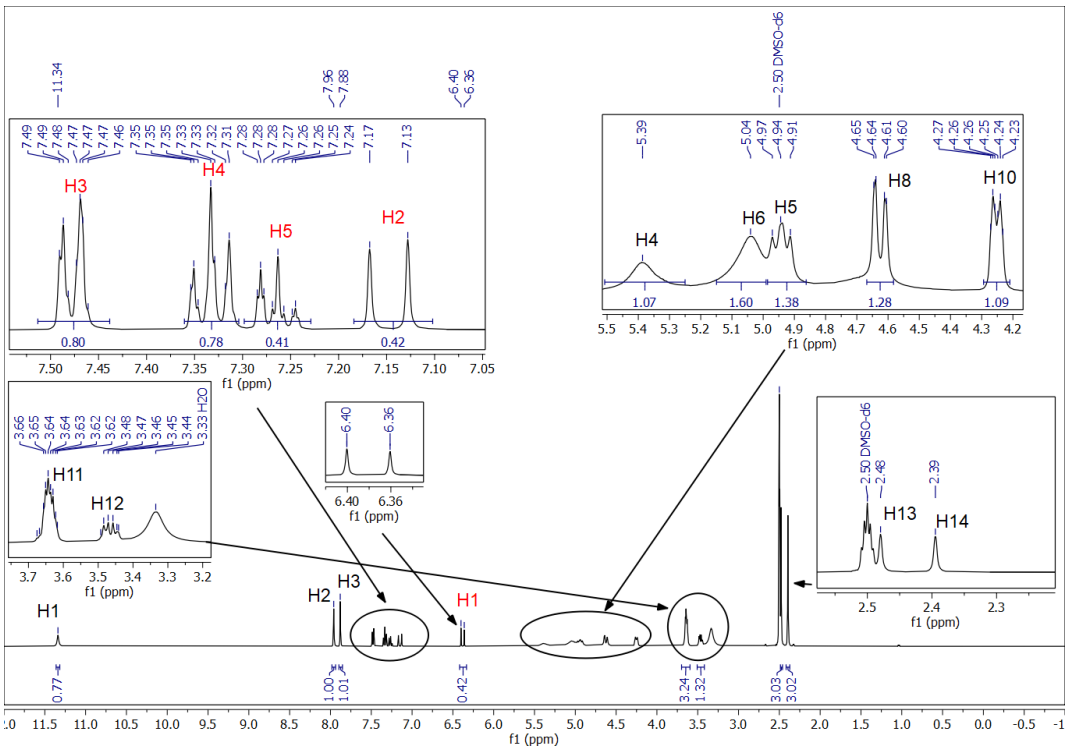

Figure A 51: ^{1}H-NMR spectrum of riboflavin and sodium cinnamate in DMSO-d_6 at a molar ratio of NaCinn/RF = 0.4. Red: Protons of NaCinn; Black: Protons of RF.

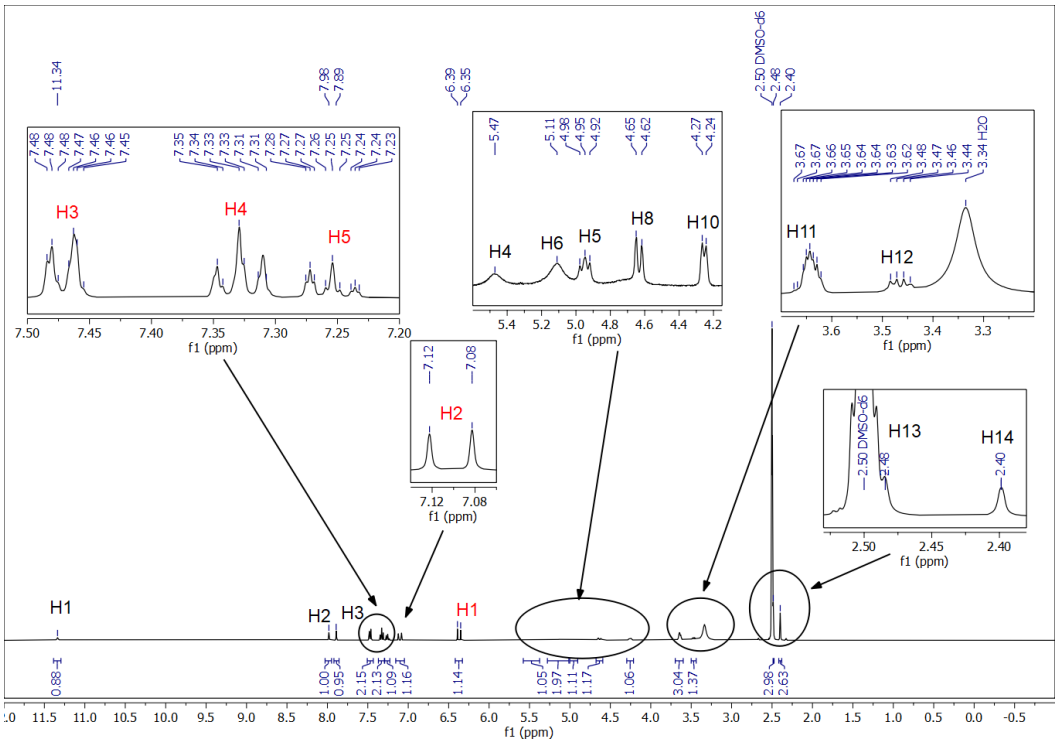

Figure A 52: ^{1}H-NMR spectrum of riboflavin and sodium cinnamate in DMSO-d_6 at a molar ratio of NaCinn/RF = 1. Red: Protons of NaCinn; Black: Protons of RF.

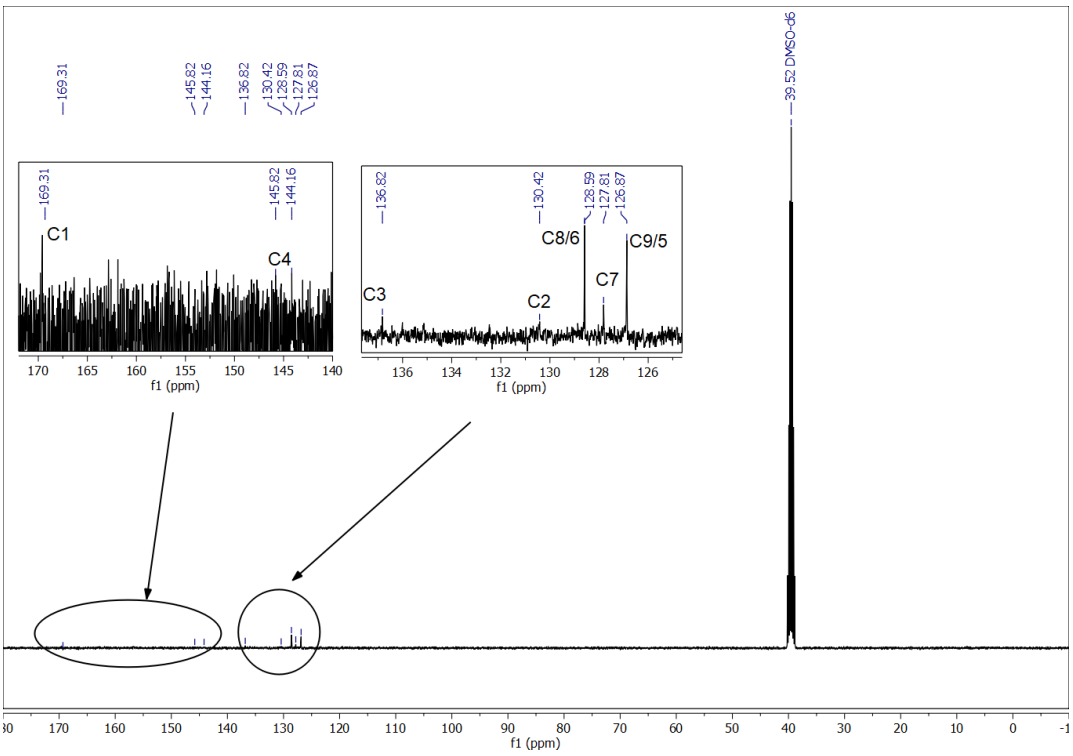

Figure A 53: ^{13}C-NMR spectrum of sodium cinnamate in DMSO-d_6 (saturation).

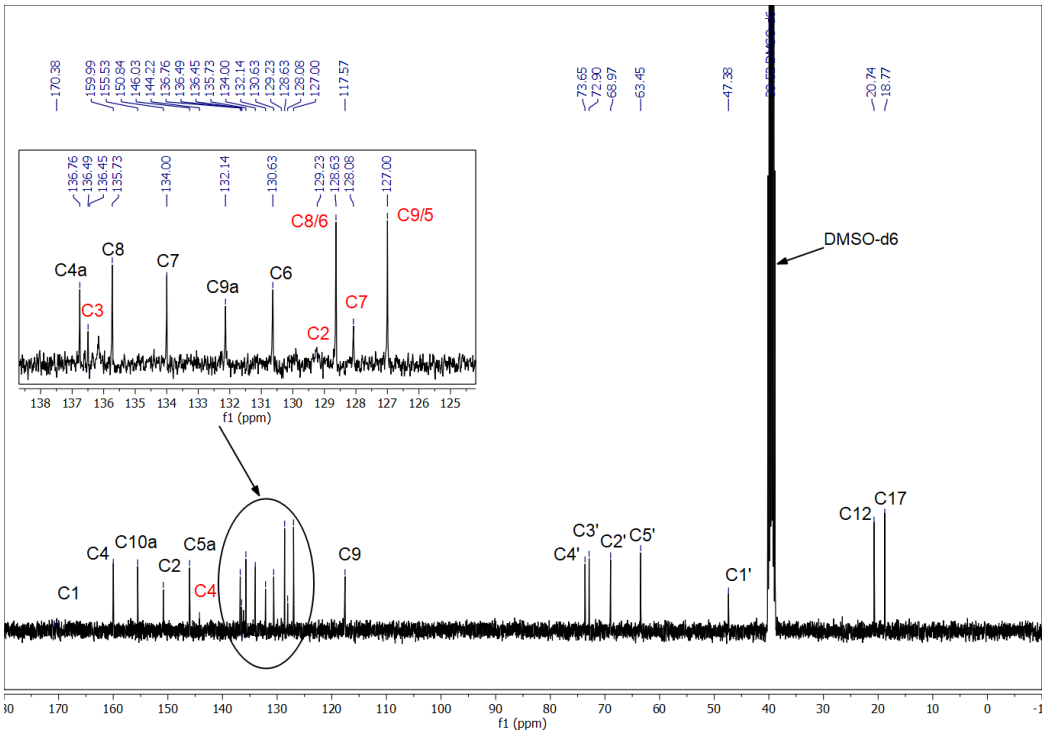

Figure A 54: ^{13}C-NMR spectrum of riboflavin and sodium cinnamate in DMSO-d_6 at a molar ratio of NaCinn/RF = 0.4. Red: Carbons of NaCinn; Black: Carbons of RF.

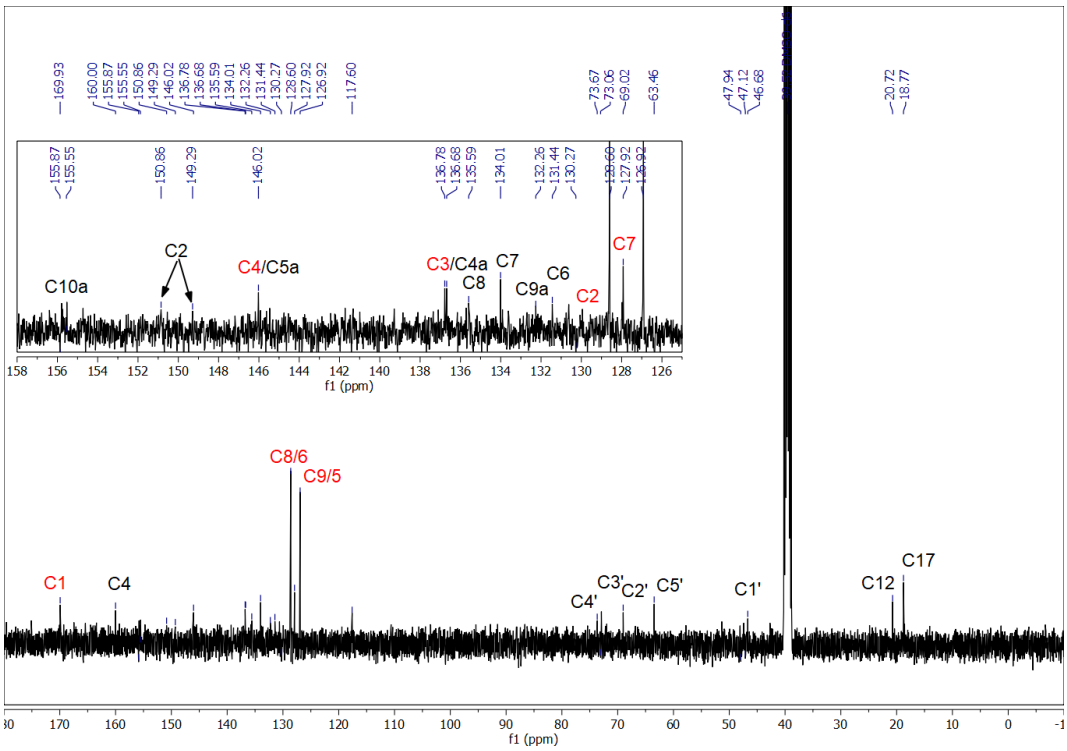

Figure A 55: ^{13}C-NMR spectrum of riboflavin and sodium cinnamate in DMSO-d_6 at a molar ratio of NaCinn/RF = 1. Red: Carbons of NaCinn; Black: Carbons of RF.

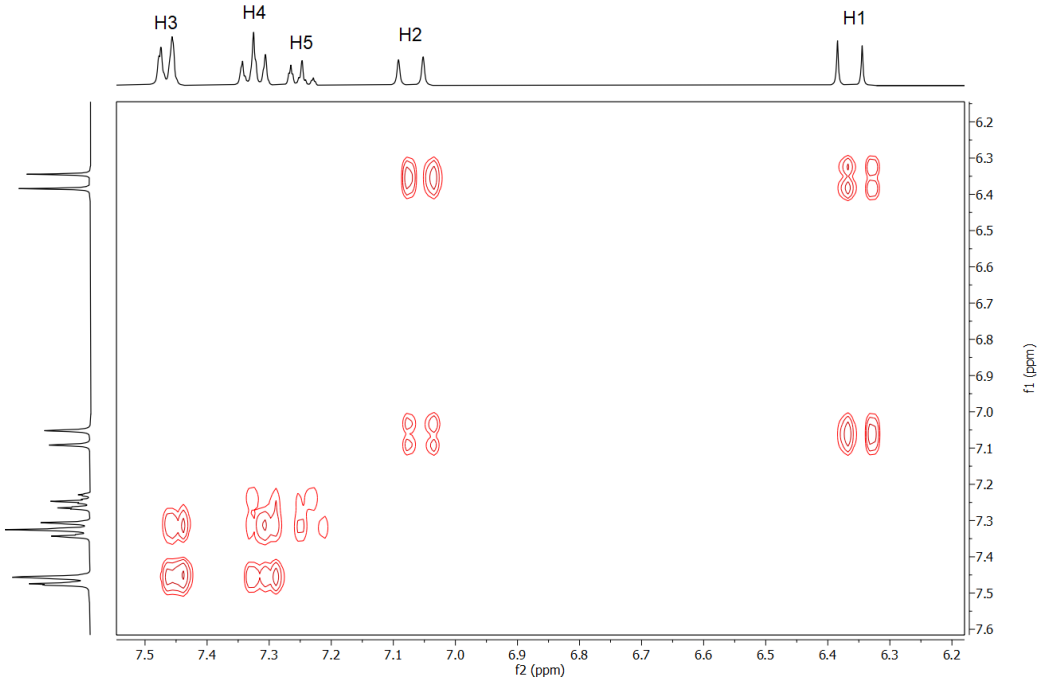

Figure A 56: COSY NMR spectrum of sodium cinnamate in DMSO-d_6 (saturation).

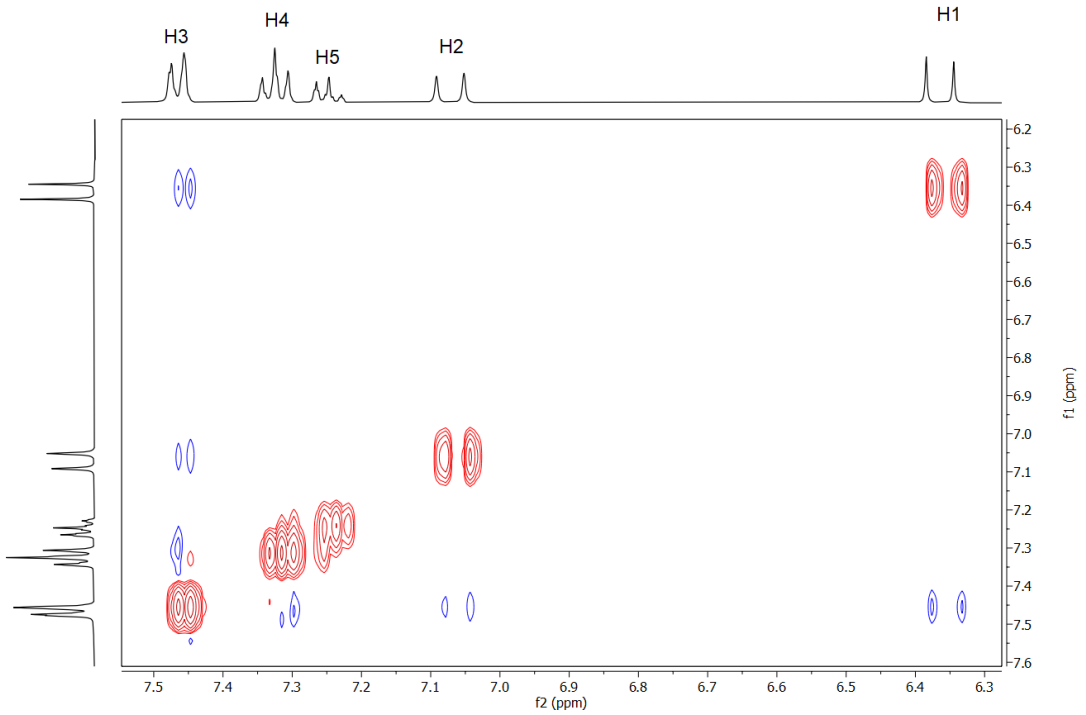

Figure A 57: NOESY NMR spectrum of sodium cinnamate in DMSO-d_6 (saturation).

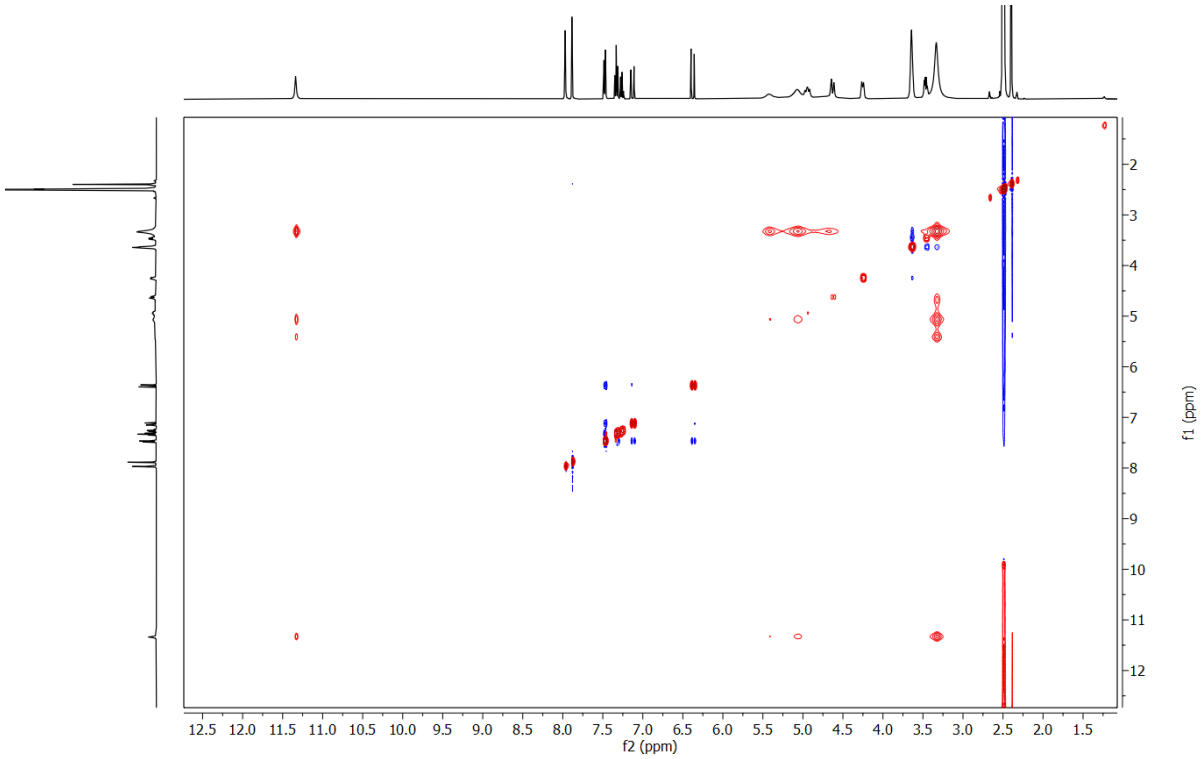

Figure A 58: NOESY NMR spectrum of riboflavin and sodium cinnamate in DMSO-d_6 at a molar ratio of NaCinn/RF = 1.

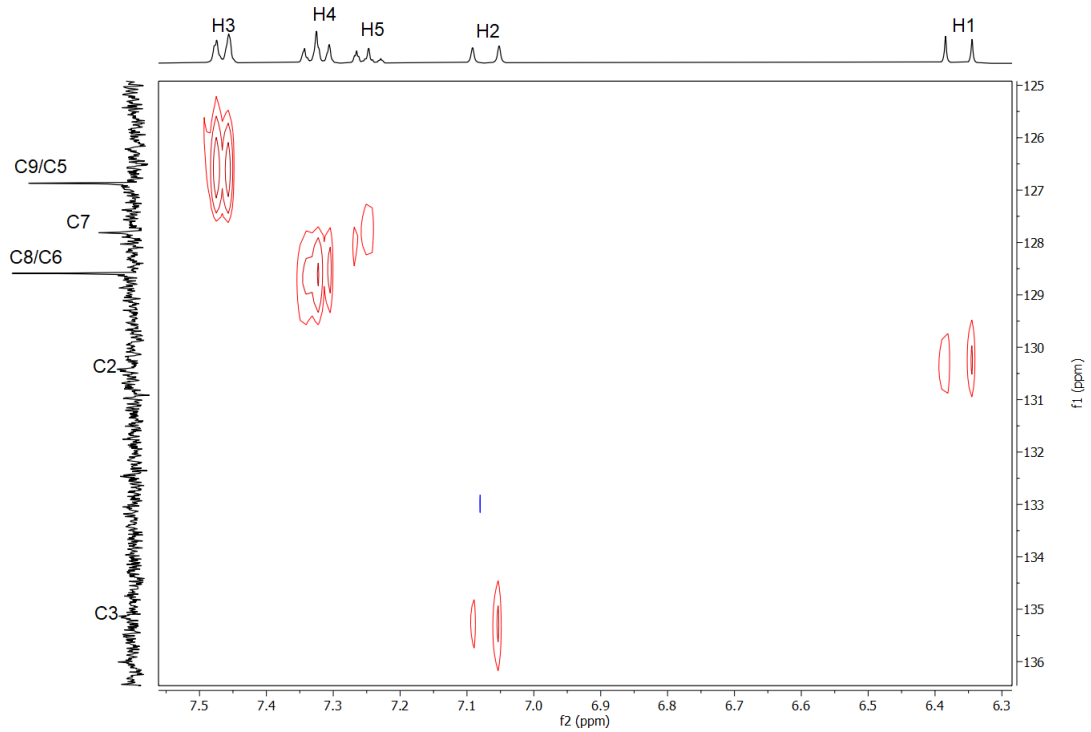

Figure A 59: HSQC NMR spectrum of sodium cinnamate in DMSO-d_6 (saturation).

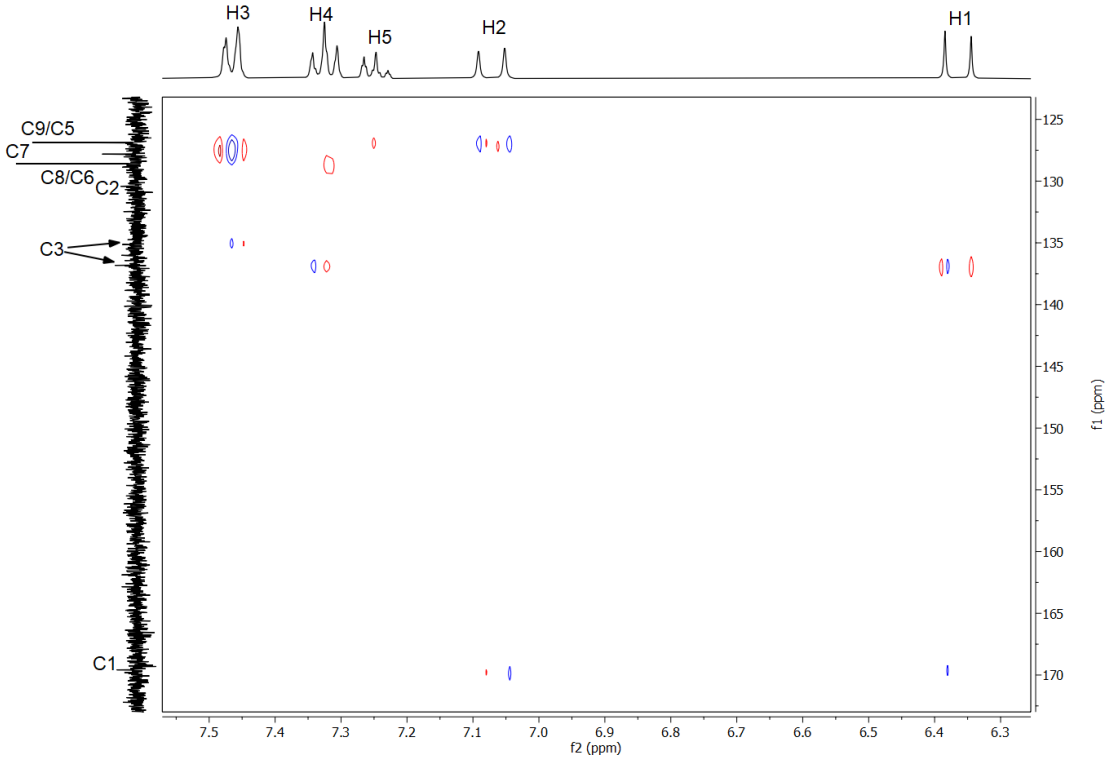

Figure A 60: HMBC NMR spectrum of sodium cinnamate in DMSO-d_6 (saturation).

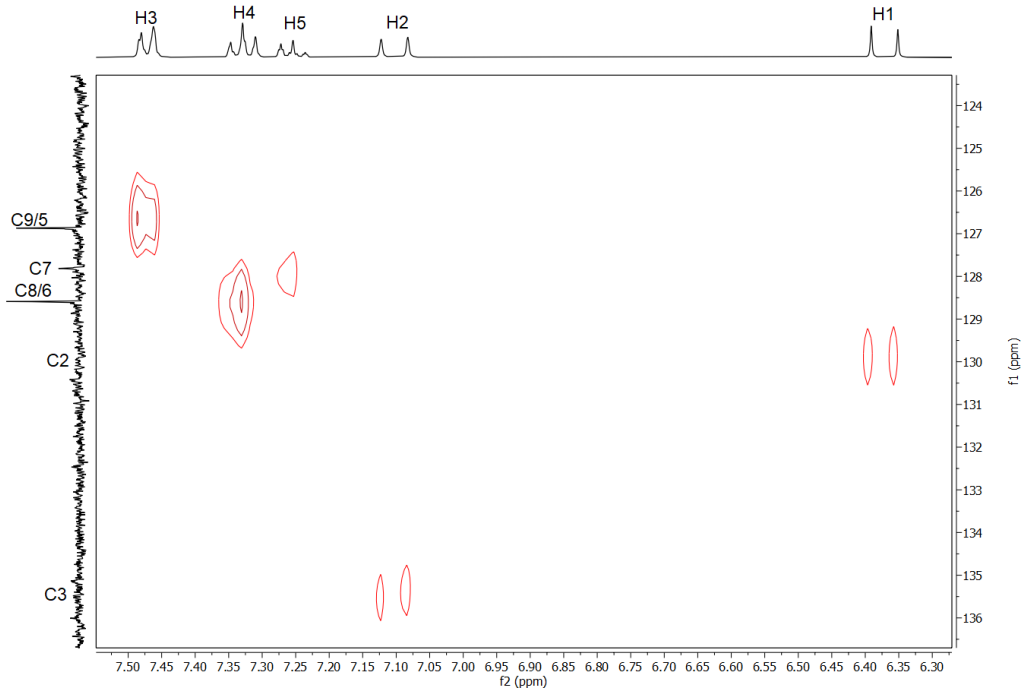

Figure A 61: HSQC NMR spectrum of sodium cinnamate and riboflavin in DMSO-d_6 at a molar ratio of NaCinn/RF = 1.

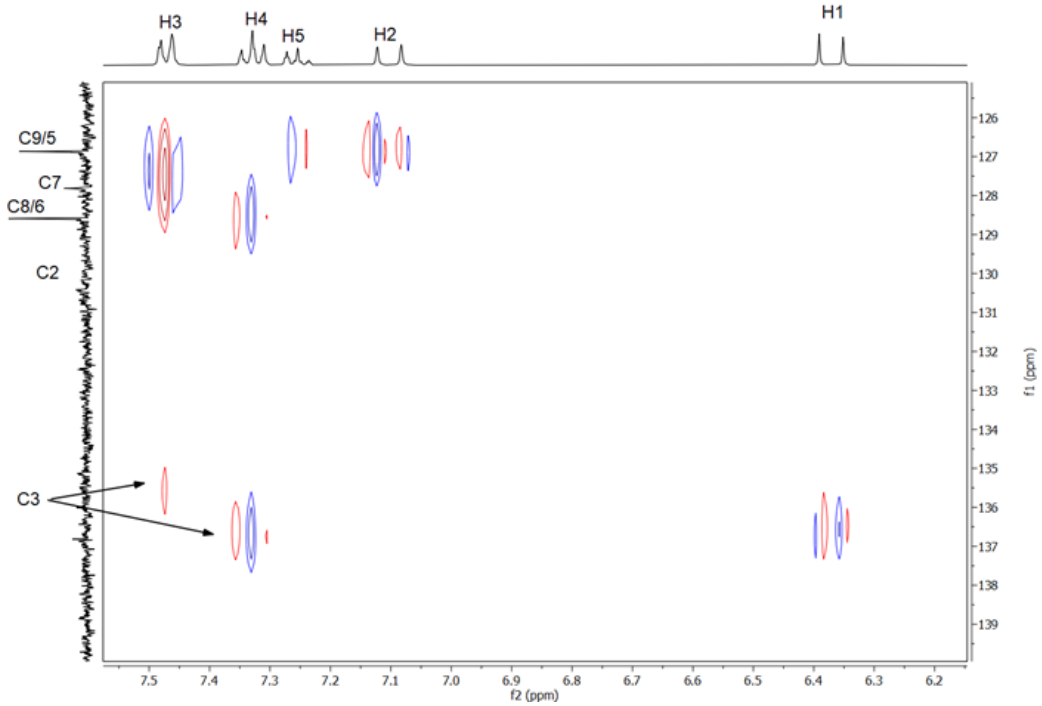

Figure A 62: HMBC NMR spectrum of riboflavin and sodium cinnamate in DMSO-d_6 at a molar ratio of NaCinn/RF = 1.

Table A 109: δ_{exp}: Chemical shift of the protons of sodium cinnamate from Figure A 50, chemical shift of NaCinn's protons in DMSO-d_6 from Figure A 51 and Figure A 52 at the molar NaCinn/riboflavin ratios 0.4 and 1. Δδ: Change of the chemical shift of NaCinn's protons in presence of RF at the molar ratios 0.4 and 1 relatively to NaCinn in pure DMSO-d_6. Last three columns: Splitting pattern, coupling constants and attribution of the protons for the NMR spectra were equal for both molar ratios. The chemical shift of the protons was attributed via the splitting, the coupling constants, the COSY NOESY, HSQC and HMBC NMR spectra (Figure A 56-Figure A 62) and with the help of the calculated shift $\boldsymbol{\delta_{calc.}}$[273] Left = deshielding/shift downfield, d = doublet, td = triplet of doublets, tt = triplet of triplets.

	NaCinn		NaCinn/RF =		NaCinn/RF =		General information for all spectra		
Proton	**δ_{calc} (ppm)**	**δ_{exp} (ppm)**	**δ_{exp} (ppm)**	**Δδ (ppm)**	**δ_{exp} (ppm)**	**Δδ (ppm)**	**Splitting/ J (Hz)**		**Attributed by**
1	6.60	6.36	6.38	Left: 0.02	6.37	-	d	^{3}J(1-2) = 15.91	Integral Coupling
2	8.04	7.07	7.15	Left: 0.08	7.10	Left: 0.03	d	^{3}J(1-2) = 15.91	Integral Coupling HMBC
3	7.16	7.46	7.47	-	7.47	-	td	^{3}J(3-4) = 7.22, ^{4}J 3-5) = 1.56	Splitting Integral NOESY:H2/1 COSY: H4; HMBC
4	7.29	7.33	7.33	-	7.33	-	tt	^{3}J(3/5-4) = 7.17	Splitting Integral COSY: H3/5
5	7.32	7.25	7.26	-	7.25	-	tt	^{3}J(4-5) = 7.21, ^{4}J(3-5) = 1.56	Splitting Integral

Table A 110: δ_{exp}: Chemical shift of the carbon atoms of sodium cinnamate in DMSO-d_6 from Figure A 53, chemical shift of the carbon atoms of sodium cinnamate at a molar ratio of NaCinn/riboflavin of 0.4 and 1 from Figure A 54 and Figure A 55. Δδ: Change of the chemical shift of NaCinn's carbons of NaCinn in presence of riboflavin relatively to NaCinn in pure DMSO-d_6. Left = deshielding/shift downfield; Right = shielding/ shift upfield. In Brackets: Signal not certain due to strong noise for pure NaCinn in DMSO-d_6. The signals were attributed via the HSQC and HMBC spectrum from Figure A 59-Figure A 62 and with calculated chemical shift $\delta_{calc.}$[273]

	NaCinn				NaCinn/RF = 1				NaCinn/RF = 0.4	
	δ_{calc} (ppm)	**δ_{exp} (ppm)**	**HSQC**	**HMBC**	**δ_{exp} (ppm)**	**Δδ (ppm)**	**HSQC**	**HMBC**	**δ_{exp} (ppm)**	**Δδ (ppm)**
C1		169.31		H1,H2	169.93	Left: 0.62	-	-	170.38	Left: 1.07
C4	136.1	145.82/ 144.16*	-	-	Not vis.	-	-	-	144.22	(Left: 0.06)
C3	144.7	136.82	H2	H3, H4,H1	136.78/ 136.68	Right: 0.14	H2	H4,H1	136.50/ 136.45	Right: 0.37
C2	116.5	130.42	H1	-	130.27	Right: 0.15	H1	-	129.23	Right: 1.19
C8/ C6	126.7	128.59	H4	H4	128.60	-	H4	H4	128.63	Left: 0.04
C7	125	127.81	H5	H3	127.92	Left: 0.11	H5	H3	128.08	Left: 0.27
C9/ C5	126.7	126.87	H3	H2, H3,H5	126.92	Left: 0.05	H3	H3,H5, H2	127.00	Left: 0.13

Table A 111: δ_{exp}: Chemical shift of the protons of riboflavin in presence of sodium cinnamate from Figure A 51 and Figure A 52 at a molar ratio of NaCinn/RF of 0.4 and 1 in DMSO-d_6. Δδ: Change of the chemical shift of RF in presence of NaCinn relatively to RF in pure DMSO-d_6 from Figure A 8. The splitting was equal for both molar ratios, the coupling for both ratios is given in the last two columns. Left = deshielding/shift downfield; Right = shielding/ shift upfield, s = singlet, d = doublet, t = triplet, m = multiplet.

	NaCinn/RF = 0.4		NaCinn/RF = 1			NaCinn/RF = 0.4	NaCinn/RF = 1
Proton	**δ_{exp} (ppm)**	**Δδ (ppm)**	**δ_{exp} (ppm)**	**Δδ (ppm)**	**Splitting**	**J (Hz)**	**J (Hz)**
1	11.34	-	11.34	-	s		
2	7.96	Left: 0.06	7.98	Left: 0.08	s		
3	7.88	Left: 0.02	7.89	Left: 0.03	s		
4 (OH)	5.39	Left: 0.28	5.47	Left: 0.36	s (broad)		
5	4.94	Left: 0.02	4.95	Left: 0.03	t	J_2(5-8) = 11.68	J_2(5-8) = 11.75
6 (OH)	5.04	Left: 0.18	5.11	Left: 0.25	s (broad)		
7 (OH)	-	-		-	-		
8	4.63	Left: 0.03	4.63	Left: 0.03	d	J_2(8-5) = 13.40	J_2(8-5) = 13.75
9 (OH)	-	-		-	-		
10	4.25	-	4.25	-	d	J_3(10-7) = 9.72	J_3(10-7) = 8.98
11	3.64	--	3.64	-	m		
12	3.46	-	3.46	-	m		
13	2.48	-	2.48	-	s		
14	2.39	-	2.40	-	s		

Table A 112: δ_{exp}: Chemical shift of the carbon atoms of riboflavin in presence of sodium cinnamate in DMSO-d_6 at a molar ratio of NaCinn/RF of 1 from Figure A 55. Δδ: Change of the chemical shift of riboflavin due to the presence of NaCinn in DMSO-d_6 relative to RF in pure DMSO-d_6 from Figure A 9. "Left = deshielding/shift downfield; Right = shielding/ shift upfield; Shifts in brackets, are not certain as the signal to noise ratio was too low. For C1', C4a, C2 and C10a several peaks were found.

Carbon	**δ_{exp} (ppm)**	**Δδ (ppm)**	**Carbon**	**δ_{exp} (ppm)**	**Δδ (ppm)**
4	160.00	-	**9**	117.60	Left: 0.38
10a	155.87/155.55	Left: 0.05-0.37	**4'**	73.67	Left: 0.38
2	150.86/149.29	(Right: 1.71)	**3'**	73.06	Left: 0.25
5a	146.02	Left: 0.06	**2'**	69.02	Left: 0.22
4a	136.78/136.68	Left. 0.26-0.36	**5'**	63.46	Left: 0.34
8	135.59	Right:0.08	**1'**	47.94/47.12/46.68	Left: 0.83; Right: 0.43
7	134.01	Right: 0.29	**12**	20.72	Right: 0.04
9a	132.26	(Right: 1.75)	**17**	18.77	-
6	131.44	Left: 1.05			

7.11.9 Riboflavin 5'-monophosphate sodium salt in presence of sodium ferulate in deuterium oxide

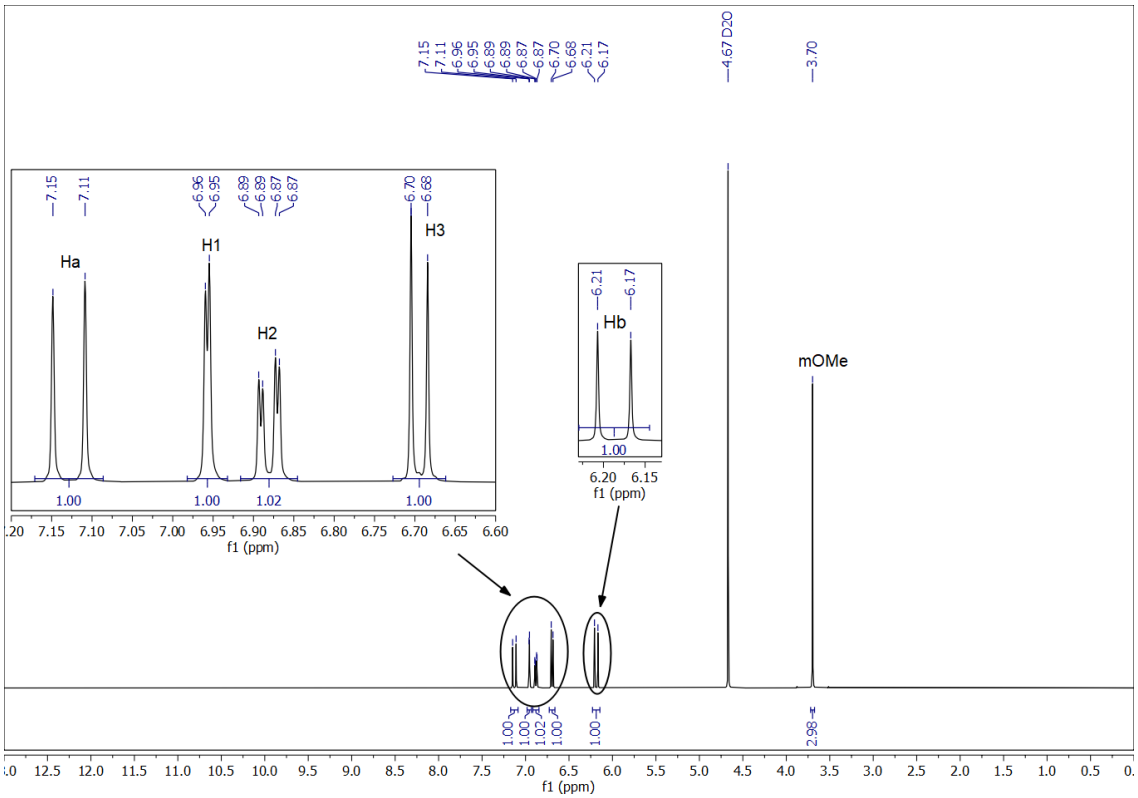

Figure A 63: ^{1}H-NMR spectrum sodium ferulate in deuterium oxide (saturation).

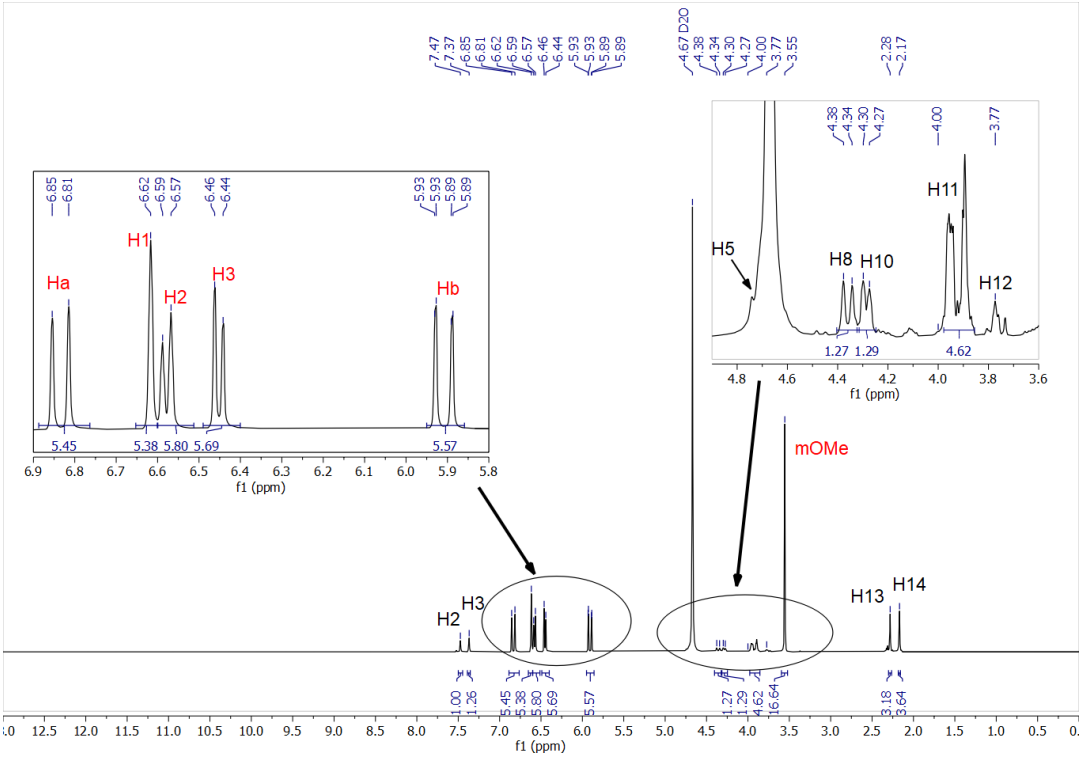

Figure A 64: ^{1}H-NMR spectrum of riboflavin 5'-monophosphate with sodium ferulate in deuterium oxide at a molar ratio of Na-4-OH-3-OMe-Cinn/RF-PO_4 = 5.5. Red: Protons of sodium ferulate; black: Protons of RF-PO_4 sodium salt.

Table A 113: Attribution of the protons of sodium ferulate in deuterium oxide to the ^{1}H-NMR signals from Figure A 63 with corresponding the splitting and coupling constants. The shift was also compared with the theoretical shift δ_{calc} from an increment table.[273] d = doublet; dd = doublet of doublets; s = singlet.

Proton	δ_{calc} (ppm)	δ (ppm)	Number of protons	Splitting	J (Hz)
1	6.73	6.96	1	d	^{4}J(1-2) = 1.99
2	7.77	6.88	1	dd	^{3}J(2-3) = 8.26, ^{4}J(1-2) = 1.99
3	6.50	6.69	1	d	^{3}J(2-3) = 8.26
a	8.04	7.13	1	d	^{3}J(a-b) = 15.95
b	6.58	6.19	1	d	^{3}J(a-b) = 15.95
OMe		3.70	3	s	-

*Table A 114: Attribution of the protons of riboflavin 5'-monophosphate sodium salt at a molar ratio of sodium ferulate/RF-PO$_4$ = 5.5 from Figure A 64 in deuterium oxide. Δδ: Change of chemical shift compared to the signals of pure RF-PO$_4$ due to the presence of sodium ferulate in deuterium oxide from the Figure A 14. Left = deshielding/shift downfield; Right = shielding/ shift upfield; J = coupling constant; s = singlet, d = doublet, m = multiplet, vis. = visible * overlap with signal of deuterium oxide.*

Proton	δ_{exp}	Number of protons	Splitting	J (Hz)	Δδ (ppm)
1	Not vis.	1	-	-	-
2	7.47	1	s	-	Right: 0.10
3	7.37	1	s	-	Left: 0.07
4 (OH)	Not vis.	1	-	-	-
5	4.7*	1	-	*	Right: 0.15
6 (OH)	Not vis.	1	-	-	-
7 (OH)	Not vis.	1	-	-	-
8	4.36	1	d	^{2}J(8-5) = 13.50	Right: 0.10
10	4.29	1	m	^{2}J(8-5) = 10.05	Left: 0.06
11	3.93	3	m		-
12	3.77	1	m		-
13	2.28	3	s	-	Right: 0.05
14	2.17	3	s	-	-

Table A 115: Attribution of sodium ferulate's protons at a molar ratio of sodium ferulate/RF-PO$_4$ = 5.5 in deuterium oxide from Figure A 64. ∆δ: Change of chemical shift of sodium ferulate's protons due to the presence of RF-PO$_4$ relative to sodium ferulate in pure deuterium oxide from Figure A 63 and Table A 113. Right = shielding/ shift upfield, s = singlet, d = doublet.

Proton	δ_{exp} (ppm)	Number of protons	Splitting	J (Hz)	Δδ (ppm)
1	6.62	1	s	-	Right: 0.34
2	6.58	1	d	^{3}J(2-3) = 8.30	Right: 0.30
3	6.45	1	d	^{3}J(2-3) = 8.30	Right: 0.24
a	6.83	1	d	^{3}J(b-a) = 16.04	Right: 0.30
b	5.91	1	d	^{3}J(b-a) = 16.04	Right: 0.28
OMe	3.55	3	s	-	Right: 0.15

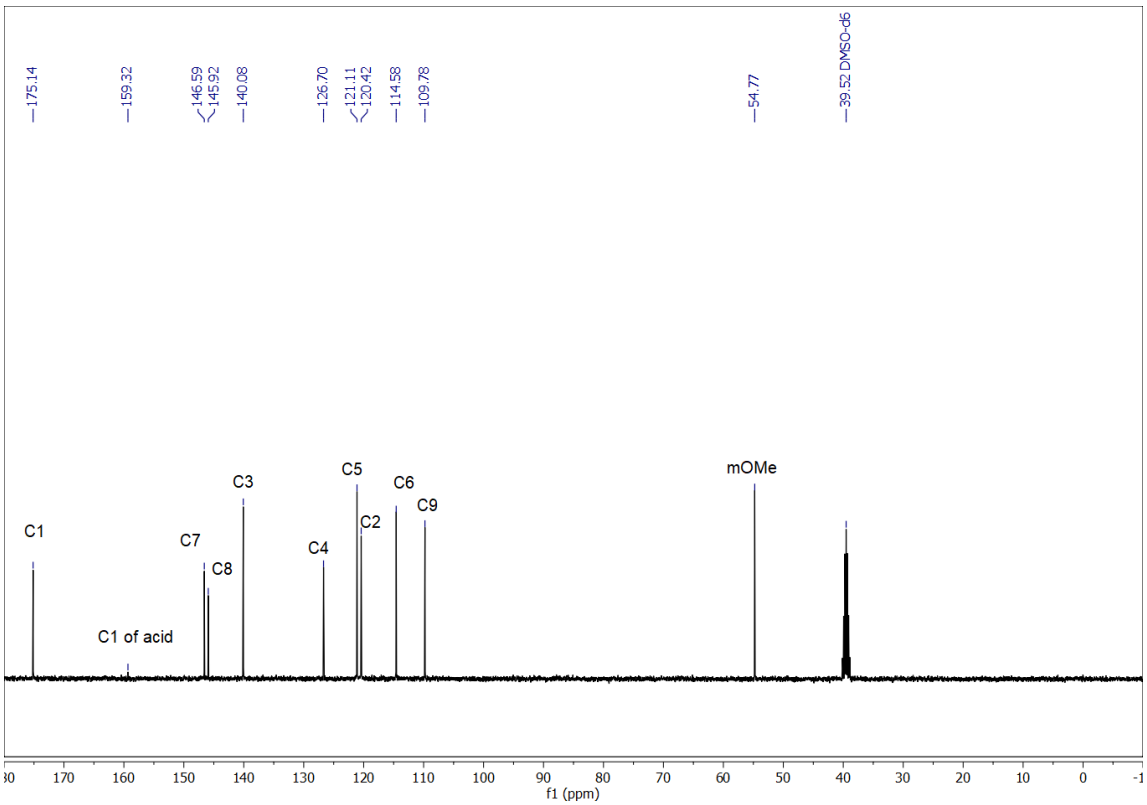

Figure A 65: ^{13}C-NMR spectrum of sodium ferulate in deuterium oxide (saturation). To have a reference an NMR tube with deuterated dimethyl sulfoxide was inserted.

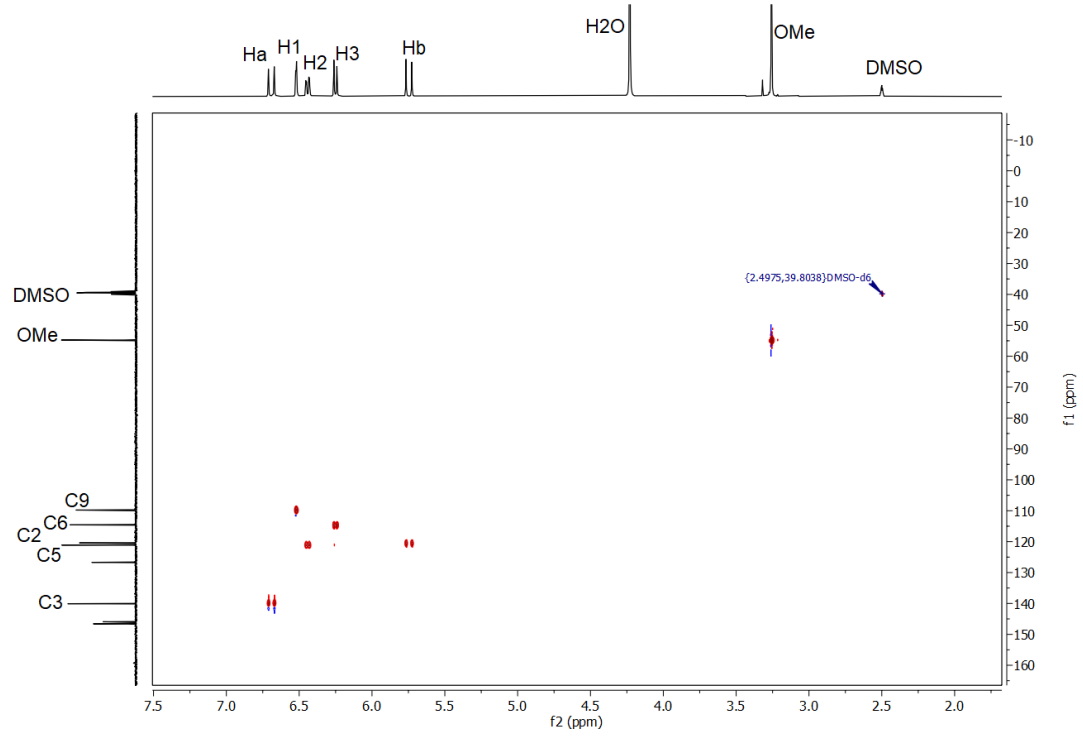

Figure A 66: HSQC NMR spectrum of sodium ferulate in deuterium oxide (saturation). To have a reference signal, an NMR tube with deuterated dimethyl sulfoxide was inserted to record the ^{1}H and ^{13}C-NMR spectrum.

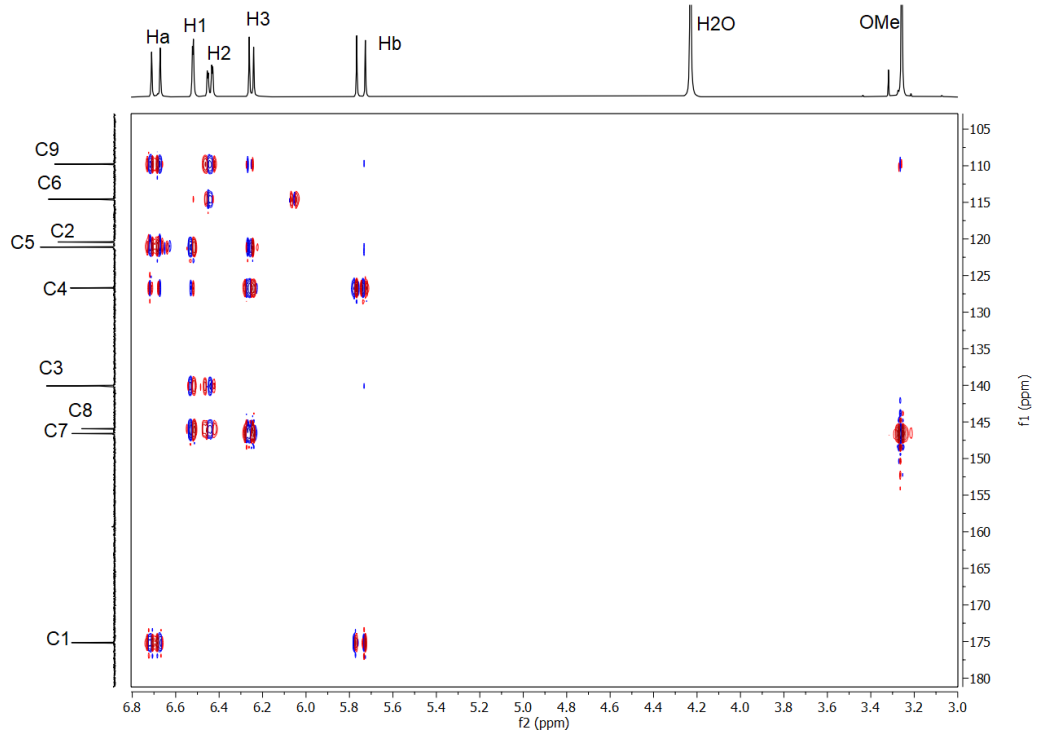

Figure A 67: HMBC NMR spectrum of sodium ferulate in deuterium oxide (saturation). To have a reference signal, an NMR tube with deuterated dimethyl sulfoxide was inserted to record the ^{1}H- and ^{13}C-NMR spectrum.

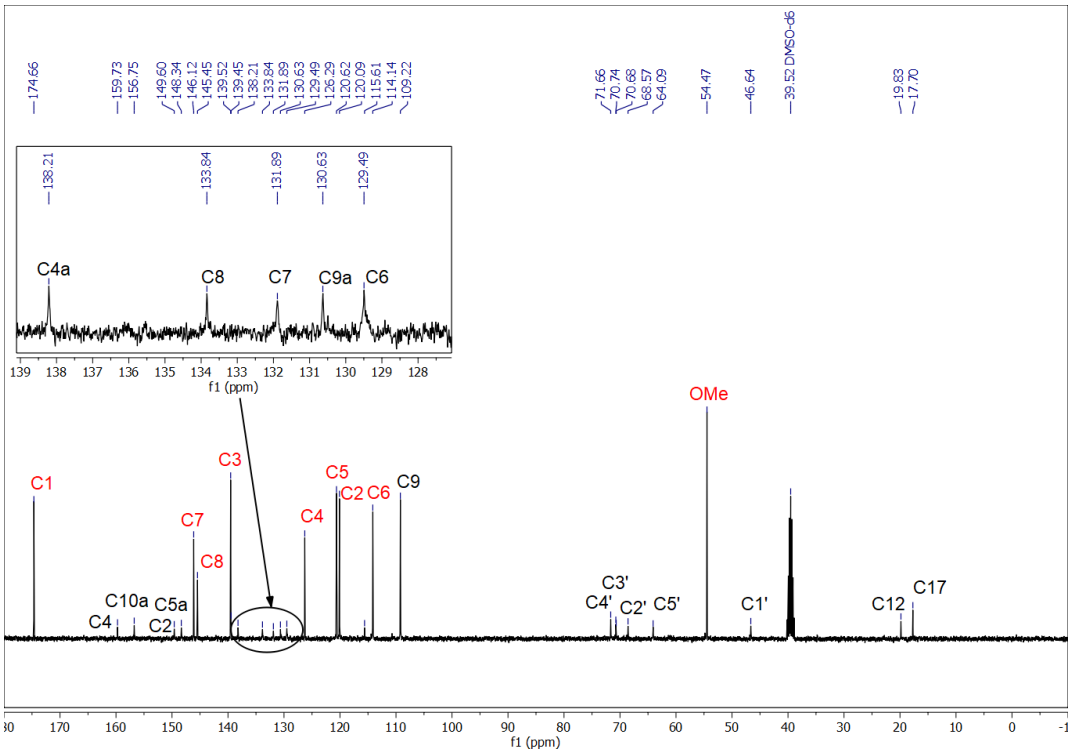

Figure A 68: ^{13}C-NMR spectrum of sodium riboflavin 5'-monophosphate with sodium ferulate in deuterium oxide at a molar ratio of ferulate/RF-PO_4 = 5.5. To have a reference signal an NMR tube with deuterated dimethyl sulfoxide was inserted to record the^{13}C-NMR spectrum. Red: Carbons of sodium ferulate; black: Carbons of RF-PO_4.

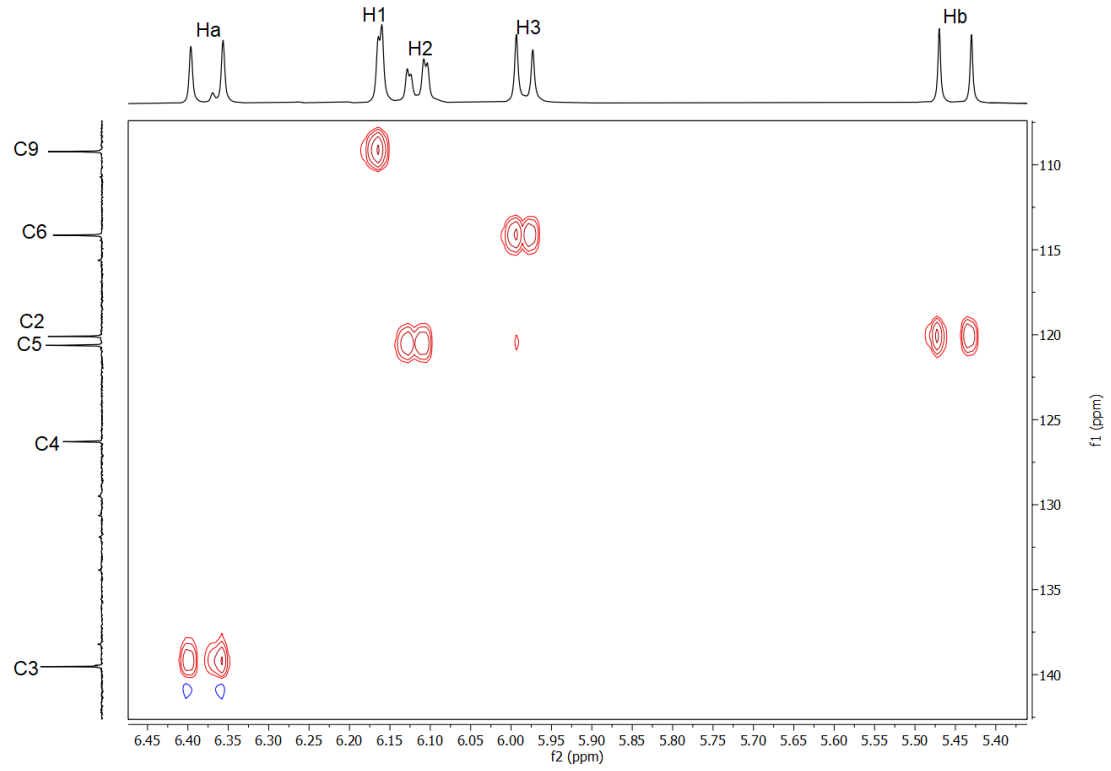

Figure A 69: HSQC NMR spectrum of aromatic sodium ferulate carbon atoms at a molar ratio of ferulate/sodium riboflavin 5'-monophosphate = 5.5 in deuterium oxide. To have a reference signal, an NMR tube with deuterated dimethyl sulfoxide was inserted to record the ^{13}C-NMR spectrum.

Table A 116: Attribution of ^{13}C-NMR signals from Figure A 65 to sodium ferulate's carbon atoms via the cross-peaks in the HSQC spectrum from Figure A 66 and HMBC from Figure A 67. The purchased ferulate was not entirely deprotonated. Thus, the acid's signal was also visible at 159.32 ppm.

Carbon	δ_{calc} (ppm)	δ (ppm)	HMBC	HSQC
1	-	175.14 (acid: 159.32)	Ha, Hb	-
7	147.0	146.59	OMe, H3	-
8	140.8	145.92	H3, H2, H1	-
3	144.7	140.08	Hb, H2, H1	Ha
4	129.6	126.70	Ha, Hb, H1, (H2), H3	-
5	120.0	121.11	Hb, H3	H2
2	116.5	120.42	H1, Ha	Hb
6	115.5	114.58	H2, H1	H3
9	110.7	109.78	Ha, Hb, H2, H3, OMe	H1
m-OMe	-	54.77	OMe	OMe

Table A 117: Attribution of the carbon atoms of sodium riboflavin 5'-monophosphate in presence of sodium ferulate in deuterium oxide at a molar ratio of ferulate/RF-PO_4 = 5.5 from Figure A 68. ∆δ: Change of chemical shift compared to the ones in absence of sodium ferulate from Figure A 15. Left = deshielding/shift downfield; Right = shielding/ shift upfield. C3' and C4a were present as two signals.

Carbon	δ_{exp} (ppm)	Δδ (ppm)	Carbon	δ_{exp} (ppm)	Δδ (ppm)
4	159.73	Left: 0.53	**9**	115.61	Right: 0.37
2	156.74	Left: 0.35	**4'**	71.66	Left: 0.18
10a	149.60	Right: 0.15	**3'**	70.74/70.68	Left: 0.30
4a	139.45/138.21	Left: 1.01; Right: 0.23	**2'**	68.57	Left: 0.30
5a	148.34	Right: 0.10	**5'**	64.09	Right: 0.84/0.79
8	133.84	Left: 1.14	**1'**	46.64	Left: 0.16
7	131.89	Right: 0.37	**12**	19.83	Left: 0.12
9a	130.63	Left: 0.37	**17**	17.70	Left: 0.12
6	129.49	Left: 0.50			

Table A 118: Attribution of sodium ferulate's carbon atoms in presence of sodium riboflavin 5'-monophosphate in deuterium oxide at a molar ratio of ferulate/RF-PO_4 = 5.5 from Figure A 68. ∆δ: Change of chemical shift compared to the signals in absence of RF-PO_4 from Figure A 65. Right = shielding/ shift upfield; The carbons were identified via the HSQC spectrum in Figure A 69. C9 was present as two signals.

Carbon	δ (ppm)	Δδ (ppm)	HSQC
1	174.66	Right: 0.48	-
7	146.12	Right: 0.47	-
8	145.45	Right:0.47	-
3	139.52	Right: 0.56	Ha
4	126.29	Right: 0.41	-
5	120.62	Right: 0.49	H2
2	120.09	Right: 0.33	Hb
6	114.14	Right: 0.44	H3
9	109.22; (110.70)	Right: 0.56	H1
m-OMe	54.47	Right: 0.30	OMe

7.11.10 Vitamin K3

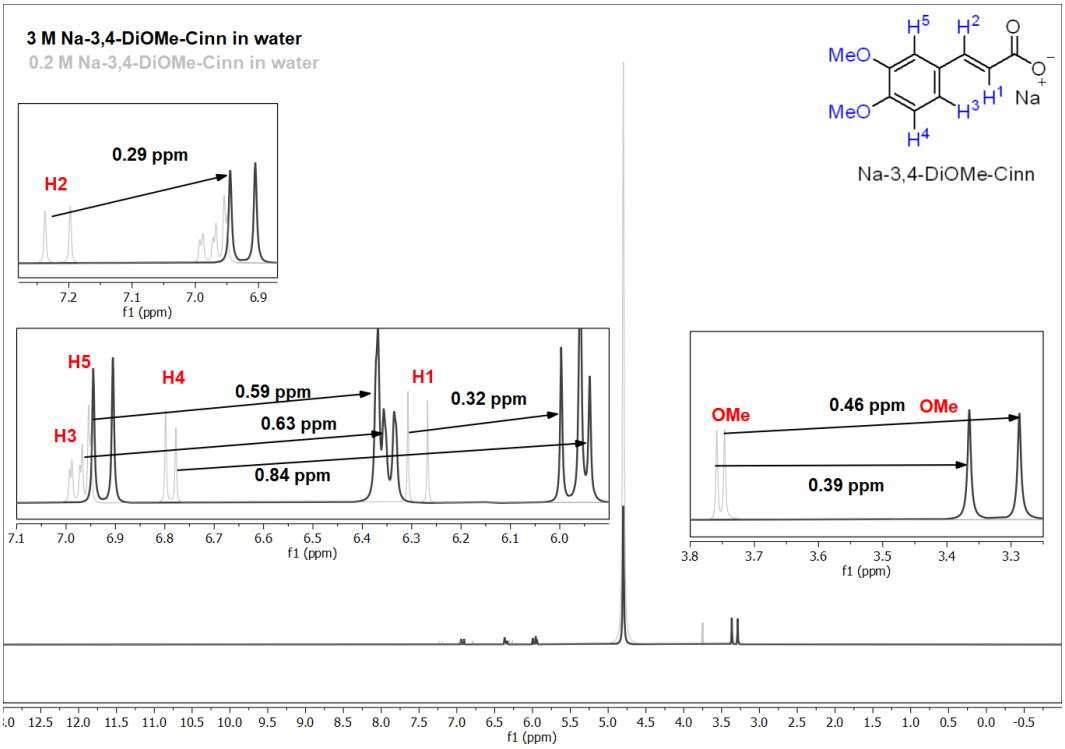

Figure A 70: Superimposed ^{1}H-NMR spectrum of an aqueous 0.2 mol·kg^{-1} and 3 mol·kg^{-1} sodium 3,4-dimethoxycinnamate solution. Red: protons of 3,4-dimethoxycinnamate. The arrows show the change of the chemical shift due to the variation of the concentration. Water peak: 4.8 ppm.

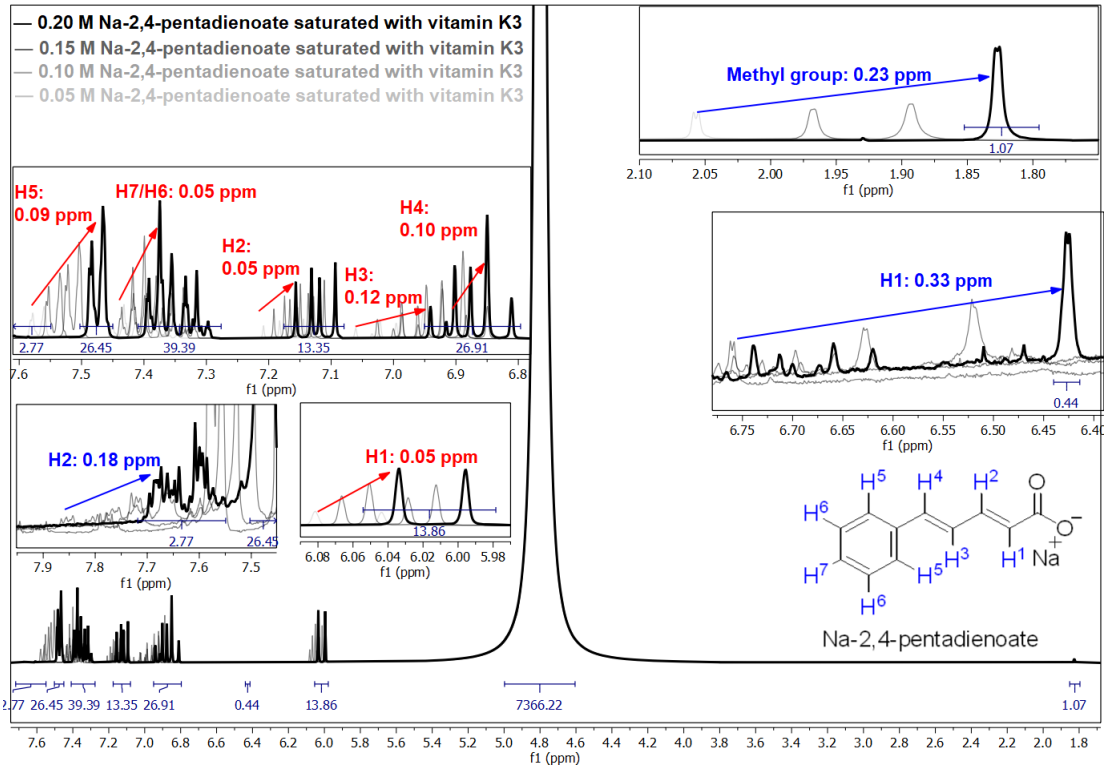

Figure A 71: Superimposed ^{1}H-NMR spectra of distinct aqueous solutions of sodium 5-phenyl-2,4-pentadieonate solutions saturated with vitamin K3. Protons of vitamin K3: blue; protons of sodium salt: red. Water peak: 4.8 ppm.

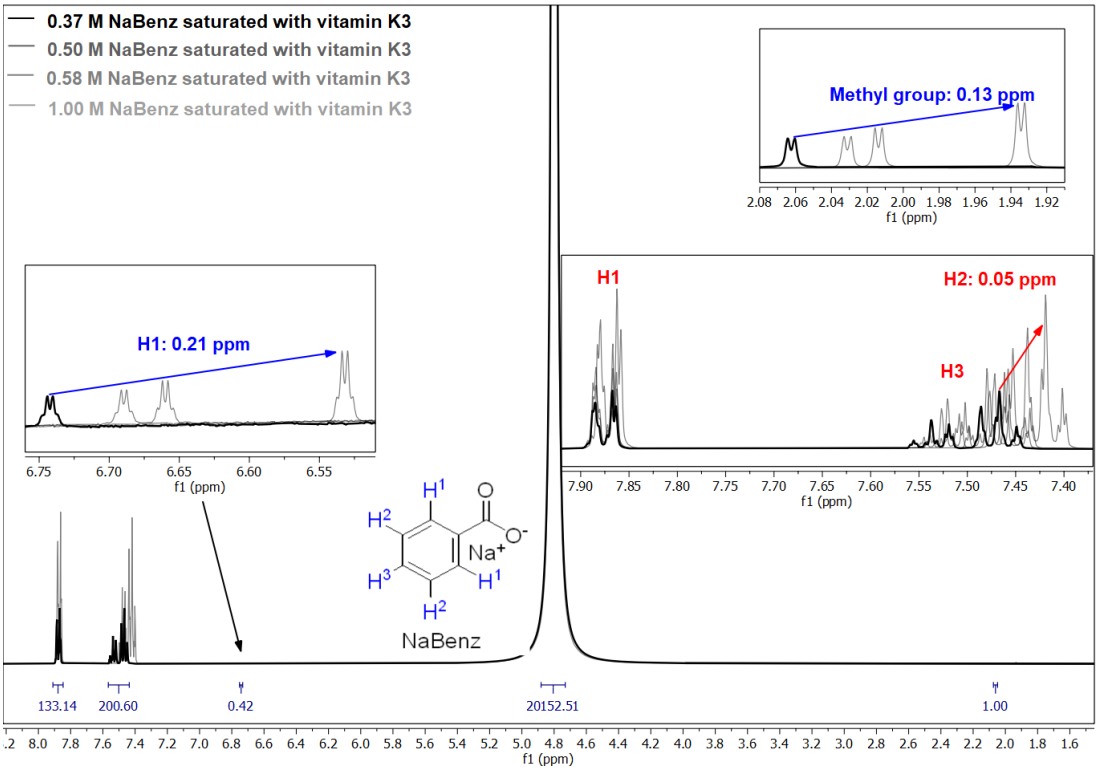

Figure A 72: Superimposed ^{1}H-NMR spectra of distinct aqueous solutions of sodium benzoate solutions saturated with vitamin K3. Protons of vitamin K3: blue; protons of sodium salt: red. H2 of vitamin K3 is covered by the aromatic protons of NaBenz. Water peak: 4.8 ppm.

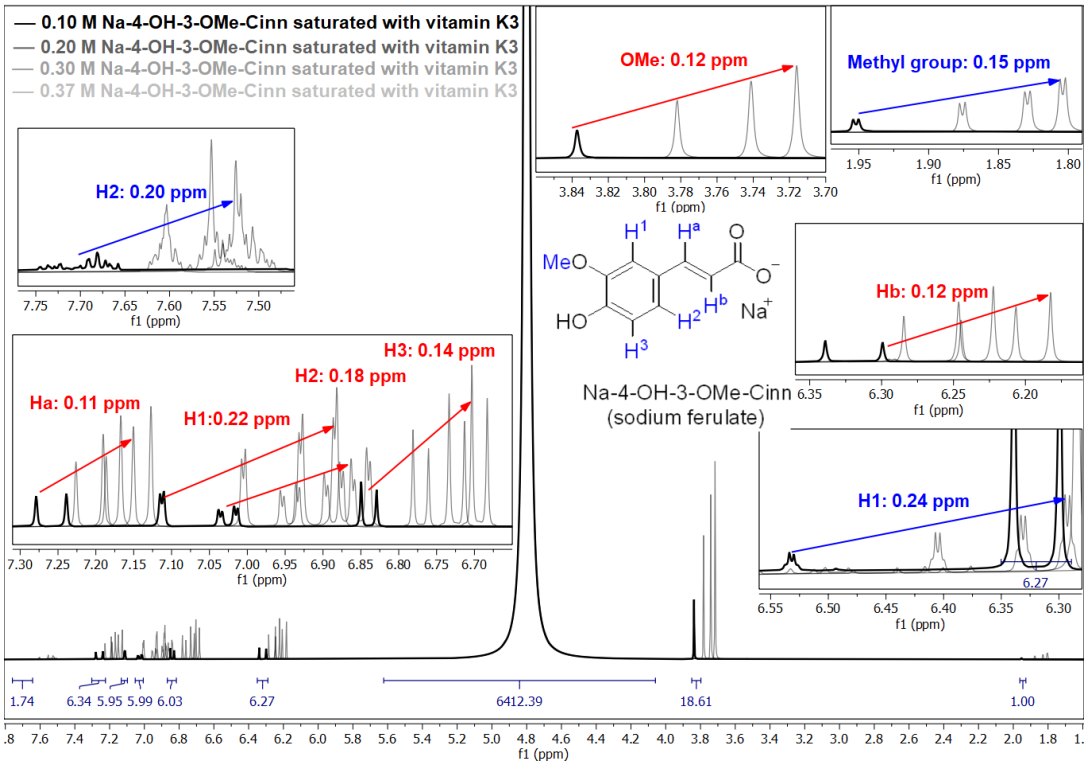

Figure A 73: Superimposed ^{1}H-NMR spectra of distinct aqueous solutions of sodium ferulate saturated with vitamin K3. Protons of vitamin K3: blue; protons of sodium salt: red. Water peak: 4.8 ppm.

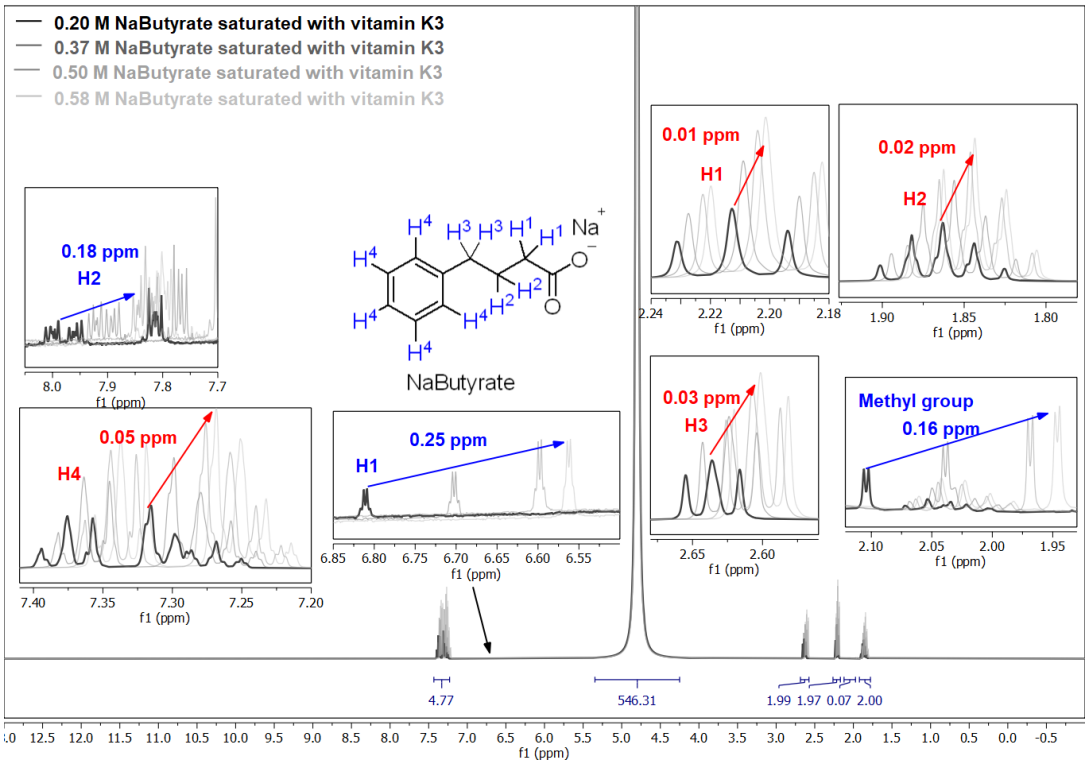

Figure A 74: ^{1}H-NMR spectrum of distinct aqueous solutions of sodium 4-phenylbutyrate saturated with vitamin K3 in water. Protons of vitamin K3: blue; protons of sodium salt: red.

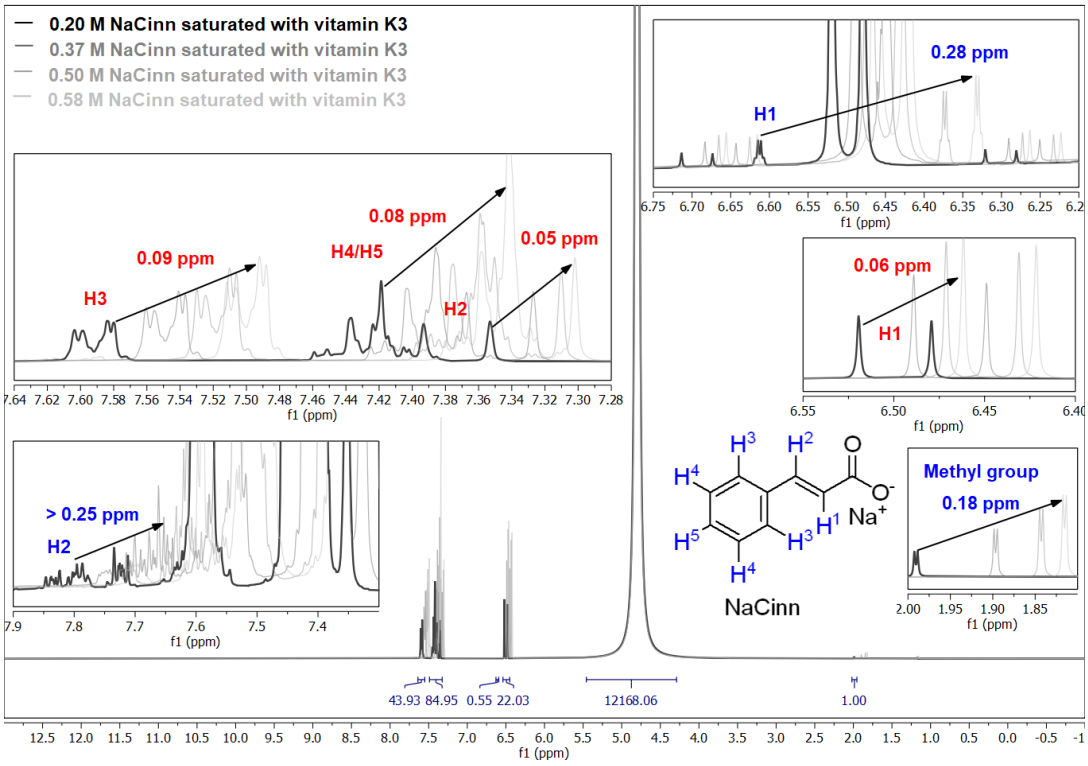

Figure A 75: ^{1}H-NMR spectrum of distinct aqueous solutions of sodium cinnamate saturated with vitamin K3 in water. Protons of vitamin K3: blue; protons of sodium cinnamate: red. Water peak: 4.8 ppm.

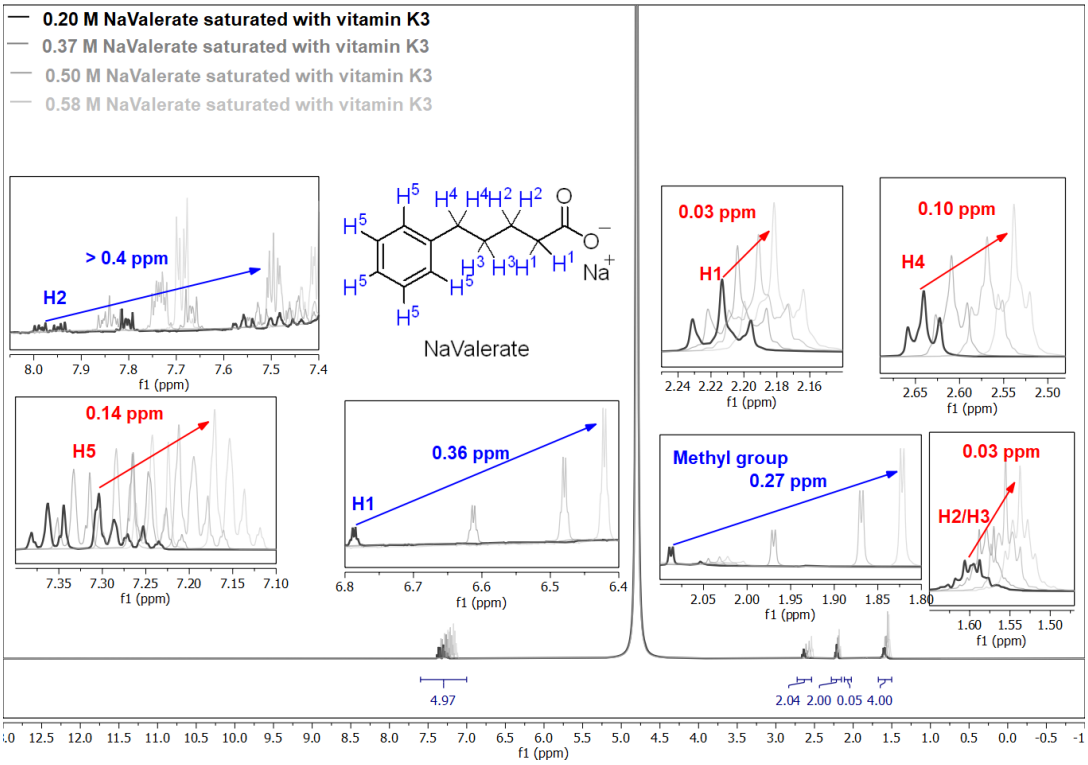

Figure A 76: ^{1}H-NMR spectrum of distinct aqueous solutions of sodium 5-phenylvalerate saturated with vitamin K3 in water. Protons of vitamin K3: blue; protons of sodium salt: red. Water peak: 4.8 ppm.

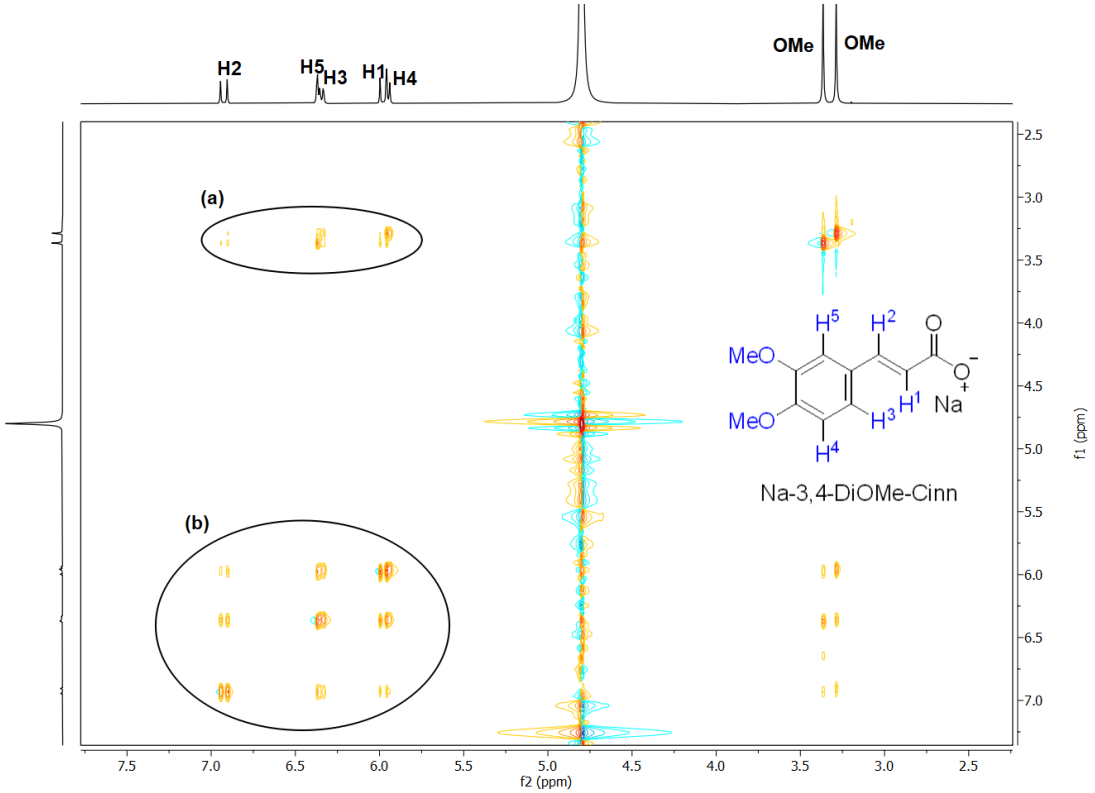

Figure A 77: NOESY spectrum of an aqueous 3 mol·kg^{-1} sodium 3,4-dimethoxycinnamate sample. (a) Cross-peaks of the methoxy groups with all aromatic protons; (b) Cross peaks between all aromatic protons.

7.11.11 Folic acid

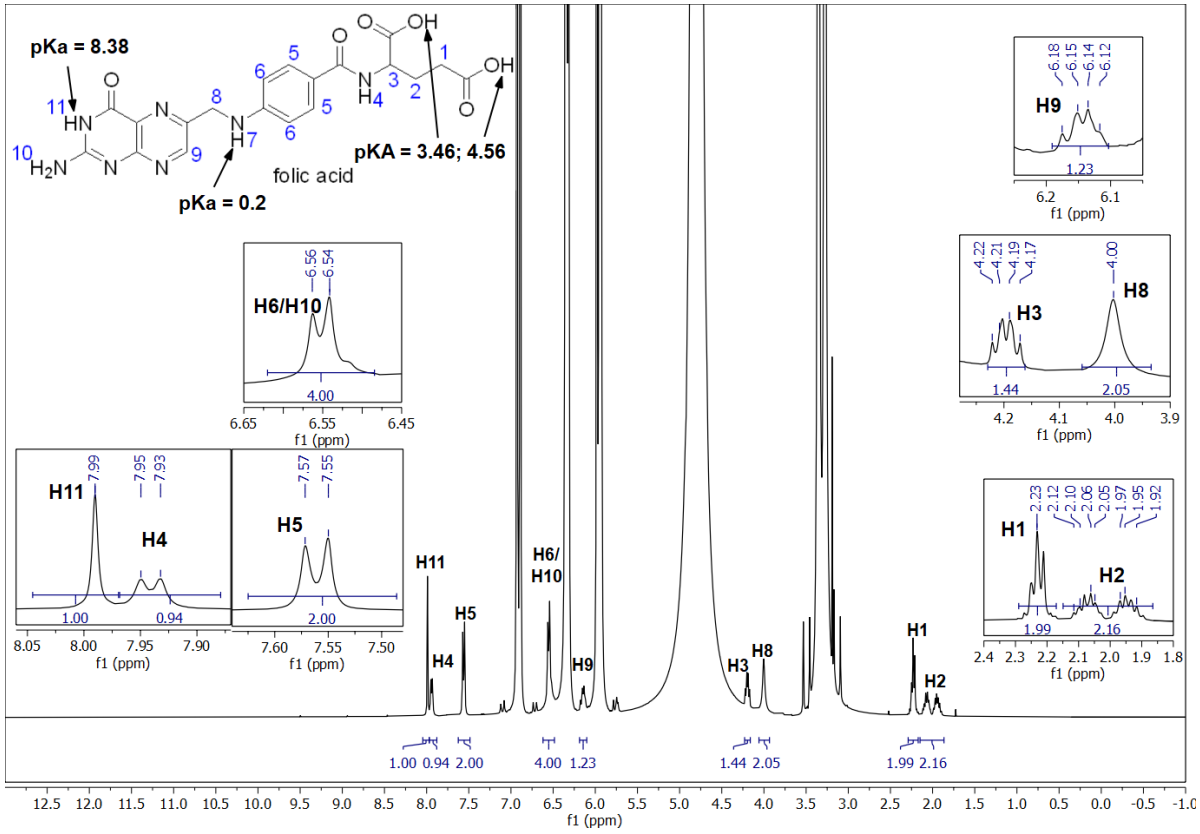

Figure A 78: ^{1}H-NMR spectrum of folic acid (saturation) in an aqueous 3.0 mol·kg^{-1} Na-3,4-DiOMe-Cinn solution.

7.11.12 Solubility of caffeine in aqueous sodium vanillate solutions

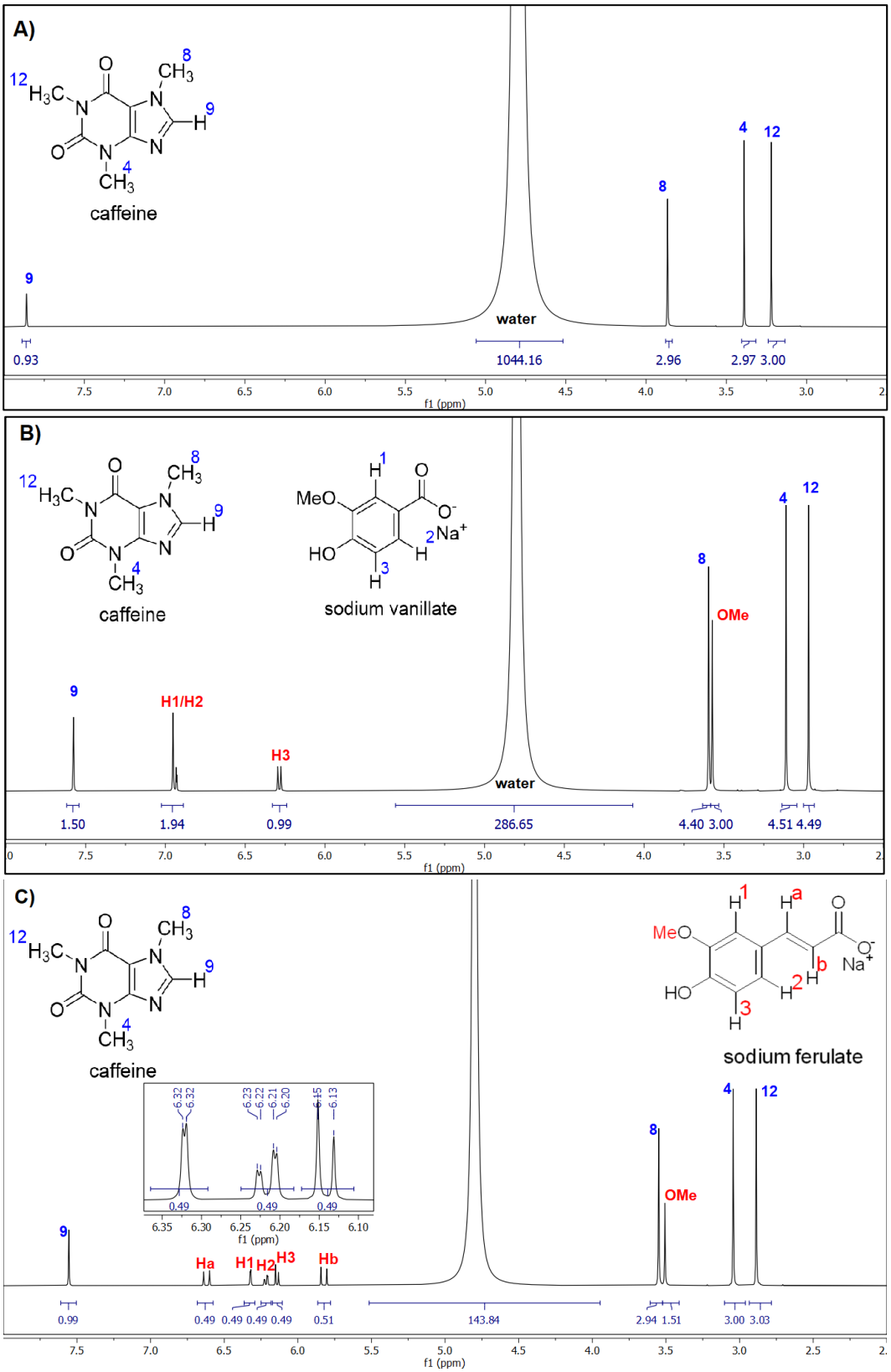

Figure A 79: ^{1}H-NMR spectrum of caffeine (saturation) in pure water (A) and in an aqueous 0.37 mol·kg^{-1} sodium vanillate (B) and sodium ferulate (C) solution. Protons of caffeine: blue; protons of vanillate and ferulate: red.

7.11.13 Compatibility of riboflavin, vitamin K3, folic acid and caffeine in an aqueous sodium polyphenolate solution

Due to an overlap with other peaks and due to the huge solvent signal, some protons were not found in the spectra of this section. Note that the ferulate content differed slightly from sample to sample, although the mother solution was the same. The reason was that water was trapped in the powder, which was removed via filtration.

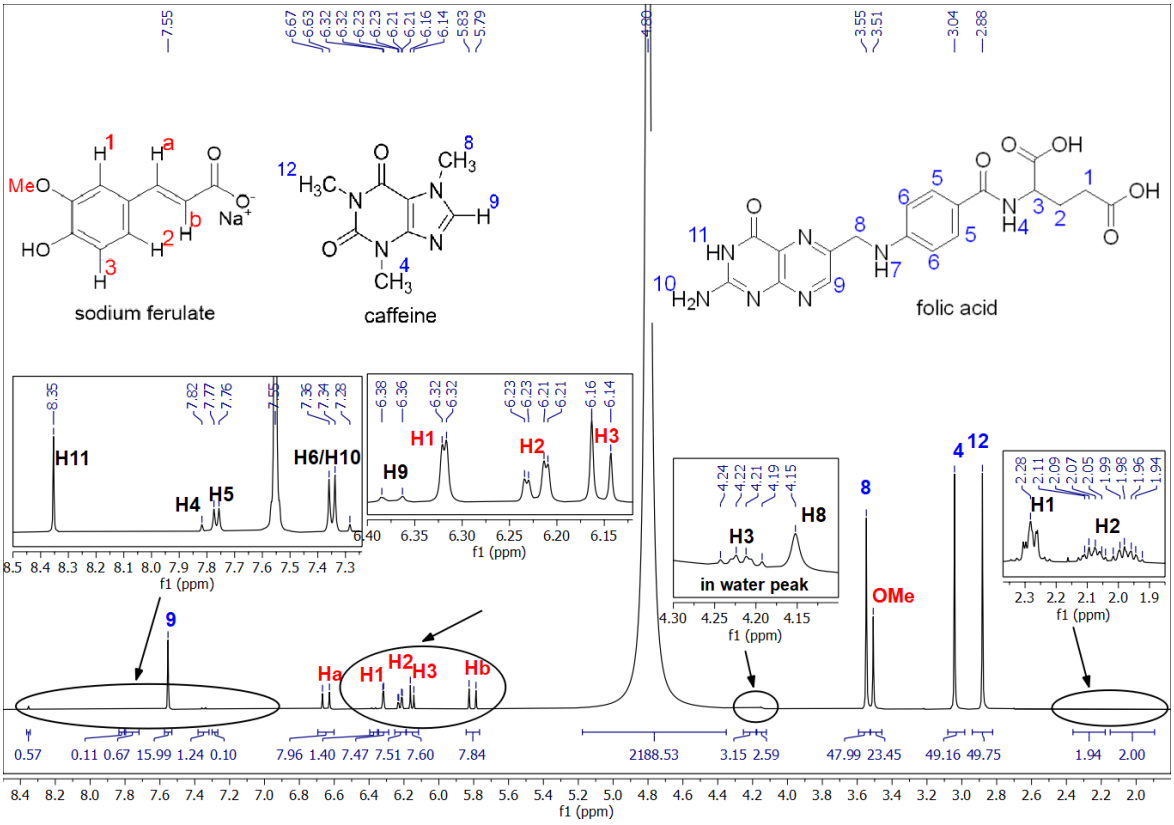

Figure A 80: ^{1}H-NMR spectrum of caffeine and folic acid (saturation) in an aqueous 0.37 mol·kg^{-1} sodium ferulate solution. Protons of caffeine: blue; protons of folic acid: black; protons of ferulate: red.

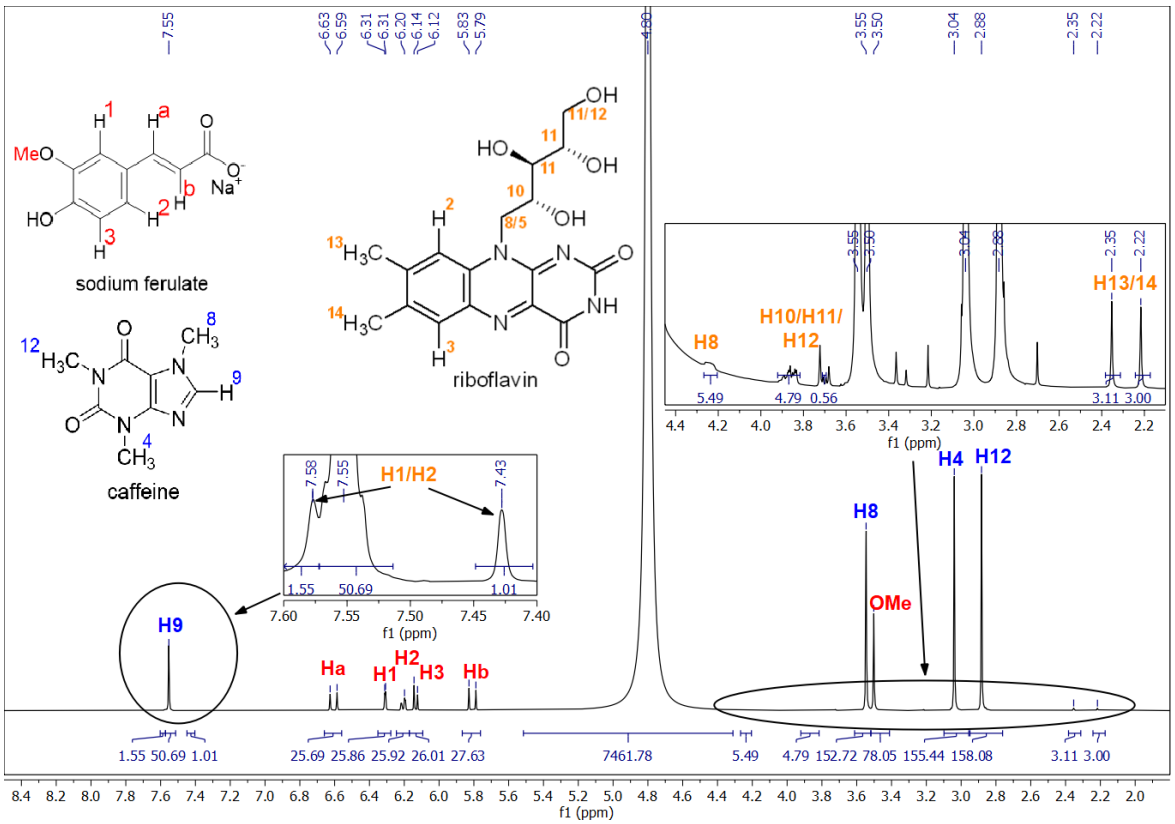

Figure A 81: ^{1}H-NMR spectrum of caffeine and riboflavin (saturation) in an aqueous 0.37 mol·kg^{-1} sodium ferulate solution. Protons of caffeine: blue; protons of riboflavin: orange; protons of ferulate: red.

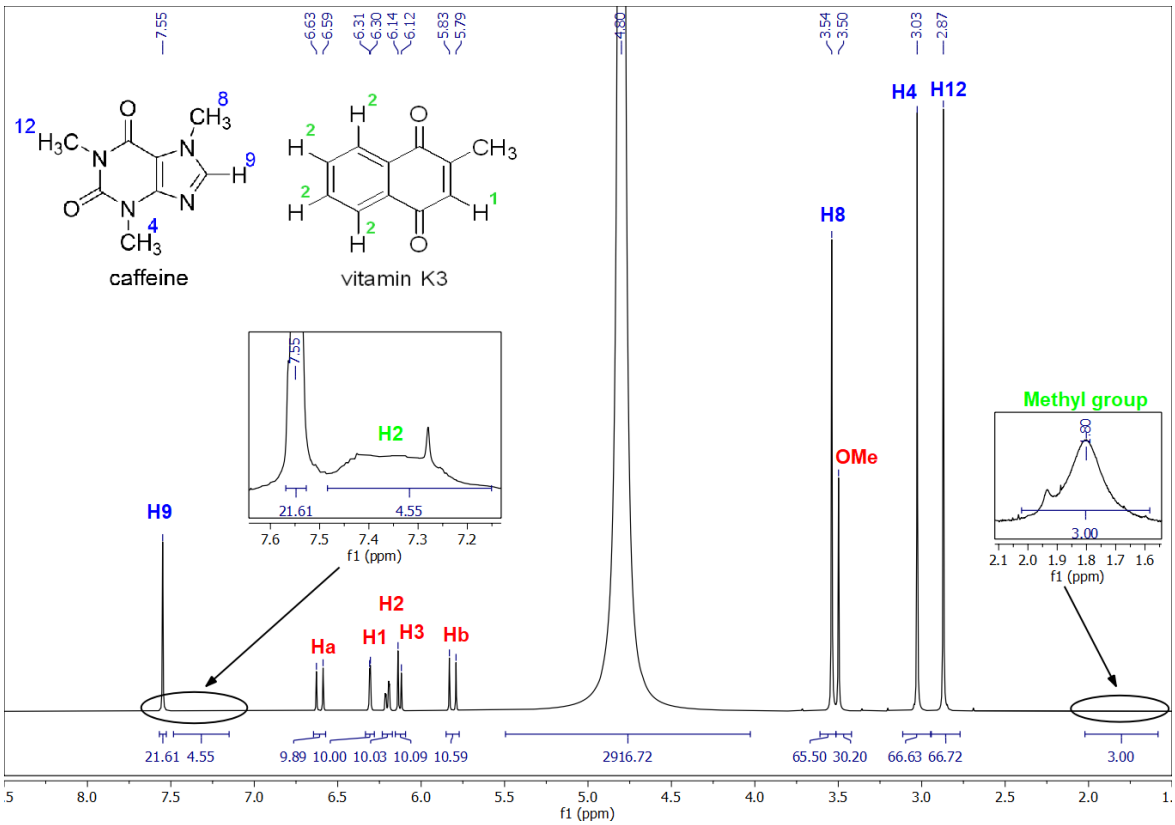

Figure A 82: ^{1}H-NMR spectrum of caffeine and vitamin K3 (saturation) in an aqueous 0.37 mol·kg^{-1} sodium ferulate solution. Protons of caffeine: blue; protons of vitamin K3: green; protons of ferulate: red.

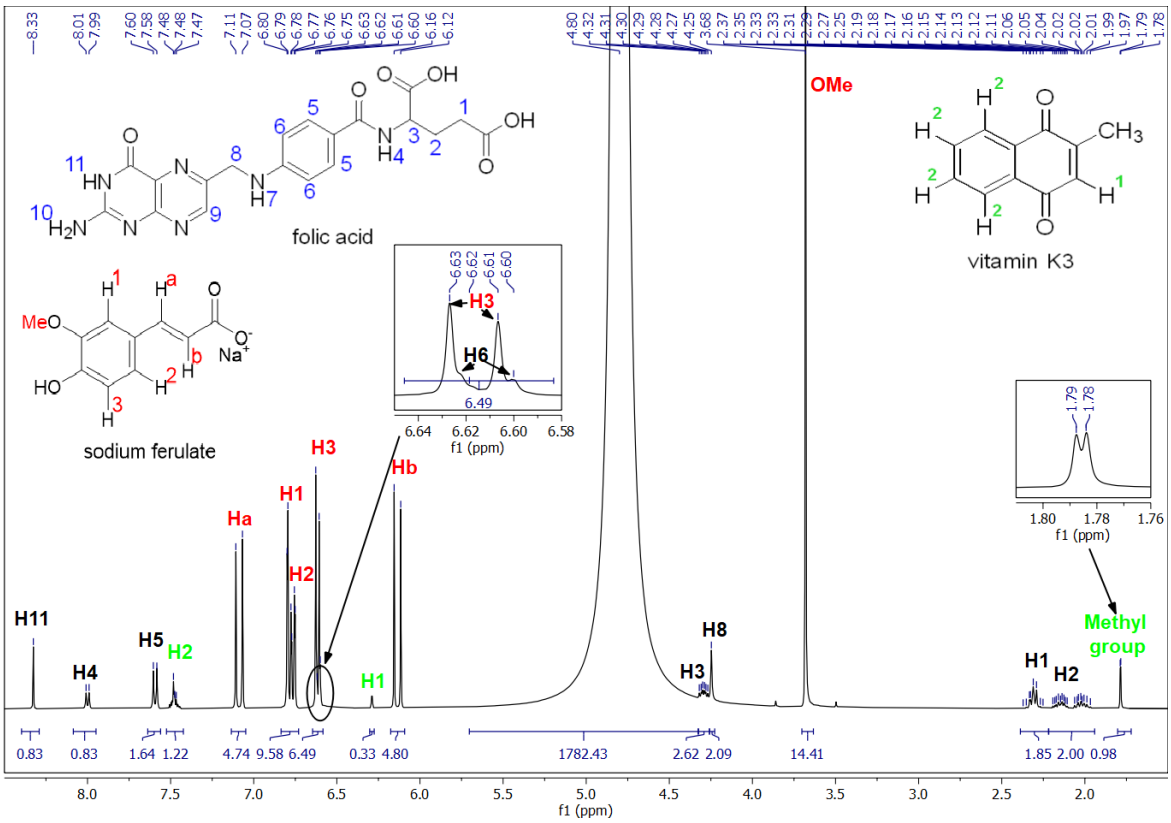

Figure A 83: ^{1}H-NMR spectrum of folic acid and vitamin K3 (saturation) in an aqueous 0.37 mol·kg^{-1} sodium ferulate solution. Protons of folic acid: black; protons of vitamin K3: green; protons of ferulate: red.

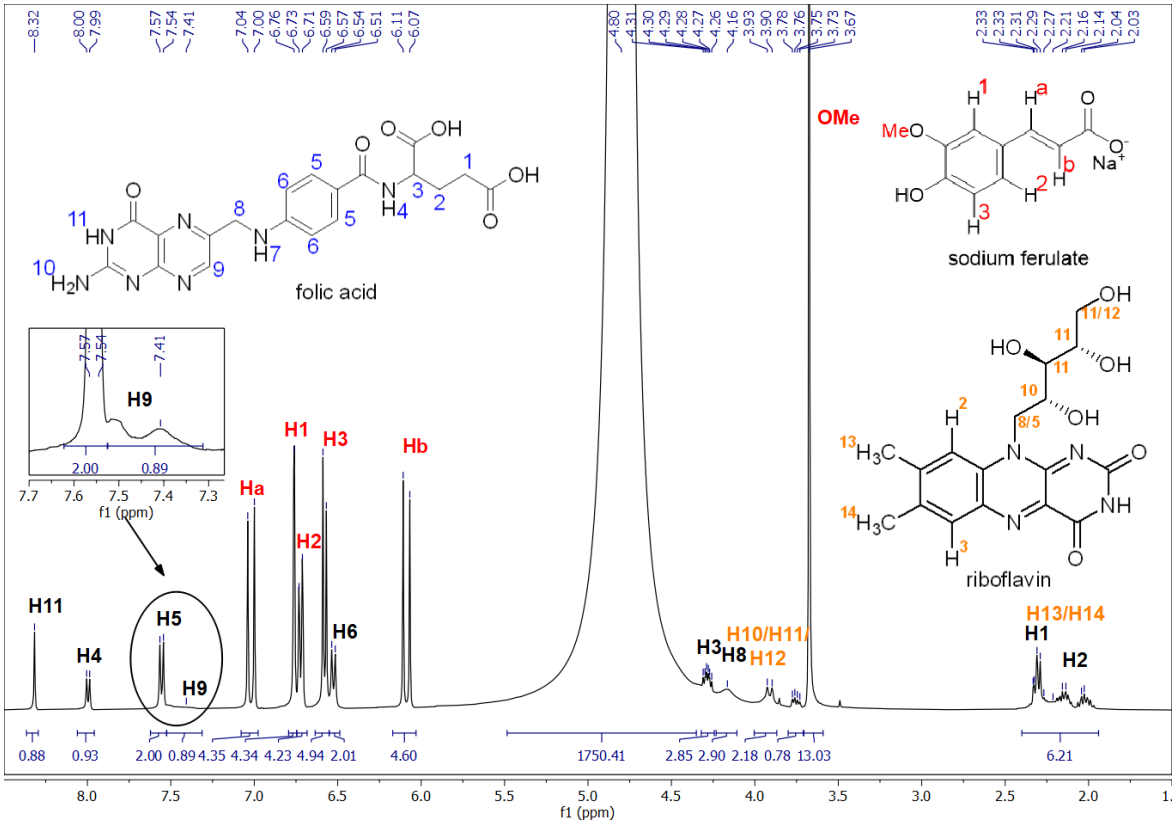

Figure A 84: ^{1}H-NMR spectrum of folic acid and riboflavin (saturation) in an aqueous 0.37 mol·kg^{-1} sodium ferulate solution. Protons of folic acid: black; protons of riboflavin: orange; protons of ferulate: red.

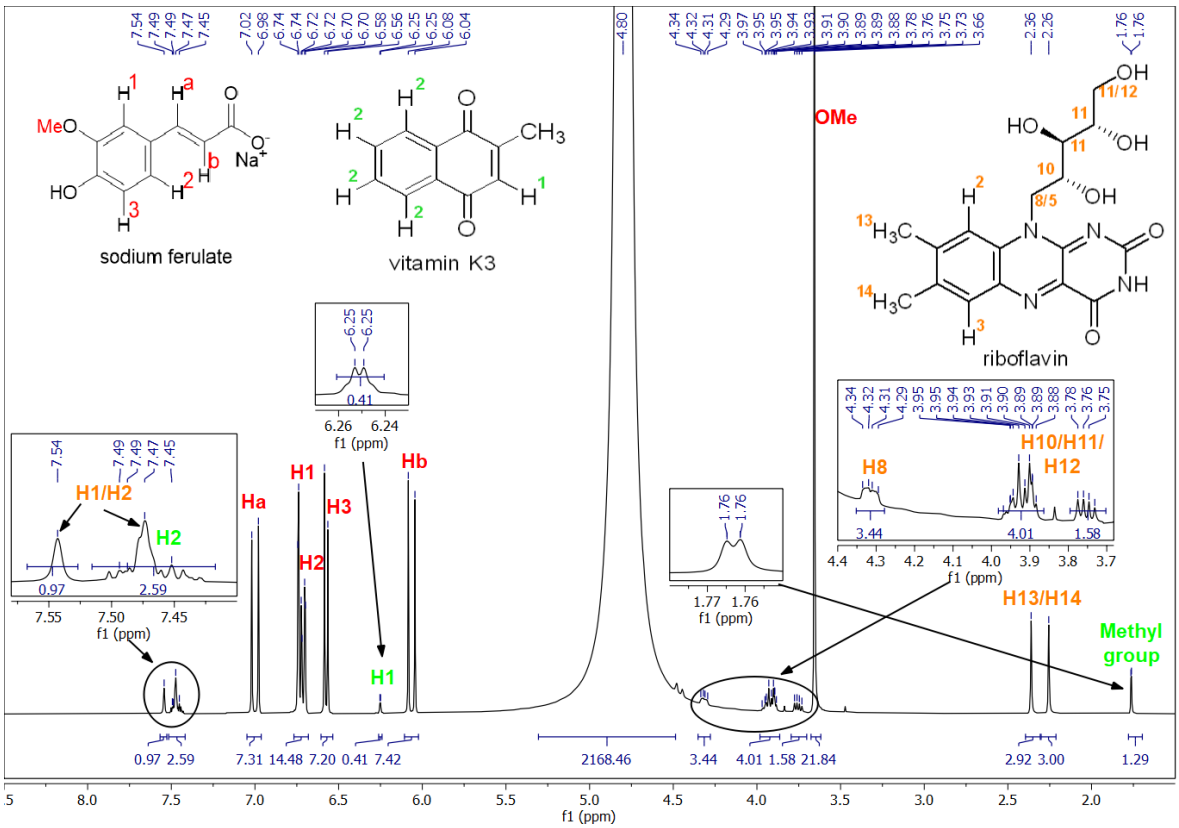

Figure A 85: ^{1}H-NMR spectrum of vitamin K3 and riboflavin (saturation) in an aqueous 0.37 mol·kg^{-1} sodium ferulate solution. Protons of vitamin K3: green; protons of riboflavin: orange; protons of ferulate: red.

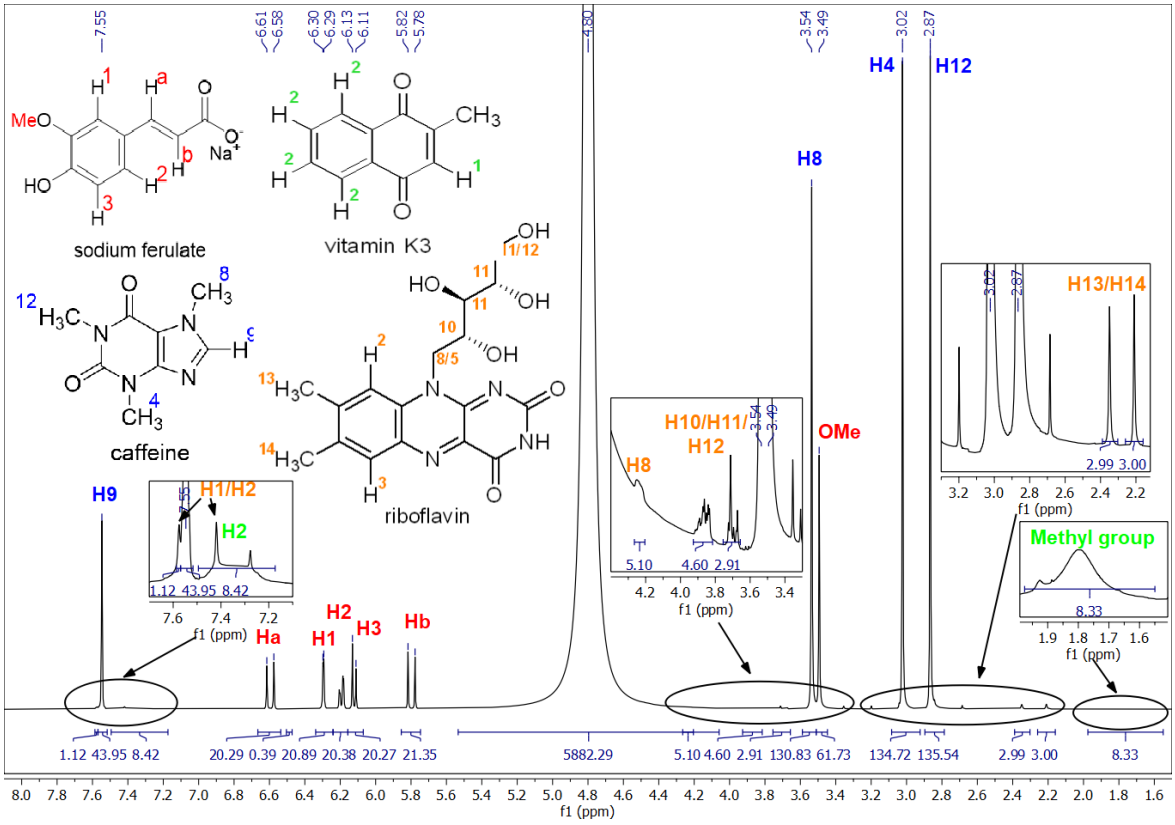

Figure A 86: ^{1}H-NMR spectrum of caffeine, vitamin K3 and riboflavin (saturation) in an aqueous 0.37 mol·kg^{-1} sodium ferulate solution. Protons of caffeine: blue; protons of vitamin K3: green; protons of riboflavin: orange; protons of ferulate: red.

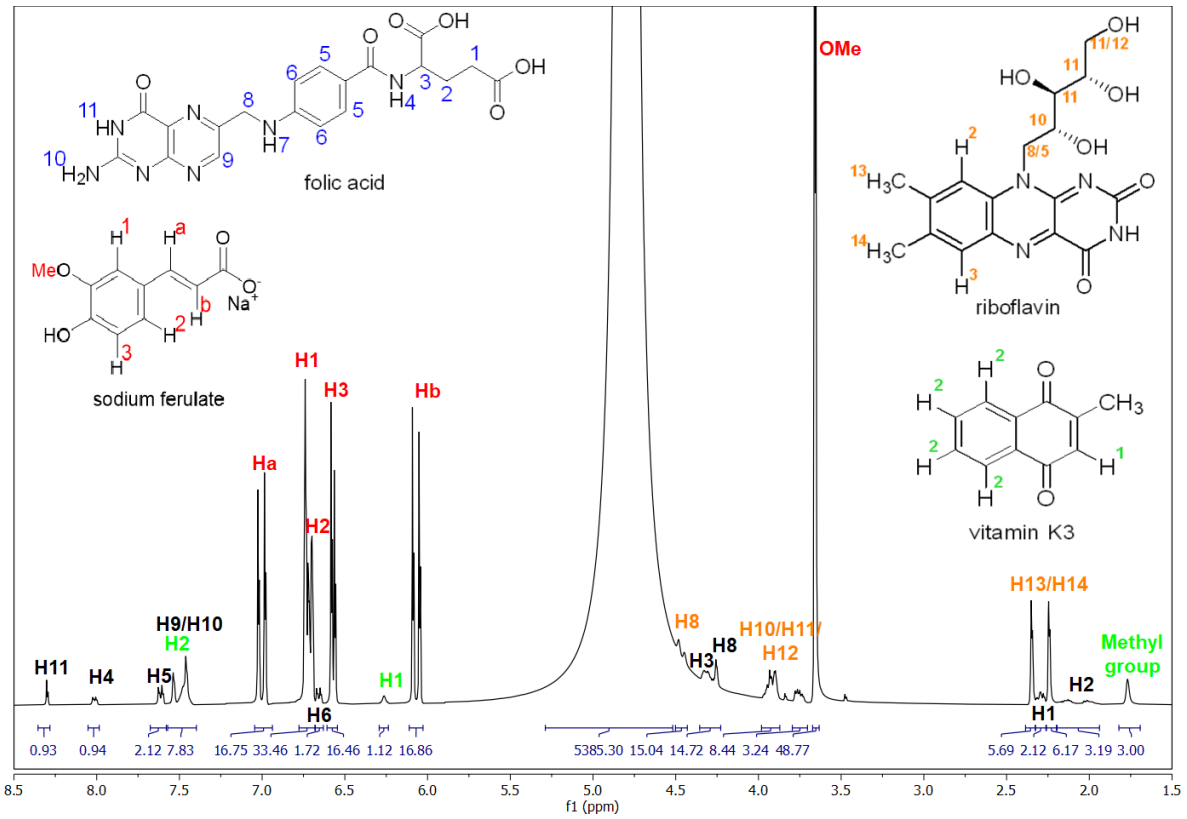

Figure A 87: ^{1}H-NMR spectrum of folic acid, vitamin K3 and riboflavin (saturation) in an aqueous 0.37 mol·kg^{-1} sodium ferulate solution. Protons of folic acid: black; protons of vitamin K3: green; protons of riboflavin: orange; protons of ferulate: red.

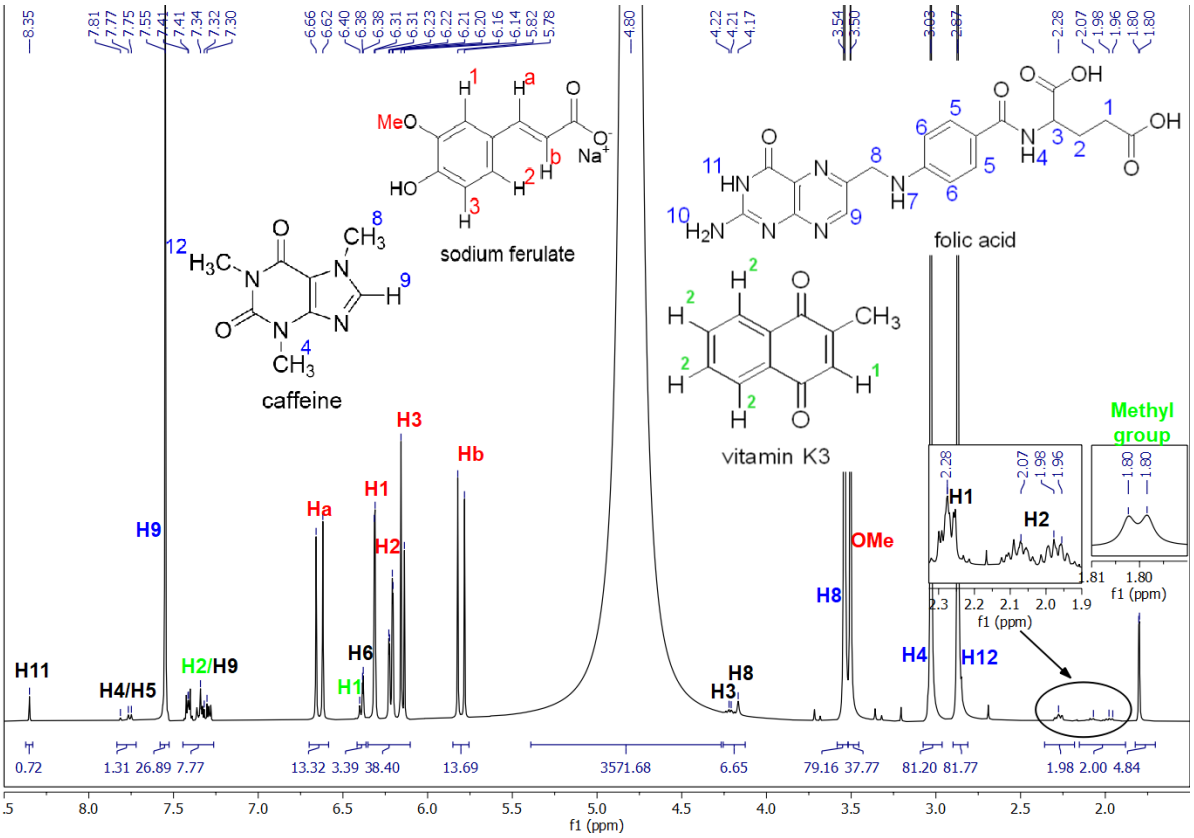

Figure A 88: ^{1}H-NMR spectrum of caffeine, vitamin K3 and folic acid (saturation) in an aqueous 0.37 mol·kg^{-1} sodium ferulate solution. Protons of caffeine: blue; protons of vitamin K3: green; protons of folic acid: black; protons of ferulate: red.

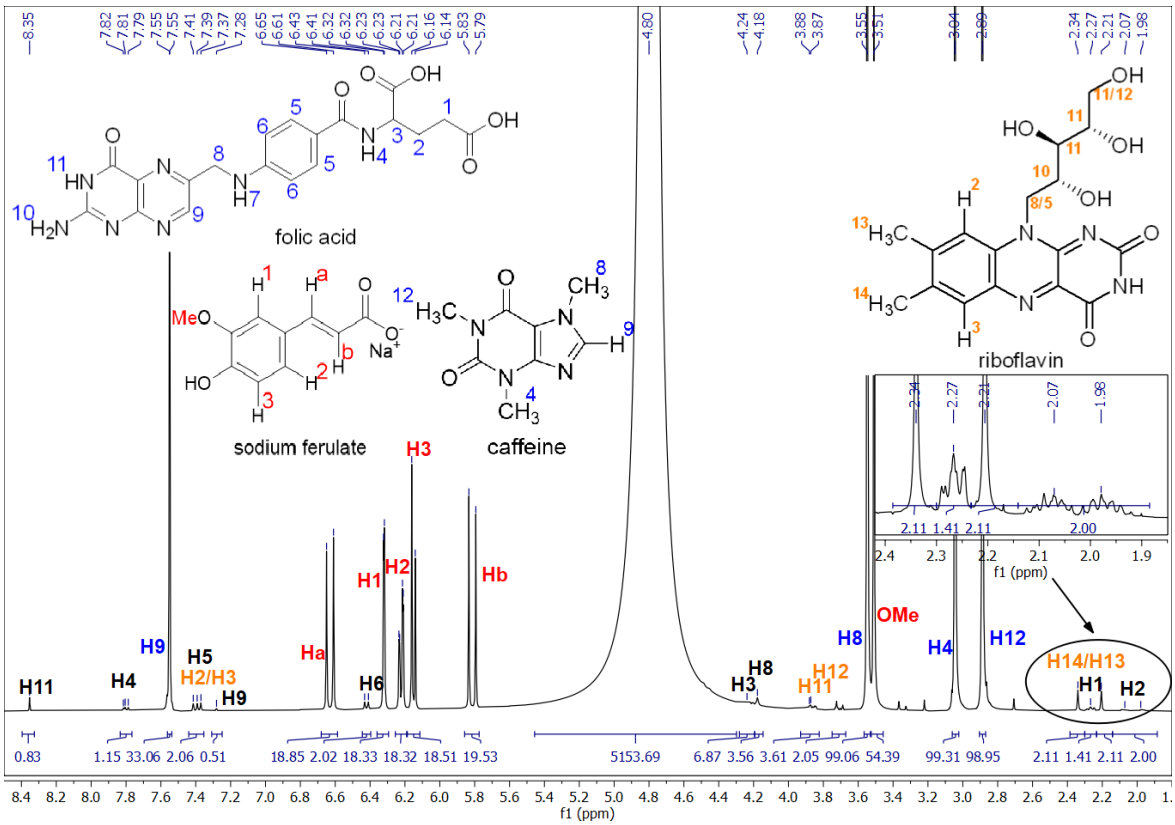

Figure A 89: ^{1}H-NMR spectrum of caffeine, riboflavin and folic acid (saturation) in an aqueous 0.37 mol·kg^{-1} sodium ferulate solution. Protons of caffeine: blue; protons of folic acid: black; protons of riboflavin: orange; protons of ferulate: red.

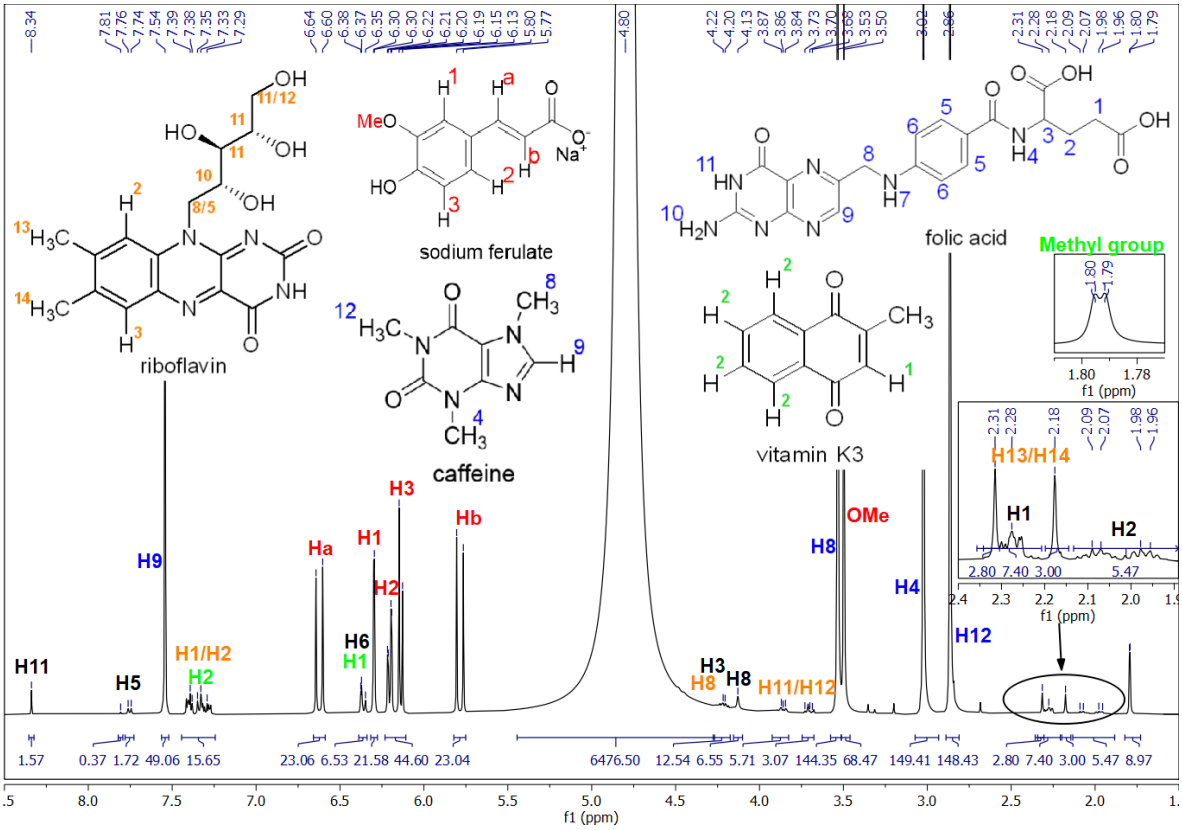

Figure A 90: ^{1}H-NMR spectrum of caffeine, vitamin K3, riboflavin and folic acid (saturation) in an aqueous 0.37 mol·kg^{-1} sodium ferulate solution. Protons of caffeine: blue; protons of vitamin K3: green; protons of folic acid: black; protons of riboflavin: orange; protons of ferulate: red.

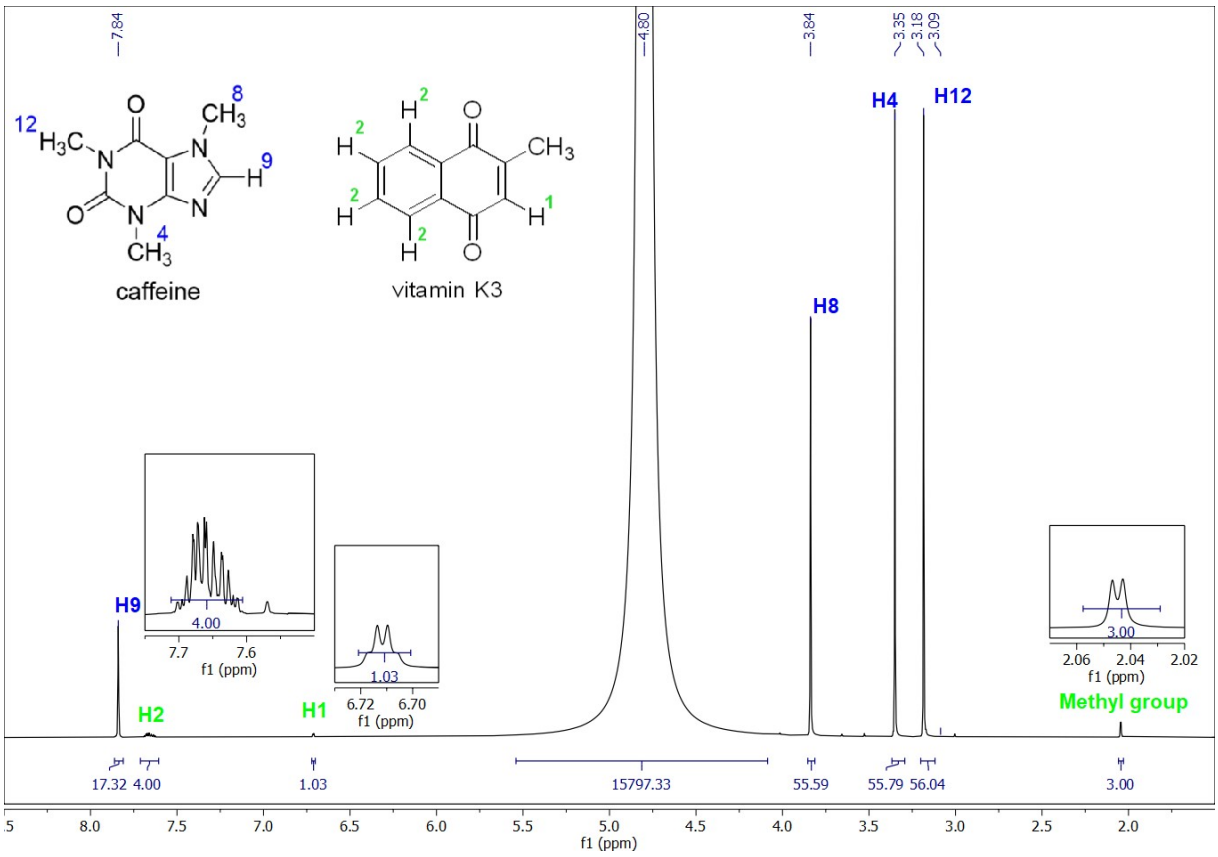

Figure A 91: ^{1}H-NMR spectrum of caffeine and vitamin K3 in water (saturation). Protons of caffeine: blue; protons of vitamin K3.

7.12 Photodegradation of riboflavin

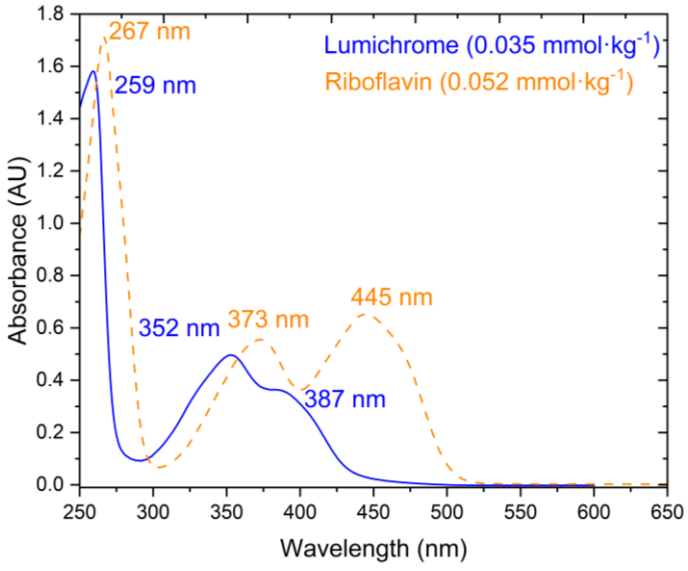

Figure A 92: UV-Vis-absorption spectrum of riboflavin and lumichrome in water.

Table A 119: LC-MS results for the photodegradation of riboflavin in pure water (saturation) after illumination with an LED-plant lamp for 5 h.

M-H$^+$ (g·mol^{-1})	Photodegradation products	Formula	Intensity in ion extract
377.1457	Riboflavin	$C_{17}H_{20}N_4O_4$	10^5
243.0878	Lumichrome	$C_{12}H_{10}H_4O_2$	10^5
301.0931	Carboxymethylflavin	$C_{14}H_{12}N_4O_4$	10^3
375.1302	Cyclodehydroriboflavin	$C_{17}H_{18}N_4O_6$	10^4
315.1086	3-(7,8-Dimethyl-2,4-dioxo-3,4-dihydrobenzo[g]pteridin-10(2H)-yl) propanoic acid	$C_{15}H_{14}N_4O_4$	10^4
285.0983	Formylmethylflavin	$C_{14}H_{12}N_4O_3$	10^4

Table A 120: LC-MS results for the photodegradation of riboflavin (48 mg·kg^{-1}) in presence of sodium ferulate at a molar ratio of 25 after illumination with an LED-plant lamp for 15 h. The photodegradation products with molar mass 570 and 705 seemed to be adducts of ferulic acid and riboflavin. RF = riboflavin.

M-H$^+$ (g·mol^{-1})	Photodegradation products	Formula	Intensity in ion extract
369.0983 (at least 4 different types)	2 x ferulic acid – H_2O – H_2	$C_{20}H_{18}O_8$	10^5
243.0876	Lumichrome	$C_{12}H_{10}H_4O_2$	10^4
301.0931	Carboxymethylflavin	$C_{14}H_{12}N_4O_4$	10^3
375.1299	Cyclodehydroriboflavin	$C_{17}H_{18}N_4O_6$	10^3
570.1978	Adduct of: RF + ferulic acid	$C_{30}H_{24}N_4O_7$	10^4
705.1944	Adduct of 4x ferulic acid – 4x H2O	$C_{38}H_{34}O_{12}$	10^4

*Table A 121: LC-MS results for the photodegradation of riboflavin (48 mg·kg^{-1}) in presence of sodium cinnamate at a molar ratio of 25 after illumination with an LED-plant lamp for 15 h. *Probably dimers/trimers/tetramers of cinnamic acid with riboflavin and decomposition products of riboflavin, as riboflavin has four nitrogen, while some of the degradation products have only two. RF = riboflavin.*

M-H$^+$ (g·mol^{-1})	Photodegradation products	Formula	Intensity in ion extract
425.1714	*	$C_{23}H_{24}N_2O_6$	10^3
676.2648	*	$C_{39}H_{37}N_3O_8$	10^3
692.2612	*	$C_{39}H_{37}N_3O_9$	10^3
793.3437	3x cinnamic acid + RF - CO	$C_{44}H_{48}N_4O_{10}$	10^3
889.3403	*	$C_{46}H_{52}N_2O_{16}$	10^3
847.3189	*	$C_{46}H_{46}N_4O_{12}$	10^3
243.0876	Lumichrome	$C_{12}H_{10}N_4O_2$	10^3
375.1299	Cyclodehydroriboflavin	$C_{17}H_{18}N_4O_6$	10^3

Table A 122: LC-MS results for the oxidation of sodium caffeate in water.

M-H$^+$ (g·mol^{-1})	Photodegradation products	Formula	Intensity in ion extract
313.0730	2x caffeic acid -H_2O - CO	$C_{18}H_{14}O_8$ / $[C_{18}H_{14}O_8]^+$	10^3
403.0673	2x caffeic acid	HCOO)$^-$	

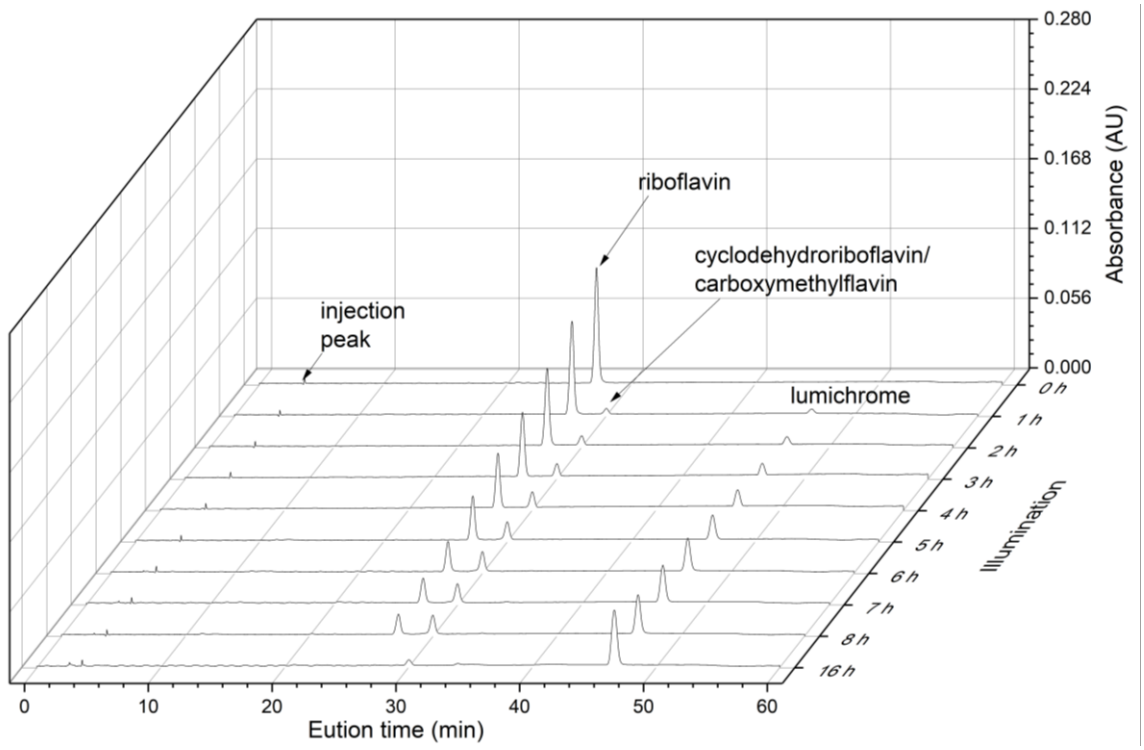

Figure A 93: Chromatographic evolution of the photodegradation of riboflavin (48 mg·kg^{-1}) in Millipore water upon illumination with an LED-plant lamp.

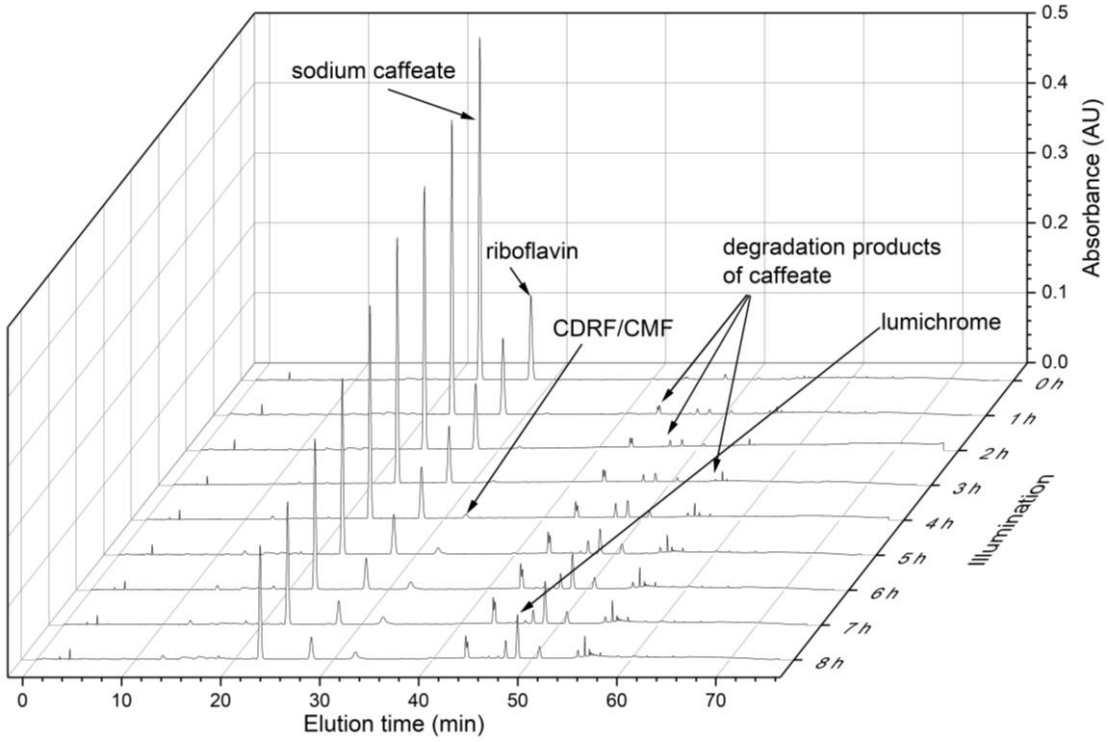

Figure A 94: Chromatographic evolution of the photodegradation of riboflavin (48 mg·kg^{-1}) in aqueous sodium caffeate solution at a molar caffeate/riboflavin ratio of 6 upon illumination with an LED-plant lamp. CDRF = cyclodehydroriboflavin; CMF = carboxymethylflavin.

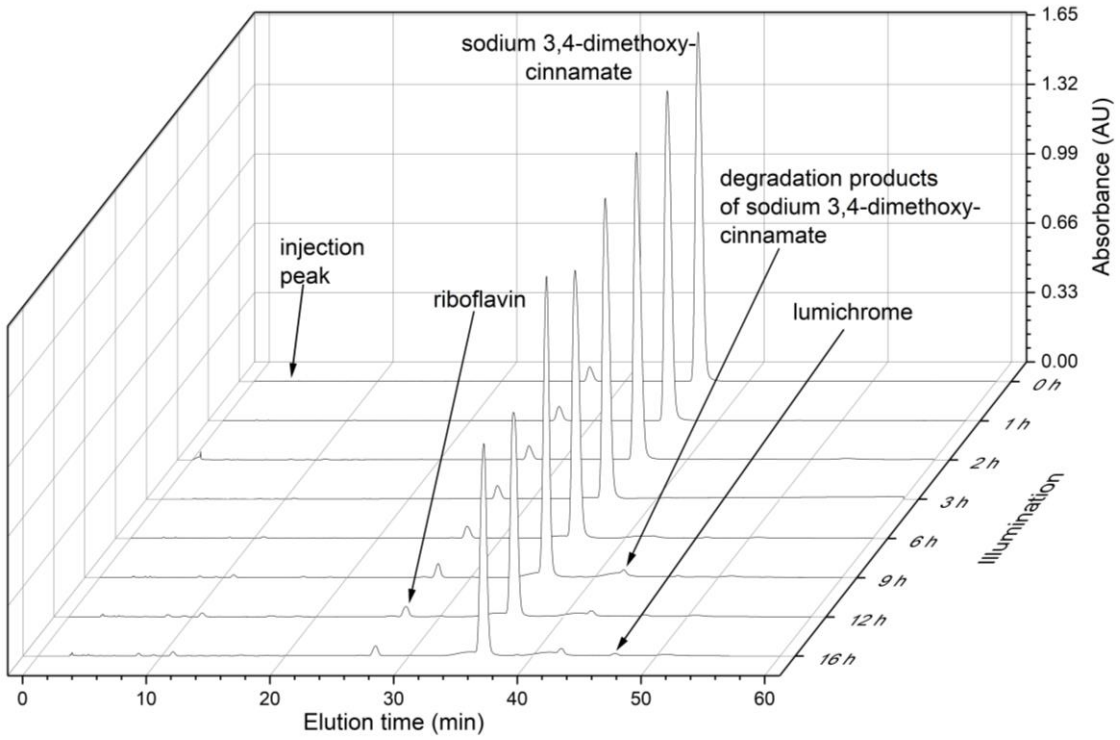

Figure A 95: Chromatographic evolution of the photodegradation of riboflavin (48 mg·kg^{-1}) in aqueous sodium 3,4-dimethoxycinnamate solution at a molar Na-3,4-DiOMe-Cinn/RF ratio of 25 upon illumination with an LED-plant lamp. CDRF = cyclodehydroriboflavin; CMF = carboxymethylflavin.

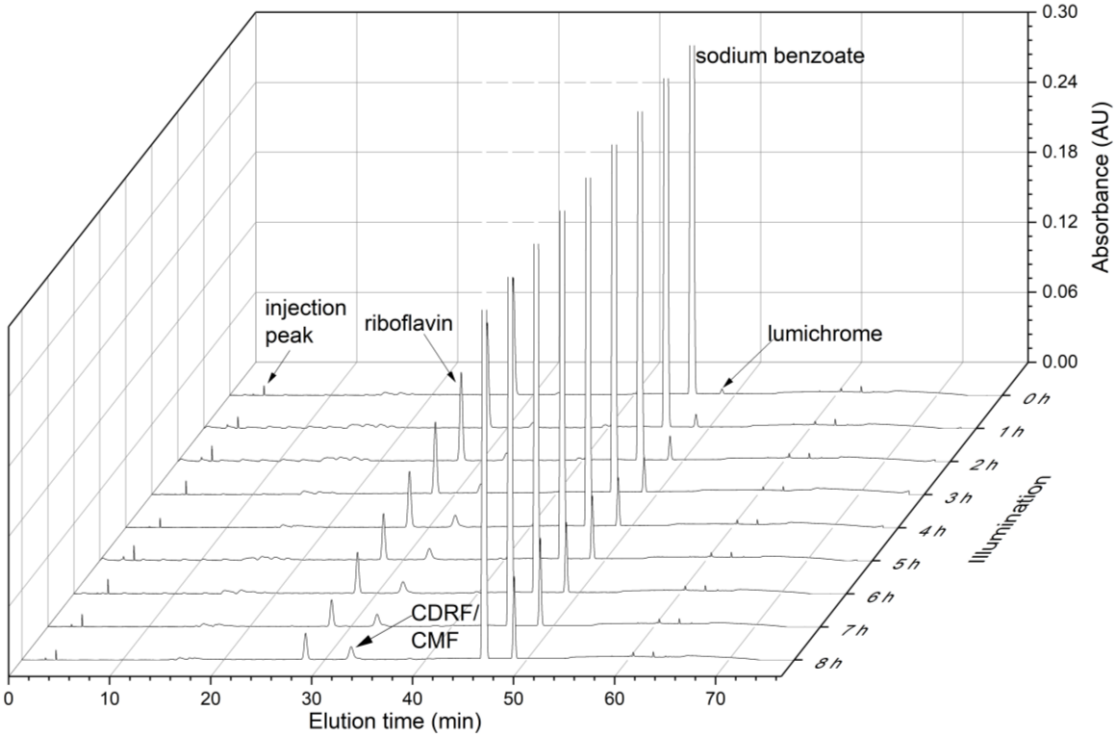

Figure A 96: Chromatographic evolution of the photodegradation of riboflavin (48 mg·kg^{-1}) in aqueous sodium benzoate solution at a molar NaBenz/RF ratio of 50 upon illumination with an LED-plant lamp. CDRF = cyclodehydroriboflavin; CMF = carboxymethylflavin.

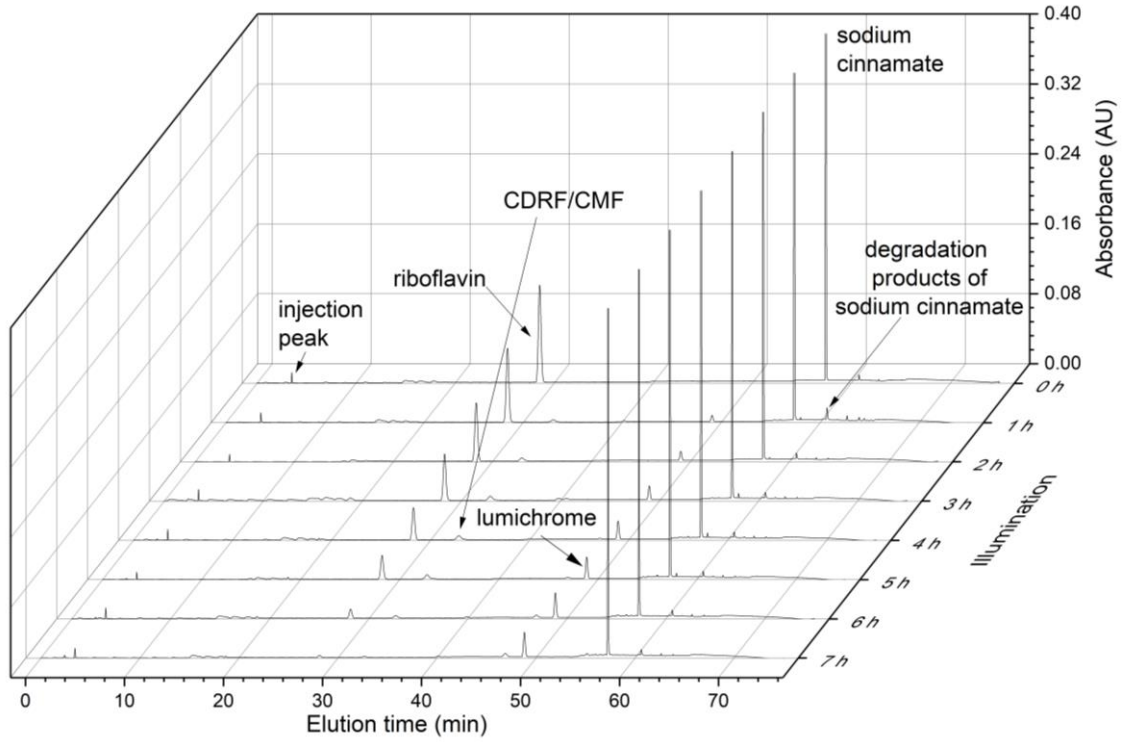

Figure A 97: Chromatographic evolution of the photodegradation of riboflavin (48 mg·kg^{-1}) in aqueous sodium cinnamate solution at a molar NaCinn/RF ratio of 6 upon illumination with an LED-plant lamp. CDRF = cyclodehydroriboflavin; CMF = carboxymethylflavin.

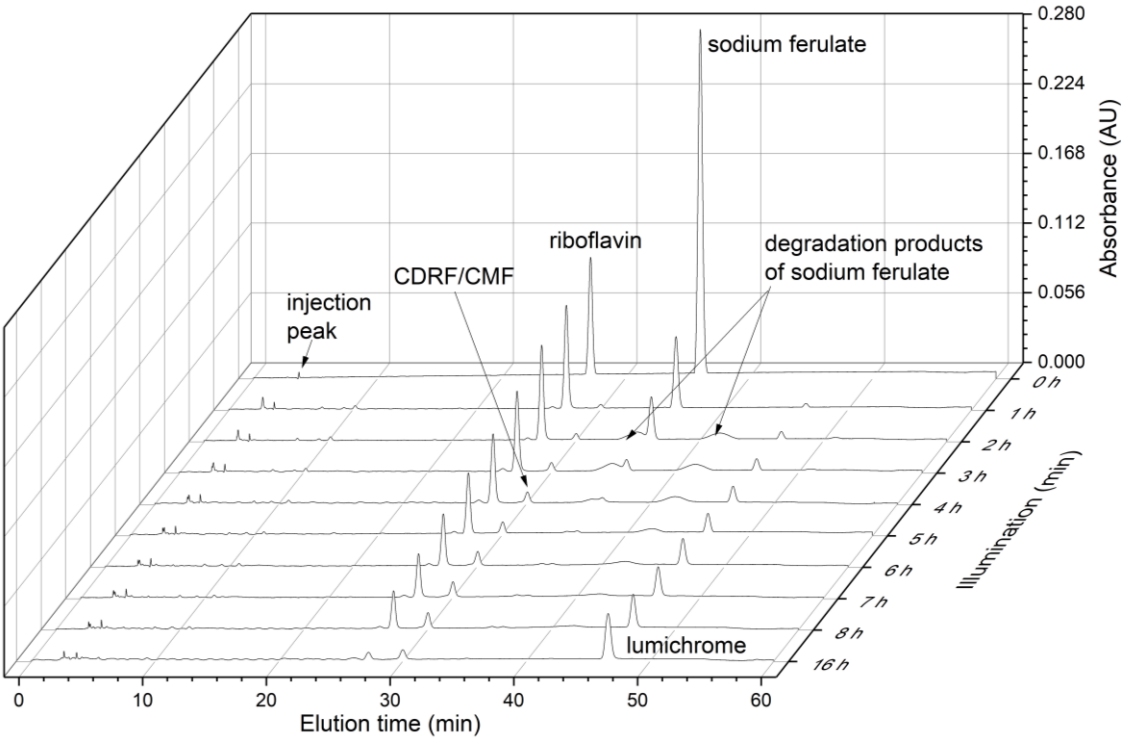

Figure A 98: Chromatographic evolution of the photodegradation of riboflavin (48 mg·kg^{-1}) in aqueous sodium ferulate (Na-4-OH-3-OMe-Cinn) solution at a molar ferulate/riboflavin ratio of 6 upon illumination with an LED-plant lamp. CDRF = cyclodehydroriboflavin; CMF = carboxymethylflavin.

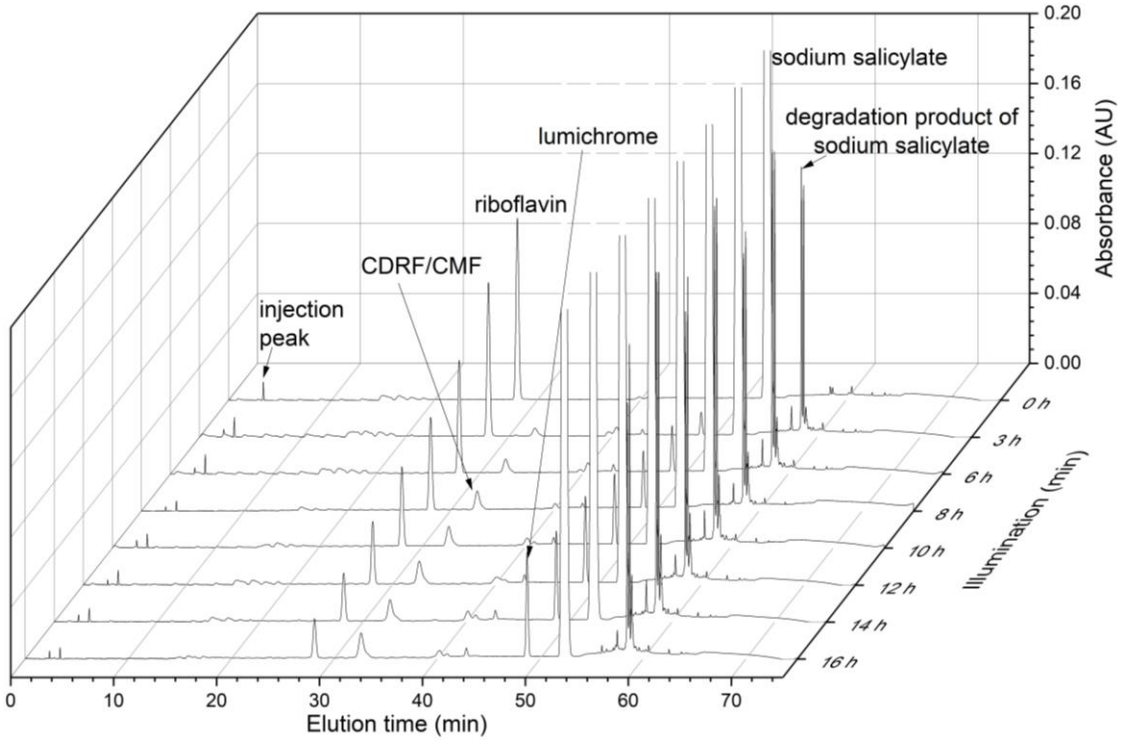

Figure A 99: Chromatographic evolution of the photodegradation of riboflavin (48 mg·kg^{-1}) in aqueous sodium salicylate (Na-2-OH-Benz) solution at a molar Na-2-OH-Benz/RF ratio of 50 upon illumination with an LED-plant lamp. CDRF = cyclodehydroriboflavin; CMF = carboxymethylflavin.

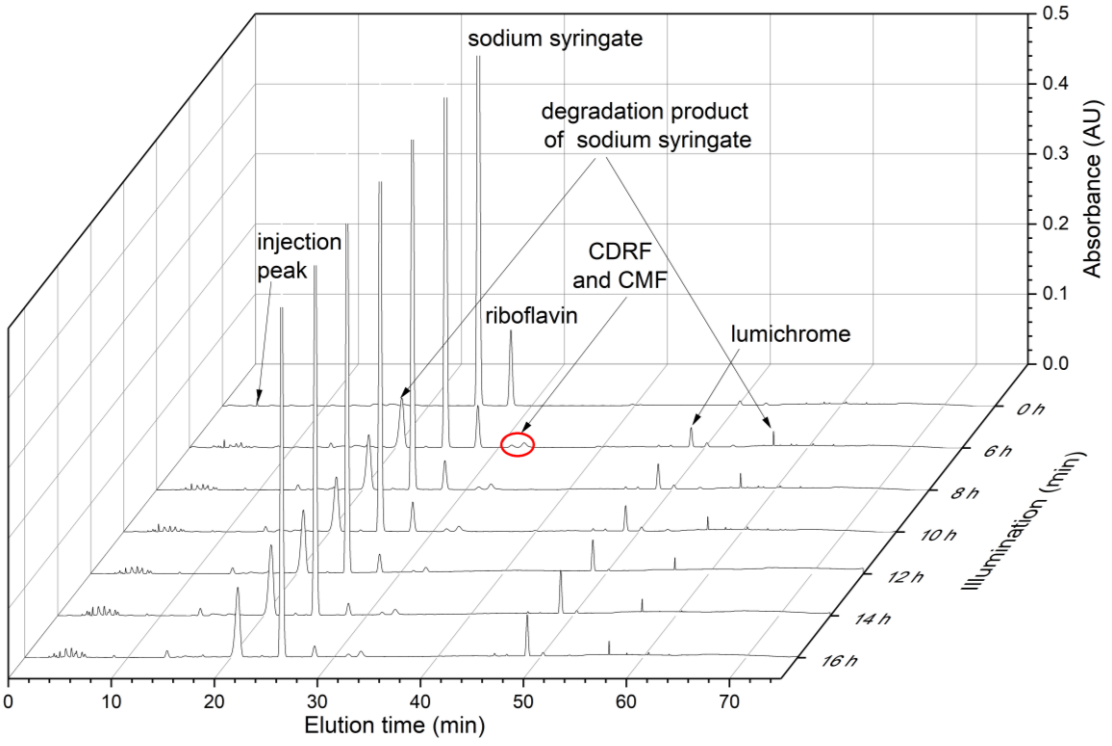

Figure A 100: Chromatographic evolution of the photodegradation of riboflavin (48 mg·kg^{-1}) in aqueous sodium syringate (Na-4-OH-3,5-DiOMe-Benz) solution at a molar Na-4-OH-3,5-DiOMe-Benz /RF ratio of 25 upon illumination with an LED-plant lamp. CDRF = cyclodehydroriboflavin; CMF = carboxymethylflavin.

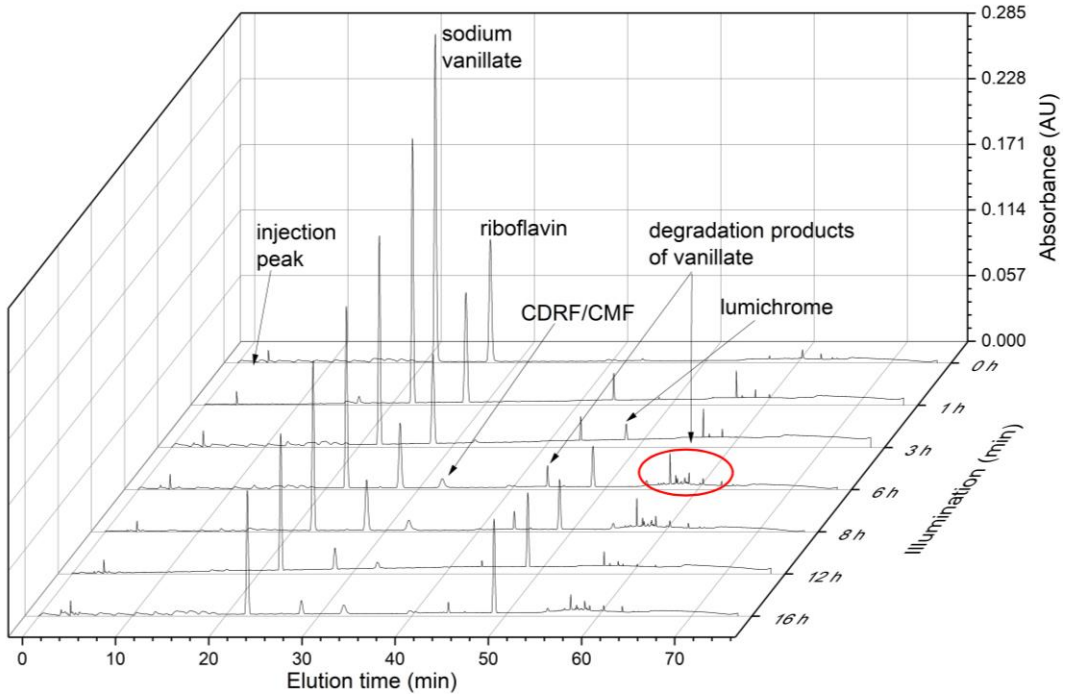

Figure A 101: Chromatographic evolution of the photodegradation of riboflavin (48 mg·kg^{-1}) in aqueous sodium vanillate (Na-4-OH-3-OMe-Benz) solution at a molar Na-4-OH-3-OMe-Benz/RF ratio of 6 upon illumination with an LED-plant lamp. CDRF = cyclodehydroriboflavin; CMF = carboxymethylflavin.

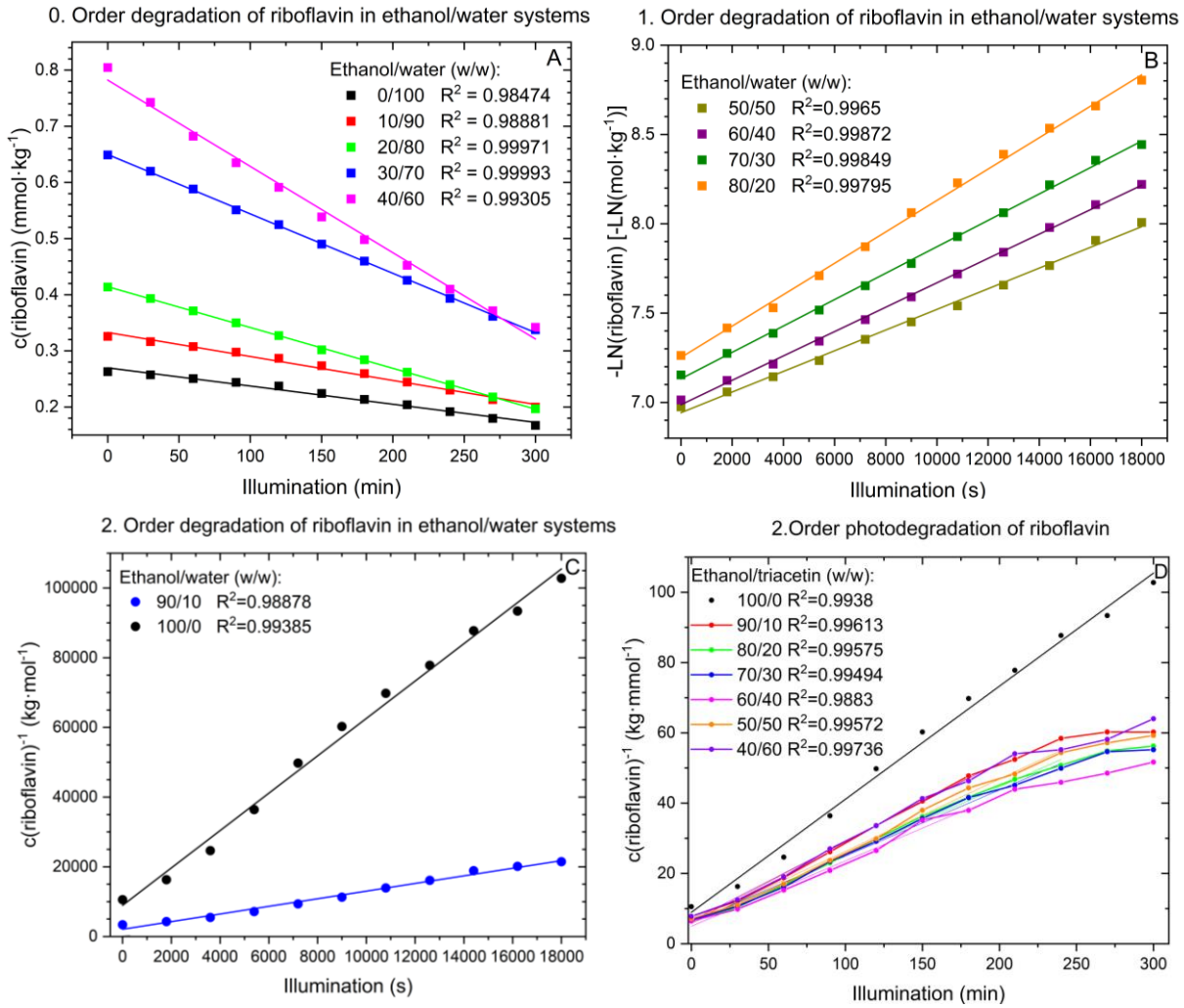

Figure A 102: Photodegradation of riboflavin in binary water/ethanol systems (A-C) and in the binary ethanol/triacetin system (D).

Table A 123: Zero, first and second order rate constants for the photodegradation of riboflavin in the binary water/ethanol and ethanol/triacetin system.

Water/ethanol (w/w)	k_0 (mol·kg^{-1}·s^{-1})
100/0	-5.396·10^{-9}
90/10	-7.119·10^{-9}
80/20	-1.212·10^{-8}
70/30	-1.767·10^{-8}
60/40	-2.567·10^{-8}
Water/ethanol (w/w)	**k_1 [ln(mol·kg^{-1})·s^{-1}]**
50/50	-5.787·10^{-5}
40/60	-6.826·10^{-5}
30/70	-7.392·10^{-5}
20/80	-8.791·10^{-5}
Water/ethanol (w/w)	**k_2 (kg·mol^{-1}·s^{-1})**
10/90	1.094
0/100	5.363

Ethanol/triacetin (w/w)	k_2 (kg·mol^{-1}·s^{-1})
90/10	3.806
80/20	3.237
70/30	3.139
60/40	3.103
50/50	3.422
40/60	3.748

7.13 High pressure liquid chromatography

7.13.1 Elution methods

Table A 124: Left: *Elution method for the RP-18 column from Knauer.* Riboflavin: *27.2 min.* Right: *Elution method for the RP-18 column 4.6 Nucleodur C18 Isis 5 µm.* Riboflavin: 28 min. *Solvent A = Millipore water with 0.1 vol.% trifluoroacetic acid; solvent B = acetonitrile*.

Time (min)	Solvent A (%)	Solvent B (%)
15	90	10
40	80	20
50	80	20
53	90	10
60	90	10

Time (min)	Solvent A (%)	Solvent B (%)
10	95	5
15	90	10
35	90	10
40	80	20
50	80	20
60	10	90
62	10	90
70	95	5
75	95	5

Table A 125: Elution method for the RP-18 column 4.6 Nucleodur C18 Isis 5 µm. Folic acid was eluted at 19.7 min. Solvent A = Millipore water with 0.1 vol.% trifluoroacetic acid; solvent B = acetonitrile.

Time (min)	Solvent A (%)	Solvent B (%)
15	95	5
30	90	10
35	90	10
37	10	90
39	10	90
42	95	5

7.13.2 Calibration curves for riboflavin

The concentration of RF was determined the RP-18 column from Knauer or with the RP-18 column 4.6 Nucleodur C18 Isis 5 µm. Because of RF's poor water-solubility, only a calibration for low RF concentrations would be possible. To have a wider detection range (six points between 0.1 mmol·kg^{-1} and 2 mmol·kg^{-1} riboflavin), the two calibration solutions for the RP-18 column from Knauer were prepared in an aqueous 9.97 g·kg^{-1} sodium ferulate solution, see Table A 126.

For the quantification of the compounds with the RP-18 column 4.6 Nucleodur C18 Isis 5 µm, two calibration curves of RF in an aqueous solution of 9.97 g·kg^{-1} sodium caffeate as solubilizer were recorded (seven points between 0.1 mmol·kg^{-1} and 2 mmol·kg^{-1} riboflavin), see Table A 127. Each concentration of one calibration curve was injected three times. The HPLC measurement setup is given in section 3.7.

Table A 126: Calibration curves for riboflavin in an aqueous sodium ferulate solution for the RP-18 column from Knauer at 445 nm.

Slope (V·s kg·mmol^{-1})	Intercept (V·s)	Correlation coefficient R^2
6.769	-0.02	1
6.714	-0.01	0.9999
averaged	**averaged**	**-**
6.74 ± 0.03	**0.017 ± 0.007**	-

Table A 127: Calibration curves for riboflavin in an aqueous sodium caffeate solution for the RP-18 column 4.6 Nucleodur C18 Isis 5 µm at 445 nm.

Slope (V·s kg·mmol^{-1})	Intercept (V·s)	Correlation coefficient R^2
6.745	-0.02	1
6.708	-0.10	0.9994
averaged	**averaged**	**-**
6.73 ± 0.02	**0.06 ± 0.04**	-

7.13.3 Calibration curves for aromatic sodium salts

Two calibration curves of the sodium caffeate, ferulate, salicylate, benzoate, vanillate, cinnamate, syringate and 3,4-dimethoxycinnamate in water were recorded with the RP-18 column 4.6 Nucleodur C18 Isis 5 µm, see Table A 128-Table A 135. Therefore, each concentration of one calibration curve was injected twice. The solutions were prepared via dissolution of the salt in water or via neutralization of the corresponding acid with self-made sodium hydroxide solution.

Table A 128: Calibration curves for sodium caffeate in water for the RP-18 column 4.6 Nucleodur C18 Isis 5 µm at 323 nm. Due to the high oxidative sensitivity of caffeate, the deviation of the calibration curves was nearly 9 %. Seven points from 0.1-12 mmol·kg^{-1}.

Slope (V·s kg·mmol^{-1})	Intercept (V·s)	Correlation coefficient R^2
5.57	0.1	0.9983
5.46	0.74	0.9977
averaged	**averaged**	**-**
5.51 ± 0.06	**0.4 ± 0.3**	-

Table A 129: Calibration curves for sodium cinnamate in water for the RP-18 column 4.6 Nucleodur C18 Isis 5 µm at 270 nm. Six points from 0.1-1 mmol·kg^{-1}.

Slope (V·s kg·mmol^{-1})	Intercept (V·s)	Correlation coefficient R^2
10.51	0.1	0.9999
10.599	0.1	0.9998
averaged	**averaged**	**-**
10.55 ± 0.05	**0.091 ± 0.005**	-

Table A 130: Calibration curves for sodium vanillate in water for the RP-18 column 4.6 Nucleodur C18 Isis 5 µm at 292 nm. Six points from 0.12-13 mmol·kg^{-1}.

Slope (V·s kg·mmol^{-1})	Intercept (V·s)	Correlation coefficient R^2
3.036	0.18	0.9999
2.992	0.24	0.9998
averaged	**averaged**	**-**
3.01 ± 0.02	**0.21 ± 0.03**	-

Table A 131: Calibration curves for sodium ferulate in water for the RP-18 column 4.6 Nucleodur C18 Isis 5 µm at 323nm. Five points from 0.46-2.3 mmol·kg^{-1}.

Slope (V·s kg·mmol^{-1})	Intercept (V·s)	Correlation coefficient R^2
10.455	-0.171	0.9970
9.897	0.05	0.9977
averaged	**averaged**	**-**
10.2 ± 0.3	**0.1 ± 0.1**	-

Table A 132: Calibration curves for sodium salicylate in water for the RP-18 column 4.6 Nucleodur C18 Isis 5 µm at 302 nm. Six points from 0.1-8 mmol·kg^{-1}.

Slope (V·s kg·mmol^{-1})	Intercept (V·s)	Correlation coefficient R^2
1.915	0.025	0.9982
2.014	0.071	0.9993
averaged	**averaged**	**-**
1.96 ± 0.05	**0.05 ± 0.02**	-

Table A 133: Calibration curves for sodium benzoate in water for the RP-18 column 4.6 Nucleodur C18 Isis 5 µm at 273 nm. Eight points from 0.1-10 mmol·kg^{-1}.

Slope (V·s kg·mmol^{-1})	Intercept (V·s)	Correlation coefficient R^2
0.5053	0.056	0.9990
0.5043	0.046	0.9998
averaged	**averaged**	**-**
0.5048 ± 0.0005	**0.051 ± 0.005**	-

Table A 134: Calibration curves for sodium syringate in water for the RP-18 column 4.6 Nucleodur C18 Isis 5 µm at 274 nm. Seven points from 0.1-8 mmol·kg^{-1}.

Slope (V·s kg·mmol^{-1})	Intercept (V·s)	Correlation coefficient R^2
5.543	0.22	0.9997
5.617	0.20	0.9998
averaged	**averaged**	**-**
5.58 ± 0.04	**0.21± 0.01**	-

Table A 135: Calibration curves for sodium 3,4-dimethoxycinnamate in water for the RP-18 column 4.6 Nucleodur C18 Isis 5 µm at 323 nm. Five points from 0.43-2.5 mmol·kg^{-1}.

Slope (V·s kg·mmol^{-1})	Intercept (V·s)	Correlation coefficient R^2
9.458	0.305	0.9987
9.255	0.495	0.9987
averaged	**averaged**	**-**
9.4 ± 0.1	**0.4 ± 0.1**	-

7.13.4 Calibration curves for folic acid

Table A 136: Calibration curves for folic acid in an aqueous sodium vanillate solution for the RP-18 column 4.6 Nucleodur C18 Isis 5 µm at 290 nm.

Slope (V·s kg·mmol^{-1})	Intercept (V·s)	Correlation coefficient R^2
11.132	-0.0312	0.9999
10.852	0.0045	0.9992
10.616	-0.0112	0.9998
averaged	**averaged**	**-**
10.9 ± 0.2	**-0.01 ± 0.01**	-

Eidesstattliche Erklärung

Ich erkläre hiermit an Eides statt, dass ich die vorliegende Arbeit ohne unzulässige Hilfe Dritter und ohne Benutzung anderer als der angegebenen Hilfsmittel angefertigt habe; die aus anderen Quellen direkt oder indirekt übernommenen Daten und Konzepte sind unter Angabe des Literaturzitats gekennzeichnet.

Weitere Personen waren an der inhaltlich-materiellen Herstellung der vorliegenden Arbeit nicht beteiligt. Insbesondere habe ich hierfür nicht die entgeltliche Hilfe eines Promotionsberaters oder anderer Personen in Anspruch genommen. Niemand hat von mir weder unmittelbar noch mittelbar geldwerte Leistungen für Arbeiten erhalten, die im Zusammenhang mit dem Inhalt der vorgelegten Dissertation stehen. Die Arbeit wurde bisher weder im In- noch im Ausland in gleicher oder ähnlicher Form einer anderen Prüfungsbehörde vorgelegt. Ich versichere an Eides statt, dass ich nach bestem Wissen die reine Wahrheit gesagt und nichts verschwiegen habe.

Regensburg, den _____ _____

Nadja Ulmann